



EXPLORE *in* MANITOBA

Report of Activities 1997

DISCOVER *the* MANITOBA ADVANTAGE



**Manitoba
Energy and Mines**



MANITOBA ENERGY AND MINES

MINISTER, Hon. David Newman

Room 314, Legislative Building
Winnipeg, MB R3C 0V8
(204) 945-4601 Fax: (204) 945-8374

A/DEPUTY MINISTER, Garry Barnes

Room 314, Legislative Building
Winnipeg, MB R3C 0V8
(204) 945-4172 Fax: (204) 945-8374

BRANCH/SECTION STAFF

360 - 1395 Ellice Avenue, Winnipeg, MB R3G 3P2

MARKETING

Fax: (204) 945-8427

Director	Jim Crone	945-1874	Library Website Coordinator	Monique Lavergne	945-6584
Business Development	Lyle Skinner	945-6585	Media Relations and		
	Gary Ostry	945-6564	Convention Coordinator	Elaine Stevenson	945-2691
Mineral Exploration			Information Resources		
Assistance Program	Shelly Lizak	945-6586	Manager	Dave Baldwin	945-6551

GEOLOGICAL SERVICES

Fax: (204) 945-1406

A/Director	Christine Kaszycki	945-6549	Flin Flon Office:		
Geology/Precambrian	Ric Syme	945-6556	143 Main Street, Flin Flon, MB R8A 1K2		
Sedimentary and			Tom Heine	687-1633	
Industrial Minerals	Christine Kaszycki	945-6549		(Fax) 687-1623	
Geoscience					
Information Services	Paul Lenton	945-6553	Core Storage, 10 Midland Street, Winnipeg ;		
Thompson Office:			Core Shed, University of Manitoba; and Rock Storage		
204 - 59 Elizabeth Road, Thompson, MB R8N 1X4	Peter Theyer	677-6886	Facility, Perimeter Hwy. at Brady Road	Doug Berk	945-6550
		(Fax) 677-6888			(Fax) 948-2164

MINES

Fax: (204) 945-8427

Director	Art Ball	945-6505	Brandon Office:		
Mining Recording	Sheena Shetty	945-6528	340-Ninth Street, Brandon, MB R7A 6C2		
Mining Engineering	Barry Hadfield	945-6517	Doug Bender	726-7118	
				(Fax) 726-6749	
The Pas Office:			Russell Office:		
3rd and Ross Avenue, P.O. Box 2550, The Pas, MB R9A 1M4	Fred Heidman	627-8268	402 Main Street N., Russell, MB R0J 1W0	Jack Adams	773-3343
		(Fax) 627-8387			(Fax) 773-2411

PETROLEUM AND ENERGY

Fax: (204) 945-0586

Director	Bob Dubreuil	945-6573	Virden Office:		
Geology/Administration/	Carol Martiniuk	945-6570	227 King Street W., P.O. Box 1359, Virden, MB R0M 2C0		
Special Projects			Bruce Dunning	748-1557	
Computer Programmer	Keith Lowdon	748-1627		(Fax) 748-2208	
Engineering and Inspection	John Fox	945-6574	Waskada Office:		
Energy Efficiency			106 Railway Avenue, P.O. Box 220, Waskada, MB R0M 2E0		
and Alternative Energy	Grant McVicar	945-3674	Lorne Barsness	673-2472	
				(Fax) 673-2767	

ADMINISTRATIVE SERVICES

Fax: (204) 945-1406

A/Executive Director	Craig Halwachs	945-3675	Computer Services	Andy Bibik	945-2172
Personnel Services	JoAnne Reinsch	945-4437			

For a complete list of staff and e-mail addresses, visit our website at <http://www.gov.mb.ca/em>

Manitoba
Energy and Mines
Geological Services



**REPORT OF
ACTIVITIES
1997**

1997

This publication is available in large print, audiotape or braille on request

Errata

Report of Activities 1997

GS-19

Page 123: In Table GS-19-1, locations of coreholes are incorrect:

M-1-97 Selkirk	NTS 62I/2 5553900N 354875N 228.9 m	<i>replace with:</i>	11-22-13-5E 62I/2 5553900N 654875E 228.9 m
M-2-97 Selkirk	NTS 62J/2 5551275N 352860E 233.2 m	<i>replace with:</i>	4-16-13-5E 5551275N 652860E 233.2 m
M-3-97 Selkirk	16-32-13-15E 5557255N 357475E 230.1 m	<i>replace with:</i>	NTS 62I/2 9-35-13-5E 5557255N 657475E 230.1 m

Page 127: Diamond drill log intervals identified in Table GS-19-2 for M-1-97 should be replaced with:

89.5-89.2	with 98.5-99.2
89.2-89.4	with 99.2-99.4
89.4-89.9	with 99.4-99.8
89.9-101.6	with 99.8-101.6



**Minister of
Energy and Mines**
Minister responsible for Manitoba Hydro

Room 314
Legislative Building
Winnipeg, Manitoba, CANADA
R3C 0V8



I am pleased to present this report on the 1997 geoscientific activities of Manitoba Energy and Mines.

The 1997 **Report of Activities** is a synopsis of recent work conducted by the geological staff of the Department. It is designed and presented in a format that will give the mining industry an informative summary of this past summer's geological work, with a view to assisting their exploration plans for the coming year. In releasing the **Report of Activities** at the 1997 Manitoba Mining and Minerals Convention, we hope to stimulate discussion at the convention and produce fruitful consultations between industry geologists and my staff.

In support of Manitoba's mineral strategy, field activities were focused in the traditional mining areas of Manitoba as well as in frontier parts of the province. Work continued in established mining camps at Flin Flon, Snow Lake and Lynn Lake to support exploration for copper/zinc and gold mineralization. In the Thompson Nickel Belt, a major new initiative was launched this year that harnesses the cooperative efforts of the exploration industry, geological survey staff and the universities in developing the geological framework for exploration in this highly productive area. In frontier areas, such as the northern Superior Province, work continued on regional multimedia geochemical surveys to identify prospective areas for exploration. New mapping programs were implemented in this region as part of a federally sponsored NATMAP initiative designed to better understand the volcanic, structural and tectonic evolution of greenstone belts.

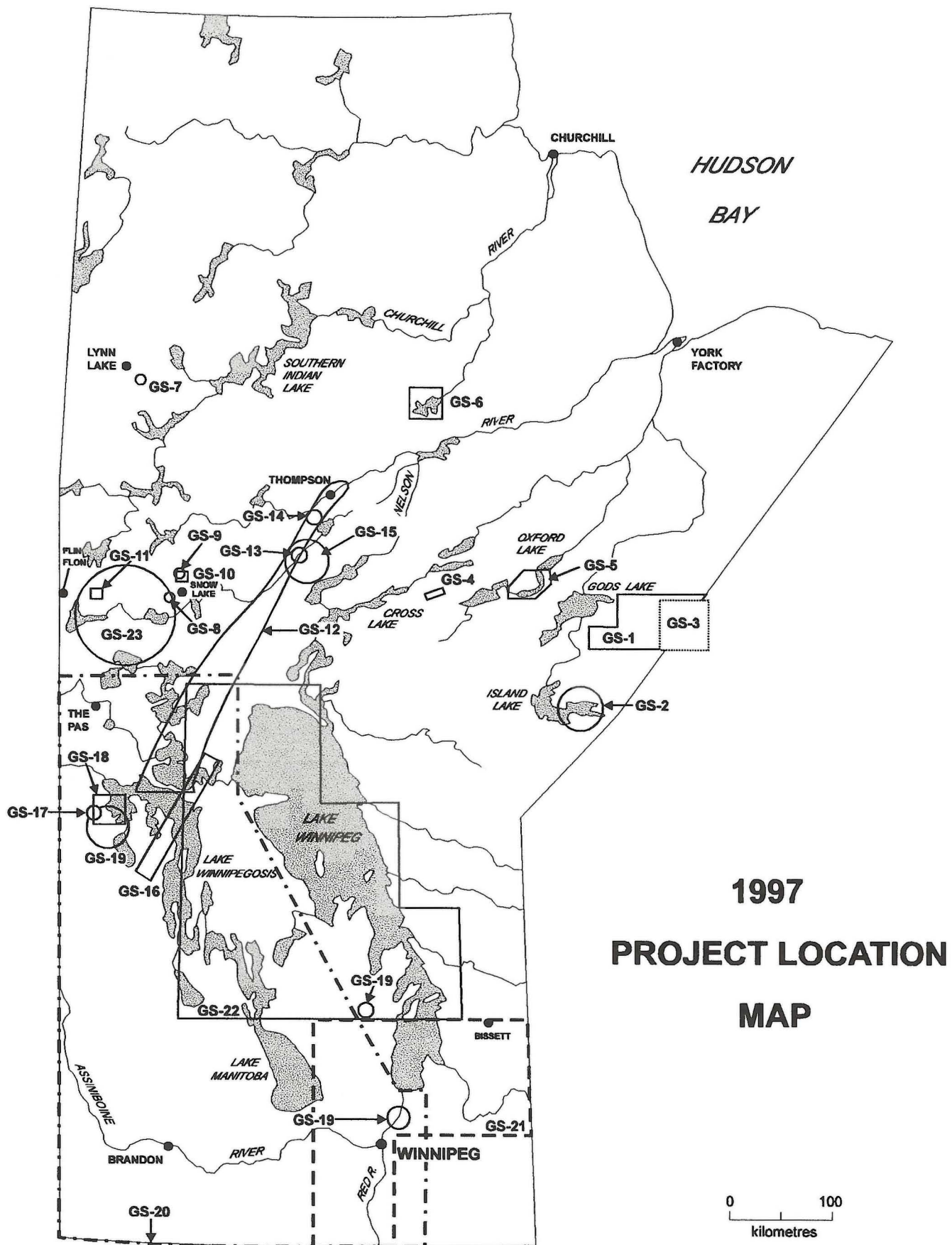
In southern Manitoba, the recognition of microdisseminated precious metal mineralization has opened up exciting exploration opportunities in areas outside of the traditional "gold-hunting grounds".

We hope that the Report of Activities and our exploration incentives will stimulate your interest and promote further mineral exploration in Manitoba.

Yours sincerely,

David Newman





GS-1

TABLE OF CONTENTS

Minister's Message

Introductory Summary
by W.D. McRitchie

SUPERIOR PROVINCE

GS-1	Operation Superior: Multimedia Geochemical Surveys in the Edmund Lake and Sharpe Lake Greenstone Belts, Northern Superior Province, Manitoba (NTS 53K) by M.A.F. Fedikow and E. Nielsen	4
GS-2	Structural Setting of the Au-Bearing Quartz Veins at the Henderson Island Gold Deposit (Ministik Mine), Island Lake, Manitoba by S. Lin and H.D.M. Cameron	6
GS-3	Geology of the Little Stull Lake Area (part of NTS 53K/10) by M.T. Corkery, T. Skulski and J.B. Whalen	13
GS-4	Geology and Geochemistry of the Eastern Part of the Carrot River Greenstone Belt, Northwestern Superior Province, Manitoba (part of NTS 63I/16) by D.C. Peck, P. Theyer, J. Liwanag and C. Chandler	18
GS-5	Geological Investigations in the Knee Lake Area, Northwestern Superior Province (parts of NTS 53L/15 and 53L/14) by E.C. Syme, M.T. Corkery, A.H. Bailes, S. Lin, H.D.M. Cameron and D. Prouse	37
GS-6	Geology of the Assean Lake Area (parts of NTS 64A/1,2,7,8) by Ch. Böhm	47

LYNN LAKE DISTRICT

GS-7	Geochemical and Structural Analysis of Gold Mineralization at the Burnt Timber Mine, Lynn Lake (part of NTS 64C/15) by D.C. Peck and A.M. Eastwood	50
------	--	----

FLIN FLON-SNOW LAKE DISTRICT

GS-8	Geochemistry of Paleoproterozoic Volcanic Rocks in the Photo Lake Area, Flin Flon Belt (parts of NTS 63K16) by A.H. Bailes	61
GS-9	Geological Settings and Genesis of Gold Mineralization in the Snow Lake Area (NTS 63K/16) by G.H. Gale	73
GS-10	Squall Lake Project: Geology and Gold Mineralization North of Snow Lake (NTS 63K/16NE) by D.C.P. Schledewitz	79
GS-11	Geology of the Lac Aimée-Naosap Lake Area (NTS 63K/13SE and 63K/14SW) by H.P. Gilbert	84

THOMPSON-CROSS LAKE DISTRICT

GS-12	The Thompson Nickel Belt Project: Aims and Objectives by D.C. Peck	99
GS-13	Thompson Nickel Belt Project: Progress on a New Compilation Map of the Thompson Nickel Belt (parts of NTS 63J, 63O and 63P) by J.J. Macek	101
GS-14	Thompson Nickel belt Project: Petrographic and Chemical Characterization of Major Lithologies (parts of NTS 63J, 63O and 63P) by C.R. McGregor	102
GS-15	Revised Stratigraphy of the Setting Lake Area (parts of NTS 63O/1, 2 and 63J/15) by H.V. Zwanzig	103
GS-16	Stratigraphy and Lithologies of Selected Drill Core from the Lake Winnipegosis Komatiite Belt (parts of NTS 63B, 63C and 63G) by P. Theyer	109

SOUTHERN MANITOBA-INTERLAKE REGION

GS-17	Geology, Geochemistry and Geophysics of Prairie-type Microdisseminated Mineralization in West Central Manitoba (NTS 63C) by J.D. Bamburak, R.K. Bezys, M.A.F. Fedikow and I. Hosain	112
GS-18	A Geochemical Study of Saline Brine Sediments as a Guide to Prairie-type Microdisseminated Mineralization and Other Precious Metals in West Central Manitoba (NTS 63C) by R.K. Bezys, E.B. Ducharme, J.D. Bamburak, and M.A.F. Fedikow	118
GS-19	Stratigraphic and Industrial Mineral Core hole Drilling Program 1997 (NTS 63C) by R.K. Bezys and J.D. Bamburak	123
GS-20	Geochemical Characterization of Black Shales in Manitoba's Phanerozoic by M.A.F. Fedikow, R.K. Bezys, J.D. Bamburak and R.G. Garrett	129
GS-21	Quaternary Geological, Engineering Geological, and Hydrogeological Initiatives in the Red River Valley, Interlake, and Southeastern Manitoba by G. L. D. Matile and L. H. Thorleifson	131
GS-22	Tufa Mounds, Upwellings and Gravity Springs in the Central and Northern Interlake Region, Manitoba (parts of NTS Areas 62O, 62P, 63B and 63G) by W.D. McRitchie and C. A. Kaszycki	133

MANITOBA GENERAL

GS-23	The Use of Rare Earth Element Analyses in the Exploration for Massive Sulphide Type Deposits in Volcanic Rocks - Progress Report by G.H. Gale, L.B. Dabek and M.A.F. Fedikow	147
GS-24	Geoscience Information Services Projects by P.G. Lenton	156

A diskette containing tables of analytical data presented in this report is available at the price of \$2.00 from:

Manitoba Energy and Mines
Marketing Branch, Publication Sales
1395 Ellice Avenue, Suite 360
Winnipeg, MB R3G 3P2
Canada

Telephone (204) 945-4154
Fax (204) 945-8427
e-mail publications@em.gov.mb.ca

INTRODUCTORY SUMMARY

by W. D. McRitchie

McRitchie, W. D., 1997: Introductory Summary; in Manitoba Energy and Mines, Geological Services Report of Activities 1997, p 1-3.

GENERAL

During 1997, Geological Survey programming in Manitoba continued to build in momentum, along with other government initiatives directed at stimulating increased levels of exploration and investments in the province's mineral sector. The strategic plan of the Department of Energy and Mines, now in its third year, includes the introduction of more favourable taxation policies, an enhanced Mineral Exploration Assistance Program (MEAP), Prospector Assistance, one window permitting procedures and increased funding for geological surveys (\$3.6 million in 1997) to generate new maps and information that will underpin the exploration efforts of the private sector.

In January, the Geological Services Branch (GSB) was reorganized into two new sections, a Precambrian Survey and a Sedimentary and Industrial Minerals Section (SIMS), each headed by new Chief Geologists. These field-oriented units will be supported by a Geoscience Information Services Unit (including a digital cartography component) and an Administrative Services Unit. SIMS also oversees the activities and functions of the Rock Preparation Laboratory at Midland Street. In April, 1997, management of the Branch's Analytical Laboratory on Logan Avenue was transferred to the Manitoba Technology Centre along with established commitments to continue servicing/supporting mineral explorationists in the province.

The programs of the GSB have been reviewed on several occasions over the last few years and feedback from industry and other client groups was used to frame out a new five year plan. This formed the basis for discussions at a joint GSB/Geological Survey of Canada (GSC) Regional Needs Workshop convened January 16, 17th, 1997, in Winnipeg, the objective being to develop an expanded program including contributions from the GSC. The resulting document entitled Manitoba's Geoscience Needs was distributed in June to all members of the Mineral Exploration Liaison Committee, the National Prospector and Developers Association, all explorationists active in the province and northern communities whose wellbeing depends on mineral development. It is intended that the plan be reviewed and amended annually to ensure that the work of the Branch remains relevant and is focused on areas of importance to industry.

Components of the new plan include Memoranda of Agreements with various companies where joint work is being undertaken, multi-agency, multi-disciplinary CAMIRO- (Canadian Mining Industry Research Organization) sponsored projects in the Thompson and Snow Lake regions, new GSC/GSB NATMAP (National Mapping Program) initiatives in the northern Superior Province and Southeast Manitoba, and a new hydrogeological project in the Williston basin involving the provincial Water Resources Branch, the GSC and the GSB. Existing commitments to conclude the Shield Margin (NATMAP) program in the Flin Flon/Snow Lake region and the Capital Region study around Winnipeg are integral to the aims of the plan. In addition, the GSB has subsequently become involved in discussions with the GSC and a wide array of provincial agencies, as well as potential contributors from the United States, to scope out new programs that would contribute toward a better understanding of the major flood event on the Red River that occurred in April/May of this year.

FLIN FLON/SNOW LAKE

In the north, this years field program continued to balance work in established mining districts (Flin Flon/Snow Lake and Thompson) with new mapping and geochemical surveys in under-explored regions such as the northern Superior Province.

In May, the preliminary manuscript of the 1:100 000 geological compilation for the Shield Margin project was completed and displayed at the Geological Association of Canada Annual Meeting in Ottawa. Editing of this preliminary map continues with the goal of having a final compilation complete for public release in November, at the 1997 Manitoba Mining and Minerals Convention. Papers for inclusion in a Canadian Journal of

Earth Sciences Special Volume dedicated to the Shield Margin Project, are in preparation and a Shield Margin NATMAP CD-ROM will be completed six months after releasing the final hardcopy maps.

Detailed mapping of the Flin Flon mine "rhyolitic package" exposed on Millrock Hill provided new insights into the nature and location of this horizon. 1:20 000 mapping in the Naosap-Aimée-Alberts area defined a major NE-trending fault zone that represents a crustal scale structural break separating lithologically, stratigraphically and structurally distinct volcanic suites. At Snow Lake, a new 1:20 000 scale geological mapping program, initiated at Squall Lake to upgrade existing maps and to provide a more detailed geological and structural framework for gold exploration in this region, demonstrated that the pre-metamorphic Birch Lake Fault is an imbricate splay of the McLeod Road Thrust. New mapping at Herblet, Osborne and north of Snow Lake enhanced the stratigraphic and structural understanding of this region, as input to the new 1:50 000 compilation. The relationship between the geological structures and gold mineralization is the subject of a Masters Thesis at the University of Manitoba.

Detailed mapping of the host rocks to a number of gold deposits and occurrences in the vicinity of the New Britannia Mine showed that the mineralization occurs predominantly in altered mafic pyroclastic and intrusive rocks along early structures and predates the end of the latest metamorphism.

Rare earth element studies of rhyolites and sulphides from massive sulphide deposits in the Flin Flon-Snow Lake area indicate that light rare earths, Europium in particular, are depleted in alteration zones around VMS deposits, and are enriched in exhalite-tuff associated with the massive sulphide lenses. Data from the Spruce Point Deposit suggests that the Eu enrichment may be a useful tool in the exploration for VMS deposits.

Mineral Deposit Series Reports 63K/10 and 63N/3 will be released at the November Convention.

The Flin Flon Regional Office continues to be active, providing advice to the mineral exploration and mining communities in the region. As with other regional offices, the communications capabilities have been expanded with the establishment of an Internet e-mail account.

LYNN LAKE

At Lynn Lake a pilot lithogeochemical/structural study of the Burnt Timber gold mine was carried out with the cooperation of Black Hawk Mining Incorporated. Field mapping and drill core investigations suggest a predominant structural control for the gold-pyrite-quartz mineralization.

THOMPSON BELT AND CHURCHILL SUPERIOR BOUNDARY ZONE

On June 1st, a major three year research initiative was launched to investigate the factors controlling nickel mineralization in the Thompson Belt. The project is co-sponsored by six companies (Cominco Ltd., Falconbridge Ltd., Hudson Bay Exploration and Development Company Ltd., Inco Ltd., Teck Corporation and WMC International Ltd.). NSERC support for an Industrial Research Chair Application (Laurentian University) has been confirmed, and approval of a collaborative research and development grant (University of Manitoba, l'Université du Québec a Montreal, University of Alberta, GSB, GSC) is under consideration. The methodology will involve integration of archival and newly generated geological, mineralogical, geochemical, geochronological and geophysical data using GIS technology. Several interrelated field investigations were completed during the 1997 season. Basaltic and komatiitic flows at Mystery, and Mid lakes and north of Setting Lake were sampled as were several mafic dykes. New 1:50 000 geological compilations will be completed for the entire area between Moak and Setting lakes by February 1998, under a MOU between INCO and the GSB. Subsequent work will extend this coverage south, to link up with previous compilations south of Ponton. Drillcore studies focused on the relatively undeformed ultramafic and mafic intrusive rocks from the sub-Paleozoic segment of the TNB, including

samples from Cedar Lake, William Lake and the Minago River to Setting Lake region.

At Assean Lake, new mapping was undertaken as part of a cooperative program involving the University of Alberta, with joint funding provided through NSERC, GSB and the Swiss government. Geochronological sampling at Assean Lake, Paint Lake and Cross Lake, augmented by archived samples from Sipiwesk Lake, will provide new isotopic ages for much of the Churchill-Superior Boundary region.

On Setting Lake, rocks belonging to the Ospwagan Group were traced along the full 45 km of the lake. The Ospwagan Group, the newly identified Grass River Group terrestrial sediments, and the Archean basement gneisses and tonalite gneiss each occupy separate fault-bounded folds or panels, and each is intruded by a different set of Proterozoic dykes or sills.

Systematic mineralogical examination of Ospwagan Group supracrustal rocks was undertaken to expand the existing characterization of the lithostratigraphy and provide new constraints guiding exploration for nickel.

NORTHERN SUPERIOR PROVINCE

One of the primary objectives of Manitoba's Northern Superior Project is to better understand the volcanic, structural and tectonic evolution of greenstone belts in this sector of the province. Central to this objective is an understanding of the Oxford-Knee Lake Belt, the largest contiguous greenstone belt in the area. Accordingly, a team of geologists visited the region during the summer and undertook to remap the extensive shoreline exposures on southern and central Knee Lake, looking for key and distinct lithological associations and major structural breaks pointing toward unique structural and stratigraphic packages. This resulted in a better definition of the stratigraphy in rocks of the Hayes Group, identification of facies within a rhyolite complex and flanking volcanoclastic rocks, identification of stratiform alteration zones in Hayes Group basalts, and a lithological and structural reinterpretation of the Oxford Group. Associated geochronological sampling and dating will improve the understanding of the age relationships within and between the sundry stratigraphic panels.

Also under Operation Superior, the second phase of multi-media geochemical surveys was completed in the Red Sucker Lake region. Open Files containing preliminary results from Phase 1 (1996) were released in March and May, together with the results of the regional till sampling conducted jointly by the GSB/GSC. New 1:20 000 scale geological mapping was undertaken at Little Stull-Rorke and Kistigan lakes and reconnaissance mapping and geochemical/geochronological sampling was carried out in the Stull Lake area in cooperation with the GSC and Ontario Geological Survey (OGS). Two reports are under development, interpreting and compiling all geophysical data from assessment files relating to past exploration in the northern Superior Province. The first report and 21 accompanying maps (encompassing portions of NTS areas 53K, 53L, and 63I), will be released in November in conjunction with the Department's Annual Convention.

Thematic mapping and geochemical studies in the eastern part of the Carrot River Greenstone Belt characterized a 2 km thick section of Archean Oceanic crust. Locally intensive sea floor hydrothermal alteration and associated Fe-Cu-Zn sulphide mineralization is taken to indicate significant potential for as yet undiscovered VMS mineralization. In addition, a potential for gold mineralization exists along an east-northeast striking deformation zone containing abundant quartz-sulphide vein networks. Recent forest fires have resulted in new exposures of metre-thick spinifex-textured komatiite flows that provide an excellent opportunity to record textural sequences and document geochemical and petrographic characteristics.

A major new project to better understand the factors controlling gold mineralization in the northern Superior, this year focused on Henderson (High Rock) Island, Island Lake. At this location, detailed geological mapping highlighted the importance of late structures (at high angles to the dominant regional deformation zones), in localizing the gold mineralization.

A 1:250 000 digital geological compilation covering the core of the northern Superior (NTS areas 53L, 53M, 63I, 63P) has been compiled as a base for all other work. A new 1:250 000 compilation of bedrock geology in

NTS area 63H (Norway House) was also completed.

The M. Sc. Thesis documenting the mineralogy and genesis of Fe-Ti-V oxide mineralization in the Pipestone Lake Anorthositic Complex (PLAC) has been completed. The thesis confirmed a magmatic origin for the oxides and indicates that the PLAC was derived from four separate influxes of chemically similar magma. The research is ongoing and will better characterize the petrogenetic and metallogenic significance of widespread anorthositic magmatism throughout the Pikwitonei Domain and the Cross Lake-Kiskitto Lake region during the late Archean.

SE MANITOBA

In the Rice Lake belt a NATMAP field tour familiarized participants active in the Western Superior NATMAP and Northwestern Superior LITHOPROBE projects with the geology of the region. Examination of the geology and PGE tenor of the gabbroic upper portion of the Bird River Sill was undertaken in collaboration with Gossan Resources Ltd. Sampling and detailed mapping was carried out on the Chrome property.

CENTRAL MANITOBA

In central Manitoba, mapping, stratigraphic drilling and geochemical sampling of Devonian high calcium limestone units, and salt springs near Mafeking continued to evaluate the potential for Prairie-Type micro-disseminated gold mineralization in cooperation with Birch Mountain Resources. Elsewhere along the Mesozoic escarpment, numerous samples were taken as part of a regional study evaluating the potential for significant occurrences of black shale and bentonite. To the east, in the Grand Rapids and Gypsumville regions, numerous new fresh water artesian springs and tufa mounds were confirmed in the Central Interlake where geochemical investigations of the groundwater are evaluating the potential for Mississippi-Valley-Type mineralization in the Silurian and Ordovician sequences. Bedrock fracture measurements were taken on outcrops and in numerous quarries throughout the Interlake to better define the structural controls that may have influenced paleokarst development and subsequent deposition of silica, kaolin and other types of mineralization. At Arborg, three holes were drilled in an attempt to better define the extent of buried channels containing Cretaceous kaolin.

SOUTHERN MANITOBA

Further south, work in the Capital Region focused on compiling a database south of latitude 50° N. Documentation of surficial deposits was extended through 1:100 000 scale mapping, in NTS areas 52L, 62H and 62I, together with clay sampling on a 10K grid to help define flood-related deposits and new dyke construction material. Discussions between the provincial Water Resources Branch, the GSC, GSB and other parties concerned with groundwater resources, have led to the implementation of a new multi-year hydrogeological study focused on the Winnipeg region, but also extending to define the subsurface architecture of the broader Williston Basin margin in Manitoba.

A manuscript identifying the regional geologic and geomorphic controls that impact on the physical environment of Lake Winnipeg is nearing completion, with publication as part of a GSC Open File scheduled for the Fall.

Three holes (two to basement) were drilled to better define the regional geological setting of the Precambrian basement in the Selkirk area, where new exploration interests are currently active looking for nickel and platinum group metals. Two of the holes intersected ultramafic rocks and iron formation similar to those known in the Bird River greenstone belt to the east. Compilation of a 1:250 000 bedrock geology map for NTS area 62I (Selkirk) is advanced, with the intention of releasing this map in November.

In Winnipeg, the Geoscience Information Services Section continued to make progress in phasing in a wide array of new GIS capabilities, and enlarging the Branch's presence on the Website. The 1:1 000 000 scale Wetlands Map, produced in cooperation with the University of Alberta and LINNET corporation was completed in ArcInfo, and numerous new customized colour geological maps have been developed using the Branch's new plotter. In preparation for a new 1:1 000 000 scale Quaternary map of the province, a digital compilation of Quaternary and aggregate index maps for the province has been initiated,

a provincial basemap imported into MAPINFO, and test plots of scanned and vectorized map data are currently being evaluated.

The Branch continued to provide geological input to land use issues including aboriginal land claims, selection of candidate areas for the Endangered Spaces Campaign, and proposals for creation of new potentially restrictive land-use designations such as ecological reserves, rezoning of provincial parks etc.. The Branch is also represented on the MEAP panel evaluating the technical attributes of private sector exploration proposals seeking financial assistance. In May, the Branch hosted an Enzyme-leach Workshop for industry explorationists in Winnipeg, and a Prospector training Workshop in Thompson. Numerous field tours and demonstrations were given throughout the summer, to Aur Resources, TVX and Claude Resources in the Flin Flon and Snow Lake areas, for Birch Mountain at Mafeking, Falconbridge, REA and the GSC in the Bissett district, and with the GSC and OGS in the northern Superior region and at Thompson.

Displays highlighting various aspects of Manitoba's geological potential were generated for several major conferences, such as the PDAC (Toronto), Mines Ministers (St. John's, Newfoundland), GAC/MAC (Ottawa), and Calgary Mining Forum (Calgary).

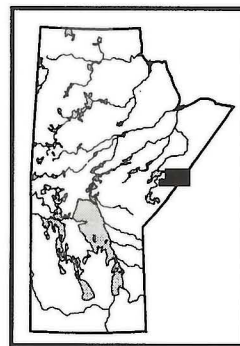
I would like to take this opportunity to express my sincere thanks to all the staff of the Geological Services Branch who contributed to this, the last, summary of their programs, that I will have the pleasure to compile. I am also deeply indebted to the present and past staff of the Branch and associated agencies especially those in the GSC, for the support they have given me in assisting and directing the affairs and programs of the Geological Services Branch over the last two decades. The experience has been an exceptionally rewarding one and a pleasure and a privilege to take part in.

W. D. McRitchie,
September 17th, 1997.

GS-1 OPERATION SUPERIOR: MULTIMEDIA GEOCHEMICAL SURVEYS IN THE EDMUND LAKE AND SHARPE LAKE GREENSTONE BELTS, NORTHERN SUPERIOR PROVINCE, MANITOBA (NTS 53K)

by M.A.F. Fedikow and E. Nielsen

Fedikow, M.A.F. and Nielsen E. (1997): Operation Superior: multimedia geochemical surveys in the Edmund Lake and Sharpe Lake greenstone belts, northern Superior Province, Manitoba (NTS 53K); in Manitoba Energy and Mines, Minerals Division, Report of Activities, 1997, p. 4-5.



SUMMARY

Rock, till, b-horizon, humus and vegetation samples were collected for geochemical analysis during the months of June, July and August, 1997, from 286 sites within the Edmund Lake and Sharpe Lake greenstone belts in the northern Superior Province. In addition, 169 samples of till were collected for kimberlite indicator mineral identification and analysis. Multielement geochemical analysis of these sample types will expand the geochemical database initiated in 1996 (Fedikow *et al.*, 1996) for application to mineral exploration in this part of the province.

1997 SURVEY

Year two of a five year, helicopter and fixed-wing assisted, belt scale (1 km site spacing), multimedia geochemical survey being conducted in northeastern Manitoba was concentrated in the Edmund Lake and Sharpe Lake greenstone belts (NTS 53K; Fig. GS-1-1). In the Edmund Lake belt, sample collection (n=149 sites) extended from the Manitoba-Ontario border (Kistigan-Little Stull Lake area) to the west shore of Edmund Lake, and in the Sharpe Lake belt (n=137 sites) sampling extended from the Manitoba-Ontario border to the west end of Sharpe Lake (Fig. GS-1-2).

Sample collection, preparation and analytical protocols for the 1997 survey are consistent with those established for the 1996 survey (Fedikow *et al.*, 1996). Some modifications to the 1997 sample collection have been effected based on the preliminary evaluation of geochemical data from the 1996 survey. Vegetation samples collected in 1997 were restricted to non-burned black spruce (*Picea mariana*) crowns because geochemical contrast is elevated in this tissue type.

Analyses are unavailable at the time of writing. Sample preparation for all media is currently underway.

1996 SURVEY




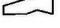

Preliminary results of multimedia geochemical surveys conducted in the Echimamish River, Carrot River and Munro Lake greenstone belts have been released as: 1) open file report OF97-1 (Fedikow *et al.*, 1997a), which provides geochemical data for an area south of Max Lake along the Echimamish River greenstone belt; and 2) open file report OF97-2 (Fedikow *et al.*, 1997b) for the entire survey area. The latter open file is presented in 6 parts with data analysis for rock (Part 1); till (<2 µm and <63 µm size fractions) (Part 2); b-horizon soil (Part 3); humus (Part 4); vegetation (Part 5); and kimberlite indicator minerals (Part 6). Sample coordinates (UTM) and analytical data for these sample types are included on two diskettes with the hardcopy reports. Revisions to Part 6 (Kimberlite Indicator Mineral Survey Results) were undertaken by C. Kaszycki.

A third report based on the quantification of metal flux in vegetation (Sailerova, in prep.) has been completed and is currently being prepared for publication.

Regional till mineralogical and geochemical results from a companion survey undertaken in 1996 (Matile and Thorleifson, 1996) have been released as open file OF97-3 (Matile and Thorleifson, 1997). This regional survey provides a reference set of data for background geochemical and kimberlite indicator mineral trends.

In addition to multiple areas of high contrast geochemical response, two areas of particular interest were identified in zones where intense forest fires provided excellent bedrock exposure. Area 1 occurs south of Max Lake and west of Aswapiswanan Lake, where bare outcrop ridges exposed: (1) locally sulphidized oxide facies (chert-magnetite) iron formation and a garnet-rich, rusty weathered volcanoclastic (?) sedimentary rock (garnetite);

TARGET AREAS FOR MULTI-MEDIA GEOCHEMICAL SAMPLING

-  1997 Multi-media geochemical surveys
-  1996 Multi-media geochemical surveys
-  Limits of greenstone, gabbro/sediment belts
-  Proposed survey boundary
-  Faults

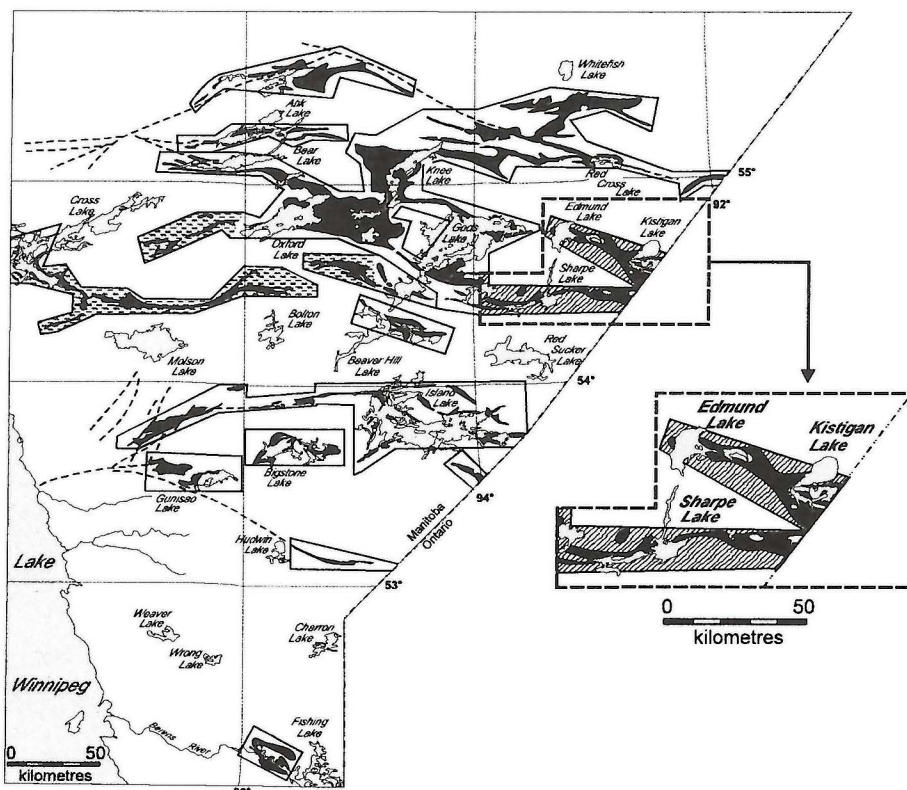


Figure GS-1-1: Location map for Superior Province greenstone belt samples in the 1997 Operation Superior multimedia geochemical survey.

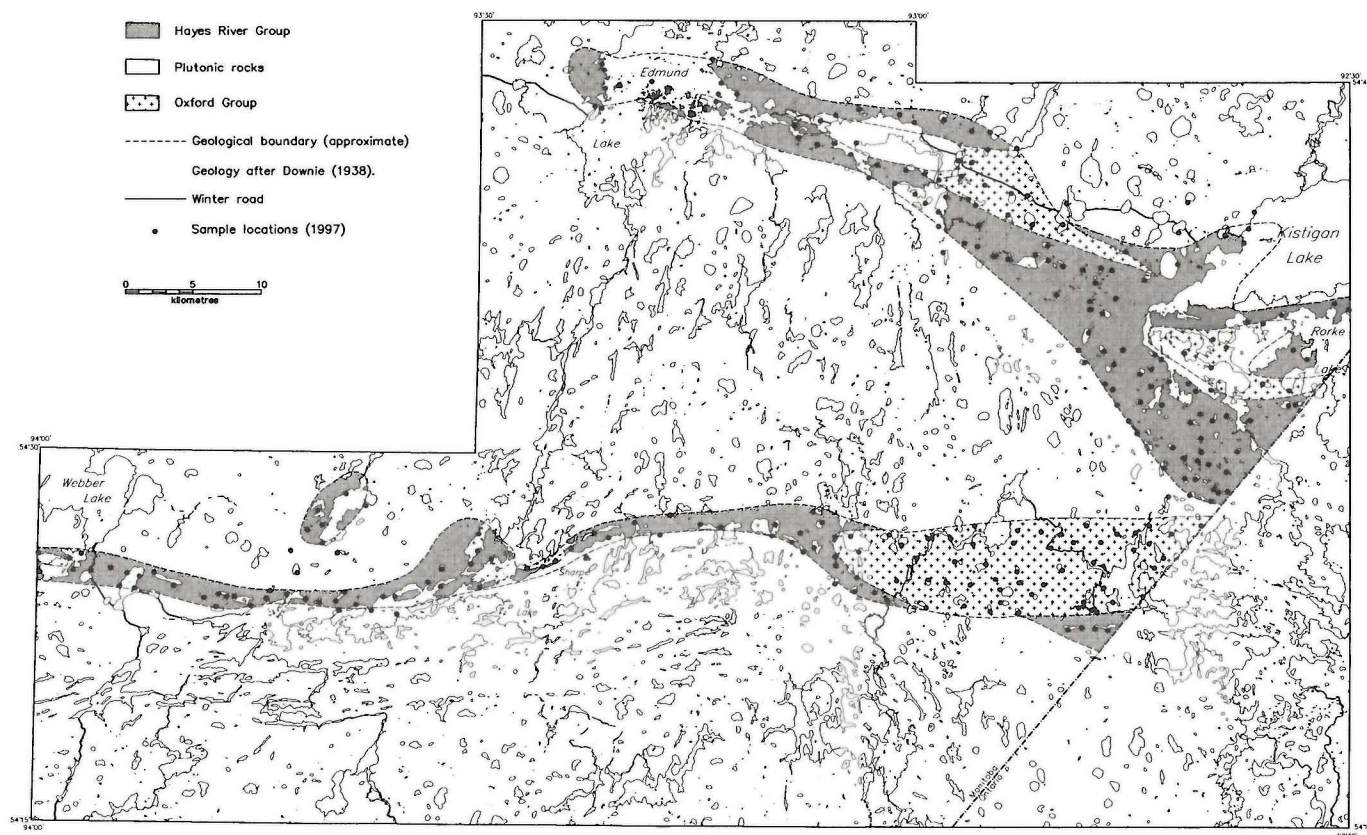


Figure GS-1-2: Location of 1997 multimedia geochemical sampling sites in relation to the boundaries for the Edmund Lake and Sharpe Lake greenstone belts.

and (2) silicified, epidotized and strongly rusty weathered pillow basalts with associated crosscutting garnet-chlorite veins, and strongly rusty weathered beds of felsic volcanoclastic sedimentary rocks. These rocks are exposed over an area of approximately 30 km² (10 km x 3 km) and the zone can be extended eastward under vegetation cover for an additional several kilometres towards Aswapiswanan Lake based on the airborne magnetic signature of the oxide facies iron formation.

The second area of interest occurs west of Peridotite Island south of the Carrot River, where coarsely spinifex-textured ultramafic flows and associated oxide facies iron formation and thick (0.5 - 1.0 m) magnetite-rich rocks are exposed. In this area, another zone of interest occurs on the shores of the Carrot River, also west of Peridotite Island, where rusty-weathered fragmental and quartz-phyric rhyolite hosts disseminated and veinlet base metal and iron sulphide mineralization. The rusty weathered character of the felsic volcanic rocks associated with this mineralization is extensive. The geology of the Carrot River area is discussed by Peck *et al.* (GS-4, this volume).

Each of these two areas of interest are also characterized by high contrast multimedia geochemical signatures. The ability to identify these altered and mineralized zones with potential for base and precious metal mineralization, while in the field, clearly demonstrates the benefits of landing a helicopter at approximately 1 km intervals, particularly in areas of recent forest fires. The unexpected benefit of the multimedia geochemical survey has resulted in new mapping projects (*e.g.*, Peck *et al.*, GS-4, this volume) to take advantage of the improved exposure.

ACKNOWLEDGMENTS

We greatly acknowledge the considerable skills of Messrs. D. O'Donnell and C. Taylor, Provincial Helicopters Ltd. (Lac du Bonnet) in safely accessing sample sites for 1997. Eddie and Stella Cull, Red Sucker Air Services Ltd., are thanked for logistical support throughout the 1997 season. Messrs. Graham Carlyle and Cameron Toews provided able assistance during the sampling program.

REFERENCES

- Fedikow, M.A.F., Nielsen, E. And Sailerova, E.
1996: Operation Superior: multimedia geochemical surveys in the Echimamish River, Carrot River and Munro Lake greenstone belts, northern Superior Province, Manitoba (NTS 53L and 63I); in Manitoba Energy and Mines, Minerals Division, Report of Activities 1996, p. 5-8.
- Fedikow, M.A.F., Nielsen, E. And Conley, G.G.
1997a: Operation Superior: 1996 Multimedia geochemical data from the Max Lake area (NTS 63I/8, 9 and 53L/5 and 12); Manitoba Energy and Mines, Mineral Resources Division, Open File Report OF97-1, 34 p. with diskette.
- Fedikow, M.A.F., Nielsen, E., Conley, G.G. and Matile, G.L.D.
1997b: Operation Superior: multimedia geochemical survey results from the Echimamish River, Carrot River and Munro Lake greenstone belts, northern Superior Province, Manitoba (NTS 53L and 63I); Manitoba Energy and Mines Open File Report OF97-2.
- Matile, G.L.D and Thorleifson, L.H.
1996: Regional till compositional trends, northeastern Manitoba; in Manitoba Energy and Mines, Minerals Division, Report of Activities 1996, p. 9-10.
- Matile, G.L.D. and Thorleifson, L.H.
1997: Till geochemical and indicator mineral reconnaissance of northeastern Manitoba; Manitoba Energy and Mines, Mineral Resources Division, Open File Report OF97-3, 174 p.
- Sailerova, E.
(in prep): Geochemical flux in black spruce (*Picea mariana*) crowns and the correlation with root water uptake: effects of sample site drainage and tree and crown morphology on crown twig and outer bark metal concentrations; Manitoba Energy and Mines, Mineral Resources Division, Geological Report.

GS-2 STRUCTURAL SETTING OF THE AU-BEARING QUARTZ VEINS AT THE HENDERSON ISLAND GOLD DEPOSIT (MINISTIK MINE), ISLAND LAKE, MANITOBA

by Shoufa Lin and H. D. Malcolm Cameron

Lin, S. and Cameron, H.D.M. (1997): Structural setting of the Au-bearing quartz veins at the Henderson Island gold deposit (Ministik Mine), Island Lake, Manitoba; in Manitoba Energy and Mines, Minerals Division, Report of Activities, 1997, p. 6-12.

SUMMARY

Gold exploration in the Superior province has traditionally been focused on Archean structures parallel to the main structural trends in the greenstone belts. This study draws attention to late structures, at high angle to the main structural trends, that are potentially also important for gold mineralization. For example, the emplacement of Henderson Island Au-bearing quartz veins is controlled by a dextral ductile-brittle fault. The fault, associated quartz veins and mineralized zone are late features relative to the dominant, Archean foliation and folds in the area. The quartz veins and the fault cut a north-trending mafic dyke, potentially Proterozoic in age, suggesting that gold mineralization could be much later than traditionally assumed.

INTRODUCTION

A structural study of the western Superior Province in Manitoba was started in 1997 as a component of the Manitoba Geological Services Branch northern Superior projects, and more recently the western Superior NATMAP Project (with OGS and GSC). The main purpose of this study is to better understand the structural evolution of selected greenstone belts in the area and in particular the structural settings of mineral deposits (especially gold deposits). This structural study, in concert with other geological, geochemical and geochronological work, can lead to a better understanding of the tectonic evolution of the greenstone belts and the western Superior Province as a whole.

In the summer of 1997 we started working in the Island Lake and Knee Lake greenstone belts. During our work at Island Lake, besides regional structural mapping, we did detailed work at the Henderson Island (formerly High Rock Island) gold deposit (Ministik Mine; Fig. GS-2-1), including grid-mapping at a scale of 1:50. This report is mainly concerned with the structural setting of the deposit was previously briefly described by Theyer (1990). The exploration history of the deposit is summarized in Richardson and Ostry (1996).

The deposit consists of gold-bearing quartz veins, the most important of which is the "main vein" described below. According to Bighorn

Development Corporation (1987, cited in Richardson and Ostry, 1996), the reserves contained in the vein are 390 000 tonnes grading 12 g/tonne (0.35 oz/tonne) gold. Mineralization consists of free gold, pyrite, chalcopyrite, galena and tellurides. Gold occurs as fine grains within the sulphide minerals and as coarse specks and "nuggets" (Richardson and Ostry, 1996).

GEOLOGICAL SETTING

The Henderson Island gold deposit occurs across the intrusive contact between a granitoid pluton and mafic metavolcanic rocks at the southern margin of the Island Lake greenstone belt (Fig. GS-2-2). The pluton is tonalitic to granodioritic in composition and gneissic near its contact with the mafic rocks in the north. The mafic rocks are metamorphosed to amphibolite facies and are very strongly deformed. They bear a well defined foliation that strikes approximately east, parallel to the granitoid-supracrustal contact, and dips steeply ($\sim 70^\circ$) to the north. The mafic rocks are intruded by abundant tonalitic to granodioritic dykes, presumably associated with the pluton, that are mostly parallel to the foliation.

Two generations of folding are recognized in both the granitoid and the supracrustal rocks. The earlier folds (F_1) are very tight to isoclinal (Fig. GS-2-3). The dominant foliation (S_1) described above is axial planar to the F_1 folds (Fig. GS-2-3). It is locally folded by F_2 , which is open to tight and lacks an axial planar foliation (Fig. GS-2-4).

STRUCTURES AT THE HENDERSON ISLAND GOLD DEPOSIT

Faults

The main structure at the Henderson Island gold deposit is a ductile-brittle fault (the main fault) that hosts the gold-bearing quartz veins (Figs. GS-2-5 and 6). The fault strikes $\sim 355^\circ$ and dips $\sim 85^\circ$ to the east. It cuts at right angle across the pluton-greenstone contact and the contact-parallel foliation. The associated slickenside striae plunge $\sim 30^\circ$ south (Fig. GS-2-7), indicating that the movement is oblique. The offset of foliation-subparallel dykes and the pluton-greenstone contact, the drag of the foliation and the dykes, and the geometry of the associated *en echelon* and sigmoidal quartz veins described below all indicate dextral shear (Figs. GS-2-5 and 6), with some west-side-up dip-slip component. Total horizontal displacement along the fault is ~ 9 m, of which ~ 6 m is accomplished by brittle faulting and ~ 3 m by ductile shearing.

Smaller-scale shear zones/faults of variable orientations also occur at the deposit and in the surrounding area. Most of these structures belong to one of the following three groups: (1) SE-trending brittle-ductile dextral shear zones (Fig. GS-2-4), (2) NE-trending sinistral brittle faults, and (3) N-S-trending dextral faults parallel to, and thus interpreted to be kinematically related to, the main fault described above. Group 3 faults are observed to cut both group 1 and group 2 faults (Fig. GS-2-8) and group 1 faults cut the F_2 folds described above (Fig. GS-2-4). Therefore, the group 3 faults, and by inference the main fault, postdate the F_2 folding. All the faults postdate peak metamorphism.

Au-bearing quartz veins and their structural setting

Au-bearing quartz veins at the Henderson Island gold deposit include the main vein, *en echelon* veins and some foliation-parallel veins (Figs. GS-2-5 and 6).

The main vein occurs in the centre of, and is parallel to, the main fault and cuts a subparallel mafic dyke (Fig. GS-2-5). It is exposed continuously for ~ 50 m (Fig. GS-2-5) and intermittently for ~ 180 m (Theyer, 1990). Drilling indicated a minimum strike length of 520 m and a minimum depth of 245 m (Bighorn Development Corporation, 1987, cited in Richardson and Ostry, 1996). Its exposed width varies from <0.5 m to ~ 2 m.

The *en echelon* veins occur on both sides, and mostly within 1.5 m, of the main vein (Figs. GS-2-5 and 6). They cut across the foliation and are

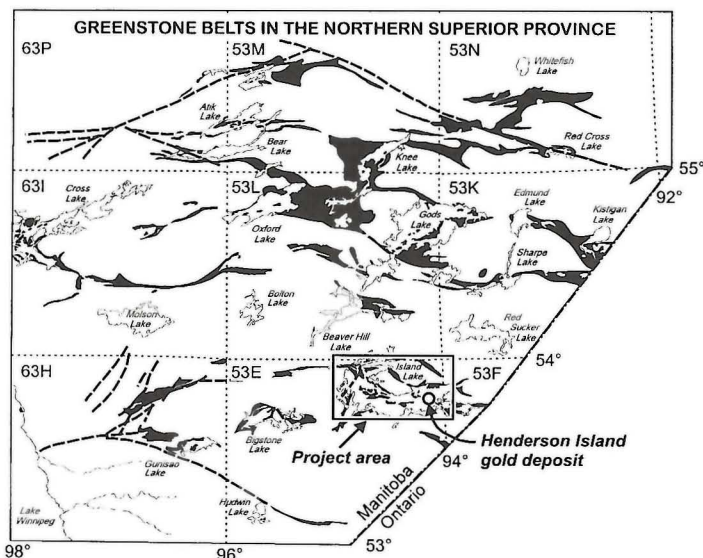
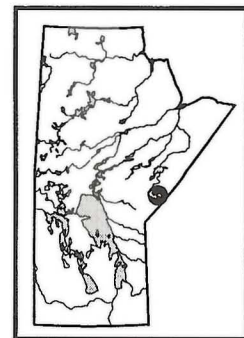


Figure GS-2-1: Location map, showing the location of Island Lake and the Henderson Island gold deposit (Ministik Mine) in Manitoba.

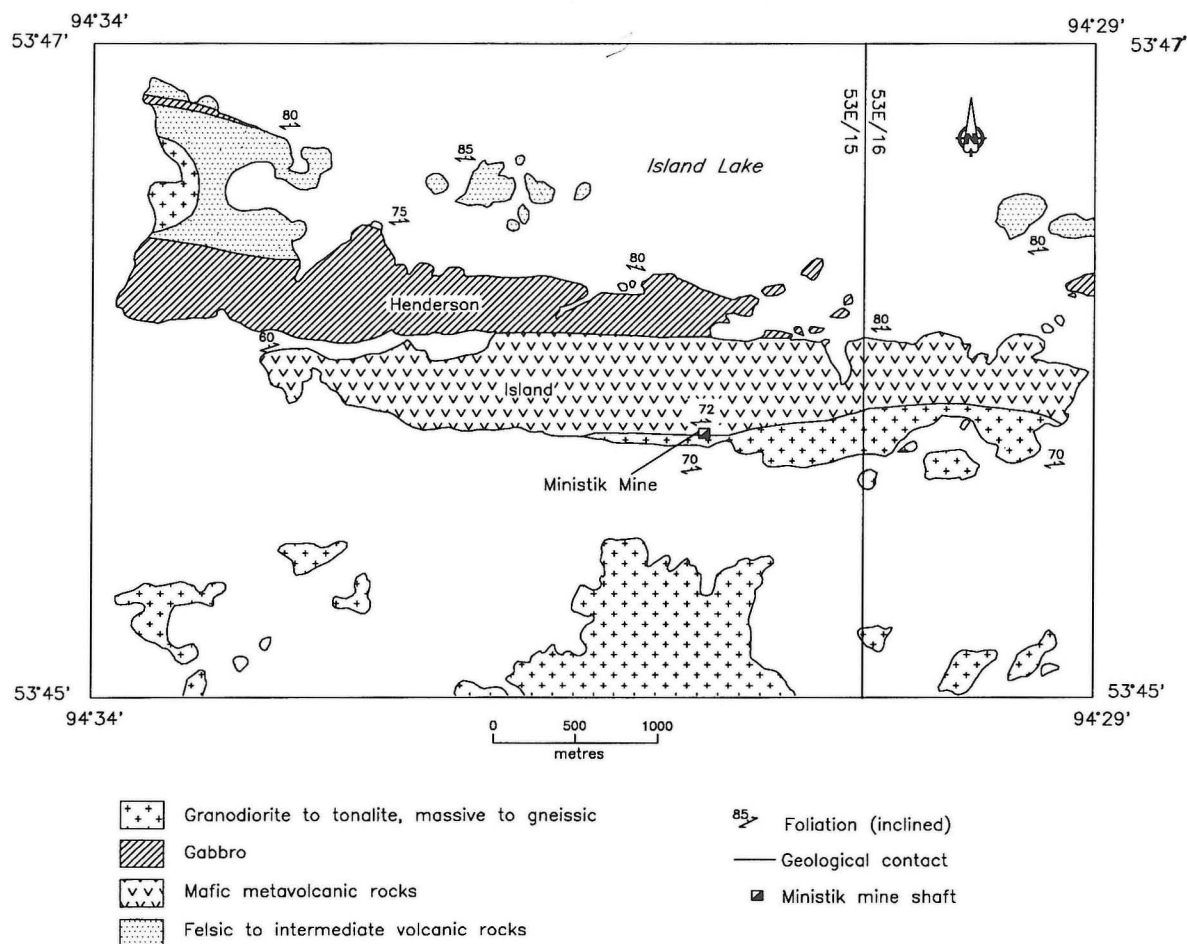


Figure GS-2-2: Simplified map of the Henderson Island area, showing the geological setting of the Henderson Island gold deposit (Ministik Mine).

oblique to the main vein, both on the horizontal surface and on vertical section (Figs. GS-2-6 and 9), a geometry supporting oblique movement along the fault. Some of veins are sigmoidal. These veins have variable length and width; most of them are <1 m long and <15 cm wide. The foliation-parallel veins only occur locally. They are mostly <1 m long and <cm wide. The following observations constrain the relative timing of emplacement of the three types of quartz veins and their structural setting:

The main vein is spatially controlled, and is itself deformed, by the main fault (Figs. GS-2-5, 6 and 7).

The *en echelon* veins, some of which have sigmoidal shape, are unambiguously related to the dextral shearing.

Some *en echelon* veins cut across the group 3 faults that are kinematically related to the main fault (Fig. GS-2-8).

Many *en echelon* veins are continuous with the main vein (Fig. GS-2-10), supporting the notion that the two types of veins are kinematically related.

The *en echelon* veins and the foliation-parallel veins cuts one another (Fig. GS-2-11), indicating that they are approximately contemporaneous. At one location, a former vein curves into a latter one, supporting this interpretation.

These observations indicate that the three types of quartz veins all emplaced during, and are kinematically related to, the dextral shearing along the main fault. By inference, the associated mineralization is also

interpreted to be related to the dextral shearing along the fault, an interpretation supported by the observation that the zone of alteration and mineralization spatially coincides with the zone influenced by deformation along the fault (Figs. GS-2-5 and 6).

SUMMARY, DISCUSSION AND IMPLICATIONS FOR EXPLORATION

Figure GS-2-12 summarizes the main features of the Henderson Island gold deposit. The emplacement of the Au-bearing quartz veins are controlled by a dextral ductile-brittle fault. The fault, the associated quartz veins and the mineralization zone cut at right angle across, are late features relative to, the main (Archean) structures (the dominant foliation and the F_1 and F_2 folds) in the area. Notably, the quartz veins and the fault also cut a north-trending mafic dyke. The age of the mafic dyke is unknown but could potentially be Proterozoic. It is also unknown whether the emplacement of the mafic dyke was controlled by the main fault, or the dyke was pre-faulting and may have controlled the location of the faulting and mineralization, or the spatial association between the dyke and the faulting and mineralization is coincidental.

Gold exploration in the Superior province has traditionally been focused on Archean structures parallel to the main structural trends in the greenstone belts. We hope that this study could draw attention to late structures at high angle to the main structural trends that are potentially also important for gold mineralization.

REFERENCES

Richardson, D.J. and Ostry, G. (revised by W. Weber and D. Fogwill)
1996: Gold deposits of Manitoba; Manitoba Energy and Mines,
Economic Geology Report ER 86-1 (2nd edition).

Theyer, P.
1990: Mineral occurrence studies and documentation in the Island
Lake area (NTS 53E/10, 53E/15, 53E/16, 53F/13); in Manitoba
Energy and Mines, Minerals Division, Report of Activities,
1990, p. 125-127.

Gilbert, H.P., Neale, K.L., Weber, W., Corkery, M.T. and McGregor, C.R.
1983: Island Lake (NTS 53E/15SE and parts of 53E/16SW);
Manitoba Energy and Mines, preliminary map 1983 I-1, scale
1:20 000.

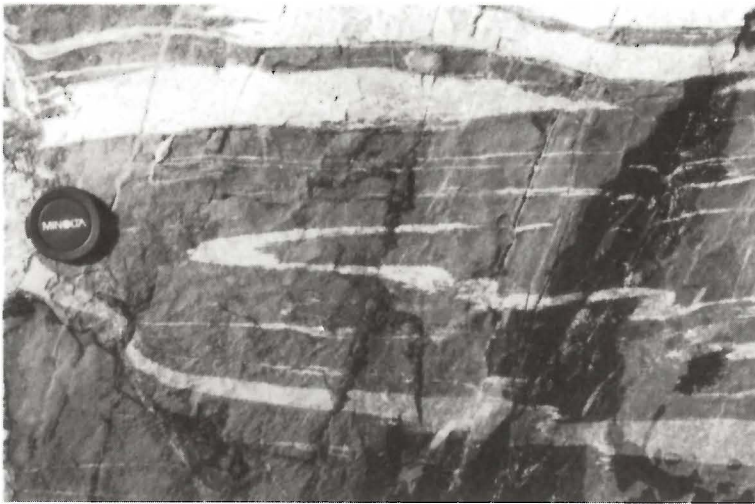


Figure GS-2-3: Isoclinal F_1 folds in mafic metavolcanic rocks (amphibolite). The well developed axial planar foliation (S_1) is the dominant foliation in the area.

Figure GS-2-4: S_1 foliation overprinted by F_2 folds. No axial planar foliation is associated with the F_2 folds. The F_2 folds are cut by SE-trending brittle-ductile dextral shear zones (above and below the hammer and parallel to the hammer handle).



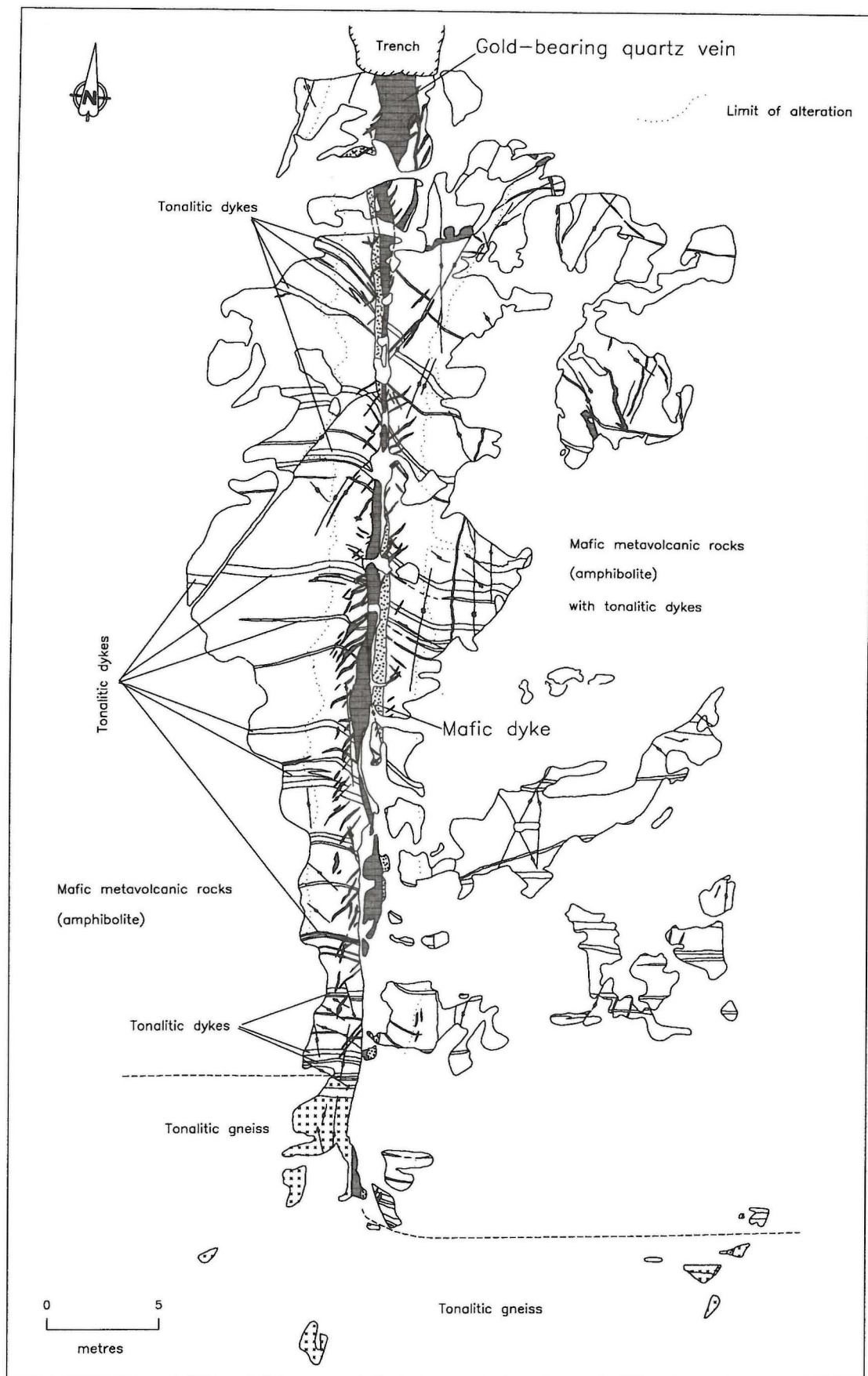


Figure GS-2-5: Simplified map of a stripped outcrop at the Henderson Island gold deposit. Original map at a scale of 1:75.



Figure GS-2-6: Photo of the central part of the area shown in Figure GS-2-5. The main (quartz) vein is spatially associated with the centre of the main fault. Note the drag of the foliation and the foliation-parallel dykes as a result of dextral shearing along the fault and the en echelon quartz veins, some of which are sigmoidal. Also note that the zone of alteration (darker coloured) spatially coincides with the zone of dextral shearing. Right is approximately north-northwest. Horizontal edge is ~10 m.

Figure GS-2-7: Slickenside striae in the main fault. The faulted rock is the main (quartz) vein described in the text. Looking west.



Figure GS-2-8: A north-trending (group 3) dextral fault cuts a SE-trending brittle-ductile shear zone. Both are cut by a quartz vein that is part of the en echelon veins. East is right. Pen in the centre right for scale.

Figure GS-2-9: Sectional view of the main vein and associated en echelon veins. Looking south.



Figure GS-2-10: Photo showing en echelon quartz veins continuous with the main vein (under the lens cap).

Figure GS-2-11: Photo showing the crosscutting relationship among en echelon veins and foliation-parallel veins. Veins A, B and C are foliation parallel, and veins D and E are part of en echelon veins. Vein A cuts vein D and vein E cut veins A, B and C.



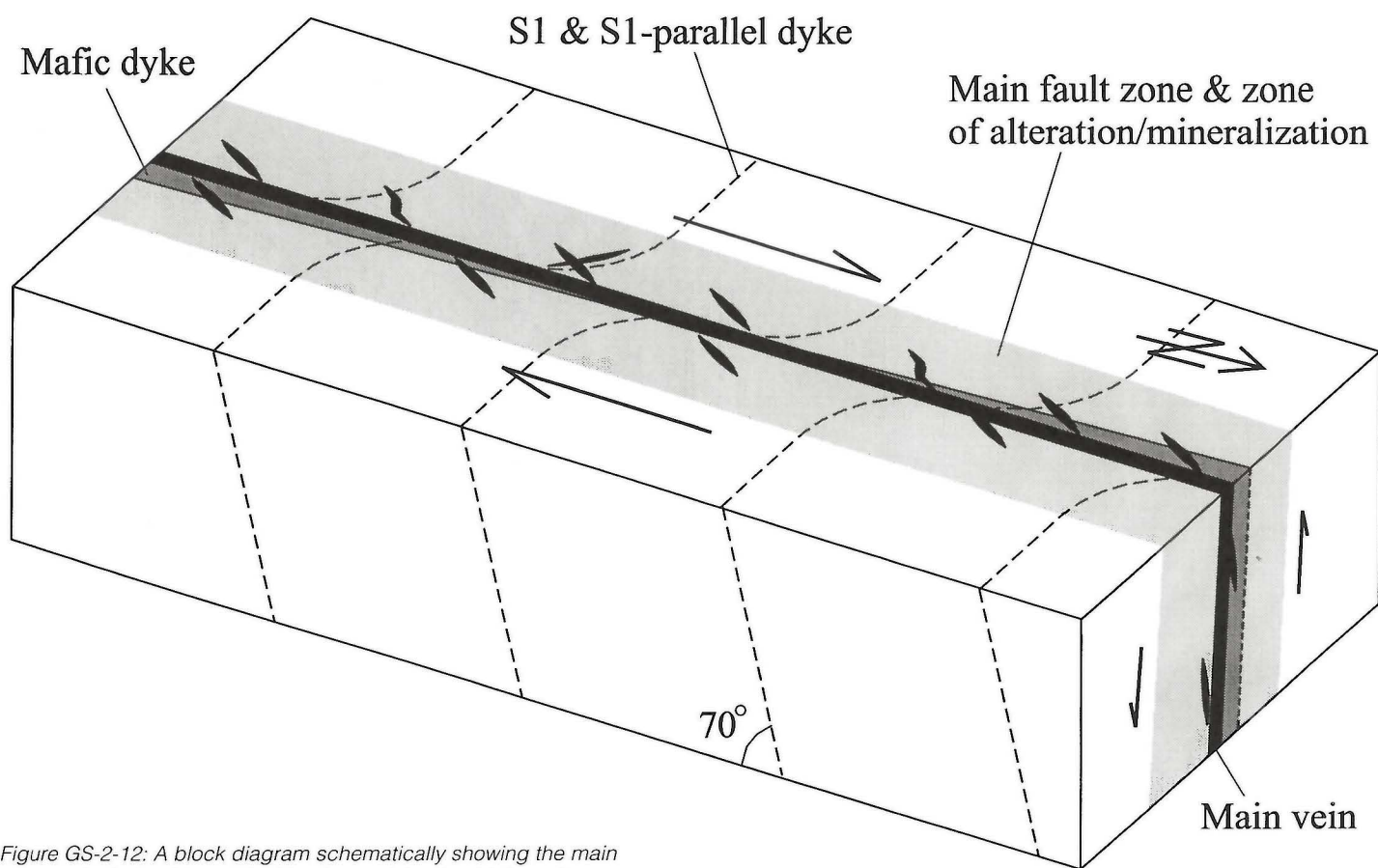
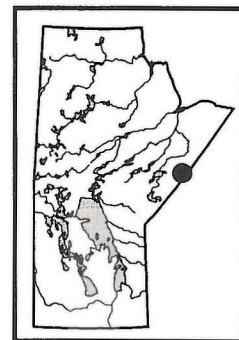


Figure GS-2-12: A block diagram schematically showing the main structural relationships at the Henderson Island gold deposit.

GS-3 GEOLOGY OF THE LITTLE STULL LAKE AREA (PART OF NTS 53K/10)

by M. Timothy Corkery, T. Skulski¹ and J. B. Whalen¹

Corkery, M.T., Skulski, T. and Whalen, J.B. (1997): Geology of the Little Stull Lake area (part of NTS 53K/10); in Manitoba Energy and Mines, Minerals Division, Report of Activities, 1997, p. 13-17.



SUMMARY

The Little Stull Lake greenstone belt is divided into four structural panels each with distinctive supracrustal assemblages whose contacts are defined by deformation zones. From south to north these assemblages are: 1) basalt and associated gabbro intrusions, 2) subaerial sandstone and conglomerate, 3) a diverse assemblage of intermediate to felsic tuffs, breccias, associated volcanoclastic rocks and epiclastic sedimentary rocks, all of which were deposited in a marine setting, and 4) basalt, including one occurrence of komatiitic basalt.

New lithologic, geochemical, structural and geochronologic data collected during this study will be critical to interpret the setting of known mineral deposits and to better assess the mineral development potential of the region. This work includes cooperative mapping in Western Superior NATMAP Project involving the Ontario Geological Survey, Geological Survey of Canada and Manitoba Geological Services Branch.

INTRODUCTION

The Little Stull Lake map area is a moderately well exposed extension of the northern segment of the Stull Lake greenstone belt in

Ontario. The belt extends from Ontario through the Rorke - Little Stull lakes area northwest to the Edmund Lake and is on strike with the Gods Lake greenstone belt to the west (Fig. GS-3-1). This mapping represents the second in a series of programs within the Archean greenstone belts in the Stull Lake map sheet - NTS 53K that straddles the Ontario-Manitoba border.

The Stull-Kistigan project entails 1:20 000 scale geological mapping of supracrustal belts and plutonic rocks within selected portions of 53K in Manitoba. Mapping programs are ongoing in the Edmund - Margaret lakes area (Corkery, 1996a) and the Little Stull-Kistigan lakes area (Corkery *et al.*, 1997), and future mapping is planned for the Sharpe Lake area. Previous mapping in the region consists only of 1:250 000 coverage by Downie (1937).

Mapping in the summer of 1997 focused on the supracrustal rocks in the Little Stull-Kistigan-Rorke lakes area of (53K/10) (Corkery, *et al.* 1997).

Regional Setting

Supracrustal rocks in the Little Stull Lake area have historically been subdivided into Hayes River Group and Oxford Group. The original

¹ Geological Survey of Canada, Ottawa, Ontario

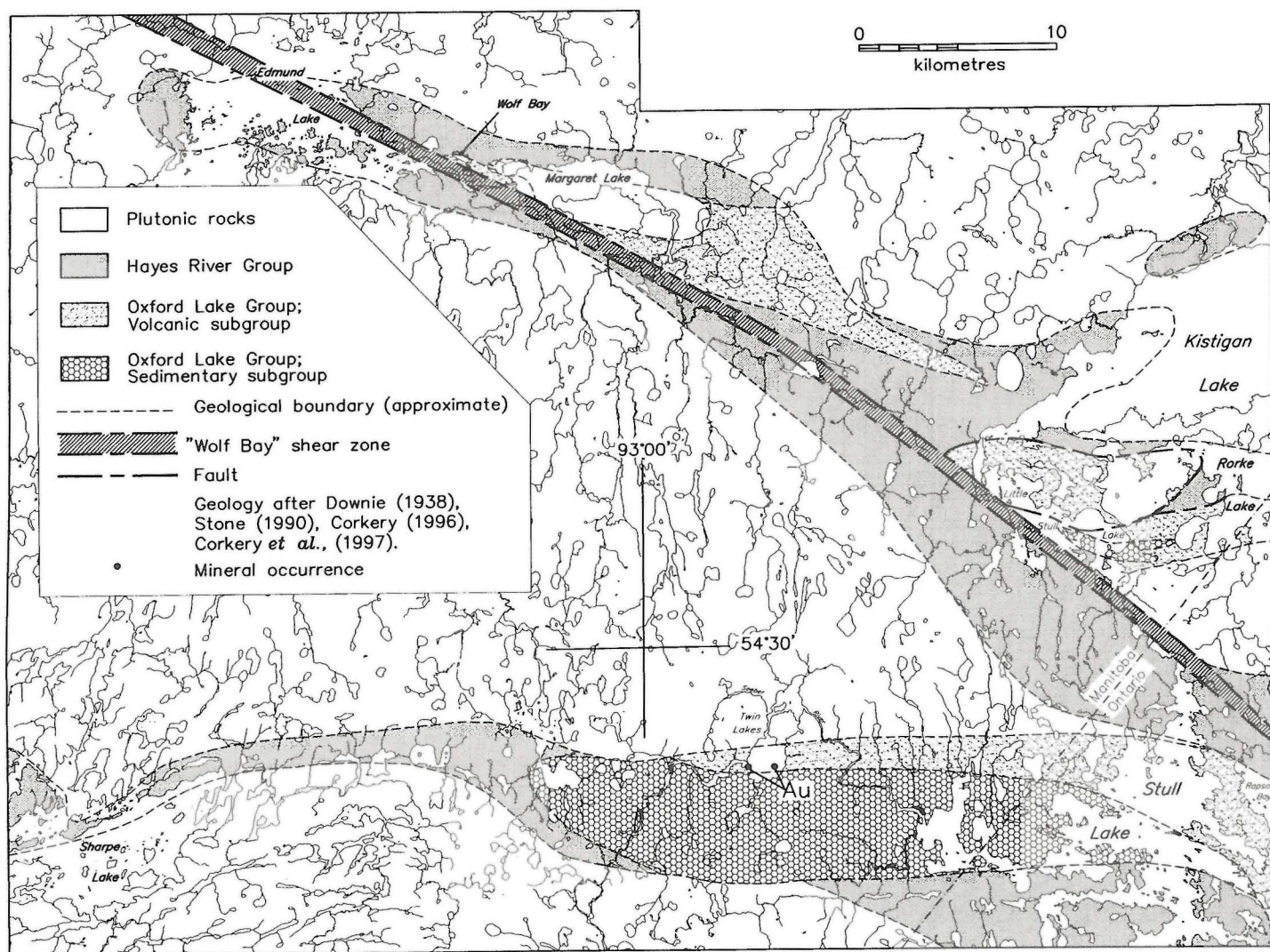


Figure GS-3-1: Regional geologic setting and major subdivisions in the Stull Lake region.

subdivision into the two groups was based on the distinction between a predominantly volcanic sequence, the Hayes River Group, ranging from basaltic through rhyolitic composition with minor intercalated sedimentary rocks, and a younger, unconformable overlying sequence, the Oxford Group, dominated by sedimentary rocks and marked at the base by polymictic conglomerates. In the 1970's a major mapping program in the greenstone belts to the west in the Gods, Knee, Oxford lakes area reevaluated the supracrustal sequences and Hubregtse (1985), in redefining the Oxford Group, separated it into a lower metavolcanic and volcanoclastic subgroup and an overlying metasedimentary subgroup. These subgroups were then included in the new Oxford Lake Group (Hubregtse, 1985).

Previous Work

Existing maps for the Stull Lake area date back to work by Downie (1937) at 1:250 000 scale, and a reconnaissance map of the Little Stull Lake area by Corkery (1989). To the northwest, the southeast portion of the Edmund Lake was mapped by Corkery (1996a) and this summer a study of the Oxford Lake - Knee Lake belt was initiated with a 1:20 000 scale mapping program in the south and central Knee Lake (Syme *et al.* GS-5, this volume).

In Ontario the Downie (1937) map represents the earliest regional geologic synthesis. Satterly of OGS also published a map of the Stull Lake area in 1937. More recent mapping was done by Riley and Davies (1967) and the supracrustal belt was reexamined by Thurston *et al.* (1987). Stone and Pufahl (1995) remapped the Stull Lake belt at 1:50 000 scale as part of an ongoing regional mapping program. Stone and Halle (in press) report on mapping in the Sachigo, Stull and Yelling lakes area of Ontario.

Current Research Directions

In addition to geologic map production, one of the prime objectives of the program is to better understand the primary volcano-sedimentary environments, structural and tectonic evolution of greenstone belts in the Northern Superior Province. To that end cooperative teams of geologists, from the Geological Survey of Canada, Ontario Geological Survey and Manitoba Geological Services Branch are working together under the auspices of the Western Superior NATMAP, to provide new lithologic, geochemical, structural and geochronological information for the region. These teams are pursuing a number of individual lines of research, but with the same goals (*e.g.* Syme *et al.*, GS-5 this volume).

Our mapping in the Little Stull Lake area was coordinated with similar regional mapping in Ontario by D. Stone of the Ontario Geological Survey. A joint release of a 1:50 000 scale geologic map for parts of Kistigan Lake (NTS 53K 10) and Ney Lake (NTS 53K 9) is planned for early December 1997, and a 1:100 000 scale compilation map for the Stull Lake greenstone belt is tentatively planned for late 1998.

SUPRACRUSTAL ROCKS

At Little Stull Lake the belt is divided into four structural panels (Fig. GS-3-2), each comprising distinctive supracrustal assemblages (Table GS-3-1) and whose contacts are faulted. From south to north these assemblages are: 1) basalt and associated gabbro intrusions, 2) subaerial sandstone and conglomerate, 3) a diverse assemblage of intermediate to felsic tuffs, breccias, associated volcanoclastic rocks and epiclastic sedimentary rocks, and 4) basalt, including one occurrence of komatiitic basalt. Some of the panels and bounding deformation zones are traced 50 km northwest to Edmunds Lake (Fig GS-3-1).

TABLE GS-3-1

Structural and geologic subdivisions of the rocks in the Little Stull Lake area from this paper, previously assigned nomenclature is included for comparison.

Structural Panel	Supracrustal subdivisions	Correlative units
Rapson Bay panel	Rapson Bay mafic complex	Hayes River Group
Little Stull Lake panel	Little Stull Lake arkosic sedimentary rocks	'sedimentary' subgroup of the Oxford Lake Group
Rorke Lake panel	Rorke Lake assemblage * 'Minnow' Bay 'volcanic' * sequence 'Sickle' Bay 'greywacke' sequence * 'Lodge' Bay 'volcanic' sequence * Isthmus 'volcanoclastic' sequence	'volcanic' subgroup of the Oxford Lake Group
Kistigan Lake panel	Kistigan Lake basalts	Hayes River Group

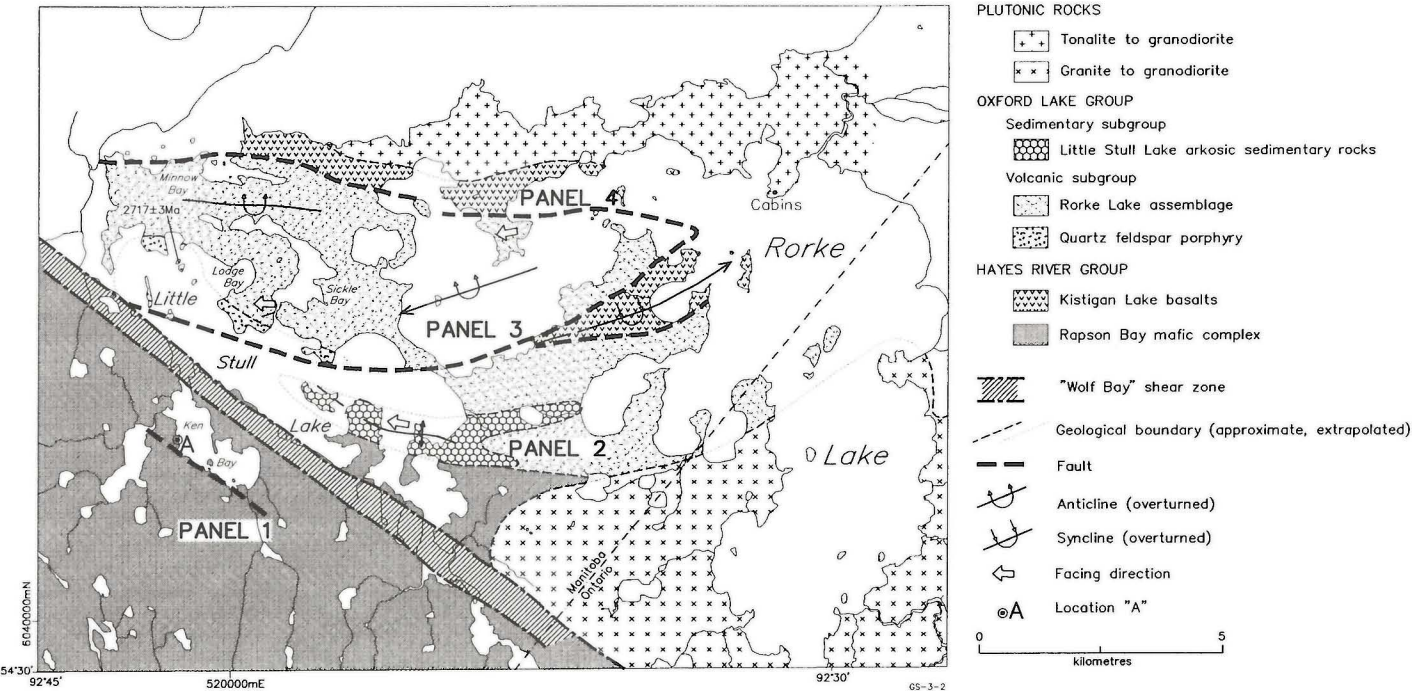


Figure GS-3-2: General geology of the Little Stull, Rorke, and Kistigan lakes area.

Panels 1 and 4 are dominated by mafic volcanic flows and synvolcanic intrusions interpreted to belong to the Hayes River Group. Panel 2 consists of subaerial sedimentary rocks equivalent to the 'sedimentary' subgroup of the Oxford Lake Group. Panel 3 has been interpreted as 'volcanic' subgroup of the Oxford Lake Group.

An age of 2717 ± 1 Ma (Davis and Moore, 1991) for a quartz feldspar porphyry intrusion on the north shore of Little Stull Lake is a minimum age for the rocks in panel 3. Thirty kilometres to the northeast on Margaret Lake, a fault bounded sequence interpreted as the most northwesterly part of panel 3 (Fig GS-3-1) yielded a preliminary (207/206) U-Pb zircon age of 2783 Ma (2% discordant) (Heaman, pers. comm., 1997) from a felsic pyroclastic rock. These data can be interpreted to indicate a significant time span (77 m.y.) between the volcanic and sedimentary subgroups of the Oxford Lake Group.

Rapson Bay mafic complex

To the south of the "Wolf Bay" shear zone on Little Stull Lake (Fig. GS-3-2), a northeast trending assemblage of deformed and metamorphosed basalts and gabbros forms the southern element of the supracrustal belt (panel 1). This assemblage can be traced from Rapson Bay in Ontario through Little Stull Lake and west to Edmund Lake. The thickest and best preserved portions of this assemblage occur in the Rapson Bay area where it comprises "north facing, pillowed volcanic mafic flows and minor sandstone" (Stone and Pufahl, 1995).

In the Little Stull Lake area, where primary features are well preserved, the basalts include pillowed and massive aphyric flows. Locally the pillowed basalt is spherulitic, and in places the spherulites coalesce into a pale green pillow core (see also Peck *et al.*, GS-4 and Syme *et al.*, GS-5, this volume) Epidote domains occur sporadically.

Up to 50% of the mafic volcanic assemblage in panel 1 consists of gabbro sills, interpreted as synvolcanic. Most gabbro is medium grained, equigranular and composed of amphibole, chlorite and plagioclase with minor magnetite and pyrite. On the southwest shore of Little Stull Lake, gabbro has 3 to 5% euhedral, tabular plagioclase phenocrysts, up to 2.5 cm long. The thickest sill (≈ 800 m) is on the northwest end of Ken Bay. This, as with other weakly deformed sills, retains a subtle decimeter scale differentiation layering of mesogabbro, melagabbro, and locally leucogabbro and anorthositic gabbro. Several gabbro pegmatite zones in mesogabbro layers of the sill in Ken Bay were sampled for U-Pb geochronology to provide a minimum age for the basalts. Minor tonalite to granodiorite intrusions cut the Rapson Bay basalt along the Stull River to the south of Little Stull Lake and in Ken Bay.

Little Stull Lake arkosic sedimentary rocks

Panel 2 occurs as a wedge of fluvial-alluvial sandstone and conglomerate (Fig. GS-3-2) at the east end of Little Stull Lake. Primary features are generally well preserved on the clean exposures in a recently burned area along the southeast end of Little Stull Lake. The sedimentary sequence occurs in an anticline that is cored by arkosic sandstones overlain by conglomerate.

The sandstones are dominantly creamy yellow weathering and pale blue-green when broken, and comprise feldspar-rich, quartz-poor arkose to arkosic wacke. The wacke contains a distinctive dark green to brown lithic sand fraction. Rare interbeds of brown weathering, green-grey wacke occur with increasing abundance up section. Cross-bedding occurs on small to large scales, generally as bed sets. Sandstones generally contain a few per cent pebbles as lags scattered along the foresets in thicker trough cross-beds (Fig. GS-3-3). Bottomsets and the lower few centimetres of the foresets in thicker beds may contain black magnetite-rich placers. Interbeds of pebbly sandstone are common. A gradational upward increase in the abundance of clasts and matrix-support conglomerate layers on the west shore of Peninsula A (Fig. GS-3-2).

Polymictic, clast-supported, pebble to boulder conglomerate abruptly overlies the sandstones. The conglomerate is thick-bedded with increasing bed thickness and clast size up section. Clasts are well rounded, spherical and highly variable in rock type, but plutonic clasts are generally absent. Feldspathic greywacke typically forms the matrix to the conglomerates.

In the central Rorke Lake area, along strike from the subaerial sequence, a few scattered outcrops of more recrystallized and deformed metasedimentary rocks and related volcanoclastic rocks are more like the Rorke Lake assemblage and have been mapped as such.

Rorke Lake assemblage

Intermediate to felsic volcanic tuff and breccia, and interbedded marine volcanoclastic and epiclastic rocks outcrop on the north shore of Little Stull Lake and central Rorke Lake. These rocks, herein termed the Rorke Lake assemblage, can be grouped into four distinctive associations: 1) the 'Lodge' Bay 'volcanic' sequence of aphyric intermediate to felsic tuff and breccia, 2) the 'Sickle' Bay 'greywacke' sequence of greywacke turbidites, argillite, and oxide facies iron formation, 3) the 'Minnow' Bay 'volcanic' sequence of feldspar phyric intermediate to felsic tuff and breccia and derived volcanogenic sedimentary rocks, and 4) the Isthmus 'volcanoclastic' sequence of generally hornblende phyric mafic breccias and derived volcanoclastic rocks (possibly high-potassium volcanic rocks or shoshonites).

The aphyric intermediate to felsic volcanic rocks of the 'Lodge' Bay 'volcanic' sequence include tuff and lapilli tuff occurring in >5 cm thick beds, and poorly sorted breccias (block- to ash-sized) in <1.5 m beds (Fig. GS-3-4). Many thin tuff beds display normal grading and some reverse grading at the base. Rip-ups and intraclasts are common in the coarser units. The thicker beds are interpreted to be pyroclastic in origin, but some may have been resedimented as debris flows. Most beds display basal scours, up to 15 cm deep, below the thicker beds. They are typically interbedded with the argillite and iron formation, and on a larger scale, with the greywacke turbidites. Interbeds of thickly- to thinly-laminated, magnetite-bearing, cherty iron formation are up to 30 cm thick and occur sporadically throughout the assemblage. Thinly laminated, pyritic, black argillite forms interbeds up to 15 cm thick. Sedimentary structures include, flame structures, and rip-ups and argillite intraclasts.

Brown to light brown weathering greywacke to feldspathic sandstone of the 'Sickle' Bay 'greywacke' sequence form units up to 100 m thick, or individual interbeds and sets of beds between aphyric felsic pyroclastic beds. These sandy interbeds are 5 - 15 cm thick and become more abundant and thicker (up to 2.5 m) up section. Higher in the succession light brown to creamy beige weathering, thick-bedded, plagioclase-rich sandstones are interlayered with the feldspar phyric intermediate to felsic tuffs, breccias and conglomerates. Graded bedding is common, and other turbidite bedforms can be distinguished in well preserved sections.

Feldspar and quartz feldspar phyric andesite to rhyolite and associated sedimentary rocks of the 'Minnow' Bay 'volcanic' sequence (Fig. GS-3-2) are interpreted to conformably overlie the aphyric volcanic and greywacke sedimentary succession. This abrupt change to porphyritic volcanic rocks and derived sedimentary rocks provides a distinctive characteristic for the upper part of the succession. The dominant rock type is medium- to thick-bedded, creamy yellow weathering feldspar phyric or quartz feldspar phyric rhyodacitic tuff. Lapilli tuff, and block-and-ash-debris flows dominate the sequence in 'Minnow' Bay at the southwest end of Kistigan Lake (Fig GS-3-2).

Throughout the upper part of the Rorke Lake assemblage, clast-support and matrix-support conglomerates are interbedded with the volcanic rocks. Clasts are well rounded with poor to moderate sphericity. Up to 90% are a variety of intermediate to felsic composition porphyries, while the remainder includes chert, basalt, gabbro and sedimentary rocks (no granitoid clasts). Bedding ranges from 1 to 5 m thick. Clasts range from pebbles to boulders (up to 1 m in diameter) and only rarely display sorting. Some metre-size boulders occur in beds less than 3 m thick. This large clast-to-bed thickness ratio is interpreted to indicate deposition by sediment debris flow.

Along the southeast shore of the west bay of Rorke Lake, deformed, intermediate to mafic fragmental rocks of the Isthmus 'volcanoclastic' sequence, include tuff, lapilli tuff and tuff breccia interlayered with reworked volcanoclastic and epiclastic rocks. Several outcrops contain hornblende phyric intermediate to mafic fragmental beds that may be shoshonitic (Fig. GS-3-5). These exposures are near the fault zone bounding panel 2 and 3, where primary and tectonic interlayering are difficult to distinguish. However, the dominance of pyroclastic rocks, volcanoclastic greywacke and conglomerate sedimentary rocks suggest that the deformed assemblage is part of the nearby Rorke Lake assemblage in Panel 3.

The 'Lodge' Bay 'volcanic' sequence is intruded on the south side by a tabular, 5 km long, composite intrusion. Phases in this intrusion range from feldspar phyric andesite on the north side to quartz-feldspar phyric rhyolite at the eastern termination. The age of 2717 Ma reported by Davis and Moore (1991) is from this intrusion, which is similar to the tuff in upper porphyritic portions of the assemblage. Samples have been collected for geochronology and geochemistry to test this relationship.



Figure GS-3-3: Planar cross bedded pebbly sandstone with magnetite placers marking foreset bedding from the Little Stull Lake Arkosic Suite.

Figure GS-3-4: Aphyric lapilli tuff bed from the Rorke Lake assemblage.

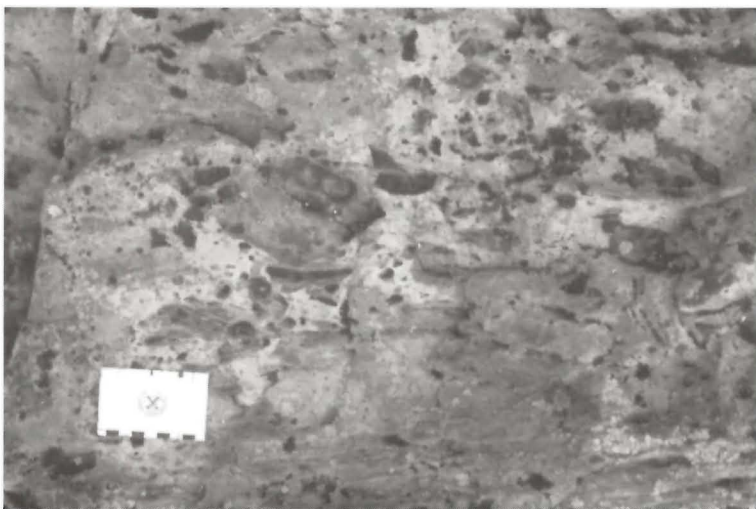


Figure GS-3-5: Shoshonitic hornblende porphyritic intermediate fragmental debris flow bed from the south shore of the west bay of Rorke Lake.

A marine environment for deposition of the Rorke Lake assemblage is indicated by the graded bedding and other density-current bedforms in the greywacke sandstones, iron formations and laminated argillites. However, the well rounded nature of the clasts in most of the conglomerates indicates subaerial provenance. The environment of deposition is interpreted to be a marine basin adjacent to islands with active intermediate to felsic volcanism.

Kistigan Lake basalts

Rocks in Panel 4 are similar to those in Panel 1, dominated by pillowed and massive basalt and associated gabbro. Rare oxide facies iron formation is interbedded with the basalts. An isolated occurrence of high magnesium volcanic flows (komatiite?) occurs on the north shore of Rorke Lake. It is bounded on the north by a deformation zone and separated from the basaltic sequence by an intrusion of the marginal phase of the Kistigan tonalite.

INTRUSIVE ROCKS

An oval tonalite to granodiorite body intrudes the north flank of the supracrustal belt in the south Kistigan Lake area (Fig. GS-3-2). The intrusion consists of medium- to coarse-grained, well foliated hornblende granodiorite to tonalite. A strong regional alteration has replaced most of the hornblende with biotite and epidote, and locally the rock is strongly silicified and laced with a quartz carbonate stockwork.

Three phases can be distinguished in the intrusion. A coarse grained equigranular tonalite to granodiorite predominates, whereas finer grained, slightly more mafic tonalite to quartz diorite forms the south margin of the intrusion. The phases have a similar texture, are locally interlayered and contacts are generally gradational over 1 - 2 metres. The third variant is medium to coarse granodiorite similar to the dominant phase but contains a few per cent elongate, up to 1 by 7 cm long, and randomly oriented microcline megacrysts.

STRUCTURE

Two periods of deformation are identified in the map area. An early regional deformation produced an east-west foliation (S_1) that is axial planar to tight to isoclinal folds (F_1). Large-scale younging reversals in the Rorke Lake assemblage form a series of westerly facing, steeply plunging (F_1) synclines and anticlines. An anticline that cores the Little Stull Lake arkosic sedimentary rocks also faces west. The early deformation and an associated fabric is best identified in Panel 3. A subsequent deformation is responsible for a gradational zone of overprinting and deflecting of S_1 fabrics in the vicinity of major deformation zones. All of the observed contacts between the Panels are marked by faults.

The contact between the Kistigan Lake basalts and the Rorke Lake assemblage is defined by an east-trending fault through the north side of the small bay on the south west end of Kistigan Lake. The fault extends through the north west end of Rorke Lake and turns south west into Little Stull (Fig GS 3-2). If this boundary is a single continuous fault the geometry suggests that it may be folded in the east west fabric. This possible deformation event, indicating early tectonic assembly of the supracrustal belt, is not considered in this paper. In the Little Stull Lake area, the fault is part of the east-west trending shear zone separating andesitic pillowed flows of the Rorke Lake assemblage on the north shore from crossbedded sandstones of the Little Stull Lake arkosic sedimentary rocks. The contact between these two assemblages is not exposed to the east of Panel 2.

The "Wolf Bay" shear zone (Corkery, 1996b) has been traced from northwest Edmund Lake through Margaret Lake along the south shore of Little Stull Lake and to the east end of Rapson Bay on Stull Lake. This shear zone features mylonites and phylonites (Fig. GS-3-6) and tectonic interleaving of numerous rock types. Kinematic indicators are consistently dextral and a strike slip movement with south side up is indicated by the shallow southeast to horizontal lineations.

ECONOMIC CONSIDERATIONS

Shear zone related gold is a characteristic feature of deformation zones throughout this region. Prospecting in the 1930's and exploration beginning in the 1960's identified the Little Stull Lake area as having a high potential for gold. Mineral showings occur on an island in Ken Bay south of Little Stull Lake and on an island in north central Stull Lake. Noranda Exploration Limited reported 3 500 000 t grading 2.7 to 15.8 grams gold/tonne in 4 zones at Twin Lakes 15 km south of Little Stull Lake (Fig. GS-3-1) Northern Miner (April 8, 1991). Westmin identified 750 000 t grading 9.3

grams gold/tonne (Richardson *et al.*, 1996) in four zones along the south shore of Little Stull Lake.

The mineralization in one of the Little Stull Lake occurrences occurred where 1) 310° trending mylonite and phylonite deforms mesogabbro 2) the resulting sheared rock has been significantly albitized and silicified 3) a closely spaced 340° to 350° trending dilational fracture cleavage, associated with the shearing, is filled with quartz carbonate veins and 4) sulphidization has produced variable amount of pyrite throughout the phylonites in the alteration zone.

The Ken Bay occurrence also occurs within a variably sheared gabbro which is less altered near the showing. A previously unreported sulphide rich zone, located on the north shore of Ken Bay, northwest along strike from the Ken Bay occurrence, has been sampled for assay. This zone is >1 m thick and occurs in sheared gabbro crosscut by a young tonalite dyke (location A on Preliminary Map 1997 S-1).

REFERENCES

- Corkery, M.T.
1981: Little Stull Lake area; **in** Manitoba Department of Energy and Mines, Mineral Resources Division, Report of Field Activities, 1981, p. 43-44.
- Corkery, M.T.
1989: Little Stull Lake area (Part of NTS 53K/10); Preliminary Map 1989S-1, 1:20 000.
- Corkery
1996a: Geology of the Edmund Lake area; **in** Manitoba Energy and Mines, Minerals Division, Report of Activities, 1996, p. 11-13.
- Corkery
1996b: Northeast Edmund Lake (53K/11NE); Manitoba Energy and Mines, Minerals Division, Preliminary Map 1997S-1, 1:20 000.
- Corkery M.T., Skulski T., and Whalen, J.B.
1997: Geology of the Little Stull Lake area (part of 53K 10); Manitoba Energy and Mines, Minerals Division, Preliminary Map 1997S-1
- Davis, D.W. and Moore, M.
1991: Geochronology in the Western Superior Province: summary report - May 1991; Internal Report, Jack Satterley Geochronology Laboratory, Royal Ontario Museum, Toronto, 7 p.
- Downie, D.L.
1937: Stull (Mink) Lake area, Manitoba; Geological Survey of Canada, Paper 37-3, 26 p.
- Gilbert, H.P.
1985: Geology of the Knee Lake-Gods Lake area; Manitoba Energy and Mines, Geological Services, Geological Report GR83-1B, 76 p.
- Hubregtse, J.J.M.W.
1985: Geology of the Oxford Lake-Carrot River area; Manitoba Energy and Mines, Geological Services, Geological Report GR83-1A, 73 p.
- Richardson, D.J. and Ostry G. (Revised by W. Weber and D. Fogwill)
1996: Gold Deposits of Manitoba, Manitoba Energy and Mines, Minerals Division, Economic Geology Report ER86-1 (2nd Edition), 114 p.
- Riley, R.A. and Davies, J.C.
1967: Stull Lake sheet, District of Kenora (Patricia Portion); Ontario Department of Mines, Preliminary Map P.426, scale 1:126 720
- Satterley, J.
1937: Geology of the Stull Lake Area; **in** Ontario Department of Mines, Annual Report 46, Part 4, p.1-31.
- Stone, D. and Pufahl, P.
1995: Geology of the Stull Lake Area; Northern Superior Province, Ontario; **in** Summary of Field Work and other Activities 1995, Ontario Geological Survey, Miscellaneous Paper 164, p.48-51.
- Thurston, P.C., Cortis, A.L. and Chivers, K.M.
1987: A reconnaissance re-evaluation of a number of northwestern greenstone belts; evidence for an early Archean crust; **in** Summary of Field Work and Other Activities 1987, Ontario Geological Survey, Miscellaneous Paper 137, p.2-24.

GS-4 GEOLOGY AND GEOCHEMISTRY OF THE EASTERN PART OF THE CARROT RIVER GREENSTONE BELT, NORTHWESTERN SUPERIOR PROVINCE, MANITOBA (PART OF NTS 63I/16).

by D.C. Peck, P. Theyer, J. Liwanag¹ and C. Chandler²

Peck, D.C., Theyer, P., Liwanag, J. and Chandler, C., 1997: Geology and geochemistry of the eastern part of the Carrot River greenstone belt, northwestern Superior Province, Manitoba (part of NTS 63I/16); in Manitoba Energy and Mines, Minerals Division, Report of Activities 1997, p. 18-36.

SUMMARY

The eastern part of the Carrot River greenstone belt (CRGB) represents a relatively undeformed section of juvenile Archean crust that developed as two distinctive supracrustal sequences, viz.: (1) a lower mafic-ultramafic series dominated by komatiite, tholeiitic basalt and plutonic equivalents, and subordinate, ferruginous sediments; and, (2) an upper calc-alkaline series, incorporating subaqueous andesite and dacite lavas, associated intermediate pyroclastic rocks and fine-grained clastic sedimentary rocks. Pillow lavas and layered mafic-ultramafic intrusions are consistently north facing, suggesting a homoclinal structure for this section of the CRGB.

The lower, mafic-ultramafic series is characterized by the occurrence of spectacular and widespread quench textures in the volcanic units. The principal lithologies are: (1) pillowed, commonly spherulitic basalt; (2) layered peridotite-gabbro sills; (3) spinifex-textured komatiite; (4) megacrystic and plagioclase phyric basalt and melagabbro; and, (5) basaltic pyroxenite flows and sills. Spectacular spinifex textures occur in komatiite flows near the base of the mafic-ultramafic sequence. Field and geochemical observations document three cycles of basaltic and komatiitic magmatism.

The upper part of the supracrustal succession is dominated by pillowed andesite, massive and brecciated dacite flows and tuff, and fine-grained siltstone and mudstone. The upper series is distinguished from the underlying mafic-ultramafic succession by its calc-alkaline affinities, the absence of iron formation and increased amounts of clastic sedimentary rocks. These features may reflect an evolution from an abyssal, oceanic rift to an island arc regime.

Geochemical variation within the mafic and ultramafic series principally reflects olivine and clinopyroxene fractional crystallization involving several generations of chemically similar komatiitic to tholeiitic magma derived from a depleted mantle source similar to that for modern mid-ocean ridge basalts. Komatiites, despite developing very coarse-grained olivine spinifex textures, are relatively Fe-rich and range to basaltic komatiite compositions. Efficient separation of feldspathic residual liquids towards the top of ultramafic magma chambers, followed by prolonged plagioclase fractionation in the gabbroic residuum, can account for the observed association of high-Fe basalt, high-Mg basalt and komatiite. Additional controls on the observed chemical compositions include metasomatism associated with seafloor alteration, assimilation of crustal rocks, and crystal sorting in flows and sills. Intermediate volcanic rocks have calc-alkaline compositions and are strongly enriched in lithophile elements in comparison to the mafic-ultramafic series.

Several moderate to strong conductors in the eastern CRGB relate to thick, commonly stratiform pyrrhotite-rich gossans that locally contain pyrite, chalcopyrite, sphalerite and, rarely, galena. The sulphide zones are commonly developed along mafic flow boundaries in the lower series or in association with andesite, dacite and siltstone in the upper series. Some of the sulphide bodies are oblique to layer contacts and follow northeast-trending shear zones. Sampling and limited assay work returned little evidence of few significant base or precious metal enrichment in these sulphide bodies. Features that may indicate the potential for VMS deposits in the eastern CRGB include extensive hydrothermal alteration in the footwall to some of the larger sulphide bodies, the abundance of mafic and/or ultramafic intrusions (heat engines) and the coincidence of ultramafic-mafic and intermediate-felsic magmatism. The eastern CRGB may also be prospective for magmatic nickel sulphide deposits and epigenetic Au deposits.

INTRODUCTION

This report describes aspects of the geology, lithogeochemistry and mineral potential of the eastern part of the CRGB (Fig. GS-4-1). The study area is located approximately 50 km west of Oxford House and 140 km southeast of Thompson (Fig. GS-4-1). Field studies focused on detailed mapping along well exposed corridors across the CRGB, documentation of komatiites and related lithologies, documentation and sampling of sulphide occurrences and systematic lithogeochemical sampling. Geological documentation described in this report is principally based upon detailed mapping in the vicinity of the western part of Wakehau Lake (western section) and the eastern part of Peridotite Island (eastern section) (Figs. GS-4-2, 3). Lithogeochemical studies were principally directed towards: (1) in conjunction with field observations, determining the petrogenetic and tectonic evolution of the eastern CRGB; (2) evaluation of metal abundances of major sulphide gossans to determine the potential for VMS and Au deposits; and, (3) assessing the potential for Ni, Cu and PGE mineralization in mafic and ultramafic intrusive rocks.

GENERAL GEOLOGY

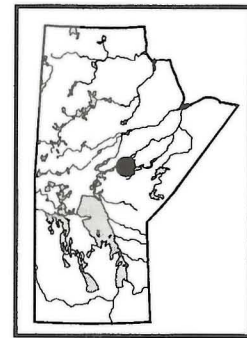
The CRGB is a <2.5 km wide, 50 km long, east-northeast trending volcanic belt in the Gods Lake Domain of the northwestern Superior Province (Fig. GS-4-1). Hubregtse (1985) mapped the CRGB and correlated the rocks with the Hayes River Group - a composite, predominantly basaltic volcanic sequence accounting for the lower portions of the exposed greenstone belts in the Knee- Gods- Oxford-Island lakes region (Hubregtse, 1985). Additional descriptions of the geology and mineral potential of the CRGB are provided by Wright (1926, 1932), Barry (1959), Southard (1977), Gilbert (1985) and Syme *et al.* (GS-5, this volume). The petrology and mineral potential of ultramafic rocks exposed on Peridotite Island is described by Davidson (1974).

The age of the CRGB and adjacent granitic rocks is unknown. An U/Pb zircon age of 2830 Ma was obtained for a felsic volcanic unit within the Hayes River Group at Knee Lake (Syme *et al.*, 1993). During the current study, five samples were collected for U-Pb geochronology, including two samples from the younger, granitic terranes to the north and south of the greenstone belt (Wakehau Lake area), two samples of pegmatitic gabbro from a large, layered mafic dyke of probable Paleoproterozoic age (south shoreline of Wakehau Lake), and one sample of pegmatitic gabbro from a layered gabbro body on Eagle Island (see Fig. GS-4-2 for sampling locations).

Within the study area, the CRGB is <1 to 2.5 km wide and comprises abundant mafic to ultramafic volcanic and intrusive rocks and subordinate intermediate flows and pyroclastic rocks (Fig. GS-4-2). Minor fine-grained metasedimentary rocks, including oxide-facies banded iron formation, ultramafic debris, mafic mudstone and intermediate siltstone, are locally developed. The CRGB is intruded by granite and granodiorite plutons to the south, and by tonalite, granodiorite and diorite to the north, all of which are correlated with the Bayly Lake Complex (Gilbert, 1985; Hubregtse, 1985). The granitic rocks also intrude the central part of the CRGB, dividing it into western and eastern segments (Hubregtse, 1985). The current study focuses on the eastern segment, where abundant additional bedrock exposures resulted from a forest fire in 1989.

LITHOSTRATIGRAPHY

The general geology depicted on Figure GS-4-2 consolidates new mapping data from the current study with geological observations shown on Hubregtse's (1985) 1:50 000 scale map for the Carrot River area. Type lithostratigraphic sections for the eastern CRGB (Figs. GS-4-2, 3) are based on 1:20 000 mapping along flagged grid lines and more detailed 1:100 to



¹ Department of Geological Sciences, University of Manitoba, Winnipeg, Manitoba

² Department of Geology, Brandon University, Brandon, Manitoba

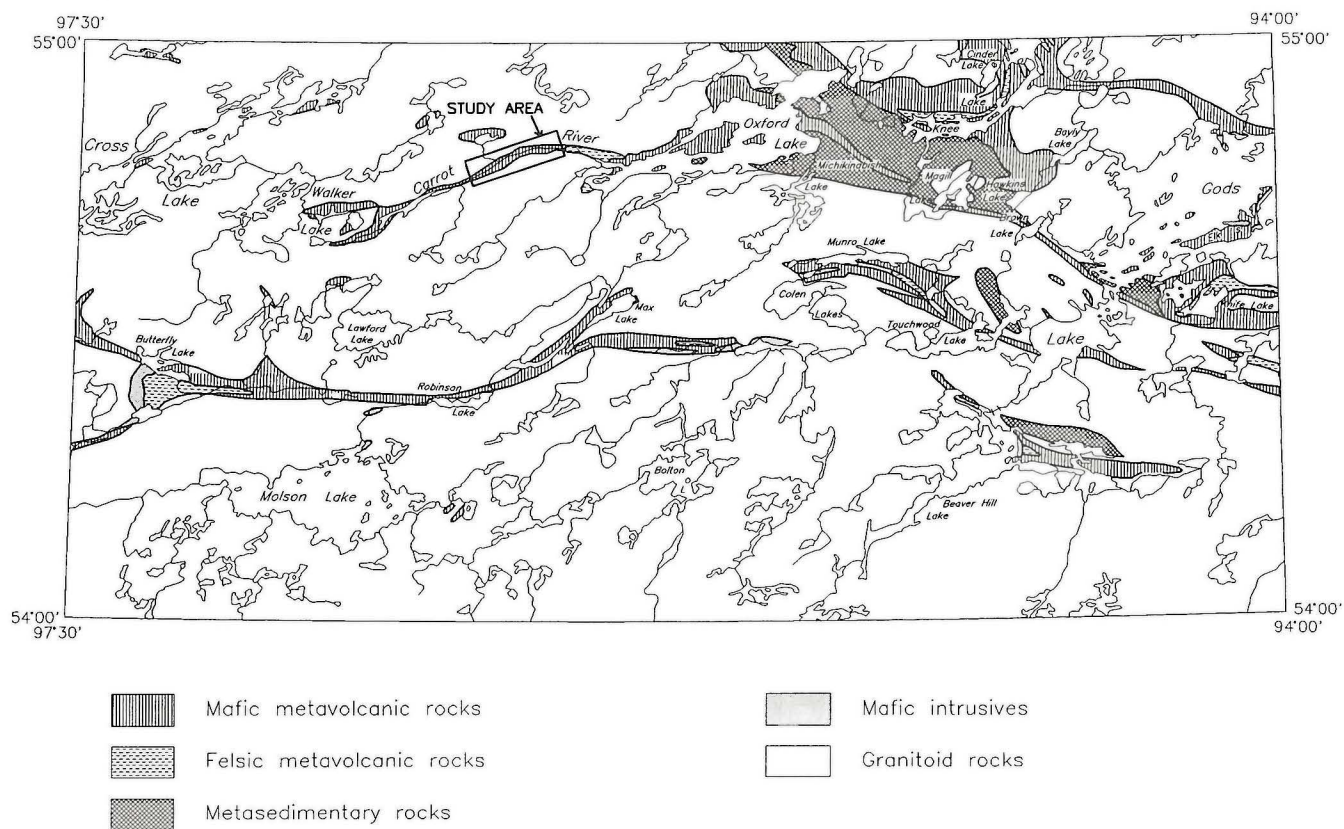


Figure GS-4-1: Location of the study area in the eastern part of the Carrot River greenstone belt.

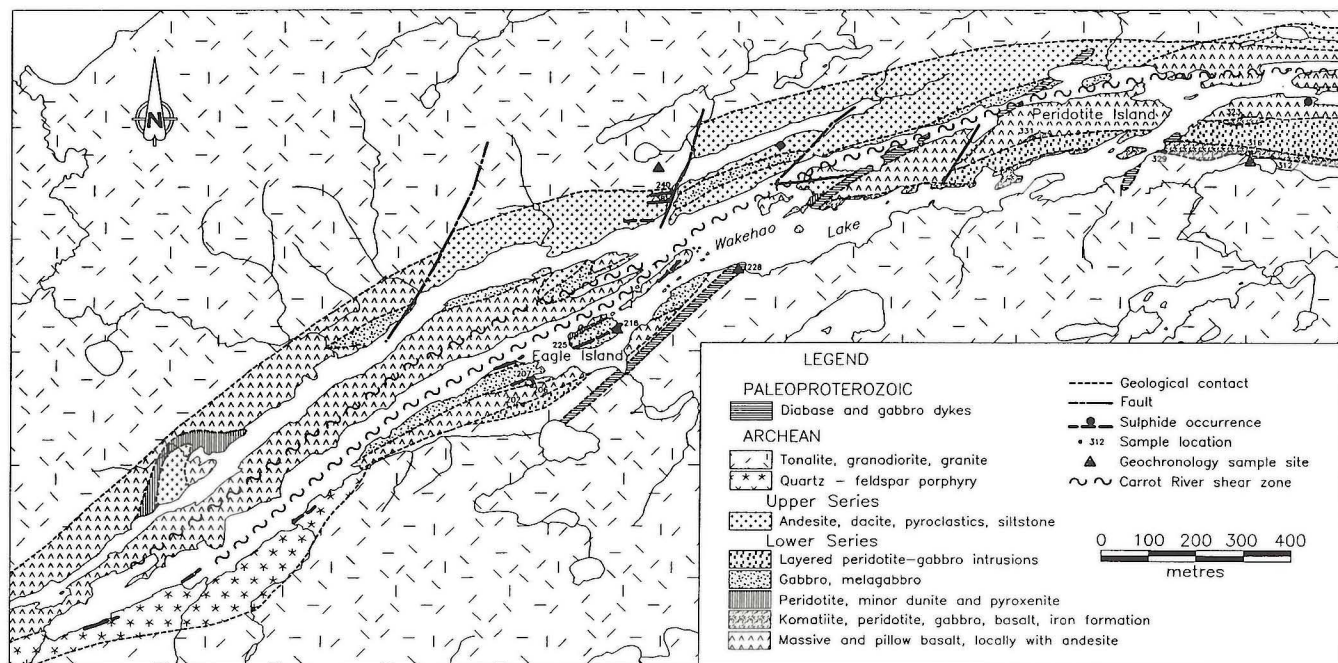


Figure GS-4-2: General geology of the eastern part of the Carrot River greenstone belt. Geology modified from Hubregtse (1985).

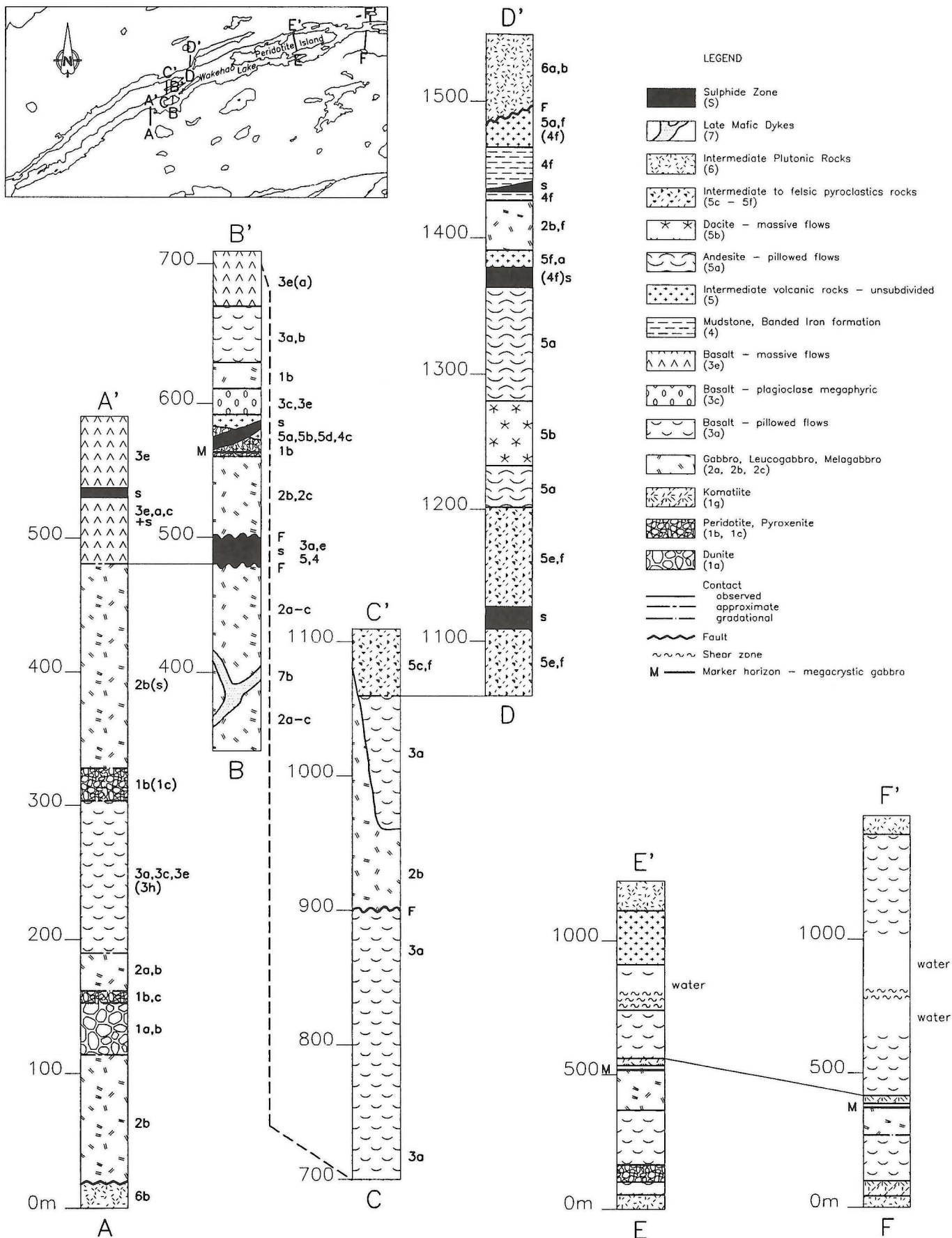


Figure GS-4-3: Detailed lithostratigraphic sections for the eastern part of the Carrot River greenstone belt. Refer to the text for detailed unit descriptions. Note that the scale for section lines A-A' to D-D' is larger than for sections E-E' and F-F'.

1:5000 scale mapping in selected, critical areas of outcrop. The type sections provide a means of correlating within the CRGB and a basis for comparison with other occurrences of the Hayes River Group (e.g., Hubregtse, 1985; Syme *et al.*, GS-5, this volume).

Western Section - Wakehao Lake

The western section is a composite based on 1:1000 scale grid mapping along 4 staggered but overlapping section lines (A-A' to D-D') covering an area of ca. 1 x 2 km adjacent to the western end of Wakehao Lake (Fig. GS-4-3). The corrected composite section is ca. 1.5 km long and extends into the granitic terranes on both the northern and southern boundaries of the greenstone belt. All primary facing indicators suggest that the entire western section is north-facing. No evidence of large scale folding was encountered. Minor, asymmetric drag folds occur in the vicinity of the major zone of shearing (herein referred to as the Carrot River shear zone) that affects units in the middle parts of the section and strikes at a slightly oblique angle to the trend of the Carrot River within the study area (Fig. GS-4-2). Numerous steeply dipping planar faults cut the stratigraphy and cause apparent lateral displacement on the scale of several centimetres to several metres. These include both northerly-trending and easterly-trending faults which exhibit either a dextral or a sinistral sense of movement. Given the lateral continuity of marker layers (see below), the north-trending faults do not appear to have caused significant disruption of the stratigraphy within the study area. However, repetition or dislocation of units along layer-parallel easterly-trending faults cannot be ruled out.

The contact between the lower series and the granitic terrane to the south was not observed and may be faulted based on from air photo interpretation. The granitic rocks include massive and foliated coarse-grained tonalite and granodiorite, and quartz and feldspar phyrlic granodiorite. The lowermost member of the lower series is a fine-grained to medium-grained gabbro. This is overlain by an approximately 75 m thick layered mafic-ultramafic intrusion, comprising a basal, 45 m thick layered dunite-peridotite-pyroxenite body and an overlying 30 m thick melagabbro-gabbro body (station 202, Fig. GS-4-2). The contact between these two bodies is gradational, ca. 1 m thick, and is denoted by the first appearance of plagioclase in the ultramafic unit, the gradual upward increase in modal plagioclase content from <5 to >50% and the disappearance of olivine (Fig. GS-4-4). The peridotite body can be subdivided into several layered units but, in general, displays a steady increase in pyroxene at the expense of olivine, to the north. Deuteric alteration emanating from the upper part of the ultramafic sequence, cuts the overlying gabbroic rocks along irregular, cm-wide veins. These veins strike at nearly 90° to the gabbro-ultramafic contact and contain coarse-grained plagioclase and a tan-coloured amphibole.

The gabbro is overlain by ca. 120 m of of basaltic rocks, including abundant pillowed flows, amygdaloidal pillows, amoeboid pillows, and porphyritic flows containing up to 60% medium-grained plagioclase

phenocrysts and rare megacrysts. The upper part of the basalt sequence contains north-northwest trending zones of intense brecciation and veining. The veins are planar to irregular, <20 cm wide and include variable proportions of quartz, epidote, calcite, plagioclase and sulphides (pyrrhotite ± chalcopyrite). The vein networks appear to have formed by hydrofracturing processes and subsequent open-space filling and may reflect proximal seafloor hydrothermal alteration.

The basalt sequence is overlain by a second layered mafic-ultramafic complex (station 206, Fig. GS-4-2). The base of this complex has a minimum thickness of 20 m and comprises fine- to medium-grained peridotite which grades upward into pyroxenite and plagioclase pyroxenite. A gradational modal contact (Fig. GS-4-4), similar to that observed in the lower mafic-ultramafic body, separates the plagioclase peridotite from overlying gabbroic rocks that range in composition from melagabbro to leucogabbro. The gabbroic rocks include a 100 to >200 m thick body, comprising several texturally- and/or modally distinctive layers, which is exposed on Eagle Island in Wakehao Lake (see station 216, Fig. GS-4-2). On line B-B' (Fig. GS-4-3), detailed mapping of the gabbro body delineated 9 major layers (L1 to L9), including (from base to top, thickness in parentheses): L1 (>10 m) - coarse-grained leucogabbro; L2 (30 m) - coarse-grained to medium-grained leucogabbro with diffuse gabbroic bands; L3 (25 m) - medium-grained leucogabbro with pyrrhotite-bearing granophyric gabbro pods, layers and veins, and displaying minor cm-scale modal layering; L4 (1 m) - fine-grained gabbro; L5 (2 m) - modally-layered (cm-scale) fine-grained gabbro, coarse- to medium-grained leucogabbro and quartz gabbro; L6 (8 m) - medium-grained gabbro with minor, irregular patches of pegmatitic, vari-textured gabbro; L7 (6 m) - irregular mixing between fine-grained gabbro, medium-grained leucogabbro and pegmatitic, locally dendritic quartz-bearing gabbro, with abundant, stratiform, lenticular zones of disseminated pyrrhotite + chalcopyrite mineralization; L8 (3 m) - thinly-banded (2 cm - 15 cm) coarse-grained quartz gabbro/diorite, medium-grained leucogabbro and fine-grained gabbro with local, lenticular pyrrhotite-rich bands containing up to 15% sulphides; L9 (>10 m) - a distinctive coarse-grained gabbro/leucogabbro characterized by randomly-orientated acicular amphibole crystals.

The layered gabbro body is overlain by massive and pillow basalt containing local amygdaloidal units. Along section B-B' the layered gabbro body is in fault contact with a sulphide-bearing volcanic unit including crystal-lithic tuff of intermediate composition, mafic mudstone and disseminated to semi-massive pyrrhotite mineralization. The tuffaceous unit was only observed on the western shoreline of Eagle Island, where it comprises a massive, very fine-grained quartz-sericite-albite-amphibole matrix and <10% broken, angular quartz and plagioclase phenocrysts and rare andesitic to dacitic lithic fragments.

The layered gabbro unit continues for ca. 60 m to the north of the felsic tuff unit. The gabbro adjoins a >20 m thick, poorly exposed ultramafic-



Figure GS-4-4: Gradational modal contact between underlying peridotite and overlying poikilitic melagabbro at station 202 (see Fig. GS-4-2 for location).

mafic body (lower contact not observed) that comprises peridotite, poikilitic peridotite, olivine pyroxenite, pyroxenite, melagabbro and plagioclase megaphyric gabbro. The plagioclase megaphyric unit is commonly 2-5 m thick and contains up to 30% blocky, idiomorphic and partially resorbed, up to several cm wide plagioclase megacrysts. The plagioclase megaphyric gabbro also displays a distinctive, wavy contact with underlying leucogabbro and/or pyroxenite layers (Fig. GS-4-5) that may have been created by magmatic turbidity currents. This package of ultramafic and mafic rocks, together with overlying spherulitic basalts, forms a texturally unique and mappable marker unit that has been correlated between the western and eastern sections over a distance of ca. 10 km (Figs. GS-4-2, 3).

The second ultramafic-mafic body is intrusive into an ca. 15 m thick supracrustal sequence that includes interbedded felsic tuff, massive and hyaloclastic dacite flows, heterolithologic mafic volcanic breccia and mafic mudstone. This sequence is overlain by >100 m of plagioclase phyric, aphyric and spherulitic pillow basalt and andesite, minor, <10 m thick, massive basalt flows and associated gabbro. Pillow breccia and amoeboid pillows are commonly observed in this area. The spherulitic basalts are commonly undeformed and preserve delicate budded pillow structures, concentric zoning and primary aspect ratios (Fig. GS-4-6). The spherules are commonly <1 cm circular objects that occur between the core and rim of pillows and are distributed in a symmetric manner around the pillow axis, commonly forming widely scattered haloes close to the selvage and becoming more abundant towards the core (Fig. GS-4-6). Smaller pillows locally display core areas composed entirely of contiguous, densely packed spherules. The spherules may have resulted from quenching of the lava,

resulting in radial, skeletal growth of plagioclase about irregularly spaced nucleation centres.

The spherulitic basalt sequence is locally intruded by thicker bodies of globular-textured gabbro and plagioclase pyroxenite. The globular texture is similar in appearance to ocellar textures in komatiites in which partial melts derived from country rock or unconsolidated sediments remain suspended as immiscible droplets that retain spherical forms. In the study area, these globular forms rarely exceed 10 cm in diameter and have a dioritic to tonalitic mineralogy. In the megaphyric gabbro unit, resorption textures indicate that the large plagioclase phenocrysts contained in the rocks were not in equilibrium with the matrix. The culmination of this resorption process also generated rounded spheroids of gabbroic to tonalitic composition that resemble the leucocratic globules in the globular-textured gabbro.

The middle of the stratigraphy of the CRGB, along section C-C' (Fig. GS-4-3) is characterized by >300 m of highly sheared volcanic rocks and younger gabbroic intrusions that were deformed by the Carrot River shear zone. The southern part of this section consists of pillow basalt and local spherulitic basalt. An east-northeast trending fault separates the basalts from a medium-grained gabbro body which intrudes both pillow basalt and conformably overlying sheared quartz + albite + sericite + biotite schists that are interpreted to represent intermediate to felsic pyroclastic rocks. The main structural elements associated with the Carrot River shear zone are asymmetric drag folds, local crenulation cleavages, quartz and/or carbonate and/or sulphide veining, extreme flattening of pillows and pervasive grain size reduction.

Figure GS-4-5: Undulating contact between weakly porphyritic plagioclase pyroxenite (bottom), thin plagioclase phyric leucogabbro (middle) and plagioclase megaphyric gabbro (top). Note the sheared plagioclase megacrysts (white) along the layer contacts and the partial digestion of megacrysts in the leucogabbro layer.



Figure GS-4-6: Concentric structures in plagioclase phyric and spherulitic pillow lava sequence from the Wakehao Lake area. Pillows typically display spherule-free glassy rims, inner, thin, spherule-rich zones and coarser grained, plagioclase phyric or aphyric cores. Note intense feldspar + quartz + carbonate alteration (seafloor?) along irregular veinlets in the lowermost, brecciated pillow unit. Facing direction is toward the top of the photo.

The upper part of the stratigraphy is documented along section D-D' (Fig. GS-4-3) and consists of andesitic and dacitic flows and tuffs, fine-grained siltstone and mudstone. Stratiform sulphide-rich layers (discussed below) are locally developed. All of the volcanic rocks types are intruded by aphyric or plagioclase phyric gabbro dykes. In comparison to basaltic flows occurring to the south, the intermediate flows display less definitive pillow structures, are more commonly amygdaloidal and plagioclase phyric, and develop block flows up to 5 m thick. Flow breccias are associated with hyaloclastite and incorporate angular andesite fragments in a fine-grained to aphanitic matrix of intermediate composition. Massive flows developed pillows up to 7 m long and 3 m wide and commonly contain both plagioclase and amphibole (formerly pyroxene?) phenocrysts up to 3 mm long. Siltstone and mudstone form several, thin interflow beds and an *ca.* 40 m thick, thinly-bedded sequence near the top of the section (D-D'; Fig. GS-4-3). Sulphide mineralization occurs in a semi-conformable zone of intense recrystallization and silicification within the metasedimentary unit.

The contact between the volcanic sequence and the granitic unit to the north is faulted. However, the granitic rocks immediately to the north of the uppermost volcanic unit contain abundant cm- to m-size inclusions of layered gabbro and amphibolite which may have been derived from the CRGB.

Eastern Section

The eastern section focused on new exposures of komatiites occurring to the south of the Carrot River in the vicinity of Peridotite Island (Fig. GS-4-2). Komatiites associated with oxide facies iron formation were recently observed in the eastern CRGB (Fedikow *pers. comm.*, 1996) during a multimedia geochemical survey (Fedikow *et al.*, 1996). Section E-E' represents a traverse across Peridotite Island and two islands to the southeast of Peridotite Island (Fig. GS-4-2). In this area, the southern margin of the CRGB comprises tonalitic rocks which intrude massive and pillow basalt. Peridotite, interlayered with silicate and/or oxide facies iron formation and mudstone, is exposed on the two islands. The peridotites were the subject of Ni-Cu exploration by several companies, the most recent of which was Canex Placer Limited (1971 to 1973). An M.Sc. thesis dealing with the geology of the Carrot River ultramafic complex was completed by Davidson (1974). The peridotite body is best exposed along the south shoreline of Peridotite Island, and comprises fine-grained dunite, peridotite and pyroxenite. The ultramafic rocks display local cm-scale modal layering, grade upward into melagabbro and gabbro, and are intrusive into overlying pillow basalt. A large part of the southeastern section of Peridotite Island is underlain by melagabbro, plagioclase pyroxenite, gabbro and plagioclase megaphyric gabbro (described below) that intrude into pillow basalt. An assemblage of mafic and ultramafic rocks, in which spinifex textured komatiitic dykes intrude fault-displaced blocks of peridotite and dunite, is exposed in the south-central part of Peridotite Island (station 331, Fig. GS-4-2). This occurrence of komatiitic rocks is considered to be stratigraphically equivalent to komatiite exposed to the east (Figs. GS-4-2, 3), based largely on the presence of the megaphyric gabbro marker layer.

The komatiite-gabbro sequence is overlain by massive, pillowed and commonly spherulitic basalt including many well preserved flows having pillows up to 8 x 3 m in size. A 3 m wide plagioclase pyroxenite dyke striking 070° cuts the spherulitic pillow basalt sequence in the north-eastern part of Peridotite Island. Similar dykes are observed in the lower and middle parts of the stratigraphy at several other localities in the study area. The basaltic rocks continue to the north shore of the island where they become strongly deformed within the Carrot River shear zone. The north section of line E-E' comprises strongly sheared intermediate schists that have been correlated with the intermediate volcanic units exposed along section line D-D' (Figs. GS-4-2, 3; Hubregtse, 1985).

At the base of section line F-F' (Fig. GS-4-2), tonalites intrude pillow basalt and ultramafic komatiites. The komatiites are locally interlayered with thin, laminated sedimentary rocks, including fine-grained silty beds enriched in ultramafic detritus and siliceous siltstone. North of the komatiites are a sequence of mafic volcanics and high level mafic to ultramafic intrusions. The shallow intrusive rocks are gabbroic to pyroxenitic in composition and include the above mentioned plagioclase megaphyric marker layer, which in this area commonly displays glomeroporphyritic textures. This megaphyric gabbro is overlain by a second sequence of

komatiites (station 323; see below) which are in turn overlain by massive and pillow basalt. The Carrot River shear zone passes through an island at the east end of the Carrot River and near the top of section F-F' (Fig. GS-4-3), where a basaltic protolith has been reduced to sericitic phyllite. The northern segment along section line F-F' is composed of pillowed flows intruded by the granitoid rocks that form the northern boundary of the greenstone belt.

Stratigraphic setting and petrology of the komatiites

Owing to their excellent preservation, a significant effort was made in documenting the textural characteristics of the komatiitic units exposed in the southeastern part of the study area, where the stratigraphically lower portion of the CRGB hosts ultramafic komatiites at two and, possibly, three stratigraphic levels. (Figs. GS-4-2, 3). The lowermost komatiite sequence is exposed at several locations. The following descriptions are principally based on observations made at two of these locations.

Stations 312 and 316 are located to the north and west of a small lake south of the Carrot River (Fig. GS-4-2). At station 312, two komatiite flows are exposed immediately to the north of the younger tonalitic rocks. Field observations are augmented by petrographic observations made on drill core obtained from two holes, one of which intersected part of the lower flow (#314) and the second of which (#311) intersected the stratigraphically lowermost portion of the upper flow and continued into the top of the lower flow (Fig. GS-4-7). One complete and two partially exposed ultramafic flows are present within the 64 cm section intersected by the drillholes. Only the top of the lowermost flow is exposed. It is approximately 40 cm thick (Fig. GS-4-7) and comprises a radial, plumose, bookleaf and randomly ordered pyroxene spinifex. This unit is overlain by olivine mesocumulate (unit A), interpreted to represent the stratigraphic base of a 44 cm thick flow unit (Fig. GS-4-7). The olivine mesocumulate is overlain by a coarser-grained layer containing what is interpreted as skeletal plagioclase (?) with minor interstitial hornblende (unit C). This unit grades into a spinifex-textured (pyroxene?) layer that contains interstitial skeletal plagioclase (unit D). Only the olivine-rich cumulate base of the uppermost flow (20 cm thick) is exposed.

Lithologic and textural studies were carried out on polished core from the two drillholes collared in this outcrop. Drillhole #314 is 24 cm long and primarily intersects spinifex textured (chain olivine) peridotite. Olivine cumulate was intersected at the bottom of the drillhole and also occurs as a 2 cm thick layer between 12 and 14 cm (downhole depth). Drillhole #311 intersects olivine mesocumulate with subrounded olivine crystals, up to 1.2 mm in diameter, which are locally embedded in pyroxene oikocrysts. The lower portion of this drillhole intersects olivine cumulate in which olivine crystals are characterized by amoeboid shapes that imply disequilibrium crystallization, likely from a melt supersaturated in olivine. The reason for the discrepancy between the geology of the outcrop surface and that of the drillholes is not evident.

Several contiguous komatiitic flows are exposed in an outcrop (station 316) approximately 22 x 12 m, located about 200 m west-northwest of station 312 (Fig. GS-4-2). Individual flows were distinguished by means of interpreted lithologies and textures visible on the weathered surface. Olivine-dominated flows occur in contact with pyroxenitic flows or are separated by fine grained oxide facies iron formation or finely comminuted ultramafic debris (hyaloclastite?). A detailed cross section (A-B, Fig. GS-4-8) through part of this outcrop identified parts of three ultramafic flows separated by thinly bedded ultramafic clastic rocks and/or oxide facies iron formation. Textures and key contacts are illustrated in Figures GS-4-9, 10 and 11. Ultramafic komatiites in association with pillowed basalt, bedded ultramafic sediment, and or silicate facies iron formation have been also observed in outcrops along strike and to the west, and likely relate to the mafic-ultramafic sequences exposed on and to the south of Peridotite Island.

An approximately 4.3 m thick komatiitic ultramafic flow occurs at station 323, approximately 400 m north of the ultramafic flows described from stations 312 and 316 (Figs. GS-4-2, 12). Excellent outcrops along an escarpment expose magnificent spinifex textures (Figs. GS-4-12, 13). The base of the flow consists of olivine cumulate grading abruptly into a complex sequence of spinifex textures, details of which are shown on Figure GS-4-12. The flow occurs within a complex sequence of komatiitic basalt and spherulitic pillow basalt flows, interlayered pyroxenite, leucogabbro, gabbro,

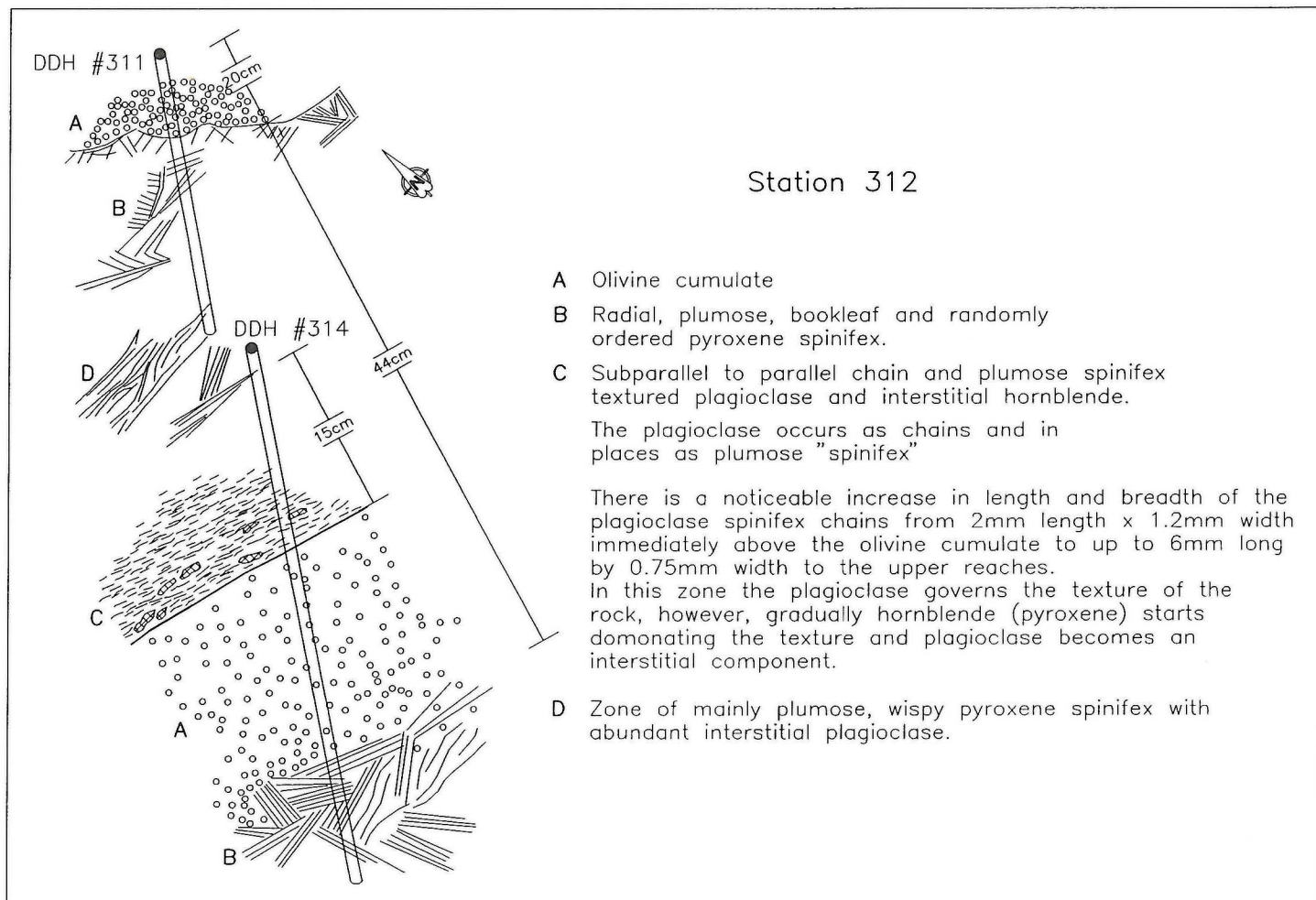


Figure GS-4-7: Lithologies and rock textures of komatiite flows exposed at station 312.

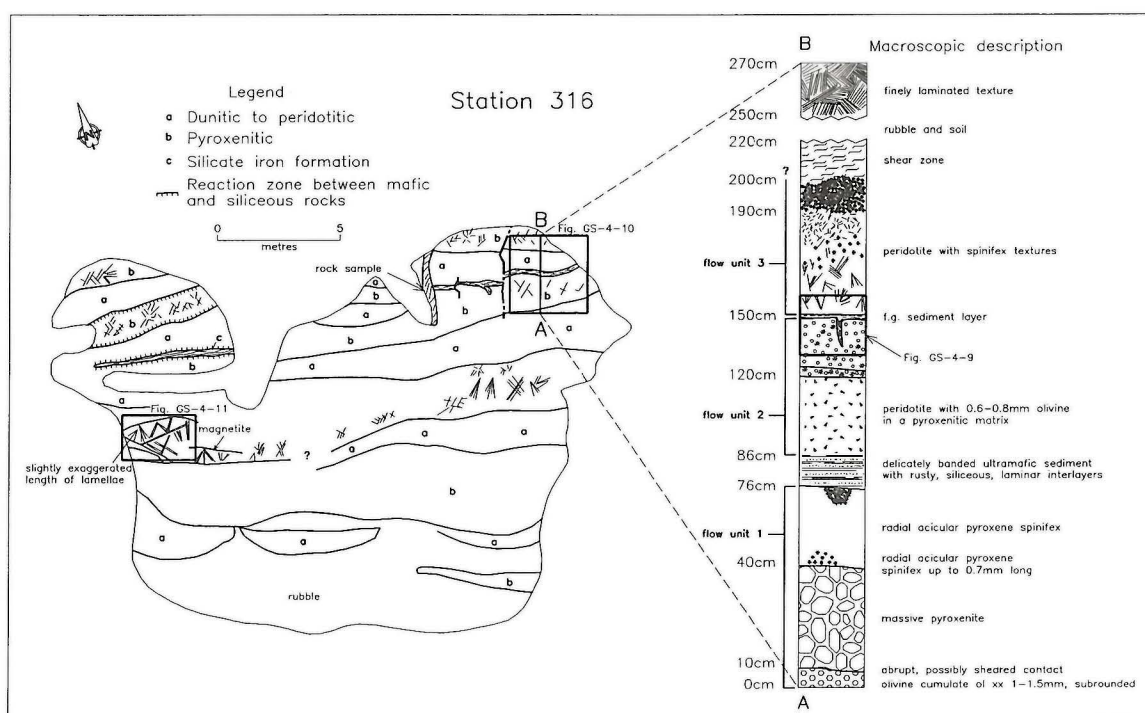


Figure GS-4-8: Plan and detailed section of komatiites exposed at station 316.



Figure GS-4-9: Peridotitic komatiite overlain by thin siliceous sedimentary unit and spinifex textured pyroxenitic komatiite (station 316). Photo height is 50 cm. See Figure GS-4-8 for location.



Figure GS-4-10: Fine grained laminated ultramafic detrital sediments and siliceous sediments deposited between massive and spinifex textured komatiitic flows (station 316). Photo height is 80 cm. See Figure GS-4-8 for location.

Figure GS-4-11: Coarse, platy olivine spinifex in komatiite flow, station 316. See Figure GS-4-8 for location.



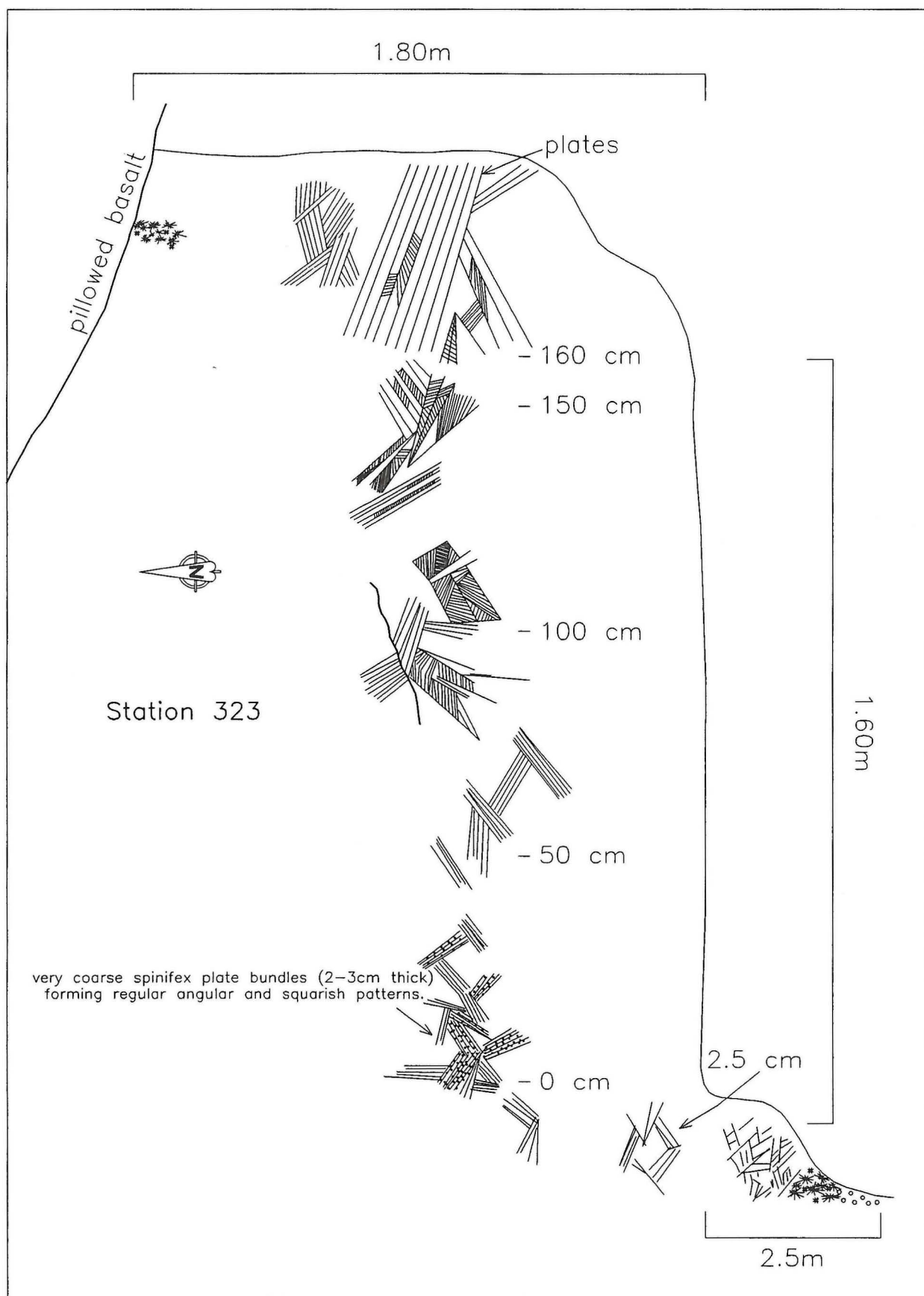


Figure GS-4-12: Details of spinifex textures exposed in a rock face at station 323

Figure GS-4-13: Coarse spinifex textures in komatiite flow, station 323. See Figure GS-4-2 for location.

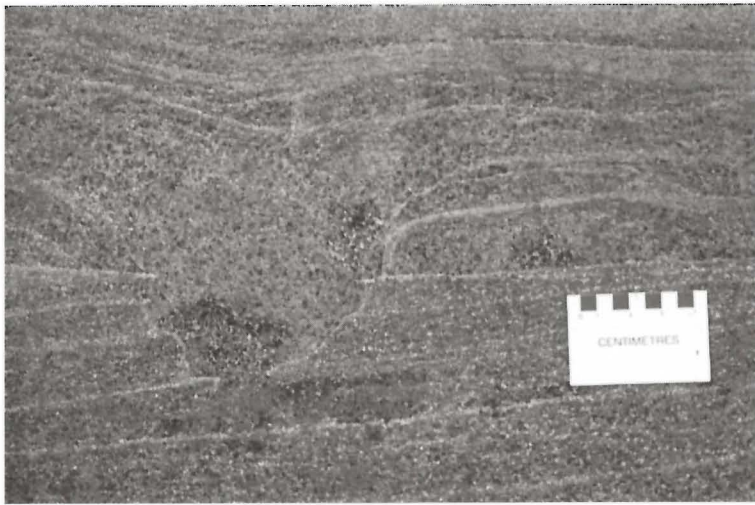
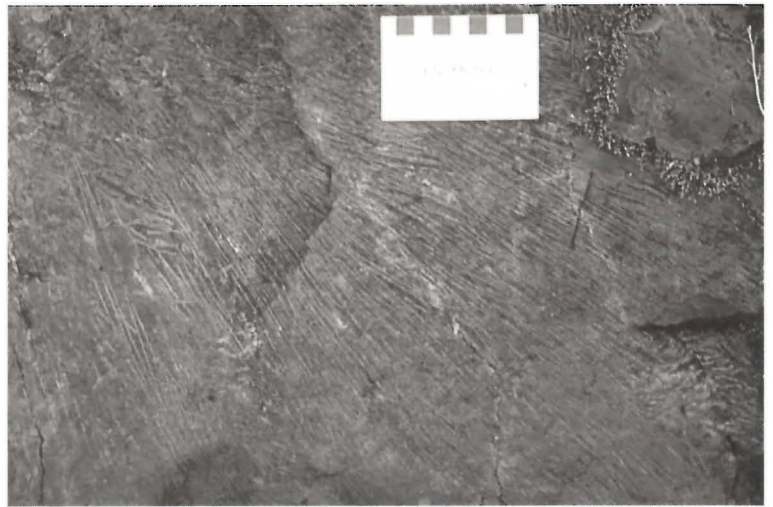


Figure GS-4-14: Trough structure in a layered Paleoproterozoic gabbro dyke, station 228, Wakehao Lake.

melagabbro and plagioclase phyric gabbro. It is situated approximately 700 m to the north of the tonalite body which defines the southern boundary of the CRGB, and represents the uppermost komatiite unit on section lines E-E' and F-F' (Fig. GS-4-3). Geochemical studies (below) indicate that most of the komatiitic and spatially associated gabbroic and basaltic units were cogenetic.

GEOLOGICAL SYNTHESIS

The major lithofacies exposed in the study area can be correlated between the western and eastern sections. Lateral facies changes may be represented by the absence of komatiites and iron formations in the eastern section, and a paucity of intermediate volcanic rocks and sulphide bodies in the middle portions of the western section. In terms of the general abundance and distribution of rock types, the CRGB is most similar to platform type, 'iron' assemblages found at the base of many late Archean greenstone belts, and of particular prominence in the Sachigo and Abitibi Subprovinces of the Superior Craton in Ontario (Thurston, 1994). The upper portion of the CRGB within the study area is a much more evolved supracrustal section, characterized by abundant andesite, dacite and allied pyroclastic units, contains a greater proportion of detrital sedimentary rocks, and is apparently devoid of ultramafic rocks.

At Oxford Lake, the lower, mafic portion of the Hayes River Group is dominated by basalts, but also contains ultramafic rocks. The character of the rocks, as described by Hubregtse (1985), is similar to the lower ultramafic-mafic succession in the Carrot River belt, particularly with respect to the development of quench textures, spherulitic and plagioclase phyric

basalt flows and megaphyric units. However, the andesitic to dacitic sequence exposed in the CRGB is not recognized as part of the Hayes River Group at Oxford Lake. The intermediate to felsic volcanic rocks at Oxford Lake are primarily included in the younger Oxford Lake Group, and have been ascribed to shoshonitic volcanism in an arc environment following development of the Hayes River Group (Brooks *et al.*, 1982). Syme *et al.* (GS-5, this volume) describe a mafic-felsic association for the Hayes River Group at Knee Lake that may be more comparable to the CRGB.

LATE DYKES

Two large mafic dykes and several smaller dykes occur within the study area. The dykes commonly retain their primary mineralogy and clearly post-date the last major deformation along the Carrot River shear zone. They are petrologically similar to Paleoproterozoic mafic dykes occurring in other parts of the northwestern Superior Province (*e.g.*, Molson dyke swarm; Scoates and Macek, 1978). The dykes typically strike east-northeasterly, but there is no consistent orientation within the study area. The dykes commonly display chilled margins against the supracrustal rocks and include three major types: (1) <1 m wide, planar to irregular, massive diabase dykes; (2) medium-sized, >1 to <20 m wide, branching, plagioclase phyric and aphyric gabbro dykes; and, (3) large, >20 m to <150 m wide, layered, differentiated olivine gabbro-gabbro-leucogabbro-diorite dykes. The dykes are very abundant in the central and eastern parts Eagle Island, and at several locations along the southern shoreline of the Carrot River.

The largest dyke observed in the study area is exposed along the southern shoreline of Wakehao Lake. Several sedimentary-type structures

are developed in the dyke, including scours (Fig. GS-4-14), 'drop stones', truncated layering and size-graded layering. Layer structures suggest a southward facing direction for the dyke. The well-developed cross-bedding structures and symmetric scours are interpreted to indicate crystallization and deposition along a gently sloping floor as opposed to a steeply-inclined wall. Therefore, the dyke may, in fact, represent a sill that has been rotated sufficiently to expose a cross-section through the layered units. Accordingly, the dyke may predate a period of tilting during the Paleoproterozoic. The age of the dyke is being investigated by L. Heaman (University of Alberta), based on two samples of pegmatitic gabbro collected during this study (station 228, Fig. GS-4-2).

In addition to the mafic dykes, numerous felsic porphyry dykes, including quartz, quartz + plagioclase and plagioclase phyric dykes are present in the eastern CRGB. The dykes generally appear to postdate all of the supracrustal rocks in the area, although in one location, a quartz + plagioclase phyric granitic dyke is intruded by a megaphyric gabbroic dyke, confirming that some of the granitic bodies were contemporaneous with the mafic and ultramafic magmatism.

GEOCHEMISTRY

Representative samples obtained from all of the major lithologic units in the study area were analyzed for major, trace and rare-earth elements at the Geoscience Laboratories, Sudbury, Ontario. Analytical results and methods are given in Tables GS-4-1 and GS-4-2. The following description is based on a preliminary analysis of the geochemical data.

The major element geochemistry of the igneous rock samples investigated have been plotted on the simple ternary cation plot designed by Jensen (1976), which provides a general classification scheme for metavolcanic rocks. Samples from the current study define two principal compositional trends (Fig. GS-4-15). Komatiitic, peridotitic, gabbroic and some basaltic rocks define a staggered Fe-enrichment trend (komatiitic and tholeiitic trends; Fig. GS-4-15). The komatiites, excluding one sample, plot in the basaltic komatiite field. The second trend relates to the intermediate volcanic rocks from the upper series, which exhibit calc-alkaline compositions ranging from basalt to rhyolite. A few of the basalt and gabbro samples plot in the calc-alkaline field and do not follow the Fe-enrichment trend. These samples were collected from the lower series, and their distinctive compositions may indicate an early stage of arc magmatism in the CRGB.

Selected trace and rare-earth element (REE) data are reported in Table GS-4-2 and representative analyses for the major rock types are plotted on a series of mantle and mid-ocean ridge basalt (MORB) normalized spider diagrams (Figs. GS-4-16 to 19). Komatiite samples display flat REE patterns relative to MORB but are slightly enriched in lithophile trace elements such as U, Th and Cs (Fig. GS-4-16). Some of the samples display negative Eu and Sr anomalies which could relate to seafloor alteration and selective removal of these elements. The REE profiles for the komatiites is consistent with derivation from a MORB-like depleted mantle source.

A similar flat REE pattern is demonstrated by rocks belonging to the lowermost of the mafic-ultramafic bodies encountered along the western section (station 202, Fig. GS-4-2). The selected samples include Mg-rich peridotite, melagabbro and gabbro (Fig. GS-4-17), all of which display absolute abundances of REE that are similar to those of the komatiite samples. The negative Sr and Eu anomalies displayed by the peridotite samples is mirrored by corresponding positive anomalies in the overlying gabbros, which also exhibit strong enrichment in the strongly incompatible elements (Cs, Rb, Ba, K; Fig. GS-4-17). All of the rocks are enriched in Th and U, possibly indicating assimilation of crustal materials or contamination of the mantle source. These geochemical trends are consistent with the gabbroic rocks being related to the ultramafic units by fractional crystallization and accumulation of plagioclase-saturated residual liquids in the upper part of the intrusion.

A comparison of selected basalt samples from the western and eastern cross sections reveals significant differences in the REE abundances (Fig. GS-4-18), with the eastern basalts displaying relatively flat, mantle-like profiles and the western basalts displaying strong enrichment in the light REE (La to Nd) (Fig. GS-4-18). These differences likely reflect variations in the source composition and degree of partial

melting and are not readily explained by alteration (the rocks are not visibly altered), assimilation or fractional crystallization. The primitive basalts have similar major, trace and REE abundances to the adjacent basaltic komatiites, and it appears likely that these basalts were derived from komatiitic parent liquids.

Intermediate volcanic rocks from the western section display two major trends on mantle-normalized REE plots (Fig. GS-4-19). Tuffaceous rocks have extremely fractionated REE patterns with light REE abundances >20 times mantle values but heavy REE abundances of ca. 2 times mantle values (Fig. GS-4-19). Andesitic and dacitic flows display higher heavy REE abundances of ca. 6 times mantle values, but similar, strongly fractionated middle to light REE patterns (Fig. GS-4-19). The trends for the flow units are characteristic of volcanic rocks erupted in arc environments. On MORB-normalized multi-element plots (not shown), these intermediate volcanic rocks display similar, incompatible element-enriched patterns to the evolved basalts from the western section (Fig. GS-4-18), and both suites of rocks display distinct negative Nb and Ti anomalies that typify most Proterozoic and Phanerozoic arc-related volcanic sequences.

The geochemical results augment field observations and suggest that at least two major styles of magmatism occurred within the eastern CRGB - an early komatiite-tholeiite suite and a later calc-alkaline suite. The results also suggest that there was significant overlap between these two volcanic regimes. Major geochemical trends in the volcanic and plutonic rocks from the study area largely reflect partial melting processes and differences in source compositions, whereas more subtle trends relate to crystal fractionation, contamination and localized hydrothermal alteration.

ECONOMIC GEOLOGY

The CRGB has been explored by several companies over the past 30 years, principally for base metals (Cu-Zn-Pb) and Au. In addition, ultramafic rock occurrences on or adjacent to Peridotite Island have been explored for Ni. Detailed accounts of the exploration results are given by Southard (1977) and Hubregtse (1985). The best assay results obtained to date relate to massive to semi-massive sulphide bodies along the southern shoreline of the Carrot River, and include one assay which returned 17.4% Zn and 9.6% Pb from a 0.61 m chip sample (Barry, 1960). Drill core samples from a <2 m wide massive sulphide band occurring at the contact between greywacke and felsic tuff to the south of Peridotite Island contain up to 3% Zn over 1.5 m (Southard, 1977). Government aeromagnetic data and open assessment file reports reveal a clustering of linear, east-northeast trending, moderate to strong EM anomalies extending along the Carrot River and terminating ca. 500 m to the south of the west end of Peridotite Island. To date, most of the exploration in the study area has targeted these conductors. Additional drilling tested a strong linear magnetic anomaly immediately to the south of the west end of Peridotite Island, and in a peridotite-gabbro-basalt sequence exposed in the eastern part of Peridotite Island.

Several known and newly discovered sulphide occurrences were investigated during the current study. Assay results for grab and chip samples obtained from these occurrences are given in Table GS-4-3. Anomalously high Au abundances were obtained from a mineralized felsic tuff exposed on the southwestern side of Eagle Island (station 225, Fig. GS-4-2). Anomalously high Cu abundances were obtained from a weakly mineralized layered gabbro body exposed in a small bay to the west of Eagle Island (station 207, Fig. GS-4-2). Elevated Zn abundances (860 ppm) were obtained from two easterly-striking sulphide-rich bodies developed within fine-grained, intermediate metasedimentary rocks in the upper part of the stratigraphy to the north of Wakehao Lake (stations 238 and 240, Fig. GS-4-2).

Based on field observations obtained during the current study, four major styles of sulphide mineralization are exposed in the area. These include: (1) massive to semi-massive pyrrhotite ± chalcopyrite ± pyrite ± sphalerite in tabular to lenticular metre-wide zones, several metres to hundreds of metres in length; (2) local, disseminated pyrrhotite-chalcopyrite mineralization in peridotite; (3) disseminated pyrite and/or pyrrhotite ± sphalerite ± chalcopyrite in quartz veins associated with the major east-northeast trending shear zone; and, (4) disseminated pyrrhotite ± chalcopyrite in gabbroic and basaltic rocks. The most continuous sulphide body in the study area strikes east-northeasterly along the southwestern

Table GS-4-1

Major element geochemistry for metavolcanic and metaplutonic rocks from the eastern part of the Carrot River greenstone belt

Sample #	Location	Rock Type	SiO ₂	TiO ₂	Al ₂ O ₃	Fe ₂ O ₃	MnO	MgO	CaO	Na ₂ O	K ₂ O	P ₂ O ₅	LOI	TOTAL	Mg#	CaO/Al ₂ O ₃	Al ₂ O ₃ /TiO ₂
98-97-202-1	West Section	Peridotite	38.9	0.25	4.94	14.0	0.16	30.0	2.90	N.D.	0.02	0.07	8.94	100.1	80.9	0.59	19.8
98-97-202-3	West Section	Peridotite	39.7	0.25	5.23	14.1	0.16	29.5	3.12	N.D.	0.02	0.07	8.76	100.9	80.6	0.60	20.9
98-97-202-7	West Section	Plagioclase Pyroxenite	41.5	0.36	10.4	13.1	0.19	22.0	6.89	0.13	0.02	0.07	6.17	100.8	76.9	0.66	28.9
98-97-202-8	West Section	Melagabbro	47.3	0.37	13.1	10.5	0.21	15.4	6.91	1.52	0.94	0.07	4.19	100.4	74.4	0.53	35.3
98-97-202-9	West Section	Melagabbro	50.6	0.40	12.0	9.12	0.21	14.3	8.25	1.51	1.44	0.07	3.07	101.0	75.7	0.69	29.9
98-97-202-10	West Section	Gabbro	51.7	0.52	12.1	9.98	0.22	11.5	9.60	2.66	0.24	0.08	1.93	100.5	69.5	0.80	23.2
98-97-203-1	West Section	Aphyric Basalt	54.8	0.92	15.9	6.17	0.12	7.28	8.01	3.16	N.D.	0.12	2.63	99.14	70.0	0.50	17.3
98-97-208-3	West Section	Intermediate Volcanic	53.4	0.87	15.6	9.31	0.17	5.13	9.70	1.20	0.35	0.12	3.07	98.98	52.2	0.62	18.0
98-97-210-1	West Section	Amygdaloidal Basalt	57.7	0.83	15.1	6.31	0.15	5.05	8.41	2.36	0.21	0.11	2.47	98.69	61.3	0.56	18.2
98-97-216-1	West Section	Leucogabbro	46.7	0.45	19.8	6.71	0.11	6.75	13.1	2.15	0.07	0.10	3.01	98.90	66.6	0.66	43.9
98-97-216-5	West Section	Gabbro	49.4	0.89	14.6	10.8	0.17	8.12	10.9	1.99	0.54	0.13	2.14	99.57	59.8	0.75	16.4
98-97-216-7	West Section	Gabbro	49.5	1.24	13.3	14.5	0.19	6.47	9.12	2.35	N.D.	0.14	2.26	99.03	46.9	0.69	10.7
98-97-216-10	West Section	Vari-textured Gabbro	51.1	1.52	13.5	13.4	0.20	6.00	7.97	3.08	N.D.	0.18	2.33	99.23	46.9	0.59	8.9
98-97-216-12	West Section	Leucogabbro	48.9	1.55	13.5	15.4	0.18	5.79	8.22	3.11	N.D.	0.18	2.12	98.95	42.7	0.61	8.7
98-97-221-1B	West Section	Altered Basalt	54.9	0.78	15.7	7.24	0.19	5.27	7.70	1.82	2.32	0.12	2.10	98.15	59.1	0.49	20.1
98-97-225-1A	West Section	Intermediate Tuff	66.6	0.36	15.2	3.72	0.05	1.61	3.23	3.82	1.55	0.21	2.08	98.38	46.2	0.21	42.2
98-97-228-1	West Section	Gabbro Pegmatite Pod	49.4	2.05	12.8	17.8	0.27	4.31	8.86	2.29	0.19	0.23	1.39	99.61	32.4	0.69	6.2
98-97-234-2	West Section	Felsic Crystal Tuff	67.2	0.64	15.5	1.68	0.03	1.79	4.08	4.43	1.02	0.23	2.14	98.77	67.9	0.26	24.2
98-97-236-1	West Section	Dacite Pillow Lava	62.8	0.79	15.8	5.20	0.08	2.50	4.04	5.09	0.67	0.34	1.59	98.83	48.8	0.26	20.0
98-97-236-2	West Section	Plag.-Phyric Andesite	57.9	0.76	15.6	6.61	0.13	3.24	8.70	2.51	0.42	0.33	3.26	99.45	49.3	0.56	20.5
8-97-246-1	West Section	Basalt	48.2	0.67	11.8	13.1	0.21	11.9	11.3	1.04	0.33	0.19	1.90	100.6	64.2	0.96	17.6
98-97-319-1	East Section	Basaltic Komatiite	47.0	0.88	6.95	16.2	0.32	15.3	11.0	0.90	0.12	0.09	1.63	100.4	65.1	1.59	7.9
98-97-320-1	East Section	Komatiite	47.5	0.77	6.27	15.2	0.27	17.4	10.4	0.63	0.07	0.09	2.31	100.9	69.4	1.66	8.1
98-97-321-1	East Section	Peridotite	41.4	0.47	3.59	13.7	0.12	29.2	3.95	0.24	0.05	0.08	7.48	100.1	80.9	1.10	7.6
98-97-322-1	East Section	Komatiite	46.3	0.79	6.37	15.3	0.27	18.0	9.95	0.65	0.11	0.09	2.33	100.1	70.0	1.56	8.1
98-97-323-4	East Section	Megacrystic Gabbro	49.7	1.03	12.5	14.1	0.19	7.68	8.94	3.17	0.22	0.09	1.21	98.89	51.9	0.71	12.2
98-97-323-6	East Section	Basaltic Komatiite	47.2	0.76	10.0	13.9	0.19	14.7	10.6	0.74	0.77	0.07	1.87	100.8	67.6	1.06	13.2
98-97-323-9A	East Section	Peridotite	40.4	0.33	3.83	11.0	0.14	32.0	4.27	0.01	0.02	0.05	8.27	100.4	85.2	1.11	11.6
98-97-323-10	East Section	Spinifex Komatiite	46.0	0.62	7.54	14.3	0.20	18.0	9.92	0.38	0.11	0.07	3.24	100.4	71.3	1.32	12.2
98-97-323-11	East Section	Komatiite	45.9	0.59	7.10	14.2	0.20	19.1	9.60	0.32	0.06	0.07	3.25	100.3	72.8	1.35	12.0
98-97-323-12	East Section	Plag.-Phyric Diabase	49.5	0.66	12.3	13.2	0.21	10.6	10.9	1.87	0.22	0.09	1.21	100.8	61.4	0.88	18.7
98-97-323-13	East Section	Pillow Basalt Core	49.3	0.74	12.4	12.5	0.21	9.78	11.6	1.77	0.10	0.09	0.94	99.37	60.7	0.94	16.7
98-97-329-4	East Section	Komatiite	44.0	0.64	5.20	14.3	0.20	23.8	7.67	0.44	0.08	0.08	4.23	100.7	76.7	1.48	8.1
98-97-329-6	East Section	Basaltic Komatiite	46.7	0.86	6.90	15.7	0.28	16.0	11.3	0.95	0.13	0.09	1.65	100.5	66.9	1.6	8.0

Notes: All data are expressed in weight %. Analyses were performed at the Geoscience Laboratories, Sudbury, Ontario, using X-ray fluorescence spectrometry.

Mg# = 100*Mg/(Mg+Fe), where Fe is total Fe expressed as FeO. N.D. = not determined by this method.

Table GS-4-2

Selected major, trace and rare earth element abundances in metavolcanic and metaplutonic rocks from the eastern part of the Carrot River greenstone belt

Sample #	Location	Rock Type	MgO	Al ₂ O ₃	Fe ₂ O ₃ ^T	MnO	TiO ₂	P ₂ O ₅	Sc	V	Cr	Co	Ni	Cu	Zn	Ga	Rb	Sr	Y
98-97-202-1	Western Section	Peridotite	30.0	4.94	14.02	0.16	0.25	0.07	19.4	110	2800	108	1050	6.9	63.2	4.90	0.55	10.0	5.19
98-97-202-3	Western Section	Peridotite	29.5	5.23	14.05	0.16	0.25	0.07	20.5	112	1800	112	1010	14.0	45.1	5.21	0.35	10.2	5.93
98-97-202-7	Western Section	Plagioclase Pyroxenite	22.0	10.4	13.08	0.19	0.36	0.07	29.0	156	1500	88.8	426	3.2	57.4	8.41	0.25	6.32	11.7
98-97-202-8	Western Section	Melagabbro	15.4	13.1	10.47	0.19	0.37	0.07	39.4	173	1200	52.4	166	5.2	54.8	9.60	30.9	82.9	8.07
98-97-202-9	Western Section	Melagabbro	14.3	12.0	9.12	0.19	0.40	0.07	46.9	196	1000	44.2	155	9.3	50.6	9.41	38.6	81.7	9.74
98-97-202-10	Western Section	Gabbro	11.5	12.1	9.98	0.20	0.52	0.08	46.4	227	740	41.0	126	18.7	49.1	10.7	5.82	287	11.7
98-97-203-1	Western Section	Aphyric Basalt	7.28	15.9	6.17	0.12	0.92	0.12	56.6	333	303	45.8	114	52.3	67.9	16.7	3.09	155	20.3
98-97-208-3	Western Section	Intermediate Volcanic	5.13	15.6	9.31	0.15	0.87	0.12	51.0	293	309	48.6	129	88.3	79.5	13.0	9.94	106	18.9
98-97-212-2	Western Section	Gabbro	8.35	15.8	12.7	0.19	1.45	0.16	31.8	255	371	48.7	145	236	133	16.0	0.51	193	21.9
98-97-214-1	Western Section	Plagioclase Pyroxenite	7.38	13.2	7.7	0.10	1.21	0.51	16.3	133	370	32.8	213	68.7	79.0	18.1	1.12	547	24.5
98-97-216-1	Western Section	Leucogabbro	6.75	19.8	6.71	0.10	0.45	0.01	29.8	154	790	33.0	80.2	29.3	39.3	15.5	2.38	152	10.2
98-97-216-5	Western Section	Gabbro	8.12	14.6	10.8	0.16	0.89	0.13	42.1	260	94	40.5	54.2	113	57.3	15.5	13.0	149	19.5
98-97-216-7	Western Section	Gabbro	6.47	13.3	14.5	0.20	1.24	0.14	39.4	349	8	45.3	34.4	108	66.9	16.9	0.91	108	21.1
98-97-216-9	Western Section	Gabbro	8.78	14.6	13.5	0.20	1.23	0.14	44.1	302	19	42.1	40.6	27.4	61.5	16.0	6.12	110	21.0
98-97-216-12	Western Section	Leucogabbro	5.79	13.5	15.4	0.19	1.55	0.18	37.8	367	15	48.8	39.1	13.0	88.0	18.4	1.56	141	23.9
98-97-221-1B	Western Section	Altered Basalt	5.27	15.7	7.25	0.19	0.78	0.12	53.1	296	113	16.7	62.4	69.2	69.5	16.7	61.0	126	16.1
98-97-225-1A	Western Section	Intermediate Tuff	1.61	15.2	3.72	0.06	0.36	0.21	5.8	48	14	11.9	17.2	43.5	37.1	16.9	39.2	187	8.07
98-97-228-1	Western Section	Pegmatitic Gabbro Dyke	4.31	12.8	17.8	0.30	2.05	0.23	41.6	364	14	51.0	49.1	136	142.1	20.1	5.17	126	36.0
98-97-234-2	Western Section	Felsic Crystal Tuff	1.79	15.5	1.68	0.04	0.64	0.23	20.6	128	54	6.6	62.1	9.8	26.9	17.5	29.6	173	21.5
98-97-236-1	Western Section	Dacite Pillow Lava	2.50	15.8	5.20	0.10	0.79	0.34	15.8	141	60	18.6	45.3	37.4	62.1	17.7	27.5	197	22.7
98-97-236-2	Western Section	Plag.-Phyric Andesite	3.24	15.6	6.61	0.15	0.76	0.33	19.5	139	60	23.2	81.5	9.0	69.7	17.1	10.5	213	24.2
98-97-237-1	Western Section	Andesite Pillow Lava	5.84	16.2	9.52	0.15	0.97	0.35	18.7	137	185	29.6	137	112	66.0	15.4	9.32	256	23.3
98-97-243-1	Western Section	Dunite	OR	1.33	8.03	0.09	0.06	0.05	8.3	44.0	1400	97.7		18.5	33.7	2.26	0.65	2.65	1.34
98-97-243-2	Western Section	Peridotite	44.7	2.72	9.82	0.11	0.17	0.15	11.7	70.4	1200	111	2480	47.8	39.9	2.98	0.60	6.90	2.15
98-97-245-2	Western Section	Megacrystic Gabbro	9.01	16.0	14.4	0.22	1.03	0.18	36.4	25.0	301	55.1	148	110	63.1	15.6	10.1	189	14.4
98-97-246-1	Western Section	Basalt	11.9	11.8	13.1	0.25	0.67	0.19	37.3	255	829	69.4	257	68.6	71.4	13.8	11.9	48.6	15.2
98-97-249-1	Western Section	Olivine Norite Dyke	24.2	10.5	12.6	0.21	0.31	0.05	29.8	132	2500	82.0	600	61.9	56.3	7.76	4.69	59.8	7.21
98-97-251-1	Western Section	Intermediate Tuff	3.96	21.1	5.54	0.07	0.65	0.14	11.7	95.6	53	14.7	41.4	6.1	43.3	18.4	62.6	71.2	11.2
98-97-251-2	Western Section	Pillow Basalt	11.6	9.64	15.8	0.24	1.01	0.09	31.2	213	1200	69.5	419	15.3	94.1	12.9	3.68	118	24.3
98-97-319-1	Eastern Section	Basaltic Komatiite	15.3	6.95	16.2	0.30	0.88	0.09	30.8	202	1800	84.9	504	26.2	120	11.4	1.28	51.8	14.1
98-97-320-1	Eastern Section	Komatiite	17.4	6.27	15.2	0.26	0.77	0.09	29.0	188	1900	87.7	709	34.2	94.5	9.88	0.75	35.5	11.9
98-97-321-1	Eastern Section	Peridotite	29.2	3.59	13.7	0.13	0.47	0.08	17.1	103	1300	104	1600	43.1	67.0	5.60	2.71	11.8	7.06
98-97-322-1	Eastern Section	Komatiite	18.0	6.37	15.3	0.26	0.79	0.09	28.0	185	1700	95.3	797	274	98.6	10.1	4.19	38.6	12.0
98-97-323-4	Eastern Section	Megacrystic Gabbro	7.68	12.5	14.1	0.20	1.03	0.09	32.5	253	570	54.0	123	219	79.2	15.4	10.3	111	19.6
98-97-323-6	Eastern Section	Basaltic Komatiite	14.7	10.0	13.9	0.19	0.76	0.07	28.8	202	1400	73.4	539	16.7	94.6	12.9	39.7	50.3	14.0
98-97-323-8	Eastern Section	Melagabbro	10.0	13.4	16.6	0.20	1.05	0.09	38.8	273	401	59.3	104	232	99.4	16.0	2.11	74.0	19.7
98-97-323-9A	Eastern Section	Peridotite or Websterite	32.0	3.83	11.0	0.15	0.33	0.05	17.8	112	1700	101	OR	25.3	40.1	5.38	0.40	3.38	5.91
98-97-323-10	Eastern Section	Spinifex Komatiite	18.0	7.54	14.3	0.20	0.62	0.07	33.7	214	1900	90.2	647	92.1	66.4	10.9	2.64	17.6	11.6
98-97-323-11	Eastern Section	Basaltic Komatiite	19.1	7.10	14.2	0.18	0.59	0.07	30.8	207	2300	94.5	875	88.5	72.5	10.1	0.58	6.26	10.7
98-97-323-12	Eastern Section	Plag.-Phyric Diabase	10.6	12.4	13.2	0.20	0.66	0.09	33.6	229	590	56.6	177	28.6	72.4	14.4	7.00	105	16.0
98-97-323-13	Eastern Section	Pillow Basalt - Core	9.78	12.3	12.5	0.21	0.74	0.09	35.7	251	590	58.3	170	93.8	69.7	14.9	2.41	83.5	17.9
98-97-329-1	Eastern Section	Olivine Pyroxenite	26.6	4.94	12.7	0.15	0.66	0.07	21.3	144	>3000	92.7	1360	24.5	80.4	7.15	22.1	22.8	9.94
98-97-329-4	Eastern Section	Basaltic Komatiite	23.8	5.20	14.3	0.20	0.64	0.08	22.6	151	1600	106	1290	69.8	74.1	8.08	4.37	32.1	10.6
98-97-329-6	Eastern Section	Basaltic Pyroxenite	16.0	6.90	15.7	0.25	0.86	0.09	29.0	194	1900	91.3	638	69.6	96.9	11.1	4.55	72.2	16.0

Notes: Major element data were determined using both X-ray fluorescence spectrometry (XRF) and inductively-coupled plasma mass spectrometry (ICP-MS) at the Geoscience Laboratories, Sudbury, Ontario. Zirconium was determined by XRF. Cr was determined using XRF for samples listed in Table GS-4-1, and ICP-MS for the remaining samples. All other elements were determined by ICP-MS. OR = analyte out of range.

Table GS-4-2 (continued)

Sample #	Location	Rock Type	Zr	Nb	Mo	Ag	Cd	Sn	Sb	Li	Be	Cs	Ba	La	Ce	Pr	Nd	Sm	Eu
98-97-202-1	Western Section	Peridotite	13	0.58	0.47	0.00	0.03	0.20	0.31	1.55	0.47	0.24	9.79	0.910	2.26	0.33	1.55	0.53	0.13
98-97-202-3	Western Section	Peridotite	12	0.57	0.82	0.00	0.03	0.44	0.45	1.23	0.45	0.19	5.58	0.965	2.56	0.38	1.79	0.58	0.12
98-97-202-7	Western Section	Plagioclase Pyroxenite	18	0.89	0.35	0.00	0.06	0.32	0.15	11.4	0.52	0.10	9.05	1.52	4.80	0.84	4.15	1.31	0.32
98-97-202-8	Western Section	Melagabbro	22	0.80	0.21	0.00	0.05	0.19	0.21	58.7	0.68	1.29	744	1.57	3.57	0.51	2.33	0.76	0.53
98-97-202-9	Western Section	Melagabbro	25	0.86	0.25	0.00	0.05	0.27	0.23	38.0	0.62	1.42	1380	1.73	3.96	0.58	2.60	0.91	0.78
98-97-202-10	Western Section	Gabbro	32	1.16	0.52	0.01	0.07	0.83	0.52	21.2	0.57	0.28	246	2.13	4.98	0.71	3.35	1.11	0.47
98-97-203-1	Western Section	Aphyric Basalt	OR	2.46	0.89	0.01	0.05	0.49	0.20	39.6	0.80	0.24	112	4.54	10.9	1.51	7.02	2.01	0.67
98-97-208-3	Western Section	Intermediate Volcanic	62	2.29	1.48	0.01	0.04	0.49	1.12	29.5	0.53	0.84	134	4.29	9.69	1.33	6.13	1.89	0.58
98-97-212-2	Western Section	Gabbro	74	3.28	0.95	0.01	0.18	2.53	2.53	10.7	0.85	0.05	22.5	4.79	12.1	1.90	9.50	2.80	0.94
98-97-214-1	Western Section	Plagioclase Pyroxenite	180	6.74	1.06	0.03	0.07	1.67	0.38	17.0	3.16	0.17	52.8	51.0	114	14.44	59.74	12.31	2.61
98-97-216-1	Western Section	Leucogabbro	28	1.14	2.07	0.01	0.04	0.25	0.80	20.5	0.63	0.14	25.4	1.65	4.19	0.66	3.26	1.05	0.44
98-97-216-5	Western Section	Gabbro	56	2.40	1.13	0.01	0.10	1.95	0.96	18.4	0.64	0.61	144	3.76	9.56	1.42	6.87	2.09	0.77
98-97-216-7	Western Section	Gabbro	74	3.08	0.72	0.13	0.07	0.47	0.31	19.3	0.78	0.18	27.5	4.14	10.9	1.62	7.64	2.36	0.76
98-97-216-9	Western Section	Gabbro	61	2.71	0.50	0.10	0.04	0.51	0.38	30.4	0.54	0.38	96.4	2.82	8.57	1.40	7.08	2.15	0.76
98-97-216-12	Western Section	Leucogabbro	97	4.38	1.43	0.16	0.06	0.71	0.28	22.4	0.69	0.23	32.0	7.26	16.3	2.29	10.61	3.04	1.06
98-97-221-1B	Western Section	Altered Basalt	66	2.16	1.22	0.01	0.14	2.01	0.73	36.8	0.91	3.32	238	5.09	10.6	1.37	6.06	1.62	0.66
98-97-225-1A	Western Section	Intermediate Tuff	150	5.10	1.39	0.22	0.07	0.90	0.87	21.2	1.18	1.61	374	17.2	36.0	4.09	13.65	2.22	0.88
98-97-228-1	Western Section	Pegmatitic Gabbro Dyke	120	6.21	1.24	0.19	0.15	1.57	1.78	9.59	1.04	0.40	51.1	6.83	18.1	2.83	14.37	4.44	1.46
98-97-234-2	Western Section	Felsic Crystal Tuff	170	6.20	3.05	0.24	0.06	1.80	0.13	24.1	1.17	0.84	193	35.8	78.6	8.50	29.09	4.50	1.26
98-97-236-1	Western Section	Dacite Pillow Lava	190	8.51	0.89	0.27	0.05	1.11	0.15	19.8	1.30	1.43	227	14.5	33.4	4.25	16.86	3.64	1.03
98-97-236-2	Western Section	Plag.-Phyric Andesite	180	8.03	1.41	0.26	0.07	1.18	0.29	18.8	0.87	0.36	130	16.7	37.6	4.80	18.60	3.81	1.21
98-97-237-1	Western Section	Andesite Pillow Lava	170	8.23	3.85	0.27	0.09	0.95	0.10	21.1	0.99	0.18	114	14.6	33.9	4.37	17.09	3.60	0.92
98-97-243-1	Western Section	Dunite	OR	0.25	0.27	0.00	0.02	0.41	0.41	1.82	0.46	0.10	3.93	0.498	1.09	0.14	0.62	0.15	0.06
98-97-243-2	Western Section	Peridotite	13	0.35	0.74	0.03	0.06	1.89	1.25	1.91	0.31	0.03	8.71	0.672	1.52	0.22	0.95	0.24	0.06
98-97-245-2	Western Section	Megacrystic Gabbro	54	1.45	0.78	0.08	0.06	0.49	0.13	20.5	0.57	0.10	48.6	2.27	5.58	0.82	4.27	1.50	0.59
98-97-246-1	Western Section	Basalt	49	1.37	0.51	0.07	0.08	0.43	0.09	20.3	0.62	0.38	48.1	2.06	5.06	0.78	3.82	1.33	0.50
98-97-249-1	Western Section	Olivine Norite Dyke	32	0.93	0.57	0.01	0.06	0.40	0.09	7.37	0.63	0.23	65.4	3.11	6.55	0.81	3.42	0.84	0.29
98-97-251-1	Western Section	Intermediate Tuff	130	4.59	0.71	0.02	0.04	0.54	0.91	44.3	1.20	2.79	70.0	23.0	46.57	5.15	18.94	3.27	1.09
98-97-251-2	Western Section	Pillow Basalt	94	2.81	1.00	0.01	0.08	1.40	3.23	15.4	0.72	0.81	39.6	4.79	12.37	1.86	9.64	3.21	1.02
98-97-319-1	Eastern Section	Basaltic Komatiite	50	1.96	1.10	0.01	0.19	3.84	0.22	20.9	1.79	0.14	12.6	2.18	5.99	1.01	5.53	1.97	0.86
98-97-320-1	Eastern Section	Komatiite	47	1.36	0.47	0.01	0.09	0.90	0.07	13.2	0.68	0.12	7.48	1.72	4.73	0.80	4.24	1.55	0.55
98-97-321-1	Eastern Section	Peridotite	27	0.78	2.22	0.05	0.11	3.23	0.44	2.80	0.70	0.49	7.01	1.14	3.29	0.53	2.99	0.99	0.28
98-97-322-1	Eastern Section	Komatiite	47	1.35	1.86	0.01	0.22	6.66	0.70	11.0	0.81	0.57	14.8	1.71	4.77	0.82	4.70	1.63	0.43
98-97-323-4	Eastern Section	Megacrystic Gabbro	73	1.98	0.55	0.02	0.12	1.93	0.20	17.0	0.68	0.68	86.6	3.47	8.67	1.31	6.83	2.40	0.83
98-97-323-6	Eastern Section	Basaltic Komatiite	52	1.31	0.51	0.01	0.07	0.98	0.40	33.6	0.56	3.28	121	2.43	5.99	0.92	4.67	1.62	0.56
98-97-323-8	Eastern Section	Melagabbro	65	1.81	0.92	0.01	0.13	1.24	0.15	23.0	0.53	0.22	56.2	3.18	8.08	1.23	6.50	2.28	0.83
98-97-323-9A	Eastern Section	Peridotite or Websterite	20	0.40	0.26	0.00	0.03	0.40	0.08	2.54	0.34	0.26	4.53	0.645	1.70	0.27	1.52	0.55	0.24
98-97-323-10	Eastern Section	Spinifex Komatiite	36	0.82	0.74	0.01	0.07	1.06	0.35	7.90	0.55	0.44	14.8	1.08	2.98	0.51	2.73	1.11	0.34
98-97-323-11 0.36	Eastern Section	Basaltic Komatiite	34	0.75		0.27	0.01	0.05	0.44	0.07	5.17	0.51	0.13	6.68	1.08	2.91	0.47	2.58	1.02
98-97-323-12	Eastern Section	Plag.-Phyric Diabase	55	1.61	1.09	0.01	0.04	0.70	0.20	19.4	0.61	0.49	46.1	2.68	6.61	0.97	4.70	1.57	0.50
98-97-323-13	Eastern Section	Pillow Basalt - Core	54	1.55	0.99	0.01	0.06	1.45	0.39	18.8	0.54	0.24	36.6	2.26	5.77	0.89	4.51	1.63	0.55
98-97-329-1	Eastern Section	Olivine Pyroxenite	37	1.12	1.02	0.01	0.09	1.76	0.55	15.5	0.86	5.21	14.0	1.56	4.37	0.73	3.91	1.37	0.48
98-97-329-4	Eastern Section	Basaltic Komatiite	42	1.11	3.05	0.01	0.10	2.21	0.14	3.57	0.62	0.62	4.65	1.62	4.68	0.78	4.14	1.43	0.42
98-97-329-6	Eastern Section	Basaltic Pyroxenite	57	1.80	8.71	0.01	0.14	2.17	0.18	11.5	0.84	0.72	7.38	2.38	6.71	1.10	6.24	2.01	0.80

Table GS-4-2 (continued)

Sample #	Location	Rock Type	Tb	Gd	Dy	Ho	Er	Tm	Yb	Lu	Hf	Ta	W	Tl	Pb	Bi	Th	U
98-97-202-1	Western Section	Peridotite	0.11	0.58	0.85	0.19	0.54	0.08	0.51	0.08	0.42	0.07	0.34	0.01	0.58	0.03	0.22	0.06
98-97-202-3	Western Section	Peridotite	0.13	0.63	0.95	0.21	0.64	0.09	0.64	0.09	0.41	0.05	0.36	0.01	1.37	0.04	0.22	0.07
98-97-202-7	Western Section	Plagioclase Pyroxenite	0.26	1.43	1.95	0.41	1.16	0.17	1.00	0.15	0.59	0.07	0.14	0.01	0.47	0.02	0.30	0.07
98-97-202-8	Western Section	Melagabbro	0.17	0.89	1.28	0.30	0.84	0.13	0.87	0.13	0.60	0.07	0.24	0.32	0.93	0.03	0.28	0.08
98-97-202-9	Western Section	Melagabbro	0.20	1.04	1.55	0.35	1.05	0.15	1.01	0.15	0.66	0.07	0.30	0.40	0.92	0.05	0.34	0.08
98-97-202-10	Western Section	Gabbro	0.25	1.32	1.84	0.41	1.21	0.19	1.19	0.18	0.86	0.13	0.32	0.07	2.55	0.10	0.44	0.10
98-97-203-1	Western Section	Aphyric Basalt	0.43	2.32	3.32	0.72	2.03	0.31	1.96	0.30	1.79	0.19	0.43	0.06	2.47	0.04	0.95	0.25
98-97-208-3	Western Section	Intermediate Volcanic	0.39	2.15	3.21	0.70	2.04	0.31	1.91	0.30	1.60	0.17	1.14	0.09	2.78	0.07	0.87	0.26
98-97-212-2	Western Section	Gabbro	0.53	3.05	3.62	0.79	2.21	0.33	2.07	0.33	1.84	0.25	0.31	0.01	9.14	0.48	0.38	0.11
98-97-214-1	Western Section	Plagioclase Pyroxenite	1.16	9.43	5.22	0.85	1.96	0.25	1.59	0.24	4.44	0.42	0.83	0.02	7.93	0.15	8.15	1.90
98-97-216-1	Western Section	Leucogabbro	0.21	1.16	1.70	0.36	1.01	0.15	0.95	0.14	0.72	0.08	0.72	0.03	1.92	0.03	0.17	0.05
98-97-216-5	Western Section	Gabbro	0.42	2.31	3.31	0.70	2.06	0.31	1.83	0.30	1.57	0.16	0.31	0.14	3.53	0.03	0.35	0.10
98-97-216-7	Western Section	Gabbro	0.48	2.62	3.56	0.78	2.22	0.35	2.18	0.33	1.93	0.21	0.21	0.01	1.36	0.04	0.41	0.12
98-97-216-9	Western Section	Gabbro	0.46	2.54	3.60	0.76	2.22	0.35	2.12	0.33	1.72	0.20	0.24	0.05	1.32	0.04	0.40	0.11
98-97-216-12	Western Section	Leucogabbro	0.59	3.25	4.42	0.91	2.55	0.41	2.57	0.40	2.73	0.32	0.25	0.03	1.50	0.02	0.61	0.17
98-97-221-1B	Western Section	Altered Basalt	0.34	1.91	2.55	0.57	1.59	0.25	1.53	0.23	1.67	0.18	0.48	2.01	3.04	0.06	1.37	0.41
98-97-225-1A	Western Section	Intermediate Tuff	0.28	1.90	1.38	0.27	0.72	0.12	0.78	0.11	3.34	0.51	2.96	0.46	3.35	0.07	3.20	0.87
98-97-228-1	Western Section	Pegmatitic Gabbro Dyke	0.89	5.13	6.56	1.40	3.83	0.57	3.65	0.55	3.35	0.46	0.38	0.04	1.56	0.03	0.72	0.19
98-97-234-2	Western Section	Felsic Crystal Tuff	0.61	4.28	3.55	0.77	2.23	0.35	2.30	0.35	3.93	0.61	0.70	0.12	2.45	0.04	4.00	3.25
98-97-236-1	Western Section	Dacite Pillow Lava	0.56	3.61	3.83	0.79	2.33	0.36	2.36	0.35	4.01	0.64	0.58	0.12	3.54	0.05	1.57	0.37
98-97-236-2	Western Section	Plag.-Phyric Andesite	0.62	3.88	3.99	0.83	2.38	0.38	2.46	0.38	3.78	0.58	0.66	0.05	4.18	0.06	1.44	0.37
98-97-237-1	Western Section	Andesite Pillow Lava	0.57	3.62	3.92	0.82	2.36	0.36	2.34	0.37	3.60	0.58	1.27	0.03	2.98	0.05	1.37	0.34
98-97-243-1	Western Section	Dunite	0.03	0.17	0.20	0.04	0.13	0.02	0.16	0.03	0.14	0.02	0.12	0.02	0.97	0.08	0.06	0.03
98-97-243-2	Western Section	Peridotite	0.05	0.28	0.35	0.08	0.23	0.04	0.27	0.04	0.22	0.04	0.53	0.01	3.41	0.02	0.08	0.02
98-97-245-2	Western Section	Megacrystic Gabbro	0.34	1.89	2.49	0.54	1.45	0.22	1.39	0.20	1.24	0.12	0.22	0.08	1.17	0.03	0.32	0.09
98-97-246-1	Western Section	Basalt	0.32	1.69	2.50	0.54	1.54	0.23	1.49	0.24	1.23	0.11	0.14	0.08	0.58	0.05	0.18	0.04
98-97-249-1	Western Section	Olivine Norite Dyke	0.18	0.93	1.18	0.27	0.76	0.13	0.82	0.12	0.71	0.09	0.27	0.03	1.34	0.03	0.59	0.15
98-97-251-1	Western Section	Intermediate Tuff	0.37	2.55	2.01	0.41	1.10	0.18	1.10	0.16	3.08	0.43	2.12	0.69	2.12	0.02	3.81	0.93
98-97-251-2	Western Section	Pillow Basalt	0.62	3.61	4.41	0.95	2.61	0.40	2.38	0.37	2.26	0.21	0.58	0.11	2.06	0.03	0.44	0.11
98-97-319-1	Eastern Section	Basaltic Komatiite	0.37	2.15	2.57	0.53	1.40	0.21	1.27	0.20	1.24	0.11	0.45	0.01	1.68	0.47	0.22	0.11
98-97-320-1	Eastern Section	Komatiite	0.30	1.73	2.07	0.43	1.18	0.18	1.04	0.16	1.09	0.09	0.30	0.01	0.68	0.39	0.18	0.07
98-97-321-1	Eastern Section	Peridotite	0.19	1.13	1.33	0.27	0.70	0.11	0.65	0.10	0.64	0.06	0.42	0.05	4.41	0.74	0.11	0.04
98-97-322-1	Eastern Section	Komatiite	0.32	1.86	2.20	0.45	1.21	0.18	1.07	0.16	1.14	0.11	0.34	0.06	8.84	0.59	0.19	0.06
98-97-323-4	Eastern Section	Megacrystic Gabbro	0.50	2.87	3.58	0.76	2.09	0.30	1.91	0.29	1.79	0.16	0.54	0.10	2.92	0.38	0.47	0.13
98-97-323-6	Eastern Section	Basaltic Komatiite	0.36	1.97	2.52	0.53	1.45	0.22	1.26	0.20	1.36	0.11	0.42	0.39	1.23	0.17	0.31	0.08
98-97-323-8	Eastern Section	Melagabbro	0.48	2.75	3.49	0.76	2.05	0.31	1.81	0.28	1.64	0.15	0.24	0.02	1.55	0.16	0.38	0.10
98-97-323-9A	Eastern Section	Peridotite or Websterite	0.14	0.76	1.04	0.23	0.58	0.09	0.54	0.08	0.46	0.04	0.44	0.01	0.38	0.07	0.06	0.02
98-97-323-10	Eastern Section	Spinifex Komatiite	0.28	1.47	2.06	0.44	1.23	0.18	1.07	0.17	0.90	0.07	0.28	0.04	1.29	0.15	0.11	0.04
98-97-323-11	Eastern Section	Basaltic Komatiite	0.25	1.33	1.84	0.39	1.05	0.16	0.96	0.16	0.81	0.06	0.14	0.01	0.35	0.18	0.10	0.03
98-97-323-12	Eastern Section	Plag.-Phyric Diabase	0.34	1.87	2.60	0.57	1.59	0.25	1.51	0.23	1.30	0.11	0.35	0.08	1.13	0.11	0.38	0.10
98-97-323-13	Eastern Section	Pillow Basalt - Core	0.37	2.00	2.91	0.63	1.76	0.28	1.64	0.26	1.31	0.12	0.37	0.04	1.76	0.11	0.32	0.09
98-97-329-1	Eastern Section	Olivine Pyroxenite	0.26	1.51	1.81	0.37	0.97	0.14	0.87	0.13	0.91	0.25	0.77	0.11	2.95	0.09	0.15	0.05
98-97-329-4	Eastern Section	Basaltic Komatiite	0.27	1.59	1.91	0.39	1.08	0.16	0.94	0.15	0.97	0.12	0.78	0.05	2.42	0.46	0.17	0.05
98-97-329-6	Eastern Section	Basaltic Pyroxenite	0.40	2.31	2.79	0.59	1.54	0.24	1.40	0.22	1.45	0.16	0.34	0.05	2.86	0.21	0.25	0.09

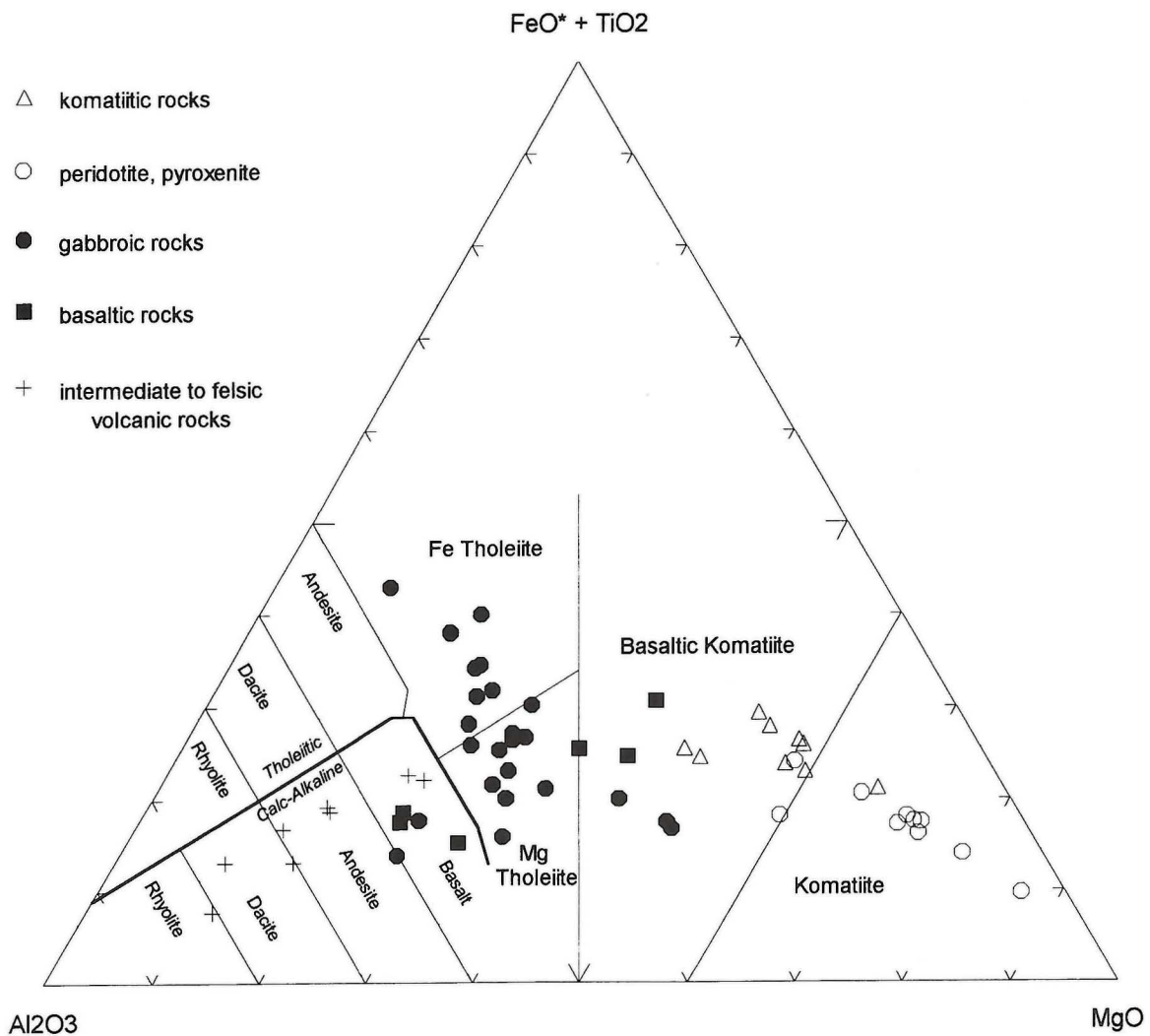


Figure GS-4-15: Jensen cation plot (Jensen, 1976) for volcanic rocks from the Carrot River greenstone belt.

shoreline of Wakehao Lake and through a series of small islands toward the middle of the lake (Fig. GS-4-2). This zone is <3 to 10 metres wide and is characterized by variable amounts (<10 to >50%) of fine- to medium-grained pyrrhotite with local, subordinate pyrite, magnetite, chalcopyrite and sphalerite in a fine-grained mafic to intermediate silicate matrix. Several other sulphide bodies of similar appearance occur in the Wakehao Lake area. Field observations suggest that at least some of these sulphide bodies formed prior to deformation along the Carrot River shear zone. The local development of intense, irregular but generally north-trending vein networks within relatively undeformed basaltic, gabbroic and ultramafic units within the lower parts of the stratigraphy may signify an early period of sea-floor type alteration, now reflected by quartz, sulphide, chlorite, epidote, feldspar, amphibole and carbonate veins. The large proportion of gabbroic to ultramafic intrusive rocks in the CRGB may have provided heat sources capable of driving sub-seafloor hydrothermal convection cells.

The tectonic environment for the CRGB appears to be similar to platform-type, "iron" assemblages described by Thurston (1994), which are characterized by a wide variety of volcanic rocks (komatiite, basalt, andesite, dacite, rhyolite) and abundant oxide or sulphide facies iron formation, and which occur adjacent to large granitic batholiths. Within the Abitibi Subprovince, the "iron" assemblages tend to be older than adjacent greenstone assemblages, and host several Ni sulphide deposits in

association with 2.7 Ga komatiites. Fyon *et al.* (1992) imply that the abundance of VMS deposits in the Abitibi greenstone belt is in part related to the tectonic setting reflected in abundant komatiitic volcanism. In this scenario, komatiites indicate areas of anomalously high heat flow. Where the komatiites are associated with derivative intermediate to felsic volcanics (icelandites and silica-rich rhyolites), the possibility existed for long-lived magma chambers capable of sustaining and focusing seafloor alteration systems and generating VMS deposits. Although none of the intermediate volcanic rocks examined from the CRGB appear to be directly related to the mafic-ultramafic magmatism, the mafic-ultramafic series does occur with thin layers of mineralized intermediate pyroclastic rocks. Also, the great abundance of plagioclase phryic units in the lower part of the stratigraphy suggests that the potential for generating felsic differentiates clearly existed. Detailed tectonic analysis, mineral deposits studies and precise age determinations are required before the potential for VMS deposits in the CRGB can be firmly established.

The potential for epigenetic gold deposits in the study area requires additional evaluation, focusing on the structural evolution along the major shear zones, and on the correlation between gold abundance, stratigraphic position, lithology and vein mineralogy. Assay results obtained to date indicate a weak association between Au and sulphide-bearing intermediate pyroclastic rocks (Table GS-4-4; Southard, 1977).

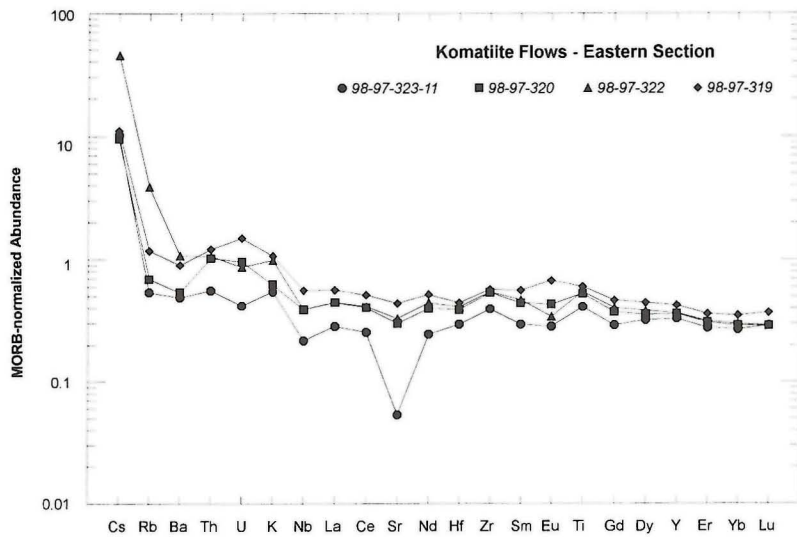


Figure GS-4-16: MORB-normalized spider diagram for komatiitic flows from the eastern part of the Carrot River greenstone belt. Normalizing values are those used in the NEWPET program.

Figure GS-4-17: MORB-normalized spider diagram for samples from the layered ultramafic-mafic intrusion exposed at station 206 (see Figure GS-4-2 for location).

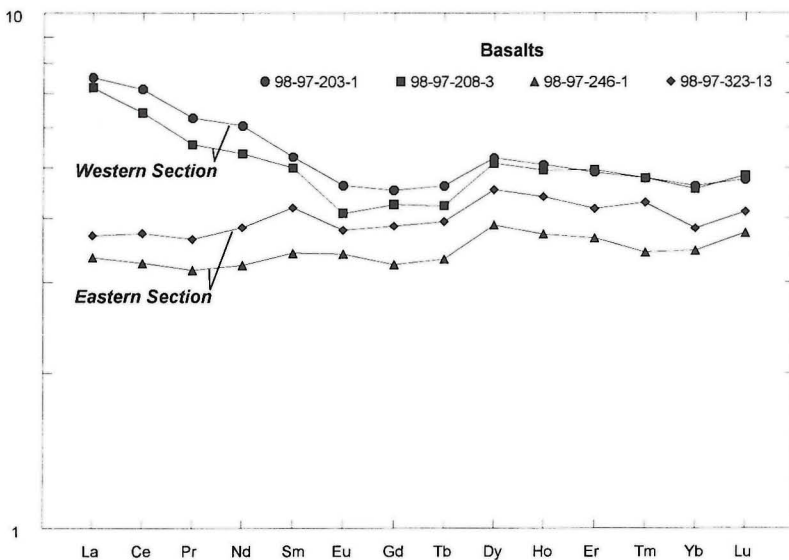
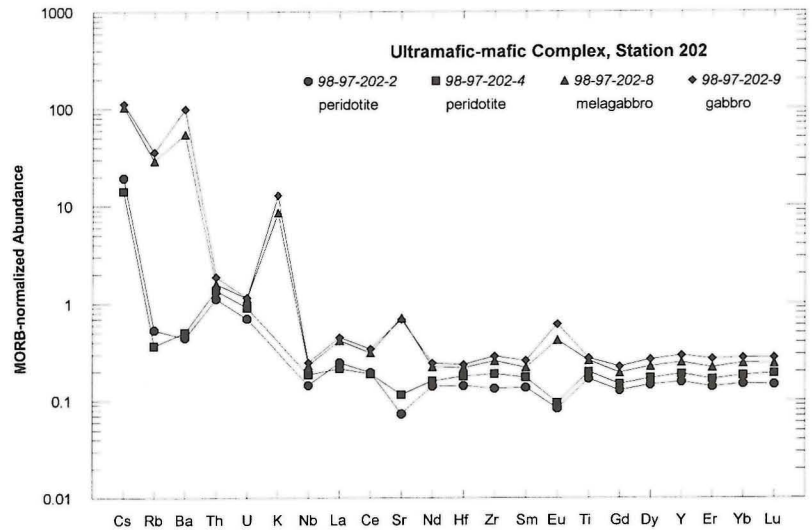


Figure GS-4-18: Primitive mantle-normalized rare-earth element abundances for basalts from the eastern and western sections. Normalizing values are those used in the NEWPET program

Figure GS-4-19: Primitive mantle-normalized rare-earth element abundances for intermediate volcanic rocks from the western section.

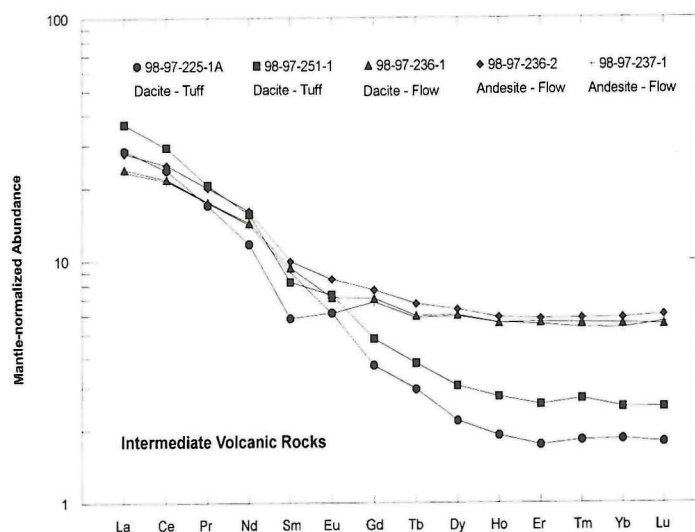


Table GS-4-3

Assays for selected sulphide occurrences from the eastern part of the Carrot River greenstone belt

Sample #	Rock Type	Au	Ag	Cu	Ni	Zn	Pb	Cr	Mo	Mn
98-97-207-4	Po + Cpy in gabbro	42	1.4	1600	48	94	<5	110	<5	1200
98-97-208-2	30 cm wide Po zone in mafic sediment	20	<0.5	460	210	750	10	64	<5	370
98-97-209-1	3 m wide Po-rich zone in basalt	17	<0.5	180	82	120	<5	53	<5	910
98-97-211-1	3 m wide Po-rich zone in basalt	<6	<0.5	130	36	52	<5	54	<5	550
98-97-221-1A	10 m wide Po-rich zone in basalt	<6	<0.5	140	36	50	<5	55	<5	430
98-97-225-1B	Minor Po + Cpy veins in dacitic tuff	420	<0.5	190	17	43	6.0	11	<5	270
98-97-234-1	Disseminated Po in felsic tuff	<6	<0.5	140	86	77	5.0	11	<5	340
98-98-238-1	Disseminated Po in siltstone	9	0.8	230	250	860	<5	200	<5	850
98-97-240-1	Disseminated Po in siltstone	<6	<0.5	60	250	860	8	19	<5	220
97-97-329-3	Minor, disseminated Po in komatiite	<6	nr	nr	nr	nr	nr	nr	nr	nr

Notes: Assays performed at Envirotec Laboratories, Winnipeg, using inductively-coupled plasma - optical emission spectrometry (base metals and Ag) and Pb fire assay - atomic absorption spectrometry (Au). Au reported in ppb. All other elements are reported in ppm.

Table GS-4-4

Precious metal, CO₂, S and Se abundances in gabbroic rocks from the eastern part of the Carrot River greenstone belt

Sample #	Au	Pt	Pd	CO ₂	S	Se	S/Se
98-97-213-1	29	<10	<5	0.19	1.10	430	25,580
98-97-216-1	<3	<10	<5	0.38	0.05	70	7,140
98-97-216-2	<3	<10	<5	0.55	0.14	140	10,000
98-97-216-4	3.5	<10	<5	0.40	0.12	85	14,120
98-97-216-5	83	<10	<5	0.20	0.17	220	7,730
98-97-216-6	<3	<10	<5	0.30	N.D.	N.D.	-
98-97-216-7	<3	<10	7.2	0.20	0.11	360	3,060
98-97-216-8A	5.1	<10	7.1	0.42	0.59	600	9,830
98-97-216-8B	6.9	<10	<5	1.00	0.54	670	8,050
98-97-216-8C	<3	<10	<5	0.62	1.20	1300	9,230
98-97-216-9	<3	<10	<5	0.10	N.D.	20	-
98-97-216-11A	<3	<10	<5	0.14	1.10	1500	7,330
98-97-216-11B	<3	<10	<5	0.39	0.61	1100	5,550
98-97-216-11C	<3	<10	<5	0.17	0.30	440	6,820
98-97-216-11D	76	<10	<5	0.12	0.97	1400	6,930
98-97-216-12	<3	<10	6.8	0.13	0.11	360	3,060
98-97-216-13	<3	<10	<5	0.08	0.28	690	4,060
98-97-219-3	64	<10	5.7	0.12	0.87	490	17,760
98-97-323-8	<3	<10	<5	0.13	0.38	1200	3,170

The potential for Ni mineralization in the ultramafic rocks of the CRGB is also poorly constrained. The Ni occurrences documented to date are largely from drill core intersection of disseminated pyrrhotite and chalcopyrite in the ultramafic intrusion developed along the south shoreline of Peridotite Island. Canex Placer completed a ground geophysical and drilling program in the early 1970s, but no higher grade Ni sulphide mineralization was detected. Peridotite layers with disseminated sulphide mineralization commonly contain between 0.3 and 0.5% Ni, with local enrichment to 0.7% Ni (Southard, 1977). Davidson (1974) attributes all of the Ni sulphide mineralization to sulphurization during serpentinization, citing the random distribution of the sulphide enrichment and the correlation of Ni sulphide abundance with the intensity of serpentinization. The geochemical data obtained during the current study indicate that the majority of mafic and ultramafic rocks in the eastern CRGB were not substantially modified by assimilation of crustal materials during their emplacement. However, some of the peridotite samples appear to be depleted in Ni relative to the komatiites (Fig. GS-4-20). This feature suggests that some of the peridotites crystallized from komatiitic liquids that had lost a portion of the Ni that was inherited from the mantle source region, possibly by prior separation of a magmatic sulphide component (Fig. GS-4-20) or during subsequent metasomatism.

On Eagle Island, S-rich country rocks occurring below a poorly exposed ultramafic intrusion represent a potential source for sulphur (Figs. GS-4-2, 3). In addition, the globular-textured gabbroic rocks that occur in association with the komatiites in the eastern part of the study area may provide evidence of crustal contamination and warrant further study.

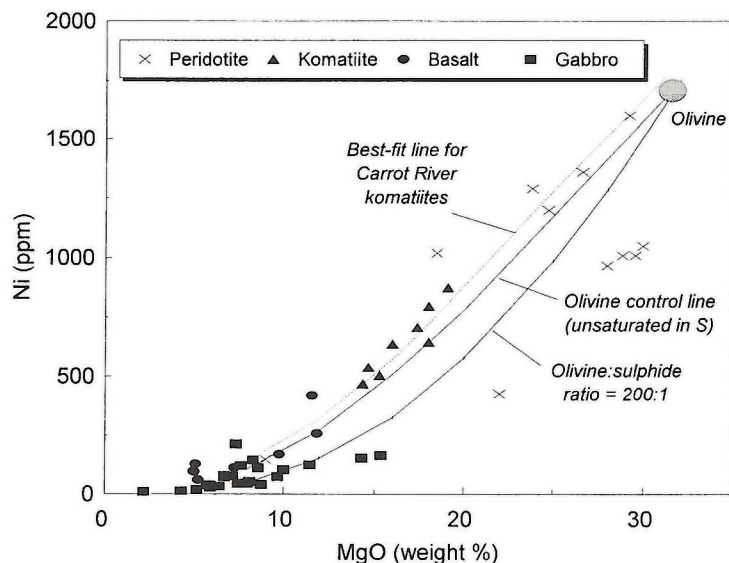


Figure GS-4-20: MgO-Ni plot for ultramafic and mafic rocks from the eastern CRGB. Theoretical curve for olivine-controlled fractional crystallization and sulphur-saturated, olivine + sulphide fractionation are derived from Naldrett (1989, Fig. 7.4). Best-fit line assumes olivine control for the Carrot River komatiite samples.

A suite of samples collected from the Eagle Island layered gabbro body were analyzed for Au, Pt, Pd, S, Se and CO₂ in order to evaluate the potential for platinum-group element + magmatic sulphide mineralization. Sulphides are concentrated into the upper parts of the layered gabbro, where losenge-shaped, <20 cm wide x 1-5 m long disseminations of pyrrhotite and minor chalcocopyrite are developed in vari-textured granophyre-bearing gabbro, coarse-grained leucogabbro and fine-grained gabbro. The layered gabbro body appears to be coeval and comagmatic with adjacent peridotite bodies. Mixing between different lithologies occurred locally generating hybrid rock types enriched in sulphides. Table GS-4-4 lists the assay results for samples from the layered gabbro body (station 216, Fig. GS-4-2) and additional sulphide-bearing gabbro samples. Four samples contained anomalously high gold, with values ranging from 29 to 83 ppb (Table GS-4-4). However, none of the samples contained anomalously high Pt or Pd, with most of the values being below the limit of detection for the method used (<5 ppb for Pd; <10 ppb for Pt). Given a komatiitic parent liquid for the gabbroic rocks (based on REE data described above), the high Au and low Pt and Pd values are problematic. The S/Se ratios for most of the samples exceed those typical of the mantle (1000 to 5000), indicating a hydrothermal or sedimentary sulphide component may be present in the rocks. The low total PGE abundances could reflect prior extraction of the PGE during fractional crystallization of a sulphide phase.

ACKNOWLEDGMENT

J.M. Pacey is thanked for preparing many of the figures contained in this report.

REFERENCES

- Barry, G.S.
1959: Geology of the Oxford House-Knee Lake areas; Manitoba Department of Mines and Natural Resources, Mines Branch, Publication 58-3, 39p.
- Brooks, C., Ludden, J., Pigeon, Y. and Hubregtse, J.J.M.W.
1982: Volcanism of shoshonite to high-K andesite affinity in an Archean arc environment, Oxford Lake, Manitoba; Canadian Journal of Earth Sciences, v. 19, p. 55-67.
- Davidson, D.D.
1974: The Carrot River Ultramafic Complex. Unpublished M.Sc. thesis, Acadia University, 154 p.
- Fedikow, M.A.F. and Nielsen E.
1997: Operation Superior: Multimedia geochemical survey in the Edmund and Sharpe Lake greenstone belts, northern Superior Province, Manitoba (NTS 53 K); in Manitoba Energy and Mines, Minerals Division, Report of Activities 1997. Fyon, J.A., Breaks, F.W., Heather, K.B., Jackson, S.L., Muir, T.L., Stott, G.M. and Thurston, P.C.
1992: Metallogeny of metallic minerals in the Superior Province of Ontario; in Geology of Ontario, Ontario Geological Survey, Special Volume 4, Part 2.
- Gilbert, H.P.
1985: Geology of the Knee Lake-Gods Lake area; Manitoba Energy and Mines, Geological Report GR83-1B, 76 p.
- Hubregtse, J.J.M.W.
1985: Geology of the Oxford Lake-Carrot River area; Manitoba Energy and Mines, Geological Report GR83-1A, 73 p.
- Jensen, L.S.
1976: A new cation plot for classifying subalkalic volcanic rocks; Ontario Department of Mines, Miscellaneous Paper 66.
- Naldrett, A.J.
1989: Magmatic sulphide deposits, Clarendon Press, New York, 186 p.
- Southard, G.G.
1977: Exploration history compilation and review, including exploration data from canceled assessment files, for the Gods, Knee and Oxford Lakes areas, Manitoba; Manitoba Department of Mines, Resources and Environmental Management, Mineral Resources Division, Open File Report 77/5, 93 p.
- Syme E.C., Weber, W. and Lenton P.G.
1993: Manitoba geochronology database; Manitoba Energy and Mines, Geological Services, Open File OF 93-4. Syme, E.C., Corkery, M.T., Bailes, A.H. Lin, S., Cameron H.D.M., and Prouse, D.
1997: Geological investigations in the Knee Lake area, northwestern Superior Province (parts of NTS 53L 14, 15) in Manitoba Energy and Mines, Minerals Division, Report of Activities 1997.
- Thurston, P.C.
1994: Archean volcanic patterns; in Archean Crustal Evolution, Developments in Precambrian Geology 11, (K.C. Condie, ed.), Elsevier 1994.
- Wright, J.F.
1926: Oxford and Knee lakes area, Northern Manitoba; Geological Survey of Canada, Summary Report, 1925, pt. B.
- Wright, J.F.
1932: Geology and gold prospects of the areas about Island, Gods and Oxford lakes, Manitoba; Canadian Mining and Metallurgical Bulletin, v. 25, no. 244.

GS-5 GEOLOGICAL INVESTIGATIONS IN THE KNEE LAKE AREA, NORTHWESTERN SUPERIOR PROVINCE (PARTS OF NTS 53L/15 AND 53L/14)

by E.C. Syme, M.T. Corkery, A.H. Bailes, S. Lin, H.D.M. Cameron, and D. Prouse

Syme, E.C., Corkery, M.T., Bailes, A.H., Lin, S., Cameron, H.D.M. and Prouse, D. (1997): Geological investigations in the Knee Lake area, northwestern Superior Province (parts of NTS 53L/15 and 53L/14); in Manitoba Energy and Mines, Minerals Division, Report of Activities, 1997, p. 37-46.

SUMMARY

The largest greenstone belt in northwest Superior Province, the Oxford Lake - Knee Lake Belt, is key to our understanding of the volcanic, structural, tectonic and metallogenic evolution of the region. We began a renewed study of the belt in southern and central Knee Lake, which we mapped at a scale of 1:20 000. This first year of a multi-year project resulted in better definition of stratigraphy within metavolcanic rocks of the Hayes River Group; identification of facies within a rhyolite complex and flanking volcanoclastic sedimentary rocks; identification of stratiform alteration zones in Hayes River Group basalts; lithologic and structural reinterpretation of the Oxford Lake Group; and the definition of regional faults and shear zones which bound stratigraphic panels. New lithologic, geochemical, structural and geochronologic data collected during this study will be critical for interpreting the setting of known mineral deposits and to better assess the mineral development potential of the region. This work is one component of the newly established Western Superior NATMAP Project, a collaborative geoscience endeavor involving the Ontario Geological Survey, Geological Survey of Canada and MGSLB.

INTRODUCTION

One of the primary objectives of Manitoba's Northern Superior projects is to better understand the volcanic, structural and tectonic evolution of greenstone belts in the Manitoba portion of Sachigo subprovince/Gods Lake domain. Central to this objective is an understanding of the largest contiguous greenstone belt in the Sachigo,

the Oxford Lake - Knee Lake Belt (Fig. GS-5-1). Multidisciplinary stratigraphic, geochemical, structural and geochronological studies of this belt are being conducted as part of the Western Superior NATMAP Project. These studies are anticipated to result in the types of advances made during the Shield Margin NATMAP Project in the Paleoproterozoic Flin Flon greenstone belt (e.g., Lucas *et al.*, 1996).

To begin a renewed study of the Oxford Lake - Knee Lake Belt we mapped the extensive shoreline of southern and central Knee Lake (Fig. GS-5-2) at a scale of 1:20 000. This area was chosen because it provided both across- and along-strike exposure, and existing 1:50 000 maps (Gilbert, 1985) formed an excellent base on which to integrate new observations. Given the success of the 1997 program at Knee Lake we plan to extend this regional mapping upgrade to northern Knee Lake in 1998 and to Oxford Lake/Gods Lake in 1999.

Regional setting

Supracrustal rocks in the Oxford Lake - Knee Lake Belt have been assigned to two principal stratigraphic entities, the Hayes River Group and Oxford Lake Group (Gilbert, 1985 and references therein). These Groups are the principal focus of our recent work in that they have more potential to host gold and base metal deposits than the voluminous granitoid terrains in the Superior Province.

The Hayes River Group (ca. 2830 Ma at Knee Lake, D. Davis, pers. comm. 1986) is a predominantly volcanic sequence dominated by pillowed

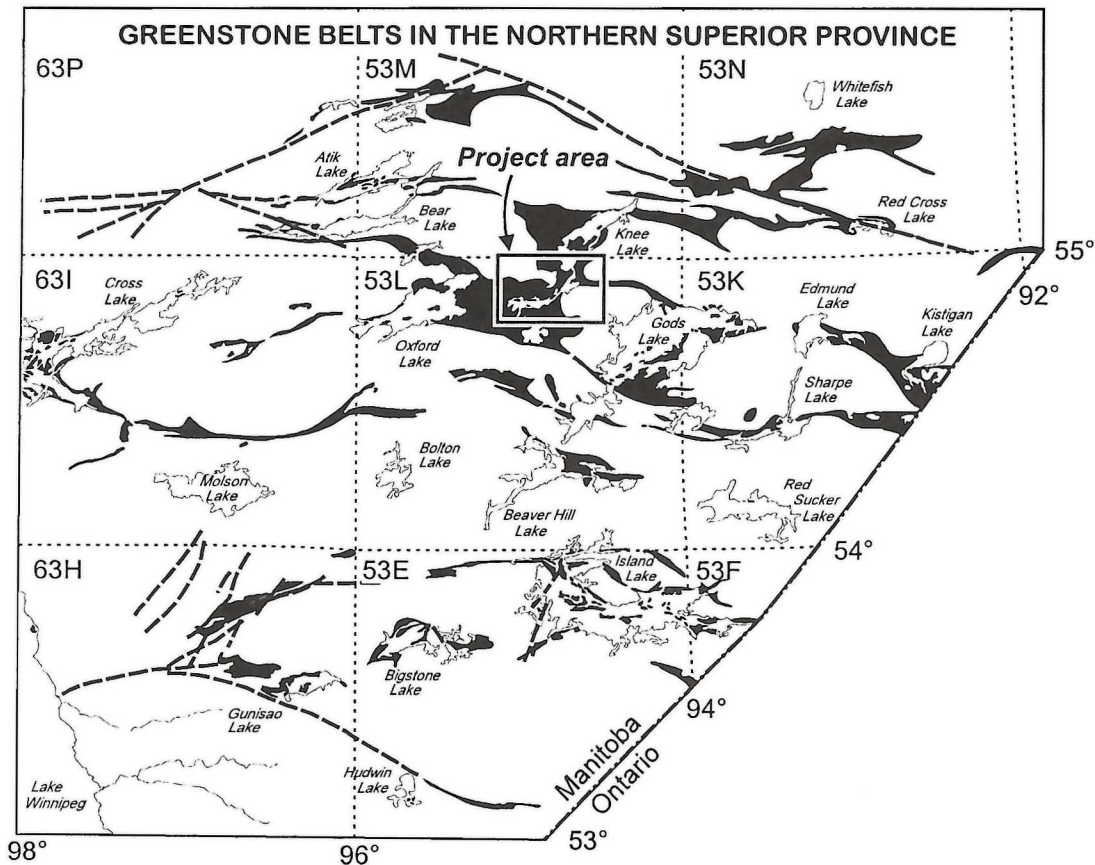


Figure GS-5-1: Location of the Knee Lake project area with respect to other greenstone belts in the northern Superior Province of Manitoba. Major regional faults are shown as dashed lines. The area depicted in Figure GS-5-2 is outlined.

basalt and related gabbro, minor intermediate to felsic volcanic rocks and minor volcanogenic sedimentary rocks. At Knee Lake the volcanic rocks have been described in terms of five volcanic 'cycles' (Hubregtse, 1976), each comprising a lower, tholeiitic basalt section and an upper, calc-alkalic, intermediate to felsic portion locally containing sedimentary rocks and iron formation. At Knee Lake the entire Hayes River Group section is estimated to be 9.7 km thick (Gilbert, 1985); neither the base nor top is exposed. It represents the upper portion of the Hayes River Group, the lower portion being that exposed on Oxford Lake (Manitoba Energy and Mines, 1987). The base of the Hayes River Group has been intruded by tonalitic to granitic plutons and related gneisses of the Bayly Lake Complex (2883-2730 Ma, D. Davis, pers. comm. 1986).

The Oxford Lake Group is a younger (*ca.* 2706 Ma at Oxford Lake, D. Davis, pers. comm. 1986), largely sedimentary succession which lies unconformably on Hayes River Group volcanic rocks at Gods Lake (Gilbert, 1985). It consists of a lower, dominantly 'volcanic' subgroup of limited extent, overlain by more extensive sedimentary rocks extending in a 12 km wide belt from Oxford Lake to Magill Lake (40 km; Gilbert, 1985; Manitoba Energy and Mines, 1987). Volcanic rocks in the lower subgroup are shoshonitic to calc-alkalic in character (Hubregtse, 1976; Brooks *et al.*, 1982; Gilbert, 1985) and include fragmental and flow rocks; in this report we consider the fragmental rocks to be epiclastic (conglomerates) rather than volcanogenic (reworked pyroclastic rocks; Gilbert, 1985). Stratigraphic relations within the Oxford Lake Group suggest that the sedimentary rocks were deposited in shallow- to deep-water basinal environments (Manitoba Energy and Mines, 1987).

Current research directions

A number of interdependent lines of research are actively being pursued during this regional reinterpretation of the Oxford Lake - Knee Lake Belt. Samples that have been collected within the context of our 1997 mapping will result in new geochemical, geochronological and structural data to be integrated into a new map for the belt. Research directions being pursued during this project include:

1. Stratigraphy and geochemistry of the Hayes River Group:
 - can a stratigraphy be defined and mapped within the Hayes River Group?
 - do the reported mafic-to-felsic volcanic cycles exist without structural breaks?
 - what do volcanic/sedimentary facies say about provenance of fragmental units?
 - what is the tectonic environment in which the volcanic rocks were emplaced?
2. Stratigraphic and structural setting of 'Hayes River Group' sedimentary rocks:
 - do they actually belong to the Hayes River Group?
 - what sedimentary environment do they represent?
 - what is their structural relationship to Hayes River Group volcanic rocks?
3. Stratigraphy and geochemistry of the Oxford Lake Group:
 - are there important distinctions between the 'volcanic' and 'sedimentary' portions (Gilbert, 1985) of the Group?
 - what are the contact relations between the 'volcanic' subgroup, the Hayes River Group, and sedimentary portions of the Oxford Lake Group?
 - what are the environments in which these rocks were deposited?
 - what is the tectonic environment in which these distinctive alkaline and calc-alkaline rocks were erupted?
4. Structural geology:
 - what are the main faults, shear zones and folds in the Knee Lake belt, and how are they related in the structural evolution of the belt?
 - are there early structures which have juxtaposed unrelated stratigraphic components?
5. Geochronology:
 - what is the range of ages for the Hayes River Group - are there structurally juxtaposed or repeated parts of the section?
 - what is the age of 'Hayes River Group' sediments?
 - what is the range of ages represented in the 'volcanic' and 'sedimentary' portions of the Oxford Lake Group - is this entity in fact a composite of a number of unrelated components?
 - what are the ages of major structures?
6. Tectonics:
 - what do the stratigraphy and structure relations in the Knee Lake belt

say about the tectonic evolution and setting of the constituent rocks?

- what does the tectonic environment suggest about the possible development of base metal and gold deposits?

7. Mineral deposits:

- what is the setting of known mineral showings in the Knee Lake area, in the context of new interpretations?
- does the Hayes River Group have features that would suggest potential for VMS-type mineralization?
- does the volcanic subgroup of the Oxford Lake Group have base metal mineral potential?
- how does the structural framework of the Knee Lake area compare with areas (*e.g.*, Island Lake) that have gold showings?
- what implications do the new tectonic interpretations have regarding the potential for mineral deposits in the Oxford-Knee-Gods lakes area?

HAYES RIVER GROUP

The Hayes River Group is arched broadly around the Bayly Lake complex (Gilbert, 1985), a composite batholithic granitoid terrain. The volcanic section is largely monoclinical, facing south and east between Cinder Lake and southern Knee Lake (Fig. GS-5-2). Hayes River Group volcanic and volcanogenic sedimentary rocks on southern and central Knee Lake are cut by major faults and shear zones coinciding largely with the lake basins; as a result the stratigraphic relation between basalts on the north side of Knee Lake and those on the south side are not known.

Basalt, basaltic andesite

Subaqueous, pillowed and massive mafic flows comprise the major portion of the Hayes River Group in the Knee Lake area (Fig. GS-5-2). In order to construct a regional stratigraphy in the Hayes River Group we attempted a first-order subdivision the mafic sequence on the basis of readily identifiable field characteristics. Each regionally extensive unit was sampled for geochemical analysis.

Most mafic flows in the Hayes River Group at Knee Lake are aphyric and typically have a very pale buff to cream and pale grey green weathering colour, in some places due to widespread pervasive epidotization. Three regional scale units were defined: aphyric flows, spherulitic flows ('variolitic' flows of Gilbert, 1985), and plagioclase phyric flows:

1) Aphyric flows include pillowed, composite and massive types. Pillowed flows are characterized by medium to small, bun shaped to irregular pillows with narrow selvages and thin interpillow hyaloclastite. Composite flows have a massive base and pillowed top, or massive core and pillowed margins and top. Massive flows may or may not have amoeboid pillow breccia tops.

2) Spherulitic flows form highly distinctive marker units up to 700 m thick within Hayes River Group stratigraphy. In these flows, cm-scale concentrically zoned objects interpreted as devitrification structures occur in pillow margins and coalesce to a dense mass in pillow cores (Fig. GS-5-3). They were interpreted as variolites (immiscible liquid segregations in lava) by Gilbert (1985) but were found overprinting amoeboid pillow breccias and hyaloclastite during this study and are thus clearly subsolidus in origin (Fig. GS-5-4). Regardless of the mode of origin of the concentrically zoned structures their presence is a fundamental characteristic of these units. Contacts between km-scale spherulitic and aphyric units are sharp, and there is no small-scale intercalation of the two flow types. Spherulitic flows also differ from non-spherulitic flows in that pillows tend to be larger, elongate ('mattress-' and 'mega-' pillows) and have thicker selvages and interpillow hyaloclastite than aphyric flows.

3) Plagioclase phyric flows occur in westernmost central Knee Lake, underlying a greywacke turbidite section, and at south central Knee Lake. Flows are morphologically similar to aphyric basalts, the only difference being the presence of 1-5 mm plagioclase phenocrysts (up to 20%).

Mafic rocks on the east side of the fault located along the southeast shore of Knee Lake (Fig. GS-5-2) include dark green weathering amphibolites that differ in metamorphic grade and contained tectonic fabrics from Hayes River Group basalt and basaltic andesite to the north. These mafic metavolcanic rocks contain almandine amphibolite facies mineral assemblages, as opposed to the greenschist mineral assemblages, and include prominent tectonic fabrics (*e.g.* Sellers Lake shear zone, Fig. GS-5-2) that are not present northwest of the fault (a feature which indicate that this fault probably involves significant offset). Mafic volcanic rocks southeast

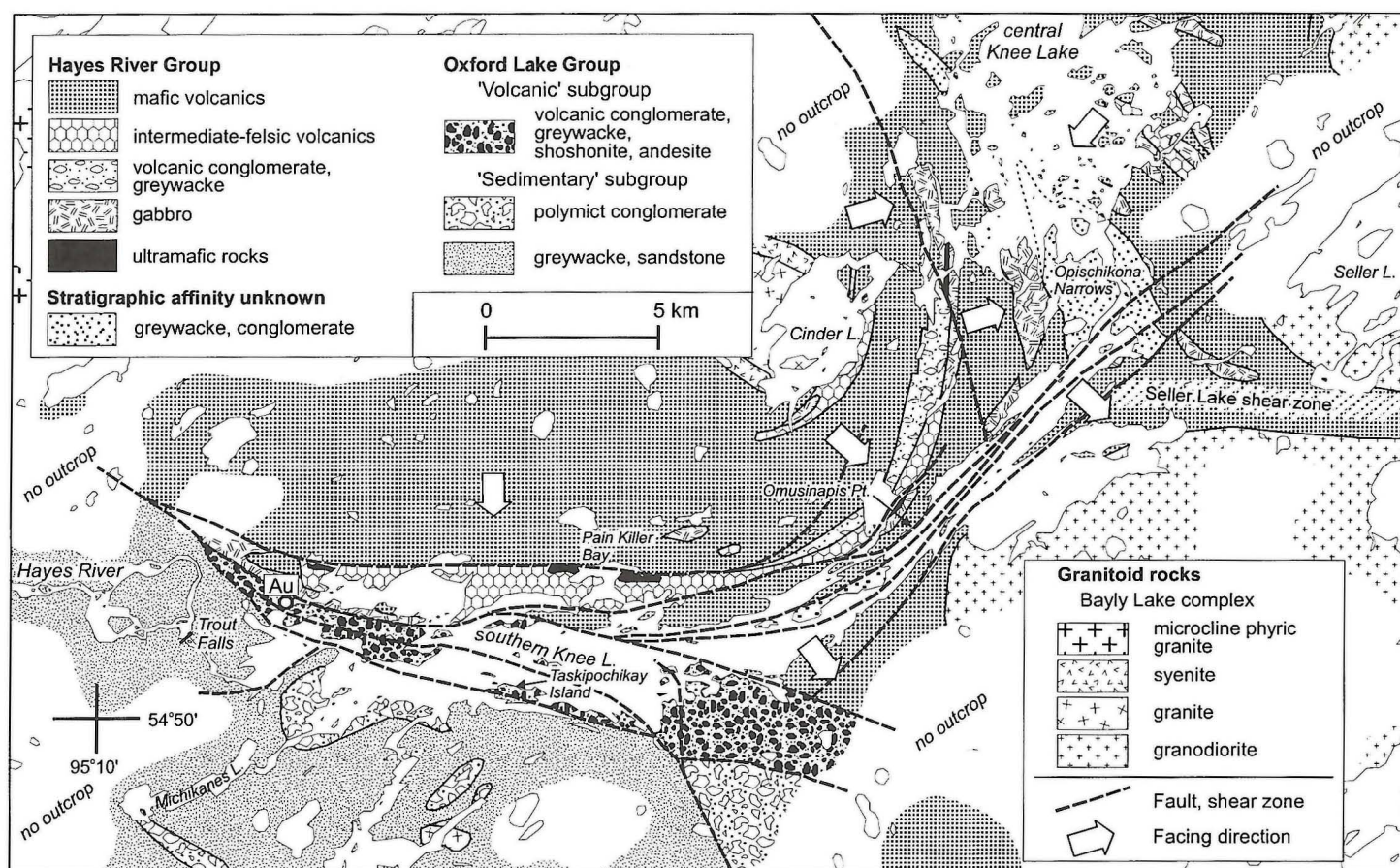
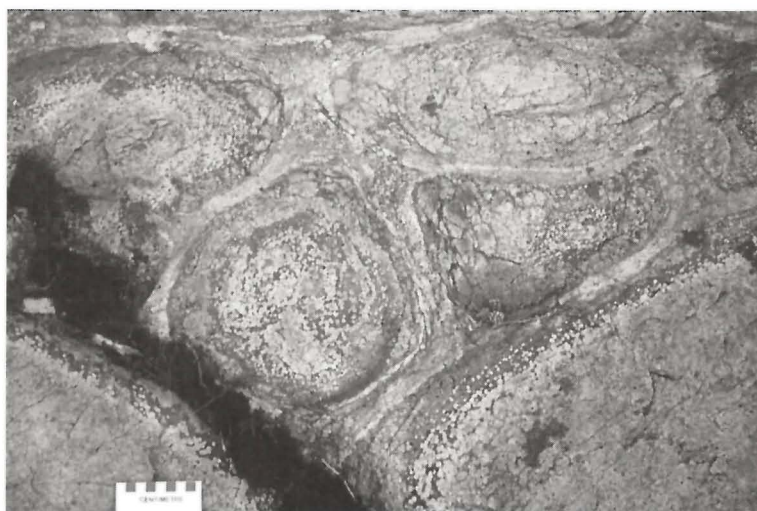


Figure GS-5-2: General geology of south and central Knee Lake, modified from Manitoba Energy and Mines (1987) and Gilbert (1985).

Figure GS-5-3: Spherulitic basalt, Hayes River Group. Oval, concentrically zoned structures interpreted as domains of devitrification become larger and more abundant from the pillow margin to the pillow core. Map scale units composed of spherulitic flows form stratigraphic markers within the Hayes River Group mafic volcanic sequence.



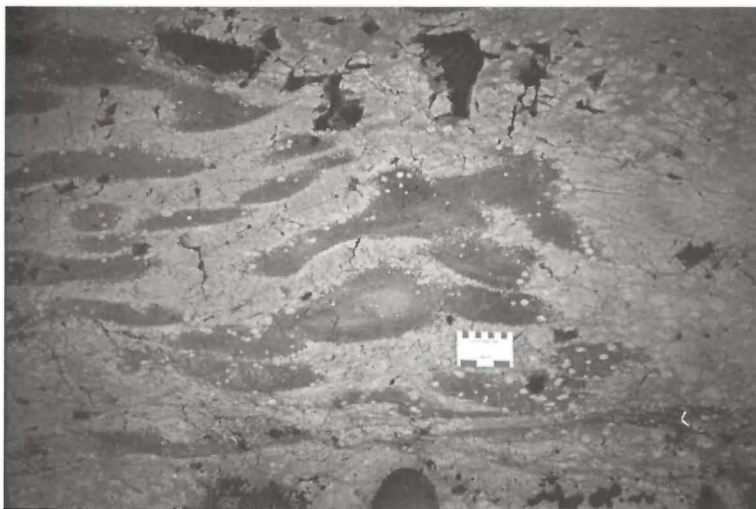


Figure GS-5-4: Spherulites as in Figure GS-5-3 overprinting amoeboid pillows and hyaloclastite in a basalt flow-top breccia. This relationship demonstrates that the oval structures are not immiscible silicate liquid segregations, but formed after the flow had quenched.

of the fault will be examined in 1998 to determine whether they should continue to be included in the Hayes River Group or whether they are part of a separate unit.

Felsic volcanic, volcanoclastic and sedimentary rocks

A 1.2 km wide zone of felsic volcanic, volcanoclastic and sedimentary rocks occurs on the north shore of southern Knee Lake, between two large domains of Hayes River Group basalt and basaltic andesite (Fig. GS-5-2). Gilbert (1985) considered this zone of felsic volcanic and sedimentary rocks to represent an episode of felsic volcanism in the contiguous and otherwise dominantly mafic Hayes River Group. Although the felsic volcanic rocks face south and southeast, similar to the underlying Hayes River Group basalts, the contact between these felsic and mafic domains is commonly marked by a fault (Fig. GS-5-2). For this reason the present configuration of the mafic and felsic units is a product of faulting rather than stratigraphic superposition and, consequently, relationships between the felsic and mafic domains are uncertain.

Figure GS-5-5 show sections across the felsic volcanic and volcanoclastic unit from three localities: Pain Killer Bay, north of Omusinapis Point and central Knee Lake. The Pain Killer Bay section is dominated by massive rhyolite and a high level, possibly subvolcanic, intrusive body of quartz feldspar porphyry, whereas those north of Omusinapis Point and central Knee Lake sections are dominantly volcanoclastic and sedimentary. The volcanoclastic and sedimentary portions were interpreted by Gilbert (1985) to have been derived from the "more proximal" rhyolite-dominated section on Pain Killer Bay. Descriptions of the rhyolite-dominated (Pain Killer Bay felsic complex) and the volcanoclastic/sedimentary-dominated (Omusinapis Point and central Knee Lake) sections follow.

Pain Killer Bay felsic complex

At Pain Killer Bay a 1.5 km wide fault-bounded panel that includes quartz feldspar porphyry, massive and fragmental rhyolite flows and lesser felsic volcanoclastic rocks (Fig. GS-5-5) forms a northeast trending sequence trending counterclockwise to the bounding faults. Consequently, the total exposed felsic stratigraphic section (ca. 2.5 km) is considerably thicker than the width of the fault panel (Fig. GS-5-2).

The Pain Killer Bay felsic complex is cored by a high level, composite, porphyritic felsic intrusion. This body is at least 1 km thick and trends northeast, subparallel to primary layering in the overlying felsic volcanic

sequence. Small felsic intrusions also form irregular bodies, dykes and sills in the overlying section. The porphyritic felsic intrusion is a multicomponent body composed of very fine grained, pale green- to green-grey rhyolitic phases that vary in the abundance and size of contained feldspar and quartz phenocrysts. Creamy yellow euhedral to subhedral tabular feldspars (1-5 mm) are characteristic, with subordinate commonly subhedral quartz phenocrysts (1-2 mm). The multicomponent character, presence of miarolitic cavities (Fig. GS-5-6), and cobbles of similar quartz-feldspar porphyry in stratigraphically overlying volcanoclastic units suggests that the intrusion was high level and probably subvolcanic. A megacrystic phase characterized by large (2 cm) microcline phenocrysts intrudes the main quartz feldspar porphyry and locally forms domains up to several hundred metres in width. It is uncertain whether this phase is a later intrusion or comagmatic with the main quartz-feldspar porphyry body.

Overlying the felsic intrusion is a section that contains 3 'formations': at the base a 50-100 m thick sedimentary section, in the middle a 650-700 m thick sequence dominated by massive and fragmental rhyolite flows, and at the top a >800 m thick volcanoclastic formation (Fig. GS-5-5).

The lowermost formation consists of delicately layered and/or laminated felsic siltstone and thinly bedded feldspathic sandstone containing 20-30% detrital feldspar in a fine grained felsic matrix.

The middle formation is dominated by massive feldspar ± quartz phyrlic rhyolite flows, fragmental flows, and felsic, lapilli-bearing, crystal tuff. Interlayers of coarse felsic volcanoclastic breccia, feldspathic greywacke, felsic volcanoclastic conglomerate and reworked tuff and lapilli tuff occur throughout the sequence.

The topmost formation has a gradational contact with the underlying sequence, with an upward transition from flows to a heterolithic sequence including both volcanoclastic/sedimentary and pyroclastic rocks. The dominant component of the upper sequence is massive, unsorted, thick bedded (to >4 m thick) granule-, pebble-, and rarely cobble-bearing conglomerate containing porphyritic, felsic volcanic clasts in a feldspar crystal-rich sandy matrix. Feldspar phyrlic fragments and matrix are similar in composition and texture, such that in many outcrops only the mafic clasts can readily be observed. These conglomerates are interlayered with heterogeneous felsic breccia, massive rhyolite, and crystal-lapilli tuff. The top portion of this formation is a foliated and sheared quartz-feldspar phyrlic massive rhyolite, truncated by a fault.

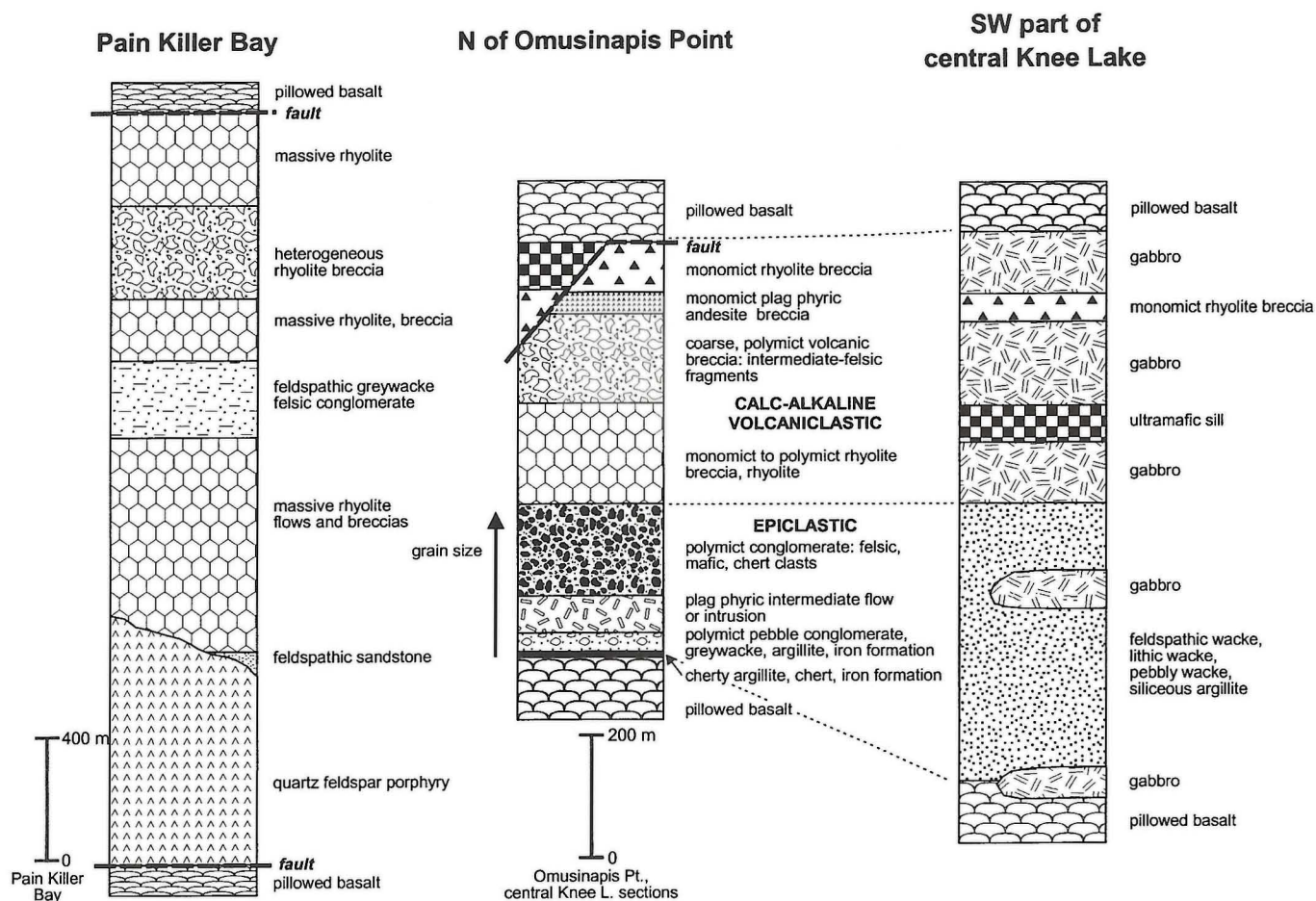


Figure GS-5-5: Stratigraphic sections through a prominent felsic volcanic - volcanoclastic/sedimentary unit within the Hayes River Group, southern Knee Lake. Note that the Pain Killer Bay section is at a different scale than the other two sections.



Figure GS-5-6: Miarolitic cavity (1.5 cm oval structure above scale card) in quartz-feldspar porphyry, Pain Killer Bay felsic complex. These structures indicate that this body was emplaced at a relatively high level, allowing a gas phase in the magma to exsolve.

Intermediate-felsic volcanoclastic rocks, polymictic conglomerate, greywacke-argillite

Volcanoclastic sedimentary rocks interpreted to be stratigraphically equivalent to the Pain Killer Bay felsic complex extend for 15 km northeast of Pain Killer Bay (Fig. GS-5-2) and are exposed in shoreline sections north of Omusinapis Point (the site of Knee Lake Lodge) and on southwestern central Knee Lake. Descriptions of the two volcanoclastic/epiclastic-dominated sections north of Omusinapis Point and central Knee Lake follow. Together with the Pain Killer Bay section they are thought to record the interplay between constructive volcanic (vent complex?) and destructive epiclastic processes in the felsic dominated interval (Fig. GS-5-5). Unlike

the section on Pain Killer Bay, which is fault bounded, those to the north both appear to be stratigraphically conformable with underlying and overlying basalts.

North of Omusinapis Point the volcanoclastic sedimentary section rests conformably on green weathering, pillowed, Hayes River Group basalts. The section is composed of a number of distinct stratigraphic members which can be broadly grouped into a lower epiclastic and upper volcanoclastic member (Fig. GS-5-5). The lowermost part of the section is dominated by relatively fine grained sedimentary rocks: polymict pebble conglomerates, argillites and wackes. These give way upwards to coarser,

polymict, pebble-cobble-boulder conglomerates with a significant felsic volcanic component. Rhyolite breccias and massive rhyolites overlie the polymict conglomerates, and are in turn overlain by a number of coarse volcanoclastic breccias, containing intermediate to felsic fragments, that comprise the top of the exposed section. This sequence records a significant hiatus in mafic volcanism during which were first deposited basinal facies volcanic conglomerates and wackes. The rounding observed in felsic pebbles suggests that some of the volcanoclastic material was eroded and transported in a subaerial environment before being deposited in a marine basinal setting. The influence of calc-alkalic intermediate to felsic volcanism in this interval increases in importance upwards, with the deposition of coarse heterolithic debris flow deposits. An important feature of this section is that although it is stratigraphically equivalent to Pain Killer Bay central vent complex rhyolites, it includes a wide variety of intermediate, felsic and even mafic detritus.

In easternmost central Knee Lake a turbidite section 450-500 m thick overlies pillowed aphyric and plagioclase phyric basalt and is provisionally correlated with the conglomerates and wackes in the lower, epiclastic portion of the Omusinapis Point section (Fig. GS-5-5). The sediments include feldspathic wacke, pebbly wacke, siltstone, argillite, siliceous argillite, and rare mafic accretionary lapilli tuff layers. Sandy beds contain turbidite bedforms including normal grading, parallel lamination, flame structures, ripups and scours. Sand-sized material (0.5-1 mm) includes feldspar, lithic grains, and minor quartz. Pebbles (<1 cm) are predominantly aphyric, grey to white felsic and intermediate volcanic lithologies. The upper part of the sedimentary section is intruded by gabbro; rafts within the gabbro include ultramafic rocks and monomict rhyolite breccias, a sequence which parallels that at Omusinapis Point (Fig. GS-5-5).

An important point to be made from the stratigraphic relations described above is that there is no simple, proximal to distal facies relationship between the Pain Killer Bay felsic complex and the breccias, conglomerates and turbidites comprising the clastic portion of Gilbert's (1985) unit 2 (felsic volcanic and subvolcanic rocks, related sedimentary rocks). Indeed, our stratigraphy suggests that the epiclastic and volcanoclastic members of the sequence may be unrelated. Stratigraphy suggests the less mature volcanoclastic deposits prograded over the epiclastic units, and that both show a west to east, proximal to distal facies relationship. Note also that the volcanoclastic part of the section contains a wide variety of presumably calc-alkaline, intermediate to felsic lithologies, and thus is not simply a clastic apron on rhyolites in the west. The volcanoclastic section may include breccias related to the Pain Killer Bay rhyolite, but only as components of a sequence with complex provenance.

STRATIGRAPHIC AFFINITY UNKNOWN

Greywacke, pebble conglomerate (Opischikona Narrows sediments)

At Opischikona Narrows a sedimentary sequence occupies a structural basin created by fold interference (Fig. GS-5-2). Gilbert (1985) shows these sedimentary rocks to be part of the Hayes River Group, but the age of the sequence is equivocal in that its stratigraphic and structural relationships with the underlying Hayes River Group basalts are equivocal. Accordingly, we prefer at this time to depict these rocks as having unknown stratigraphic affinity. Samples for U-Pb geochronology were collected in order to determine the range of ages of detrital zircons, the youngest of which would provide a maximum age of deposition.

Chert-magnetite iron formation and argillite mark the base of the sedimentary section in the few locations where it is exposed. Greywacke, pebbly sandstone and conglomerate form the bulk of the overlying stratigraphic section. A range of primary sedimentary structures are preserved, indicative of deposition in both subaerial and submarine environments.

Nowhere has an unambiguous stratigraphic relationship been documented to indicate a conformable or unconformable contact between the Opischikona Narrows sediments and the underlying Hayes River Group basalts. The contact between the basalt sequence and the sediments is intruded by gabbro on both the east and west sides of the structure. In the one location, where the contact is exposed, iron formation overlies a massive, aphanitic and vesicular mafic rock that could be either a chilled

high level gabbro or a massive flow in the Hayes River Group basalts.

The dominant lithologies in the sedimentary package consist of marine turbidite greywacke, siltstone and polymictic conglomerate. Slump structures, soft sediment deformation, scours and channeling indicate proximal deposition. Sedimentary structures within the turbidites include graded bedding, parallel lamination, rare convolute lamination and mudstone intervals. Conglomeratic beds range from poorly sorted matrix-rich turbidites to poorly stratified unsorted debris flow deposits. Clasts are dominantly well rounded, pebble to cobble size, intermediate to felsic volcanic, and smaller percentages of mafic volcanic and sedimentary (including iron formation) clasts.

Sandstone and pebbly sandstone interpreted to have been deposited in a subaerial environment occur in several locations within the Opischikona Narrows sedimentary package. These rocks consist of trough cross-bedded greywacke and pebbly greywacke, some within well developed channels. Composition of the sands and clasts are the same as in the marine portion of the section. Stratigraphic control is not sufficiently constrained to define the location of these sequences within the section. These rocks never occur at the base of the section, but are within 150 m of the base on the northeast side of the structure.

OXFORD LAKE GROUP

The Oxford Lake Group on Knee Lake is depicted on existing maps (Gilbert, 1985) to include both volcanic fragmental-dominated and greywacke-dominated members. We informally refer to these two members of the Oxford Lake Group as the 'volcanic' and 'sedimentary' subgroups (Fig. GS-5-2). Our work indicates that the 'volcanic' subgroup, although composed dominantly of volcanic clasts, is epiclastic rather than pyroclastic/volcanoclastic as originally mapped by Gilbert (1985). The relationship between the 'volcanic' and 'sedimentary' subgroups is not clear at this time, with the possibility that they are not contiguous or related sequences.

'Volcanic' subgroup: polymictic conglomerate, greywacke, shoshonite

Gilbert (1985) includes a diverse sequence of 'porphyritic volcanic rocks and related sedimentary rocks' in the Oxford Lake Group in southern Knee Lake. In this unit he includes shoshonite flows, andesite flows, heterolithic pyroclastic rocks and sedimentary rocks. Our interpretation of the bedded fragmental rocks is that they comprise a wide variety of polymictic conglomerates and greywackes; true pyroclastic rocks are rare or absent. This distinction is important in that the facies of this mixed volcanic/sedimentary package are clearly dominated by polymict subaqueous debris flow deposits emplaced in a basinal setting, coeval with alkalic and calc-alkalic magmatism.

On Knee Lake the mixed unit of conglomerates and volcanic rocks is entirely fault bounded - no stratigraphic relationships exist between it and the Hayes River Group or the greywacke-dominated member of the Oxford Lake Group (Fig. GS-5-2). Similar rocks on Oxford Lake have been dated at 2706 \pm 4/-2 Ma (D. Davis, pers. comm. 1986; Manitoba Energy and Mines, 1987). Due to the polydeformed and faulted nature of the incompletely-exposed sequence on southern Knee Lake, a complete stratigraphic sequence cannot be established.

During this study sedimentary units were sampled for geochronology, to determine the range of ages of detrital zircons and provide a maximum age for the deposition of the sediments. A suite of samples was also collected from lava flows and conglomerate clasts to define their geochemical characteristics and constrain the tectonic setting in which the volcanic rocks were emplaced.

Taskipochikay Island

Shoshonite flows on Taskipochikay Island (Fig. GS-5-2) are pillowed, coarsely and abundantly plagioclase phyric (to 10 mm), grey weathering, and dark grey on fresh surfaces. Pillows are elongate, up to 1 m wide by several m long (to 5 m); this elongation is in part primary and in part a function of the high degree of deformation observed on horizontal surfaces due to the subhorizontal stretching developed in Oxford Lake Group rocks. Vertical exposures reveal medium sized, bun shaped pillows. The pillows contain deformed carbonate-filled amygdaloids up to 10 cm long and 5 mm wide. Pillow selvages are thick and laminated hyaloclastite occurs between pillows.

Polymictic conglomerate on and directly north and northwest of Taskipochikay Island (Fig. GS-5-2) comprises a stratified sequence of thick (1 - >5 m) massive conglomerates, thin bedded (50 - 100 cm) planar-bedded conglomerates, conglomeratic scour channels (Fig. GS-5-7), and thin bedded, normally graded pebble conglomerate with sandstone-siltstone interbeds and isolated large boulders. Clasts are subangular to rounded and are entirely volcanic in origin, including: light grey aphyric rhyolite, grey-green aphyric basalt/andesite, dark grey aphyric shoshonite, plagioclase phyric shoshonite, quartz feldspar porphyry, felsic plagioclase-hornblende porphyry, and light grey aphyric andesite. Some of the conglomerates are ultra-coarse grained despite the intense subhorizontal stretching lineation (*e.g.*, shoshonite clasts up to 45 x 300 cm, rhyolite clasts up to 20 x 120 cm). All of the conglomerates are matrix-supported and poorly sorted; the matrix is mafic in composition, possibly shoshonitic. The general environment of deposition is clearly marine, evidenced by the presence of intercalated pillowed shoshonite as well as the primary structures and bedforms in the sediments. Sedimentary structures suggest deposition of the conglomerates within the channelized portion of a sedimentary fan, proximal to source. The rounding exhibited by many clasts may have been produced in a subaerial environment prior to marine deposition. One interpretation is that this conglomeratic sequence was deposited from subaqueous debris flows adjacent to a subaerial calc-alkaline - alkaline volcanic island of Oxford Lake Group age.

East of Taskipochikay Island

Polymictic conglomerates 5 km east of Taskipochikay Island form a unit more than 640 m thick, with a faulted base and overlain by volcanogenic greywackes (see below). Like the conglomerates north of Taskipochikay Island these clastic sediments also are dominated by mafic, intermediate to felsic, porphyritic and aphyric volcanic clasts, but show some important distinctions. First, primary structures tend to be better preserved due in large part to the absence of a strong stretching lineation; only a weak subvertical stretching lineation is present. These conglomerates tend to be thick bedded (>10 m), massive to normally graded, very poorly sorted, and largely clast-supported in the lower parts of beds. Grading, from cobble-pebble base to sandy bed tops, is conspicuous. Clasts (including boulders to 1 m diameter) are well rounded to subangular (Fig. GS-5-8). Some clasts have at least one and perhaps two generations of cleavage that predate incorporation into the conglomerate. Mafic intrusive clasts (diorite, gabbro, pyroxenite) form a small proportion of the clast population. Rare ultramafic conglomerate beds (see below) are intercalated with the 'normal' volcanic-derived conglomerates. A significant portion of the lower part of this sequence, interlayered with conglomerate, includes finer grained sediments such as greywacke, siltstone, pebbly wacke, mafic argillite, siliceous argillite and chert. Superb preservation of primary sedimentary structures in these sediments (grading, lamination, flame structures, load casts, syn-sedimentary folding; Fig. GS-5-9) clearly indicates that the clastic beds were deposited from turbulent subaqueous density currents.



Figure GS-5-7: Conglomeratic channel cutting finer grained clastic deposits, 'volcanic' subgroup of the Oxford Lake Group, Taskipochikay Island. Tops are to the right.



Figure GS-5-8: Slump deposit, 'volcanic' subgroup of the Oxford Lake Group. Large (to several metres) angular blocks of lithified sediment are incorporated in a pebble-cobble conglomerate.

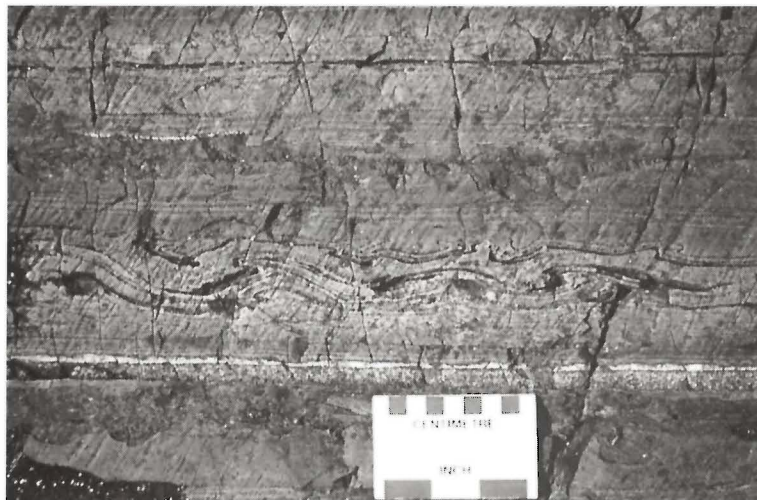


Figure GS-5-9: Sedimentary structures in sequence of siliceous argillite, argillite and mafic wacke, 'volcanic' subgroup of the Oxford Lake Group. Beds face toward top of photograph. Above scale card: synsedimentary folds in siliceous argillite. Scale card rests on a mafic wacke bed with flame structures, scours and load structures at its base.

More than 370 m of greywacke, with minor units of argillite, siliceous argillite, chert, and iron formation, overlies the conglomerates described above. The greywacke is distinctive relative to other wackes in the Oxford Lake Group in that much of the unit appears to be derived from a single andesitic volcanic source. The greywacke is composed primarily of plagioclase crystals (phenoclasts) 1-3 mm in size at the base of beds and <1 mm at the top of graded (A) divisions. These normally graded beds are 10-100 cm thick, typically forming Bouma AB sequences (parallel laminated B divisions at bed tops). Other turbidite structures preserved include scours and flame structures. The greywackes are locally interlayered with metre-scale normally graded conglomerate beds in which the dominant clasts are rounded, plagioclase phyric (1-5 mm, 50%) andesite. Pebbles of an identical porphyritic andesite, and rhyolite, occur as isolated clasts in some greywacke beds. Fine grained sediments form units to about 10 m thick within the greywacke section. These sediments include interlayered (0.2 - 40 cm) grey to cream chert and dark grey to black mafic argillite. Both the chert and argillite display abundant syn-sedimentary folds. Thin, cm-scale mafic wacke beds in this fine grained sequence form graded beds with bases scoured into underlying cherts. The mafic argillites contain locally abundant, disseminated specular hematite.

Ultramafic conglomerate, or conglomerate composed almost entirely of ultramafic and mafic materials, form highly distinctive units within the conglomeratic section 6-7 km east of Taskipochikay Island (Fig. GS-5-2). Pebble- to cobble-sized clasts in the conglomerate (Fig. GS-5-10) include serpentinite, pyroxenite, peridotite, gabbro, basalt and massive sulphide (pyrite); the latter are up to 10 cm in size. The matrix is fine grained bright green recrystallized ultramafic sand now apparently dominated by actinolite (Gilbert, 1985). Beds are 0.5-1.5 m thick and bedforms include normal and, more rarely, reverse size grading as well as lenticular scour channels, in which a coarse pebbly base grades to a finer pebbly top. Clearly these conglomerates were derived from a single source, presumably a subaerially exposed ultramafic-mafic plutonic massif. The presence of rare foliated ultramafic clasts in the conglomerate suggests that portions of this ultramafic-mafic massive were deformed. Geochemistry of the constituent clasts will help to define the nature and origin of the source rocks - one possibility is that the ultramafic-mafic plutonic rocks and associated basalts represent components of oceanic crust.

The environment of deposition for the conglomerates, greywackes and argillites in this section is unambiguously marine. Rare pillowed andesite flows in the conglomeratic sequence attest to a subaqueous regime. Graded conglomerate beds, turbidite sedimentary structures in greywackes, and syn-sedimentary folding in interlayered cherts and cherty argillites are consistent with deposition below wave base. The rounding observed in many clasts, however, is more likely to have occurred in a fluvial rather than a purely marine environment. We conclude that, like the mixed sedimentary and volcanic section on Taskipochikay Island, the epiclastic rocks are the products of erosion and stream transport in a subaerial environment. At least some of the sediments appear to have been derived from active volcanoes (e.g., plagioclase crystal-rich greywacke). The clastic material, once delivered to the sea, was remobilized into a subaqueous

sedimentary fan. The suggestion that some clasts contain deformation fabrics that predate deposition opens the possibility that the source terrain included not only Oxford Lake Group calc-alkaline volcanoes but perhaps also deformed, older volcanic material (possibly Hayes River Group age).

'Sedimentary' subgroup: greywacke, conglomerate

The 'sedimentary' subgroup of the Oxford Lake Group (Fig. GS-5-2) is not a simple continuous sequence of metasediments. With the data collected to date, the complexities of this area could not be resolved; however, some conclusions can be drawn from the observations made: 1) a narrow wedge (up to 2.2 km thick) of subaerial fluvial sediments at the west end of the lake is in probable fault contact with 2) clearly marine sediments (approximately 3 km thick) to the southeast, which are flanked to the south by 3) about 6 km of sandstone and conglomerate of unknown depositional environment. The primary depositional variations within these sedimentary packages is further complicated by an abrupt increase to amphibolite grade mineral assemblages across an east northeast trending shear zone that marks the contact with the 'volcanic' subgroup.

A wedge of subaerial fluvial sandstone and conglomerate at the southwest end of Knee Lake extends up the Hayes River past Trout Falls (Fig. GS-5-2). The sandstones are dominantly light grey weathering, medium- to coarse-grained, feldspar-rich, quartz-poor greywacke to subarkose. Crossbedding occurs on small to large scales, generally as bed sets. The sandstones locally contain a few per cent pebbles, either as a basal lag, or scattered along foreset beds in some trough crossbeds. Interbeds of pebbly sandstone are common. Clast supported, polymictic, pebble-cobble conglomerates interlayered with the sandstones are thick bedded; bedding and clast size increase up section. Clasts are highly variable with respect to rock type, are well rounded and display a well developed sphericity.

The 'sedimentary' subgroup displays an abrupt change in the character where Hayes River empties into Knee Lake. At this locality the fluvial sequence to the west is replaced by a probable marine sequence of sedimentary rocks that is dominated by turbidite sandstone and siltstone, with lesser amounts of conglomerate, argillite and iron formation. The dominant turbidite component consists of light grey weathering, medium- to fine-grained greywacke, feldspathic greywacke and siltstone. These are intercalated with numerous 2 - >5 m thick unsorted, polymictic, clast supported, pebble to cobble conglomerate beds. Laminated argillite and chert-magnetite iron formation locally form thick (> 30 m) to thin (2-10 cm) interbeds throughout the sequence.

STRUCTURE

Preliminary results of structural analysis of Knee Lake Belt suggests that it has been affected by multiple generations of folding. At the mesoscopic scale, the earliest folds recognized (F_1) are very tight to isoclinal with a locally developed axial planar cleavage (S_1). They are overprinted by F_2 folds which are also very tight to isoclinal but have a generally well developed axial planar cleavage (S_2). The S_2 is locally refolded by open F_3 folds. Very tight to isoclinal folds (F_1 or F_2) are also recognized at the

mesoscopic scale, in many parts of the Knee Lake Belt, based on younging direction reversal, fold asymmetry change and repetition of lithological units. At several localities, clasts in the conglomerate of the Oxford Lake Group contain a pre-depositional foliation, indicating that rocks of the Hayes River Group had probably been deformed before the deposition of the Oxford Lake Group. It is interesting and yet to be explained that, although deformation in the Hayes River Group is mainly concentrated in localized shear zones and many parts of the group are only very weakly deformed, rocks of the Oxford Lake Group are generally very strongly deformed.

One of the significant outcomes of our remapping is the recognition of major west-northwest and northeast-trending faults and shear zones, concentrated in the linear portions of southern Knee Lake (Fig. GS-5-2). In the shear zones, rocks are very intensely deformed (Fig. GS-5-11) and stretching lineations are well developed. In most shear zones, stretching lineations are steeply plunging.

The west-northwest-trending structures define the contact between the Hayes River Group and the Oxford Lake Group. In the Oxford Lake Group, a zone of subhorizontal lineations (Fig. GS-5-12) are bordered on both sides by zones of steep lineations and the strain in all the zones is prolate (or the strain ellipsoid is of cigar shape, as opposed to pancake shape). The deformation of such a structural association may require a very specific boundary condition. The kinematics and tectonic significance of these shear zones will be a focus of further study.

Northeast-trending faults slice the Hayes River Group and Opischikona Narrows sediments, resulting in a fault-bounded panel of sedimentary rocks extending through the centre of southern Knee Lake

(Fig. GS-5-2). Presumably related structures bound the Pain Killer Bay felsic complex, and an isoclinally folded panel of Hayes River Group basalts south of Opusinapis Point.

The ages of the west-northwest and northeast-trending faults and shear zones is not precisely established pending dating of the 'volcanic' subgroup of the Oxford Lake Group and Opischikona Narrows sediments. Granodiorite dykes in amphibolite east of Opusinapis Point contain laminated mafic tectonite xenoliths, indicating that at least some deformation predates emplacement of voluminous granitoid plutons of the Bayly Lake complex.

The Seller lake shear zone (Fig. GS-5-2) is an easterly-trending, km scale structure that is inferred to exist from examination of limited shoreline exposure on Knee Lake and from descriptions of rocks south of Seller Lake (Gilbert, 1985). Tectonites within the zone comprise layered amphibolite and felsic rocks, and are at a higher metamorphic grade than structurally juxtaposed basalts of the Hayes River Group. The Seller Lake structure is clearly older than the northeast-trending fault set against which it is truncated (Fig. GS-5-2) but more detail on its character awaits further work.

METAMORPHISM

Two distinct metamorphic zones are observed within the supracrustal assemblages. Lower to middle greenschist facies metamorphic mineral assemblages characterize the Hayes River Group and 'volcanic' subgroup of the Oxford Lake group throughout the area with one exception: to the east of the northeast trending fault through Omusinapis Point, where Hayes River Group basalts contain amphibolite facies mineral assemblages.

Figure GS-5-10: Conglomerate composed entirely of ultramafic-mafic detritus, 'volcanic' subgroup of the Oxford Lake Group. Large gabbroic clast above scale card contains a tectonic fabric which predates deposition of the conglomerate. Dark clasts (2-3 cm) are serpentinite. Large clast left of the scale card is pyroxenite.

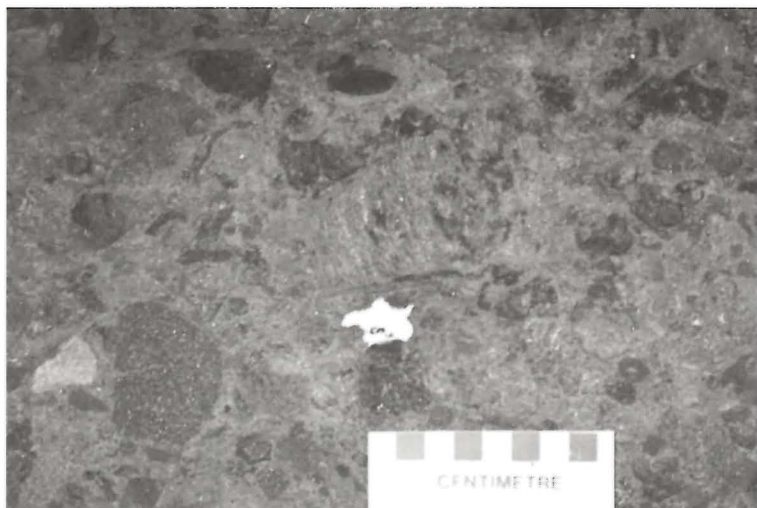


Figure GS-5-11: Phyllonite in the shear zone at the contact between the Hayes River Group and the 'volcanic' subgroup of the Oxford Lake Group. The stretching lineation at this outcrop is steeply plunging.

Similarly rocks of the Seller Lake shear zone contain amphibolite facies mineral assemblages. These rocks are abruptly truncated at the northeast trending fault zone and directly to the west the supracrustal rocks are at greenschist grade. A second major break occurs between the 'volcanic' subgroup and the 'sedimentary' subgroup of the Oxford Lake Group on the south side of Knee Lake. The change from greenschist to amphibolite grade is rather abrupt; however, there is a stepwise increase in metamorphic grade, recrystallization and regional deformation to the south, with each increase apparently controlled by faults. In the fluvial greywacke sequence there is no garnet and primary features are well preserved. To the south in the marine sediments garnet occurs in mafic interbeds in the iron formation. At the south end of a long bay near the west end of Knee Lake the sandstones are highly recrystallized with patches of very coarse grained incipient mobilisate.

ECONOMIC GEOLOGY

Implications for volcanogenic massive sulphide deposits

The potential for volcanogenic massive sulphide (VMS) deposits in the Knee Lake area resides within the subaqueous volcanic stratigraphy of the Hayes River Group. These rocks include both extensive tholeiitic basalt packages as well as calc-alkaline intermediate to felsic flows and volcanoclastic rocks (Hubregtse, 1976), suggesting that at least part of the Hayes River Group was emplaced in an arc environment. The association

of VMS deposits with volcanic arc rocks is common; for example, virtually 100% of the economic VMS deposits in the Paleoproterozoic Flin Flon Belt occur in juvenile arc sequences (Syme and Bailes, 1993), and in the best documented cases are more specifically associated with intra-arc rifting (Syme *et al.*, in prep.). At this early stage in our investigations the general volcanic environment within the Hayes River Group appears not dissimilar to that in existing VMS camps.

More specific factors suggesting VMS potential include the presence of a large, proximal felsic volcanic complex (Pain Killer Bay), presence of coarse felsic volcanoclastic rocks, and identification this year of altered basalts. Hayes River Group basalts are unusually pale weathering throughout most of the Knee Lake area. This low grade pervasive alteration locally intensifies such that the basalts weather white, are very light grey on fresh surfaces, and primary structures are obliterated. The alteration appears to result in an epidote/clinozoisite - albite - quartz rock, with patchy rust gossans locally developed in the most intensely altered rocks in the Pain Killer Bay area. Chemical analyses of the altered and less-altered rocks are pending.

Implications for gold deposits

A previously reported gold occurrence at the west end of Knee Lake (Fig. GS-5-2) was visited during the course of the mapping program. A minor gossan with disseminated pyrite was observed in gabbro and deformed gabbro on the north side of the shear zone that separates the Hayes River and Oxford Lake groups. Regionally the association of gold with gabbro and sheared gabbro is significant, *e.g.*, at the Westmin-Tanqueray deposits on Little Stull Lake and on the north side of Noranda's Twin Lakes deposits. However, a variety of rock types are associated with gold throughout the region (Richardson and Ostry, 1996): greywacke and iron formation in pillowed basalt at Gods Lake gold mine, felsic volcanic rocks and polymictic conglomerate at the Twin Lakes Seeber River deposits, and at the contact between mafic volcanic rocks and tonalite to granodiorite in the Henderson Island gold deposit described by Lin (GS-2, this volume). It is apparent that the significant characteristic common to these deposits and showings is major alteration zones in association with late ductile-brittle deformation zones.

The complex series of younger shear zones above is interpreted to represent part of a regionally extensive anastomosing network of long lived deformation zones. Significant gold occurrences or deposits have been reported in association with extensions of the Knee Lake shear zones to the west in the west Oxford Lake-Carrot River area, and to the east in Gods Lake and Little Stull Lake areas.

REFERENCES

- Brooks, C., Ludden, J., Pigeon, Y. and Hubregtse, J.J.M.W.
1982: Volcanism of shoshonite to high-K andesite affinity in an Archean arc environment, Oxford Lake, Manitoba; Canadian Journal of Earth Sciences, v. 19, p. 55-67.
- Gilbert, H.P.
1985: Geology of the Knee Lake - Gods Lake area; Manitoba Energy and Mines, Geological Services, Geological Report GR83-1B, 76 p.
- Hubregtse, J.J.M.W.
1976: Volcanism in the western Superior Province in Manitoba; in B.F. Windley (Ed.), Early History of the Earth; Wiley, New York, p. 279-287.
- Lucas, S.B., Stern, R.A., Syme, E.C., Reilly, B.A. and Thomas, D.J.
1996: Intraoceanic tectonics and the development of continental crust: 1.92-1.84 Ga evolution of the Flin Flon Belt, Canada; Geological Society of America Bulletin, v. 108, p. 602-629.
- Manitoba Energy and Mines
1987: Bedrock Geology Compilation Map Series, Oxford House, NTS 53L, 1:250 000.
- Richardson, D.J. and Ostry G. (Revised by W. Weber and D. Fogwill)
1996: Gold Deposits of Manitoba, Manitoba Energy and Mines, Minerals Division, Economic Geology Report ER86-1 (2nd Edition), 114 p.



Figure GS-5-12: Very strongly deformed conglomerate in the 'volcanic' subgroup of the Oxford Lake Group. The elongate clasts define a subhorizontal lineation. The aspect ratios of the clasts are up to 1:100 on the horizontal surface and only ~1:3 on the vertical surface (the lower right corner).

GS-6 GEOLOGY OF THE ASSEAN LAKE AREA (PARTS OF NTS 64A 1,2,7,8)

by Ch. Böhm¹

Böhm, Ch. (1997): Geology of the Assean Lake area (parts of NTS 64A/1,2,7,8); in Manitoba Energy and Mines, Minerals Division, Report of Activities, 1997, p. 47-49.

SUMMARY

Preliminary U-Pb zircon age data for a representative felsic igneous gneiss sampled from the northwestern part of Assean Lake reveal a pre- 3.0 Ga origin, and therefore calls into question the proportion of Proterozoic material previously suggested for this region.

INTRODUCTION

Shoreline exposures on Assean Lake, from the southwest end to the Awupak narrows in the northeast, were mapped during the 1996 and 1997 field seasons with the assistance of R. Belsham, E. Chaboyer, and T. Bochonko. The new findings supplement earlier mapping by Corkery (1985) and Corkery and Lenton (1990).

The area covered forms part of the Superior Boundary Zone (SBZ) (previously called Churchill-Superior Boundary Zone). The coverage includes the northwestern margin of the Split Lake Block (SLB), and the southeast margin of the Orr Lake Block (OLB). The SLB is interpreted as a marginal segment of the Superior Province and predominantly consists of reworked Archean felsic and mafic gneisses. Representative lithologies in the OLB are orthogneiss, intrusive granitic, pegmatitic, metasedimentary and volcanogenic rocks of unknown affinity. Thus the SBZ in the map

area is a heterogeneous crustal segment of mostly uncertain origin and age (Archean and/or Proterozoic).

The Assean Lake deformation zone, which separates the SLB and the OLB, consists of cataclastic rocks and mylonites derived from both domains. The more restricted Lindal Bay fault zone along the northern part of Assean Lake, separates a southern slice from the main part of the OLB.

One objective of this study is to evaluate the presence and extent of Archean tectono-metamorphism and magmatism - prior to the Paleoproterozoic orogenic overprint - along the northwestern Superior cratonic margin. The objective of further mapping and sampling on Assean Lake is to unravel the provenance, evolution and relationship of the main lithologies of the SBZ and tectonic domains within it.

GENERAL GEOLOGY

The distribution of the major geological domains and their structural subdivisions are illustrated in Figure GS-6-1. The Assean Lake deformation zone separates rock assemblages of the SLB and the OLB, which are distinct in composition and metamorphic grade. Based on petrographic

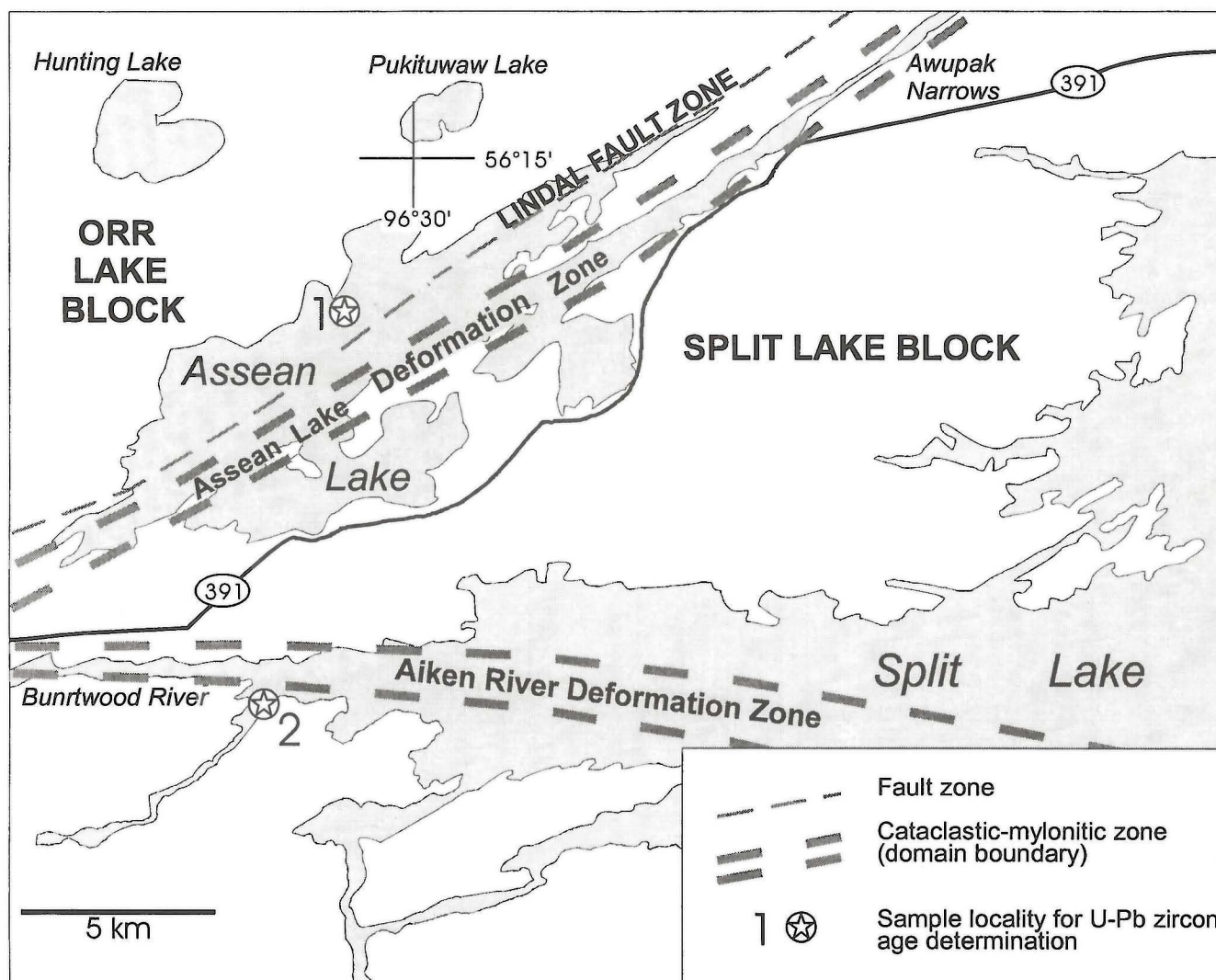
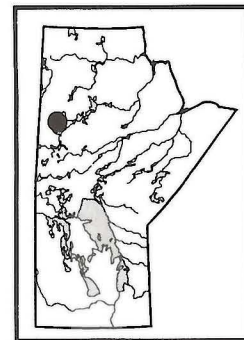


Figure GS-6-1: General geology of the Assean Lake area.

and field observations, the Archean lithologies of the SLB represent granulites, which underwent medium and low grade retrogression. In contrast, mineral parageneses of the gneisses in the OLB show no evidence of relic granulite grade texture but indicate partially retrogressed medium to upper amphibolite grade. Both the lithologies in the SLB and OLB underwent extensive polyphase deformation including the development of an early metamorphic layering, folding, development of a regional fabric, migmatitization, cataclasis and small-scale refolding followed by late shearing and faulting.

The following structural zones and corresponding lithologies are described from south to north. Unit numbers refer to Preliminary Map 1997S-3 (Böhm, 1997).

SLB - SUPERIOR PROVINCE (UNITS 1 TO 4)

The main lithologies in the SLB on Assean Lake are mafic and felsic granulites that are the product of polyphase metamorphism. Metamorphic mineral assemblages and relic granoblastic textures are preserved from both Archean and Paleoproterozoic tectono-metamorphic events.

Amphibolite, metagabbro and associated gneiss (1) are massive and compositionally layered. They occur as lensoid bodies and rafts in tonalite-granodiorite gneiss (2). The primary layering in the mafic lenses is locally at an angle to the metamorphic layering in the felsic gneiss, suggesting that deformation of the mafic granulites included boudinage and rotation. Formation of coarse-grained hornblende-plagioclase melt pods after primary pyroxene-plagioclase±hornblende is attributed to high grade metamorphism at about 2696 Ma (Böhm *et al.*, 1997). The tonalite-granodiorite gneiss (2) intruded prior to and/or during this high grade metamorphic event. Unit 2 felsic gneiss contains up to 25% hornblende as pseudomorphs after pyroxene and primary hornblende. Schlieren-like layers of hornblende and hornblende-plagioclase neosome, in the felsic granulites, are parallel to the metamorphic layering.

Layered hornblende and hornblende-biotite gneiss (3) is most likely the product of agmatization and formation of tonalite-granodiorite neosome, derived from units 1 and 2. Minor bodies of granite, augen gneiss and pegmatite (4) are either syntectonic melt products, from the felsic granulites formed during the main migmatization phase, or formed from later boudinated dykes, which crosscut the mafic and felsic granulites.

ASSEAN LAKE DEFORMATION ZONE

A major northeast-trending belt of cataclastic rocks and mylonites follows Assean River (Awupak Narrows) and continues along Little Assean Lake. A northern cataclastic zone can be distinguished from a mylonitic zone in the south. Based on structural and petrographic mapping, the relatively narrow southern mylonite zone is mainly composed of layered mylonites (5), derived from units 1 to 4, and consistently shows dextral shearing (minor Z folds, shear bands, c-s structure and rotated clasts).

In the northern cataclastic zone, highly deformed gneisses from both the SLB and the OLB were identified. They include layered tonalitic to granitic and mafic cataclastic gneiss (6a), potentially derived from units 1 to 4, and the OLB cataclastic gneiss and mylonites (6b), potentially derived from units 7 and 8. Shearing in this cataclastic zone is also dextral. Extensive intrafolial folding of the primary and metamorphic layering with doubly plunging minor folds indicates refolding during migmatitic and cataclastic deformation.

A key outcrop along the northern rim of the cataclastic zone shows a set of mafic dykes (12) crosscutting, and thus postdating the cataclastic structures in metavolcanic and metasedimentary gneisses (units 7 and 8). Moreover, a weak internal fabric is developed in the mafic dyke, parallel and potentially related to the mylonitic fabric in the southern mylonite zone. The main phase of cataclastic deformation might be contemporaneous with the development of the dominant regional fabric and migmatization, which occurred prior to dyke emplacement and late mylonitic deformation. However, the intense cataclasis and mylonitization in the Assean Lake deformation zone pervasively overprinted earlier structures. Even the composition of these tectonites was not always clearly recognized.

Along the south shoreline of the Awupak Narrows, leucocratic granitic gneiss (13) most likely represents a mylonitic to cataclastic marginal zone of the ca. 1820 Ma old Fox Lake granite (Heaman, unpubl. data).

Therefore mylonitization, which affects all lithologies in the Assean Lake deformation zone, must have occurred after ca. 1820 Ma.

OLB - Assean Lake south segment (units 7, 8, 10, 11)

Mafic and felsic schists and gneisses of presumably volcanogenic and sedimentary origin (units 7 and 8, respectively) form the main lithologies between the Assean Lake deformation zone and the Lindal Bay fault zone. Depending on the degree of deformation, part of units 7 and 8 might be identified as rocks equivalent to OLB lithologies north of the fault zone (see below).

Granitic to tonalitic and pegmatitic gneisses (10 and 11) are exposed mainly along the southeast shoreline of the northeast bay. In general, units 7 to 11 are strongly layered, foliated and isoclinally folded. Compared to unit 2 in the SLB domain, the felsic gneisses in the southern OLB are not interlayered with mafic gneisses and lack of granulitic texture.

Lindal Bay fault zone

A relatively narrow northeast-trending fault zone in the southern part of the OLB lithological assemblage on Assean Lake is subparallel and contemporaneous with the Assean Lake deformation zone. Whereas the northeastern part of the fault zone is relatively well defined and nicely traced by the northeastern branch of Assean Lake (Lindal Bay), its southwestern continuation is less definite. Shearing tends to be sinistral along the fault zone.

OLB - Assean Lake main segment (units 7 to 12)

Layered amphibolites (7: metabasalt to meta-andesite) form a larger complex in the most northeastern part of Assean Lake and include minor lenses of ultramafic and volcanogenic metasedimentary rocks. Amphibolite is locally interlayered with greywacke-derived gneiss or forms lensoid bodies within the metasediments (8).

Metasedimentary rocks (8) in the northern part of Assean Lake include staurolite-bearing metagreywacke, garnet-biotite gneiss and interlayered psammitic and pelitic gneiss. Coarse-grained mobilizate pods in pelitic layers in metagreywacke contain cordierite-sillimanite-garnet in a quartz feldspar matrix formed during medium to high grade peak metamorphism.

In the western part of the lake, hornblende-magnetite-bearing migmatitic feldspathic gneiss (9) is closely associated with metasedimentary rocks (8) as well as igneous gneisses (10). Contacts are generally subconcordant and deformed. Minor metagabbroic dykes and sills intrude the felsic migmatites (9).

The predominant rocks along the northern shoreline are tonalite to granodiorite gneisses (10). Their texture ranges from compositionally layered to massive or pegmatitic, depending on primary composition and degree of deformation. Where associated with amphibolite, the tonalite to granodiorite gneisses contain hornblende-rich layers and/or disseminated hornblende, similar to the tonalite-granodiorite gneiss (2) in the SLB.

Bodies of leucocratic granite and granitoid pegmatite (11) are most abundant in the northeast of Assean Lake and generally grade into tonalite-granodiorite gneisses (10). All pegmatites are deformed in the late mylonitization.

Along the northern shoreline of Assean Lake numerous mafic, ultramafic and gabbroic dykes (12) were intruded into units 10, 11, and locally 8. The width of the generally east-west trending dykes ranges from a few decimetres to tens of metres. Contacts with the felsic gneiss and pegmatites (11) are commonly discordant to slightly oblique. In addition, a highly foliated transitional zone of (±hornblende) biotite-rich schists and quartzo-feldspathic lenses with minor sulphides, is generally developed (mafic pegmatite). In a few cases, the mafic dykes are crosscut by pegmatites, the latter being boudinaged. The margins of the mafic dykes are always fine-grained, whereas the central parts range from fine-grained (basaltic) to coarser-grained (diabasic, metagabbroic) depending on degree of deformation and width of the dyke.

PRELIMINARY U-PB ZIRCON AGE DETERMINATIONS AND GEOLOGICAL CONSEQUENCES

Preliminary U-Pb zircon age data for a representative tonalite-granodiorite gneiss (9) from the northwestern Assean Lake (Fig. GS-6-1, U-Pb zircon sample locality #1) provide evidence for the presence of pre-

3.0 Ga old crust in the SBZ. Since the dated sample represents the predominant lithology along the northwestern Assean Lake, a pre- 3.0 Ga origin for most of the gneisses in the OLB must be considered. In addition, preliminary U-Pb zircon age data for a felsic augen gneiss from the mouth of the Burntwood River into Split Lake (Fig. GS-6-1, U-Pb zircon sample locality #2) similarly indicate a pre- 3.0 Ga origin for the southern part of the SBZ. The new geochronological results are in clear contrast to the traditional interpretation of the SBZ as a crustal segment of the Churchill Province, formed during Paleoproterozoic Churchill-Superior collision. Since composition and metamorphic grade of the main lithologies are different in the SLB and OLB segments, the SBZ in the Assean Lake area most likely represents a segment of Archean crust that was separate from the Superior Province during 2696 Ma regional high grade metamorphism (Böhm *et al.*, 1997). The main elements of the SBZ could have been amalgamated to the northwestern margin of the Superior craton during the late Archean, particularly if the main part of the OLB also turns out to be Archean.

The new age determinations and the current geochronological investigations on lithologically comparable units from distinct tectonic domains will potentially reveal the full extent and exact age of the high grade Archean crustal segments along the northwestern margin of the Superior craton.

REFERENCES

- Böhm, Ch.O.
 1997: Geology of the Assean Lake area (part of 64A 1,2,7,8); Manitoba Energy and Mines, Minerals Division, Preliminary Map 1997S-3.
- Böhm, Ch.O. Heaman, L.M. and Corkery, M.T.
 1997: Tectonic evolution of the western Superior craton margin: U-Pb zircon results from the Split Lake Block, Geol. Assoc. Can. Program Abstr., A-14.
- Corkery, M.T.
 1985: Geology of the lower Nelson River project area; Manitoba Energy and Mines, Geological Report GR82-1, 66p.
- Corkery, M.T. and Lenton, P.G.
 1990: Geology of the lower Churchill river region; Manitoba Energy and Mines, Geological Report GR85-1 (maps GR85-1-5 to GR85-1-9)

GS-7 GEOCHEMICAL AND STRUCTURAL ANALYSIS OF GOLD MINERALIZATION AT THE BURNT TIMBER MINE, LYNN LAKE (PART OF NTS 64C/15)

by D. C. Peck and A. M. Eastwood¹

Peck, D.C. and Eastwood, A.M., 1996. Geochemical and structural analysis of gold mineralization at the Burnt Timber mine, Lynn Lake (part of NTS 64C/15); in Manitoba Energy and Mines, Report of Activities, 1997, p. 50-60.

SUMMARY

Geological and geochemical studies of the Burnt Timber mine indicate that the gold mineralization is contained in zones of intense deformation and silicification within the Johnson shear zone, a laterally continuous ductile to brittle deformation zone. Introduction of gold into mafic to intermediate metavolcanic rocks and subordinate intermediate metasedimentary rocks occurred prior to a major period of folding that post-dated easterly trending regional isoclinal folding, and ductile deformation along the shear zone. Mineralization consists of open space fillings, in both metavolcanic and metasedimentary rocks, which produced auriferous quartz-pyrite veins. Gold mineralization also occurs in aplite and quartz veins that cut a penetrative foliation related to ductile deformation along the Johnson shear zone. The Burnt Timber deposit is therefore similar to several other gold occurrences along the Johnson shear zone, which were formed during a period of brittle deformation subsequent to a period of intense ductile deformation. At the Burnt Timber mine, a later period of folding and cleavage development post-dates deposition of the gold mineralization.

Despite the structural complexities and metasomatism associated with the development of the veins and intense cataclasis and folding, the protolith composition in the host supracrustal rocks can be recognized using immobile trace element geochemistry. Preliminary results suggest that the host rocks have a strong affinity to calc-alkaline andesitic units occurring to the east of the deposit, rather than to tholeiitic basalt sequences that are documented to the north of the mine site. It does not appear that the host-rock composition played a significant role in localizing the gold.

INTRODUCTION

The Burnt Timber (BT) gold deposit is hosted by the Southern volcanic belt of the Wasekwan Group in the Lynn Lake greenstone belt (Fig. GS-7-1). It is situated along the Johnson shear zone, a >40 km long, easterly-striking linear deformation zone that hosts a number of gold deposits and occurrences (Fedikow *et al.*, 1991). The BT deposit was mined by open pit methods from 1993 to 1996. The deposit is reported to have contained 1.23 million tonnes of ore at startup, with an average grade of 2.85 g of gold per tonne (Richardson and Ostry, 1996). The deposit occurs in the hanging wall of the T1 fault, a late (post-mineralization) brittle fault developed along and sub-parallel to the Johnson shear (Fig. GS-7-1, 2).

The current study was prompted by discussions held between MEM and Black Hawk Mining Incorporated. Difficulties resolving primary lithologies in and adjacent to the BT Mine have precluded establishment of a definitive mine stratigraphy. These difficulties reflect limited outcrop in the area, intense reworking of primary textures and compositions during the development of the Johnson shear zone and the T1 fault, and a lack of detailed structural and geochemical data. A preliminary geochemical and structural study was undertaken in order to address these problems.

The principal objectives of the current study are: (1) better characterize the chemistry and textures of the host rocks; (2) investigate the controls on gold mineralization at the BT Mine.

GEOLOGY OF THE BURNT TIMBER GOLD DEPOSIT

The geology of the BT deposit is summarized by Eastwood (*in* Richardson and Ostry, 1996). A general geological map for the BT mine area, based strictly on 1:50,000 mapping (Gilbert *et al.*, 1980), is given in Figure GS-7-2. Gold mineralization occurs as finely distributed native gold associated with fine-grained disseminated and fracture-controlled pyrite, minor galena and/or chalcopyrite and, rarely, sphalerite. The host rocks are sheared and strongly altered metabasaltic and possible metasedimentary rocks that are correlative with a regionally extensive, easterly-striking sequence of metagreywackes and metabasalts (units 2

and 9, Gilbert *et al.*, 1980, Cockeram Lake sheet).

Gold mineralization in the Burnt Timber deposit occurs largely to the north and within 40 metres of the T1 fault. However, local high grade auriferous quartz veins occur to the north of the main deposit. Gold mineralization occurs in north-dipping fracture zones within hanging wall metavolcanic and metasedimentary rocks. The zones are recognized by increasing abundances of quartz and/or pyrite veins that commonly contain carbonate and chlorite. Within the main ore zones, gold grades correlate with the intensity of shear lamination, silicification, pyritization and brittle fracturing. Mineralization also occurs in association with pyrite-quartz veins that cut folded and fractured aplite and granite veins. The highest grades are present in rocks containing both pyrite and galena (Richardson and Ostry, 1996).

Pervasive silicification and polyphase deformation have obliterated primary fabrics and modified the chemistry of the host rocks. Intense carbonate + talc + chlorite alteration is largely confined to unmineralized ultramafic schists (pyroxenitic dykes) and unmineralized metavolcanic rocks in the immediate footwall environment. Granitic veins and dykes, broadly conformable with the predominant S_1 cleavage (easterly-striking), are commonly observed in the hanging wall sequence.

PRELIMINARY STRUCTURAL STUDIES AT THE BURNT TIMBER MINE

The Burnt Timber deposit is located on the southern limb of a major, easterly trending anticlinal fold (Gilbert *et al.*, 1980) and within an east-trending zone of ductile to brittle deformation (Johnson shear zone). Structural studies at the BT mine have focused on the relationships between a penetrative foliation (S_1), mineralized quartz-pyrite veins and a series of northeast-plunging folds with northwest-trending axial planes (F_2 folds). Preliminary structural and petrographic studies suggest that the S_1 fabrics in the Burnt Timber mine reflect intense ductile deformation along the Johnson shear zone (Fig. GS-7-2), including granulation, annealing and tectonically-induced compositional banding. Fabrics related to regional isoclinal folding have not been recognized. The F_2 folds were first recognized during mining, and they clearly post-date the penetrative S_1 foliation. F_2 folds are asymmetric, tight, inclined folds that affected all of the units observed in the hanging wall, including all mineralized quartz, sulphide and granitic veins. Minor structures associated with F_2 folding include crenulation cleavages, parasitic folds, intrafolial folds defined by granite and quartz veins, boudinage and kink folds.

The T1 fault separates mineralized hanging wall rocks from barren footwall rocks. Eastwood (*in* Richardson and Ostry, 1996) described the T1 fault as a post-mineralization fault that strikes N70° to N80° E and dips at approximately 60° N. The fault is characterized by tectonic breccia and fault gouge, and is several tens of centimetres to a few metres wide. The T1 fault forms a pronounced lineament recognizable on air photographs, and truncates all major fold structures and foliations in the hanging wall sequence.

More detailed structural investigations are planned for 1998.

PETROLOGY OF THE MINE SEQUENCE

Thirty samples were collected from drillhole 95-BTE-01 (Fig. GS-7-2), which intersected hanging wall supracrustal rocks containing numerous quartz, quartz + pyrite and granitic veins, the T1 fault and footwall metabasaltic rocks. Sampling focused on the least altered supracrustal rocks, but it was not possible to completely avoid pyrite mineralization or quartz veins.

The major rock units recognized in the drill core include: (1) 0 to 70 m; fine- to medium-grained, dark green to grey, mafic to intermediate metavolcanics ("hanging wall metabasalts"; mine terminology); (2) 70 to 80 m; pale green, fine grained, schistose intermediate metavolcanics; (3)

¹ Black Hawk Mining, Inc., Lynn Lake, Manitoba

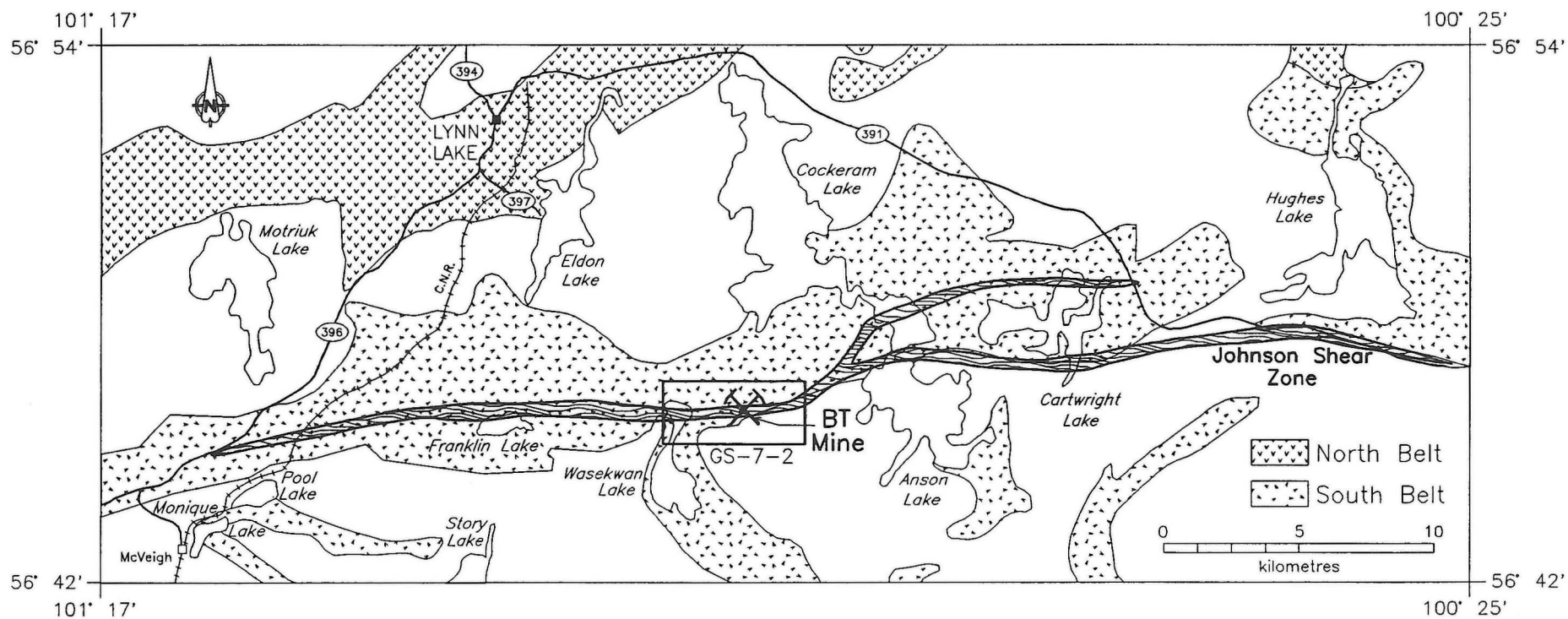


Figure GS-7-1: Location of the Burnt Timber gold mine, Lynn Lake greenstone belt.

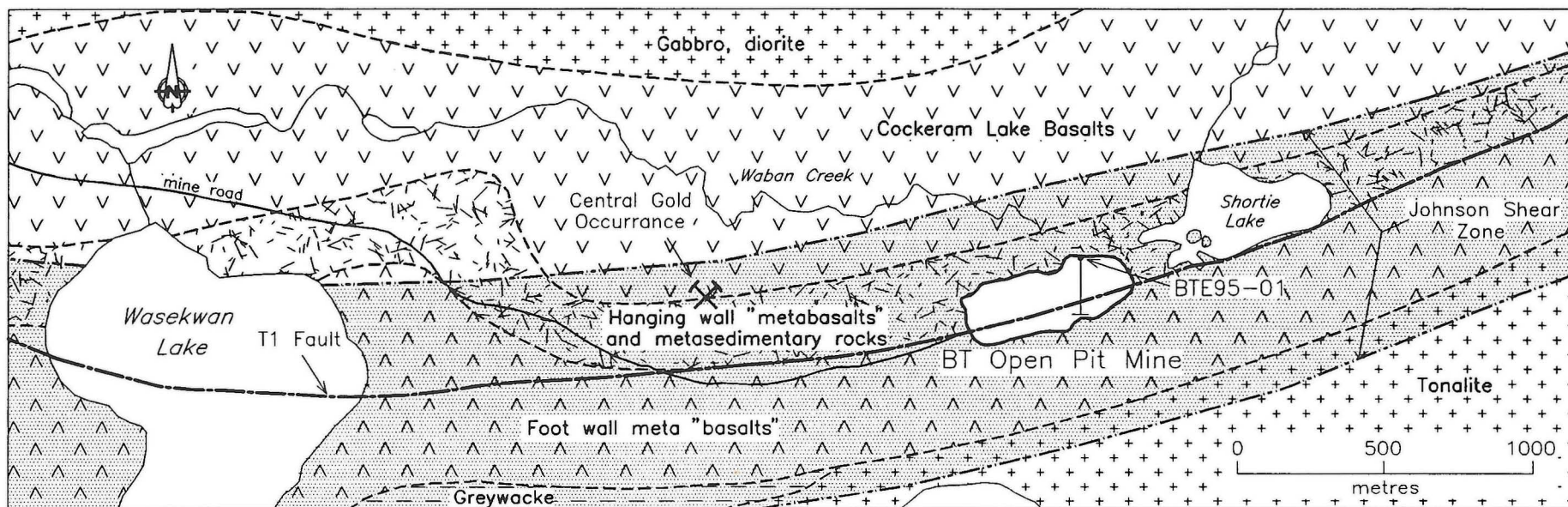


Figure GS-7-2: General geology of the Burnt Timber mine area. Geology modified from Gilbert et al. (1980).

80 to 102 m; biotite-rich, intermediate schists (possible metasedimentary rocks) and granitic veins; (4) 103 to 105 m; mafic to ultramafic schist adjoining chloritic fault gouge that defines the T1 fault; and, (5) >105m; dark green, schistose and carbonatized footwall "metabasalt" (mine terminology).

The hanging wall metabasalts locally contain up to 10% subhedral, variably preserved plagioclase phenocrysts. However, most of these rocks are aphyric, finely laminated and foliated and consist of biotite + albite + quartz \pm amphibole \pm K-feldspar \pm chlorite \pm sericite \pm magnetite, consistent with greenschist facies metamorphism. In thin section, the metabasaltic rocks display a microlamination that formed during ductile deformation, and sense of motion indicators such as rotated porphyroclasts, augen tails and shear bands suggest a predominant dextral motion along the penetrative S_1 foliation plane. Hanging wall rocks of intermediate to felsic composition are enriched in biotite and quartz at the expense of amphibole and albite, and tend to develop a more planar and finely laminated cleavage in comparison to basaltic units. Even in the granitic veins, which cut and therefore postdate the S_1 fabric in the metavolcanic rocks, a penetrative fabric that is subparallel with the S_1 cleavage, is developed. This suggests a protracted period of deformation along the Johnson shear zone. A spaced cleavage (S_2 fabric) is locally developed along axial planes of F_2 minor folds, and needle-like amphibole porphyroblasts are parallel to the S_2 cleavage and locally preserve the S_1 cleavage in the form of magnetite inclusion trails. Thin to thick (<1 cm to several tens of cm) fine- to medium-grained, polygonal quartz, calcite, quartz + calcite, and granitic veins occur throughout the hanging wall metabasalts. Many of the veins are sub-parallel but clearly discordant to the primary shear fabric in the host rocks but have been folded and recrystallized during the F_2 folding event and post-date the development of the spaced cleavage. Late sericite alteration has affected some of the quartz veins.

Pyrite mineralization is sporadically developed within quartz (carbonate) veins and as disseminations throughout all of the principal rock types in the hanging wall sequence. Pyrite typically occurs in fine-grained monomineralic veinlets and as fine-grained disseminations in quartz and granitic veins. Trace amounts of sphalerite and chalcopyrite locally occur in association with pyrite. All of the sampled pyrite-bearing veins contain anomalous concentrations of gold (Table GS-7-1).

The footwall metabasalts display similar megascopic features to the least deformed hanging wall metabasalts, including the mineralogy, grain size and style and intensity of veining. In thin section, however, the footwall rocks are distinguished by a less well-defined mylonitic fabric, more intense carbonate alteration and better preservation of igneous textures.

The intermediate schists separating the hanging wall and footwall metabasalts are distinguished from the metabasalts by a more pronounced tectonic (S_1) fabric and higher quartz (disseminated and vein) contents. The schistose metavolcanics occurring between 70 to 80 m depth appear to represent a gradual textural and mineralogical transition from the basalts to the north to the intermediate schists to the south. The intermediate schists are well foliated and biotite-rich, and grade from protomylonite to mylonite, in which the S_1 fabric is defined by alternating, <0.1 to 1 mm wide quartzo-feldspathic and semi-pelitic bands (biotite \pm chlorite \pm sericite \pm albite). Thin, conformable quartz + carbonate veins are commonly present in the schists, as are pink to white, K-feldspar and muscovite-bearing aplite and medium-grained granitic veins.

The nature of the protolith for the intermediate schists is equivocal. Along the wall of the mine, the schists have the appearance of fine-grained clastic metasedimentary or volcanoclastic rocks (greywacke, siltstone, mudstone or intermediate, reworked pyroclastic rocks), based on irregular, megascopic (cm-scale) compositional banding and enrichment in biotite and quartz in comparison to the adjacent metavolcanic rocks. However, neither drill core nor petrographic studies revealed conclusive sedimentary features in the schists. The primary fabrics of all of the hanging wall rocks, including many of the quartz and granitic veins, has been largely obliterated by tectonic reworking during the development of the S_1 and S_2 fabrics. Throughout the BT mine area, the intensity of foliation and the abundance of veins increases gradually, although not systematically, towards the T1 fault. The history of movement along the T1 fault is not known, although

the fault truncates both S_1 and S_2 foliations and related folds, and appears to superimpose tectonically and mineralogically distinctive blocks (mineralized and mylonitic hanging wall sequence; unmineralized, carbonatized and less deformed footwall metabasalts).

GEOCHEMISTRY OF THE MINE SEQUENCE

Thirty core samples from DDH# 95-BTE-01 were analysed for major elements, Au, Ag, S, Cu, Pb and Zn and selected lithophile trace elements at Manitoba Energy and Mines' Analytical Laboratories. A subset of these samples was analysed for additional trace and rare-earth elements (REE) at Activation Laboratories (Ancaster, Ontario). The data are presented in Tables GS-7-1 and GS-7-2.

Controls on gold abundance

No correlation exists between Au abundance and proximity to the T1 fault, however, Au contents are known to correlate with the intensity of pyrite mineralization and abundance of quartz veins. Graphical and statistical analysis of the data returned few significant correlations between rock compositions and gold content. A weak positive correlation between Au, S and Cu abundances exists (e.g., Fig. GS-7-3). A weak negative correlation exists between Au, Ba and K abundances (e.g., Fig. GS-7-4). The lack of significant correlations between the abundances of Au and lithophile trace elements, base metals and major elements suggests that the localization of the mineralization was not controlled by the host rock chemistry. Even the talc-carbonate schist, which appears to cut the S_1 fabric (pyroxenite dyke?), contains anomalous Au mineralization. The most important control on Au deposition appears to have been structural - i.e., ground preparation associated with deformation along the Johnson shear zone. Emplacement of gold-bearing quartz and pyrite veins followed development of the S_1 cleavage and predated F_2 folding.

Geochemical characteristics of the host rocks

In comparison to proximal basaltic units of the Southern Belt (Syme, 1985; Peck, 1986) the hanging wall metabasalts (including andesitic rocks) have lower Mg# (28 to 55; Table GS-7-1), CaO (<7.4%) and TiO₂ (<0.86%) and much higher K₂O (1.3 to 3.4%). They are very different in composition to basaltic andesites and andesites from either the Cockerm Lake or McVeigh Lake metabasaltic sequences (Gilbert *et al.*, 1980; Syme, 1985), which display higher TiO₂ and FeO at equivalent SiO₂ abundances. In terms of major element abundances, andesites from the Hughes Lake and Cartwright Lake calc-alkaline suites (Syme, 1985; Peck, 1986) are the best known analogues for the Burnt Timber metabasalts, although the low CaO and high total alkali abundances of the Burnt Timber samples are distinctive. Calcium abundances in the Burnt Timber metabasalts correlate strongly with loss on ignition, MgO, Cr, Ni and Sc, suggesting preferential addition of carbonate to the most primitive basaltic units. The footwall metabasalts contain lower SiO₂, Al₂O₃ and K₂O and higher Fe₂O₃, MgO and TiO₂ than most of the hanging wall metabasalts.

Two samples from the transitional schistose metavolcanic unit (70 to 80 m) are characterized by extremely low CaO contents, and contain lower TiO₂ and P₂O₅ than the hanging wall metabasalts.

The siliceous schists have distinctive low TiO₂, CaO and P₂O₅ abundances and, unlike the hanging wall basalts, display systematic chemical changes approaching the T1 fault (Tables GS-7-1, 2). These changes include increasing Al₂O₃, Fe₂O₃, CaO and MgO and corresponding decreasing SiO₂ abundances. These changes could be primary (magmatic differentiation; graded sedimentary bed) or relate to systematic metasomatism during the development of the gold mineralization.

In DDH# 95-BTE-01, the T1 fault truncates a MgO-rich schist. One sample of the schist contains 10.3% MgO, much greater than any of the basaltic units intersected in the drillhole. The high LOI value is consistent with extensive alteration and development of a secondary talc + carbonate assemblage from a pyroxenite or melagabbro precursor.

The major and trace element geochemistry indicates that most of the metabasaltic rocks are andesites having calc-alkaline affinities, with a few samples falling in the basaltic andesite and basalt fields (e.g., see total alkali - silica diagram, Fig. GS-7-5). A few samples have apparent alkaline affinities (possibly related to potassic alteration along the Johnson shear zone) but most are sub-alkaline in composition (Fig. GS-7-5). At this stage, it is not possible to quantify the effects of metasomatism in the rocks,

Table GS-7-1
Major, trace and precious metal abundances in drill core 95-BTE-01, Burnt Timber Mine
Major Elements

Sample#	Depth (m)	Rock Type	SiO ₂	Al ₂ O ₃	Fe ₂ O ₃	CaO	MgO	Na ₂ O	K ₂ O	TiO ₂	P ₂ O ₅	MnO	LOI	S	TOTAL
			%	%	%	%	%	%	%	%	%	%	%	%	%
Hangingwall															
98-95-100-1	9.4	Gabbro	48.3	19.09	7.74	7.23	2.44	5.47	2.17	0.84	0.45	0.13	4.9	0.07	98.8
98-95-100-2	15.85	Andesite	54.4	15.73	10.37	4.54	3.09	2.93	2.15	0.78	0.20	0.12	3.5	0.25	98.1
98-95-100-3	18.3	Andesite	59.7	15.92	9.51	4.09	2.33	2.41	2.23	0.72	0.17	0.11	2.3	0.18	99.7
98-95-100-4	23.2	Andesite	58.5	15.67	9.16	5.38	2.46	3.18	1.45	0.78	0.20	0.14	2.5	0.05	99.5
98-95-100-5	26.2	Andesite	57.8	15.42	9.36	4.87	2.29	2.98	2.72	0.75	0.19	0.12	3.1	0.15	99.8
98-95-100-6	31	Andesite	54.0	15.53	8.99	4.61	2.43	2.97	3.42	0.75	0.18	0.11	3.4	0.09	96.5
98-95-100-7	33.55	Andesite	58.1	15.50	8.91	4.48	2.55	3.55	2.15	0.76	0.17	0.14	3.6	0.11	100.0
98-95-100-8	36.1	Andesite	58.8	15.83	8.83	5.27	2.25	2.26	2.93	0.75	0.16	0.14	2.9	0.02	100.1
98-95-100-9	39.15	Andesite	57.4	15.93	10.03	5.03	2.80	3.23	1.50	0.86	0.17	0.16	2.7	0.04	99.8
98-95-100-10	43.9	Andesite	58.6	15.24	9.13	4.64	2.41	3.26	1.89	0.80	0.19	0.14	2.9	0.02	99.2
98-95-100-11	47.5	Andesite	58.5	14.89	8.94	4.44	2.50	3.45	1.89	0.80	0.17	0.14	3.6	0.00	99.3
98-95-100-12	51.25	Andesite	55.2	14.93	8.85	5.39	3.64	3.43	1.89	0.78	0.17	0.12	4.4	0.09	98.9
98-95-100-13	55.4	Basalt	50.9	12.79	9.11	7.03	5.76	3.45	1.26	0.80	0.17	0.15	7.1	0.50	99.0
98-95-100-14	59	Andesite	56.2	14.49	9.15	5.96	3.10	2.61	2.83	0.76	0.17	0.16	4.6	0.27	100.3
98-95-100-15	61.35	Andesite	57.2	14.96	9.68	4.53	2.82	3.17	2.90	0.75	0.16	0.12	3.2	0.47	99.0
98-95-100-16	66.4	Andesite	49.4	12.60	9.50	7.38	7.25	1.41	2.68	0.74	0.19	0.15	7.9	0.19	99.4
98-95-100-17	70.6	Andesite	57.0	13.59	9.48	4.32	5.20	3.31	1.32	0.30	0.06	0.13	3.4	0.13	98.2
98-95-100-18	74.4	Andesite	59.2	13.42	8.80	3.24	4.26	4.20	2.00	0.33	0.05	0.12	3.5	0.39	99.5
98-95-100-19	77.8	Aplite	62.7	13.92	4.38	3.87	1.37	7.46	0.47	0.33	0.12	0.07	2.8	1.64	99.1
98-95-100-20	81.4	Schist	66.5	12.73	7.63	0.69	3.81	3.26	2.02	0.34	0.09	0.12	1.8	0.23	99.2
98-95-100-21	84.5	Schist	64.2	13.41	9.23	0.76	4.12	2.60	2.72	0.33	0.08	0.17	1.9	0.21	99.7
98-95-100-22	88.6	Schist	58.6	13.71	9.64	1.90	5.65	3.20	2.59	0.34	0.06	0.15	2.6	0.15	98.6
98-95-100-23	90.4	Schist	52.2	14.52	11.01	3.86	6.00	2.74	3.13	0.56	0.06	0.13	5.0	0.11	99.3
98-95-100-24	95.5	Granite Vein	71.6	11.79	6.08	1.17	0.85	4.50	0.76	0.29	0.08	0.04	1.6	1.14	99.9
98-95-100-25	98	Granite Vein	67.5	12.78	5.34	1.63	1.34	5.46	0.80	0.31	0.12	0.05	2.0	0.74	98.1
98-95-100-26	101	Granite Vein	66.6	11.22	6.47	3.11	1.81	4.16	0.88	0.27	0.10	0.06	2.9	0.69	98.3
98-95-100-27	103.6	Mafic Schist	39.3	8.75	9.02	12.20	10.26	2.14	1.00	0.98	0.03	0.23	13.4	0.44	97.8
Footwall															
98-95-100-28	105.5	Basalt	48.0	14.49	10.17	6.44	5.64	2.63	2.35	1.00	0.21	0.13	8.2	0.08	99.3
98-95-100-29	109.7	Basalt	44.4	13.05	10.44	9.31	5.96	2.72	0.89	0.99	0.18	0.15	10.6	0.07	98.8
98-95-100-30	110.7	Basalt	47.8	14.93	11.20	7.37	4.38	3.60	0.58	1.10	0.20	0.15	8.0	0.13	99.4

Trace Elements

Sample#	Depth (m)	Rock Type	Cu	Ba	Rb	Sr	V	Cr	Co	Ni	Cu	Zn	Au
			ppm	ppm	ppm	ppm	ppm	ppm	ppm	ppm	ppm	ppm	ppb
Hangingwall													
98-95-100-1	9.4	Gabbro	347	987	37	782	162	20	26	7	347	108	34
98-95-100-2	15.85	Andesite	150	846	44	215	164	52	36	16	150	132	30
98-95-100-3	18.3	Andesite	115	544	47	253	161	27	31	12	115	119	<6
98-95-100-4	23.2	Andesite	58	564	28	277	176	22	35	11	58	118	<6
98-95-100-5	26.2	Andesite	68	680	56	224	169	24	29	10	68	115	7
98-95-100-6	31	Andesite	58	761	75	195	216	18	30	7	58	144	10
98-95-100-7	33.55	Andesite	66	461	46	246	191	18	25	7	66	108	332
98-95-100-8	36.1	Andesite	52	774	64	238	180	18	27	7	52	105	9
98-95-100-9	39.15	Andesite	54	547	33	270	192	21	29	<5	54	122	<6
98-95-100-10	43.9	Andesite	31	541	36	261	178	19	32	<5	31	124	14
98-95-100-11	47.5	Andesite	44	470	39	234	179	18	29	<5	44	112	47
98-95-100-12	51.25	Andesite	67	395	46	235	172	116	38	36	67	102	33
98-95-100-13	55.4	Basalt	105	309	29	153	216	401	40	120	105	127	1072
98-95-100-14	59	Andesite	74	642	58	206	159	29	35	15	74	138	41
98-95-100-15	61.35	Andesite	66	552	67	171	158	24	30	17	66	120	455
98-95-100-16	66.4	Andesite	81	335	63	145	236	652	47	202	81	124	266
98-95-100-17	70.6	Andesite	92	203	29	102	252	120	37	34	92	119	32
98-95-100-18	74.4	Andesite	197	193	42	69	214	39	44	11	197	81	1307
98-95-100-19	77.8	Aplite	51	114	11	155	83	60	28	17	51	25	3773
98-95-100-20	81.4	Schist	110	226	41	67	79	<10	23	<5	110	127	234
98-95-100-21	84.5	Schist	206	285	50	47	125	<10	32	<5	206	298	203
98-95-100-22	88.6	Schist	88	242	54	78	210	28	33	13	88	148	95
98-95-100-23	90.4	Schist	75	406	64	98	256	113	42	46	75	73	54
98-95-100-24	95.5	Granite Vein	119	178	17	71	<20	<10	40	<5	119	97	260
98-95-100-25	98	Granite Vein	54	205	18	95	47	<10	31	<5	54	27	405
98-95-100-26	101	Granite Vein	74	328	21	133	63	56	31	10	74	124	211
98-95-100-27	103.6	Mafic Schist	43	253	28	228	256	911	56	350	43	1560	297
Footwall													
98-95-100-28	105.5	Basalt	78	539	45	220	233	137	37	50	78	113	32
98-95-100-29	109.7	Basalt	106	226	17	180	250	351	49	101	106	102	<6
98-95-100-30	110.7	Basalt	106	171	14	212	257	60	43	22	106	99	<6

Table GS-7-2

Rare earth and selected additional trace element abundances in drill core 95-BTE-01, Burnt Timber Mine

Sample#	Depth (m)	Rock Type	Sc	Ga	Ge	Y	Zr	Nb	Mo	Sn	Sb	Cs
	<i>Hangingwall</i>		ppm	ppm	ppm	ppm	ppm	ppm	ppm	ppm	ppm	ppm
98-95-100-1	9.4	Gabbro	46	18	1.6	24.6	68.9	4.0	2.6	0.8	0.63	0.20
98-95-100-3	18.3	Andesite	27	18	1.7	21.5	74.3	3.2	2.6	1.1	0.42	0.51
98-95-100-7	33.5	Andesite	28	18	1.5	18.4	63.6	2.8	0.8	0.9	0.34	0.64
98-95-100-10	43.9	Andesite	27	18	1.7	17.9	68.8	3.2	2.1	2.3	0.22	0.44
98-95-100-12	51.2	Andesite	27	17	1.4	18.5	61.9	2.8	3.5	1.2	0.69	0.83
98-95-100-13	55.4	Basalt	27	15	1.5	18.5	62.7	3.0	0.9	1.0	0.42	0.61
98-95-100-15	61.4	Andesite	26	17	1.4	21.8	78.7	3.3	1.2	0.9	0.41	0.73
98-95-100-16	66.4	Basalt	28	14	1.3	16.5	58.7	3.5	0.9	0.7	0.49	0.90
98-95-100-19	77.8	Aplite	9	15	1.9	8.0	107	7.0	13.1	0.6	0.79	0.15
98-95-100-20	81.4	Schist	21	12	1.4	16.0	35.1	1.2	1.2	0.5	0.52	0.92
98-95-100-21	84.5	Schist	24	13	1.5	16.0	32.5	1.0	1.3	0.9	0.28	0.81
98-95-100-23	90.4	Schist	38	14	1.2	16.6	34.9	1.0	0.7	0.5	0.30	1.53
98-95-100-24	95.5	Schist	19	11	1.1	20.2	46.3	1.5	0.8	0.7	0.19	0.29
98-95-100-25	98	Granite Vein	21	12	1.3	28.2	42.1	1.4	0.6	0.7	0.18	0.46
98-95-100-27	104	Granite Vein	30	10	1.6	12.4	25.6	1.1	2.8	0.6	1.18	1.25
98-95-100-28	106	Granite Vein	30	17	1.5	17.3	69.6	4.3	0.4	0.7	0.64	0.23
	<i>Footwall</i>											
98-95-100-29	10:	Basalt	35	16	1.5	22.3	63.1	3.6	0.6	1.2	0.53	0.28
98-95-100-30	111	Basalt	37	17	1.2	26.6	71.7	4.1	1.5	1.0	0.85	0.28

Sample#	Depth (m)	Rock Type	La	Ce	Pr	Nd	Sm	Eu	Gd	Tb	Dy	Ho
	<i>Hangingwall</i>		ppm	ppm	ppm	ppm	ppm	ppm	ppm	ppm	ppm	ppm
98-95-100-1	9.4	Gabbro	5.70	13.5	1.57	8.47	2.82	0.990	3.28	0.65	4.22	0.87
98-95-100-3	18.3	Andesite	9.60	20.6	2.21	10.0	3.22	0.907	3.20	0.61	3.75	0.73
98-95-100-7	33.5	Andesite	7.56	16.5	1.80	9.28	2.42	0.906	2.61	0.48	3.09	0.64
98-95-100-10	43.9	Andesite	8.21	18.7	1.97	9.62	2.58	0.945	2.66	0.49	3.22	0.63
98-95-100-12	51.2	Andesite	7.66	16.7	1.90	9.34	2.75	0.866	2.86	0.53	3.09	0.66
98-95-100-13	55.4	Basalt	7.84	17.9	1.96	9.52	2.69	0.903	2.90	0.54	3.17	0.66
98-95-100-15	61.4	Andesite	8.97	19.7	2.26	10.7	2.94	0.882	3.36	0.56	3.47	0.78
98-95-100-16	66.4	Basalt	8.07	17.2	1.83	8.53	2.31	0.798	2.63	0.47	2.73	0.61
98-95-100-19	77.8	Aplite	27.1	51.3	4.65	18.1	3.31	0.853	3.16	0.34	1.40	0.24
98-95-100-20	81.4	Schist	2.47	5.94	0.64	3.59	1.11	0.351	1.39	0.35	2.35	0.58
98-95-100-21	84.5	Schist	2.60	6.14	0.65	3.48	1.07	0.358	1.47	0.34	2.37	0.58
98-95-100-23	90.4	Schist	3.31	7.47	0.85	4.22	1.33	0.539	1.83	0.38	2.46	0.58
98-95-100-24	95.5	Schist	4.12	10.1	0.94	5.05	1.62	0.450	1.86	0.44	2.96	0.72
98-95-100-25	98	Granite Vein	5.32	13.6	1.33	6.76	2.11	0.550	2.70	0.58	4.12	0.96
98-95-100-27	104	Granite Vein	5.09	10.3	1.16	5.69	1.65	0.620	1.77	0.32	1.97	0.41
98-95-100-28	106	Granite Vein	9.94	21.6	2.31	11.1	2.87	0.942	3.02	0.49	3.08	0.60
	<i>Footwall</i>											
98-95-100-29	10:	Basalt	8.11	16.0	1.88	9.47	2.92	1.01	3.23	0.60	3.81	0.82
98-95-100-30	111	Basalt	7.25	15.0	1.71	9.35	3.07	0.942	3.37	0.71	4.24	0.93

Sample#	Depth (m)	Rock Type	Er	Tm	Yb	Lu	Hf	Ta	W	Tl	Th	U
	<i>Hangingwall</i>		ppm	ppm	ppm	ppm	ppm	ppm	ppm	ppm	ppm	ppm
98-95-100-1	9.4	Gabbro	2.63	0.356	2.48	0.452	2.06	0.930	202	0.35	0.62	0.15
98-95-100-3	18.3	Andesite	2.36	0.324	2.57	0.421	2.25	0.558	11:	0.34	1.66	1.04
98-95-100-7	33.5	Andesite	1.99	0.287	2.21	0.371	2.05	0.395	84.8	0.35	1.41	0.71
98-95-100-10	43.9	Andesite	2.03	0.288	2.40	0.385	2.16	0.610	123	0.29	1.55	0.73
98-95-100-12	51.2	Andesite	2.00	0.300	2.14	0.355	2.00	0.469	104	0.30	1.22	0.71
98-95-100-13	55.4	Basalt	1.95	0.273	1.93	0.319	2.00	0.350	63.3	0.28	1.23	0.80
98-95-100-15	61.4	Andesite	2.30	0.343	2.65	0.439	2.45	0.498	92.7	0.45	1.66	1.14
98-95-100-16	66.4	Basalt	1.73	0.239	1.82	0.307	1.82	0.429	85.3	0.43	1.43	1.11
98-95-100-19	77.8	Aplite	0.72	0.100	0.75	0.131	2.97	0.889	161	0.12	6.63	3.42
98-95-100-20	81.4	Schist	1.82	0.286	2.34	0.367	1.10	0.414	122	0.28	0.86	0.59
98-95-100-21	84.5	Schist	1.79	0.292	2.05	0.380	1.03	0.344	98.1	0.39	0.65	0.54
98-95-100-23	90.4	Schist	1.78	0.260	2.01	0.333	1.06	0.304	86.3	0.39	0.36	0.32
98-95-100-24	95.5	Schist	2.28	0.365	2.75	0.484	1.51	1.02	374	0.06	0.82	0.61
98-95-100-25	98	Granite Vein	3.13	0.481	3.67	0.622	1.38	0.740	326	0.08	0.82	0.59
98-95-100-27	104	Granite Vein	1.22	0.181	1.38	0.214	0.73	0.132	44.1	0.27	0.32	0.39
98-95-100-28	106	Granite Vein	1.90	0.268	1.90	0.311	1.89	0.353	44.0	0.28	1.32	0.58
	<i>Footwall</i>											
98-95-100-29	10:	Basalt	2.47	0.332	2.42	0.377	1.85	0.325	37.7	0.14	0.82	0.47
98-95-100-30	111	Basalt	2.67	0.372	2.93	0.476	2.20	0.613	47.1	0.19	0.79	0.37

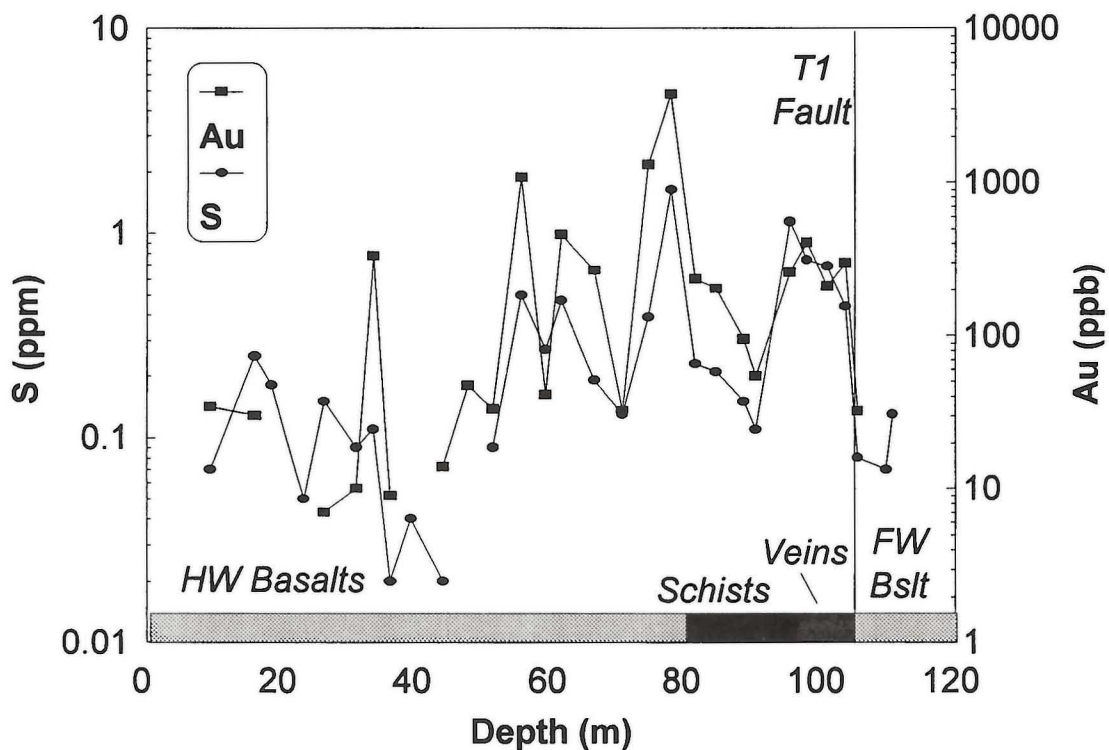


Figure GS-7-3: Variation in gold and sulphur abundance with depth, DDH# 95-BTE-01, Burnt Timber mine.

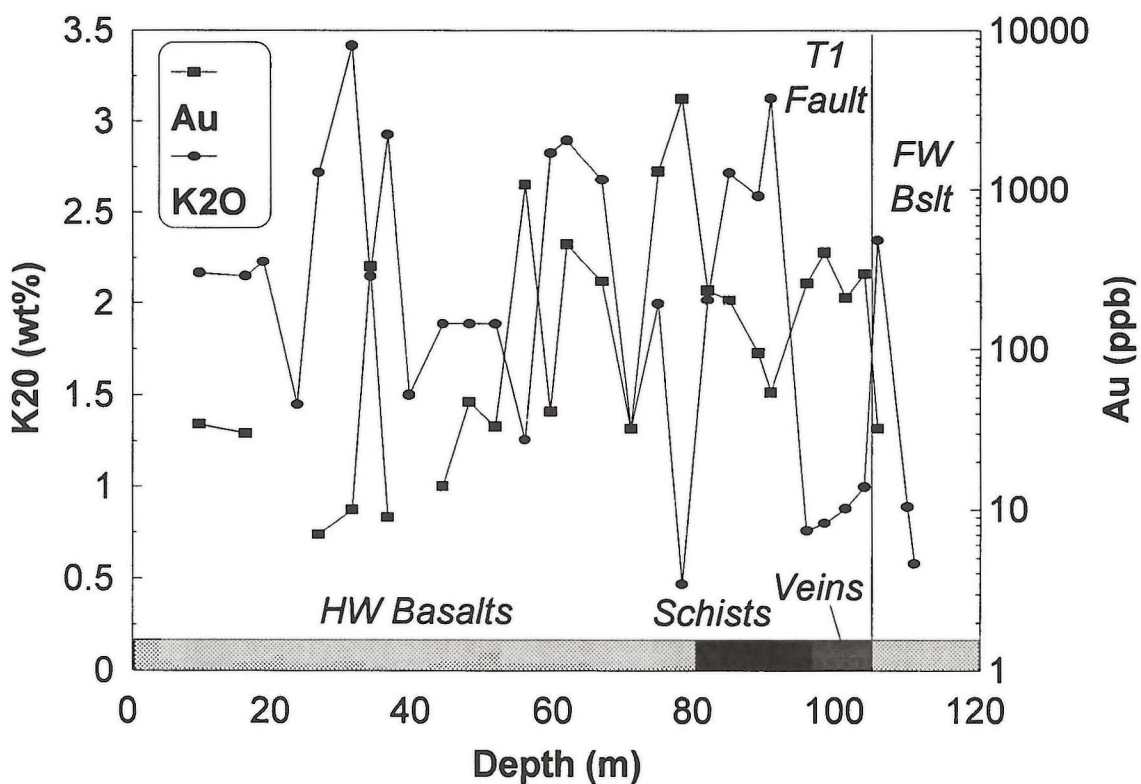


Figure GS-7-4: Variation in gold and K₂O abundance with depth, DDH# 95-BTE-01, Burnt Timber mine.

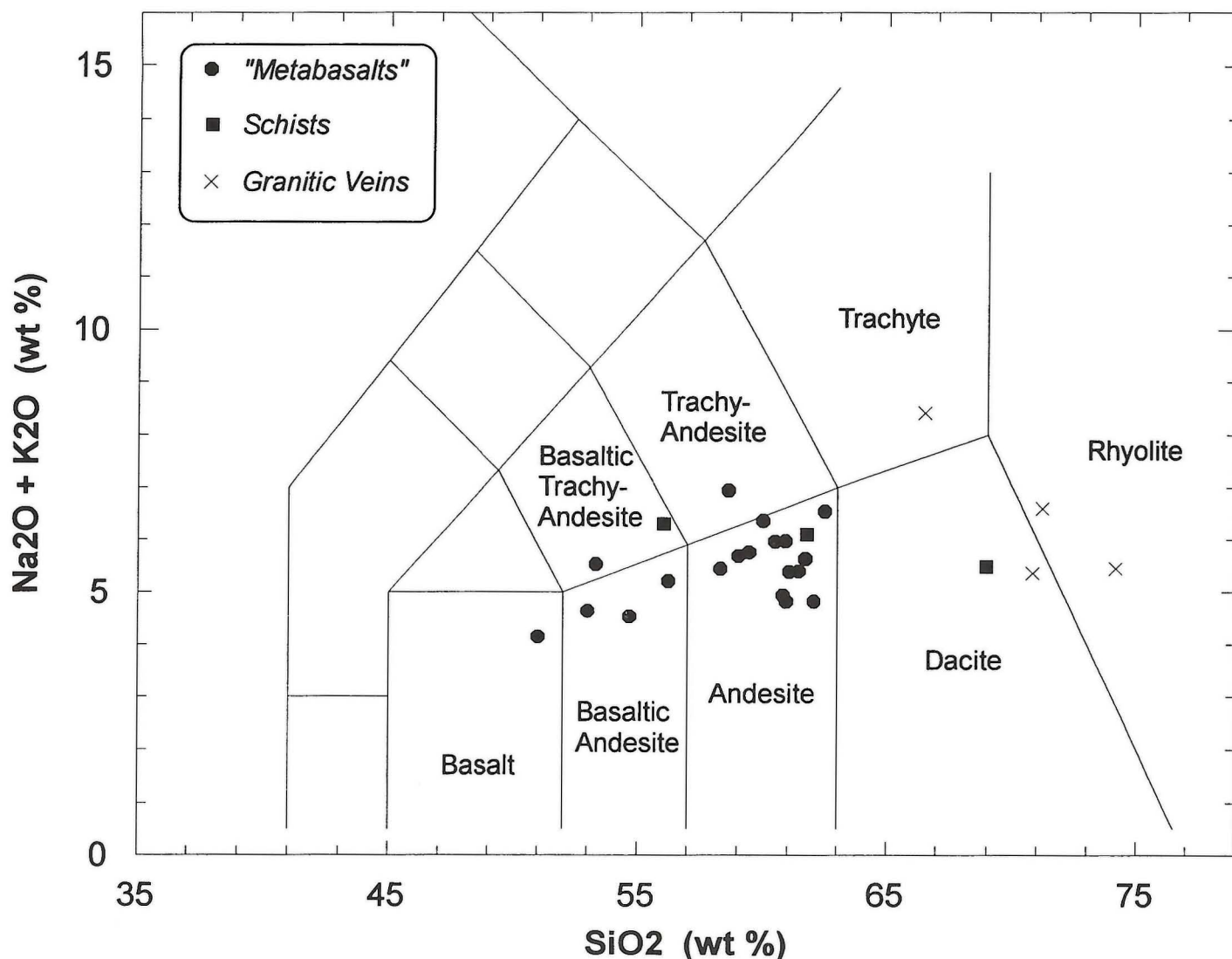


Figure GS-7-5: Total alkali - silica diagram (LeMaitre, 1989) for metavolcanic rocks intersected by DDH# 95-BTE-01.

and meaningful investigations of primary compositions based on major and lithophile trace elements will require better documentation of mineral assemblages and element mobility.

Inter-element correlations in metabasaltic rocks

Several significant correlations were identified for the metabasaltic rocks (including hanging wall and footwall units; Tables GS-7-1, 2). Of relevance here are the following results: (1) Si has a strong positive correlation with W, Ga and Th, and a strong inverse relationship with Ca, Mg, Cr, V, Ni, Fe and Sc, possibly reflecting a primary fractionation trend; (2) Fe has a strong positive correlation with Sc, Y, Nb, and the middle (in terms of atomic weight) of the rare-earth element (REE) group (*e.g.*, Gd to Er) - likely a primary trend; (3) K varies sympathetically with Rb and all of the light REE (*e.g.*, La, Ce, Pr, Nd) and is negatively correlated with Sc and the middle REE - this is likely a primary trend as there is no evidence for REE mobility; (4) Sc and Y display strong positive correlations with the heavy REE, a feature indicative of pyroxene crystallization.

These observations suggest that some primary fractionation trends typical of basaltic lavas were preserved in the BT mine area, despite the extensive quartz veining and introduction of carbonate and sulphide minerals. Nonetheless, the most lithophile and mobile trace elements, such as La, Th, U, Ti, Cs, Rb, attain their highest abundances in the most siliceous and K-rich rocks (Table GS-7-2). This could be interpreted as a primary feature associated with fractional crystallization or sedimentation, or a secondary feature, associated with the introduction of quartz veins and mobile, lithophile elements. The consistent correlations appear to indicate

a primary process, as does the fact that some of these mobile trace elements have strong positive correlations with immobile elements.

Figures GS-7-6 to GS-7-11 are multi-element spider diagrams (spidergrams) normalized to standard elemental abundances for mid-ocean ridge basalt (MORB). Metabasaltic rocks (Fig. GS-7-6, 7) have patterns typical of basaltic (andesitic) rocks from arc environments, and are characterized by pronounced negative Nb and Ti anomalies and LREE enrichment. Intermediate schists have a distinctive chemical signature, and a U-shaped profile (from La to Lu). A gabbro sample (98-95-100-1; Table GS-7-1) is chemically distinct from all of the metabasalts, with a flat REE pattern and a strong lithophile element enrichment typical of evolved tholeiitic basalt (Fig. GS-7-9). The talc-carbonate schist has an erratic MORB-normalized chemical profile (Fig. GS-7-9), but is most similar to the footwall metabasalts. Granitic veins also display strong negative Nb and Ti anomalies and have U-shaped REE profiles similar to the intermediate schists (Fig. GS-7-10). A gold-enriched aplite vein (98-95-100-19, Table GS-7-1, 2) is strongly enriched in LREE and lithophile elements compared to the granitic vein samples (Fig. GS-7-10).

A comparison of the MORB-normalized chemical profiles for the major units highlights the compositional similarities between the hanging wall and footwall metabasalts and the intermediate schists (Fig. GS-7-11). The intermediate schists (80 to 95 m) have similar lithophile element abundances, but much lower REE abundances, and are strongly depleted in LREE in comparison to the metabasalts. Conceivably, the intermediate schists were derived from protoliths of similar composition to the

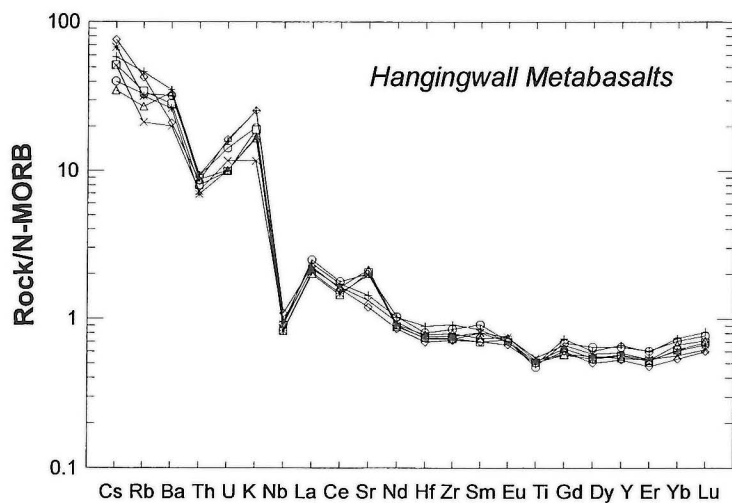


Figure GS-7-6: MORB-normalized spidergram for the Burnt Timber hanging wall metabasalts.

Figure GS-7-7: MORB-normalized spidergram for the footwall metabasalts.

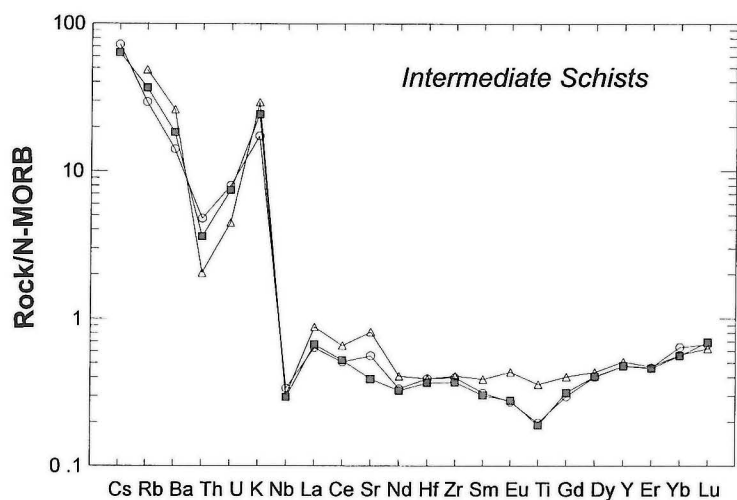
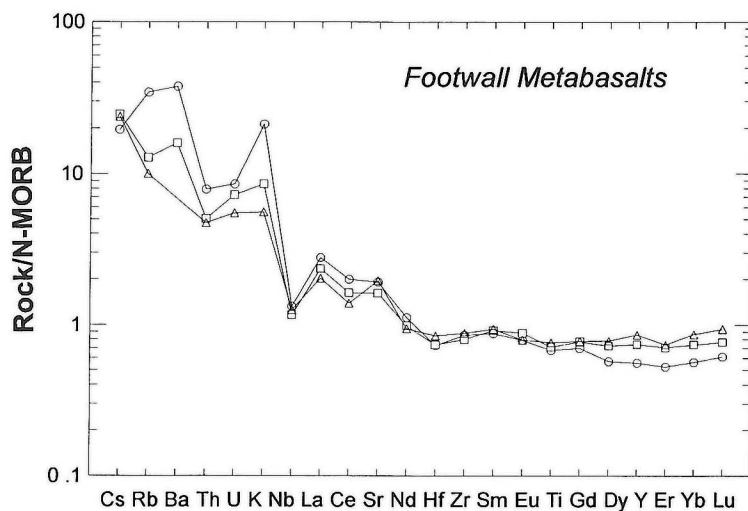


Figure GS-7-8: MORB-normalized spidergram for the intermediate schists.

Figure GS-7-9: MORB-normalized spidergram for the gabbro and MgO-rich schist units.

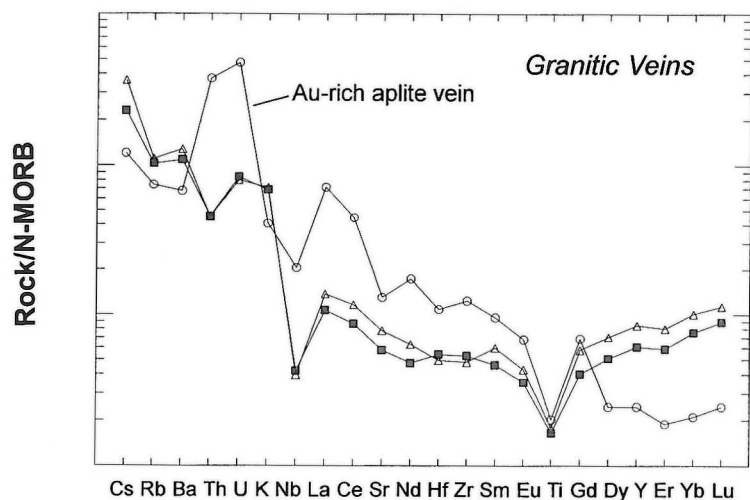
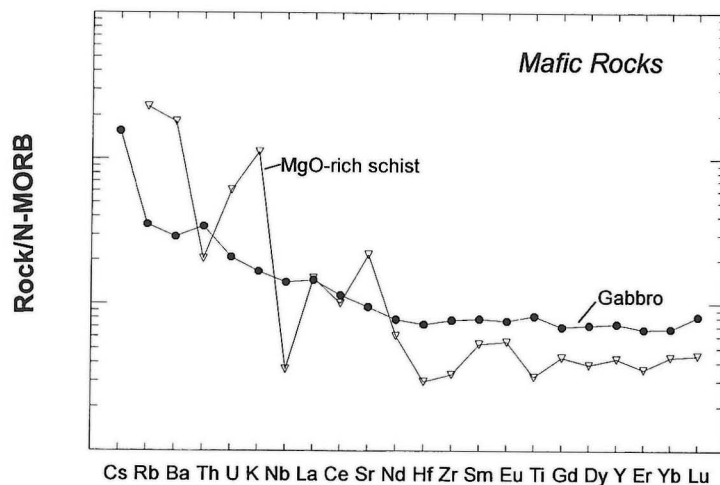


Figure GS-7-10: MORB-normalized spidergram for the Burnt Timber granitic veins.

metabasalts, through intense ductile deformation and concomitant hydrothermal alteration along the Johnson shear zone. Accordingly, the schists would require addition of K and Si and removal of Ca, Sr, Ti, and specific REE (La to Dy). Alternatively, the schists represent an intermediate metasedimentary or pyroclastic rock deposited between two andesitic units (hanging wall and footwall "metabasalts").

A plot of Nb/Y versus Th/Nb (Fig. GS-7-12) illustrates that the metabasaltic rocks from the Burnt Timber mine plot in the calc-alkaline basalt field. The pronounced negative Nb anomalies of the metabasalts (Figs. GS-7-6, 7) also suggest an arc origin. In relation to proximal andesitic suites from the Cartwright Lake and Hughes Lake areas (Gilbert *et al.*, 1980; Peck, 1986; Syme, 1985), the Burnt Timber rocks are depleted in high field strength elements including Ti, Zr, Y and Nb. This may suggest a more refractory source for the Burnt Timber metabasaltic rocks.

GENESIS OF THE GOLD MINERALIZATION

Although petrographic studies indicate that possibility of pervasive metasomatism involving addition of K, Si and lithophile elements and leaching of Ca and Mg, metasomatic effects do not appear to account for the distribution of sulphide and gold mineralization. Based on petrographic observations, metasomatic effects occurred both prior to and following the Au mineralization. The geochemistry of the hanging wall metavolcanic

rocks indicates that gold was not concentrated in any specific, chemically favourable lithology. Implicitly, the mineralization was controlled by prevailing structural patterns, yet gold occurs in a variety of lithologic types with a range of relative mechanical competencies. This contrasts with the Cartwright Lake area, where only the most siliceous and competent units contain Au-bearing quartz-sulphide veins (Peck, 1986; Peck *et al.*, 1995). Results from the current study also constrain the timing of the introduction of the gold. Based on available structural observations, the bulk of the gold was introduced following the transition from ductile deformation along this part of the Johnson shear zone. The early ductile regime produced the penetrative S_1 schistosity and planar tectonic lamination, which is cut by later mineralized quartz and granitic veins. Brittle deformation likely produced fracture sets that, at least locally, were oblique to the S_1 schistosity, and hosted early quartz and granitic veins, and later-formed mineralized quartz and sulphide veins.

The T1 fault appears to have superimposed two chemically similar metavolcanic packages which experienced distinctly different tectonic and metasomatic effects. Whereas Au mineralization, mylonitization and silicification are focused in the hanging wall units, the footwall metabasalts are less deformed, more intensely carbonatized and are not known to contain significant gold mineralization. At first glance, this would suggest the T1 fault acted as the pathway for the fluids which were preferentially channelled into the hanging wall. However, structural observations

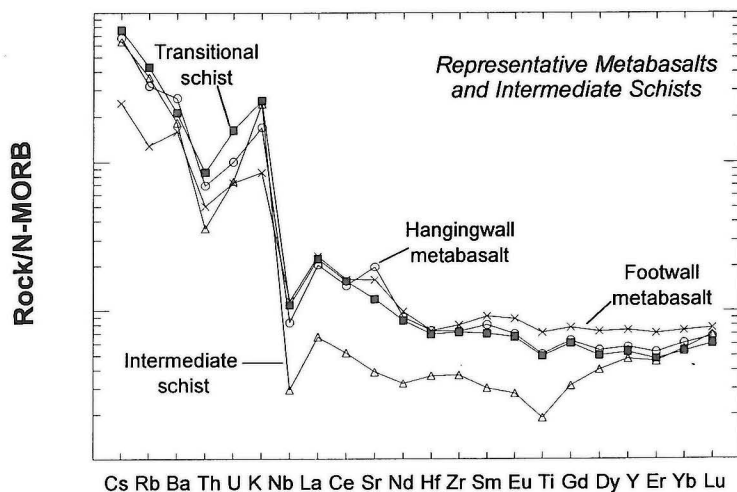
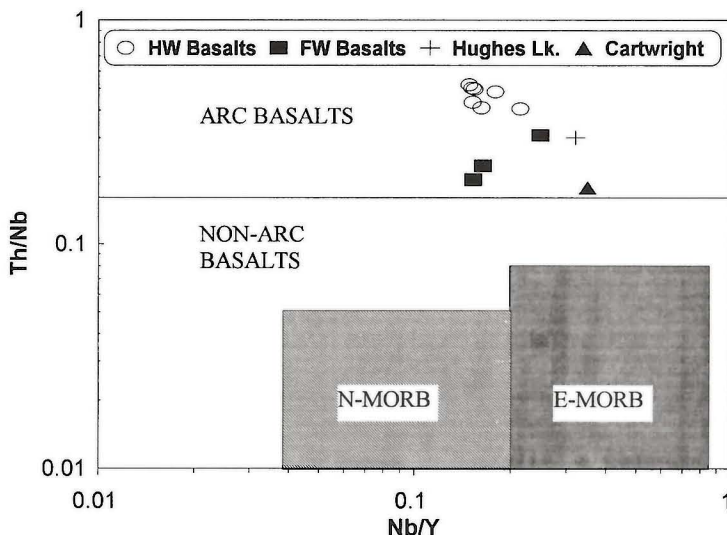


Figure GS-7-11: MORB-normalized spidergram comparing profiles for average metabasalt, intermediate schist and selected metavolcanic rocks from the Southern Volcanic belt, Lynn Lake.

Figure GS-7-12: Nb/Y versus Th/Nb plot for the metabasalts. Fields for normal-type MORB (N-MORB) and enriched-type MORB (E-MORB) are derived from Swinden (1996). Data for andesites from the Cartwright Lake and Hughes Lake areas are taken from Peck (1986) and Syme (1985).



demonstrate that mineralization occurred prior to D_2 and following emplacement of some of the quartz and granitic veins and pyroxenitic dykes. Resolving the amount and sense of movement which occurred along the T1 fault will be a major focus of future studies. Detailed structural and petrographic studies, supported by additional lithogeochemistry, are also being planned in order to better constrain the timing and controls on gold mineralization at the Burnt Timber deposit.

ACKNOWLEDGEMENTS

Mr. Paul Pawliw of Black Hawk Mining Inc. is thanked for providing technical support. J.M. Pacey prepared several figures.

REFERENCES

- Fedikow, M.A.F., Ferreira, K.J. and Baldwin, D.A.
1991: The Johnson shear zone - A regional metallogenic feature in the Lynn Lake area. Manitoba Energy and Mines, Mineral Deposit Thematic Map Series, Map 91-1.
- Gilbert, H.P., Syme, E.C. and Zwanzig, H.V.
1980: Geology of the metavolcanic and volcanoclastic metasedimentary rocks in the Lynn Lake area; Manitoba Energy and Mines, Geological Paper GP80-1, 118 p.
- LeMaitre, R.W.
1989: A classification of igneous rocks and glossary of terms; Blackwell Scientific Publications, Oxford, U.K., 193 p.
- Peck, D. C.
1986: The geology and geochemistry of the Cartwright Lake area: Lynn Lake greenstone belt, northwestern Manitoba; Unpublished M.Sc. thesis, University of Windsor, 270 p.
- Peck, D.C., Cameron, H.D.M. and Layton-Matthews, D.
1995: Geological and geochemical studies in the southern part of the Lynn Lake greenstone belt, Northwestern Manitoba (parts of NTS 64C/11, 64C/14 and 64C/15); in Manitoba Energy and Mines, Report of Activities, 1995, p. 4-10.
- Richardson, D.J. and Ostry, G.
1996: Gold deposits of Manitoba; Manitoba Energy and Mines, Economic Geology Report ER86-1 (second edition), 114 p.
- Swinden, H.S.
1996: The application of volcanic rock geochemistry to the metallogeny of volcanic-hosted sulphide deposits in central Newfoundland, in Trace element geochemistry of volcanic rocks: Application for massive sulphide exploration, (ed.) D.A. Wyman; Geological Association of Canada, Short Course Notes v. 12, p. 329-358.
- Syme, E.C.
1985: Geochemistry of metavolcanic rocks in the Lynn Lake belt; Manitoba Energy and Mines, Geological Report GR84-1, 84 p.

GS-8: GEOCHEMISTRY OF PALEOPROTEROZOIC VOLCANIC ROCKS IN THE PHOTO LAKE AREA, FLIN FLON BELT (PART OF NTS 63K16)

by Alan H. Bailes

Bailes, A.H. (1997): Geochemistry of Paleoproterozoic volcanic rocks in the Photo Lake area, Flin Flon Belt (part of NTS 63K16); in Manitoba Energy and Mines, Minerals Division, Report of Activities, 1997, p. 61-72.

SUMMARY

Precise (XRF, ICP-MS) geochemical analyses of selected volcanic rocks from the Photo Lake area were acquired in 1996 and 1997 as a follow up to detailed mapping (1:5 000 and 1:10 000 scale) undertaken in 1994 (Bailes and Simms, 1994; Bailes *et al.*, 1994) and 1996 (Bailes, 1996; Bailes *et al.*, 1996). These analyses demonstrate that the Photo Lake sequence is tholeiitic, bimodal (mafic/felsic), with an island arc geochemical signature. Furthermore, all volcanic rocks in the Photo Lake area belong to the "evolved arc" portion of the Snow Lake arc assemblage (as defined by Bailes and Galley, 1996).

Until discovery of the Photo Lake Cu-Zn-Au VMS deposit, all Cu-rich deposits were located in the "primitive arc" (e.g. the Anderson area Cu-rich deposits). This study confirms that the Cu-rich Photo Lake deposit is hosted by "evolved arc" rhyolites and that it represents a new and unique VMS environment in the Snow Lake district. An examination of the chemistry of felsic volcanic rocks in the Photo Lake area suggests that the VMS-hosting Photo Lake rhyolite is correlative with the Ghost Lake rhyolite but not necessarily with felsic volcanic gneisses that occur northwest of Bolloch Lake or between Squall Creek and the Ham pluton.

INTRODUCTION

This report concludes a cooperative project conducted by Manitoba Energy and Mines (MEM) and Hudson Bay Exploration and Development (HBED). The objective of the project was to provide a sound geological framework for future exploration activities in the Photo Lake area after the 1994 discovery of a Cu-Zn-Au rich volcanic-hosted massive sulphide (VMS) zone, now the Photo Lake mine, in the Snow Lake arc assemblage at the east end of the Flin Flon Belt (Fig. GS-8-1).

The mapping shows that the Photo Lake VMS deposit occurs within a different stratigraphic setting than other VMS deposits in the Snow Lake area (Bailes *et al.*, 1996a). Geochemistry of the volcanic rocks at Photo Lake was undertaken so that this potentially productive package could be more completely characterized and more easily followed and recognized elsewhere.

The geology of the Photo Lake area (Fig. GS-8-2) is reported in Bailes (1996). In summary, the area is underlain by ca. 1.89 Ga metavolcanic and associated synvolcanic intrusive rocks, intruded by the synkinematic Chisel Lake layered mafic to ultramafic pluton. All rocks are overprinted by lower to middle almandine amphibolite facies mineral assemblages that were produced during a ca. 1.81 Ga regional metamorphic event that reached approximately 5 kb and 535° C at Photo Lake (Menard and Gordon, 1995). The volcanic and sedimentary rocks at Photo Lake include an 'older' and 'younger' sequence. The 'older' sequence consists largely of felsic flows, volcanoclastic rocks and derived gneisses whereas the 'younger' sequence comprises dominantly mafic volcanoclastic rocks of the Threehouse formation. The Photo Lake VMS deposit is hosted by the Photo Lake rhyolite, in the 'older' volcanic sequence.

Bailes and Simms (1994) reported evidence for a potential unconformity at the base of the younger Threehouse sequence, which they suggested explains angular truncation of 'older' stratigraphic units at its base. However re-examination of a critical outcrop during the 1997 field season suggests that this may not be a valid interpretation and that the two sequences are conformable.

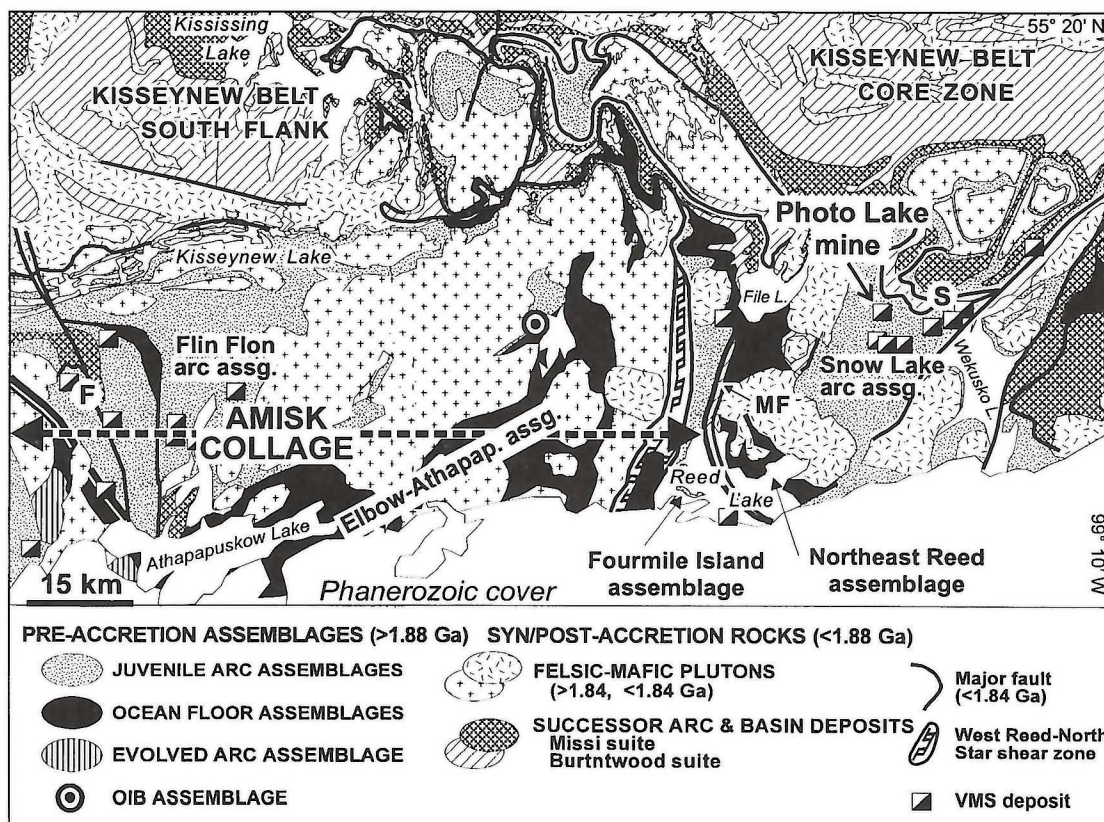
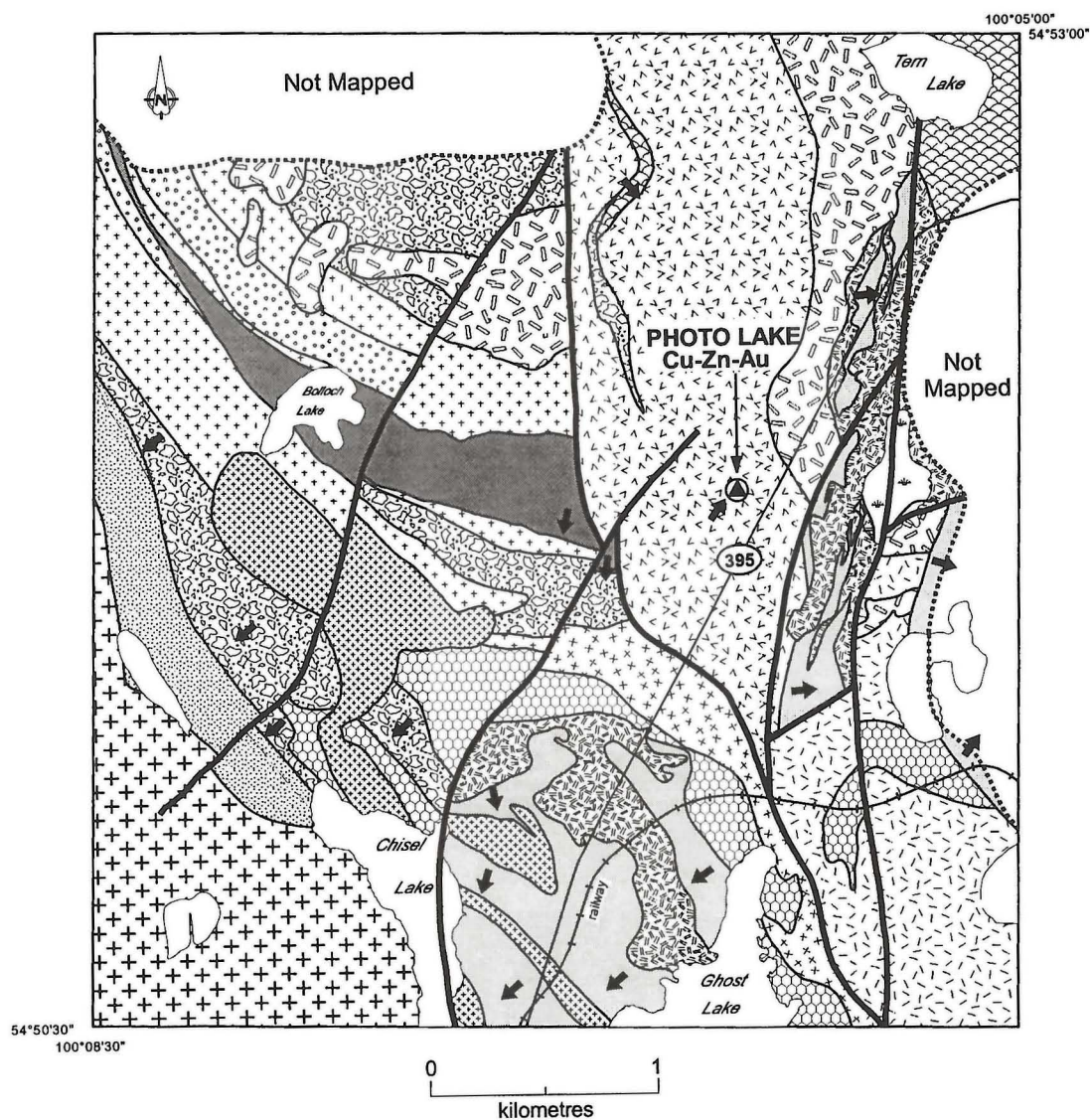


Figure GS-8-1: Simplified geological map of the central and eastern portion of the Flin Flon Belt showing major tectonostratigraphic assemblages and plutons, and locations of mined VMS deposits. F: Flin Flon, S: Snow Lake, ML: Morton Lake fault zone. Filled rectangle shows location of Photo Lake map area.



INTRUSIVE ROCKS

Synkinematic And Undivided Intrusive Rocks

- Chisel Lake Pluton: gabbro, pyroxenite and peridotite
- Fine- to medium-grained gabbro

Younger (Syn-Threehouse) Intrusive Rocks

- Porphyritic gabbro

Older Synvolcanic Intrusive Rocks

- Quartz porphyry, quartz-plagioclase porphyry

JUVENILE ARC VOLCANIC AND SEDIMENTARY ROCKS

Younger Volcanic And Sedimentary Rocks

- Threehouse basalt and andesite
- Threehouse mafic wacke and breccia

Older Volcanic And Sedimentary Rocks

- Heterolithic felsic breccia
- Bolloch Lake rhyolite
- Ghost Lake rhyolite
- Undivided rhyolite
- Dacite volcaniclastic rocks (Powderhouse dacite?)
- Ghost Lake "andesite"
- Undivided heterolithic mafic volcaniclastic rocks
- Porphyritic basalt
- Bolloch Lake basalt

— Faults

← Facing direction

Figure GS-8-2: Simplified geology of the Photo Lake area from Bailes et al. (1996).

SAMPLING AND ANALYTICAL PROCEDURES

Samples were collected specifically for geochemical analysis. They are mainly from mesoscopically least altered rocks, but do include some altered rocks. Both sample types were trimmed to remove weathered surfaces, joints and veinettes, and contain a minimum number of amygdaloids. Samples collected from clearly altered rocks or to test for suspected alteration have not been used on any geochemical plots in this report without being clearly identified. Samples were analyzed for a complete spectrum of whole rock, trace and rare earth elements using a combination of XRF (XRAL Laboratories) and ICP-MS (University of Saskatchewan) analytical procedures.

GEOCHEMISTRY

Mafic volcanic rocks

Although mafic flows are a minor rock lithology in the Photo Lake area (Figure GS-8-2), geochemical discriminants for potential tectonic environment of emplacement of mafic rocks (e.g. Pearce, 1996) are better documented than for felsic rocks. Thus, basalt geochemistry is important for establishing the tectonic environment of deposition for the intercalated and much more voluminous felsic volcanic host rocks of the Photo Lake VMS deposit. With this objective in mind 2 samples of Bolloch Lake basalt and 9 samples of Threehouse Lake basalt and its subvolcanic gabbro feeders were analyzed for major, trace and rare earth elements.

The Bolloch Lake (BLB) and Threehouse (THB) mafic flows are basalt to basaltic andesites in composition with major element compositional ranges as follows (see also Table GS-8-1):

	Bolloch Lake mafic flows	Threehouse mafic flows
SiO ₂	51.5-54.2 wt. %	51.6-52.1 wt. %
MgO	3.4-4.7 wt. %	5.1-7.6 wt. %
CaO	8.1-10.2 wt. %	8.2-10.58 wt. %
Al ₂ O ₃	14.6-15.8 wt. %	13.9-17.2 wt. %
TiO ₂	0.57-0.70 wt. %	0.30-0.43 wt. %
Ni	<10 ppm	5-28 ppm
Cr	7-9 ppm	10-195 ppm

They are subalkaline (Figs. GS-8-5 and 6), tholeiitic (Figs. GS-8-3a, 3b and 6a) and similar to other arc basalts lower in the Snow Lake Arc Assemblage (Bailes and Galley, 1996).

Both BLB and THB display typical arc signatures on MORB-normalized trace element diagrams (Fig. GS-8-4) including positive Th and negative Nb anomalies, depleted Zr and Hf, and a trough at Ti. They display the enrichment in light rare earth elements (LREE; Fig GS-8-3c) and elevated ratios such as Th/Yb (Fig. GS-8-3d) that characterize stratigraphically higher "evolved arc" rocks in the Snow Lake arc assemblage (Bailes and Galley, 1996). Both BLB and THB display similar patterns to other "evolved arc" mafic volcanic rocks on Figure GS-8-4 (Moore, Bolloch, Threehouse, Lost) and are readily distinguished from patterns displayed by the stratigraphically underlying "primitive arc" basalts (Welch) and overlying MORB basalts (Snow Creek). Although they display broadly similar patterns on the MORB-normalized trace element diagrams to the Moore Lake basalt (Fig. GS-8-3), they are distinctly less enriched in high field strength elements (HFSE, e.g. Zr, Y, Ti), large ion lithophile elements (LILE, e.g. Th) and LREE elements. The unique chemistry of BLB and THB relative to other basalts in the Snow Lake area is further reflected in the other geochemical plots in Figures GS-8-3 and 4.

Geochemistry of BLB and THB mafic flows demonstrates that they have island affinity and belong to the "evolved arc" sequence of the Snow Lake arc assemblage. Along with other "evolved arc" basalts they display features that reflect complex conditions of magma genesis where older crustal fragments and previously formed arc segments added a diversity to magma generation that is not evident in the underlying "primitive arc" Welch basaltic andesites and boninitic flows.

Felsic volcanic rocks

Most VMS deposits in the Flin Flon and Snow Lake mining districts are spatially associated with rhyolite flows (Syme and Bailes, 1993). This association of VMS deposits with felsic volcanic rocks is clearly evident

for the Photo Lake Cu-Zn-Au VMS deposit which is located in a thick, monotonous sequence of massive, aphyric to sparsely porphyritic felsic rocks and derived felsic gneisses informally termed the Photo Lake rhyolite (PLR; Bailes, 1996). Two similar, large, but fault-bounded, bodies of felsic rocks also occur in the Photo Lake map area but have uncertain relationships to PLR. They are informally referred to as the Ghost Lake rhyolite (GLR), occurring northeast of Ghost Lake, and the Bolloch Lake rhyolite (BLR), located northwest and southeast of Bolloch Lake (Fig. GS-8-2).

A total of 24 XRF plus ICP-MS geochemical analyses of PLR (14 analyses), GLR (6) and BLR (4) rhyolites were undertaken with the following objectives: (1) to identify any subtle chemostratigraphy in PLR; (2) to provide criteria to make stratigraphic correlations between PLR and other the rhyolite bodies at Ghost Lake and Bolloch Lake, and (3) to characterize the VMS-hosting PLR as a method of identifying this prospective unit elsewhere in the Snow Lake area. Additionally, 9 geochemical analyses of the Ghost Lake andesite (GLA) and 3 of the Powderhouse dacite (PWD) were undertaken with two objectives in mind: (1) to determine the original composition and affiliations of GLA, which owes its present, largely andesitic, composition to alteration, and (2) to compare rocks mapped as Powderhouse dacite in the Photo Lake area with those occurring in the type area south of the Chisel Lake Zn-rich VMS deposits.

On an AFM diagram (Fig. GS-8-6a) Photo Lake area felsic rocks (large symbols) and mafic rocks (small symbols) are clearly tholeiitic. The felsic rocks fall on the boundary between metaluminous and peraluminous on a diagram of $Al_2O_3/(Na_2O + K_2O)$ vs. $Al_2O_3/(CaO + Na_2O + K_2O)$. On a diagram of Rb vs. Y + Nb (Fig. GS-8-6c) they fall in the field of volcanic arc granite (VAG; Pearce *et al.*, 1984)).

Photo Lake rhyolite (PLR)

PLR consists of a monotonous, 1 Km wide (map width) sequence of massive aphyric to sparsely porphyritic felsic flows and derived felsic gneisses that locally contain quartz amygdaloids, quartz-filled gas cavities and local massive lobes with intervening microbreccia. Although no internal subdivisions of PLR were mapped and no facing directions for these strata were observed, the rhyolites have tentatively been interpreted to top to the east-northeast on the basis of one pillow top in an intercalated mafic flow and the presence of hydrothermally altered rocks southwest of the Photo Lake VMS deposit. The Photo Lake VMS "horizon" is interpreted to be coincident with the base of an up to 90 m thick unit of intercalated heterolithologic mafic breccia that trends north-northwest (see Bailes, 1996, for discussion). The mafic breccia unit divides the felsic package equally into a stratigraphically lower (west and southwest) and upper (east and northeast) package (Figure-8-2).

A suite of 14 samples collected from least altered Photo Lake rhyolite, although displaying considerable variation in such elements as Zr (52 - 105 ppm, one at 32 ppm), shows no consistent differences between the southwest and northeast package nor to those samples collected within 100 m of the Photo Lake VMS "horizon". The variations that do exist in PLR are interpreted to be unrelated to stratigraphy and to represent the natural range of composition of this rhyolite package.

Although identified during field mapping as rhyolites, analyses of samples of PLR demonstrate them to be andesite to rhyolite in composition (62 to 82 wt. % SiO₂), with most being either rhyodacites or rhyolites (Fig. GS-8-5a). On a plot of Zr/TiO₂ vs. Nb/Y (Fig. GS-8-5b) PLR falls in the basaltic andesite, andesite and dacite fields, but assigning composition on the basis of this diagram is not recommended as Flin Flon and Snow Lake area volcanic rocks display lower than normal Zr contents (Syme and Bailes, 1993). Stern *et al.* (1995) interpret Flin Flon and Snow Lake volcanic rocks to be derived from a Zr-depleted, refractory mantle. Some of the low and high values of SiO₂ in PLR likely reflect alteration effects. This is in part attributable to the fact that some samples are from lobes (often selectively silicified in subaqueous flow complexes) and others from interlobe hyaloclastite (most susceptible to hydrothermal alteration).

Despite the apparent variation in major elements, PLR displays only minor differences on chondrite normalized REE plots (Fig. GS-8-7); this is consistent with experience elsewhere in the Flin Flon Belt where REE elements appear to be relatively immobile in volcanic rocks, even those that have been effected by weak to moderate hydrothermal alteration and subsequent regional metamorphism (Stern *et al.*, 1995; Bailes and Galley,

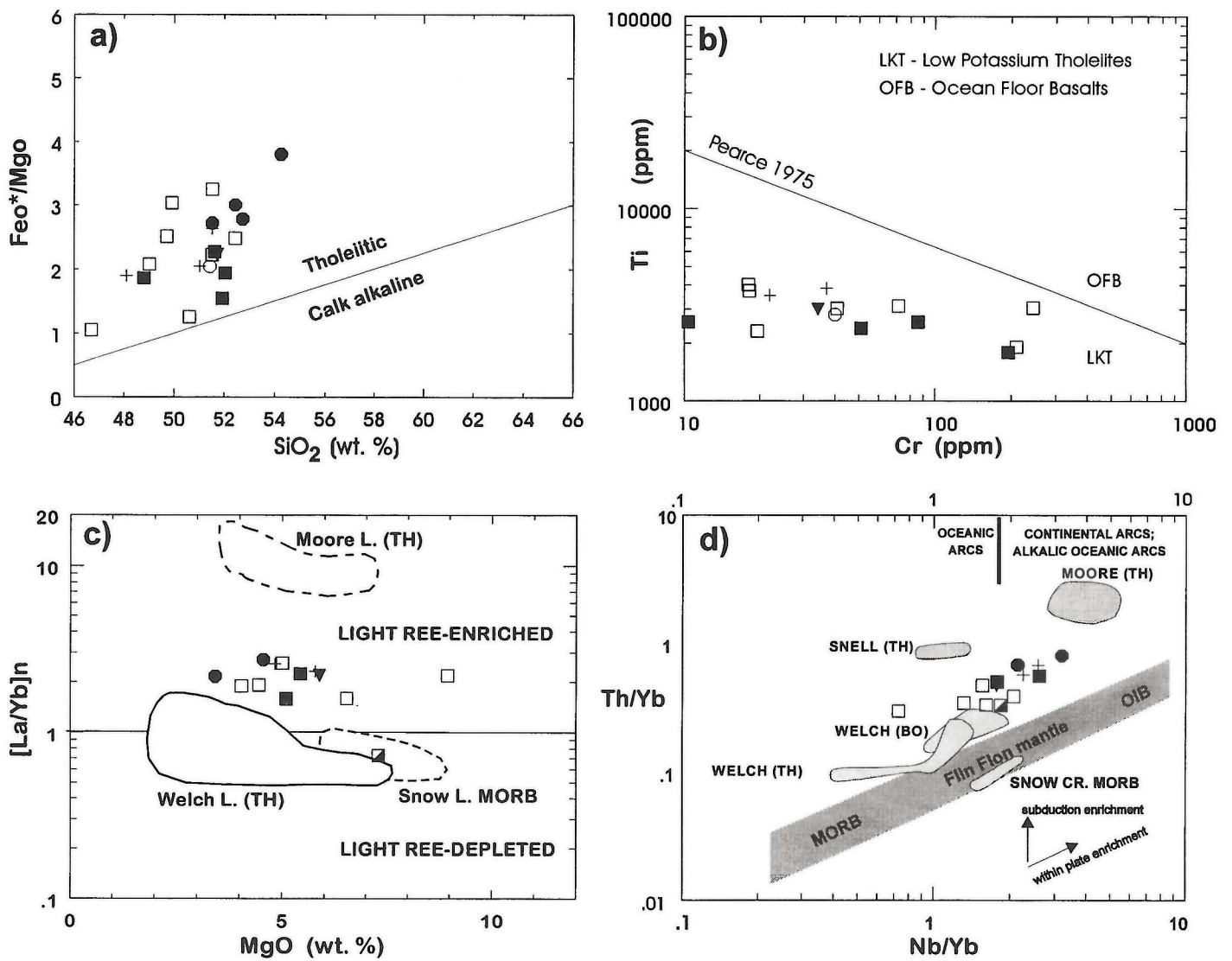


Figure GS-8-3: Photo Lake area mafic flows and synvolcanic intrusions on various geochemical discrimination diagrams: (a) SiO_2 vs. FeO^*/MgO , plot in the tholeiitic field (boundaries from Gill (1981)); (b) Cr vs. Ti , plot in island arc field (boundaries from Pearce, 1975); (c) MgO vs. $[\text{La}/\text{Yb}]_n$, plot in light REE-enriched field (boundaries from Stern et al., 1995); (d) Nb/Yb vs. Th/Yb (boundaries from Stern et al., 1995, modified from Pearce, 1983).

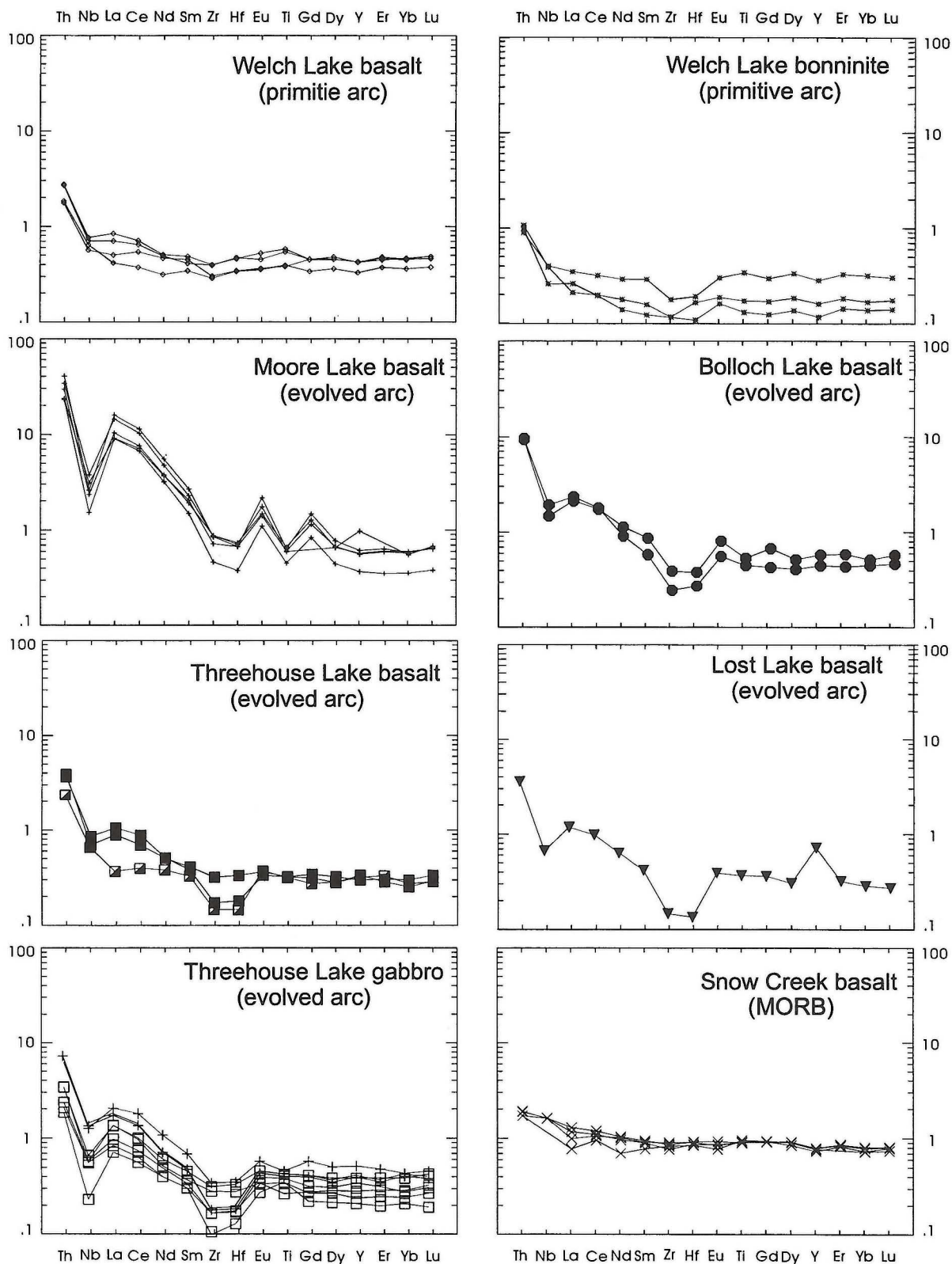


Figure GS-8-4: Least mobile elements in Photo Lake area mafic flows and synvolcanic intrusions on N-MORB-normalized incompatible element diagrams (after Sun and McDonough, 1989). Elements are arranged in order (to right) of decreasing incompatibility in MORB-source mantle.

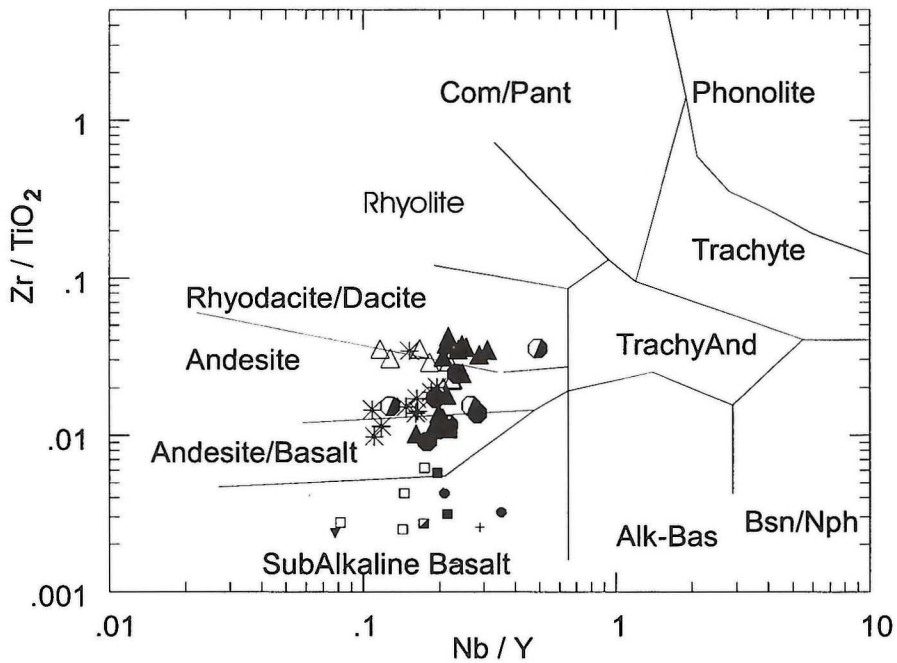
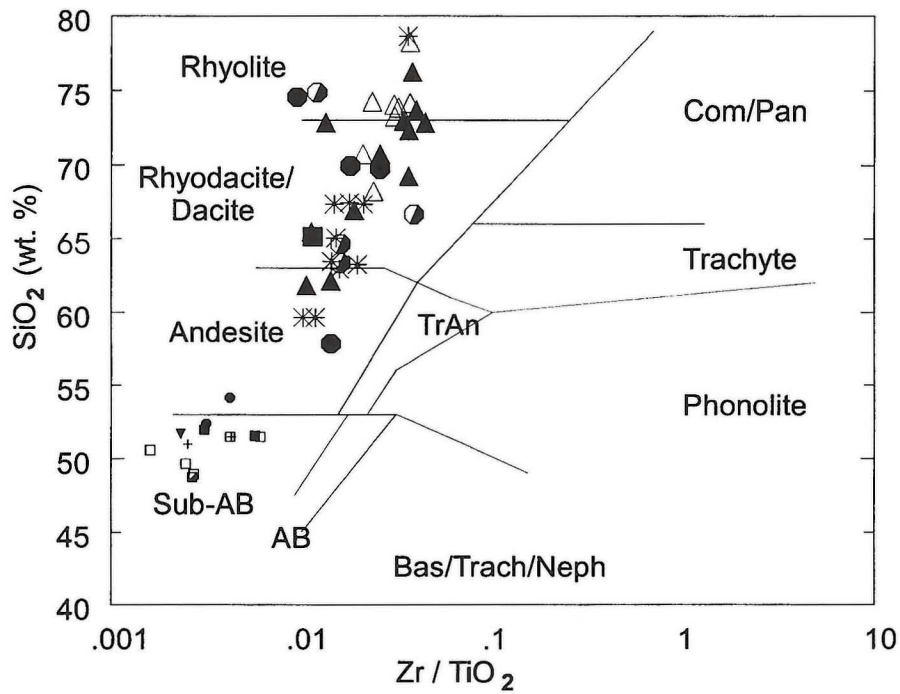


Figure GS-8-5: Photo Lake area volcanic rocks plotted on chemical rock discrimination diagrams (from Winchester and Folyd, 1977) (a) Zr/TiO_2 vs. SiO_2 ; (b) Nb/Y vs. Zr/TiO_2 .

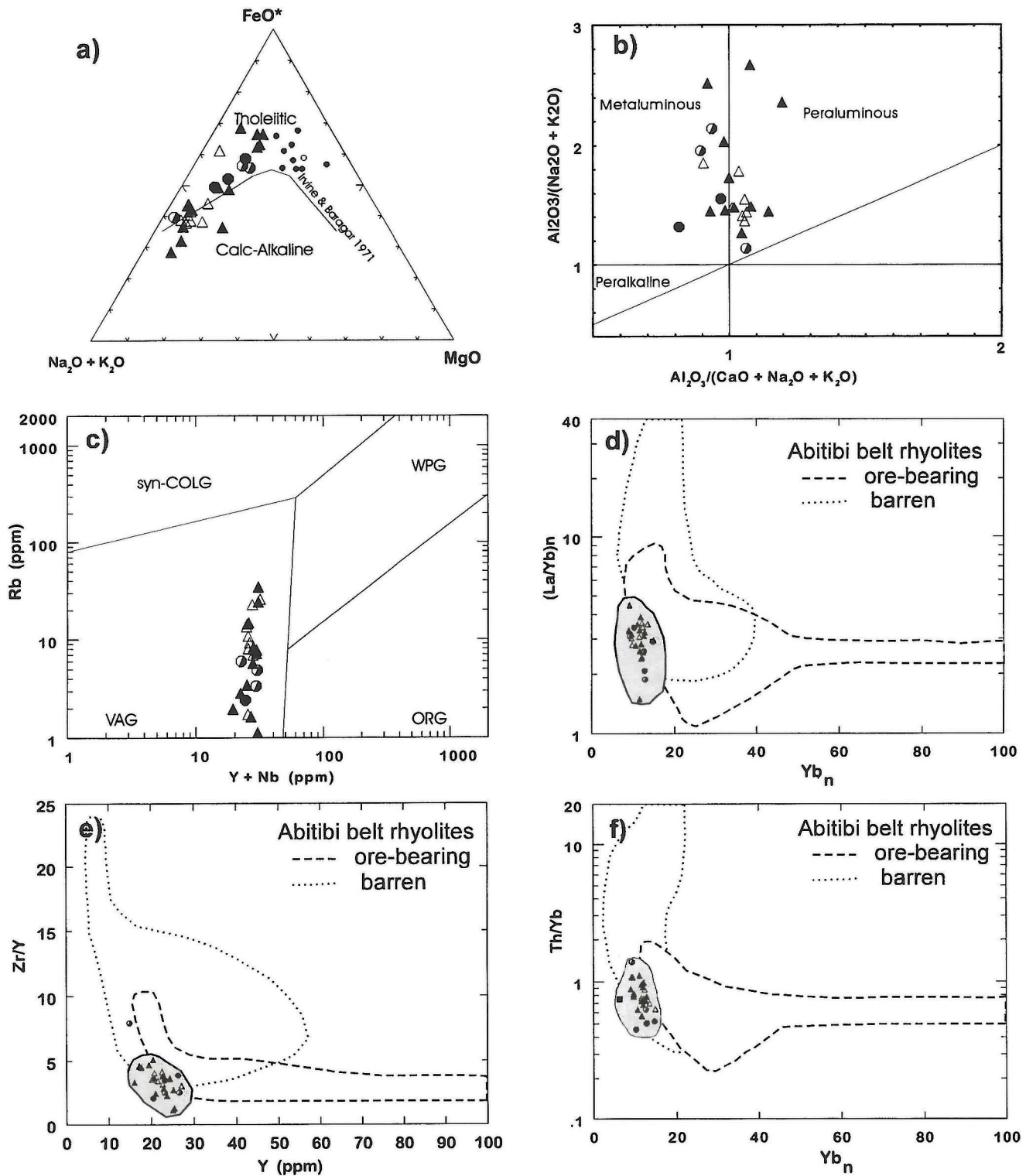


Figure GS-8-6: Photo Lake area felsic volcanic rocks on various geochemical discrimination diagrams: (a) AFM diagram (Irvine and Baragar, 1971); (b) $\text{Al}_2\text{O}_3/(\text{CaO} + \text{Na}_2\text{O} + \text{K}_2\text{O})$ vs. $\text{Al}_2\text{O}_3/(\text{Na}_2\text{O} + \text{K}_2\text{O})$ (Maniar and Piccolli); (c) $\text{Y} + \text{Nb}$ vs. Rb (Pearce et al., 1984); (d) Yb_n vs. $(\text{La}/\text{Yb})_n$ (Barrie et al., 1993); (e) Y vs. Zr/Y (Barrie et al., 1993); (f) Yb_n vs. Th/Yb (Barrie et al., 1993).

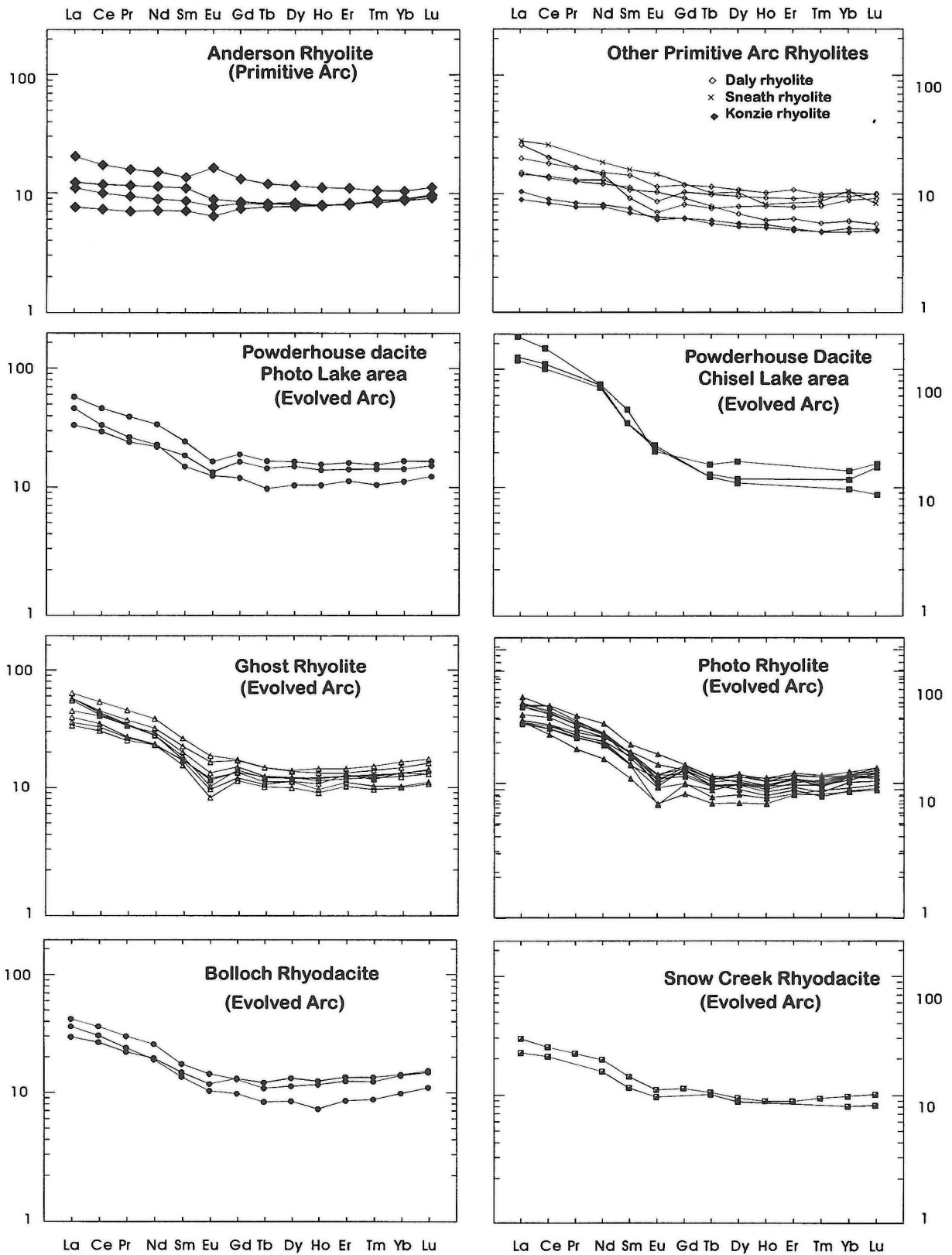


Figure GS-8-7: Photo Lake area felsic volcanic rocks and comparison analyses on chondrite-normalized REE plots (after Sun and McDonough, 1989).

Table GS-8-1a

Major element data for whole rocks, Photo Lake

SAMPLE	Rock Type	SiO ₂	Al ₂ O ₃	Fe ₂ O ₃	MgO	CaO	Na ₂ O	K ₂ O	MnO	TiO ₂	P ₂ O ₅	LOI
07-96-5589-1-1	Powderhouse dacite	58.23	13.68	14.48	2.87	3.53	6.18	0.19	0.09	0.59	0.16	<0.10
07-96-5592-1-1	Powderhouse dacite	75.02	12.37	3.36	0.55	5.25	2.22	0.32	0.07	0.46	0.37	0.5
07-96-5605-1-1	Powderhouse dacite	70.11	12.46	7.77	1.53	2.66	4.77	0.15	0.06	0.42	0.07	<0.15
07-94-5095-1-1	Ghost rhyolite	68.76	14.3	6.74	1.35	1.93	5.45	0.89	0.09	0.37	0.13	0.7
07-94-5360-1-1	Ghost rhyolite	73.29	13.2	4.09	1.09	2.94	3.72	1.18	0.06	0.32	0.11	0.6
07-94-5407-1-1	Ghost rhyolite	74.79	12.48	4.15	0.78	2.06	4.26	0.97	0.07	0.32	0.12	1.01
07-94-5403-1-1	Ghost rhyolite	71	14.24	4.3	0.6	4.43	4.27	0.6	0.09	0.33	0.13	0.74
07-96-5502-1-1	Ghost rhyolite	74.65	12.59	4.09	0.69	2.18	4.75	0.64	0.07	0.26	0.08	0.85
07-96-5510-1-1	Ghost rhyolite	78.26	10.99	3.68	0.45	1.48	4.61	0.2	0.07	0.21	0.06	0.05
07-96-5548-1-1	Ghost rhyolite	74.66	11.67	5.17	0.34	5.09	0.88	1.74	0.16	0.24	0.04	0.8
CH-90-15-1903'	Ghost rhyolite	74.37	12.38	4.82	0.66	1.46	5.01	0.75	0.09	0.28	0.17	0.75
07-94-5089-1-1	Ghost "andesite"	64.3	15.14	7.58	1.06	6.78	4.07	0.53	0.1	0.33	0.12	1.57
07-94-5090-1-1	Ghost "andesite"	63.74	14.45	9.13	2.12	5.67	3.91	0.26	0.16	0.45	0.1	0.76
07-94-5093-1-1	Ghost "andesite"	67.86	13.89	7.81	1.38	3.21	4.28	0.92	0.17	0.35	0.13	0.46
07-94-5405-1-1	Ghost "andesite"	67.88	14.48	7.24	1.87	1.84	4.84	1.23	0.13	0.4	0.1	1.23
07-94-5406-1-1	Ghost "andesite"	66.81	14.77	7.36	1.36	5.05	3.78	0.26	0.1	0.4	0.13	0.45
07-96-5497-1-1	Ghost "andesite"	63.68	14.46	9.23	2.71	5.14	3.44	0.7	0.16	0.39	0.1	0.4
07-96-5573-1-1	Ghost "andesite"	78.94	10.13	3.62	0.82	3	3.1	0.13	0.06	0.19	0.0	0.3
07-96-5573-1-2	Ghost "andesite"	60.03	15.28	10.86	2.72	6.05	4.16	0.18	0.19	0.45	0.06	0.35
07-96-5440-1-1	Ghost "andesite"	60.55	16.43	9.35	1.85	6.48	4.22	0.24	0.17	0.51	0.2	0.1
CH-90-15-597'	Ghost "andesite"	65.68	14.53	8.2	1.67	4.37	3.92	0.92	0.18	0.45	0.07	0.25
07-94-5009-1-1	Photo rhyolite	73.68	12.33	5.05	0.49	2.62	4.61	0.85	0.09	0.21	0.07	1
07-94-5011-1-1	Photo rhyolite	69.7	14.48	5.37	2.37	1.45	5.94	0.21	0.07	0.3	0.09	0.91
07-94-5044-1-1	Photo rhyolite	65.4	13.08	10.25	2.13	4.96	2.94	0.34	0.16	0.47	0.27	0.56
07-94-5058-1-1	Photo rhyolite	74.84	11.29	5.74	0.50	5.31	0.59	1.3	0.13	0.24	0.06	0.86
07-94-5120-1-1	Photo rhyolite	68.03	12.59	9.12	1.51	5.37	2.16	0.49	0.2	0.37	0.15	1.63
07-94-5128-1-1	Photo rhyolite	62.09	13.97	13.56	2.54	3.16	3.51	0.13	0.26	0.5	0.28	0.59
07-94-5242-1-1	Photo rhyolite	82.27	9.05	2.69	0.26	2.63	2.46	0.37	0.04	0.17	0.05	0.23
07-94-5244-1-1	Photo rhyolite	81.36	10.95	0.88	0.11	0.47	5.64	0.3	0.01	0.21	0.07	0.19
07-94-5248-1-1	Photo rhyolite	72.73	13.16	5.12	0.71	2.22	4.9	0.75	0.08	0.25	0.07	0.54
07-94-5257-1-1	Photo rhyolite	77.31	11.96	2.98	0.73	1.67	4.63	0.37	0.06	0.22	0.07	0.43
07-94-5267-1-1	Photo rhyolite	62.05	14.33	11.05	2.29	5.52	3.29	0.46	0.2	0.52	0.29	0.6
07-94-5270-1-1	Photo rhyolite	71.59	12.24	6.55	1.62	2.84	3.67	0.95	0.12	0.31	0.11	1.4
07-94-5291-1-1	Photo rhyolite	74.46	12.73	3.95	0.67	2.29	4.91	0.62	0.07	0.23	0.07	0.91
07-94-5399-1-1	Photo rhyolite	73.41	13.68	3.42	0.83	1.25	5.79	1.18	0.07	0.28	0.09	0.28
07-94-5400-1-1	Photo rhyolite	73.09	12.93	4.97	0.92	3.94	1.49	2.21	0.12	0.25	0.08	0.64
07-94-5031-1-1	Bolloch dacite	65.5	13.77	9.1	1.92	4.61	3.96	0.49	0.15	0.38	0.12	2.09
07-94-5106-1-1	Bolloch dacite	63.65	14.76	9.31	2.36	4.88	3.9	0.45	0.14	0.44	0.11	1.05
07-94-5110-1-1	Bolloch dacite	67.45	15.78	6.65	0.44	0.54	7.93	0.78	0.03	0.32	0.08	0.42
07-94-5103-1-1	Bolloch basalt	52.53	14.64	15.37	4.54	10.19	1.62	0.18	0.25	0.59	0.09	1.36
07-94-5067-1-1	Bolloch basalt	54.09	15.77	14.47	3.39	8.07	2.81	0.26	0.2	0.7	0.24	0.98
07-94-5300-1-1	Threehouse basalt	51.98	17.19	11.95	5.4	9.86	2.78	0.19	0.18	0.43	0.05	1.07
07-94-5304-1-1	Threehouse basalt	65.22	16.4	5.18	2.17	5.55	4.64	0.25	0.12	0.37	0.09	0.52
07-96-5461-2-1	Threehouse basalt?	52.02	16.73	13.21	5.11	8.28	3.78	0.23	0.17	0.43	0.04	0.5
07-94-5332-1-1	Threehouse gabbro	50.73	15.54	13.01	8.95	7.54	3.25	0.18	0.23	0.51	0.06	1.41
07-94-5333-1-1	Threehouse MFIV	48.91	15.64	15.46	7.29	3.51	3.32	0.18	0.21	0.4	0.09	1.42
07-94-5378-1-1	Threehouse gabbro	49.87	19.87	12.66	4.44	9.32	2.69	0.36	0.16	0.56	0.07	0.92
07-96-5427-2-1	Threehouse gabbro	52.35	15.76	14.94	4.09	8.4	2.99	0.55	0.23	0.63	0.06	0.2
07-96-5453-2-1	Threehouse gabbro	49.53	15.37	15.57	6.58	10.82	1.11	0.22	0.24	0.51	0.05	0.15
07-96-5466-1-1	Threehouse gabbro	52.46	16.91	12.83	5.07	9.27	2.52	0.3	0.2	0.39	0.05	0.25
07-94-5318-2-1	Mafic dyke	51.09	16.13	13.42	5.76	11.66	0.91	0.11	0.24	0.59	0.09	1.66
07-94-5171-1-1	Gabbro	52.09	16.79	14.48	4.86	9.57	1.05	0.12	0.24	0.68	0.12	1.15

All by XRF; major elements recalculated to 100% volatile free; total iron as Fe₂O₃

Table GS-8-1b

Trece Element Data (ppm) for Whole Rocks, Photo Lake

SAMPLE	Rock Type	Cr	Ni	Sc	V	Rb	Ba	Sr	Cs	U	Pb	Th	Zr	Y	Ta	Hf	Nb	La	Ce	Pr	Nd	Sm	Eu	Gd	Tb	Dy	Ho	Er	Tm	Yb	Lu
07-96-5589-1-1	Powderhouse dacite	6	4	46.8	0.96	302	129	0.09	0.92	2.05	1.33	81.7	23.3	0.34	2.326	5699:	8.38	19.75	2.49	11.15	3.1	0.88	3.79	0.61	4.34	0.91	2.71	0.43	2.67	0.43	
07-96-5592-1-1	Powderhouse dacite	1	14	36.8	2.42	85	339	0.05	0.54	10.88	0.98	42.4	20.5	0.16	1.26	3.64	11.14	22.05	2.71	11.59	2.56	0.83	2.86	0.43	3.14	0.71	2.21	0.32	2.15	0.36	
07-96-5605-1-1	Powderhouse dacite	12	12	24.5	0.98	125	170	0.0	0.76	5.37	1.59	102.3	26.3	0.27	2.72	6.12	13.49	29.22	3.81	16.24	3.93	1.06	4.3	0.69	4.71	1.01	3.04	0.46	3.06	0.47	
07-94-5095-1-1	Ghost rhyolite	<6	<7	22.2	3510.75	87	54	0.24	0.68	2.02	1.67	84.7	20.8	1.47	2.35	4.67	8.7	20.88	2.66	11.91	2.97	0.82	3.25	0.5	3.46	0.68	2.24	0.33	2.05	0.34	
07-94-5360-1-1	Ghost rhyolite	<6	<7	19.6	2322.84	114	76	0.16	0.8	5.04	1.89	94.1	22.6	1.23	2.53	4.92	10.03	23.64	2.84	12.09	2.93	0.68	2.97	0.48	3.48	0.75	2.56	0.37	2.57	0.39	
07-94-5407-1-1	Ghost rhyolite	<6	<7	17.5	1413.37	168	61	0.15	0.68	2.9	1.63	72.1	20.2	1.76	1.9	4.52	9.21	22.3	2.79	11.94	2.72	0.59	2.83	0.46	3.11	0.64	2.1	0.31	2.01	0.33	
07-94-5403-1-1	Ghost rhyolite	<6	<7	19.7	27 6.93	99	87	0.11	1.06	3.26	1.83	66.5	23	0.99	1.97	4.74	11.23	27.07	3.43	14.75	3.39	0.9	3.59	0.55	3.72	0.79	2.38	0.38	2.41	0.39	
07-96-5502-1-1	Ghost rhyolite	2	2	14.2	8.05	112	82	0.06	0.79	7.55	1.91	74.6	21.6	0.18	2.09	3.94	13.91	28.67	3.52	14.13	3	0.8	3.28	0.54	3.65	0.83	2.48	0.4	2.54	0.42	
07-96-5510-1-1	Ghost rhyolite	1	1	17.7	1.73	27	66	0.01	0.86	3.09	2.26	73	22.7	0.17	1.85	2.65	13.39	27.72	3.45	14.08	3.15	0.72	3.4	0.53	3.71	0.82	2.48	0.39	2.57	0.41	
07-96-5548-1-1	Ghost rhyolite	1	1	22.8	25.92	419	210	0.23	0.86	10.15	1.97	82.8	27.1	0.21	2.21	4.52	13.89	29.61	3.78	15.93	3.76	1.09	3.99	0.64	4.18	0.97	2.84	0.46	3.11	0.5	
CH-90-15-1903'	Ghost rhyolite	2	0.0	25.5	9.23	82	90	0.09	1.28	5.83	1.97	85.4	23.2	0.15	2.36	2.96	15.2	34.54	4.5	18.75	4.31	1.21	4.05	0.64	4.11	0.9	2.63	0.43	2.82	0.47	
07-94-5089-1-1	Ghost "andesite"	<6	<7	20.3	40 3.48	183	180	0.03	0.66	2.71	1.69	60.3	23.9	1.15	1.71	4.43	12.28	27.29	3.42	14.4	3.38	1.26	3.73	0.55	3.57	0.81	2.4	0.34	2.45	0.36	
07-94-5090-1-1	Ghost "andesite"	<6	<7	30.1	113 0.92	124	252	0.02	0.44	2.94	1.18	62.7	23.8	1.39	1.73	3.83	6.68	16.52	2.13	9.7	2.49	0.76	3.12	0.49	3.57	0.79	2.38	0.36	2.46	0.38	
07-94-5093-1-1	Ghost "andesite"	6	<7	22.8	5616.91	239	166	0.32	0.7	2.96	1.74	71	24.1	1.22	1.99	4.71	7.49	20.35	2.53	11.17	2.61	0.78	3.1	0.51	3.62	0.75	2.49	0.37	2.58	0.41	
07-94-5405-1-1	Ghost "andesite"	<6	<7	23.9	5713.93	118	54	0.27	0.56	1.45	1.35	68.6	24.6	1.02	1.83	3.99	8.05	18.99	2.56	11.1	2.81	0.77	3.17	0.51	3.74	0.83	2.64	0.36	2.62	0.42	
07-94-5406-1-1	Ghost "andesite"	<6	<7	24.3	64 1.43	58	142	0.0	0.59	2.11	1.49	57.3	23.7	0.9	1.63	3.88	8.28	21.64	2.54	11.41	2.93	0.81	3.25	0.52	3.9	0.82	2.57	0.41	2.59	0.37	
07-96-5497-1-1	Ghost "andesite"	2	4	29.5	11.39	252	93	0.18	0.58	5.27	1.29	58.4	19.3	0.09	1.62	2.85	4.93	11.68	1.52	7.05	2.09	0.63	2.73	0.46	3.25	0.71	2.14	0.33	2.17	0.35	
07-96-5573-1-1	Ghost "andesite"	1	1	19.7	0.74	34	189	0.08	1.49	3.86	1.6	66.3	22.6	0.15	1.72	3.42	11.19	23.99	3.04	13.14	2.94	0.91	3.2	0.52	3.65	0.84	2.48	0.39	2.51	0.4	
07-96-5573-1-2	Ghost "andesite"	1	5	34.6	0.64	28	120	0.07	0.45	8.17	0.84	44.8	17.7	0.08	1.33	1.96	2.09	5.13	0.79	4.28	1.59	0.79	2.34	0.41	2.89	0.66	2.1	0.32	2.09	0.34	
07-96-5440-1-1	Ghost "andesite"	2	1	31.7	1.16	60	164	0.04	0.52	4.97	0.99	57.4	21.4	0.13	1.73	2.51	5.76	13.28	1.77	7.89	2.11	0.75	2.78	0.47	3.38	0.78	2.35	0.37	2.37	0.41	
CH-90-15-597'	Ghost "andesite"	1	1	30.9	16.18	293	153	0.31	0.5	3.53	1.16	65.6	23.9	0.09	1.9	2.59	7.77	17.32	2.33	10.2	2.71	0.75	3.31	0.56	3.98	0.92	2.72	0.42	2.77	0.46	
07-94-5009-1-1	Photo rhyolite	6	<7	16.5	22 7.77	113	73	0.21	0.89	1.25	2.45	89.2	24.4	1.17	2.53	5.27	10.69	26.79	3.29	13.96	3.38	0.73	3.53	0.53	3.98	0.79	2.58	0.39	2.5	0.44	
07-94-5011-1-1	Photo rhyolite	<6	<7	30.8	5 1.64	15	190	0.14	0.95	3.79	2.57	104.6	20.5	0.96	2.79	6.35	12.47	32.9	4.14	17.54	3.93	1.26	3.77	0.55	3.48	0.73	2.18	0.34	2.32	0.4	
07-94-5044-1-1	Photo rhyolite	6	<7	36	46 3.43	83	197	0.08	0.53	2.35	1.4	51.5	21.1	1.18	1.44	3.93	9.37	23.05	2.96	12.86	3.21	0.88	3.2	0.48	3.32	0.66	2.09	0.3	2.23	0.35	
07-94-5058-1-1	Photo rhyolite	7	<7	23	1024.33	222	73	0.23	0.9	4.66	1.91	28.1	25.1	2.13	0.71	5.41	12.45	28.66	3.54	14.49	3.38	0.89	3.7	0.56	3.77	0.84	2.66	0.4	2.64	0.44	
07-94-5120-1-1	Photo rhyolite	<6	<7	30.1	46 5.73	100	166	0.17	0.74	1.85	1.71	65.3	22.9	0.9	1.72	4.87	9.08	22.07	2.81	12.42	2.75	0.83	3.09	0.47	3.36	0.72	2.42	0.36	2.5	0.4	
07-94-5128-1-1	Photo rhyolite	6	<7	38.2	49 1.13	53	234	<0.01	0.73	2.13	1.75	69.1	25.3	1.7	1.89	5.01	5.47	16.24	1.74	7.93	2.41	0.79	3.57	0.57	3.81	0.83	2.65	0.38	2.42	0.4	
07-94-5242-1-1	Photo rhyolite	<6	1	11.3	14 1.96	31	101	0.0	0.88	3.08	1.67	53.6	16.1	0.92	1.47	3.31	9.45	19.96	2.33	9.52	2.2	0.54	2.29	0.35	2.43	0.54	1.83	0.29	1.89	0.3	
07-94-5244-1-1	Photo rhyolite	<6	<7	11.2	7 4.89	263	61	0.14	0.92	2.07	2.13	79.1	17.2	0.98	2.12	4.21	1.94	9.64	0.68	2.88	0.94	0.26	1.28	0.27	2.31	0.61	1.97	0.31	1.99	0.34	
07-94-5248-1-1	Photo rhyolite	<6	<7	16.2	26 8.29	152	221	0.46	0.96	3.53	2.31	87.4	22.7	1	2.27	5.36	12.16	28.46	3.59	14.51	3.11	0.77	3.43	0.48	3.38	0.75	2.42	0.33	2.42	0.38	
07-94-5257-1-1	Photo rhyolite	<6	<7	13.4	19 2.85	43	147	0.04	0.86	3.47	2.07	80	17.7	1.31	2.23	4.52	12.96	29.27	3.52	14.83	3.38	0.83	3.39	0.48	3.07	0.62	1.99	0.28	1.92	0.31	
07-94-5267-1-1	Photo rhyolite	9	<7	35.1	64 5.15	236	471	0.16	0.53	2.73	1.38	53.6	23.7	1.13	1.42	3.82	9.61	23.67	3.12	13.81	3.48	1.06	3.46	0.51	3.61	0.74	2.37	0.34	2.43	0.37	
07-94-5270-1-1	Photo rhyolite	<6	<7	23.8	1214.79	125	158	0.27	0.64	1.59	1.58	76.9	20.7	1.66	1.71	5.1	9.7	23.63	2.95	12.77	2.81	0.71	2.75	0.39	2.81	0.59	1.86	0.31	2.02	0.33	
07-94-5291-1-1	Photo rhyolite	<6	1	14.6	18 7.23	66	116	0.18	0.97	2.86	2.26	87.8	24.4	1.31	2.29	5.18	14.51	31.87	3.78	14.83	3.4	0.89	3.54	0.53	3.83	0.79	2.43	0.35	2.47	0.38	
07-94-5399-1-1	Photo rhyolite	<6	0.0	17	2114.36	207	42	0.35	1.07	2.79	2.49	91.4	19.5	1.38	2.56	5.61	9.31	22.13	2.89	12.07	2.76	0.53	2.72	0.44	3.38	0.69	2.26	0.37	2.53	0.42	
07-94-5400-1-1	Photo rhyolite	<6	0.0	16.3	2934.53	499	262	0.31	0.83	3.36	2.08	32.4	25.5	1.09	0.82	5.23	13.14	29.93	3.69	15	3.35	0.8	3.64	0.53	3.94	0.83	2.54	0.39	2.67	0.4	
07-94-5031-1-1	Bolloch dacite	6	<7	27.3	24 3.36	88	128	0.01	0.85	2.47	1.66	58.7	23.2	1.24	1.54	6.17	10.36	23.91	3.04	12.87	2.96	0.95	3.11	0.48	3.43	0.79	2.45	0.38	2.63	0.43	
07-94-5106-1-1	Bolloch dacite	<6	<7	30.4	114 4.87	118	232	0.07	0.5	1.87	1.35	67.7	26.5	0.63	1.81	3.38	7.62	18.27	2.33	10.17	2.57	0.8	3.15	0.53	3.94	0.84	2.63	0.41	2.68	0.44	
07-94-5110-1-1	Bolloch dacite	<6	<7	31.5	2 6.01	54	41	0.27	0.88	1.2	2.69	118.6	14.9	1	3	7.5	9.08	20.48	2.5	9.91	2.38	0.71	2.42	0.38	2.65	0.52	1.75	0.28	1.94	0.33	
07-94-5103-1-1	Bolloch basalt	9	<7	63.4	503 0.94	30	102	<0.01	0.56	2.04	1.16	19	13	0.87	0.58	4.55	5.91	13.59	1.62	6.81	1.58	0.59	1.63	0.26	1.92	0.42	1.34	0.21	1.42	0.22	
07-94-5067-1-1	Bolloch basalt	<6	<7	51	249 0.76	55	190	0.01	0.72	1.33	1.12	29.9	16.7	0.76	0.81	3.48	5.35	13.21	1.81	8.46	2.34	0.85	2.56	0.36	2.43	0.55	1.8	0.25	1.62	0.27	
07-94-5300-1-1	Threehouse basalt	86	17	65.4	404 1.06	60	160	<0.01	0.16	1.17	0.46	13.5																			

1996). On the chondrite normalized plots, the Photo Lake rhyolite displays: an elevated light rare earth element (LREE) pattern with a negative slope to Eu; flat heavy rare earth element (HREE) patterns; and, typically, small negative Eu anomaly. The elevated, negative sloping LREE and flat normal HREE patterns displayed by PLR are characteristic of other evolved arc felsic rocks (Fig. GS-8-7) and are in marked contrast to primitive arc rhyolites (Fig. GS-8-7a and 7b) that display flat or only slightly negative REE profiles.

Ghost Lake rhyolite (GLR)

GLR consists of massive, aphyric to sparsely porphyritic felsic flows that commonly contain quartz amygdaloids, quartz-filled gas cavities and local massive lobes with intervening microbreccia. They are identical to PLR but are separated by a fault. Nine geochemical analyses of the Ghost Lake rhyolite were undertaken to test the possible equivalence of GLR and PLR.

On all plots in Figures GS-8-5 to 7, geochemical analyses of GLR and PLR are virtually indistinguishable. This is particularly true of chondrite normalized REE plots (Fig. GS-8-7), with both GLR and PLR displaying identical LREE enriched patterns, including small negative Eu anomalies for most samples. The implication is that the GLR and PLR rhyolite domains are likely part of the same felsic flow complex.

Ghost Lake andesite (GLA)

Ghost Lake "andesite" (GLA) forms narrow units within the Ghost Lake rhyolite as well as a more prominent domain extending northwest of Ghost Lake and north of Chisel Lake. GLA consists of massive aphyric flows locally characterized by large (up to 7 cm diameter) quartz-filled gas cavities. The flows include irregular domains of medium to dark green weathering melanocratic rocks and intervening areas of light green to grey weathering leucocratic rocks, with some of the rocks displaying prominent zones of rusty weathering. During previous mapping these rocks have been classified as felsic volcanic rocks and as mafic flows (Harrison, 1949; Williams, 1966; Bailes and Galley, 1992). During mapping of the Photo Lake area (Bailes *et al.*, 1996) this problematic rock lithology was mapped as separate unit, and the conclusion made that it represents a domain of hydrothermally altered felsic flows.

In order to test the assumption that GLA represents altered felsic rocks and not altered mafic rocks, a suite of 9 samples from GLA was geochemically analyzed by the same analytical procedures as other Photo Lake area rocks. On a plot of Zr/TiO_2 vs. SiO_2 (Fig. GS-8-5a), GLA is commonly more mafic than PLR, GLR or other felsic flows, but does overlap their compositional range (large symbols). GLA does not overlap the compositional range of associated mafic flows (small symbols). On a plot of Nb/Y vs. Zr/TiO_2 , a plot designed to minimize the effects of alteration by employing relatively immobile elements, the Ghost Lake "andesite" clearly plots with other Photo Lake felsic rocks and not with Photo Lake mafic rocks, supporting the interpretation that GLA was produced by alteration of associated felsic rocks.

Bolloch Lake rhyolite (BLR)

Bolloch Lake rhyolite (BLR) consists of felsic orthogneiss, northwest of Bolloch Lake, and less strongly recrystallized equivalents southeast and east of Bolloch Lake; the latter locally consists of domains (lobes?) of massive rhyolite and intervening domains of monolithologic breccia (microbreccia?). The relationship between these felsic rocks and the other major felsic units, PLR and GLR, is uncertain. This package of felsic rocks correlates along strike to the north and west with a prominent package of felsic gneisses (Harrison, 1949), so it is important to know if this unit correlates with the VMS-hosting PLR sequence.

Four samples of Bolloch Lake felsic rocks were analyzed. On a plot of Zr/TiO_2 vs. SiO_2 (Fig. GS-8-5a) they clearly plot separately from PLR and GLR with lower overall SiO_2 content (63-67 wt.%, one anomalous analysis at 75 wt.%). On chondrite normalized REE plots they show broad similarity to PLR and GLR but are not as prominently LREE enriched nor do they have the negative Eu anomaly. They do, however, display similar REE profiles as the Snow Creek rhyodacite (Fig. GS-8-7a), which lies higher in the stratigraphic section than the PLR and GLR. Thus, although the Bolloch Lake felsic rocks show some broad similarities to PLR and GLR, there is no conclusive data to suggest they are correlative with PLR and GLR and some evidence that they may correlate with felsic flows stratigraphically higher in the Snow Lake arc assemblage.

Powderhouse dacite (PWD)

Powderhouse dacite is a distinctive package of felsic volcanoclastic rocks forming the stratigraphic footwall to the Zn-rich VMS deposits at Chisel Lake. Analyzed samples from the type area south of the Chisel Lake mine display prominent elevated LREE contents (Fig. GS-8-7d) that serve to distinguish this unit from other felsic units in the Snow Lake area. A suite of dacitic volcanoclastic rocks from the southwest part of the Photo Lake area are texturally similar to the Powderhouse dacite.

In order to establish whether rocks mapped as Powderhouse dacite in the Photo Lake area are equivalent to those south of the Chisel Lake VMS deposits, 3 samples of the Photo Lake unit were analyzed. The Photo Lake dacitic volcanoclastics display lower Zr values (42-102 ppm compared to 131-152 ppm) and much lower contents of LREE (Fig. GS-8-7c). Thus the dacites in the southwest corner of the Photo Lake map area, although texturally similar, are certainly not direct equivalents and may not be related to the Powderhouse dacite at the Chisel mine site.

Comparison to Abitibi Belt rhyolites

Barrie *et al.* (1993) has identified some of the geochemical parameters that distinguish VMS-rich and VMS-poor rhyolite sequences in the Archean Abitibi Belt. Geochemical analyses of Photo Lake area felsic rocks have been plotted on these discrimination diagrams (Figs. GS-8-6d, 6e and 6f); note that the fields of Barrie *et al.* (1993) have been generalized from specific mining camps to the broader fields of "ore-bearing" and "barren". Photo Lake felsic rocks fall on the periphery of the ore-bearing field and just within the barren fields on these diagrams. They do, however, fall within the same fields as rhyolites associated with the Flin Flon area VMS deposits (Syme *et al.*, in prep.).

Bailes and Galley (1996) have previously noted that rhyolites associated with VMS deposits in Snow Lake do not display the same features as do Archean rhyolites associated with VMS deposits in the Abitibi Belt. This probably stems from derivation of Snow Lake magmas from a more depleted mantle source, as noted by Stern *et al.* (1995), with resultant fundamental variations in trace element characteristics. The implication is that trace element characteristics of VMS-rich and VMS-poor rhyolites are not necessarily transferable from one area to another and may have to be developed individually for each mining district or camp.

ECONOMIC IMPLICATIONS

VMS deposits are invariably spatially associated with rhyolite flow complexes. This examination of the geochemistry of volcanic rocks at Photo Lake is an important step in characterizing the geochemistry of the contained felsic rocks and placing limitations on correlation between the various felsic lithologies.

The mafic and felsic volcanic rocks of the Photo Lake area comprise a tholeiitic, bimodal (mafic/felsic) sequence with an island arc chemical signature. Furthermore, they belong to the "evolved arc" part of the Snow Lake arc assemblage as defined by Bailes and Galley (1996), confirming that the Cu-rich Photo Lake deposit represents a new and unique VMS environment in the Snow Lake district.

The rhyolite (PLR) that hosts the Photo Lake VMS deposit has a distinct geochemical signature that is duplicated by the Ghost Lake rhyolite and, therefore, these rhyolite domains are interpreted to be part of the same complex. This suggests that the Ghost Lake rhyolite may have potential for not only Chisel Lake Zn-rich VMS mineralization (the traditional view) but also for Photo Lake-type Cu- and Au-rich VMS mineralization. The Ghost Lake rhyolite is locally intercalated with Ghost Lake "andesite", a widely distributed altered felsic rock, further enhancing the overall potential of this rhyolite body.

The Bolloch Lake rhyolite, part of a recrystallized felsic orthogneiss sequence that extends north of the map area to the west of Squall Creek, has more affinities to the Snow Creek rhyolite than it has to the Photo Lake rhyolite. The implication is that the Bolloch Lake rhyolite may not be related to the Photo-Ghost rhyolite complex but, rather, that it may correlate with felsic rocks, such as the Snow Creek rhyolite, that occur higher in the stratigraphy of the Snow Lake arc assemblage. This interpretation, places the Bolloch Lake rhyolite in a succession that to date has not produced any known VMS deposits.

Rhyolites in the Photo Lake area do not display the same geochemical features as do VMS deposit-associated rhyolites from the Archean Abitibi Belt, although they do display similar characteristics to

VMS-hosting rhyolites at Flin Flon. Geochemical criteria developed to distinguish between "ore-bearing" and "barren" rhyolites for the Abitibi belt should be used with caution in the Proterozoic Flin Flon Belt. A project to establish geochemical criteria to distinguish "ore-bearing" from "barren" rhyolites specific to the Paleoproterozoic Flin Flon Belt is currently in progress.

ACKNOWLEDGEMENTS:

This project was supported by Hudson Bay Exploration and Development (HBED) who gave access to confidential company information, provided tours of the Photo Lake mine, and paid for geochemical analyses. I would like to acknowledge Darren Simms of HBED who was a co-investigator during the initial field investigations in 1994. I thank Gerry Kitsler of HBED who has supported this and my many other projects in the Snow Lake area. This manuscript benefited from editing comments by E. Syme (MEM).

REFERENCES:

- Bailes, A.H. and Galley, A.G.
1992: Chisel-Anderson-Stall Lakes NTS 63K/16E; Manitoba Energy and Mines, Minerals Division, Preliminary Map 1992S-1, 1:20 000
- Bailes, A.H. and Simms, D.
1994: Implications of an unconformity at the base of the Threehouse formation, Snow Lake (NTS 63K/16); in Manitoba Energy and Mines, Minerals Division, Report of Activities, p. 85-88.
- Bailes, A.H., Chackowsky, L.E., Galley, A.G., and Connors, K.A.
1994: Geology of the Snow Lake-File Lake area, Manitoba (parts of NTS 63K16 and 63J13); Manitoba Energy and Mines, Open File Report OF94-4, 1:50 000 colour map.
- Bailes, A.H. and Galley, A.G.
1996: Setting of Paleoproterozoic volcanic-associated massive sulphide deposits, Snow Lake, Manitoba; in G.F. Bonham-Carter, A.G. Galley and G.E.M. Hall, eds. EXTECH I: A multidisciplinary approach to massive sulphide research in the Rusty Lake and Snow Lake greenstone belts, Manitoba; Geological Survey of Canada, Bulletin 426, p. 105-138.
- Bailes, A.H., Simms, D., Galley, A.G. and Young, J.
1996: Geology of the Photo Lake area (NTS 63K/16); Manitoba Energy and Mines, Preliminary Map 1996S-1, 1:10 000.
- Barrie, C.T., Ludden, J.N. and Green, A.H.
1993: Geochemistry of volcanic rocks associated with Cu-Zn and Ni-Cu deposits in the Abitibi Subprovince; *Economic Geology*, v. 88, p.1341-1358.
- Harrison, J.M.
1949: Geology and mineral deposits of File-Tramping Lakes area, Manitoba; Geological Survey of Canada, Memoir 250, 92 p.
- Menard, T. and Gordon, T.M.
1995: Syntectonic alteration of VMS deposits, Snow Lake, Manitoba; in Manitoba energy and Mines, Minerals Division, Report of Activities, 1995, p. 164-167.
- Pearce, J.A.
1975: Basalt geochemistry used to investigate past tectonic environments on Cyprus; *Tectonophysics*, v. 25, p. 41-67.
- Pearce, J.A.
1996: A user's guide to basalt discrimination diagrams; in Wyman, D.A., ed, Trace element geochemistry of volcanic rocks: Applications for massive sulphide exploration; Geological Association of Canada, Short Course Notes, v.12, p. 79-113
- Pearce, J.A., Harris, N.B. and Tindle, A.G.
1984: Trace element discrimination diagrams for the tectonic interpretation of granitic rocks; *Journal of Petrology*, v. 25, p. 956-983.
- Stern, R.A., Syme, E.C., Bailes, A.H. and Lucas, S.B.
1995: Paleoproterozoic (1.90-1.86 Ga) arc volcanism in the Flin Flon Belt, Trans-Hudson Orogen, Canada; *Contributions to Mineralogy and Petrology*, v.119, p. 117-141.
- Sun, S.-s. and McDonough, W.F.
1989: Chemical and isotopic systematics of oceanic basalts; implications for mantle compositions and process; in Saunders, A.D. and Norry, M.J., eds., *Magmatism in the Ocean Basins*, Geological Society Special Publications 42, p. 313-345.
- Syme, E.C. and Bailes, A.H.
1993: Stratigraphy and tectonic setting of Early Proterozoic volcanogenic massive sulphide deposits, Flin Flon, Manitoba; *Economic Geology*, v. 88, p. 566-589.
- Syme, E.C., Lucas, S.B., Bailes, A.H. and Stern, R.A.
in prep: Role of tectonostratigraphic setting and intra-arc extension in localizing Paleoproterozoic volcanogenic massive sulphide deposits, Flin Flon Belt, Manitoba
- Williams, H.
1966: Geology and mineral deposits of the Chisel Lake map area, Manitoba; Geological Survey of Canada, Memoir 342, 38 p.
- Winchester, J.A. and Floyd, P.A.
1977: Geochemical discrimination of different magma series and their differentiation products using immobile elements; *Chemical Geology*, v. 20, p. 325-343.

GS-9 GEOLOGICAL SETTINGS AND GENESIS OF GOLD MINERALIZATION IN THE SNOW LAKE AREA (NTS 63K/16)

by G.H. Gale

Gale, G.H. (1997): Geological settings and genesis of gold mineralization in the Snow Lake area (NTS 63K/16); in Manitoba Energy and Mines, Minerals Division, Report of Activities, 1997, p. 73-78.

SUMMARY

Gold-bearing mineralization in the Snow Lake -Squall Lake area is hosted dominantly by mafic volcanic and intrusive rocks. Some of the pyroxene-bearing rocks mapped previously as intrusions are pyroclastic in origin. Pyroxene-rich intrusive and extrusive rocks are comagmatic. The mineralization is structurally controlled, postdates the intrusion of mafic sills into Missi Group rocks, and probably predates development of the Threehouse synform.

INTRODUCTION

The Nor-Acme gold deposit, mined by Howe Sound Exploration Co. Ltd. and the Britannia Mining & Smelting Co. Ltd. produced 5.8 M tonnes of 5.2 g/t Au during 1949-58. The deposit, reopened in 1995 by TVX Gold Inc., is once again a major producer in the Province. Recent studies by Galley *et al.* (1986, 1989) and Fedikow *et al.* (1989) have reported on the gold deposits in some detail. The present investigation was undertaken in order to assist explorationists in understanding the controls and genesis of gold mineralization in the area. This investigation is being undertaken in conjunction with MSc. theses studies at the University of Manitoba by Pamela Fulton and Ian Fieldhouse on the mineralogy and structural controls of mineralization. Regional geological mapping is being undertaken by D. Schledewitz (GS-10, this volume).

Froese and Moore (1980) considered the gold mineralization to be syngenetic in origin because of its localization along the contact of felsic and mafic volcanic rocks. Galley *et al.* (1986, 1989) and Harrison (1949) indicate that the gold is situated at the junction of the Nor-Acme fault and the Nor-Acme anticline.

Because this was the initial year of this study, emphasis was placed on familiarization with the geology and structural events in and around the individual deposits and occurrences; for example, investigating the genesis of "pyroxene-bearing" rocks that host some of the deposits and digitizing detailed Howe Sound Exploration Co. Ltd. geology maps.

GENERAL GEOLOGY

Most of the area has been mapped in detail at 1:2400 scale by several property holders, namely, Howe Sound Exploration Co. Ltd., Goldfields Canadian Mining Ltd. and TVX Gold Inc.. Galley *et al.* (1988) produced a 1:5000 scale map based on the Howe Sound Exploration Co. Ltd. and Goldfields outcrop geology maps. In general, the interpretation presented in Figure GS-9-1 is similar to that presented by Galley *et al.* (1988) and differs mainly in the interpretation of some of the 'pyroxene'-bearing rocks. For a description of the regional geology the reader should consult Schledewitz (this volume).

Rocks in the map area, north of the McLeod Road Fault, young to the north and northeast. The oldest rocks thick sequence of felsic volcanic rocks that occur as a large mass south and east of the New Britannia Mine and as a small body north of the mine. These rocks are in fault contact with, and are overlain, by heterolithic, dominantly mafic volcanoclastic rocks that locally contain abundant stubby crystals of amphibole pseudomorphs after pyroxene crystals. (Fig. GS-9-1). The pyroxene-bearing rocks are overlain by a unit of thinly layered biotite and quartz-rich sandstone and siltstone, greywacke and mafic sedimentary rocks. The sedimentary rocks are in turn overlain by dominantly aphyric basaltic pillow lava and associated(?) doleritic intrusions that are in fault contact with pyroxene-bearing clastic and intrusive (?) rocks north of the Birch Zone fault.

The Birch Lake Shear Zone and Missi Group sedimentary rocks with abundant 'gabbroic' intrusions occupy the eastern part of the map area.

VOLCANIC ROCKS

Felsic volcanic rocks

The felsic volcanic rocks in the map area are considered to be rhyolite and rhyodacite (Howe Sound Exploration Co. Ltd., unpublished maps; Galley *et al.*, 1988). These rocks are predominantly fragmental with a wide range in fragment size and phenocryst content and include aphyric, quartz phyric and quartz-feldspar phyric lithologies (Galley *et al.*, 1988).

Mafic volcanoclastic rocks

Mafic volcanoclastic rocks vary considerably in both composition and texture. In the southern exposures of this unit, in the vicinity of the faulted contact with the felsic volcanic rocks, it consists predominantly of mafic lapilli tuff and tuff that are interlayered with breccias containing angular lapilli- to block-sized fragments of felsic volcanic rocks that are up to 50 cm in length. The 'pyroxene' crystal content of these rocks is generally < 10%.

The abundance of felsic fragments decreases rapidly northwards and the unit consists dominantly of 'pyroxene' crystals and lapilli to block sized fragments of aphanitic scoriaceous basalt, feldspar phyric basalt, pyroxene phyric basalt and 'massive' mafic rock with > 50% 'pyroxene' crystals in a recrystallized aphanitic matrix.

Pyroxene phyric mafic volcanoclastic rocks

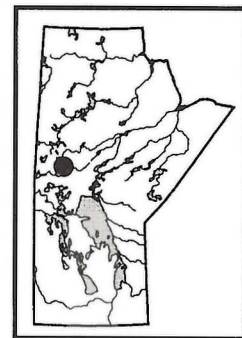
The mafic volcanoclastic rocks (Fig. GS-9-1) are characterized by the presence of stubby rectangular crystals of amphibole that range in size from < 5 mm to > 15 mm. These crystals commonly have the euhedral outlines of pyroxene, are zoned and have twins typical of pyroxene crystals. Thin sections suggest that these are unaltered pyroxene.

In the vicinity of the portal to the No. 3 Zone (Fig. GS-9-1) the volcanoclastic rocks include a tuff breccia that contains subrounded blocks (up to 40 cm) that consist of up to 20%, 15 mm euhedral pyroxene and < 10% 2 - 4 mm feldspar phenocrysts in a grey "andesitic" matrix. This breccia is interlayered with well bedded tuff and pyroxene crystal lapilli tuff with up to 80% pyroxene. Locally, the blocks define a layer in the tuff breccia. One block, with a rounded base and a flat top, disrupts layers in a tuff and is interpreted as a bomb dropped into unconsolidated tuff. Other outcrops in the vicinity of the No. 3 Zone contain blocks of amygdaloidal basalt in a matrix of lapilli tuff with pyroxene crystals.

Southeast of the Boundary Zone the volcanoclastic rocks are commonly massive and contain variable amounts of pyroxene crystals. Within and between outcrops the crystal contents vary from < 40 %, < 7 mm, crystals in a grey 'aphanitic' matrix to > 80%, > 10 mm, crystals in a similar matrix; boundaries between the different concentrations of crystals are typically irregular and gradational (Fig. GS-9-2). Locally, clean exposures of this pyroxene-rich rock exhibit rare fragments of scoriaceous aphyric and amygdular pyroxene phyric basalt that attest to the pyroclastic nature of this 'massive' rock.

In the vicinity, and northeast, of the Boundary Zone, pyroxene-crystal rich rocks are abundant and locally interlayered with tuff and lapilli tuff. Although locally 'massive' and consisting of 5-10 mm crystals in an aphanitic matrix, there is a paucity of features in both drill core and exposures that can be ascribed to flow textures or an intrusive origin, but exhibit considerable variations in both crystal size and content over short intervals of core. Elsewhere within this unit, *e.g.*, along the tailings pipeline road, a number of exposures are characterized by 1-3 m beds, 5-10 mm pyroxene crystals in a tuff matrix and 1-90% crystals (Fig. GS-9-3). Bed margins are commonly defined by tuff that is devoid of crystals, but are also defined by size and abundance grading of crystals. Amygdaloidal basalt fragments are common in some beds.

Several of the large masses of pyroxene-bearing rocks shown by Galley *et al.* (1988) as late intrusions, *e.g.*, northeast and southeast of the Boundary Zone, are reinterpreted on the basis of recently cleaned



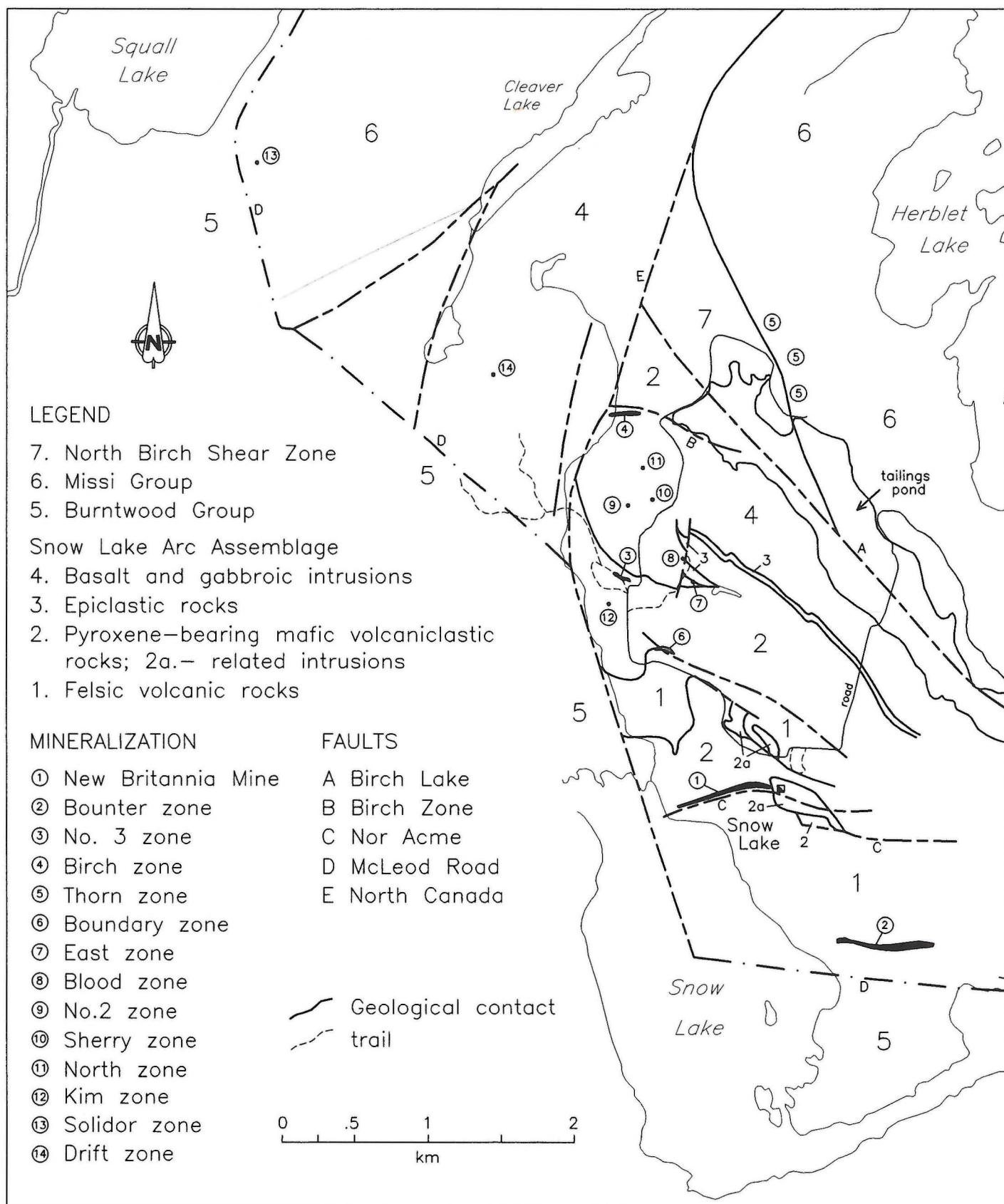


Figure GS-9-1: General geology of the New Britannia - Birch Zone area, Snow Lake.

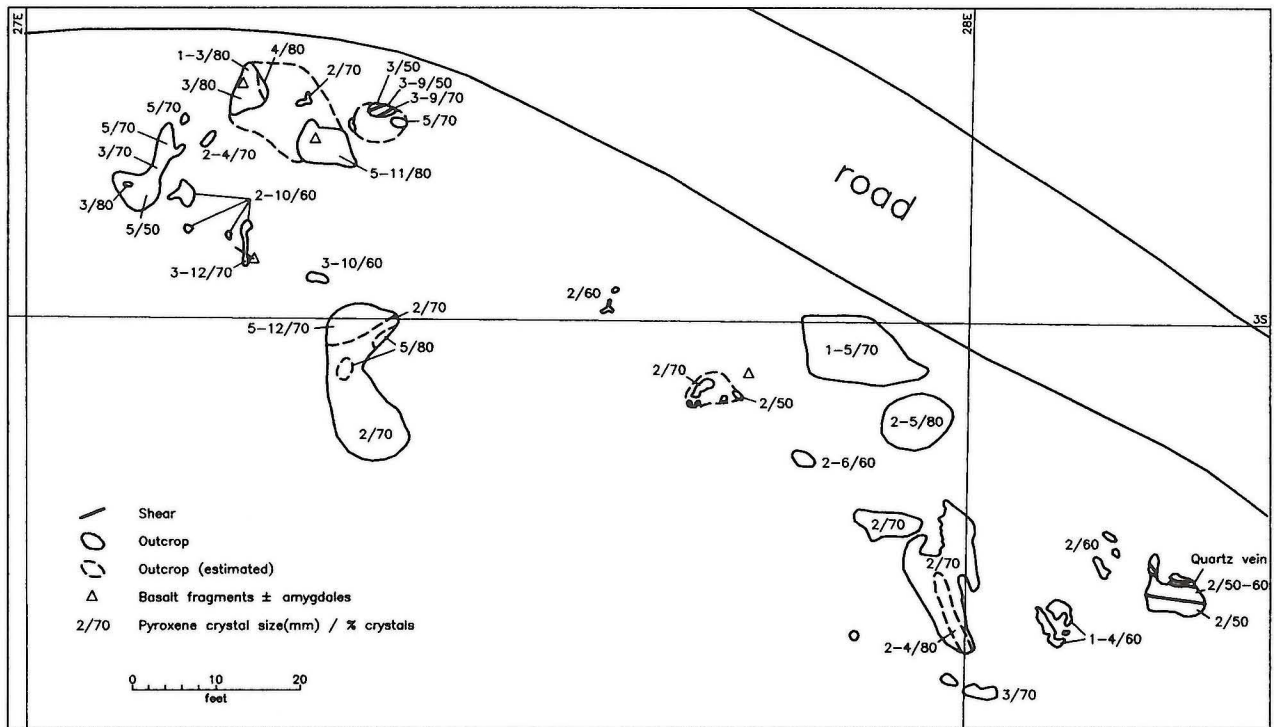


Figure GS-9-2: Distribution of pyroxene crystals in pyroclastic rocks southeast of the Boundary Zone.

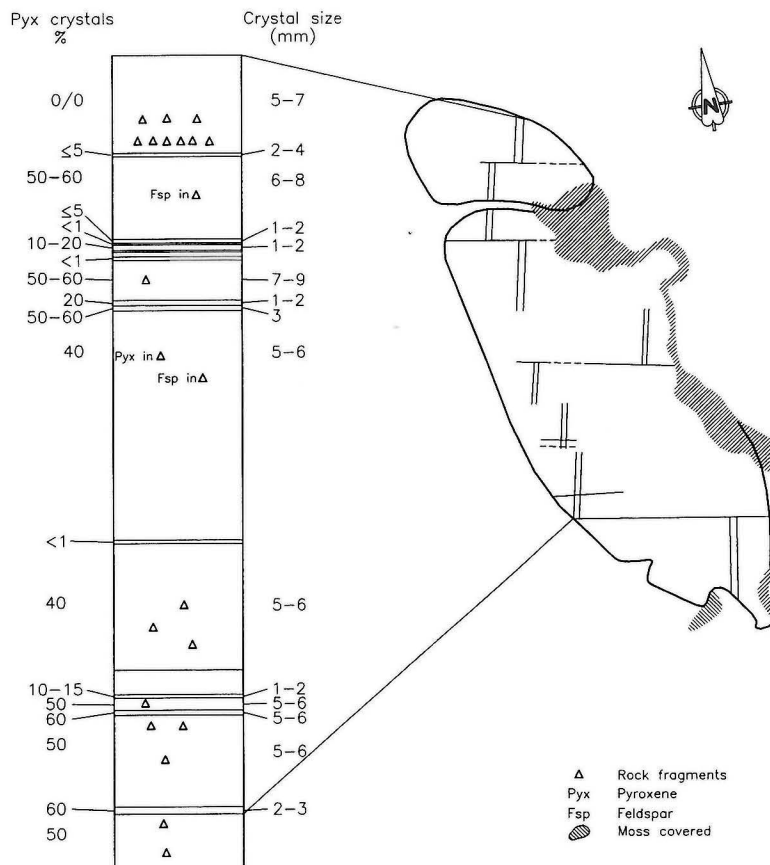


Figure GS-9-3: Tuff and tuff-breccia beds in pyroxene-rich rocks northeast of the mill complex.

exposures to be extrusive and volcanoclastic rocks. The two larger masses of pyroxene-rich rocks situated immediately north and northwest of the mill complex are lichen covered; these exposures also are probably a mixture of volcanoclastic and intrusive rocks.

Some of the pyroxene-bearing heterolithic rocks in the area are layered, contain angular felsic blocks up to 50 cm in length in a dominantly mafic matrix, are interbedded with tuff and were probably deposited as debris flows, *e.g.*, in the vicinity of the New Britannia Mine. Elsewhere, the presence of crystal lapilli tuff and tuff interlayered with blocks of pyroxene porphyritic rock as well as heterolithic mafic tuff breccia attest to a pyroclastic origin for some of these rocks, *e.g.*, in the vicinity of the No. 3 and Boundary Zones. The pyroxene crystal lapilli tuff deposits are considered to represent deposits that lost much of the original matrix in an eruption column. The collapse of a major eruption column and rapid deposition of pyroclastic ejecta would explain the variable crystal and matrix content, variable crystal size, and 'massive' nature of some of the pyroxene-rich rocks previously described as intrusions.

Massive pyroxene-rich rocks also occur as cm to metre thick dykes and as oval masses 50-100 m in diameter, *e.g.*, south east of the mill complex. These differ from the 'massive' pyroclastic rocks in that they consist almost entirely of coarse grained (> 1 cm) crystals in an aphanitic matrix. The pyroxene-rich intrusions cut rhyolitic rocks and the pyroxene-bearing pyroclastic rocks, but have not been observed cutting the younger basalts. These intrusions are interpreted here to be related to the magmatism that produced the pyroxene crystal tuffs and in part to represent feeders to the extrusive rocks rather than a separate and younger magmatic event (Galley *et al.*, 1988).

There is little evidence at this time to ascribe a subaerial origin to the pyroxene-rich rocks in this area. The presence of pillow-like shapes in similar massive rocks that occur along strike to the east, a paucity of amygdules in many of the pyroxene-phyric blocks and a crude sorting in some of the layered rocks suggests eruption of the magma into a shallow water environment.

Mafic volcanic and intrusive rocks

Aphanitic to fine grained basalt and associated dolerite occur in the northern part of the map area. The basalt (Fig. GS-9-1) includes mainly aphanitic and minor feldspar phyric pillow lava that occurs either as large units with minor fine grained dolerite dikes, or as screens within large masses of fine- to medium-grained dolerite. The pillows vary in size from flow to flow as well as within individual flows. Locally the pillows are separated by domains with 1-5 mm fragments that are considered to be of hyaloclastite origin (Fig. GS-9-4). Individual pillow outlines suggest that tops are predominantly towards the northeast. Although the pillowed flows do not display a schistosity, individual pillows are elongated and have a northeasterly plunge.

Several small masses of fine grained leucocratic rocks occur in the northern part of the area within both the basalt and dolerite, *e.g.*, near the Birch deposit (Fig. GS-9-1). These beige to grey coloured, massive to weakly schistose rocks occur as continuous units that are several metres to tens of metres thick and several hundred metres in length. These rocks are devoid of volcanic textures and occur within both massive mafic intrusions and volcanic rocks. Preliminary rock chemistry (P. Snajder, TVX Gold Inc., pers. comm., 1997) is consistent with an origin as altered mafic rocks.

EPICLASTIC ROCKS

A 40 to 50 m thick unit of epiclastic rocks occurs between pyroxene-rich rocks and the overlying basalts (Fig. GS-9-1). The contacts are not exposed. These clastic rocks include thinly bedded quartz- and biotite-rich siltstone and sandstone, greywacke and possible mafic tuff. These rocks probably represent a major break in volcanism between the pyroxene-bearing magmatism and that producing the younger aphanitic basalt.

NORTH BIRCH SHEAR ZONE

A shear zone with an exposed width of approximately 500 m extends northwestwards through Birch Lake and locally separates the volcanic rocks

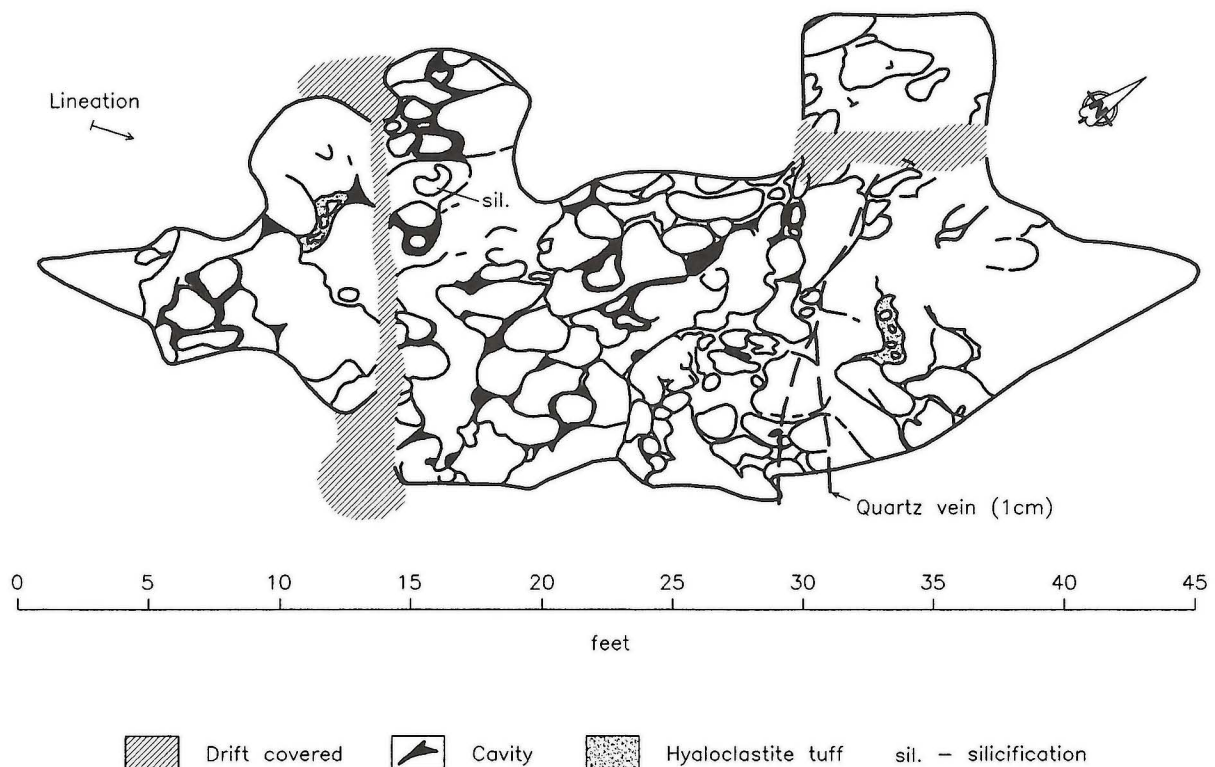


Figure GS-9-4: Outline of pillows in an outcrop northeast of the No. 3 Zone.

from Missi Group sedimentary rocks. Parts of the zone that were mapped in detail exhibit a pronounced schistosity that has a variable but overall strike of 350° and dips of 20° to 30° E. The shear zone contains lenses of aphanitic basalt, pyroxene-crystal bearing rocks of unknown origin and leucocratic quartz-feldspathic rocks that locally resemble Missi Group sedimentary rocks. The lithologic units exhibit variable degrees of deformation, *e.g.*, the pyroxene-bearing rocks vary from segments with euhedral crystals to others with crystals elongated 10 times their thickness. The zone has been affected by cross cutting zones of ferro-dolomite and amphibolitization of felsic rocks that have recrystallized to coarse grained garnet and amphibole.

MISSI GROUP AND YOUNGER ROCKS

Sedimentary rocks of the Missi Group occur east of the North Birch Shear Zone and appear to be separated from the underlying volcanic rocks by the shear zone and later faults along the eastern margin of the shear zone. Missi Group rocks are well layered and quartz- and feldspar-rich. Fine- to medium-grained recrystallized Post-Missi gabbroic intrusions are common along the western margin of the Missi Group. The intrusions range in thickness from a few meters to more than a hundred metres in the vicinity of the Thorn Zone (Fig. GS-9-1).

MINERALIZATION

In addition to the New Britannia Mine, there has been limited production from the No. 3 and Birch Zones (Fig. GS-9-1). Drilling and trenching programs have also been conducted on a number of occurrences within both the volcanic rocks as well as mafic intrusions within both the volcanic rocks and the Missi Group (Fig. GS-9-1). The only feature that the mineralization in these different settings have in common is it occurs structurally/stratigraphically above the Burntwood Group. Most of the known economic mineralization occurs in the mafic rocks that occur between the McLeod Road Fault and the North Birch Shear Zone, but significant mineralization also occurs in mafic intrusions that cut Missi Group rocks at the Thorn Zone and in the Squall Lake area. Although the alteration and mineralization have many similarities from deposit to deposit, the mineralization itself occurs in a variety of lithologic types.

The New Britannia Mine occupies a zone of recrystallized alteration within a heterolithic tuff-breccia that consists dominantly of lapilli sized particles. It is not certain if these zones of mineralization crosscut or parallel layering in the host rocks (New Britannia Mine staff geologists, TVX Gold Inc., pers. comm., 1997). However, late brittle structures postdate the mineralization and offset the ore zones. There is no obvious evidence to support the presence of an early pre-ore shear zone, but it is generally accepted by mine staff that an early concordant/discordant structure acted as a conduit for the alteration and mineralizing fluids. Recrystallization of the altered rocks during subsequent metamorphism has obliterated most of the original structural features that may have predated the alteration and mineralization. Locally, minor late vein type mobilized mineralization postdates the metamorphosed alteration. The mineralized zone is in fault contact with staurolite schists at its western margin, but is still open to the east and down dip.

The No. 3 zone occurs in a zone of deformation within pyroxene-rich volcanoclastic rocks. The economic mineralization is associated with an approximately 1 m thick quartz vein in its western part and a set of subparallel folded quartz veins at its eastern end. The thickest portion of the zone consists of a biotite-quartz rock with up to 10% finely disseminated arsenopyrite that occurs mainly between, but also outside, the two major quartz veins. High grade mineralization occurs both as angular blocks within the quartz veins and in later 'crack and seal' quartz veins. The mineralization in this zone has been superimposed upon an early shear fabric that is evident 2-3 m outside the intensely altered rocks. The mineralized zone is thickest where the subparallel quartz veins have been folded into a broad S-shaped structure with a northeasterly plunge that approximates the L>>S fabric in the biotite-quartz rock. Gold contents vary directly with the content of needle-like arsenopyrite (Staff geologists, TVX Gold Inc.; Harrison, 1949; Galley *et al.*, 1989; Fedikow *et al.*, 1989).

The Birch Zone occurs within fine grained intrusive and/or volcanic rocks. Gold is associated with needle-like arsenopyrite in a zone of beige to cream coloured quartz-rich carbonate and calc-silicate rocks. Part of

the zone has been mined by open pit. The pit is currently flooded and only a small portion of the mineralized zone is exposed. Texturally and mineralogically this zone resembles more closely the mineralization at the New Britannia Mine than that at the No. 3 Zone. The mineralization is locally foliated and has been deformed by the Birch Zone fault.

A number of other gold-bearing arsenopyrite occurrences are hosted by the fine grained mafic volcanic rocks that occur between the No. 3 and Birch Zones. These zones of mineralization are commonly hosted by a fine- to medium-grained mafic intrusion. In general, they consist of a central zone of massive quartz and biotite ± carbonate with a L>>S fabric defined by reddish brown biotite and an outer zone of quartz-amphibole-biotite in which the biotite is black. This outer zone commonly exhibits a curvilinear shear fabric, *e.g.*, Sherry Zone. At the No. 2 Zone there is a silica-rich zone that resembles the early quartz veins at the No. 3 Zone. In contrast, the quartz veins in most of the occurrences represent late fracture fillings and are devoid of arsenopyrite; they probably represent late tensional sites that postdate the alteration and mineralization.

Several occurrences are hosted by the pyroxene crystal-rich volcanoclastic rocks, *e.g.*, Kim Zone. The Kim zone is characterized by a central barren quartz vein within a quartz-biotite-rich zone with arsenopyrite. It has an outer zone of altered mafic pyroclastic rocks that consists predominantly of quartz, hornblende and black biotite.

The Boundary Zone mineralization occurs mainly within pyroxene-rich volcanoclastic rocks near a fault contact with rhyolite flows. Arsenopyrite-bearing quartz veinlets within the rhyolites probably represent a late episode of mobilization. This occurrence has been mapped in detail by Ian Fieldhouse and will be described in detail in his MSc thesis.

The Bounter zone is also hosted by mafic intrusive rocks. For a description of this deposit see Fedikow *et al.* (1989) and Galley *et al.* (1989).

The name Thorn Zone is used collectively for a number of separate, but similar, mineral occurrences located northeast of the North Birch Shear Zone. Some of these occurrences are exposed in old trenches and others areas recently stripped of overburden.

In general, in these occurrences coarse grained arsenopyrite occurs adjacent to and between quartz veins in mafic rocks that intrude the Missi Group rocks. Arsenopyrite occurs in zones of alteration adjacent to zones of late brittle deformation. Quartz-rich biotitic alteration zones contain the highest concentrations of arsenopyrite. These zones of non foliated quartz-biotite ± carbonate are surrounded by quartz-amphibole-biotite alteration in which the biotite content decreases towards the mafic host. The intensity of the wall rock alteration and the concentration of the arsenopyrite are independent of the size of the quartz veins. Several of the thicker mineralized lenses in the Thorn Zone exhibit a northeast plunge similar to that of the mineralized zones at the No. 3 and Birch Zones.

A late brittle-ductile structure in the vicinity of one of the gold-arsenopyrite occurrences contains abundant fine grained pyrrhotite and/or pyrite. This sulphide mineralization clearly postdates the alteration associated with the arsenopyrite mineralization.

SOLIDOR DEPOSITS

Gold is associated with coarse grained arsenopyrite in altered mafic sills that intrude Missi Group rocks near Squall Lake (Fedikow *et al.*, 1989). The quartz-biotite ± alteration associated with this mineralization is similar to that observed in the Thorn and No. 3 zones. Two to five cm thick quartz veins postdate both the alteration and the mineralization. The main megascopic difference between the widely separated Solidor and Thorn zones is a plunge of 10° -15° NNE on the mineralized zones at the Solidor versus 30°-35° NE at the Thorn Zone. Late mafic dikes cut across the mineralized zones at both the Solidor and the Thorn zones.

CONCLUSIONS:

The majority of the known gold arsenopyrite occurrences are located in mafic rocks that occurs structurally above the McLeod Road fault. The presence of significant gold-bearing arsenopyrite in mafic intrusions cutting folded Missi Group rocks indicates that the gold was introduced at a late stage in the development of the area from fluids of either metamorphic or magmatic derivation.

It is premature to make a definitive statement on the origin of the gold mineralization, but a number of observations relevant to its genesis

have been made during exploration of the area (John Danko, pers. comm., 1997), this study and previous studies by Harrison (1949), Fedikow *et al.* (1989) and Galley *et al.* (1989):

- there is no evidence to support a stratigraphic control or a synvolcanic origin for either the alteration or the gold mineralization
- gold is associated with fine grained needle-like arsenopyrite
- coarse grained arsenopyrite contains only minor gold except in the Squall Lake area
- gold-bearing arsenopyrite is associated predominantly with mafic rocks
- quartz veins associated with most of the mineralized zones postdate the initial mineralization
- early quartz veins of the 'crack and seal' type enclose gold-bearing arsenopyrite and altered rocks
- mineralization predates the growth of lineated reddish brown biotite
- mineralization occurs predominantly in and probably predates northeast-plunging structures that may be related to development of the Threehouse Synform.

The relative age of the fluids and the structures controlling them are uncertain. Gold deposits are restricted to those rocks that structurally overlie the McLeod Road Fault in the Snow Lake area and the contact between the Burntwood Group and the Missi Group rocks in the Squall Lake area. The contact between the sedimentary rocks of the Burntwood Group and the overlying gabbroic rocks that intrude the Missi Group at Squall Lake is considered to be a fault (Schledewitz, this volume). This interpretation has significance for gold metallogeny in this area because it implies that the gold mineralization has been structurally emplaced together with the enclosing host rocks over the Burntwood turbidites. This interpretation may also be true for the known gold-arsenopyrite mineralization in the volcanic and younger rocks at Snow Lake.

ACKNOWLEDGMENTS

Thanks to John Danko, Gerald Trembath and Peter Snajder for many fruitful discussions on the geology of the map area and for detailed information on individual mineral deposits. Ernie Guiboche, Janet Wishart and Tom Fleming provided mine tours and drill core. Special thanks to Lee-Ann Strelezki for assistance with Autocadd. Field assistance was provided by Angela Dowd and Wendy Jo Mosby.

REFERENCES:

Fedikow, M.A.F., Ostry, G., Ferreira, K.J. and Galley, A.G.
 1989: Mineral deposits and occurrences in the File Lake area, NTS 63K/16; Manitoba Energy and Mines, Geological Services, Mineral Deposit Series, Report No. 5, 277 p.

Fedikow, M.A.F., Athayde, P. and Galley, A.G.
 1993: Mineral deposits and occurrences in the Wekusko Lake area, NTS 63J/13; Manitoba Energy and Mines, Geological Services, Mineral Deposit Series, Report No. 14, 437 p.

Froese, E. and Moore, J.M.
 1980: Metamorphism in the Snow Lake area, Manitoba; Geological Survey of Canada, Paper 78-27, 16 p.

Galley, A.G., Ziehlke, D.V., Franklin, J.M., Ames, D.E. and Gordon, T.M.
 1986: Gold mineralization in the Snow Lake-Wekusko Lake region, Manitoba; **in** Gold in the Western Shield (L.A. Clark, ed.); Canadian Institute of Mining and Metallurgy, Special Volume 38, p. 379-398.

Galley, A.G., Ames, D.E. and Franklin, J.M.
 1988: Geological setting of gold mineralization, Snow Lake, Manitoba; **in** Geological Survey of Canada, Open File 1700, Geological Map, 1:5000 scale.
 1989: Results of studies on gold metallogeny of the Flin Flon belt; **in** Investigations by the Geological Survey of Canada in Manitoba and Saskatchewan during the 1984-1989 Mineral Development Agreements, Geological Survey of Canada, Open File 2133, p. 25-32.

Harrison, J.M.
 1949: Geology and mineral deposits of File-Tramping Lakes area, Manitoba; Geological Survey of Canada, Memoir 250, 92 p.

Hogg, N.
 1957: Nor-Acme Mine; **in** Geology of Canadian ore deposits, Canadian Institute of Mining and Metallurgy, Congress Volume, p. 262-275.

Kraus, J. and Williams, P.F.
 1994: Structure of the Squall Lake area, Snow Lake (NTS 63K/16); **in** Manitoba Energy and Mines, Minerals Division, Report of Activities, p. 189-193.

Schledewitz, D.C.P.
 1997: A brief review of the geology and the relationship of gold mineralization north of Snow Lake from the perspective of the current Squall Lake Project (part of 63K/16NE); **in** Manitoba Energy and Mines, Minerals Division, Report of Activities 1997, this volume.

GS-10 SQUALL LAKE PROJECT: GEOLOGY AND GOLD MINERALIZATION NORTH OF SNOW LAKE (NTS 63K/16NE)

by D.C.P Schledewitz

Schledewitz, D.C.P. (1997): Squall Lake Project: geology and gold mineralization north of Snow Lake (NTS 63K/16NE):in Manitoba Energy and Mines, Minerals Division, Report of Activities, 1997, p. 79-83.

SUMMARY

The gold mineralization in the Snow Lake area generally occurs in the hanging wall of the McLeod Road fault (e.g., New Britannia Mine). Previous studies (e.g., Galley *et al.*, 1988) have generally interpreted the mineralization to be structurally controlled and to be genetically linked to the fault. This mapping has confirmed interpretations that gold/arsenopyrite deposits in the Snow Lake area are structurally controlled, consistent with their occurrence in rocks of different composition and different ages, but linkage between the mineralization and the McLeod Road fault is not clear because the mineralization may predate the fault.

INTRODUCTION

The goal of this project is to provide a more current geological framework for mineral exploration in Snow Lake and Squall Lake areas (Fig. GS-10-1). This mapping project is being carried out in conjunction with more detailed studies dealing with the structural control on gold mineralization by Ian Fieldhouse (M.Sc., University of Manitoba), ore genesis studies by George Gale (GS-9, this volume) and ore mineralogical studies by Pam Fulton (M.Sc., University of Manitoba). A nine week field season was divided into eight weeks of mapping in the eastern half of the area, north of Snow Lake to north of Squall lake and several days mapping in the western half of the project area (Fig. GS-10-2).

The spatial relationship between the McLeod Road fault and gold mineralization makes the continuity and timing of this fault relative to other structures important. In the past the McLeod Road fault has been shown as a continuous structure (Harrison, 1949; Russell, 1957; Froese and Moore, 1980; Kraus and Williams, 1994, 1995), but mapping during this project shows that the fault is not a simple continuous structure and, in fact, consists

of a number of segments produced by offsets on younger faults (Fig. GS-10-3). The younger structures are important as they not only offset the McLeod Road fault but also offset the zones of gold/arsenopyrite mineralization.

At least some of the gold mineralization is interpreted to be pre-metamorphic, in contrast to earlier gold genesis models (e.g., Galley, 1988) that interpret the gold to be post-metamorphic in age. A pre-metamorphic interpretation is based on preliminary observations of gold-bearing post-Missi Group gabbro bodies south of Squall Lake that contain mineralized zones deformed by pre- to syn- metamorphic deformational events.

GENERAL GEOLOGY

The project area is located at the east end of the exposed Paleoproterozoic Flin Flon Belt (Fig. GS-10-1). Syme *et al.* (1995) and Lucas *et al.* (1996) have shown that this part of the Flin Flon Belt is a structural collage composed of a series of 1.89 to 1.83 Ga tectonostrophic assemblages that were juxtaposed during 1.84 to 1.80 Ga continental collision.

In the project area at Snow Lake the basic lithotectonic elements are, from southwest to northeast (Fig. GS-10-2): Snow Lake arc assemblage, Burntwood Group turbidites, undivided volcanic rocks, and Missi Group arenites. Contacts between these lithotectonic elements have typically been interpreted to be faults (Harrison, 1949; Galley *et al.*, 1988), and this is supported by >50 million year age difference between the volcanic lithologies (Snow Lake arc assemblage at ca. 1.891 Ga; David *et al.*, 1996), Burntwood Group turbidites (1.85-1.83 Ga; David *et al.*, 1996; Machado and Zwanig, 1996) and Missi Group arenites (1.85-1.83 Ga; Ansdell, 1993; Connors and Ansdell, 1994).

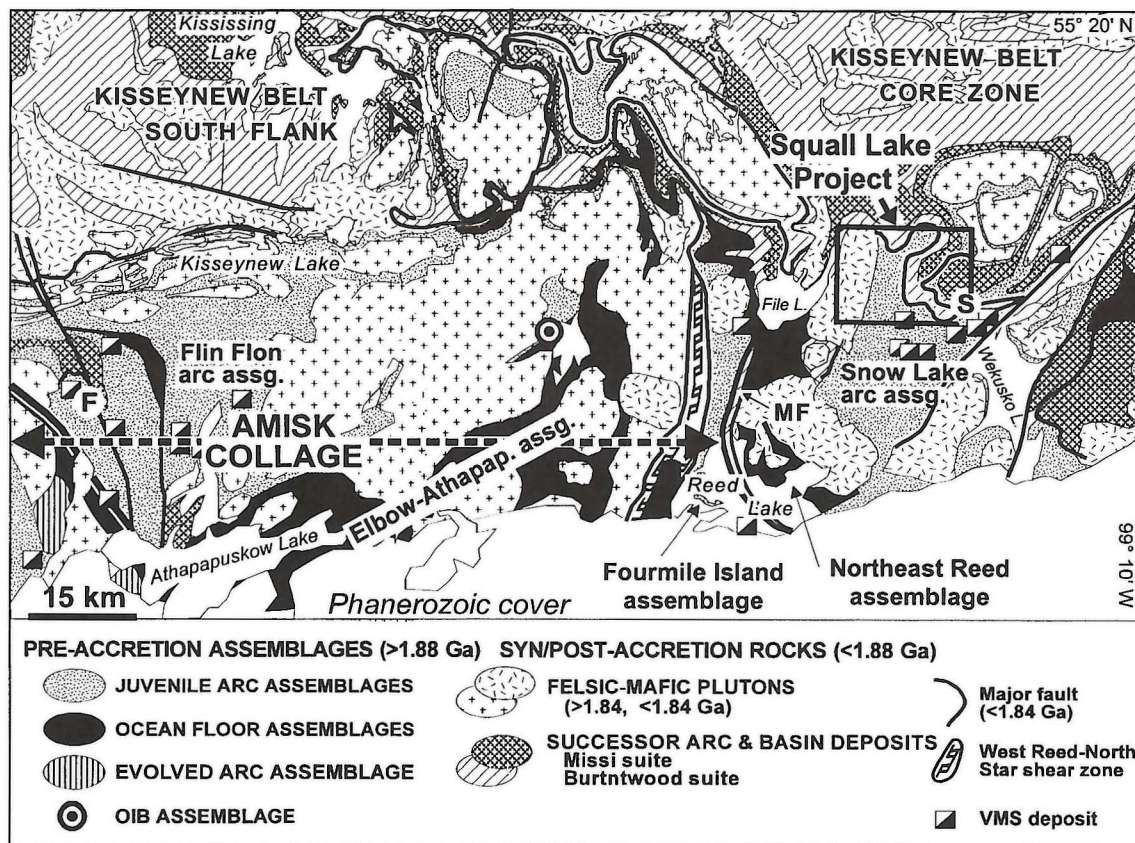


Figure GS-10-1: Geological and geographical setting of the Squall Lake project in the Flin Flon Belt.

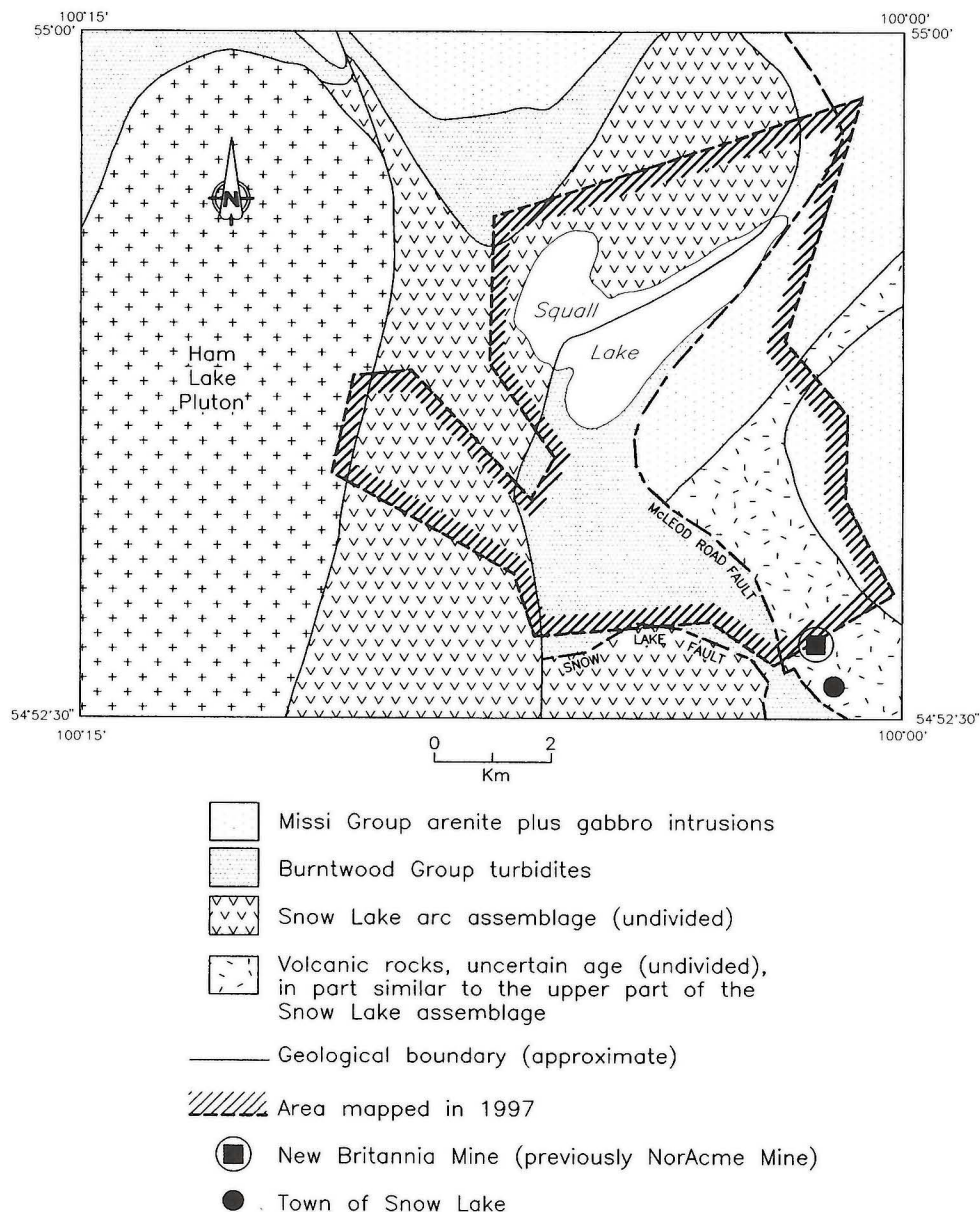


Figure GS-10-2: Outline of the Squall Lake project area showing the distribution of main lithological components and major early faults. Area mapped in 1997 is outlined.

The Snow Lake arc assemblage consists of >7 km of juvenile oceanic arc volcanic rocks. These rocks, described by Bailes and Galley (1996), were not examined in any detail during this first year of this project. They are in fault contact (Snow Lake fault) to the northwest with Burntwood Group turbidites that consist of isoclinally folded, interlayered greywacke, siltstone and mudstone, that contain lower to middle almandine facies mineral assemblages (*e.g.*, biotite + garnet ± staurolite ± sillimanite). The Burntwood Group rocks are separated from an undivided volcanic sequence to the north by the McLeod Road fault. Although undated, these volcanic rocks are tentatively correlated with similar rocks that occur in the upper part of the Snow Lake arc assemblage. Again these rocks are separated from Missi Group cross bedded arenites to the north by another fault (Birch Lake fault). The Snow Lake, McLeod Road and Birch Lake faults are all semiconformable to stratigraphy, are either pre- or syn- metamorphic, and are interpreted to be potential thrust faults.

RESULTS OF 1997 FIELDWORK

A portion of the area has been remapped (Fig. GS-10-2) and preliminary compilation map (1997 F-2) has been produced at a scale of 1:20 000. The volcanic section north of the New Britannia Mine has been subdivided into three units: aphyric basalt, intermediate to mafic volcanoclastic rocks, and rhyolite. The contacts between these units are typically sheared.

The basalt in the section north of the New Britannia Mine is fine grained, weathers dark green and occurs as both massive and pillowed flows. Initial analytical results from two samples indicates an ocean floor, MORB-like geochemistry (Bailes, per. comm. 1997). Additional sampling was undertaken during the current mapping project to verify geochemistry of this and other basalt units. The aphyric basalt is variably affected by premetamorphic alteration. The volcanoclastic rocks comprise debris flow deposits, mafic wackes and graded crystal tuffs which are described in detail by Galley (1988) and Gale (GS-9, this volume). Rhyolite bodies are

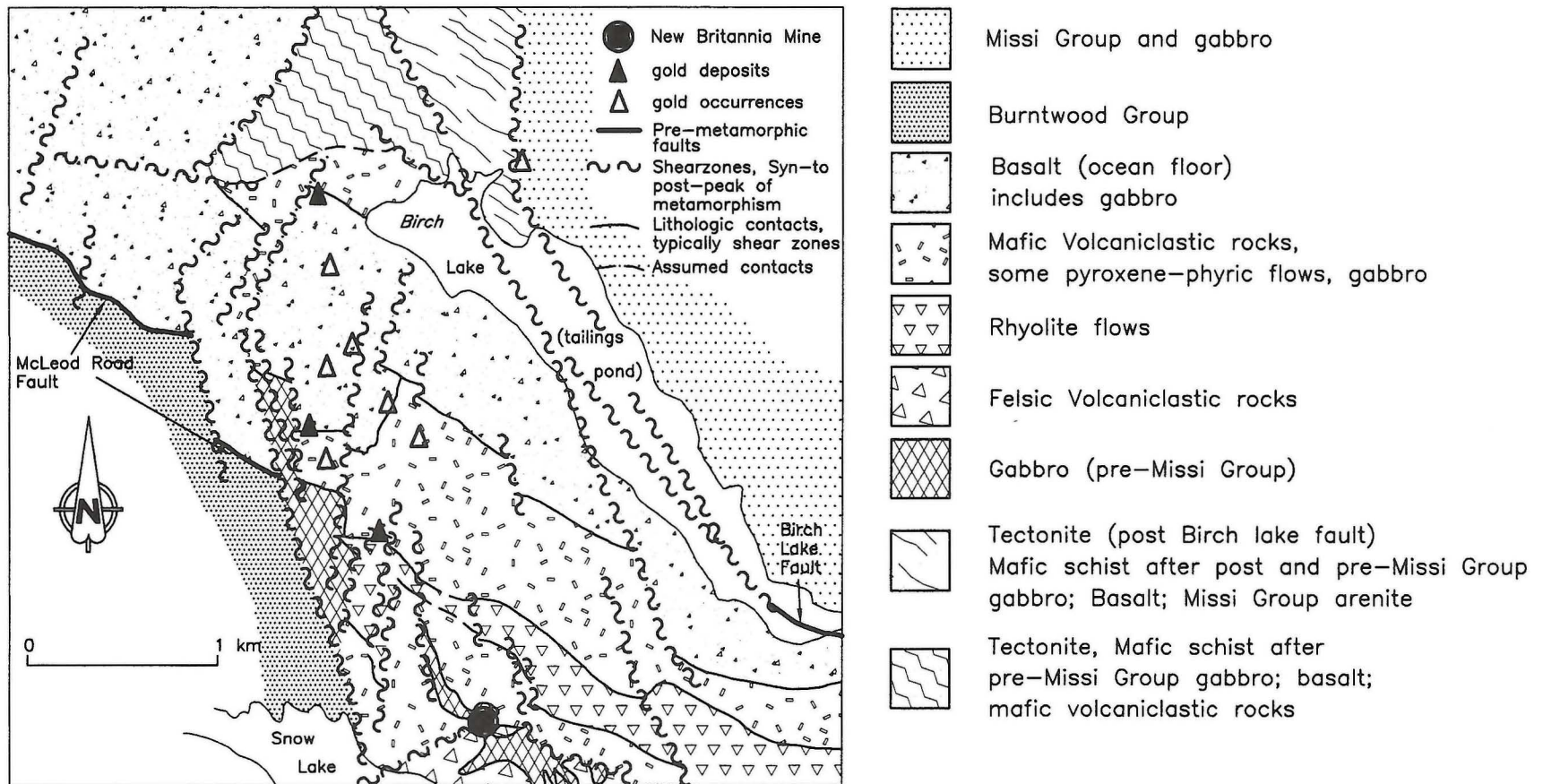
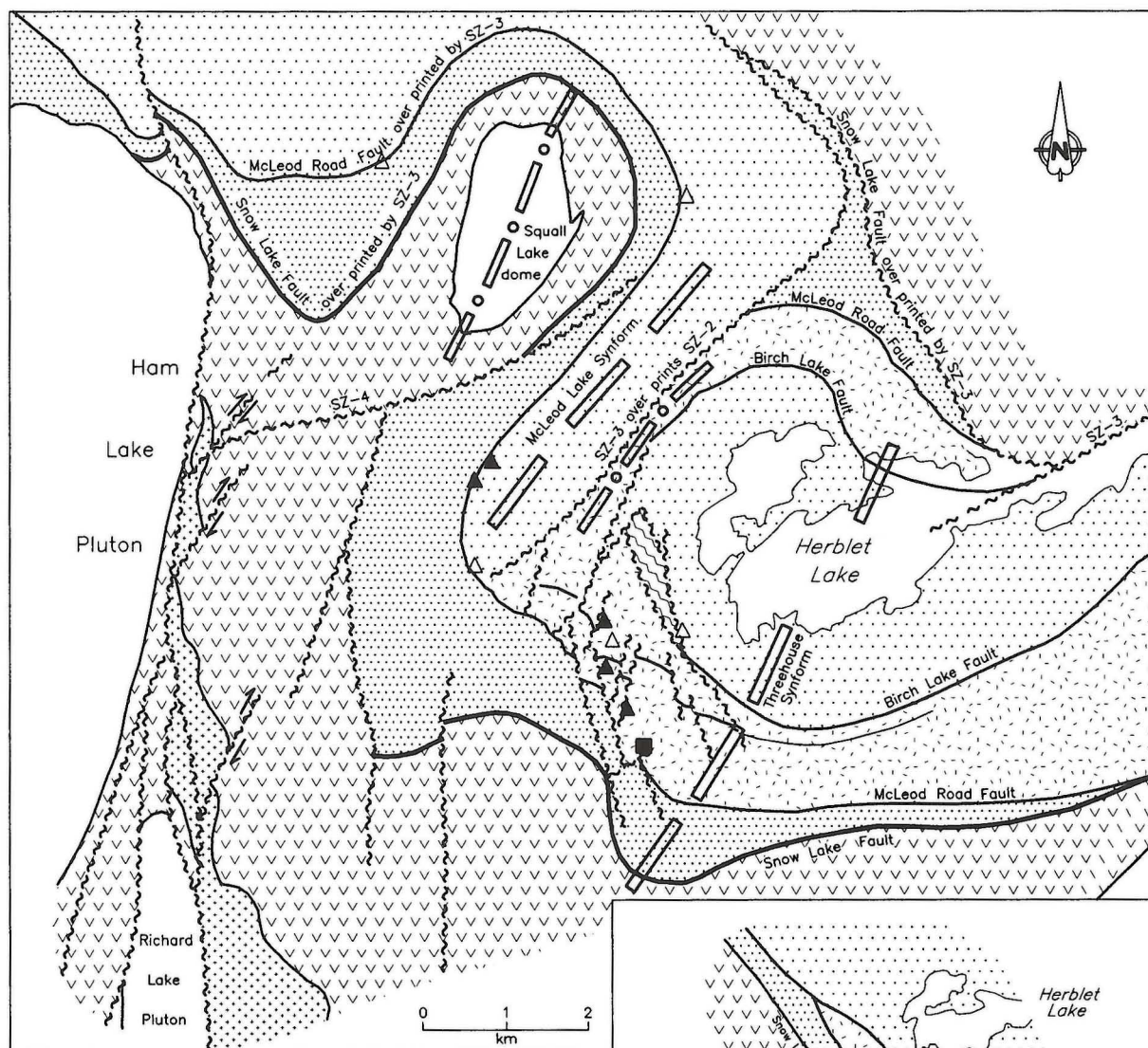


Figure GS-10-3: Reinterpreted geology north of Snow Lake based on 1997 field work. Also shown are significant faults and zones of gold mineralization.



SYMBOLS

Shear Zones

- SZ-1 Snow Lake fault
 - SZ-2 McLeod Road, Birch Lake faults
 - SZ-3 Syn- to post peak of metamorphism
 - SZ-4 Late metamorphic
- } Pre-metamorphic

Trace of Fold Axis

- F₃ Synform
- F₃ Antiform
- New Britannia Mine
- Gold deposits
- Gold occurrences

LEGEND

- Mafic tectonite, derived from pre- and post-Missi Group gabbro; Missi Group arenite; Basalt
- Missi Group and gabbro
- Burntwood Group
- Granitic rocks undivided
- Snow Lake arc assemblage, undivided and intrusive rocks
- Volcanic rocks, undivided (age uncertain) in part similar to the upper part of the Snow Lake assemblage
- Chisel Lake Pluton

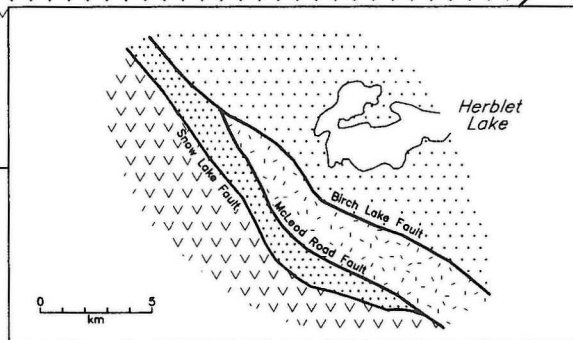


Figure GS-10-4: Simplified geology of the Squall Lake project area showing reinterpreted fault and fold trends. Inset shows a simplified structural restoration accomplished by removing effects of F_3 age folds and faults.

poorly to well foliated, variably garnetiferous, mainly massive, and aphyric to locally quartz phyrlic. The rhyolite bodies are interpreted to be extrusive as they locally contain flow lobes and flow breccia.

The basalt and mafic volcanoclastic units are structurally interleaved, but because they display a consistent north facing direction this repetition likely occurred by layer parallel faults rather than by F_1 isoclinal folding. This is consistent with local identification of pre-metamorphic shear zones along the contacts of these units. The McLeod Road fault postdates these structures as it truncates the structurally repeated stratigraphy. The McLeod Road fault is then itself offset by north-northwesterly and northeasterly syn- to post-peak metamorphic faults (Fig. GS-10-3).

In the volcanic section, the frequent occurrence of gold deposits near the boundaries of lithologic units indicates that ductility contrasts during deformation played a role in gold deposition (see also Galley, 1988). The phase of deformation that controls the gold/arsenopyrite mineralization is not clearly identified at this time. However, any structural/genetic model for the gold/arsenopyrite mineralization in the volcanic stratigraphy must take into account that gold/arsenopyrite mineralization also occurs in gabbros that postdate the Missi Group.

Post-Missi mineralization occurs above the Birch Lake fault (north of the town of Snow Lake), in the hanging wall of the McLeod Road fault, and on the southeast and northwest flanks of the Squall Lake dome (Ostry, 1990). The large volume of gabbro dykes and sills in the Missi Group arenite, minor occurrences in structurally underlying volcanic stratigraphy, and absence in the structurally underlying rocks of the Burntwood Group suggests that the Missi and Burntwood lithologies were not in contact at the time of gabbro emplacement. This implies that these rocks and the gold mineralization were juxtaposed at a later time.

A tentative interpretation that gold/arsenopyrite mineralization predates the peak of metamorphism is based on field observations of mineralization in the post-Missi Group gabbro bodies south of Squall Lake (GS-10-4). The interpretation is based on two observations. First, the gabbro, where it contains disseminated arsenopyrite, is characterized by feldspar patches, and second, these alteration patches are oriented in a lineation that formed during a pre-metamorphic deformational event. Thus, the gold-associated alteration and by extension the gold mineralization is pre- to syn metamorphic in age. Consistent with this interpretation is the observation that the most highly mineralized areas, within the altered/mottled gabbro, also form lenticular, rod-shaped areas that are elongate in the orientation of the regional stretching direction.

ECONOMIC GEOLOGY

The Snow Lake area contains the largest Paleoproterozoic lode Au deposit in Canada, the New Britannia Mine. Reopening of this mine and the adjacent mill and smelter in 1995 has greatly increased interest in Au mineralization in the area north of the town of Snow Lake. Remapping of the area north of Snow Lake during 1997 has indicated a number of previously unreported features that bear on the localization of gold mineralization and, therefore, have implications for future exploration.

Perhaps the most important outcome of this project is a new explanation for the apparent restriction of economically interesting lode gold mineralization to the area north of Snow Lake, in the structural hanging wall of the McLeod Road fault. In the past, this has been attributed to dilation of subsidiary faults during late movements on the McLeod Road fault (e.g., Galley *et al.*, 1988). An alternative explanation arising from this project is that the gold mineralization may predate the McLeod Road fault and have been carried with the host rocks as part of an allochthon soled by the McLeod Road fault. Evidence supporting the latter interpretation is the occurrence of Au-bearing gabbro intrusions in the structural hanging wall to the McLeod Road fault and a complete absence of these intrusions and accompanying Au mineralization in the footwall to the fault. According to this interpretation, the allochthon above the McLeod Road fault may have been part of a Au-rich metallogenic domain that was never present in rocks now occupying the immediate structural footwall to the fault. The implication of this relationship is that the hanging wall to the McLeod Road fault is not simply a more favourable structural environment for gold mineralization but that the footwall to the fault is unfavourable even with the right structural features present. Thus, tracing the McLeod Road fault may have important implications for identifying the distribution of the potentially more prospective

hanging wall rocks. For example, if the McLeod Road fault trends north of Squall Lake, as shown on Figure GS-10-4, then rocks east and north of Squall Lake are interesting targets for gold exploration. However, if the fault forms the southeast limb of the McLeod Lake syncline, as many workers contend (e.g., Harrison, 1949; Russell, 1957; Froese and Moore, 1980; Kraus and Williams, 1994, 1995), then this interpretation suggests that the areas east and north of Squall Lake are less likely to contain economically significant gold mineralization.

REFERENCES

- Connors, K.A. and Ansdell, K.M.
 1994: Timing and significance of thrust faulting along the boundary between the Flin Flon - Kiseeynew domains, eastern Trans-Hudson orogen; **in** Trans-Hudson Orogen Transect, LITHOPROBE Report 38, p. 112-122.
- David, J., Bailes, A.H. and Machado, N.
 1996: Evolution of the Snow Lake portion of the Paleoproterozoic Flin Flon and Kiseeynew belts, Trans-Hudson Orogen, Manitoba, Canada: implications of U-Pb geochronology of supracrustal and intrusive rocks; *Precambrian Research* v. 80 (1/2), p. 107-124.
- Froese, E. and Moore, J.M.
 1980: Metamorphism in the Snow Lake area, Manitoba; Geological Survey of Canada, Paper 78-27, 16 p.
- Galley, A.G., Ames, D.E. and Franklin, J.M.
 1988: Geological Setting of Gold Mineralization, Snow Lake, Manitoba; Geol. Surv. of Canada, Open File 1700, 7 p.
- Harrison, J.M.
 1949: File Lake area, Manitoba; Geol. Surv. Can., Map 929A with descriptive notes.
- Kraus, J. and Williams, P.F.
 1994: Structure of the Squall Lake area, Snow Lake (NTS 63K/16); **in** Manitoba Energy and Mines, Minerals Division, Report of Activities, 1994, p. 189-193.
 1995: The Tectonometamorphic History of the Snow Lake area, Manitoba, Revisited; **in** Trans-Hudson Orogen Transect, LITHOPROBE Report 48, p. 206-212.
- Lucas, S.B., Stern, R.A., Syme, E.C. and Reilly
 1996: Structural history and tectonic significance of long-lived shear zones in the central Flin Flon belt, eastern Trans-Hudson Orogen; **in** Trans-Hudson Orogen Transect, LITHOPROBE Report 48, p. 170-186.
- Machado, N. and Zwanig, H.
 1995: U-Pb geochronology of the Kiseeynew domain in Manitoba: provenance ages for metasediments and timing of magmatism; **in** Trans-Hudson Orogen Transect, LITHOPROBE Report 48, p. 133-138.
- Ostry, G.
 1990: Mineral investigations in the Squall Lake area (NTS 63N/2); **in** Manitoba Energy and Mines, Minerals Division, 1990, p. 91-94.
- Russell, G.A.
 1957: Structural studies of the Snow Lake-Herb Lake area; Manitoba Department of Mines and Natural Resources, Mines Branch, Publication 55-3, 33 p.
- Syme, E.C., Bailes, A.H. and Lucas, S.B.
 1995: Geology of the Reed Lake area (parts of NTS 63K/9 and 10); **in** Manitoba Energy and Mines, Minerals Division, Report of Activities, 1995, p. 42-60.

GS-11 GEOLOGY OF THE LAC AIMÉE-NAOSAP LAKE AREA (NTS 63K/13SE AND 63K/14SW)

by H.P. Gilbert

Gilbert, H.P. (1997): Geology of the Lac Aimée-Naosap Lake area (NTS 63K/13SE and 63K/14SW); in Manitoba Energy and Mines, Minerals Division, Report of Activities, 1997, p.84-98.

SUMMARY

Detailed 1: 20 000 scale mapping in the north-central part of the Flin Flon Belt in 1997 was extended east to the margin of the granitoid terrane at Naosap Lake (Preliminary Map 1997F-1). Parts of no less than five tectonostratigraphic assemblages occur within the relatively small (100 km²) map area, which represents less than 5% of the Flin Flon Belt (Fig. GS-11-1). Distinctive arc and arc-rift volcanic rock suites occur within these assemblages, which are separated by major regional faults. Lac Aimée fault zone (LAFZ) is a crustal-scale break that extends across the map area between the arc-derived Lac Aimée block and Animus Lake block, of inferred arc-rift affinity. The intersection of LAFZ and Sourdough Bay fault in the northeast part of the map area has been an area of active gold and base-metal exploration for the past decade.

INTRODUCTION

Geological mapping initiated in 1996 was extended in 1997 to include the west and east parts of the Lac Aimée-Naosap Lake area. The map area is contiguous with the Tartan-Embury-Mikanagan lakes area to the west (Gilbert, 1990b), and is part of a regional detailed mapping program of the Flin Flon volcanic belt initiated by Bailes and Syme (1979). The objectives of the project are as follows:

- (1) to upgrade existing maps (Bateman and Harrison, 1943; Kalliokoski, (1949) by detailed 1: 20 000 scale mapping. The results of current work will be integrated with regional 1:50 000 and 1:100 000 scale NATMAP compilation maps of the Flin Flon Belt.
- (2) To study the structure, stratigraphy, and volcanic geochemistry of the area in order to assess the tectonostratigraphic and economic significance of volcanic rock assemblages.
- (3) To investigate mineralized localities and assess their economic significance.

STRUCTURE

Five deformation periods (D_{1-5}) are recognized in the Lac Aimée-Naosap Lake area (Table GS-11-2), all of which postdate 1.88-1.87 Ma tectonic accretion of the Amisk collage (Lucas *et al.*, 1996). Lac Aimée fault zone or LAFZ (named 'Mikanagan Fault' in Kalliokoski, 1949, and 'Mikanagan Fault system' in some cancelled assessment files) bisects the map area and juxtaposes stratigraphically and structurally contrasting Lac Aimée and Animus Lake fault blocks (Figs. GS-11-2, 3). The fault zone is analogous to major tectonic zones elsewhere in the Flin Flon Belt (*e.g.*, Elbow Lake Shear Zone; Ryan and Williams, 1993, 1994; Syme, 1995) that were initiated during tectonic accretion of the Amisk collage, and underwent subsequent reactivation. LAFZ is a system of branching faults that originate at the southwest end of Lac Aimée, bifurcate round the lake, and converge to the northeast in a highly attenuated, gneissic zone that corresponds to a conspicuous, subvertical break on the LITHOPROBE deep seismic profile (Fig. GS-11-4). Mills Island fault slice, a lensoid enclave within the fault zone, is bounded by faults that extend along the northwest and southeast shorelines of Lac Aimée.

The earliest recognized structures in the map area that postdate tectonic accretion of the Amisk collage consist of north- to west-trending F_1 folds (with parallel S_1 regional foliation) in Animus Lake block (Fig. GS-11-3). Eleven anticline-syncline pairs with moderately to steeply dipping axial planes are overturned to the northeast. The F_1 structures are refolded in an open synform (F_2 or F_4 - see below) with a moderate to steep west-southwest plunge. In contrast to this pattern, the regional trend of lithologic units and S_1 foliation in Lac Aimée block is west to southwest, indicating this fault block was not contiguous with Animus Lake block during D_1 , and the blocks may have rotated during tectonic transport and final juxtaposition along LAFZ after D_1 .

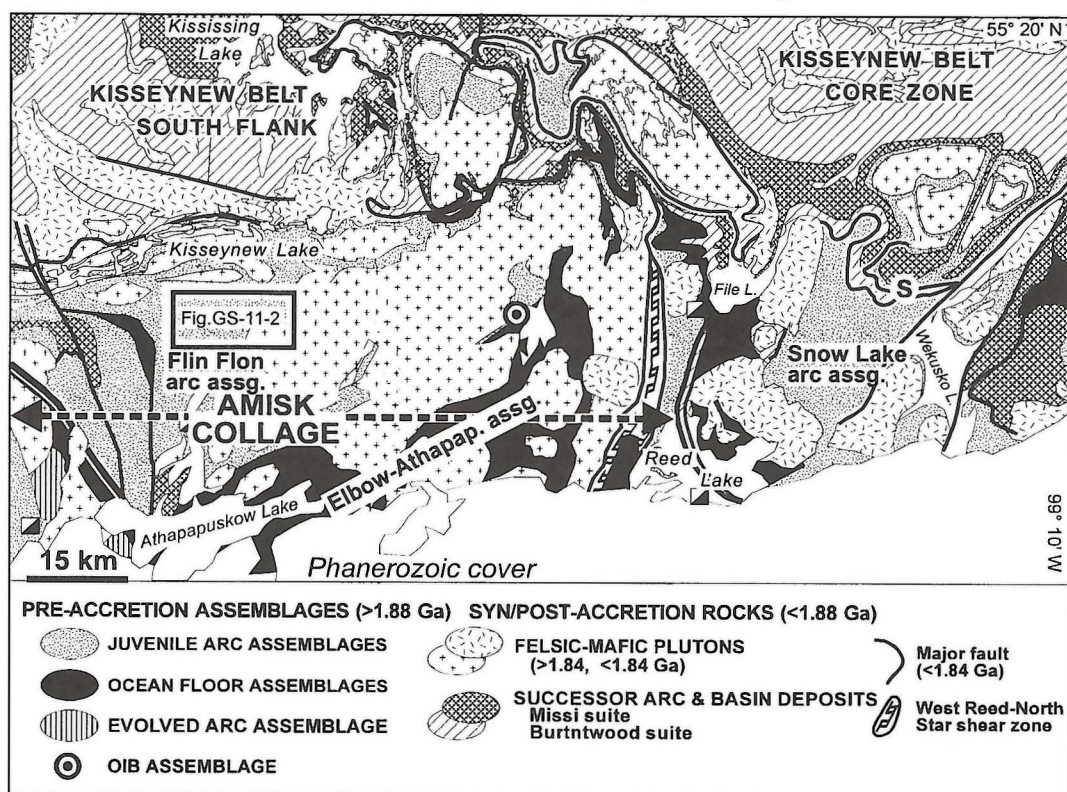


Figure GS-11-1: Simplified geological map of the central part of the Flin Flon Belt, showing the Amisk collage and major tectonostratigraphic assemblages and plutons. F: Flin Flon; S: Snow Lake. Outlined area shows location of map in Figure GS-11-2.

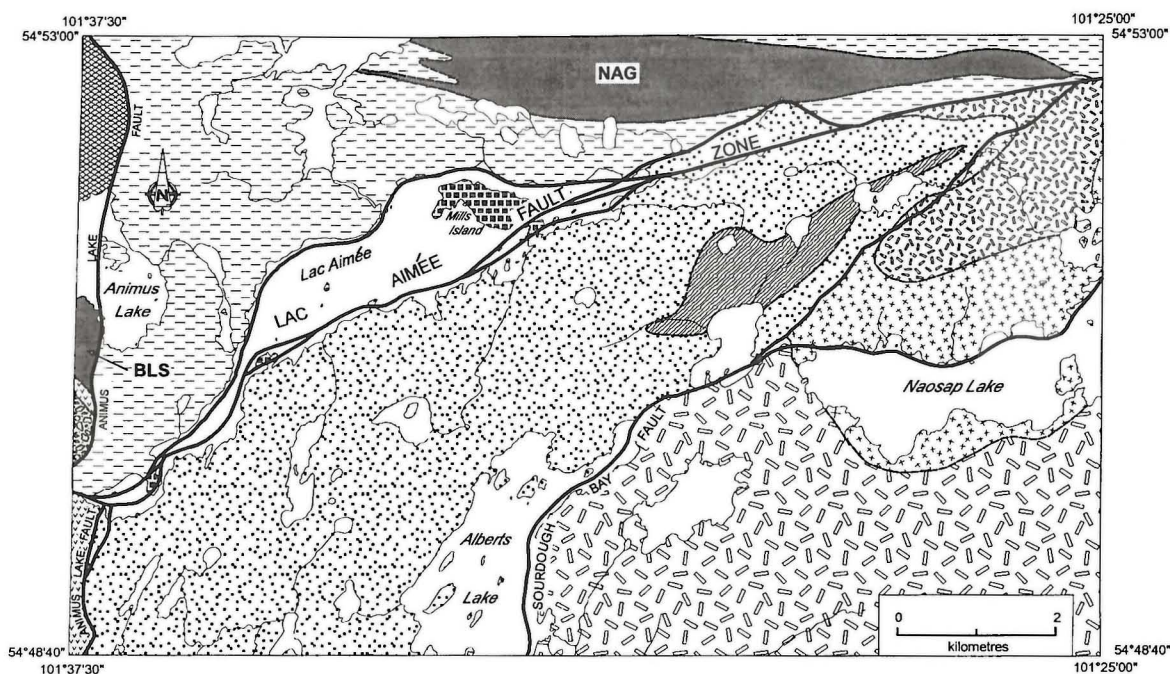
Table GS 11-2.
Deformation history of Amisk collage in the Lac Aimée-Naosap Lake area
(post 1.88-1.87 Ma tectonic accretion and initiation of Lac Aimée fault zone).

Lac Aimée Block

- D₁** Regional W- to SW-trending S₁ foliation; inferred related major folds. Juxtaposition of Lac Aimée and Animus Lake blocks along Lac Aimée fault zone.
- D₂** Major tight to isoclinal folds (deform S₁); axial planes trend W to SW. Minor F₂ folds and L₂ plunge W to SW and NE. Minor F₂ folds within Lac Aimée fault zone plunge moderately to steeply NW.
- D₃** SE-trending S₃ strain-slip cleavage associated with broad open flexure of major F₂ folds in Lac Aimée block.
- D₄** Regional NE-trending open fold in Animus Lake block (defined by curvilinear axial traces of F₁ folds), attributed to sinistral movement along Kiseynew/Flin Flon boundary, part of crustal-scale deformation of Amisk collage (Ashton, 1993).
- D₅** Brittle faulting and shearing within fault blocks. Reactivation of block-bounding faults (e.g., Animus Lake fault offset by reactivated Lac Aimée fault zone).

Animus Lake Block

- D₁** Major tight to isoclinal folds with moderately- to steeply-dipping axial planes, overturned to NE. Regional N- to W-trending S₁ foliation.
- D₂** Warping of F₁ fold axial traces. Minor F₂ folds and L₂ plunge W to SW.



INTRUSIVE ROCKS

- Late tonalite-granodiorite/gabbro, hornblendite
- Early tonalite-granodiorite/gabbro, gabbro-norite

AMISK COLLAGE

Arc

- Lac Aimée fault block
- Mills Island fault slice
- Sourdough Bay fault block
- Tartan Lake fault block

Arc-rift

- Mikanagan Lake fault block
- Animus Lake fault block

BLS Batters Lake sill

NAG North Aimée gabbro

Swordfish Lake turbidites (age unknown)

Figure GS-11-2: Main structural subdivisions, faults and intrusive units in the Lac Aimée-Naosap Lake area.

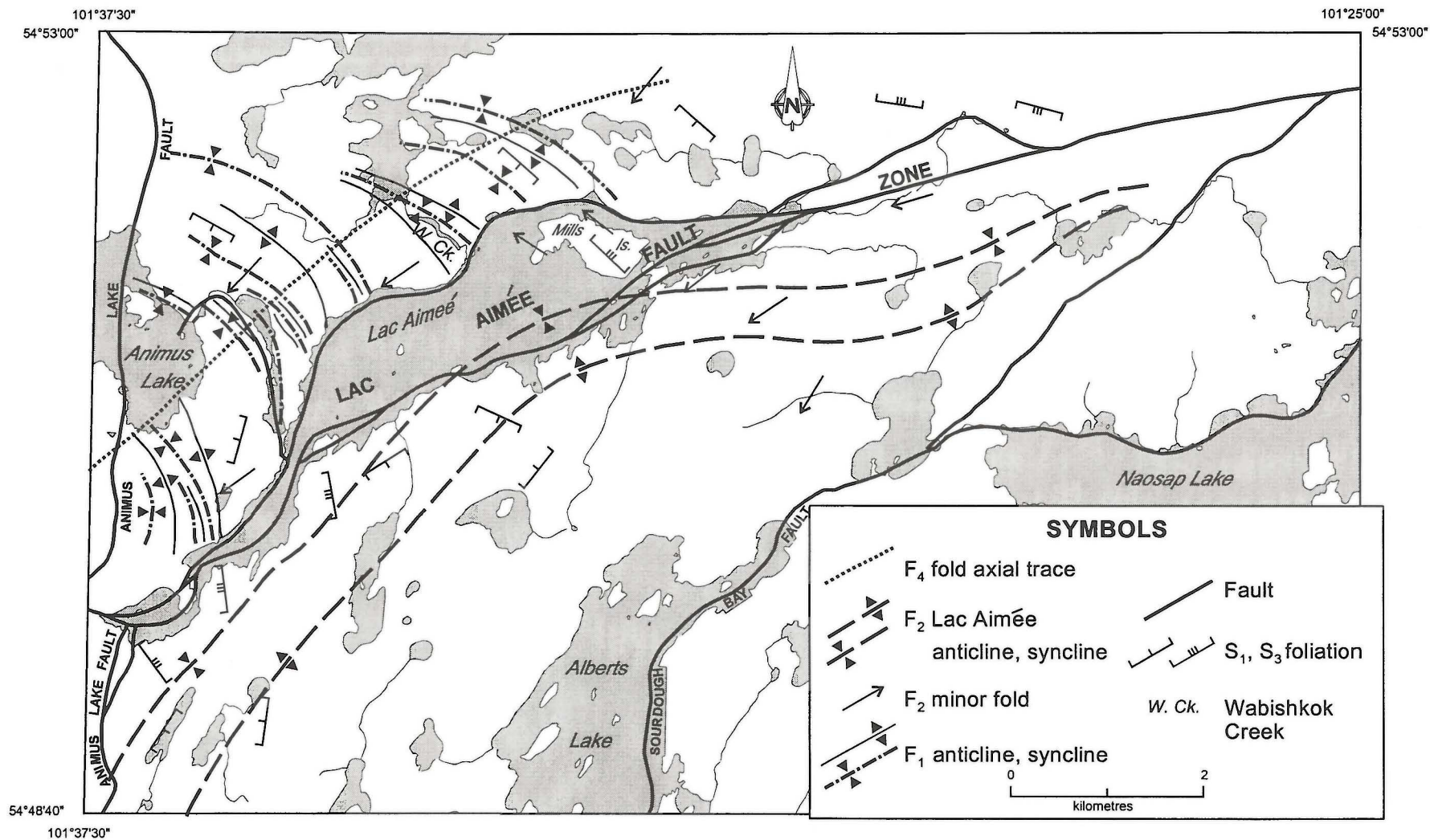


Figure GS-11-3: D₁-D₅ major and selected minor structural elements in the Lac Aimée-Naosap Lake area.

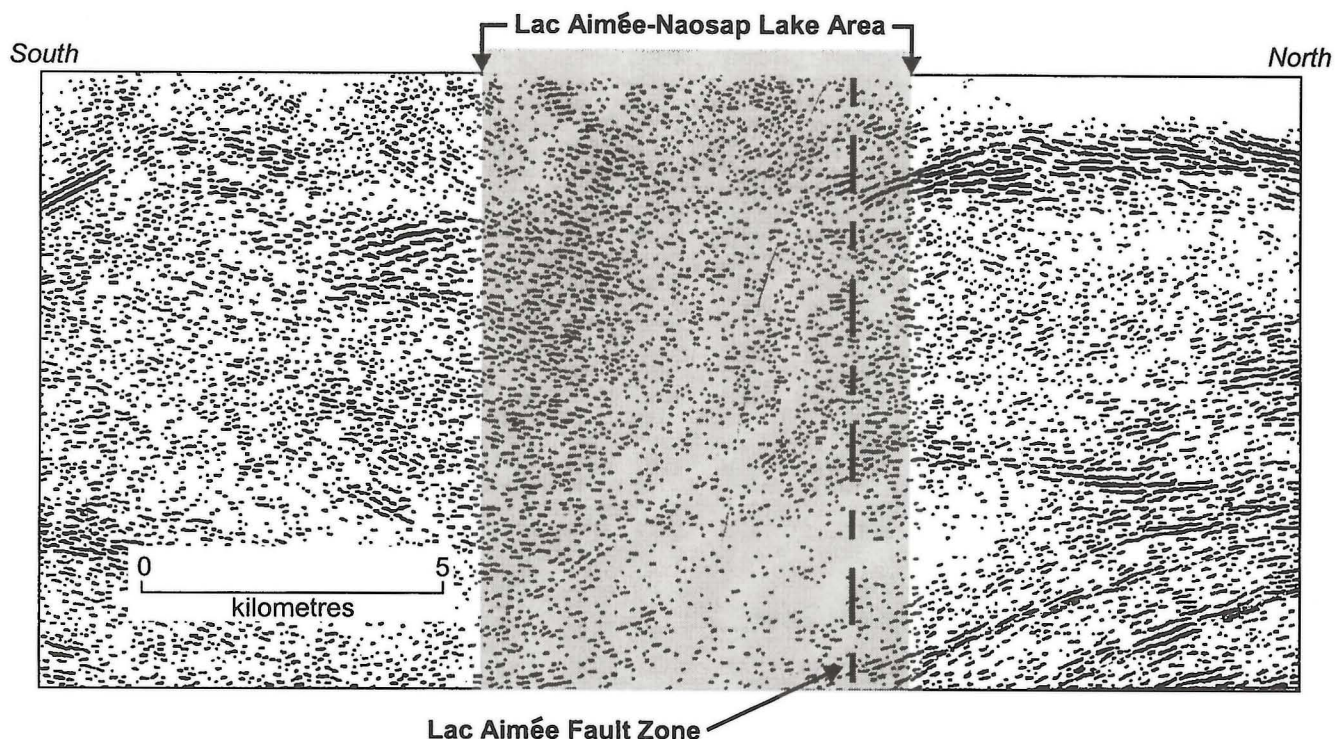


Figure GS-11-4: LITHOPROBE transect line 7A (Lucas *et al.*, 1994), showing the subvertical structural break in the pattern of reflectors corresponding to Lac Aimée fault zone. Shaded area shows the segment of line 7A that extends along the north/south gravel road in the east part of the map area (Preliminary Map 1997F-1).

Major, tight to isoclinal, west- to southwest-trending folds in Lac Aimée block are designated F_2 because they deform the regional S_1 foliation (Gilbert, 1996a); S_1 is roughly parallel to the axial surfaces of F_2 folds, except in fold closures. Inferred F_1 folds with axial planes parallel to S_1 in Lac Aimée block are assumed to have been refolded and incorporated into F_2 structures. Minor F_2 folds and related linear structures (L_2) in both Lac Aimée and Animus Lake blocks are largely coincident and plunge mainly west to southwest (Fig. GS-11-5a,c), suggesting the fault blocks were juxtaposed prior to D_2 . Whereas D_2 resulted in major folds in Lac Aimée block, D_2 may have been limited to minor folding of S_1 and warping of F_1 folds in Animus Lake block. Minor F_2 folds within LAFZ plunge northwest (Fig. GS-11-5b), possibly due to rotation of originally west to southwest-plunging folds during emplacement of Mills Island fault slice.

D_3 deformation resulted in strain-slip cleavage (S_3) that trends consistently southeast, parallel to the axial trend of broad open flexures of the major F_2 folds in Lac Aimée block. The cleavage occurs sporadically along the northwest side of Lac Aimée block, in LAFZ and in the northeast part of Animus Lake block.

The regional northeast-trending open synform in Animus Lake block, delineated by the curvilinear pattern of F_1 axial traces, is part of a regional flexure in the north central part of the Flin Flon Belt ('Embury Lake fold' of Stauffer, 1990) and is attributed to D_4 , possibly related to late sinistral movement along the Kisseynew-Flin Flon boundary that resulted in crustal scale deformation of the Amisk collage (Ashton, 1993). Alternatively, the northeast-trending synform in Animus Lake block may be a D_2 structure, consistent with the early emplacement of nappes along the Kisseynew boundary (Zwanig and Schledewitz, 1992).

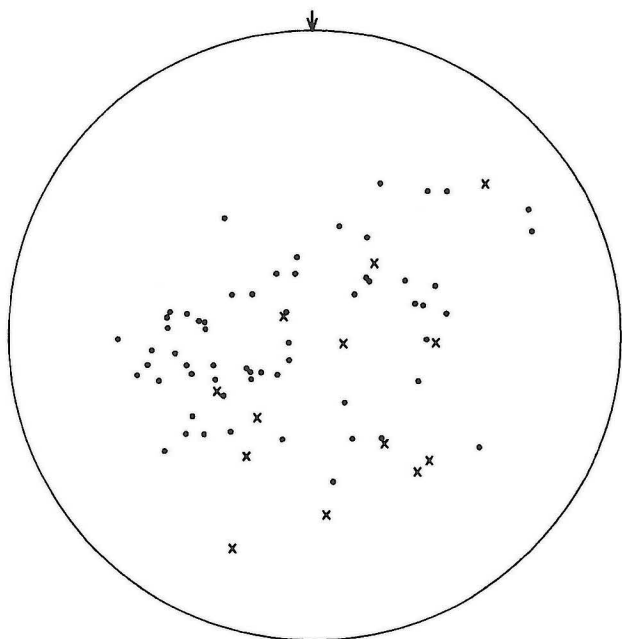
The final deformation period (D_5) resulted in brittle faulting and shearing within blocks, and reactivation of block-bounding faults (*e.g.*, displacement of Animus Lake fault by LAFZ; Fig. GS-11-3). Fault breccia within Sourdough Bay fault that contains well foliated felsic porphyry and basalt blocks (Gilbert, 1996a) is also attributed to D_5 . Intra-block faulting, which probably occurred both during and prior to D_5 , includes strike-slip shears and faults at high angles to the regional foliation that are both associated with pronounced topographic lineaments. Several west- to northwest-trending allochthonous fault slices within the Animus Lake mafic volcanic section are attributed to late (D_5) deformation.

STRATIGRAPHY

Stratigraphic details of Lac Aimée and Mikanagan Lake blocks have been previously described (Gilbert, 1986, 1990a, 1996a). New geochemical data (reported below) confirm that these blocks are tectonostratigraphically distinct (Gilbert, 1996a, b), but Mikanagan Lake rocks are re-interpreted as arc-rift rather than ocean-floor in origin, on the basis of their geochemical affinity with arc-rift basalt elsewhere in the Flin Flon belt (Syme *et al.*, in prep.) Current mapping focused on Animus Lake block, Mills Island fault slice, and Sourdough Bay block.

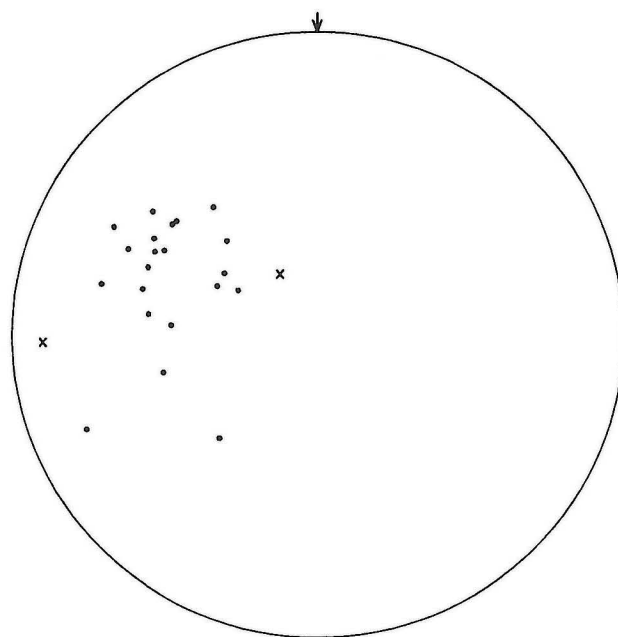
Animus Lake block

Animus Lake block consists almost entirely of mafic volcanic flows (with related gabbro) that are lithologically and stratigraphically similar to Mikanagan Lake basalt. Geochemical data for Animus Lake basalt are not yet available but the geochemical signature is expected to indicate an arc-



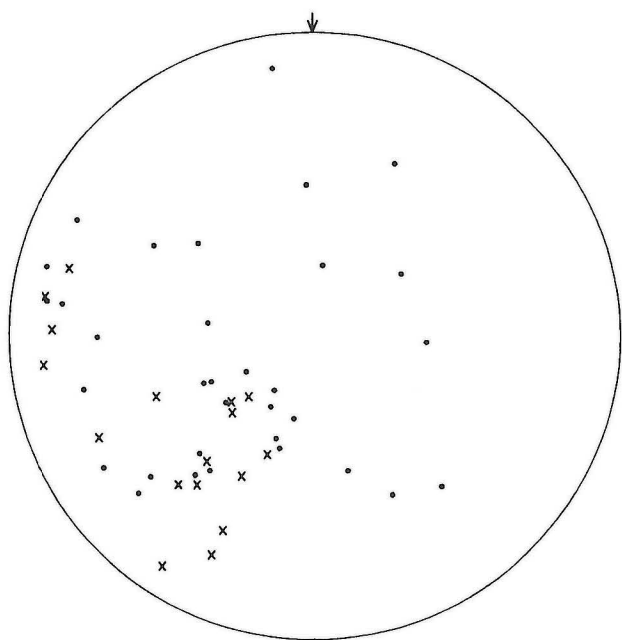
• F_2 minor fold axis × L_2 linear structure

Figure GS-11-5a: Lower hemisphere stereographic plot of F_2 minor folds and related L_2 linear structures in Lac Aimée block.



• F_2 minor fold axis × L_2 linear structure

Figure GS-11-5b: Lower hemisphere stereographic plot of F_2 minor folds and related L_2 linear structures in Lac Aimée fault zone.



• F_2 minor fold axis × L_2 linear structure

Figure GS-11-5c: Lower hemisphere stereographic plot of F_2 minor folds and related L_2 linear structures in Animus Lake block.

rift provenance, equivalent to that of Mikanagan Lake rocks. Animus Lake basalt is typically pillowed and only moderately deformed, facilitating mapping of the detailed structural pattern after extensive outcrop stripping (Preliminary Map 1997F-1).

Pale to medium gray green or beige weathering basalt is massive to slightly foliated, with 0.5-1.5 m ovoid pillows (Fig. GS-11-6); larger pillows (up to 2.5 x 1.5 m) are rare. The flows are generally aphyric, but sparse (<10%) plagioclase phenocrysts occur in a few flows; vesicles and amygdalites (quartz, carbonate) are not common. Irregular flow-breccia zones (up to 1 m wide) and interpillow chert occur in less than one per cent of the section. Polygonal cooling fractures are locally developed in mafic flows and interflow gabbros. The upper greenschist to lower amphibolite regional metamorphic grade of Animus Lake basalt increases toward the northeast corner of the map area, where garnet and anthophyllite (?) occur in the metavolcanic rocks and derived hornblende gneiss.

Several fine grained sedimentary units occur within the Animus Lake mafic volcanic section. Two minor greywacke/siltstone units close to the west margin of Animus Lake block are interpreted as fault slices, derived from a 300 m wide turbidite formation immediately to the west at Swordfish Lake (Gilbert, 1990b). Similar fine grained sedimentary units up to 24 m thick occur at and close to the south margin of North Aimée gabbro, a major sill (interpreted as penecontemporaneous with Amisk volcanism) that extends along the north side of the map area (Fig. GS-11-2). Contact relationships between these metasedimentary rocks and adjacent basalt are unknown, but the occurrence of contact metamorphic hornblende and diffuse metamorphic lamination in metasediments adjacent to the gabbro sill indicates the intrusion is relatively younger, and suggests the metasediments are coeval with Amisk volcanism.

Medium to dark green weathering mafic tuff occurs at and close to the south margin of North Aimée gabbro, east of Wabishkok Creek (Preliminary Map 1997F-1). These presumably conformable units are 4 m to over 15 m wide and include fine grained tuff with detrital plagioclase grains, and very fine grained, diffusely laminated mafic tuff. By contrast, fault-bound intermediate to mafic volcanic fragmental rocks occur within the pillowed basalt sequence at two localities west of Wabishkok Creek. These west-trending enclaves, oblique to the northwest orientation of the regional structure, consist of strongly foliated to protomylonitic volcanic breccia and tuff that have no counterparts in the local stratigraphy.

Sulphide-facies iron formation outcrops intermittently for over 2 km parallel to the north margin of the map area in the northeast part of Animus Lake block. The unit is associated with a prominent electromagnetic conductor that extends from the south shore of Wabishkok Lake east toward the west shore of Naosap Lake for a total strike length of 10.5 km (Gale and Eccles, 1988; P. Bachnick, pers. comm., 1997). The iron formation extends as a skialithic enclave through North Aimée gabbro; the exposed width is 6 m where the formation intersects the gravel road to Wabishkok Creek, and 20 m at the westernmost exposure 2 km further west (Preliminary Map

1997F-1). The formation is 18.3 metres thick in diamond drill core 3 km from the east end of the unit (P. Bachnick, pers. comm., 1997). Pyrite and pyrrhotite (\pm minor chalcopyrite and arsenopyrite) occur as stringers, aggregates and massive sections up to 25 cm wide within a diverse lithologic sequence that includes siliceous siltstone, sporadic chert laminae, feldspathic greywacke, graphitic argillite and sericite-chlorite schist. The metasedimentary rocks are partly carbonatized and characterized by locally subhorizontal foliation that is commonly highly contorted, resulting in dislocated rootless folds. The section is intruded by sulphide-bearing quartz veins and massive to weakly foliated plagioclase porphyry dykes up to 9 m wide. The felsic porphyry, which locally contains conspicuous arsenopyrite, is associated with the iron formation over a strike length of at least 3.9 km (P. Bachnick, pers. comm., 1997). An isolated occurrence of sulphide iron formation occurs within the gabbro 220 m north of the first unit; it is not known whether this occurrence is due to structural repetition or represents a separate stratigraphic unit. Aphyric basalt (<60 m thick) occurs adjacent to the iron formation at one location; sporadic skialithic enclaves (1->20 m wide) of basalt and related chlorite schist occur elsewhere in the mafic sill.

Mills Island fault slice

Mills Island fault slice broadly corresponds to the outline of Lac Aimée and stratigraphic details are thus known only from islands and peninsulas that occur within the bounding faults. The best available section occurs at Mills Island in the north part of the lake, where diverse volcanic and sedimentary rocks are variously altered to chlorite \pm carbonate \pm sericite schist (Preliminary Map 1997F-1). There is a conspicuous stratigraphic and lithologic discontinuity between Mills Island fault slice and Animus Lake block; however, most lithologic types within the fault slice have counterparts within both Lac Aimée and Sourdough Bay blocks, either of which may be stratigraphically equivalent.

Diverse lithologic units are structurally juxtaposed by internal faults in the north part of Mills Island fault slice (Table GS-11-3). Bedding in these units trends east-west, discordant to the northeast to east-northeast trend of the bounding faults. Both north and south margins of the section (units A and E, Table GS-11-3) are highly sheared over 100 to 150 m widths, and consist of chlorite \pm sericite schist that is pervasively carbonatized. Numerous 1-7 m wide shear zones with variable carbonate and quartz veining occur within the section. Graded feldspathic greywacke (B) and reworked tuff (C) face south-southwest at several localities, but the relative ages of the structurally intercalated units are uncertain. Turbiditic sediments locally display normal to reverse grading in greywacke and siltstone, which are interbedded at a scale of 15-75 cm. A slumped block and synsedimentary folds were locally observed, but depositional features other than bedding are rarely preserved. Disseminated pyritohedra (20%, up to 4 mm) are prominent in siliceous siltstone at one locality. Magnetite-bearing tuff (D) contains up to 8% magnetite as disseminated cubes (0.5-1.5 mm),

Figure GS-11-6: Aphyric pillow basalt of possible arc-rift type at the south shore of Animus Lake.



Table GS-11-3.**North/south section through Mills Island fault slice in the north part of Lac Aimée.**

Unit	Width (m)	Lithologies
A	275	Chlorite-carbonate schist; quartz-sericite-chlorite-carbonate schist. Derived from volcanic and possible sedimentary rocks. North part of section is extensively carbonatized.
B	275	Greywacke-siltstone turbidite.
C	260	Mafic tuff (a) very fine grained (b) fine grained with detrital plagioclase grains. Sporadic magnetite over southern 120 m section. Derived mafic schist and gneiss.
D	20	Magnetite-bearing mafic tuff, chlorite schist. A disrupted quartz vein in a sheared zone at one locality contains mafic schist screens with pyrite-chalcopryrite-malachite mineralization.
E	>150 <380	Chlorite-carbonate schist; quartz-sericite-chlorite-carbonate schist.

and up to 15% detrital plagioclase. Magnetite is locally remobilized into microfractures and thin (2 mm) stringers. The turbiditic sedimentary rocks within Mills Island fault slice have not been age-dated. Lithologically equivalent sequences elsewhere in the Flin Flon Belt include arc-related detritus coeval with Amisk volcanism (pre-1.88 Ga) and later deposits (*ca.* 1.85 Ga) contemporaneous with 'successor arc' volcanism (Bailes and Syme, 1989; Stern *et al.*, 1993; David *et al.*, 1993, 1996; Ansdell *et al.*, 1995; Lucas *et al.*, 1996).

The southwest part of Mills Island fault slice consists of mafic volcanic fragmental rocks that are exposed at the peninsula near the southwest end of Lac Aimée. Mafic tuff, crystal- and lapilli-tuff and volcanic breccia are intercalated at a scale of 1-4 m. Subangular to subrounded fragments up to 30 x 20 cm are mainly basaltic, and display diverse aphyric, plagioclase phyrlic and amygdaloidal textures; minor felsic fragments occur in some units (Fig. GS-11-7). Carbonatization and localized silicification are characteristic. The rocks are generally strongly attenuated, except for a locally undeformed 12 m thick unit of monolithologic mafic breccia containing aphyric, amygdaloidal basalt fragments with highly irregular, angular shapes, within a lithic crystal tuff matrix (Fig. GS-11-8).

Sourdough Bay block

Four stratigraphic units are recognized in Sourdough Bay block in the western Naosap Lake area (Table GS-11-4). Contacts between these units are not exposed, and their relative ages are uncertain due to the paucity of top indicators. Superposition of A, B and C is inferred from rare graded bedding in A and B.

A 550 m wide metasedimentary formation (A) in the north part of Sourdough Bay block consists of grey weathering feldspathic greywacke, siltstone and minor argillite, intercalated at a scale of 10-75 cm. Greywacke beds locally display grading and scoured basal contacts; cyclic interlayering of greywacke and siltstone with thin (2-10 cm) argillite units is interpreted as Bouma AE turbidite zonation (Fig. GS-11-9). Limited structural data indicate these rocks are isoclinally folded in a major west-trending anticline. The metasedimentary formation appears to be stratigraphically gradational with overlying mafic wacke and laminated siltstone (B). These fine to very fine grained, dark green weathering rocks are intercalated at a scale of 0.3-1.5 m, and locally contain subordinate pale grey, intermediate to siliceous siltstone interbeds. The rocks are generally strongly foliated, with metamorphic lamination overprinting primary layering; rare undeformed zones display southeast-facing graded bedding of detrital plagioclase.

Mafic flow and fragmental rocks (C) are predominant in Sourdough Bay block. These are lithologically and stratigraphically comparable with Lac Aimée volcanic rocks and arc-type sequences elsewhere in the Flin Flon Belt, and have therefore been grouped together with Lac Aimée rocks in the Table of Formations (Table GS-11-1). Sourdough Bay volcanics are mainly aphyric with subordinate plagioclase phyrlic phases. They are



Figure GS-11-7: Heterolithic volcanic breccia of inferred mass flow origin in the south part of Mills Island fault slice.

Table GS-11-1

Table of Formations in the Lac Aimée-Naosap Lake area.

PRECAMBRIAN

POST 1.9 Ga INTRUSIVE ROCKS

- | | |
|----|--|
| 12 | Diabase (plagioclase phyric). |
| 11 | Tonalite, granodiorite; granite, aplite. |
| 10 | Gabbro, minor hornblendite. |

AMISK COLLAGE

INTRUSIVE ROCKS (INFERRED SYNVOLCANIC OR PENECONTEMPORANEOUS WITH 1.9 GA VOLCANISM).

- | | |
|---|---|
| 9 | Mafic intrusive rocks: gabbro, gabbronorite, hornblendite. |
| 8 | Felsite, plagioclase-quartz porphyry. |
| 7 | Tonalite, quartz diorite; granodiorite, granite; minor diorite. |

VOLCANIC AND SEDIMENTARY ROCKS

Lac Aimée and Sourdough Bay arc and arc-rift volcanic rocks; related turbidite-type sedimentary rocks.

- | | |
|---|--|
| 6 | feldspathic greywacke, siltstone, siliceous siltstone, argillite. |
| 5 | rhyolite, plagioclase ± quartz phyric; minor felsic tuff and related breccia. |
| 4 | basalt, basaltic andesite (aphyric to plagioclase ± proxene
phyric); volcanic breccia, tuff and diabase; related schist and gneiss. |

Fault contact

Animus Lake mafic volcanic rocks (inferred arc-rift origin); minor related sedimentary rocks.

- | | |
|---|---|
| 3 | basalt (aphyric); minor plagioclase phyric basalt, tuff, breccia and diabase; sulphide-facies iron formation, feldspathic greywacke, siltstone. |
|---|---|

Fault contact

Tartan Lake arc-type basalt.

- | | |
|---|---|
| 2 | Basalt (aphyric to plagioclase phyric). |
|---|---|

Fault contact

Mikanagan Lake arc-rift basalt.

- | | |
|---|---|
| 1 | Basalt (aphyric); minor spherulitic, plagioclase ± pyroxene
phyric basalt and diabase. |
|---|---|

Note. Unit 6 may include sedimentary rocks that postdate 1.9 Ga volcanism. Unit 8 includes both synvolcanic (1.9 Ga) and postvolcanic intrusions. The relative ages of units 10, 11 and 12 are not determined.

Figure GS-11-8: Monolithologic volcanic breccia in the south part of Mills Island fault slice, with variously quartz amygdaloidal, angular mafic blocks; interpreted as a pyroclastic deposit.

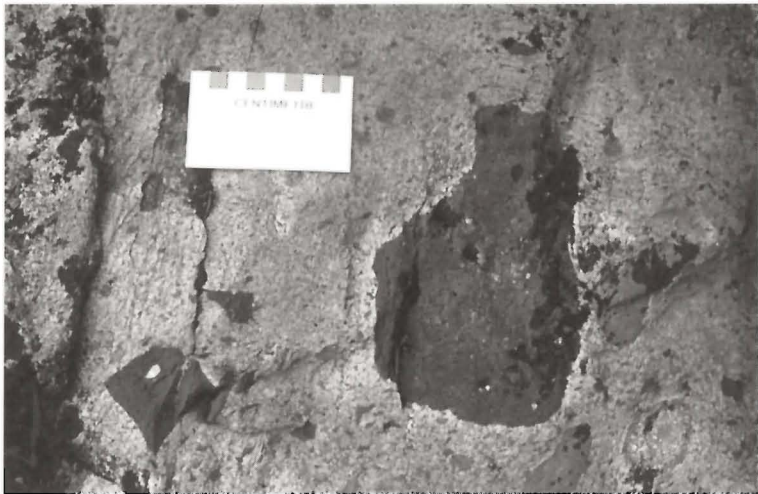


Table GS-11-4.
Stratigraphic section through Sourdough Bay block at western Naosap Lake.

Unit	Width (m)	Lithologies
D	150 >5	At east: cordierite-bearing paragneiss. At west: siliceous and argillitic siltstone.
C	>700	Basalt, locally pillowed; related volcanic breccia. Typically strongly deformed and attenuated.
B	430	Mafic wacke and siltstone, locally graded; with minor intermediate to siliceous siltstone interbeds.
A	550	Turbiditic greywacke, siltstone and minor argillite; locally graded and scoured.

strongly deformed at the north shore of western Naosap Lake (Preliminary Map 1997F-1), where highly attenuated to protomylonitic volcanic breccia and mafic tectonite are evidence for an inferred east- to northeast-trending fault roughly coincident with the shoreline. Rare pillows are locally preserved, but deformation has generally resulted in attenuation and tectonic lamination of mafic flow units. Epidosite pods and irregular masses locally contain quartzofeldspathic amygdaloids, or densely quartz-amygdaloidal zones, possibly at or close to flow tops. Most intercalated volcanic fragmental units are interpreted as flow breccia, with aphyric to plagioclase phyrlic and/or amygdaloidal mafic fragments. Several units that contain both mafic and subordinate plagioclase phyrlic felsic clasts are interpreted as mass flow deposits. Volcanic breccia is generally strongly flattened, with clast elongation ratios of 5:1 to 12:1.

A monolithologic volcanic breccia unit, over 20 m wide, occurs at the north shore of western Naosap Lake, on the north limb of the anticline that extends through a metasedimentary unit (A in Table GS-11-4; Preliminary Map 1997F-1). This unique lithology, which is interpreted as a pyroclastic deposit, consists of angular felsic fragments (1-8 cm) within a very dark grey mafic tuff matrix. Subordinate thin beds of diffusely laminated lithic tuff are intercalated with the breccia, which may be stratigraphically equivalent to unit C on the south limb of the anticline.

Metasedimentary unit D (Table GS-11-4) within the western embayment of Naosap Lake is inferred from two localities of metasedimentary rocks: siliceous to argillitic siltstone in the southwest corner of the bay, and porphyroblastic paragneiss on-strike 2.5 km further east, at the margin of the major granitoid terrane east of the map area (Preliminary Map 1997F-1). The hornfelsed paragneiss contains ovoid to pseudohexagonal, 1-3 cm porphyroblasts of cordierite (confirmation pending) ± garnet over a 150 m wide section (Fig. GS-11-10). Cordierite occurs sporadically for a further 150 m within the contiguous mafic volcanic section to the northwest, which is characterized by pervasive silicic, feldspathic and epidotic alteration (Fig. GS-11-11).

INTRUSIVE ROCKS

Intrusive rocks constitute approximately 25% of the map area and range from gabbro and hornblende to tonalite, granodiorite and felsic porphyry; these are classified by age as synvolcanic or late, postvolcanic (units 7 to 9, and 10 to 12 respectively, Table GS-11-1). Synvolcanic gabbro (9) is a major component of Animus Lake block, but equivalent intrusive rocks are insignificant in Lac Aimée block. The reverse is true for felsic porphyry (8), which is abundant in Lac Aimée block, but rare in Animus Lake block. The conformable lensoid tonalite-granodiorite stock (7) in the northeast part of Lac Aimée block predates the regional S_1 foliation and is interpreted as a subvolcanic intrusion (Gilbert, 1996a), whereas a younger age is inferred for massive tonalite-granodiorite (11) at the east margin of the map area, which truncates regional foliation in Sourdough Bay block (Preliminary Map 1997F-1). Medium- to coarse-grained melanocratic gabbro (10) in the north part of Sourdough Bay block and similar minor lensoid intrusions in Lac Aimée block are assumed to postdate 1.9 Ga volcanism.

Synvolcanic gabbro sills (9) up to 300 m wide are intercalated with Animus pillowed basalt (3). The sills are lithologically very similar to, and assumed coeval with North Aimée gabbro. Contacts with mafic flows are generally sharp (locally gradational). The medium- to coarse-grained rocks contain 40-60% hornblende in random amphibole or 'spotted' texture (equant crystals probably after pyroxene); these textures are locally intergradational. The generally massive intrusions are somewhat finer grained toward 1-10 m wide marginal zones. North Aimée gabbro (at least 850 m wide) is non-layered, in contrast to major sills of similar size west of the map area (Batters Lake, Mikanagan Lake sills; Gilbert, 1990a). Zonation is absent in North Aimée gabbro, but the intrusion locally displays igneous lamination defined by subparallel hornblende prisms and localized mottled texture due to subophitic feldspar aggregates. Very coarse grained hornblenditic zones up to 15 m across in thicker interflow sills and within North Aimée gabbro constitute approximately 5% of unit 9.



Figure GS-11-9: Feldspathic greywacke intercalated with argillitic siltstone in the turbidite formation at the north shore of western Naosap Lake.

Younger, postvolcanic gabbro (unit 10) is mesocratic to melanocratic, with massive, medium- to coarse-grained texture. Subordinate coarse- to very-coarse-grained hornblende zones are locally veined by the main gabbroic phase. Preliminary rare earth element analytical data indicate the late gabbros are conspicuously different from older, volcanic-related mafic intrusive rocks. Gabbro contacts with basalt are sharp, commonly chilled, and locally overprinted by hornblende porphyroblasts attributed to regional metamorphism. Basalt at the margin of the gabbro stock in the north part of Sourdough Bay block is amphibolitized and partly assimilated by the intrusive rock in a migmatitic contact zone. Basalt xenoliths in the contact zone are well foliated, in contrast to the massive gabbro, indicating a post-S₁ age of intrusion.

The ovoid granitoid stock (7) and felsic porphyry dykes (8) in Lac Aimée block have been previously described (units 5 and 6 in Gilbert, 1996a). Felsic porphyry dykes are abundant within LAFZ - along the northwest and southeast shores of Lac Aimée, at islands in the north part of the lake, and in the northeast part of the map area (Sap claims, Gilbert, 1996a). At least two intrusive porphyry phases are recognized: strongly foliated (pre-tectonic) and massive (post-tectonic). Foliated plagioclase-quartz porphyry, the most abundant phase, is assumed to include synvolcanic intrusions. Post-tectonic dykes include a very coarse grained

quartz-plagioclase porphyry phase that contains 20-40% quartz (up to 1 cm), 10-30% plagioclase and up to 5% disseminated pyrite; these dykes occur sporadically in Lac Aimée and Sourdough Bay blocks, and within Animus Lake fault.

GEOCHEMISTRY

Tectonostratigraphic assemblages in the Lac Aimée-Naosap Lake area are geochemically distinctive, and include both arc and arc-rift volcanic types. Trace and rare earth element contents reflect the tectonic affiliation (Table GS-11-5); variations in FeO^{total} and Mg number reflect differences in the degree of fractionation between rock suites of similar affiliation.

Lac Aimée block consists mainly of arc basalt; subordinate arc-rift basalt occurs in a narrow zone that extends laterally for 8 km within the core of Lac Aimée anticline. The arc-rift basalt, which was not recognized as a lithologic unit during the course of field mapping, is assumed to be conformable with adjacent arc basalt. Lac Aimée arc basalt is characterized by elevated LILE and LREE, and depleted HFSE relative to N-MORB (Fig. GS-11-12). The pattern is similar to that of arc volcanic rocks in the contiguous Tartan-Embury lakes area to the west, except for even more pronounced Th and LREE enrichment. Relatively low TiO₂ content in Lac Aimée arc basalt (0.3-0.9%) distinguishes these rocks from Lac Aimée arc-rift basalt (0.9-1.3% TiO₂; Fig. GS-11-13), which is also characterized by less pronounced LILE/HFSE decoupling than arc rocks (Fig. GS-11-12); LREE enrichment is moderate in Lac Aimée arc-rift basalt compared to adjacent arc rocks (average [La/Yb]_N = 2.86 for arc-rift, 4.78 for arc rocks).

Mikanagan Lake block (west of Animus Lake fault, Fig. GS-11-2) consists of arc-rift basalt that is subdivided into a low-HFSE group (TiO₂ = 0.7-1.1%) and high HFSE group (TiO₂ = 1.6-2.1%). Mikanagan Lake low-HFSE arc-rift basalt has a very similar rare earth element pattern to that of Lac Aimée arc-rift basalt, with HFSE slightly depleted relative to MORB, whereas high-HFSE basalt is enriched in HFSE relative to N-MORB.

Lac Aimée arc-rift basalt is similar to arc-rift basalt elsewhere in the Flin Flon Belt (e.g., Scotty Lake basalt, Syme *et al.*, in prep.) in having less depleted HFSE and only moderate LREE enrichment compared to arc basalt, but high Th (and, by inference, elevated LILE); this may be due to crustal contamination of the juvenile magma during ascent through the lithosphere (Syme *et al.*, in prep.). Both arc and arc-rift basalts in Lac Aimée block are distinguished from equivalent rocks elsewhere in the north central part of the Flin Flon Belt by relatively low Mg number and high FeO^{total}, indicating a relatively higher degree of fractionation (Table GS-11-5).

ECONOMIC GEOLOGY

Early exploration in the Lac Aimée-Naosap Lake area focused on structurally controlled base-metal mineralization such as the Cu occurrence within Animus Lake fault ('KD zone') in the southwest corner of the map area, originally staked in 1921 (Gilbert, 1996a). In 1949 drilling was carried out to test the base-metal potential of sulphide-facies iron formation that extends along the north margin of the map area, and the locality was actively explored over the next 35 years. Attention was diverted to precious metals following the 1986 discovery of gold in shear zones within LAFZ south of the sulphide iron formation. However, follow-up drilling of major faults yielded generally low assay values (up to 0.29 oz/tonne Au within LAFZ; up to 0.026 oz/tonne Au at the LAFZ/Sourdough Bay fault intersection; P. Bachnik, pers. comm., 1997).

Grab samples of the sulphide iron formation yielded 0.12 oz/tonne Au (Gale and Eccles, 1988). A sulphide showing at the south shore of Wabishkok Lake, on-strike with the iron formation and associated with the same EM anomaly, was examined by the author in 1986. The 4 m wide mineralized zone occurs at a basalt/gabbro contact and contains a 40 cm section of massive graphitic sulphide within mafic schist and felsite; an assay yielded 0.06% Cu, minor Ni and Zn, and trace Au.

CONCLUSIONS

The Lac Aimée-Naosap Lake area is situated in the northwest part of the Flin Flon volcanic belt (Fig. GS-11-1) at a conspicuous structural discordance within the Amisk accretionary collage (Lucas *et al.*, 1996). Lac Aimée fault zone (LAFZ), which extends southwest to northeast across



Figure GS-11-10: Semipelitic paragneiss in the western embayment of Naosap Lake, with ovoid to subhedral cordierite (?) porphyroblasts.

Figure GS-11-11: Metasomatic alteration of basalt in contact with tonalite-granodiorite at the south shore of western Naosap Lake. Epidote porphyroblasts occur within irregular to dendritic quartzofeldspathic domains.

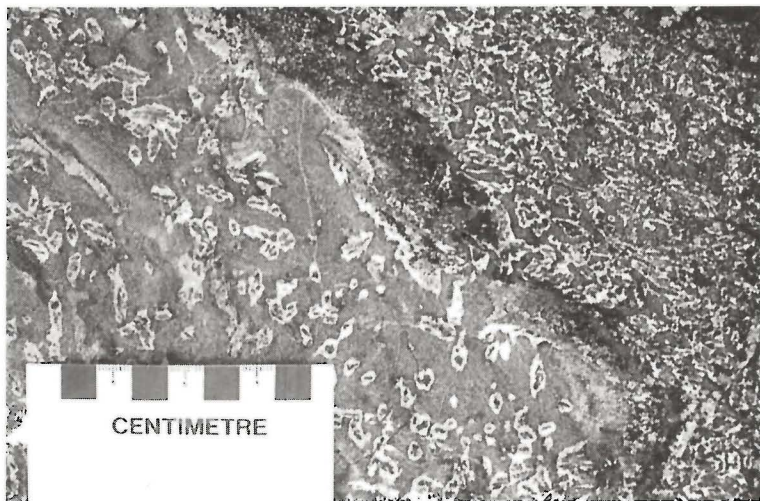


Table GS-11-5.
TiO₂, FeO^{total}, Mg number and Th averages for mafic volcanic rocksuites in the Lac Aimée area and in the Tartan-Embury-Mikanagan area to the west.

Mafic volcanic rock suite	TiO ₂ (wt. %)	FeO' (wt. %)	Mg#	Th (ppm)
Tartan-Embury Arc	0.47	9.73	0.55	0.38
Lac Aimée Arc	0.57	12.40	0.48	1.25
Lac Aimée Arc-rift	1.09	14.51	0.39	0.89
Mikanagan Arc-rift	1.67	13.09	0.49	1.29

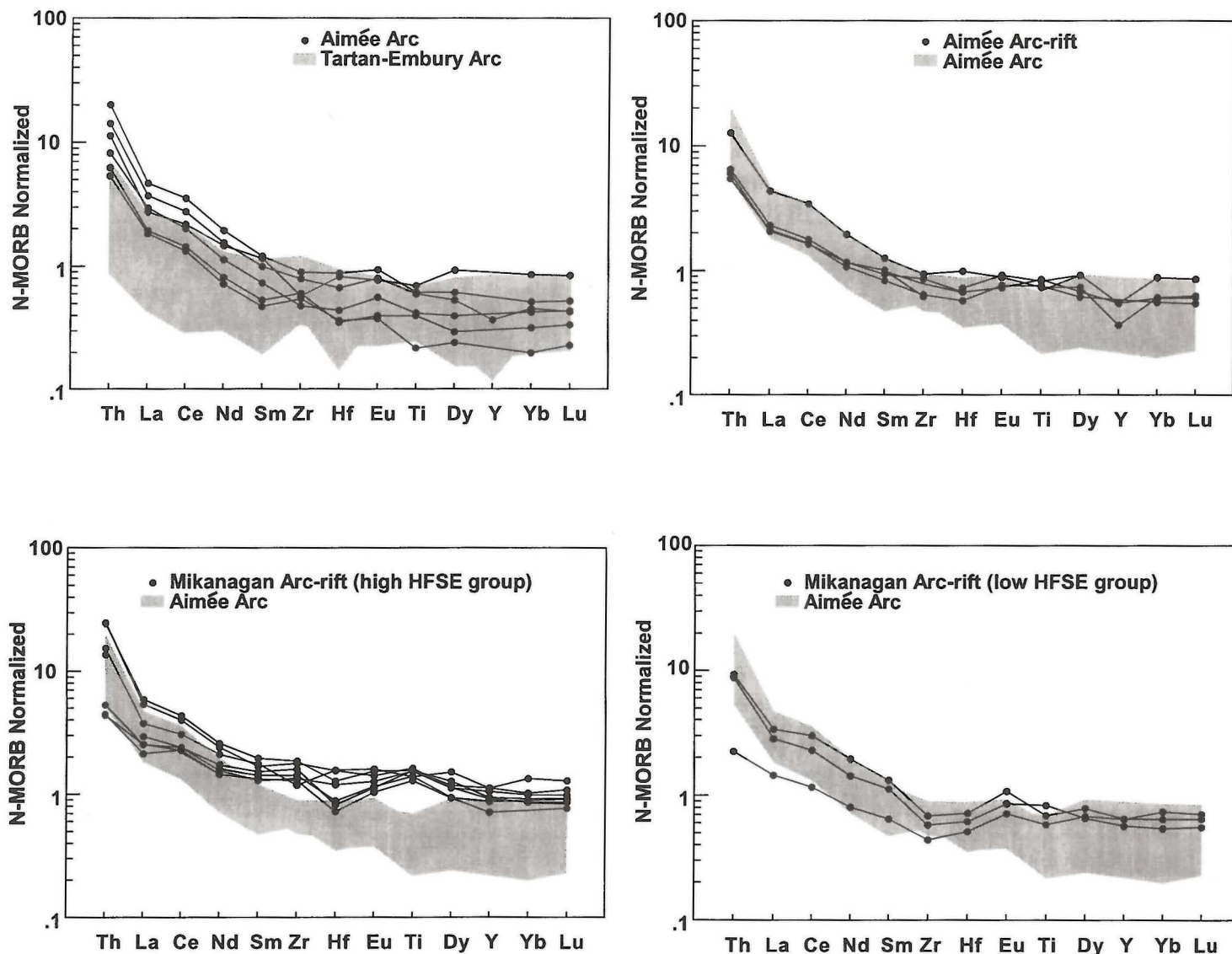


Figure GS-11-12: Rare earth element plots of mafic volcanic rocks in the Lac Aimée-Naosap Lake area and selected volcanic rock suites in the contiguous Tartan-Embury-Mikanagan lakes area to the west. N-MORB normalizing values from Sun and McDonough (1989).

the map area, represents a crustal scale structural break that can be traced on the deep seismic profile of the LITHOPROBE transect (line 7A, Lucas *et al.*, 1994). Animus Lake basalt northwest of LAFZ is characterized by isoclinal folding on north- to west-trending axes, in contrast to the northeast structural trend of rocks in Lac Aimée block, southeast of LAFZ (Figs. GS-11-2 and 3). The Animus Lake fault close to the west margin of the project area marks the west termination of Animus Lake and Lac Aimée blocks. West of the fault, Tartan Lake block (at north) and Mikanagan Lake block (at south) are separated by the layered Batters Lake gabbro sill (Gilbert, 1990a). The Sourdough Bay fault between Lac Aimée block and Sourdough Bay block in the east part of the map area is a regional structure that extends from north of Naosap Lake south to Athapapuskow Lake (Bailes and Syme, 1989).

Volcanic rock suites within the fault blocks are compositionally distinctive (see Appendix). Mikanagan Lake basalt is akin to arc-rift basalt (Syme *et al.*, in prep.; Gilbert, in prep.) whereas Tartan Lake basalt is of arc origin. Lac Aimée basalts include both arc and arc-rift volcanic types. Animus Lake basalt is provisionally interpreted as arc-rift in origin, but geochemical data are not yet available to identify these rocks.

Lac Aimée block is stratigraphically and compositionally diverse, in contrast to more homogeneous Animus, Tartan and Mikanagan Lake blocks

(Table GS-11-1). Arc-rift basalt occurs within Lac Aimée block in a zone that extends for 8 km through the core of Lac Aimée anticline; arc-type basalt is predominant elsewhere in the block. Intermediate to mafic volcanic breccia and tuff, felsic volcanic rocks and fine grained turbidite deposits are intercalated with Lac Aimée mafic volcanic flows. These rocks are intruded by felsic porphyry, minor gabbro lenses, and in the northeast part of the block, by a tonalitic stock.

Animus Lake block consists almost exclusively of pillowed aphyric basalt and abundant related gabbro which constitutes approximately 20% of the block. Narrow 1-6 m wide units of siltstone and mafic tuff occur within North Aimée gabbro in the north part of the map area (Figure GS-11-2). The mafic sill also contains two enclaves of sulphide-facies iron formation up to 20 m wide that consist of siltstone, argillite, chert and chlorite-sericite schist, with pyrite-pyrrhotite-arsenopyrite mineralization. The iron formation is brecciated and intruded by quartz veins and feldspar porphyry dykes.

Sourdough Bay block in the east part of the map area consists largely of massive to fragmental mafic volcanic rocks, interpreted as arc-related, and subordinate turbidite deposits. The supracrustal rocks are flanked by gabbro and hornblende to the north and tonalite-granodiorite to the south and east. Contact metamorphic cordierite (?) ± garnet schist occurs locally adjacent to the granitoid intrusion.

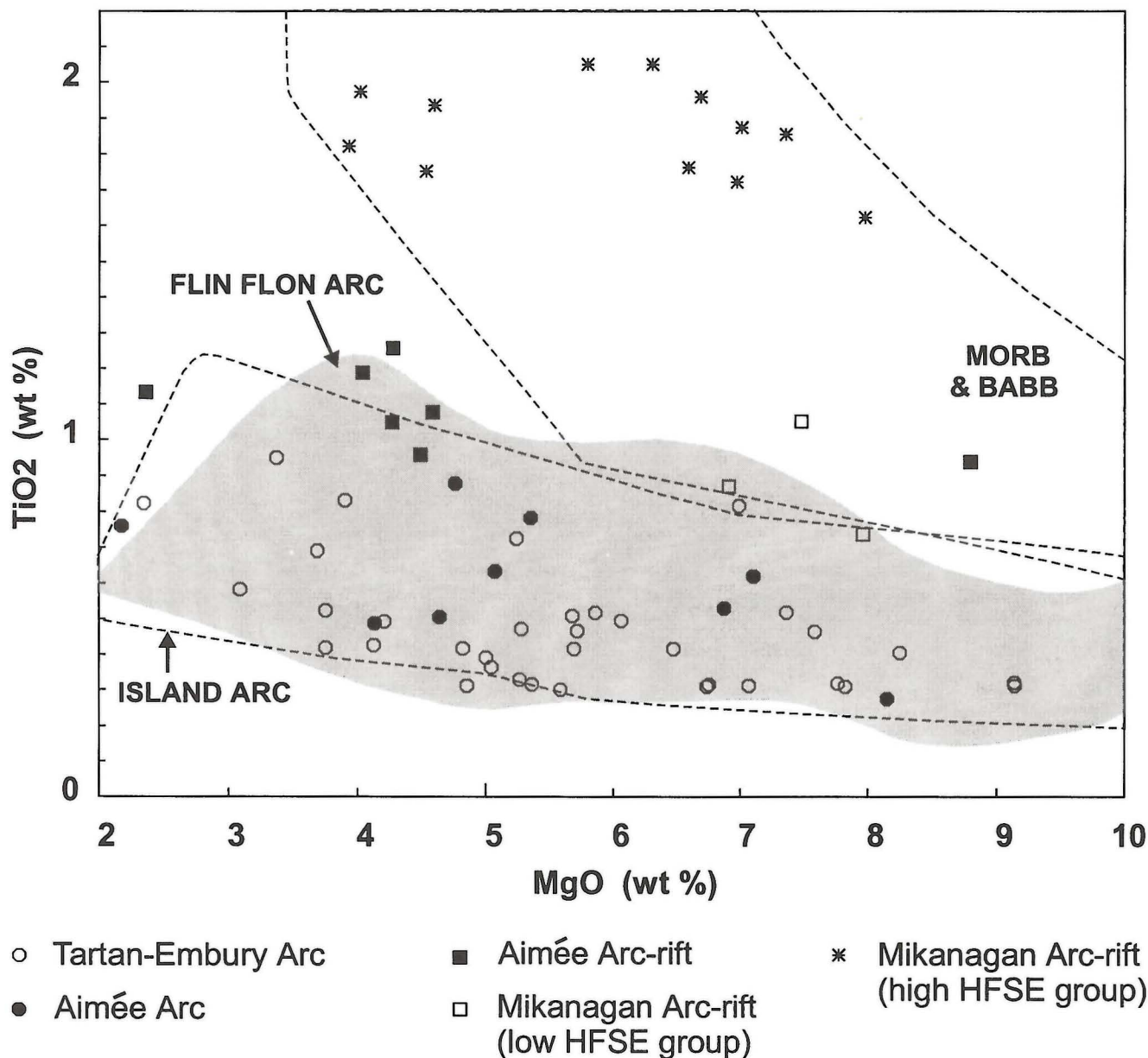


Figure GS-11-13: TiO_2 vs. MgO plot of mafic volcanic rocks in the Lac Aimée-Naosap Lake area and selected volcanic rock suites in the contiguous Tartan-Embury-Mikanagan lakes area to the west. Shaded field is for Flin Flon arc volcanic rocks (Stern et al., 1995a). Compositional fields of modern volcanic rocks after Stern et al. (1995b). MORB = mid-ocean ridge basalt; BABB = back-arc basin basalt.

Five deformation periods are recognized in the map area, post 1.88-1.87 Ga tectonic accretion of the Amisk collage and initiation of LAFZ. The discordance of D_1 structural trends in Animus and Lac Aimée blocks across LAFZ, in contrast to broadly concordant D_2 structures in these blocks (Fig. GS-11-3), indicates tectonic transport and juxtaposition of the fault blocks occurred between D_1 and D_2 . D_3 is characterized by open folding of F_2 fold axial traces and is associated with southeast-trending strain-slip cleavage. A major northeast-trending open fold delineated by the curvilinear axial traces of F_1 folds is attributed to D_4 or possibly earlier D_2 deformation. Late brittle deformation (D_5) resulted in concordant shears and high angle faults within fault blocks, and reactivation of block-bounding faults.

ACKNOWLEDGEMENTS

Field mapping this season was carried out in collaboration with Dave Prouse, who conducted 3 days mapping north of Lac Aimée, and Brian Skanderbeg who, as field assistant, made a significant contribution to the collection and evaluation of field data. Many thanks are extended to these individuals for their assistance with both geological mapping and logistical operations.

REFERENCES

- Ansdell, K.M., Lucas S.B., Connors K., and Stern, R.A.
1995: Kiseynew metasedimentary gneiss belt, Trans Hudson orogen (Canada): Back-arc origin and collisional inversion; *Geology*, v. 21, p. 1039-1043.
- Ashton, K.E.
1993: Structure of the southern flank of the Kiseynew Gneiss Belt in Saskatchewan; Trans-Hudson Orogen Transect Workshop, LITHOPROBE Report No. 34, p. 84-87.
- Bailes, A.H. and Syme, E.C.
1979: White Lake - Mikanagan Lake project; in Manitoba Department of Mines, Natural Resources and Environment, Mineral Resources Division, Report of Field Activities, 1979, p. 46-54.
- Bailes, A.H. and Syme, E.C.
1989: Geology of the Flin Flon-White Lake area; Manitoba Energy

- and Mines, Geological Services, Geological Report GR 87-1; 313 p.
- Bateman, J.D. and Harrison, J.M.
1943: Mikanagan Lake; Geological Survey of Canada Map 832A; scale 1 inch = 1 mile, with marginal notes.
- David, J., Bailes, A.H., and Machado, N.
1996: Evolution of the Snow Lake portion of the Paleoproterozoic Flin Flon and Kisseynew belts, Trans-Hudson Orogen, Manitoba, Canada; Precambrian Research v. 80 (2), p. 107-124.
- David, J., Machado, N., Bailes, A.H., and Syme, E.C.
1993: U-Pb geochronology of the Proterozoic Flin Flon Belt-Snow Lake belt: New results; Trans-Hudson Orogen Transect Workshop, LITHOPROBE Report No. 34, p. 84-87.
- Gale G.H. and Eccles, D.R.
1988: Mineral deposits and occurrences in the Flin Flon area NTS 63K/13: Part III, Weasel Bay area (63K/13NW) and Defender Lake area (63K/13NE); Manitoba Energy and Mines, Geological Services, Mineral Deposit Report No. 3, 46 p.
- Gilbert, H.P.
1986: Geological investigations in the Tartan Lake-Lac Aimée area; **in** Manitoba Energy and Mines, Minerals Division, Report of Field Activities, 1986, p. 43-48.
- Gilbert, H.P.
1990a: Geological investigations in the Tartan Lake-Mikanagan Lake area; **in** Manitoba Energy and Mines, Minerals Division, Report of Activities, 1990, p. 20-36.
- Gilbert, H.P.
1990b: Tartan-Embury Lakes; Manitoba Energy and Mines, Preliminary Map 1990F-1, 1:20 000.
- Gilbert, H.P.
1996a: Geology of the Lac Aimée-Naosap Lake area; **in** Manitoba Energy and Mines, Geological Services, Report of Activities, 1996, p. 32-39.
- Gilbert, H.P.
1996b: Geochemistry of mafic volcanic rocks in the Tartan-Embury Mikanagan Lakes area (abstract); GAC/MAC Joint Annual Meeting 1996, Program with Abstracts, Winnipeg, Manitoba, p. A36.
- Gilbert, H.P. (in prep.)
Geochemistry of arc and arc-rift volcanic rocks and the significance of intercalated turbidite deposits in the Tartan-Embury-Mikanagan lakes area, northern Flin Flon Belt, Canada.
- Lucas, S.B., Stern, R.A., Syme, E.C., Reilly, B.A. and Thomas, D.J.
1996: Intraoceanic tectonics and the development of continental crust: 1.92-1.84 Ma evolution of the Flin Flon Belt, Canada. Geological Society of America Bulletin, v. 108, p. 602-629.
- Lucas, S.B., White, D., Hajnal, Z., Lewry, J., Green, A., Clowes, R., Zwanig, H., Ashton, K., Schledewitz, D., Stauffer, M., Norman, A., Williams, P. and Spence, G.
1994: Three-dimensional collisional structure of the Trans-Hudson Orogen, Canada; **in** Proceedings of the 5th International conference on seismic reflection probing of continents and their margins. Edited by R.M. Clowes and A.G. Green. Tectonophysics, v. 232, p. 161-178.
- Kalliokoski, J.
1949: Weldon Bay; Geological Survey of Canada Map 1020A; scale 1 inch = 1 mile, with marginal notes.
- Ryan, J.J. and Williams, P.F.
1993: Structural mapping in the Elbow Lake area, Flin Flon-Snow Lake belt, central Manitoba; **in** Manitoba Energy and Mines, Geological Services, Report of Activities, 1993, p. 84-85.
- Ryan, J.J. and Williams, P.F.
1994: Structural geology of the Elbow Lake area, Flin Flon-Snow Lake greenstone belt, Manitoba; **in** Manitoba Energy and Mines, Geological Services, Report of Activities, 1994, p. 108-114.
- Stauffer, M.R.
1990: The Missi Formation: An Aphebian molasse deposit in the Reindeer Lake zone of the Trans-Hudson Orogen, Canada; **in** Lewry, J.F. and Stauffer, M.R., eds., The Early Proterozoic Trans-Hudson Orogen of North America; Geological Association of Canada Special Paper No. 37, p. 121-142.
- Stern, R.A., Lucas, S.B., Syme, E.C., Bailes, A.H., Thomas, D.J., LeClair, A.D., and Hulbert, L.
1993: Geochronological studies in the NATMAP Shield Margin Project area, Flin Flon Domain: Results for 1992-3; **in** Radiogenic Age and Isotopic Studies: Report 7, Geological Survey of Canada, Paper 93-2, p. 59-70.
- Stern, R.A., Syme, E.C., Bailes, A.H., and Lucas, S.B.
1995a: Paleoproterozoic (1.90-1.86 Ga) arc volcanism in the Flin Flon Belt, Trans-Hudson orogen, Canada; Contributions to Mineralogy and Petrology, v. 119, p. 117-141.
- Stern, R.A., Syme, E.C. and Lucas, S.B.
1995b: Geochemistry of 1.9 Ga MORB- and OIB-like basalts from the Amisk collage, Flin Flon belt, Canada: evidence for an intra-oceanic origin. Geochimica et Cosmochimica Acta, v. 59, p. 3131-3154.
- Sun, S.S and McDonough, W.F.
1989: Chemical and isotopic systematics of oceanic basalts: implications for mantle composition and processes; Geological Society Special Publication No. 42, pp. 313-345.
- Syme, E.C.
1995: 1.9 Ma arc and arc-rift assemblages and their bounding structures in the central Flin Flon Belt; **in** Trans-Hudson Orogen Transect Workshop, LITHOPROBE Report No. 48, p. 261-272.
- Syme, E.C., Lucas, S.B., Bailes, A.H. and Stern, R.A.
in prep.: Role of tectonostratigraphic setting and intra-arc extension in localizing Paleoproterozoic volcanogenic massive sulphide deposits, Flin Flon Belt, Manitoba.
- Zwanig, H.V. and Schledewitz, D.C.P.
1992: Geology of the Kissinging-Batty Lakes area: Interim Report; Manitoba Energy and Mines, Geological Services, Open File Report OF92-2, 87 p.

Appendix GS-11: Major, minor and trace element data for volcanic rocks in the Lac Aim  e-Tartan Lake-Mikanagan Lake area.

86

Sample #	Rock suite	SiO ₂	TiO ₂	Al ₂ O ₃	FeO*	MnO	MgO	CaONa ₂ OK ₂ O	P ₂ O ₅	LOI	Mg#	Ni	Cr	Sc	Zn	Rb	Ba	Sr	Cs	Hf	Zr	Y	Th	U	La	Ce	Nd	Sm	Eu	Tb	Dy	Yb	Lu (La/Yb)N			
Juvenile arc basalt, basaltic andesite																																				
32-86-0032-1	Tartan arc	54.50	0.82	17.04	5.78	0.09	6.99	9.04	4.25	1.33	0.16	1.2	0.71	60	250																					
32-86-0106-1	Tartan arc	52.46	0.72	16.97	11.38	0.17	5.24	8.28	3.05	1.54	0.19	2.8	0.49	22	64	32	110	28	408	428	0.6	0.7	39	9	0.4	0.4	4	9	6	1.5	0.5	0.3	2.0	1.26	0.19	2.60
32-86-0244-1	Tartan arc	52.68	0.52	18.21	8.53	0.13	5.86	9.55	4.01	0.40	0.11	3.0	0.59	43	108			12	216	329																
32-87-1058-1	Tartan arc	52.97	0.32	15.27	8.78	0.17	7.77	11.54	2.88	0.25	0.06		0.65	38	356			0	113	99																
32-87-1281-1	Tartan arc	53.84	0.40	13.67	9.57	0.18	8.25	10.87	2.68	0.47	0.08		0.64	46	312			10	127	85																
32-87-1406-1	Tartan arc	58.46	0.31	14.54	11.12	0.15	4.85	6.59	2.07	1.74	0.17		0.47	11	45			32	491	305																
32-87-1732-4	Tartan arc	51.53	0.31	11.12	10.66	0.21	12.42	11.73	1.31	0.61	0.10		0.71	147	1007	47	100	16	166	229	-0.2	-0.2	27	3	0.2	0.2	2	5	3	0.8	0.3	0.2	1.3	0.83	0.12	1.98
32-87-1785-1	Tartan arc	54.79	0.31	13.57	9.88	0.20	7.82	9.78	3.19	0.37	0.10		0.62	38	273			12	95	197																
32-87-1786-1	Tartan arc	50.83	0.31	18.12	9.72	0.21	7.07	11.27	1.85	0.55	0.07		0.60	31	72			19	122	208																
32-87-1789-1	Tartan arc	48.13	0.31	19.85	9.27	0.17	6.74	12.59	1.70	1.17	0.07		0.60	36	72	38	87	30	290	518	1.0	0.3	25	6	0.3	-0.1	2	6	4	1.0	0.3	0.2	1.4	1.04	0.15	1.58
32-90-4557-1	Tartan arc	56.16	0.52	15.72	11.04	0.19	3.75	8.00	1.62	1.80	0.20	2.9	0.41	12	18			28	302	461																
32-90-4563-1	Tartan arc	55.75	0.51	15.26	11.23	0.21	5.68	8.61	1.40	1.15	0.20	2.5	0.51	39	123	32	100	17	204	433	-0.2	0.6	37	9	0.4	0.4	4	9	6	1.5	0.5	0.3	2.1	1.34	0.19	2.45
32-96-0319-1	Aim��e arc	57.59	0.62	14.58	8.35	0.17	7.10	7.52	3.00	0.92	0.16	2.50	0.64	91	512			20	412	289																
32-96-0033-1	Aim��e arc	55.47	0.27	9.04	11.54	0.19	11.85	8.29	3.06	0.21	0.07	1.7	0.68						121	135			37	-10												
32-96-0037-1	Aim��e arc	59.07	0.63	13.24	12.31	0.20	5.07	5.44	2.89	1.00	0.14	3.4	0.46						298	186			81	12												
32-96-0044-1	Aim��e arc	52.17	0.88	13.97	15.17	0.23	4.76	8.95	3.39	0.31	0.17	8.6	0.39	21	18	39	104	2	117	98	0.0	1.5	39	-10	1.2	0.7	6	15	:	2.8	0.7	0.6	3.9	2.38	0.35	2.16
32-96-0056-1	Aim��e arc	59.55	0.27	9.07	11.50	0.20	8.15	8.71	1.79	0.68	0.07	3.6	0.59	40	386	48	76	10	301	198	0.0	0.7	39	-10	0.6	0.2	4	:	5	1.2	0.4	0.2	1.1	0.58	0.10	6.20
32-96-0065-1	Aim��e arc	52.11	0.53	15.05	12.66	0.22	6.87	8.95	2.73	0.79	0.09	2.6	0.53						383	190			36	-10												
32-96-0092-1	Aim��e arc	55.12	0.76	17.86	11.39	0.17	2.18	8.80	2.14	1.39	0.20	1.8	0.28	6	15	33	68	29	422	419	0.1	1.3	57	10	1.6	0.8	9	20	11	2.5	0.8	0.4	2.4	1.34	0.19	5.52
32-96-0092-2	Aim��e arc	55.74	0.78	14.76	12.28	0.23	5.35	7.57	2.33	0.79	0.17	2.3	0.47	24	155	47	117	10	320	265	0.2	1.7	64	-10	2.3	0.8	11	26	14	3.0	0.9	0.4	2.7	1.52	0.23	6.10
32-96-0147-1	Aim��e arc	55.81	0.53	14.11	14.00	0.19	6.30	5.54	2.78	0.65	0.09	3.9	0.48	11	16	46	9	9	261	142	0.2	0.9	34	-10	0.9	0.3	7	14	8	1.9	0.6	0.3	1.7	1.25	0.19	4.64
32-96-0173-1	Aim��e arc	58.29	0.50	13.89	13.18	0.19	4.64	5.53	2.89	0.79	0.09	1.1	0.42	10	13	44	109	12	341	200	0.8	0.7	44	-10	0.7	0.4	5	11	6	1.4	0.4	0.2	1.3	0.95	0.15	4.08
32-96-0230-1	Aim��e arc	57.26	0.49	14.09	13.98	0.21	4.13	6.94	2.48	0.31	0.10	0.6	0.38						70	225			38	-10												
Arc-rift basalt, basaltic andesite																																				
32-96-0016-1	Aim��e arc-rift	54.91	1.08	14.78	15.09	0.19	4.59	5.20	3.07	0.89	0.21	2.5	0.38	11	8	40	89	14	273	251	0.8	1.4	62	15	0.8	0.9	6	13	8	2.4	0.7	0.5	3.0	1.79	0.27	2.57
32-96-0041-1	Aim��e arc-rift	52.86	1.26	14.63	15.87	0.23	4.28	6.70	3.35	0.67	0.15	3.2	0.36						147	215			47	16												
32-96-0073-1	Aim��e arc-rift	55.15	1.05	14.61	14.20	0.22	4.27	6.68	3.39	0.32	0.12	2.5	0.38	12	13	43	99	5	116	113	0.1	1.4	45	15	0.7	0.5	5	12	8	2.6	0.9	0.6	4.1	2.61	0.38	1.57
32-96-0095-1	Aim��e arc-rift	57.51	1.13	13.62	15.08	0.21	2.36	5.28	3.44	1.06	0.30	4.0	0.24						296	244			77	18												
32-96-0106-1	Aim��e arc-rift	53.72	1.19	14.09	15.56	0.23	4.04	7.54	2.58	0.87	0.19	5.0	0.35						287	336			45	-10												
32-96-0149-1	Aim��e arc-rift	53.62	0.94	12.40	12.61	0.19	8.80	7.70	2.90	0.70	0.14	1.8	0.59	52	407	53	90	13	342	210	0.1	1.0	68	10	1.5	0.4	11	25	14	3.2	0.9	0.5	3.3	1.82	0.28	4.79
32-96-0150-2	Aim��e arc-rift	51.17	0.96	17.54	13.18	0.19	4.49	9.71	2.37	0.24	0.16	2.9	0.41	26	26	36	97	4	77	361	0.1	1.1	46	-10	0.6	0.4	5	12	8	2.1	0.8	0.4	2.7	1.65	0.24	2.52
32-86-0456-1	Mikanagan arc-rift (low HFSE)	51.84	1.05	15.35	9.93	0.17	7.48	9.12	4.70	0.12	0.25	4.2	0.61	41	249	51	64	5	86	240	0.1	1.2	41	15	1.0	0.6	7	16	:	2.8	0.8	0.5	2.8	1.57	0.24	3.50
32-90-4184-1	Mikanagan arc-rift (low HFSE)	50.19	0.87	16.70	12.20	0.17	6.91	8.72	3.64	0.29	0.30	3.0	0.54	36	168	44	80	6	95	316	0.1	1.4	48	17	1.1	0.5	8	21	14	3.3	1.0	0.5	3.4	1.87	0.28	3.50
32-90-4232-1	Mikanagan arc-rift (low HFSE)	50.03	0.74	15.07	13.35	0.25	7.96	9.93	2.43	0.19	0.05	4.5	0.55	66	154	54	126	4	53	123	0.1	0.0	30	17	0.2	0.1	3	8	6	1.6	0.7	0.4	2.9	2.10	0.30	1.32
32-86-0398-1	Mikanagan arc-rift (high HFSE)	52.09	2.05	15.00	10.79	0.18	6.31	7.93	3.32	1.16	0.17	2.7	0.55	34	95	34	130	27	382	189	-0.2	3.1	128	25	2.9	0.9	13	29	17	4.3	1.4	0.8	5.0	2.56	0.38	4.16
32-90-4155-1	Mikanagan arc-rift (high HFSE)	48.01	1.62	16.46	12.81	0.21	7.98	10.37	2.18	0.21	0.14	3.3	0.56	84	188	38	140	5	79	231	-0.2	1.4	90	19	0.6	-0.1	6	16	10	3.3	1.0	0.7	4.0	2.13	0.33	2.31
32-90-4480-1	Mikanagan arc-rift (high HFSE)	52.94	1.97	15.04	13.57	0.23	4.02	9.26	2.46	0.27	0.23	2.4	0.38	-6	9	31	130	5	103	347	-0.2	2.5	131	30	2.8	1.3	14	31	18	4.9	1.5	0.9	5.1	2.96	0.47	3.88
32-90-4308-1	Mikanagan arc-rift (high HFSE)</																																			

GS-12: THE THOMPSON NICKEL BELT PROJECT - AIMS AND OBJECTIVES

by D.C. Peck

Peck, D.C., 1997: The Thompson Nickel Belt Project: aims and objectives; in Manitoba Energy and Mines, Minerals Division, Report of Activities 1997, p. 99-100.

The Thompson Nickel Belt (TNB) extends southwesterly from Moak Lake in northern Manitoba, through the Interlake District, to the Manitoba - North Dakota Border (Fig. GS-12-1). Most of the belt is covered by Phanerozoic sedimentary formations; likewise most of the current knowledge pertaining to the TNB comes from the area situated between Ponton and Thompson (Fig. GS-12-1).

Meetings held in 1996, and involving Manitoba Energy and Mines, industry, the Geological Survey of Canada and representatives from several Canadian Universities, addressed the need for a major, coordinated geoscientific study of the TNB. On June 1, 1997, a new, industry-sponsored, multi-disciplinary investigation of the TNB, including its metallogeny, geology, geochemistry, geochronology and tectonic evolution, was launched. The TNB project is administered by the Exploration Technology Division of the Canadian Minerals Industry Research Organization (CAMIRO; project 97-E02) and is jointly funded by Cominco Ltd., Falconbridge Ltd., Hudson Bay Exploration and Development Ltd., Inco Ltd., Teck Corporation and Western Mining International Limited. Additional funding is provided by the Natural Sciences and Engineering Research Council of Canada. Both Manitoba Energy and Mines (MEM) and the Geological Survey of Canada (GSC) are contributing staff time, fiscal and additional resources to the TNB project. Geoscientists from Manitoba Energy and Mines, the Geological Survey of Canada, the University of Manitoba, Laurentian University, l'Université du Québec à Montréal (UQAM), the University of Alberta and the University of Saskatchewan are involved in the research and will supervise at least 5 graduate research students and post-doctoral fellows.

The TNB project builds on an ongoing CAMIRO investigation into the controls on nickel sulphide ore localization in both the TNB and Falconbridge's Raglan deposit in northern Quebec (CAMIRO project 94-E04). The new TNB project, although much broader in scope, is still focused on the genesis of nickel sulphide ores and the development of new explorations tools.

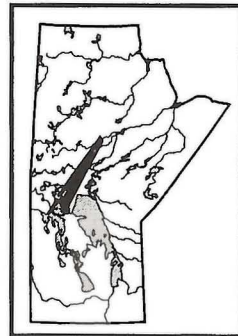
The TNB project will conclude in the year 2000. The project will concentrate on applied research in the following areas: (1) geological mapping, including compilation mapping and new thematic mapping programs; (2) petrological, lithogeochemical and petrogenetic studies of mafic and ultramafic magmatism and of the Ospwagan Group metasedimentary succession; (3) mineralogical and geochemical studies of selected nickel deposits and host rocks; (4) geochronological studies of

the Ospwagan Group metasedimentary rocks and potential Archean and Paleoproterozoic source regions; (5) geochronological studies of mafic dykes in the TNB and the Churchill-Superior boundary zone, in order to constrain the age of mafic and ultramafic magmatism and rifting; (6) integration and modeling of geophysical data; lithologic maps, lithogeochemical and geochronological data and structural information, using geographic information system technology, that will ultimately facilitate the development of a regional tectonic model.

During the current year, MEM staff were involved in several studies related to the TNB project. Work on the 1:50,000 compilation map series for the exposed part of the TNB continued, with efforts focused on the Pipe Mine to Setting Lake area (Macek, GS-13, this volume). McGregor (GS-13, this volume) has documented petrographic characteristics of carefully selected "type" specimens collected from the Ospwagan Group metasedimentary formations in the Thompson area. A subset of these samples will be analysed for a wide range of trace elements in order to characterize the geochemistry of the Ospwagan Group. Several samples will be selected for detrital zircon geochronology (N. Machado, UQAM). Zwanzig (GS-15, this volume) conducted mapping, lithogeochemical and geochronological studies in the Setting Lake area, and has provided new insights into the geology of the western margin of the TNB. Theyer (GS-16, this volume) completed a two year, detailed petrologic study of drill core from the Lake Winnipegosis Komatiite Belt in the Cedar Lake area (Cominco Ltd.) and carried out lithogeochemical sampling of komatiite, basalt and peridotite units. Sampling of mafic and ultramafic rocks present in drill core from the William Lake area (Falconbridge Ltd.), the Thompson area (Inco Ltd.) and the Minago River-Ponton region (Hudson Bay Exploration and Development Co. Ltd.) was completed (M. Burnham, Laurentian University and DCP). Additional sampling of mafic dykes and basalts was completed from outcrops along the Grass River, immediately northeast of Setting Lake, and near Mid Lake (DCP).

ACKNOWLEDGMENTS

M. Pacey is thanked for preparing the figure. The generous support provided by Cominco Ltd., Falconbridge Ltd., Hudson Bay Exploration and Development Ltd., Inco Ltd., Teck Corporation and Western Mining International Limited is gratefully acknowledged.



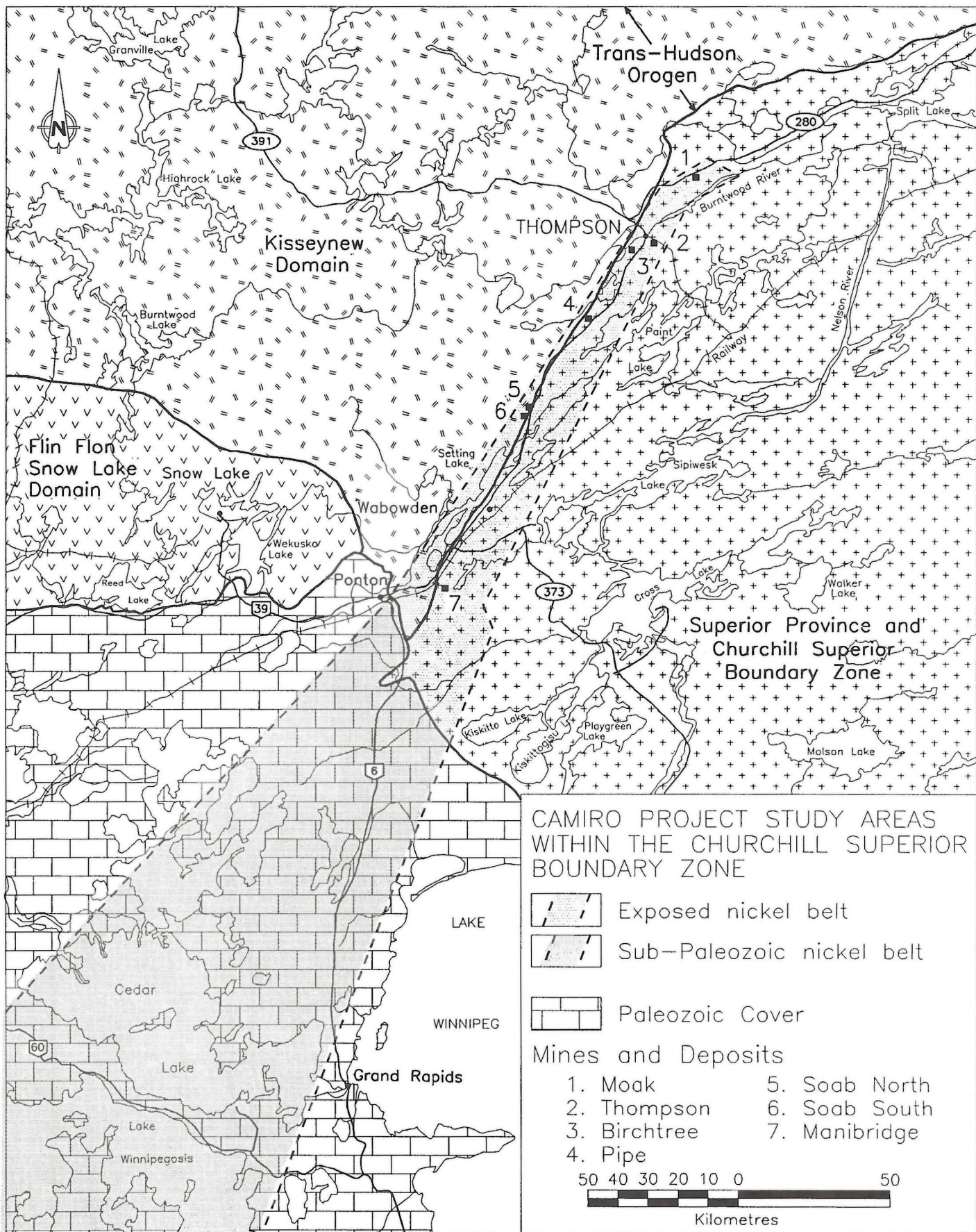


Figure GS-12-1: Location of the Thompson Nickel Belt, Manitoba.

by J. J. Macek

ACKNOWLEDGMENT

During the winter months a lithological map manuscript was completed for area A (Figure GS-13-1).

REFERENCES

Macek, J. J.,

Work on area C is expected to begin next year.



101

GS-14 THOMPSON NICKEL BELT PROJECT: PETROGRAPHIC AND CHEMICAL CHARACTERIZATION OF MAJOR LITHOLOGIES (PARTS OF NTS 63J, 63O AND 63P)

by C. R. McGregor

McGregor, C.R. (1997): Thompson Nickel belt project: petrographic and chemical characterization of major lithologies (parts of NTS 63J, 63O and 63P); in Manitoba Energy and Mines, Minerals Division, Report of Activities, 1997, p. 102.

INTRODUCTION

The most complete lithostratigraphic columns of the Oswegan Group supracrustal rocks were presented in Bleeker and Macek (1988) and Macek and Bleeker (1989). Individual lithological units are characterized by their field names but very little petrographic description is provided. Since then, exploration activity in the Thompson Nickel Belt increased and a more detailed description of the Oswegan Group lithostratigraphy is needed for field geologists as an effective guiding tool in exploration. A petrographic and geochemical program was therefore launched to better characterize all lithological units.

In order to compare the Oswegan Group rocks with reworked Archean gneiss or Kiseynew metasedimentary gneisses, analogous data will also be obtained from the gneisses. In addition, magnetic susceptibility data from all samples will be collected since a number of lithological units display distinct magnetic patterns on a regional scale.

RECENT INVESTIGATION

Laboratory work was focused on systematic mineralogical examination of the Oswegan Group supracrustal rocks. Forty-three modal analyses were completed for the Manasan Formation, 55 for the Thompson Formation and 141 for the Pipe Formation, for a total of 239 analyses.

Over sixty samples of the reworked Archean basement gneisses and migmatites along with a dozen samples from Kiseynew metasedimentary gneisses (Zwanzig, 1997, this volume) were collected

during the field season (Figure GS-14-1). Laboratory work will be conducted on these samples this fall and winter. In addition, precision chemical analyses on 75 samples (selected from the Oswegan Group rocks, reworked Archean basement gneisses and Kiseynew metasedimentary gneisses) are in progress as part of the CAMIRO project (Peck, 1997, this volume).

REFERENCES

- Bleeker, W. and Macek, J. J.
1988: Thompson Nickel Belt project - Pipe Pit Mine (part of 63O/8NE); in Manitoba Energy and Mines, Minerals Division, Report of Field Activities, 1988, p. 111-115.
- Macek, J. J. and Bleeker, W.
1989: Thompson Nickel Belt project - Pipe Pit Mine, Setting and Oswegan Lakes; in Manitoba Energy and Mines, Minerals Division, Report of Field Activities, 1989, p. 73-87.
- Peck, D. C.
1997: Thompson Nickel Belt project - aims and approach; in Manitoba Energy and Mines; Minerals Division, Report of Activities, 1997.
- Zwanzig, H. V.
1997: Revised stratigraphy of the Setting Lake area (parts of NTS 63O/1 and 2, and 63J/15); in Manitoba Energy and Mines, Minerals Division, Report of Activities, 1997.

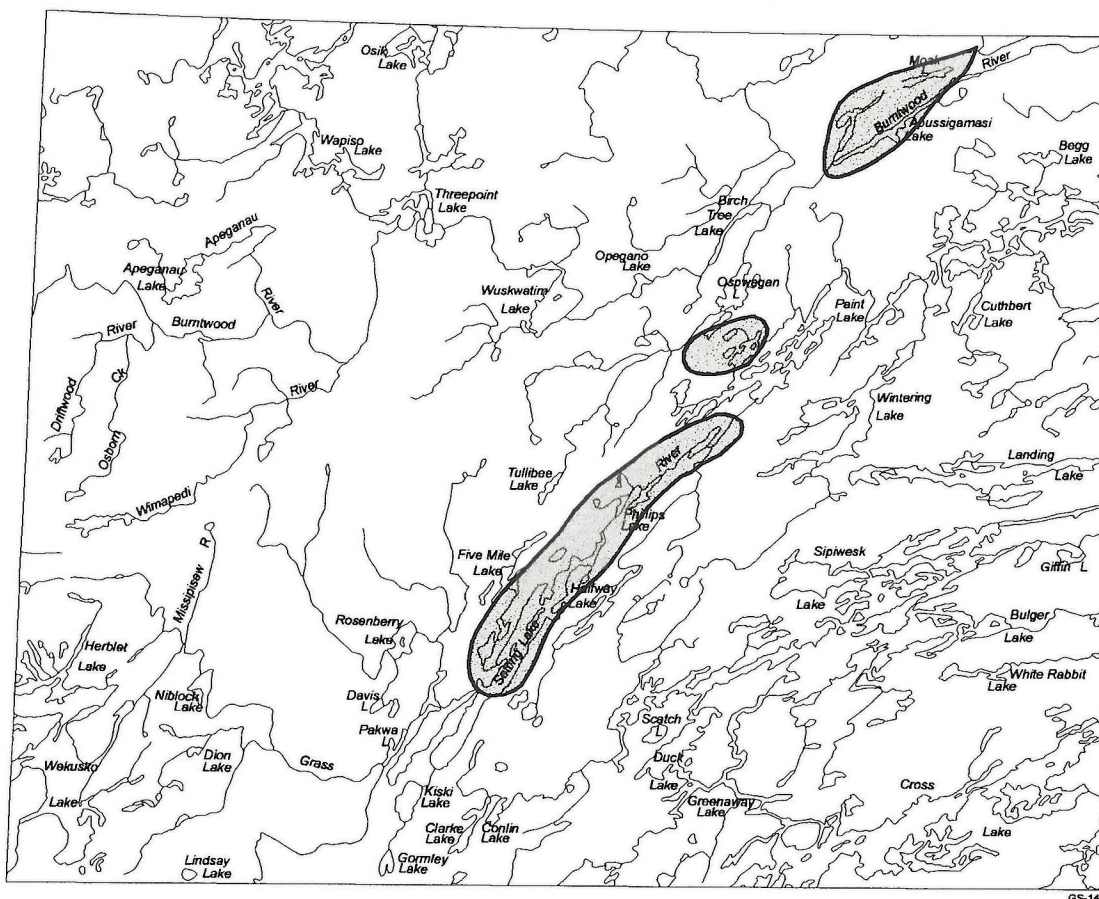
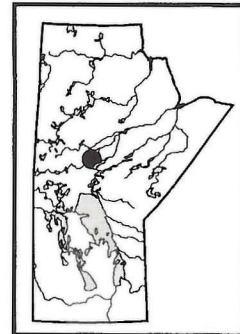


Figure GS-14-1: Sample collection areas.

GS-15 REVISED STRATIGRAPHY OF THE SETTING LAKE AREA (PARTS OF NTS 63O/1 AND 2, AND 63J/15)

by H.V. Zwanzig

Zwanzig, H.V. (1997): Revised stratigraphy of the Setting Lake area (parts of NTS 63O/1, and 2, and 63J/15); in Manitoba Energy and Mines, Minerals Division, Report of Activities, 1997, p. 103-108



SUMMARY

Five weeks of work at Setting Lake represents the first field season of remapping key areas at the boundary between the Kisseynew Gneiss Belt and the Thompson Nickel Belt. Two Paleoproterozoic sedimentary groups, Archean basement gneisses and tonalite gneiss of unknown age occupy separate fault-bounded folds or fault blocks that extend parallel to the lake. Each block is intruded by a different set of Proterozoic dykes or sills. Pegmatites occur in the entire area, and granitic to alkaline plutons in a major fault zone (Setting Lake fault). The emphasis of this year's field work was on structural mapping and defining primary stratigraphic features in the Paleoproterozoic rocks, all of which have been metamorphosed to upper amphibolite facies.

The upper part of the Oswagan Group includes fine grained sedimentary rocks, turbidite deposits, mafic sills and flows that are now traced along the full 45 km length of Setting Lake. Pebbly beds in the turbidite may have an origin in a marine channel. A younger sedimentary sequence (herein called the Grass River Group) is a >800 m thick, upward fining terrestrial deposit. It is defined from its conglomerate base to its arkose top, in as much detail as the high metamorphic grade allows. It was likely deposited in a mountainous (orogenic) environment, in part from flash floods.

INTRODUCTION

The Setting Lake area straddles the boundary between the Thompson Nickel Belt (TNB) to the southeast and the Kisseynew Gneiss Belt (KGB) to the northwest. During previous 1:25 000 scale mapping, Albino and Macek (1981a, b) defined numerous units based on the amphibolite-grade metamorphic petrology and protolith. The units were grouped into four lithostructural assemblages exposed in northeast-trending belts along Setting Lake. The assemblages are:

- S - Archean migmatites of the Superior Structural Province intruded by Proterozoic mafic dykes, reworked during the Hudsonian Orogeny and exposed on the southeast shore,

- O - Paleoproterozoic rocks of the Oswagan Group on islands along the east side,

- C - Paleoproterozoic rocks of the Churchill Structural Province exposed on central islands and along the northwest shore,

- U - Weakly foliated to gneissic intrusive rocks of unknown age.

The age of the Archean rocks has recently been confirmed near Setting Lake, and one of the unknown intrusive units has yielded a Proterozoic preliminary age (Machado pers. comm., 1997). The sedimentary rocks (C) that were suggested to be the youngest in the area and were correlated with the Sickle Group in the KGB (Albino and Macek, 1981c) have not been dated.

Field work was carried out during five weeks this summer to describe in more detail the lithostratigraphy of the Proterozoic rocks and assess their structural relationships. Sampling was conducted for geochronology and geochemistry. The work represents the first field season of remapping key parts of the southeast margin of the KGB and the adjacent parts of the TNB. The work is part of the TNB Project (Peck, GS - 12 this volume) and of a regional map compilation (Macek, this volume). The mapping and this report are focused on the primary depositional features preserved in the metamorphic rocks at Setting Lake. These features will provide the framework for a lithostratigraphic map when the fieldwork is completed. A structural analysis of the area is still in an early stage.

GENERAL GEOLOGY

The grouping of units (above) and the structure described by Albino and Macek (1981a, b, c) are fully consistent with the new mapping; however, the term 'Churchill Province' is no longer in common use. A new informal name, Grass River Group, is proposed here for the young sedimentary rocks (C). The contacts between the groups are faulted, occupied by younger intrusions or unexposed. Regional geology indicates that the

Ospwagan Group, informally introduced by Scoates *et al* (1977), lies unconformably on the Archean basement (Bleeker and Macek, 1988). Evidence exists at Setting Lake that the Grass River Group is the youngest stratigraphic division (below).

The Oswagan Group is now traced for the full 45 km length of the lake, along the islands and reefs that lie scattered over a width of 1 km closest to the Archean rocks on the southeast shore (Fig. GS-15-1). Systematic reversals in topping direction at 10-200 m intervals indicate local isoclinal folding but much of the group faces northwest. The northwest contact is the Setting Lake fault zone, characterized by 10 m of mafic Oswagan Group synmetamorphic tectonite and 10-250 m of epidotized and hematized Grass River Group. Protomylonite, mylonite, brittle faults and pseudotachylite indicate a history of protracted deformation in the zone. A composite lithologic column of the upper Oswagan Group (Fig. GS-15-1) is based on the assumptions that the northwestern part of the section faces northwest and the sedimentary rocks coarsen upward. The stratigraphic thickness is unknown.

The Grass River Group occurs in two parallel belts that also extend the full length of Setting Lake. The southeastern belt, which is in fault contact with the Oswagan Group, is 500 m wide and occupies a fault bounded and internally faulted syncline ('D' in Fig. GS-15-1). The 1000 m width that has been remapped of the northwestern belt is a northwest-topping homocline ('G' in Fig. GS-15-1). This part of the Grass River Group is shown in a stratigraphic column at the present (deformed) thickness (Fig. GS-15-1). An unexposed interval in the lower half of the column is recomposed from the southwestern belt.

The two belts of Grass River Group are separated by gneissic tonalite and granodiorite that occupy an asymmetric antiform with a moderately dipping northwest limb and a sheared, vertical southeast limb (Albino and Macek, 1981c). The structure contains gneissic hornblende-biotite granodiorite surrounded by inclusion-rich and layered orthogneiss derived from hornblende-biotite tonalite, leucotonalite and quartz diorite. The widespread inclusions are interpreted as cognate xenoliths. The layered gneiss is interpreted as highly strained dykes and transposed inclusions at the margin of an intrusive complex. Garnetiferous layers may be screens of metasedimentary rock, but no inclusions of the Grass River Group were observed; (however, see Albino and Macek, 1981a.) The contact between the complex and the Grass River Group is sheared and probably faulted. It is intruded by younger granitoid rocks in the south.

The gneissic tonalite is intruded by thin (~10 cm) dykes of fine grained gabbro to melagabbro. These are generally metamorphosed, and boudinaged parallel to the gneissosity, but are locally cross cutting. The Grass River Group is intruded by a prominent sets of dykes comprising gabbro, melagabbro and hornblende- to feldspar-phyric intermediate to felsic rocks. The dykes locally have chilled margins, cut the bedding at a low angle and are overprinted by the main (relatively late?) foliation. Some dykes are composite. Preliminary geochemical data suggest that the dykes are altered, subalkaline but with Zr:Y ratio >10. The Oswagan Group is intruded by the youngest (leucogranite) plutons in the area. In the southwestern part of the lake, the Setting Lake fault zone is intruded by the young leucogranite, hornblende granite, and a small stock and dykes ranging from alkaline monzogabbro to hornblende syenite ('C' in Fig. GS-15-1).

Hudsonian deformation involved several phases. The systematic reversals in topping on island 'F' (Fig. GS-15-1) may represent the earliest phase (D₁) in the Oswagan Group. Early minor folds (D₂?) at 'F' with a recrystallized axial planar biotite foliation are refolded by originally recumbent D₂ folds with little axial planar fabric. The interference structures and S₁ (?) are refolded by upright northeast-trending D₃ folds with local axial planar S₃ biotite foliation. D₃ probably produced the major and minor folds in the Grass River Group and in early syntectonic granitoid veins. It may have produced the anticline-syncline pair in the gneissic tonalite and

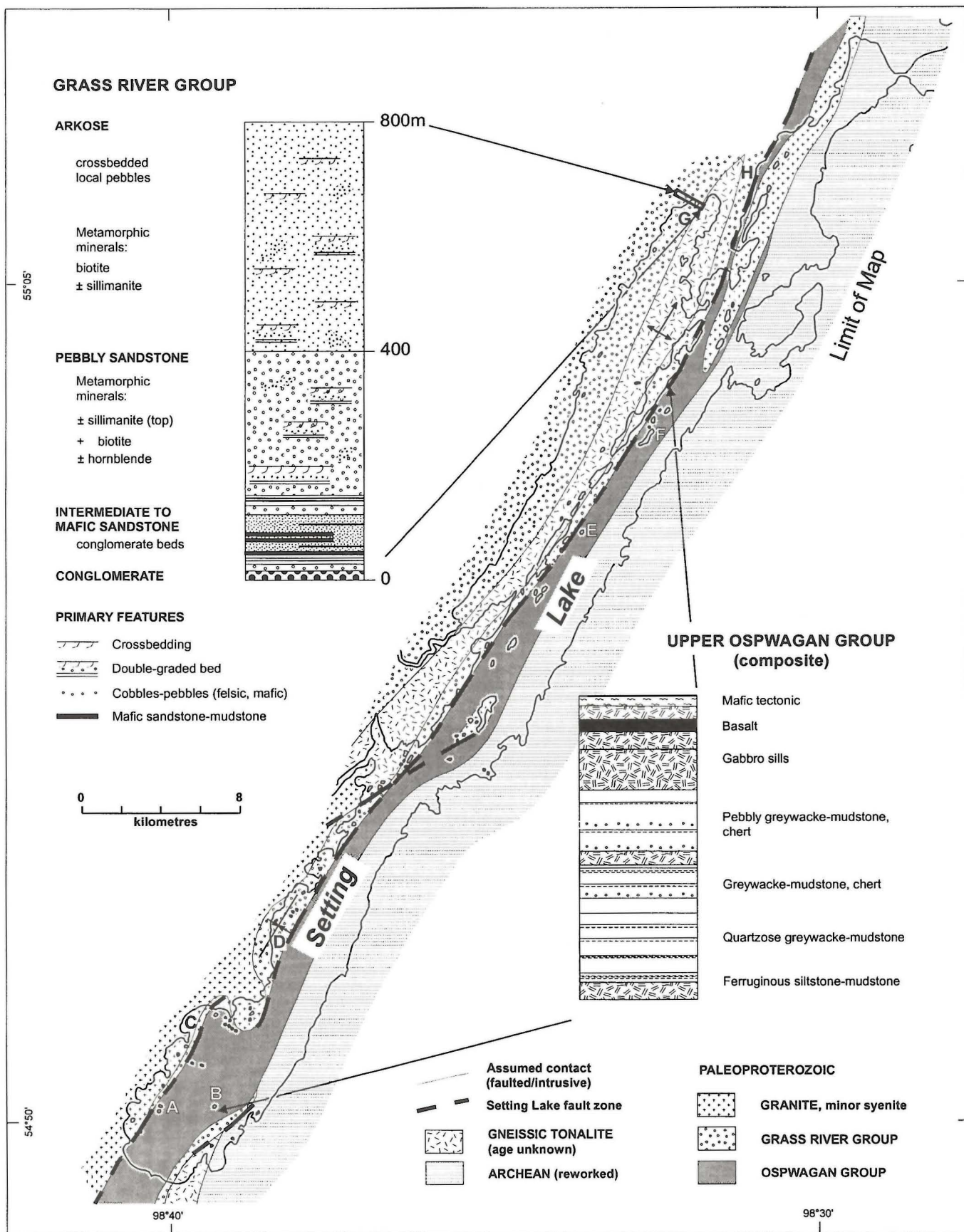


Figure GS-15-1: Simplified geology of the Setting Lake area with a stratigraphic column of the Grass River Group and a composite lithologic column of the Oswagan Group. 'A' to 'H' are locations mentioned in the text.

the Grass River Group to its southeast (Fig. GS-15-1). An important stage of SE-side-up sinistral slip with numerous kinematic indicators in the Setting Lake fault zone may also be D_3 , NE- to E-trending brittle faults and shear zones with dextral and predominantly SE-side-up slip cut the youngest intrusions and may represent D_4 .

Hudsonian metamorphism was upper amphibolite grade as indicated by sillimanite, and locally, incipient leucosome patches in the Grass River Group and gneissic granodiorite. Garnet porphyroblasts accompany some of these patches and early shear zones in the orthogneiss. Two phases of metamorphism are suggested by <3 mm long hornblende with a strong, steeply dipping lineation parallel to D_3 slip, overgrown by hornblende (<15 mm) with random to planar orientation. Hudsonian metamorphism is also indicated by hornblende crystallization in Proterozoic dykes and the enclosing Archean migmatite.

ARCHEAN MIGMATITE

The basement gneisses have complex petrography and structure that have not been revised from Albino and Macek (1981a, b). Where examined, the grey to pink gneiss blends in with early cream colored leucosome. This migmatite is cut by Proterozoic mafic dykes, and granitic or pegmatitic dykes and veins. A biotite-hornblende foliation overprints the migmatite and mafic dykes, and defines a protomylonite fabric in the granite. In some units of agmatite the proportion of Proterozoic granitoid material exceeds that of the Archean gneiss.

OSPWAGAN GROUP

Exposures with folding and faulting of the Oswagan Group on isolated islands do not allow a precise stratigraphic sequence to be defined on Setting Lake. Regionally there is a lower, fine grained sedimentary

succession, and an upper, quartzose greywacke and mafic volcanic succession as suggested in a reconstructed lithostratigraphic column (Macek and Bleeker, 1989). At Setting Lake there is amphibole- to biotite-rich pelite on the east side of several islands, but coarse grained quartzose greywacke and mafic igneous rocks predominate in the northwest. The siliciclastic rocks are turbidites that retain primary structures.

Biotite schist, amphibolite (siltstone, mudstone)

Thinly layered (<6 cm) amphibolite derived from mudstone forms the lower part (>7 m) of an upward coarsening >40 m succession of quartzose greywacke and pelite on the island at 'A' (Fig. GS-15-1). About 10 m of dark grey- to brown-weathering siltstone, or mudstone with abundant metamorphic biotite are part of a similar but highly folded succession at 'B'. At the southeastern point on island 'F' bedded (2-10 cm) and laminated pelite with 30% biotite is interlayered with greywacke at a ratio of 7:1.

Coarse grained metaturbidite

The remaining clastic rocks in the Oswagan Group form ~50 m thick upward fining and upward coarsening turbidite sequences with beds (2-200 cm) that locally grade from deformed conglomerate (with <5 cm clasts) to pelite and quartzite derived from mudstone and chert. Conglomerate:greywacke:mudstone ratios vary between 2:10:1, 0:50:1 and 0:5:1. The finer grained sequences are quartz rich, weather light grey and predominate in the southern half of the lake (Fig. GS-15-2). They commonly contain quartz-sillimanite knots (faserkiesel) in the upper part of the beds. Conglomerate bed divisions occur northeast of 'E' and grade into medium grey hornblende-bearing intermediate compositions, presumably derived from lithic wacke (Fig. GS-15-3). Identifiable clasts comprise sandstone and chert. Upper bed divisions are dark grey to brown and range from biotite- and hornblende-rich in the north to biotite-garnet-rich in the south.

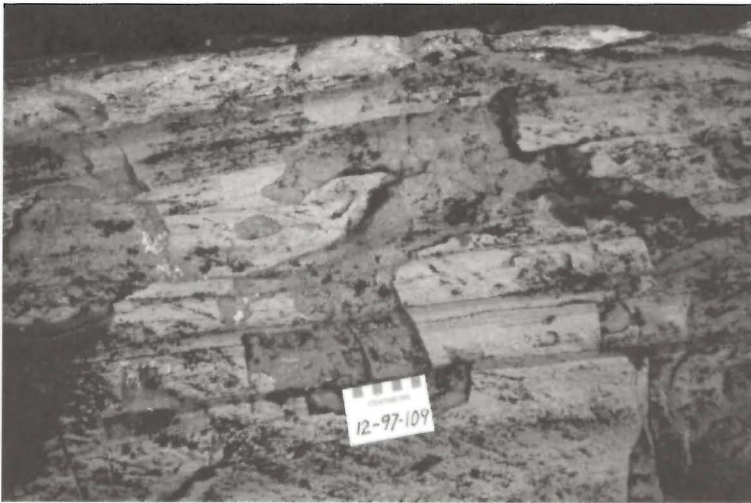
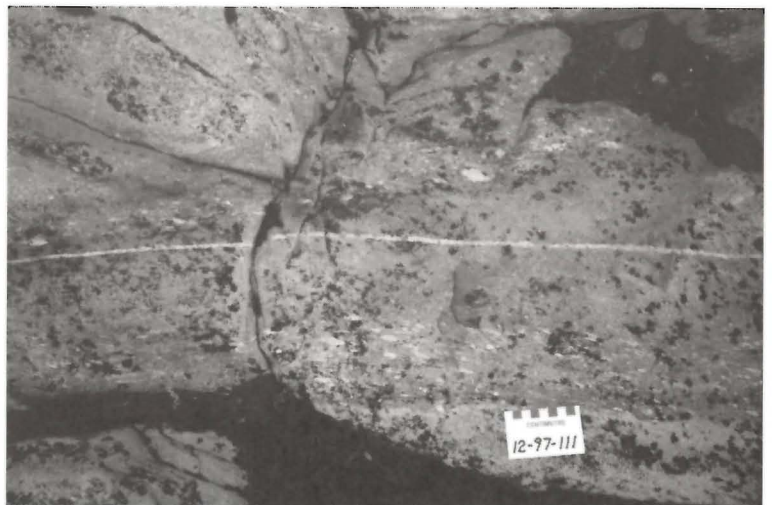


Figure GS-15-2: Oswagan Group, thin turbidite beds, with massive and graded divisions of quartz-rich, fine grained greywacke (light grey) to pelite (dark grey) from the top of a 40 m thick upward fining succession.

Figure GS-15-3: Coarse grained Oswagan Group turbidite beds with coarse-tail grading from pebbly to sandy. Pebbles comprise fine grained quartzose sedimentary rocks.



Amphibolite (gabbro and basalt)

The turbidites are overlain by dark grey-green and green amphibolite derived from gabbro sills, basalt and komatiitic basalt. Similar gabbro occurs on islands to the southeast and suggests that the lower part of the sedimentary sequence was also intruded by sills.

Recognizable pillowed and massive flows are exposed only over a stratigraphic thickness of 5-10 m on four outcrops with northwest topping recognized on three of these. Pillows are up to 3 m long and 50 cm wide. Altered rock between pillows is interpreted as hyaloclastite. One differentiated flow is 3 m thick with 70 cm of breccia at the top, overlain by 30 cm of chert. The komatiitic basalt is recrystallized to uniform fine grained amphibolite with little visible plagioclase.

Generally >90% of the mafic section is interpreted as gabbro sills (<50 m thick). Differentiated sills have a dark green to brown weathering coarse grained (<10mm) base with <15% plagioclase. The tops are grey with 60% plagioclase. The sills are interpreted as a subvolcanic part of the Ospwagan Group. They have chilled contacts and feature the same range of compositions and direction of topping as the flows.

GRASS RIVER GROUP

Various clastic lithologies are commonly interbedded in the Grass River Group but informal units are defined by the dominant clast size, and composition determined from metamorphic assemblages. The type section is the north shore of the northwest arm of Setting Lake (G in Fig. GS-15-1). Subsidiary southern and eastern sections are 8-10 km northeast of the south end of the lake and 9-10.5 km north of Setting Lake Wayside Campground (E and F). The main section, which is ~800 m thick, tops to the northwest and dips at 45-75°. Flattened pebbles suggest that the section was more than 1600 m thick before deformation. The upper half of the

group tops consistently northwest as seen in crossbedded arkose, whereas the lower half of the group lacks sedimentary tops but grades from an intermediate composition conglomerate into the arkose. The entire main section is therefore considered to face northwest, whereas the subsidiary sections are interpreted to be in a syncline.

Deformed conglomerate

The lowest unit of the Grass River Group is a deformed, polymictic, boulder to cobble conglomerate, exposed in the north for a thickness of 5-10 m. The unit is repeated several times by interbedding, folding or faulting in the southern section (D in Fig. GS-15-1). Flattened clasts in the conglomerate are up to 60 cm long, comprise mainly grey sandstone, and subequal proportions of basalt and pale grey to yellowish chert (Fig. GS-15-4). Dark grey feldspar porphyry and pink quartzofeldspathic rock that may be altered granodiorite are minor components. Some of the chert clasts are ferruginous and contain small magnetite porphyroblasts. Gabbro and melagabbro clasts, compositionally similar to the basalt clasts, increase in abundance towards the south end of the lake. The intrusive clasts are well rounded to subangular, whereas basalt and chert are tabular.

On a small island near 'E' (Fig. GS-15-1) the conglomerate overlies Ospwagan Group gabbro sills. This contact may be an unconformity, faulted or intrusive (Fig. GS-15-5). What may be the lowest bed in the Grass River Group comprises 1.5 m of granodiorite boulders (<55 cm) and smaller clasts of basalt and quartz (chert?) in a mafic to intermediate matrix. The overlying conglomerate has thick beds, with <30 cm clasts, alternating with thinner sandstone beds. The unit is overlain by para-amphibolite and pebbly sandstone. Elsewhere on Setting Lake the interlayered unit commonly has <1 m conglomerate beds intercalated with <20 cm sandstone beds that make up about 30% of the sequence.

Figure GS-15-4: Grass River Group, main conglomerate unit, with chert clasts (white to light grey) and basalt clasts (black) in subequal proportion. Abundant sandstone clasts are similar to the intermediate-composition matrix and blend in with it.



Figure GS-15-5: Granodiorite cobbles at the probable base of the Grass River Group conglomerate in a dark matrix that consists largely of flattened mafic clasts. The lower contact is with a mafic dyke (dark grey with a black margin) and may be faulted, intrusive or unconformable.

At 'D' 15 m of conglomerate is assumed to be in the southeast-facing limb of the syncline containing the eastern section. The unit has a sheared contact with gneissic granodiorite. The highly flattened clasts include light grey sandstone, white to grey quartz/chert and various types of pink granitoids. The matrix is dark, so that mafic clasts cannot be distinguished within it.

Intermediate to mafic rocks (sandstone and conglomerate)

Conglomerate is overlain in the main section by 5m of grey-green pebbly sandstone with <15 mm hornblende porphyroblasts. About 17 m of grey, laminated metasedimentary rock with fine hornblende (~8%) and biotite (~6%) grade upward into para-amphibolite. These or similar units are repeated by interbedding or faulting 150 m higher in the section. Similar units also occur above the conglomerates in the southern section. In the northeast ('H' in Fig. GS-15-1) 5 m of mafic cobble to pebble conglomerate overlies the main conglomerate. Clasts are dominated by basalt, gabbro and sandstone with only scattered chert.

Pebbly metasandstone

Medium to light grey sandstone overlies the northern conglomeratic section for a thickness of 250 m. The rock contains metamorphic biotite \pm hornblende, and local sillimanite at the top of the section. It is generally crossbedded, contains pebbles or both. Beds are 5-80 cm thick; some contain parallel biotite-rich partings or magnetite placers. Clasts and shaly rip-ups, up to 15 cm long, occur widely scattered in sorted sandstone, in clusters or pebble pavements. Green and pink layers and lenses of calc-silicate rock (<15 cm thick), interpreted to be derived from carbonate cement and concretions, locally constitute about 3% of the sandstone.

Interbeds (<1 m) of conglomerate occur mainly in the southern section. Beds commonly have normal and reverse grading. Lag deposits and truncations of foreset bedding suggest northwest tops in the lower part of the southern section (Fig. GS-15-6). Pebbles include sandstone, quartz/chert, pink to yellow fine grained granite/rhyolite and tonalite.

Quartzofeldspathic sillimanite-bearing rock (crossbedded arkose)

Light- to medium-grey weathering arkose sandstone makes up the upper 500 m of the northern section and 250 m of the mainly southeast topping part of the southern section. The metamorphic minerals in the unit are characterized by 4-30 mm long white or grey quartz-sillimanite knots (faserkiesel) that are concentrated in certain beds. Calc-silicate layers (<20 cm thick) locally make up 5% of the rock. The unit is commonly crossbedded, with a maximum amplitude of 15 cm, planar in the northern section, festoon crossbeds locally in the south. Massive beds and rare pebbly beds are generally less than 30 cm thick, but locally up to 2 m. The clasts (<10 cm), which are predominantly quartz, sandstone and fine grained felsic igneous rocks, are scattered within arkose beds or occur in clusters.

IMPLICATIONS FOR TECTONIC ENVIRONMENTS

The upper Oswagan Group at Setting Lake is a marine succession of fine grained clastic rocks to coarse grained turbidite. It was probably deposited in an extensional tectonic setting, coeval with high-MgO basaltic magmatism that produced abundant sills within the thick sedimentary cover. Pyritic mudstone intruded by gabbro is a local host of minor iron sulfide. The persistent mudstone, pelite and chert in the pelagic top of the beds suggest open marine conditions. Subangular, chert and sandstone clasts were provided by reworking a marine deposit within the depositional basin or at its margin. The accumulation of such pebbles in thick turbidite beds represents deposition in an upper fan or marine channel. Such units have little lateral continuity except along the channel or fan axis and thus only have local stratigraphic implications.

The newly named Grass River Group is interpreted to be a terrestrial deposit produced in part by flash floods. Single flood-stage units were in the order of 1 or 2 m thick. Where fully intact, they have a planar laminated base, representing a high flow regime, grading into massive sandstone, often with scattered pebbles. Lag deposits form the base of some beds. The overlying 5-50 cm thick crossbedded sandstone may represent reworking in a lower flow regime during the waning stage (Fig. GS-15-7). Shale drapes produced during ponding were ripped up in the next flood. Conglomerate beds are massive or double-graded (reverse and normal), consistent with deposition from flash floods. The coarse, angular to well rounded clasts suggest deposition in an intramountain (orogenic) environment.

Questions arise whether some of the clasts in the Grass River Group (basalt, gabbro and chert) were eroded from the uppermost part of the Oswagan Group or another deep marine deposit. The mafic conglomerate and mudstone in the Grass River Group are consistent with the subaerial erosion of oceanic crust (ophiolite), and this will be tested using geochemistry. Granitoid rocks and sandstone were clearly also eroded in a subaerial environment. The greater abundance of felsic clasts on the west side of the syncline that contains the eastern succession (Fig. GS-15-1), and in the upper half of the Grass River Group, suggests increasing erosion of a felsic igneous and sedimentary highland. The origin of such a highland and its relationship to possible ophiolite, exposed at that time, are other intriguing questions.

Further mapping and a U-Pb zircon study of detrital grains, boulders in conglomerate, mafic to felsic dykes, gneissic tonalite and younger granitoid to alkaline intrusions (N. Machado, in the planning stage) should help to determine the tectonic significance of the Grass River Group, the Setting Lake fault zone, as well as the nature and more exact location of the northwestern boundary of the TNB; (see also Böhm, this volume).

Figure GS-15-6: Grass River Group, the top of the conglomerate unit has an interbed of nearly mafic, parallel laminated sandstone overlain by a conglomerate bed with foreset layers. The foresets slope down to the south (left) and are truncated at the top by an intermediate-composition sandstone bed. The deposit probably formed at a point bar.



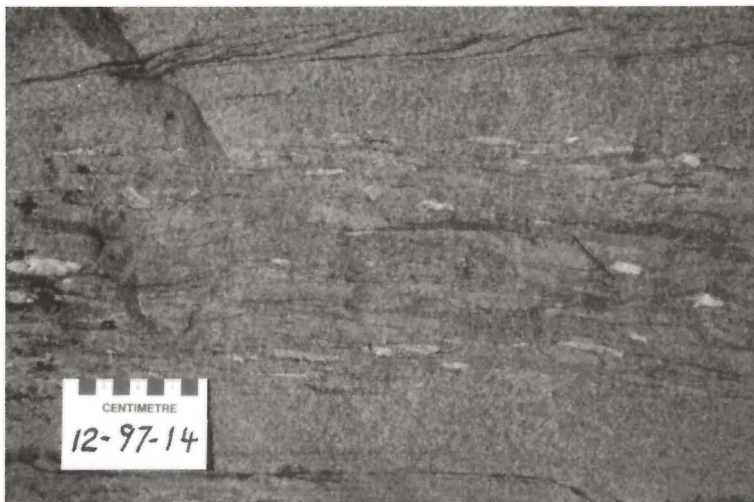


Figure GS-15-7: Grass River Group, composite pebbly sandstone bed is interpreted as a flash flood deposit with (1) a parallel laminated base (below card), (2) a coarse-tail double-graded center with pebbles and shale rip-ups (dark), and (3) a crosslaminated top.

ACKNOWLEDGEMENTS

I thank Brian Skanderbeg for his outstanding assistance in the field and acknowledge his role in making geological observations. I also enjoyed the participation of Nuno Machado of Geotop (Université de Québec à Montréal). I thank Josef Macek for helping to arrange the start of this project and for his encouraging and critical comments. We have the benefit of collaboration with Inco Ltd. Falconbridge Inc. was exceptionally generous in providing us with free accommodation in the field.

REFERENCES

Albino, K.C. and Macek, J.J.

- 1981a: Setting Lake, northeast (63O/1,2); Manitoba Energy and Mines, Mineral Resources Division, Preliminary Map 1981 T-1, 1:25 000 scale.

- 1981b: Setting Lake, southwest (63J/15); Manitoba Energy and Mines, Mineral Resources Division, Preliminary Map 1981 T-2, 1:25 000 scale.

- 1981c: Thompson Nickel Belt Project - Setting Lake; in Manitoba Energy and Mines, Mineral Resources Division, Report of Field Activities, 1981, p. 30-36. Bleeker, W. and Macek, J.J.

- 1988: Thompson nickel belt project - Pipe Pit Mine (part of 63-O/8NE; in Manitoba Energy and Mines, Minerals Division, Report of Field Activities, 1988, p. 111-115.

Macek, J.J. and Bleeker, W.

- 1989: Thompson nickel belt project - Pipe Pit Mine, Setting and Oswagan Lakes; in Manitoba Energy and Mines, Minerals Division, Report of Field Activities, 1989, p. 73-90.

Scoates, R.F.J., Macek, J.J. and Russell, J.K.

- 1977: Thompson Nickel project; in Manitoba Department of Mines Resources and Environmental Management, Mineral Resources Division, Report of Field Activities 1977, p. 47-54.

GS-16 STRATIGRAPHY AND LITHOLOGIES OF SELECTED DRILL CORE FROM THE LAKE WINNIPEGOSIS KOMATIITE BELT (PARTS OF NTS 63B, 63C AND 63G)

by P. Theyer

Theyer, P. (1997): Stratigraphy and lithologies of selected drill core from the Lake Winnipegosis Komatiite Belt (Parts of 63B, 63C and 63G); in Manitoba Energy and Mines, Minerals Division, Report of Activities, 1997, p. 109-111.

SUMMARY

Investigations of the lithostratigraphy and petrography of six drillholes, followed by detailed geochemical investigations, will provide constraints on the origin, nature and depositional regime of the ultramafic rocks in the Lake Winnipegosis Komatiite belt. Exploration for Ni-Cu deposits in this environment will benefit from this enhanced database.

INTRODUCTION

The core from six drillholes drilled by Cominco Ltd. at their Rabbit Point property were investigated. Cominco's Rabbit Point property extends from Cedar Lake in the northeast to Swan Lake in the southwest including part of the sub-Paleozoic southern extension of the Thompson Nickel Belt (Fig. GS-16-1).

This project is the continuation of a core logging program initiated in the previous year (Theyer, 1996) enhanced with complementary

lithogeochemical sampling. Since June 1, 1997 this project has been part of a major industry-sponsored, multidisciplinary investigation of the Thompson Nickel Belt (Peck, GS-12, this volume). This year's work involved logging and geochemical sampling of several closely spaced drillholes in an effort to possibly recognize regional stratigraphic and geochemical trends.

STRATIGRAPHY

In the logs to follow, primary mineralogy is presented where deduced from relict mineral textures. Primary mineral compositions are rarely preserved in the investigated core.

Drillhole RP 4 is 526.4 m long and intersects an approximately 285 m wide (uncorrected core length) sheared amphibole-chlorite-plagioclase rock sequence interlayered with several pyrrhotite- and pyrite-bearing argillite sequences.

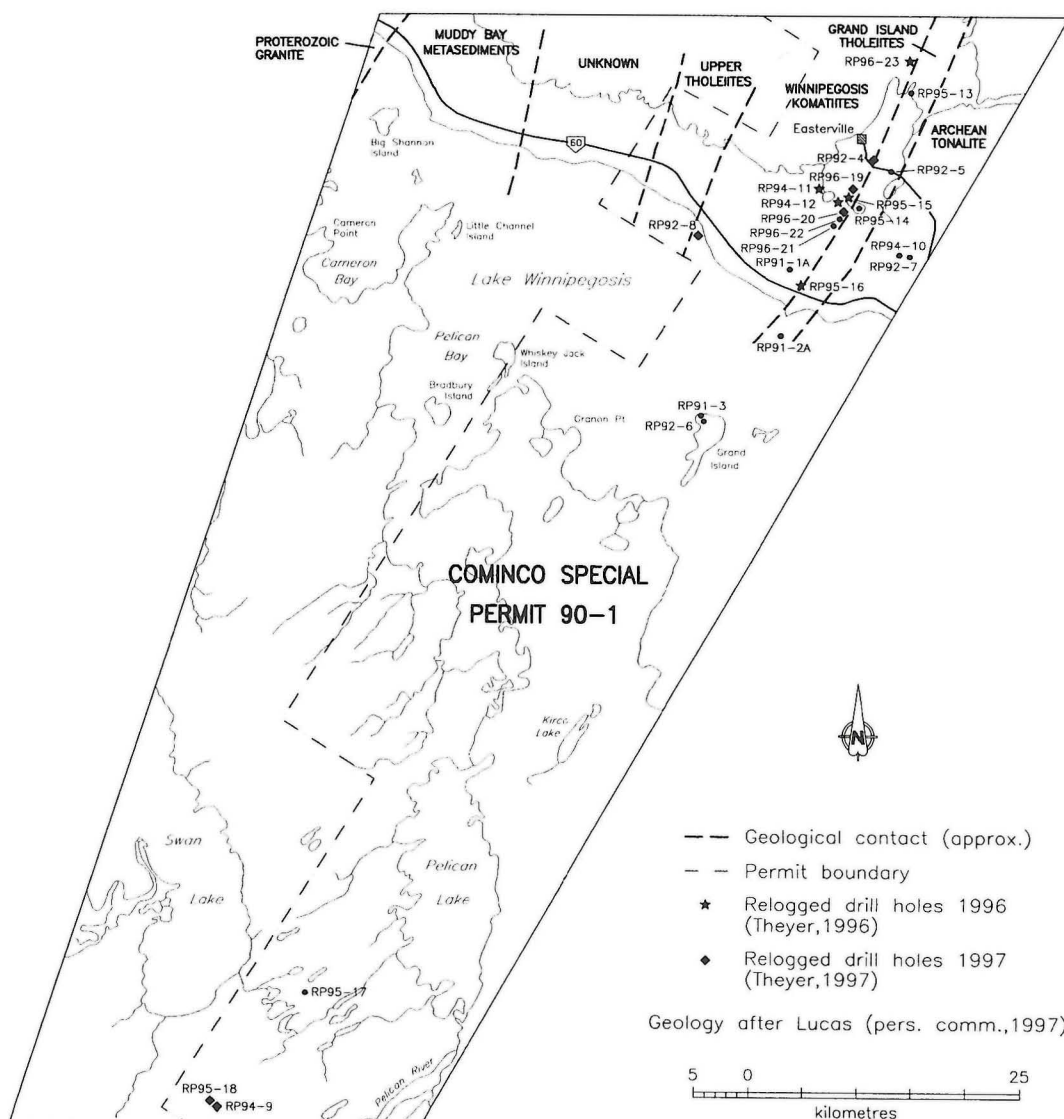


Figure GS-16-1: Location and geology of the Churchill-Superior boundary zone, Cominco Ltd. Special Permit 90-1 and of the drill holes investigated in 1996 and 1997.

From (m)	to (m)	Lithologies (Data above the regolith by Cominco LTD, from and below the regolith by the author).
0	12.19	Overburden
12.19	216.8	Paleozoic dolomite and shale
216.8	233.0	Winnipeg Sandstone
233.0	236.45	Regolith
236.5	277.2	Sheared fine grained plagioclase-amphibole-chlorite rock (basalt protolith)
277.2	82.07	Fine- to coarse-grained gabbro
482.07	492.5	Argillite with cm-thick sulphide layers containing up to 15% pyrrhotite.
492.5	526.4	Chloritized plagioclase-amphibole schist (basalt protolith)

Drillhole RP 8 is 569.1 m long and intersects an approximately 313.8 m wide (uncorrected core length) weakly differentiated gabbroic rock characterized by olivine, pyroxene and feldspar in varying proportions. Sulphides consist of up to 3% pyrrhotite and sporadic minor pyrite, predominantly concentrated in fractures.

From (m)	to (m)	Lithologies (Data above the regolith by Cominco Ltd; from and below the regolith by the author).
0	33.5	Overburden
33.5	238	Dolomite
238	254.4	Regolith
254.4	569.0	Plagioclase-pyroxene rock plus varying amounts of olivine.

Fractures are sporadically the site of black alteration comprising chlorite and magnetite. These zones could be misinterpreted as argillaceous sediment layers between individual flows. Drillhole RP 9 is 812.9 m long and intersects an approximately 125 m wide (uncorrected core length) sheared quartz-plagioclase-chlorite unit interpreted to be massive basaltic flows. Sulphides consist of trace pyrrhotite occurring predominantly in fractures.

From (m)	to (m)	Lithologies (Data above 617.6 m by Cominco Ltd; from and below 617.6 m by the author).
0	40.25	Overburden
40.25	47.10	Mesozoic clay
47.10	185.28	Silurian limestone
185.28	441.85	Ordovician limestone
441.85	472.95	Winnipeg Formation
472.95	485.10	Regolith
485.1	567.1	Argillite
567.1	567.8	Silicate facies iron formation
567.8	617.6	Argillaceous volcanoclastic rocks
617.6	812.9	Sheared and folded quartz-plagioclase chlorite schist with trace to minor pyrrhotite

Drillhole RP 18 is 884.14 m long and intersects an approximately 334 m wide (uncorrected core length) ultramafic to mafic rock sequence including gabbro, pyroxenite and peridotite.

From (m)	to (m)	Lithologies (Data above 522.85 m by Cominco Ltd; below 522.85 m by the author).
0	72.0	Overburden
72.0	464.2	Dolomite
464.2	495.15	Winnipeg Formation
495.15	522.85	Regolith
522.85	598.9	Medium- to coarse-grained gabbro
598.9	829.3	Peridotite
829.3	884.14	Dolomite and argillaceous dolomite

Drillhole RP 19 is 509.0 m long and intersects an approximately 200 m wide (uncorrected core length) ultramafic rock sequence including peridotite, pyroxenite and spinifex-textured layers.

From (m)	to (m)	Lithologies (Data above 236.2 m by Cominco LTD; below 236.2 m by the author).
0	14.5	Overburden
14.5	219.7	Limestone, dolomite and sandstone
219.7	235.5	Winnipeg Formation
235.5	236.2	Regolith
236.2	248.6	Pyroxene adcumulate
248.6	278.4	Pyroxenite with several spinifex textured layers
278.4	315.0	Peridotite and pyroxenite
315.0	456.5	Peridotite, pyroxenite, sulphide-bearing argillites and spinifex layers
456.5	463.5	Polymictic dolomite and limestone breccia
463.5	509.0	Dolomite

Drillhole RP 20 is 443.0 m long and intersects an approximately 89.5 m wide (uncorrected core length) ultramafic rock sequence including pyroxenite and spinifex textured layers concentrated in the lower parts of the drillhole.

From (m)	to (m)	Lithologies (Data above 522.85 m by Cominco LTD; below 522.85 m by the author).
0	32.0	Overburden
32.0	237.7	Paleozoic Dolomite
237.7	254.1	Winnipeg Formation
254.1	313.6	Pyroxenite
313.6	343.6	Peridotite plus abundant spinifex textured ultramafic rock layers.

ACKNOWLEDGEMENTS

M. Pacey is thanked for preparing the figure. Cominco Ltd is gratefully acknowledged for providing access to the drill core and relevant data.

Reference

REFERENCES

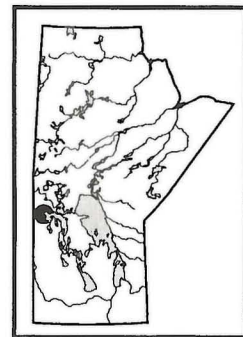
Theyer, P.

- 1996: Stratigraphy and lithologies of selected drill core from the sub-Paleozoic portion of the Thompson Nickel belt (parts of 63B, 63C and 63G); in Manitoba Energy and Mines, Minerals Division, Report of Activities, 1996, p. 91-92.

GS-17 GEOLOGY, GEOCHEMISTRY AND GEOPHYSICS OF PRAIRIE-TYPE MICRODISSEMINATED MINERALIZATION IN WEST CENTRAL MANITOBA (NTS 63C)

by J.D. Bamburak, R.K. Bezys, M.A.F. Fedikow and I. Hosain

Bamburak, J.D., Bezys, R.K., Fedikow M.A.F. and Hosain I. (1997): Geology, geochemistry and geophysics of Prairie-type microdisseminated mineralization in west central Manitoba (NTS 63C); in Manitoba Energy and Mines, Minerals Division, Report of Activities, 1997, p.112-117.



SUMMARY

Regional outcrop mapping and sampling of Devonian and Cretaceous strata in NTS 63C were carried out in support of further investigation of Prairie-type microdisseminated mineralization in the vicinity of the Mafeking quarries, which begun in 1996. The program was augmented by geochemical and geophysical surveys; brine spring, B-horizon soil, and stream sampling; and core hole drilling.

The Point Wilkins Member of the Devonian Souris River Formation contains solution chimneys that act as conduits for brines, which selectively altered a more permeable limestone unit. The resulting oxidized Dolomitic Limestone Beds and adjacent chimneys that are mineralized with siderite-altered carbonate rind and cobble-sized silica-rich sinters, indicate substantial quantities of fluid movement that may have carried base and precious metals in solution.

Black anoxic muds sampled from modern brine springs, contain trace Au, Pt and Pd, and may indicate that the Prairie-type model is still actively precipitating metals in west central Manitoba. In an attempt to detect buried metal occurrences B-horizon soils in the vicinity of the Mafeking quarries were sampled and will be analyzed by enzyme leach techniques. EM31 and VLF-16 have been completed in an effort to detect the presence of conductive material within solution chimneys in limestone. It is also hypothesized that upward movement of metal-enriched brines into overlying Cretaceous black shales may have resulted in precipitation of base and precious metals. Stream sediment and outcrop sampling were carried out to determine where mineralized shales may occur in the Porcupine Hills.

INTRODUCTION

Phanerozoic rocks in the Manitoba portion Western Canada Sedimentary Basin (WCSB) have primarily been viewed as hosts for oil and gas and industrial minerals. Sporadic attempts have been initiated, and to some degree maintained, towards the exploration for Pb-Zn deposits. Formation waters and organic-rich precipitates from Manitoba's brine springs were sampled by Stephenson (1973) for Pb-Zn. It is worth noting that Pb and Zn mineralization have been discovered in significant quantities at Pine Point (Devonian) within the WCSB. In addition, recent studies of potential base and precious metal source rocks within the WCSB have identified Ordovician metal-rich black shales at Black Island (Lake Winnipeg) (Fedikow *et al.* 1995).

PRESENT STUDY

In 1996, a detailed study of the Mafeking quarries in west central Manitoba was carried out (Fedikow *et al.*, 1996). As a result of this investigation, further analysis of the Mafeking quarries and the surrounding area was conducted in the summer of 1997.

Detailed sample collection of the Devonian Dolomitic Limestone Beds (Souris River Formation) within the Mafeking quarries and surrounding area was conducted. As well, regional outcrop mapping in NTS 63C (1:5000 and 1:50 000) was completed (Bezys *et al.*, 1997a, 1997b). The mapping program was augmented by geochemical surveys of brine spring sediments, B-horizon soils, stream sediment samples, and sampling of the black shales. Stratigraphic core hole drilling and electromagnetic geophysical surveys were also carried out.

Results from this study will be presented as a detailed report on the geology, geochemistry and geophysics of Prairie-type microdisseminated mineralization in west central Manitoba, in early 1998.

GEOLOGY

The outcropping portion of the Manitoba Devonian sequence comprises a series of complex carbonate-evaporite cycles, although within the outcrop area the evaporites have subsequently been dissolved from the outcrop area (Fig. GS-17-1). The western half of the study area, the

Porcupine Hills, consists of Cretaceous sediments.

The primary unit of interest is the Devonian Souris River Formation, which consists of the Point Wilkins Member overlain by the Sagemace Member (not present in the study area). The Point Wilkins Member consists of four rock types, in ascending stratigraphic sequence: a red and green calcareous shale (First Red Beds); fossiliferous, argillaceous limestone (Argillaceous Limestone Beds-ALB); dense, micritic and fragmental fossiliferous limestone (Micritic Limestone Beds-MLB); and a yellowish brown, finely crystalline dolomite and dolomitic limestone (Dolomitic Limestone Beds-DLB).

The bedrock in the Mafeking quarries consists of a buff coloured, mottled micritic and fossiliferous limestone that has been quarried for high-Ca limestone (MLB). These beds are overlain by a strongly oxidized, rusty red to brown, altered fossiliferous dolomitic limestone (DLB). These units vary in thickness in the north quarry from 5-10 m and 1-5 m, respectively. The oxidized nature of the DLB may be attributed to lateral fluid flow from the solution chimneys (described below) through the more permeable and oxidized unit.

In total, 163 Devonian outcrop stations were visited in the study area, excluding the Mafeking quarries. This was augmented by a drilling program, which consisted of eleven short stratigraphic core holes (see Bezys and Bamburak, GS-19, this volume). As well, the Mafeking quarries were re-mapped and are presented as Preliminary Maps 1997P-1 and 1997P-2.

SOLUTION CHIMNEYS

The Au and base metal-enriched nature of features that were to be known as "solution chimneys" in the Mafeking quarries was first recognized on a Geological Association of Canada/Mineralogical Association of Canada field trip in May 1996. Subsequent identification of the features by scanning electron microscope evaluation of samples at the Geological Survey of Canada - Calgary, established the presence of a diverse suite of native metals, including Au, base metal alloys and compounds (Fedikow *et al.*, 1996). In addition to the metals, the presence of compounds such as KCl and NaCl indicated a probable brine origin for the metals and associated compounds and heralded the documentation of a new deposit type in Manitoba, the "Prairie-type".

The solution chimneys are primarily developed within the relatively unoxidized high-Ca limestone unit (MLB) in the Mafeking quarries, although good examples of these features have been documented within the overlying oxidized member (DLB). They are recognized individually or in clusters as inverted, conical-shaped features, with a 1-8 cm thick siderite-rich rind that mantles the carbonates of both units. The solution chimneys have maximum observed dimensions of 10-25 m in width and 10 m in height, although it should be noted that the lower 10 m of the quarry is flooded. In cross section, the solution chimneys exhibit a relatively consistent lithologic progression from an outer siderite-altered carbonate rind to greenish clay infill with inclusions of elongate, cobble-sized silica-rich sinters near the rind-clay interface. Recent micropaleontological work on this material indicates a Late Devonian age based on the conodont assemblage (McCracken, 1996). The clay is probably the argillaceous residue remaining from the dissolution of Devonian limestone - a decalcified limestone. Solution chimney cores are often filled with a grey-white sand (locally with minor clay) that looks similar to the Cretaceous Swan River Formation.

OXIDIZED DOLOMITIC LIMESTONE BEDS

A gradational change from strongly oxidized reddish-brown dolomite to buff unoxidized dolomitic limestone within the DLB, occurs with distance from the solution chimneys and is apparent at several places in the North Mafeking Quarry. The chimneys occur in groups associated with broad

CRET. JUR.	GROUP/FORMATION/MEMBER		M	DEPOSITIONAL THICKNESS (METRES) AND SUMMARY LITHOLOGY	
DEVONIAN	SOURIS RIVER FORMATION	Sagemace Member	20+	Limestone, pale yellowish brown to reddish grey, microcrystalline, dense, minor argillaceous interbeds. Passes laterally to totally dolomitized sequence.	
		basal shale	2-14	Shale, dolomitic, massive, medium brownish red with some greenish mottling.	
		(evaporite dissolved)		(Davidson Evaporite)	
				(southern area only)	
		Undifferentiated carbonate beds	26	Limestone, argillaceous limestone, calcareous dolomite and dolomite. In places the carbonate beds of the Point Wilkins Member are completely dolomitized. Equivalent to the Point Wilkins Member of the north, excluding the 'First Red Beds'.	
		Point Wilkins Member			(northern area only)
			Dolomitic Limestone Beds (DLB)	5+	Orange and cream-brown, thin- to medium-bedded, finely granular dolomitic limestone and limestone locally containing stromatoporoids; typically developed near junction of Steeprock River road and Highway 10. These are the uppermost beds of the Point Wilkins Member represented in the northern part of the outcrop belt, the upper boundary of which is an erosion surface.
			Micritic Limestone Beds (MLB)	18-21	Resistant, thick-bedded, yellowish-grey, micritic and pelletoid limestone; some minor dolomitic limestone; contains scattered <i>Athyris vittata</i> ; typically developed in the Point Wilkins area and recognizable southward on islands in Swan Lake.
			Argillaceous Limestone Beds (ALB)	11-15	Thin-bedded argillaceous limestone with shaly partings, and some pelletoid limestone beds; typically developed in the Point Wilkins area.
			'First Red Beds'	2-14	Red and greenish-grey calcareous and non-calcareous shale, some silty shale and thin interbeds of argillaceous dolomite; in places some beds are brecciated; barren of fossils
		(evaporite dissolved)		(Hubbard Evaporite)	
	DAWSON BAY FORMATION	Upper Dawson Bay	5-17	Limestone, white to pale yellowish brown, highly fossiliferous with corals and stromatoporoids, in places grading to stromatoporeid biolithite. In part extremely pure high-calcium limestone (99.8% CaCO ₃), but in places variably dolomitized, especially lower part of unit.	
		Middle Dawson Bay	11-18	Calcareous shale, fossiliferous, medium grey to dark greyish red, massive (recessive).	
		Lower Dawson Bay	9-25	Gradational sequence passing upward from brown partly laminated and bituminous dolomite to grey and reddish grey dense slightly argillaceous micrite and fossiliferous micrite, which in turn grades upward to highly fossiliferous brachiopod biomicrite at top. Lower two zones thin markedly to the north.	
		Second Red Beds	6-15	Red to greenish grey dolomitic shale, commonly brecciated as a result of salt collapse.	
	ELK POINT GROUP	WINNIPEGOSIS FORMATION	0-120	Prairie Evaporite: dominantly salt with potash interbeds and minor anhydrite in basinal areas; entirely anhydrite in shelf areas (at present). Originally present throughout the entire Devonian outcrop belt, but subsequently removed by subsurface salt solution. Where preserved in subsurface, overlaps and completely buries Winnipegosis reefs with resultant thinning of evaporite section.	
			0-90	Reef facies: dolomite, very fine to medium crystalline, ranges from compact dense to subsaccharoidal, massive to medium/thick bedded, variably fossiliferous but texture largely obscured by dolomitization. Reef thicknesses tend to be relatively uniform in a given area.	
		(reef)			
		(interreef)	35	Interreef facies: dolomite, brown to black, finely laminated with black bituminous partings, in places calcareous. Lamination best defined towards top of unit.	
		Lower Winnipegosis	10-20	Lower Winnipegosis: dolomite, fine to medium crystalline, moderately granular to saccharoidal, medium to thin bedded. In part calcareous and grades laterally to Elm Point limestone facies.	
		ELM POINT FORM.	10-20	Elm Point: limestone, pale yellowish brown dense fine grained biomicrite. In part shows lighter yellowish dolomitic mottling. Pure high-calcium limestone to calcareous dolomite.	
SIL.	ASHERN FORMATION		3-18	Argillaceous dolomite and dolomitic shale, medium to dark greyish and brownish red, in places reduced to greenish grey. Local basal dolomite breccia.	
	INTERLAKE GROUP			Dolomite, white to pale yellowish buff, mostly microcrystalline dense, thin bedded, subliothographic, in part stromatolitic. Some porous biostromal interbeds towards top.	

* Units present in CBR Cement Ltd., North Quarry (Mafeking)

Figure GS-17-1: Detailed stratigraphic succession and lithologies, Devonian formations (modified after Norris et al., 1982).

synclinal forms of the strata and in these areas the surrounding DLB have been intensely altered, destroying primary sedimentary structures. In contrast, the DLB associated with the anticlinal forms are unoxidized, but may exhibit a yellow-mottled texture, which is possibly diagenetic. Transitional facies between these end members are reddish-orange mottled dolomite grading to a yellow-orange dolomitic limestone (termed leopard rock). Occasionally a few metres of bleached (beige-coloured) rock may be noted near fractures, joints, and cavities infilled with sand and clay within the DLB.

Along the southeast side of the North Mafeking Quarry, a 108 metre profile of the DLB was sampled, usually at 5 m intervals. Two or more samples were collected with a vertical separation of about 1 m. The 62 samples will be thin sectioned and analyzed to determine the physical and chemical changes that occur in the DLB, with distance from the chimneys. A second profile was sampled (11 samples), over a width of 55 m, at the northwest corner of the quarry. Sixty additional samples of DLB were collected at other locations: several within the quarry; others to the east along Highway 10, and to southeast, along the Pelican Rapids road. The results will be examined to determine the value of the DLB as a tool to guide mineral exploration.

GEOCHEMICAL SURVEYS

Brine Sediments

In early summer 1997, 203 black anoxic muds were sampled from 33 of Manitoba's west central brine springs for trace element geochemistry (see Bezys *et al.*, GS-18, this volume). The brine springs tend to have similar gross morphological characteristics with minor variation from site to site. All sites were sampled using a grid or modified grid pattern. Some spring sediments contain trace Au, Pt and Pd. Preliminary results indicate that the Prairie-type model may be applied to processes currently active in west central Manitoba. In this study, black to grey anoxic muds were sampled and values within the Churchill Superior Boundary Zone (CSBZ) were compared to those outside the CSBZ.

Enzyme Leach

B-horizon soils were sampled in the general area of both the north and south high-Ca limestone quarries near Mafeking. A total of 117 pits were hand dug along 6 east-west trending sample transects (Fig. GS-17-2). A total of 114 samples were retrieved from these pits, including 6 duplicate pairs. Samples are currently being prepared for analysis by enzyme leach; results will be reported as part of a comprehensive report on the geology, geochemistry and geophysics of microdisseminated Prairie-type mineralization.

Black Shales

Outcrops of Cretaceous Favel and Swan River formations were sampled along the Armit, Homestead and Whiskey rivers, and along creeks, situated near the Saskatchewan border, on the north side of the Porcupine Hills. A few samples were also collected along Highway 10 on the east side of the Porcupine Hills and in the Swan River valley (Figure GS-17-3). These samples will be analyzed using the same procedures as those collected for the Black Shale sub-project (See: Fedikow *et al.*, GS-20, this volume).

STREAM SEDIMENT SAMPLING

Duplicate 5 kg samples of sand and fine gravel were collected at the downstream end of sand bars within 39 streams flowing from the Porcupine Hills (Figure GS-17-3). One of the two samples was washed, sieved and concentrated using wire screens and pans. The garnet-rich silt-sized concentrates will be sent for heavy mineral analysis. Fine and coarse sands were retained for further study, but the fraction larger than 1 cm was discarded, after examination. The second 5 kg sample was washed to remove organics, coarse sieved and retained for future use.

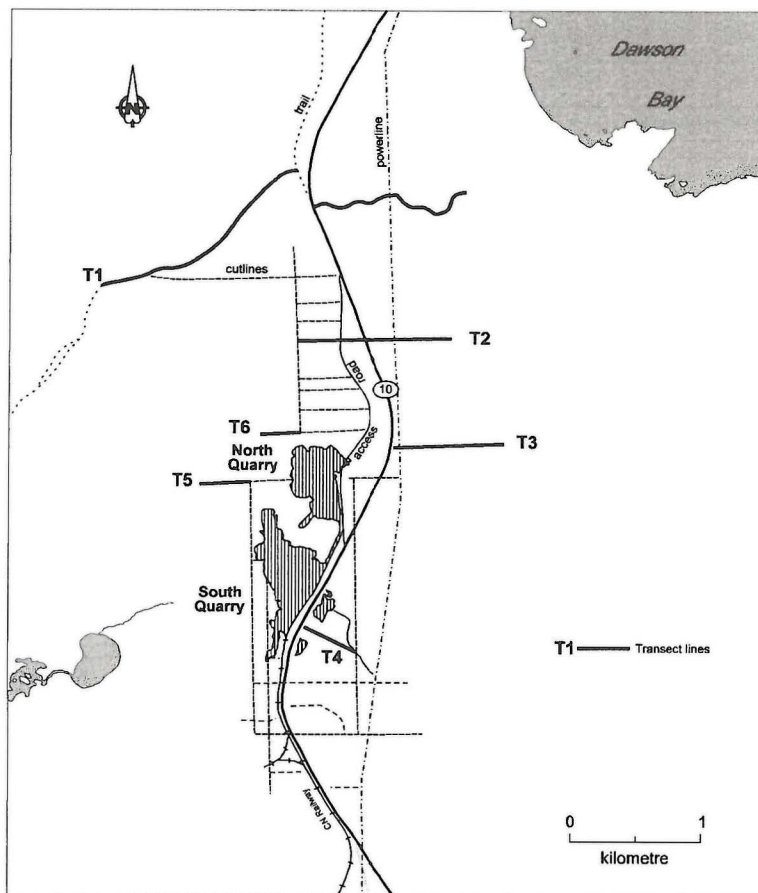


Figure GS-17-2: Enzyme Leach location map.

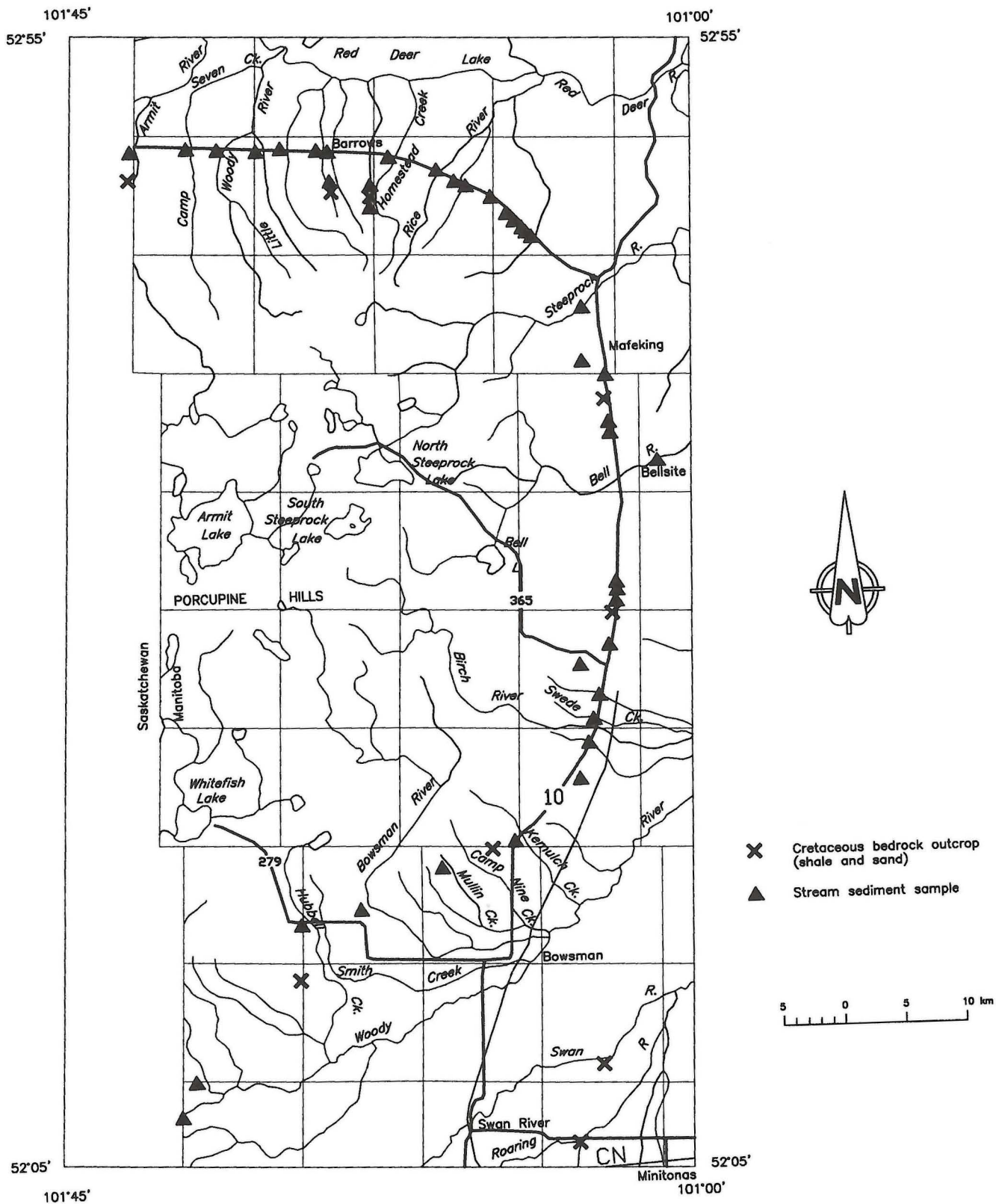


Figure GS-17-3: Stream sediment and Cretaceous black shale outcrop location map.

GEOPHYSICS

EM-31 and VLF-EM-16 Surveys in and around the Mafeking Quarries

Three days during July and one day during August 1997 were spent carrying out EM-31 and VLF-EM-16 surveys in the Mafeking quarries and surrounding areas to determine the response of electromagnetic techniques to mineralized solution chimneys.

The EM-31 and the EM-16 each require single operators and can resolve geophysical signatures explore to depths of approximately 6 and 20 metres, respectively. These depths were considered adequate for the project.

Traverses were carried out over outcropping chimneys and/or the associated rubble. A traverse around the rim of the North Mafeking Quarry incorporated the discovery chimney (Fedikow *et al.* 1996). The resulting data is shown in Figure GS-17-4. There is a definite drop in conductivity over the chimneys compared to the adjacent area - approximately 1 mmhos/m. This could be caused by the lower bulk density of the rubble compared to the surrounding solid rock. Although, this drop in conductivity is noticeable on the EM-31 instrument, it is not detected on the EM-16 unit. The EM-31 is capable of detecting smaller targets and is more sensitive to variations in conductivity. An outcropping karst structure was detected with the EM-31, manifest by higher conductivity than the surrounding area. Along the ledge on the north rim of the quarry, an area of high conductivity, up to 20 mmhos/m was outlined. This could be caused by conductive material within a karst structure.

ACKNOWLEDGMENTS

Special thanks are extended to Birch Mountain Resources Ltd. (H. Abercrombie, V. Practico, and B. Tsang) where many components of this project were made feasible with their support and funding. Thanks also to summer students E. Ducharme (Brandon University), Cory Rosolowich (University of Manitoba), and the staff of the Geological Services Branch drill crew.

REFERENCES

- Bezys, R.K., Fedikow, M.A.F., Bamburak, J.D. and Abercrombie, H.J.
1997a: Geological setting of Prairie-type Au mineralization, Mafeking Quarry, west central Manitoba, 1996 work; Manitoba Energy and Mines Preliminary Map 1997P-1, 1:5000.
- Bezys, R.K., Bamburak, J.D., and Fedikow, M.A.F.
1997b: Geological setting of Prairie-type Au mineralization, Mafeking Quarry, west central Manitoba, 1997 work; Manitoba Energy and Mines Preliminary Map 1997P-2, 1:5000.
- Fedikow, M.A.F., Bamburak, J.D., and Weitzel, J.
1995: Geochemistry of Ordovician Winnipeg Formation black shale, sandstone and their metal-rich encrustations, Black Island, Lake Winnipeg (NTS 62P/1); in Manitoba Energy and Mines, Minerals Division, Report of Activities, 1995, p. 128-135.
- Fedikow, M.A.F., Bezys, R.K., Bamburak, J.D. and Abercrombie, H.J.
1996: Prairie-type microdisseminated Au mineralization - a new deposit type in Manitoba's Phanerozoic rocks (NTS 63C/14); in Manitoba Energy and Mines, Minerals Division, Report of Activities, 1996 p. 108-121.
- McCracken, A.D.
1996: Paleontological Report: Report on 2 lower Upper Devonian (Frasnian) conodont samples from outcrop, western Manitoba (NTS 63C/14); #007-ADM-1996, Geological Survey of Canada, 3 p.
- Norris, A.W., Uyeno, T.T., and McCabe, H.R.
1982: Devonian rocks of the Lake Winnipegosis - Lake Manitoba outcrop belt, Manitoba; Manitoba Energy and Mines, Manitoba Minerals Resources Division, Publication 771, 280 p.
- Stephenson, J.F.
1973: Geochemical studies; Manitoba Department of Mines, Resources and Environment Management, Mines Branch, Geological Paper 2/73, p. 7-8.

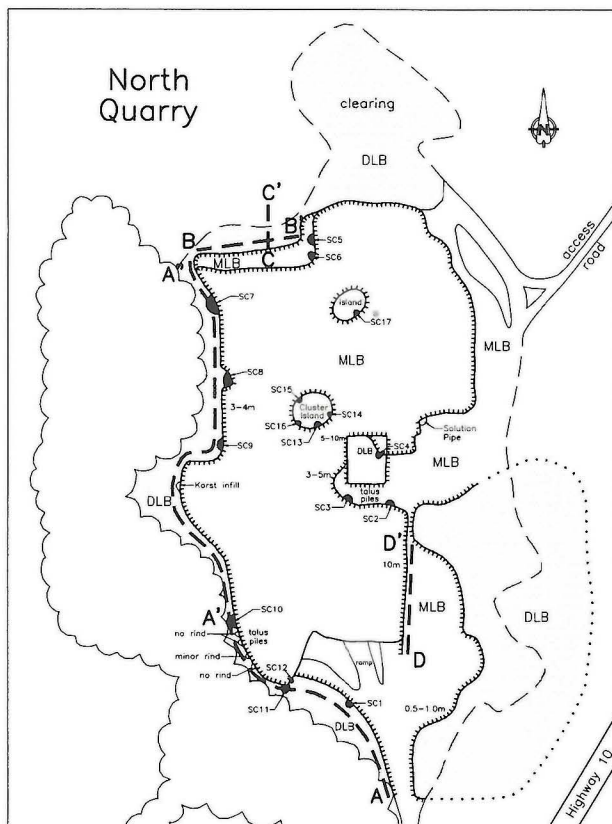


Figure GS-17-4a: North Mafeking Quarry EM-31 transect.

MAFEKING NORTH QUARRY

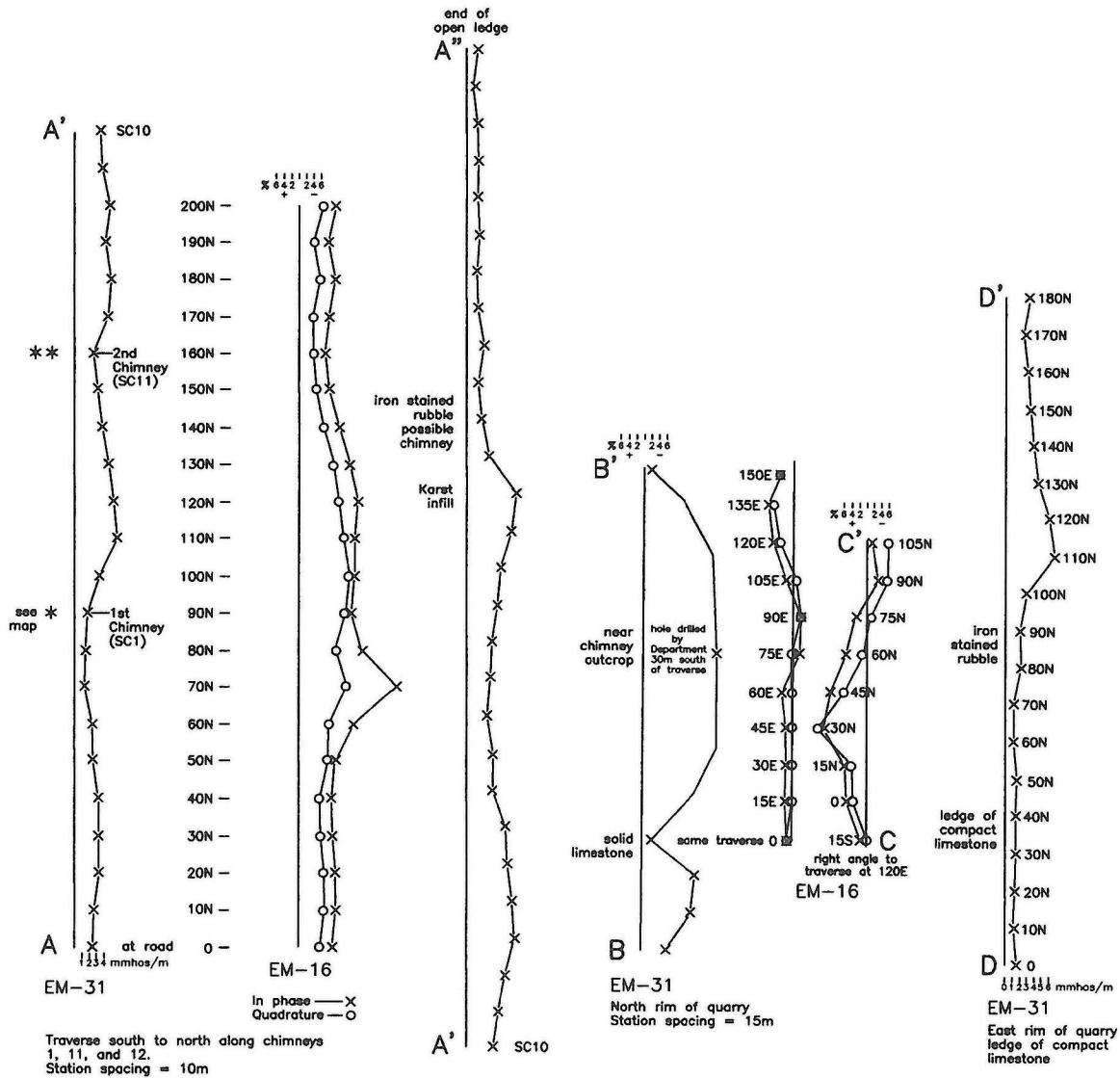


Figure GS-17-4b: North Mafeking Quarry EM-31 transect.

GS-18 A GEOCHEMICAL STUDY OF SALINE BRINE SEDIMENTS AS A GUIDE TO PRAIRIE-TYPE MICRODISSEMINATED MINERALIZATION AND OTHER PRECIOUS METALS IN WEST CENTRAL MANITOBA (NTS 63C)

by R.K. Bezys, E.B. Ducharme¹, J.D. Bamburak and M.A.F. Fedikow

Bezys, R.K., Ducharme, E.B., Bamburak, J.D. and Fedikow, M.A.F. (1997): A geochemical study of saline brine sediments as a guide to Prairie-type microdisseminated mineralization and other precious metals in west central Manitoba (NTS 63C); in Manitoba Energy and Mines, Minerals Division, Report of Activities, 1997, p. 118-122.

SUMMARY

In the summer of 1997, 203 black anoxic muds were sampled from 33 brine springs west central Manitoba. These brine springs have similar morphological characteristics although some variation occurs from site to site. All sites were sampled using a grid or modified grid pattern. Some spring sediments contain trace Au, Pt and Pd. Preliminary results indicate that the Prairie-type model for microdisseminated mineralization appears to be applicable in west central Manitoba.

In this study, black to grey anoxic muds from saline spring sites were sampled and analyzed for their metal content. Values from these spring sites within the Churchill Superior Boundary Zone (CSBZ) were then compared to those from sites outside the CSBZ.

INTRODUCTION

Exploration for precious metals utilizing the saline brines of west central Manitoba has been limited. Early descriptions of these brine springs were provided by Hind (1859), Tyrrell (1892) and Cole (1915) with more recent work completed by Petch (1987) and Jones (1991). Spring geochemistry has been studied by Cameron (1949), van Everdingen (1971), Stephenson (1973), Wadien (1984) and McKillop *et al.* (1992). Stephenson's work concentrated on the geochemistry of the brines as related to Pb-Zn-Ag mineral exploration.

In 1996, exploration focussing on the application of the Prairie-type model for microdisseminated mineralization brought renewed interest in saline springs within the study area (Fedikow *et al.*, 1996). The formation of polymetallic Prairie-type mineralization and associated alteration is attributed to oxygenated brines derived from halite evaporites within the Devonian Prairie Evaporite (Elk Point Group). Brine migration was driven by downward density flow through metal-enriched red beds, evaporites and basement strata. Metal-bearing brines were subsequently discharged at the eastern margin of the Western Canada Sedimentary Basin (WCSB), subsequent to up-dip migration and cross-strata migration due to fractures and faulting. The precipitation of Au and associated metals was constrained by oxidation-reduction reactions that involve oxidation of organic material (bitumen) and hydrocarbons, and sulphate reduction to locally produce native sulphur. The small grain size and disseminated nature of Prairie-type mineralization, the alteration mineral assemblages, and the wide distribution of bitumen in the host sedimentary rocks, indicates the temperature of deposition of the mineralization probably did not exceed 100°C (Abercrombie, 1996; Abercrombie and Feng, 1996).

SAMPLING TECHNIQUE

The study area is located in the Dawson Bay - Lake Winnipegosis area within the Devonian outcrop belt (Figure GS-18-1). Sample sites and locations are detailed in Table GS-18-1. Sampling was completed during a six week period beginning in early June and ending in mid-July of 1997. During this time interval, local water levels were higher than normal, thereby submerging some brine springs and limiting sample collection.

Black anoxic mud samples were collected from 33 brine spring sites for a total of 203 samples. Samples were collected with a plastic trowel, from 5 to 20 cm below the sediment-water interface. Initially, a grid was established at each location, and samples were collected with a spacing of 2 m. This sampling technique was later modified for two reasons: 1) at most sites, the distribution of anoxic muds is discontinuous and; 2) a greater effort was made to sample the muds proximal to discharge sites. If muds were not present near a discharge site, samples were taken as close to a discharge site as possible. Approximately 1 kg of material was collected for each sample and sealed in ZIPLOC bags for analysis. A total of 203 samples were collected; 164 have been analyzed.

BRINE SPRINGS

Gross morphology of the brine springs is generally uniform, but variations exist from one location to the next. These springs are generally flat lying to gently sloped, and contain small mounds associated with discharge sites. Springs are often perched on a "pan" of barren, glacially derived, iron stained, surficial sediment, frequently surrounded by the red salt-loving plant *Salicornia* sp. (McKillop *et al.*, 1992). At some sites, domes or hummocks are present within the brine spring and appear to represent the bedrock expression of the underlying Devonian Dawson Bay Formation where it is draped over a Winnipegosis Formation pinnacle reef.

Three types of discharge sites were observed in the study area. "Pools" or "cauldrons" are discharge sites ranging from a few centimetres to greater than a metre in depth and up to 1.5 metres in diameter. One spring, at site DB53, has a very large pool which is best described as a saline pond. The brine within these cauldrons is usually clear and overflows the rims of the pools. Brine "boils" or gas bubbles frequently percolate from these pools. The second type, abandoned or ephemeral discharge sites, are much smaller than pools, but are identifiable even when inactive and are marked by small mud volcanoes or mud pots, a few centimetres in diameter and in height. The third type of discharge site are seeps which flood a large area to a depth of one or two centimetres. The actual discharge site is very small and may not be visible. The number and type of discharge sites can vary for each spring.

A distinct spatial arrangement of vegetation was observed at the brine spring sites. Burchill (1991) and Jones (1991) described eight vegetation communities ringing the saline springs in this area, whereas McKillop *et al.* (1992) observed five vegetation communities. Trees will not grow within 5-10 metres of the discharge sites unless they are rooted on near surface bedrock outcrop or there is a source of fresh water.

Mounds of reddish brown "sinter" or "tufa" occur around the springs. They are hematitic- to limonitic-stained, gravel-like deposits that are composed of calcium carbonate. The tufa mounds rise up to one metre in height surrounding the discharge sites and are spongy, porous and friable. Reddish brown tufa can dominate the surface area of the salt flat. Red to green algae are also present within the pools and in places algal mats may cover the salt flat.

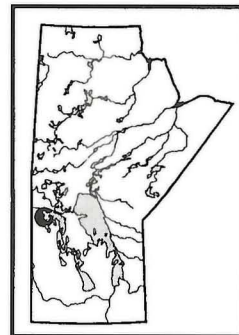
Many of the brine springs are littered with glacially transported boulders and erratics. The boulders are composed of local carbonates and Precambrian shield rocks and vary in size from a few centimetres to up one metre in diameter. Some of the boulders are extensively altered and corroded and form distorted "salt hats" in the salt flats (Fig. GS-18-2). Clusters of boulders may be present around discharge sites.

ASSAY RESULTS OF SALINE SPRING SEDIMENTS

A total of 164 brine spring sediment samples were analyzed for precious metals using fire-assay-ICP. The samples were tested for Au, Pt, and Pd (Table GS-18-1). The highest values obtained were 15 ppb Au (Station DB123) and 13 ppb Au at Station DB19. Traces of Pt and Pd were also present in samples from station DB19. Palladium showed up consistently in many of the samples.

CONCLUSIONS

Metal concentrations greater than the lower limit of detection were present in at least 20 of the brine spring sediments analyzed. The presence of low level Au, Pt and Pd in these springs indicates that metal mobilization, transport and deposition is currently active and mineralization consistent with the Prairie-type model is presently occurring in brine springs of west central Manitoba.



¹ Department of Geology, Brandon University, Brandon, Manitoba

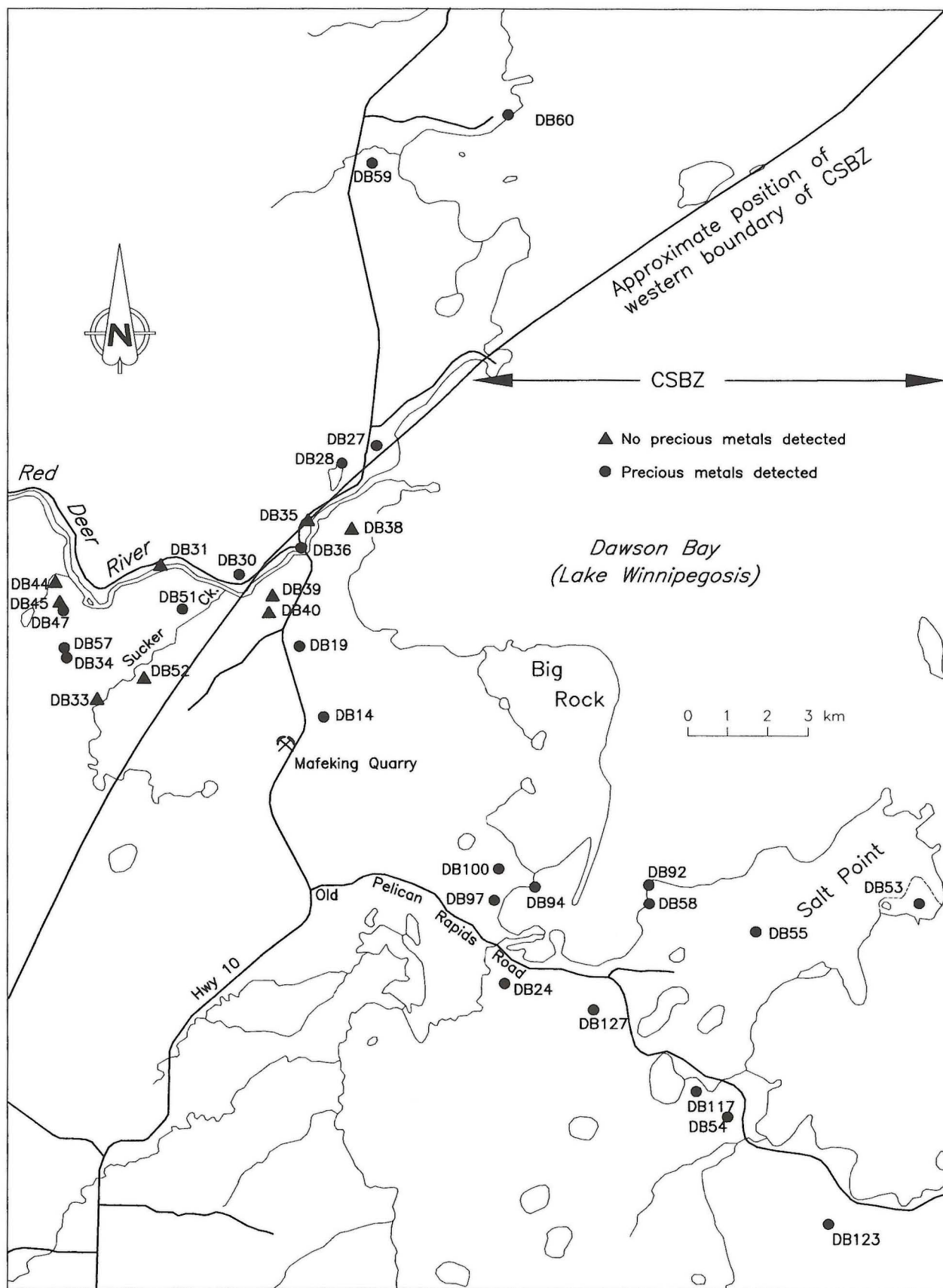


Figure GS 18-1: Location of brine springs in study area and location of the Churchill Superior Boundary Zone.



Figure GS-18-2: An example of a "salt ."

Table GS-18-1
Summary of Trace Element Geochemistry Results from Spring Sediments

Sample Number	Location	Au (ppb)	Pt (ppb)	Pd (ppb)	Sample Number	Location	Au (ppb)	Pt (ppb)	Pd (ppb)
88-97-163DB14-01	5856250N, 362775E	3	<5	<1	97-177DB28-12	5862650N, 363250E	<1	<5	<1
88-97-163DB14-04	5856250N, 362775E	4	<5	<1	88-97-179DB30-01	5859550N, 360575E	<1	<5	<1
88-97-163DB14-07	5856250N, 362775E	<1	<5	<1	88-97-179DB30-02	5859550N, 360575E	<1	<5	<1
88-97-168DB19-01	5858025N, 362175E	13	7	1	88-97-179DB30-03	5859550N, 360575E	<1	<5	<1
88-97-168DB19-03*	5858025N, 362175E	7	8	10	88-97-179DB30-04	5859550N, 360575E	<1	<5	<1
88-97-168DB19-05	5858025N, 362175E	2	7	3	88-97-179DB30-05	5859550N, 360575E	<1	<5	<1
88-97-173DB24-01	5849525N, 367325E	<1	8	<1	88-97-179DB30-06	5859550N, 360575E	<1	<5	<1
88-97-173DB24-03	5849525N, 367325E	<1	<5	<1	88-97-179DB30-07	5859550N, 360575E	<1	<5	<1
88-97-173DB24-05	5849525N, 367325E	<1	<5	<1	88-97-179DB30-08	5859550N, 360575E	<1	<5	<1
88-97-173DB24-07	5849525N, 367325E	2	<5	<1	88-97-179DB30-09	5859550N, 360575E	<1	<5	<1
88-97-173DB24-09	5849525N, 367325E	<1	<5	<1	88-97-179DB30-10	5859550N, 360575E	<1	<5	<1
88-97-173DB24-11	5849525N, 367325E	<1	<5	<1	88-97-179DB30-11	5859550N, 360575E	<1	<5	<1
88-97-173DB24-13	5849525N, 367325E	<1	<5	<1	88-97-179DB30-12	5859550N, 360575E	<1	<5	<1
88-97-173DB24-15	5849525N, 367325E	<1	<5	<1	88-97-179DB30-13	5859550N, 360575E	<1	<5	<1
88-97-173DB24-17	5849525N, 367325E	<1	<5	<1	88-97-180DB31-01	5860000N, 358725E	<1	<5	<1
88-97-173DB24-19	5849525N, 367325E	<1	<5	<1	88-97-180DB31-02	5860000N, 358725E	<1	<5	<1
88-97-176DB27-01	5863125N, 364125E	<1	<5	<1	88-97-180DB31-03	5860000N, 358725E	<1	<5	<1
88-97-176DB27-03	5863125N, 364125E	<1	<5	<1	88-97-180DB31-04	5860000N, 358725E	<1	<5	<1
88-97-176DB27-05	5863125N, 364125E	<1	<5	<1	88-97-180DB31-05	5860000N, 358725E	<1	<5	<1
88-97-176DB27-07	5863125N, 364125E	<1	<5	<1	88-97-182DB33-01	5856675N, 357175E	<1	<5	<1
88-97-176DB27-09	5863125N, 364125E	<1	<5	<1	88-97-182DB33-02	5856675N, 357175E	<1	<5	<1
88-97-176DB27-11	5863125N, 364125E	<1	<5	<1	88-97-184DB34-01	5857725N, 356425E	<1	<5	<1
88-97-176DB27-14	5863125N, 364125E	<1	<5	<1	88-97-184DB34-02	5857725N, 356425E	<1	11	<1
88-97-176DB27-15	5863125N, 364125E	<1	7	<1	88-97-184DB34-03	5857725N, 356425E	<1	<5	<1
88-97-176DB27-16	5863125N, 364125E	<1	<5	<1	88-97-184DB34-04	5857725N, 356425E	<1	<5	<1
88-97-176DB27-17	5863125N, 364125E	3	6	<1	88-97-184DB34-05	5857725N, 356425E	<1	<5	<1
88-97-176DB27-19	5863125N, 364125E	<1	<5	<1	88-97-184DB34-06	5857725N, 356425E	<1	<5	<1
88-97-177DB28-01	5862650N, 363250E	<1	<5	<1	88-97-184DB34-07	5857725N, 356425E	<1	<5	<1
88-97-177DB28-03	5862650N, 363250E	<1	<5	<1	88-97-184DB34-08	5857725N, 356425E	<1	<5	<1
88-97-177DB28-05	5862650N, 363250E	<1	<5	<1	88-97-184DB34-09	5857725N, 356425E	<1	<5	<1
88-97-177DB28-07	5862650N, 363250E	<1	<5	<1	88-97-184DB34-10	5857725N, 356425E	<1	<5	<1
88-97-177DB28-08	5862650N, 363250E	<1	11	<1	88-97-188DB35-01	5859840N, 361475E	<1	<5	<1
88-97-177DB28-09	5862650N, 363250E	<1	<5	<1	88-97-188DB35-02	5859840N, 361475E	<1	<5	<1
88-97-177DB28-10	5862650N, 363250E	<1	<5	<1					

Sample Number	Location	Au (ppb)	Pt (ppb)	Pd (ppb)	Sample Number	Location	Au (ppb)	Pt (ppb)	Pd (ppb)
88-97-188DB35-03	5859840N, 361475E	<1	<5	<1	88-97-223DB54-02	5846125N, 372900E	5	<5	<1
88-97-188DB35-04	5859840N, 361475E	<1	<5	<1	88-97-223DB54-03	5846125N, 372900E	<1	<5	<1
88-97-188DB35-05	5859840N, 361475E	<1	<5	<1	88-97-223DB54-04	5846125N, 372900E	<1	<5	1
88-97-188DB35-06	5859840N, 361475E	<1	<5	<1	88-97-223DB54-05	5846125N, 372900E	<1	<5	1
88-97-188DB35-07	5859840N, 361475E	<1	<5	<1	88-97-227DB55-01	5850775N, 373625E	<1	<5	<1
88-97-188DB35-08	5859840N, 361475E	<1	<5	<1	88-97-227DB55-02	5850775N, 373625E	<1	<5	<1
88-97-188DB35-09	5859840N, 361475E	<1	<5	<1	88-97-227DB55-03	5850775N, 373625E	<1	<5	1
88-97-188DB35-10	5859840N, 361475E	<1	<5	<1	88-97-227DB55-04	5850775N, 373625E	1	<5	<1
88-97-188DB35-11	5859840N, 361475E	<1	<5	<1	88-97-231DB57-01	5858000N, 356375E	4	7	<1
88-97-191DB36-01	5860300N, 362225E	<1	<5	<1	88-97-231DB57-02	5858000N, 356375E	<1	<5	<1
88-97-191DB36-02	5860300N, 362225E	2	<5	<1	88-97-231DB57-03	5858000N, 356375E	1	<5	1
88-97-191DB36-03	5860300N, 362225E	<1	<5	<1	88-97-231DB57-04A	5858000N, 356375E	<1	<5	1
88-97-191DB36-04	5860300N, 362225E	<1	<5	<1	88-97-231DB57-04B	5858000N, 356375E	<1	<5	1
88-97-191DB36-05	5860300N, 362225E	<1	<5	<1	88-97-232DB58-01	5851425N, 371060E	1	<5	1
88-97-195DB38-01	5860575N, 363400E	<1	<5	<1	88-97-232DB58-02	5851425N, 371060E	<1	<5	<1
88-97-195DB38-02	5860575N, 363400E	<1	<5	<1	88-97-233DB59-01	5870225N, 364000E	<1	8	2
88-97-195DB38-04	5860575N, 363400E	<1	<5	<1	88-97-233DB59-02	5870225N, 364000E	<1	<5	<1
88-97-195DB38-05	5860575N, 363400E	<1	<5	<1	88-97-233DB59-03	5870225N, 364000E	<1	8	1
88-97-195DB38-07	5860575N, 363400E	<1	<5	<1	88-97-234DB60-01	5871450N, 367450E	<1	<5	1
88-97-195DB38-08	5860575N, 363400E	<1	<5	<1	88-97-284DB92-01	5851825N, 371060E	<1	<5	1
88-97-195DB38-09	5860575N, 363400E	<1	<5	<1	88-97-284DB92-02	5851825N, 371060E	<1	<5	1
88-97-195DB38-12	5860575N, 363400E	<1	<5	<1	88-97-287DB94-01	5851925N, 368125E	3	<5	2
88-97-197DB39-01	5859300N, 361500E	<1	<5	<1	88-97-292DB97-01	5851600N, 367100E	4	<5	1
88-97-197DB39-02	5859300N, 361500E	<1	<5	<1	88-97-296DB100-01	5852400N, 367200E	1	6	1
88-97-197DB39-03	5859300N, 361500E	<1	<5	<1	88-97-317DB117-01	5846750N, 372100E	7	<5	<1
88-97-197DB39-04	5859300N, 361500E	<1	<5	<1	88-97-327DB123-01	5843350N, 372400E	7	<5	<1
88-97-197DB39-05	5859300N, 361500E	<1	<5	<1	88-97-327DB123-02	5843350N, 372400E	15	<5	<1
88-97-197DB39-06	5859300N, 361500E	<1	<5	<1	88-97-327DB123-03	5843350N, 372400E	2	<5	<1
88-97-197DB39-07	5859300N, 361500E	<1	<5	<1	88-97-331DB127-01	5848840N, 369550E	1	<5	<1
88-97-197DB39-08	5859300N, 361500E	<1	<5	<1	88-97-331DB127-02	5848840N, 369550E	<1	<5	<1
88-97-197DB39-09	5859300N, 361500E	<1	<5	<1					
88-97-197DB39-10	5859300N, 361500E	<1	<5	<1					
88-97-197DB39-11	5859300N, 361500E	<1	<5	<1					
88-97-197DB39-13	5859300N, 361500E	<1	<5	<1					
88-97-198DB40-01	5858750N, 361400E	<1	<5	<1					
88-97-198DB40-02	5858750N, 361400E	<1	<5	<1					
88-97-198DB40-03	5858750N, 361400E	<1	<5	<1					
88-97-203DB44-01	5859650N, 356125E	<1	<5	<1					
88-97-203DB44-02	5859650N, 356125E	<1	<5	<1					
88-97-206DB45-01	5859150N, 356250E	<1	<5	<1					
88-97-206DB45-02	5859150N, 356250E	<1	<5	<1					
88-97-211DB47-01	5858950N, 356350E	<1	<5	<1					
88-97-211DB47-02	5858950N, 356350E	<1	<5	<1					
88-97-211DB47-03	5858950N, 356350E	1	<5	<1					
88-97-211DB47-04	5858950N, 356350E	<1	<5	1					
88-97-211DB47-05	5858950N, 356350E	<1	<5	<1					
88-97-214DB51-01	5859000N, 359275E	<1	<5	<1					
88-97-214DB51-02	5859000N, 359275E	<1	<5	<1					
88-97-214DB51-03	5859000N, 359275E	<1	<5	<1					
88-97-214DB51-04	5859000N, 359275E	<1	<5	1					
88-97-214DB51-05	5859000N, 359275E	<1	<5	<1					
88-97-214DB51-06	5859000N, 359275E	<1	<5	1					
88-97-217DB52-01	5857200N, 358325E	<1	<5	<1					
88-97-219DB53-01	5851500N, 377725E	<1	<5	<1					
88-97-219DB53-02	5851500N, 377725E	<1	<5	1					
88-97-219DB53-03	5851500N, 377725E	<1	<5	1					
88-97-219DB53-04	5851500N, 377725E	<1	<5	1					
88-97-219DB53-05	5851500N, 377725E	<1	<5	<1					
88-97-219DB53-06	5851500N, 377725E	<1	<5	1					
88-97-219DB53-07	5851500N, 377725E	<1	<5	1					
88-97-219DB53-08	5851500N, 377725E	<1	<5	<1					
88-97-219DB53-09	5851500N, 377725E	<1	6	<1					
88-97-219DB53-10	5851500N, 377725E	<1	<5	<1					
88-97-219DB53-11	5851500N, 377725E	<1	<5	1					
88-97-219DB53-12	5851500N, 377725E	<1	<5	<1					
88-97-219DB53-13	5851500N, 377725E	<1	<5	<1					
88-97-223DB54-01	5846125N, 372900E	<1	<5	1					

*Re-assay

Nearly all brine spring sediments sampled within the Churchill Superior Boundary Zone (CSBZ) contain detectable precious metals. Five sample sites along the western side of the study area, outside of the CSBZ (stations DB31, DB33, DB44, DB45, and DB47) and two stations on the western boundary (DB30 and DB35) contained no detectable metals (Figure GS-18-1). Three stations within the CSBZ, but proximal to the western boundary, also contained no detectable precious metals. All samples east and southeast of station DB19 contained measurable precious metals. However, five stations (DB34, 47, 57, 59, and 60) west of the CSBZ had measurable metals.

Further geochemical analysis are being conducted on the brine sediments from the Lake Winnipegosis-Dawson Bay area such as INAA and ICP-AES multi-element analysis and mineral specific (sulphide) analysis. One brine spring, station DB54, is to be studied in detail with both vertical and horizontal grid sampling to determine lateral variations and facies relationships with respect to metal concentrations.

ACKNOWLEDGMENTS

Special thanks are extended to Birch Mountain Resources Ltd. (H. Abercrombie, V. Practico, and B. Tsang) where many components of this project were made feasible with their support and funding.

REFERENCES

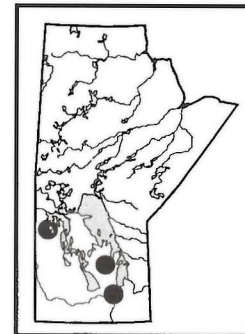
- Abercrombie, H.J.
1996: Prairie-type sedimentary Au-Ag-Cu; Short Course Notes, New Mineral Deposit Models of the Cordillera; British Columbia Geological Survey and Geological Survey of Canada, Vancouver, January, 1996.
- Abercrombie, H.J. and Feng, R.
1996: Geology of Prairie-type Au-Ag-Cu mineralization, Fort MacKay region, northeastern Alberta; in R.W. Macqueen, editor, Alberta MDA Final Report, Geological Survey of Canada Bulletin.

- Burchill, C.
1991: Vegetation - environment relationships of an inland boreal salt pan; M.Sc. Thesis, University of Manitoba, 103 p.
- Cameron, E.L.
1949: Salt, potash and phosphate in Manitoba; Department of Mines and Natural Resources, Mines Branch, Bulletin 48-9, 13 p.
- Cole, L.H.
1915: Report on the salt deposits of Canada and the salt industry; Canada Department of Mines, No. 325, Chapter V, p. 49-73.
- Fedikow, M.A.F., Bezys, R.K., Bamburak, J.D., and Abercrombie, H.J.
1996: Prairie-type microdisseminated Au mineralization - a new deposit type in Manitoba's Phanerozoic rocks (NTS 63C/14); in Manitoba Energy and Mines, Minerals Division, Report of Activities 1996, p. 108-121.
- Hind, H.Y.
1859: Reports on the North-west Territory; Report of Progress; together with a preliminary and general report on the Assiniboine and Saskatchewan exploring expedition, Canada, John Lovell, Toronto, 194p.
- Jones, G.
1991: Competitive processes and spacial patterning of plant species in inland boreal saline habitats; M.Sc. Thesis, University of Manitoba, 276 p.
- McKillop, W.B., Patterson, R.T., Delorme, L.D., and Nogrady, T.
1992: The origin, physico-chemistry and biotics of sodium chloride dominated saline waters on the western shore of Lake Winnipegosis, Manitoba; Canadian Field Naturalist, Volume 106 (4), p. 454-473.
- Petch, V.
1987: The 1986 survey of salt flats and pools along the western shore of Lake Winnipegosis, Manitoba; Archaeological Quarterly, Volume 11, p. 13-22.
- Stephenson, J.F.
1973: Geochemical studies: Summary of Geological Field Work, Department of Mines, Resources and Environmental Management, Manitoba, Geological Paper 2/73, p. 7-8.
- Tyrrell, J.B.
1892: Report on north-western Manitoba; Annual Report, Volume V, Part 1, 1891, Geological Survey of Canada, 235 p.
- Van Everdingen, R.O.
1971: Surface-water composition in southern Manitoba reflecting discharge of saline subsurface waters and subsurface solution of evaporites; Geological Association of Canada, Special Paper 9, p. 343-352.
- Wadien, R.
1984: The geochemistry and hydrogeology of saline spring waters of the Winnipegosis area, southwestern Manitoba; B.Sc. Thesis, University of Manitoba, 63 p.

GS-19 STRATIGRAPHIC AND INDUSTRIAL MINERAL CORE HOLE DRILLING PROGRAM 1997 (NTS 63C)

by R.K. Bezys and J.D.Bamburak

Bezys, R.K. and Bamburak J.D. (1997): Stratigraphic and industrial mineral core hole drilling program 1997 (NTS 63C); in Manitoba Energy and Mines, Minerals Division, Report of Activities, 1997, p.123 -128.



SUMMARY

In 1997, the drilling program carried out by the Geological Services Branch completed 17 holes for a total of 686 m. Three core holes were drilled in the Selkirk area as an extension of sub-Phanerozoic, shield margin studies in NTS 62I/2, to determine the Paleozoic and Precambrian stratigraphy. Two of these holes intersected the Precambrian. Eleven core holes were drilled in NTS 63C as a follow-up to last year's discovery of the presence of Prairie-type microdisseminated mineralization. These holes were drilled to extend solution chimney profiles in the north Mafeking Quarry and to determine the Devonian stratigraphy of the area. Three industrial minerals core holes were drilled to determine the presence of kaolin in the Sylvan area.

INTRODUCTION

Three core hole drilling projects were conducted in 1997:

- 1) Stratigraphic drilling of Paleozoic and Precambrian units in the vicinity of Selkirk (NTS 62I/2);

- 2) Stratigraphic core hole drilling in the Dawson Bay area, including north Mafeking Quarry and the surrounding Devonian outcrop belt, to investigate Prairie-type microdisseminated mineralization (NTS 63C) and;

- 3) Industrial mineral drilling (for kaolin) in the Sylvan area (NTS 62P/3).

Locations of the core holes are shown in Figure GS-19-1 and a summary of core hole data is presented in Table GS-19-1.

SELKIRK AREA DRILLING

Three core holes were drilled along Highway 59, east of East Selkirk. A total of 258.4 m were drilled including 23.5 m of Precambrian strata (M-1-97 and M-3-97). Table GS-19-2 provides a detailed corelog of the Precambrian intervals from these two core holes.

DAWSON BAY DRILLING

Eleven stratigraphic core holes were drilled in the Dawson Bay area

for a total of 376.5 m. Precambrian basement was not intersected. Of the three core holes were drilled in the north Mafeking Quarry, two were drilled for the potential intersection of a solution chimney, and one hole was drilled through the Devonian Souris River Formation Dolomitic Limestone Beds into the Dawson Bay Formation (see Bamburak *et al.*, GS-17, this volume and Fedikow *et al.*, 1996). The remaining eight core holes were drilled at various locations in NTS 63C.

INDUSTRIAL MINERAL CORE HOLE DRILLING IN THE SYLVAN AREA

Three core holes, for a total of 51.1 m, were drilled about 2 km northeast of the former community of Sylvan, to test potential for a kaolin-bearing channel as indicated by Hosain *et al.* (1995). All three holes penetrated Ordovician Red River Formation (Fort Garry Member) overlying the Selkirk Member. No kaolinitic clays were found. Additional geophysical work will be conducted to determine new targets.

ACKNOWLEDGMENTS

Thanks are extended to all staff of the Geological Services Branch drill crew.

REFERENCES

- Fedikow, M.A.F., Bezys, R.K., Bamburak, J.D., and Abercrombie, H.J.
1996: Prairie-type microdisseminated Au mineralization - a new deposit type in Manitoba's Phanerozoic rocks (NTS 63C/14); in Manitoba Energy and Mines, Minerals Division, Report of Activities, 1996, p. 106-121.
- Hosain, I.T., Ferguson, I., Ristou, J. and Cassels, J.
1995: Geophysical surveys for kaolin - Sylvan area, Manitoba; in Manitoba Energy and Mines, Minerals Division, Report of Activities, 1995, p. 140-147.

Table GS-19-1
Summary of stratigraphic and industrial minerals core hole data 1997

Hole No.	Location and Elevation (m)	SYSTEM/Formation/ (Member)	Interval (m)	Summary Lithology
M-1-97 Selkirk	NTS 62I/2 5553900N 354875E 228.9 m	ORDOVICIAN/Red River/(Selkirk)	0.0 - 76.1	Limestone; wackestone; mottled; massive; light tan brown; typical "Tyndall Stone"
		Winnipeg	76.1-98.5	75.2-76.1: Hecla Beds; irregular contacts. Blue green to steel grey to olive minor sands
		PRECAMBRIAN	98.5-112.8	
M-2-97 Selkirk	NTS 62I/2 5551275N 352860E 233.2 m	OVERBURDEN	0.0-15.0	Glacial till
		ORDOVICIAN/Red River/(Selkirk)	15.0-20.6	Limestone; wackestone; light brown tan; massive; mottled; typical "Tyndall Stone"
		Red River?	20.6-30.5	Interbeds of similar lithologies as seen above and some Precambrian fragments (karst infill?)
M-3-97 Selkirk	16-32-13-15E 5557225N 357475E 230.1 m	ORDOVICIAN/Red River/(Selkirk)	0.0-73.4	Limestone; wackestone; typical mottled; light tan brown; "Tyndall Stone"
		Winnipeg	73.4-105.9	70.5-73.4: Hecla Beds; Interbedded shales and

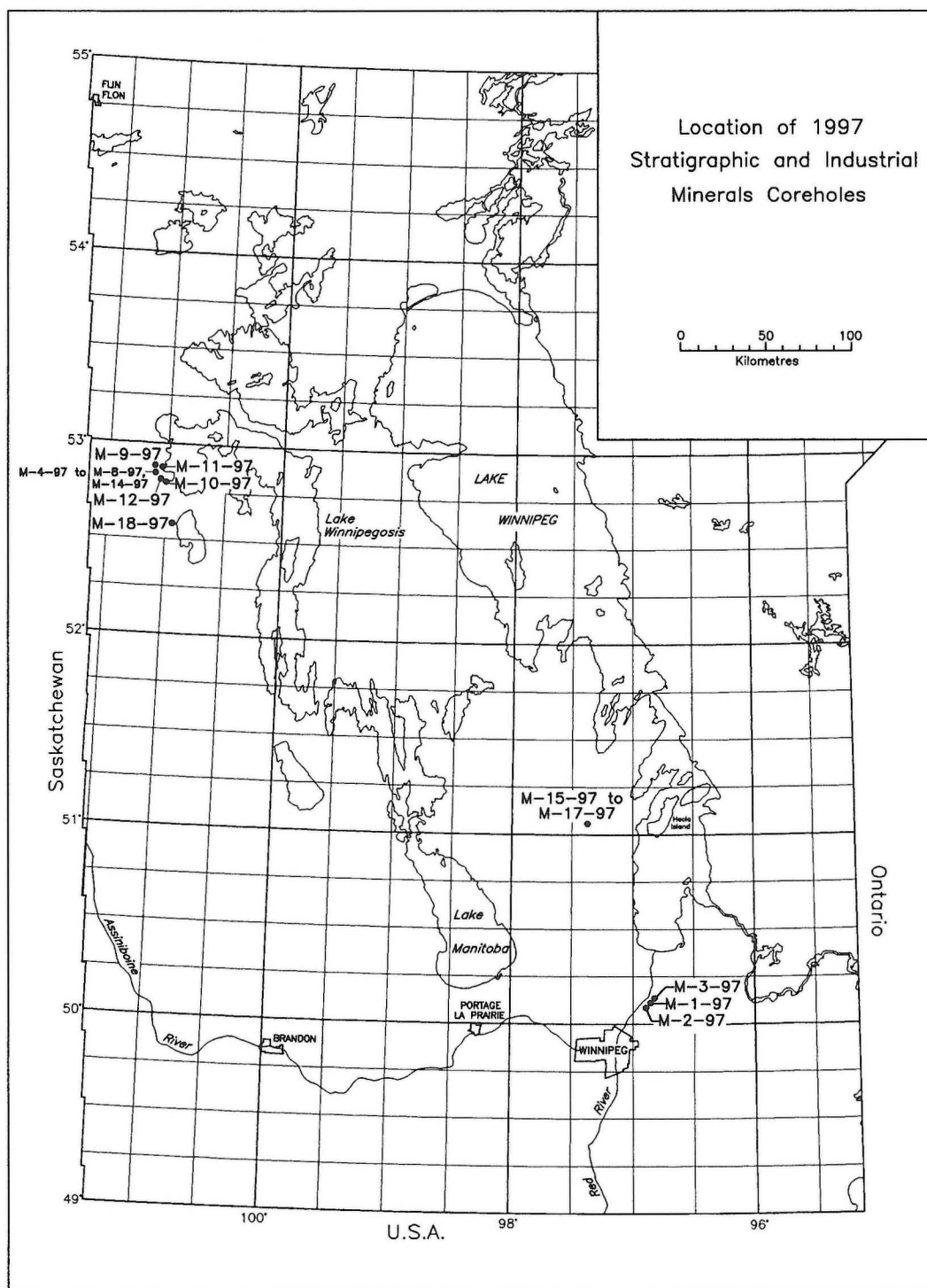


Figure GS-19-1: Location of 1997 stratigraphic and industrial minerals coreholes.

		PRECAMBRIAN	105.9-115.1	sandstones
M-4-97 Dawson Bay N. Mafeking Quarry SC-1-50° angle	7-32-44-25W 5855308N 361965E 279 m	OVERBURDEN DEVONIAN/Souris River (Point Wilkins)	0.0-1.7 1.7-3.0 3.0-9.3	Rubby limestone Dolomitic limestone beds: rusty brown; limestone to dolomitic limestone; mudstone; some intense red colouration Micritic Limestone Beds: mottled limestone; mudstone to wackestone; fossiliferous
M-5-97 Dawson Bay N. Mafeking Quarry SC-1	8-33-44-25W 5855302N 363929E 274 m	OVERBURDEN DEVONIAN/Souris River (Point Wilkins)	0.0-3.8 3.8-6.9 6.9-8.2 8.2-22.3	Boulder till; possible silica sinter pebble at the base Micritic Limestone Beds: tan limestone; wackestone; fossiliferous Sand clay infill; brown sand; some green grey clay; silica sinter pebble at the base Micritic Limestone Beds: as above; very broken
M-6-97 North Dawson Bay N. Mafeking Quarry	7-32-44-25W 5855302N 561872E 279 m	DEVONIAN/Souris River (Point Wilkins) (First Red Beds) Dawson Bay/(Upper) Dawson Bay (Middle) Dawson Bay (Lower) (Second Bed)	0.0-0.6 0.6-25.5 25.5-34.3 34.3-44.7 44.7-51.6 51.6-69.4 69.4-76.2 76.2-81.4	Dolomitic Limestone Beds: yellow orange to tan; limestone; wackestone Micritic Limestone Beds: light tan to brown; mottled limestone; fossiliferous Argillaceous Limestone Beds: light brown tan; limestone; mudstone; scattered light green clay Red brown to green limestone; mudstone Limestone: wackestone; light tan to dark brown; abundant green grey clay along fractures and bedding planes Limestone: mudstone; dark grey to light olive green Limestone: wackestone; light tan; fossiliferous Limestone: grey to dark red argillaceous mudstone
M-7-97 Dawson Bay Borrow Pit East of Mafeking Quarry	2-33-44-25W 5855935N 362619E 276 m	OVERBURDEN DEVONIAN/Souris River/(Point Wilkins) SOLUTION CHIMNEY (?)	0.0-0.4 0.4-0.5 0.5-8.3	Glacial till Rind (?): dark brown dolomitic limestone to limestone; sideritic Micritic Limestone Beds: limestone; fossiliferous; mudstone to wackestone; scattered grey clay
M-8-97 Dawson Bay Borrow Pit E. of Mafeking Quarry 55° angle	12-33-44-25W 5855935N 362619E 276 m	DEVONIAN/Souris River/(Point Wilkins)	0.0-0.2 0.2-0.3 0.3-2.0 2.0-2.2 2.2-3.5	Dolomitic Limestone Beds: limestone; light brown to brown Rind: sideritic limestone; dark brown Micritic Limestone Beds: light brown tan limestone; mudstone Pebble infill: carbonate and Precambrian fragments Micritic Limestone Beds: (as above)
M-9-97 Dawson Bay Tower Outcrop	2-8-45-25W 5858490N 361895E 274 m	DEVONIAN/Souris River/(Point Wilkins) (First Red Beds) Dawson Bay (Upper) Dawson Bay (Middle) Dawson Bay (Lower)	0.0-17.0 17.0-26.0 26.0-40.0 40.0-43.2 43.2-59.9 59.9-67.8	Micritic Limestone Beds: light tan limestone; fossiliferous; mudstone Argillaceous Limestone Beds: tan to brown limestone; mudstone; abundant red colouration, fossiliferous Interbedded green and red mudstone; calcareous and non-calcareous Limestone with some dolomite; wackestone;

		(Second Red Beds)	67.8-72.3	scattered sulphide bonding at top Grey to red calcareous shale/mudstone; fossiliferous Limestone: light green to grey to red; mudstone at the base with wackestone/packstone at the top; fossiliferous Dark red to grey argillaceous dolomite; mudstone
M-10-97 Dawson Bay East Steeprock Bridge Pelican Rapids Road	15-12-44-25W 5849594N 368079E 263 m	DEVONIAN/Dawson Bay (Lower) (Second Red Beds) Winnipegosis/(Lower)	0.0-4.7 4.7-6.2 6.2-15.5 15.5-17.6 17.6-28.8	Limestone: fossiliferous, mudstone Transitional Beds: olive grey mudstone Grey mudstone; dolomitic Transitional Beds: blue green calcareous dolomite Light brown tan packstone; porous; reefal
M-11-97 Dawson Bay Highway 10 outcrop Borrow Pit	10-5-45-25W 5857289N 362112E 282 m	DEVONIAN/Dawson Bay (Upper) Dawson Bay/(Middle) Dawson Bay (Lower) (Second Red Beds)	0.0-7.3 7.3-26.7 26.7-30.9 30.9-34.8 34.8-40.1	Limestone; wackestone; light brown tan; pyrite blebs throughout; sulphide banding at top Limestone: dark grey; mudstone; fossiliferous Limestone: light tan brown; mudstone; scattered sulphides Transitional Beds: dolomite; mudstone; brecciated Dolomite: dark red brown mudstone
M-12-97 Dawson Bay Pelican Rapids Rd. & Hwy. 10	4-21-44-25W 5851850N 362550E 283.5 m	DEVONIAN/Souris River/(Point Wilkins) (First Red Beds) Dawson Bay/(Upper) Dawson Bay/(Middle) Dawson Bay (Lower) (Second Red Beds)	0.0-1.8 31.5-42.0 42.0-48.3 48.3-56.2 56.2-67.2 67.2-74.5 74.5-78.3	Dolomitic Limestone Beds: oxide cap; dark orange brown Micritic Limestone Beds: limestone; wackestone; very broken core Argillaceous Limestone Beds: limestone; mudstone; light green with some red Limestone: dolomitic; oxidized and reduced intervals Transitional Beds: Limestone and dolomitic limestone, green grey argillaceous beds Limestone: wackestone; light brown tan Limestone: olive green to light tan; mudstone; fossiliferous Limestone: mudstone and wackestone; light tan to brown; some green argillaceous partings Dark red dolomitic mudstone
M-13-97 Dawson Bay West of Swan Lake	2-30-41-24W 5823840N 370600E 269 m	OVERBURDEN DEVONIAN/Souris River/(Point Wilkins) INFILL or SOLUTION CHIMNEY (?) CRETACEOUS or JURASSIC?	0.0-20.7 20.7-20.9 20.9-21.0 21.0-23.6 23.6-26.7	Glacial till and Lake Agassiz clay(?) Micritic Limestone Beds: calcareous dolomite; mudstone; light tan to orange - looks like rind; dark brown to olive green mudstone; dark brown to olive green mudstone/clay with muscovite flakes(?) Siliceous sinter boulder (white) Till-like material with clay (?) Clay: blue green/green grey to olive green; not sure if part of solution chimney or channel infill material
M-14-97 Dawson Bay North Mafeking Quarry	7-32-44-25W 585575N 361825E 278 m	DEVONIAN/Souris River/(Point Wilkins) SOLUTION CHIMNEY (?)	0.0-5.0 5.0-5.5	Micritic Limestone Beds: light brown tan; wackestone; poor core recovery; 5 cm of silica sinter at base Blue green to green gray clay with "micro sinters"

M-15-97 Sylvan	9-15-24-1E 5659350N 614300E 255 m	OVERBURDEN ORDOVICIAN/Red River/(Fort Garry) (Selkirk)	0.0-4.8 4.8-11.3 11.3-15.9	Clay and glacial till(?) Limestone; mudstone; light grey to tan brown yellow; some sulphide mineralization along fractures Limestone; mottled; vuggy; wackestone; abundant chert
M-16-97 Sylvan	9-15-24-1E 5659400N 614300E 255 m	OVERBURDEN ORDOVICIAN/Red River/(Fort Garry) (Selkirk)	0.0-7.0 7.0-11.9 11.9-14.4	Glacial till Limestone; mudstone; red brown, grey to tan to yellow; abundant fracturing and associated porosity Limestone; mottled; wackestone; cherty
M-17-97 Sylvan	9-15-24-1E 5659500N 614300E 255 m	OVERBURDEN ORDOVICIAN/Red River/(Fort Garry) (Selkirk)	0.0-3.0(?) 3.0-12.6 12.6-20.8	Mud and glacial till (?) Limestone: mudstone; yellow brown; fractured with some sulphides Limestone: wackestone; mottled; cherty; some clay infill

Table GS-19-2

Detailed core log of Precambrian intervals in core holes M-1-97 and M-3-97 (logged by T.C. Corkery)

Core hole M-1-97

metres	
89.5 - 89.2	Contact -Paleozoic/Precambrian -weathered zone marked by a 2 to 19 mm zone of massive pyrite - in one zone forming an oval radial growth structure. <u>Magnetite iron formation</u> - highly altered to red hematite and acicular masses of bright yellow crystals occurring both in veins disseminated and as aggregates (stilpnomelane?). <u>Oxide bearing very fine grained siliceous siltstone</u> forms thinly laminate (mm scale) interlayers. These contain disseminated, less than 0.1 mm, magnetite throughout more Fe rich layers, interlayered with quartz-p hylosilicate rich laminations. Several generations of veins, mostly carbonate with varying percentages of iron oxide are persistent throughout the hole
89.2 - 89.4	<u>Magnetite iron formation</u> Zone of dark red-purple and brown oxide alteration of massive magnetite. Still shows a relict mm scale lamination dominated by very fine grained magnetite. In some layers magnetite is recrystallized to 1 to 3 mm crystals. The dark red and brown colouration is due to late oxide and possibly hydroxide alteration. 89.4 - 89.8 <u>Oxide bearing very fine grained siliceous siltstone</u> . Return to light purple grey laminated quartz rich oxide poor iron formation or laminated IF.
89.8 - 101.6	<u>Siliceous oxide iron formation</u> Interbedded purple grey, laminated, siliceous oxide poor IF with dark purple-olive green, oxide rich laminated to massive, oxide rich IF Layering on a scale of 1-3 cm for magnetite rich bands and 3 to 5 cm for oxide poor - siliceous siltstone. 101.6 - 106.8 <u>Sulphide rich iron formation</u> Interbedded oxide bearing very fine grained siliceous siltstone 30 percent, with <u>stilpnomelane bearing, layered and laminated, oxide and sulphide iron formation</u> . Distinctive brilliant yellow stilpnomelane occurs throughout this section as does a curved cleavage dark yellow-brown opaque (sphalerite???). Minor pyrite stringers crosscut the layering. Dominant iron minerals are sulphides in this zone.
106.8 - 108.1	<u>Greywacke</u> Zone of interbedded garnetiferous greywacke, oxide iron formation and sulphide iron formation. Layering on a scale of 1 to 5 cm with lamination in the iron formations.
108.1 - 109.3	<u>Iron formation</u> Alternating hematite red and yellowish olive green iron rich metasediments. Hematitized layers are more magnetite rich and are interlayered with green amphibole rich beds. These beds appear to have a significant alteration to clay. 1 to 4 mm thick carbonate veins throughout. Sulphides more abundant near veins - dominantly pyrite with minor chalcopryite (108.5) In some sulphide zones a delicate intergrowth of pyrite with laminar intergrowth of silicate on a 0.1 mm scale. Often associated with magnetite (probably a late sulphide replacement reaction).
109.3 - 109.4	<u>Gabbro?</u> Spotted gabbroic texture for 5 to 10 cm. 1 to 2 mm aggregates of black amphibole in a more feldspathic very fine grey matrix. Sharp contact with the iron formation may be intrusive?
109.4 - 109.9	<u>Garnet porphyroblastic chlorite-amphibole schist</u> . 3 to 10 mm garnet porphyroblasts in a dark green chlorite amphibole matrix. Late black alteration veins (chlorite?) cut schist and garnets.
109.9 - 110.2	<u>Gabbro?</u> Spotted gabbroic texture as at 109.3 m.
110.2 - 110.3	<u>Alteration zone in spotted "gabbro"</u> Dark olive green clay? - unit consists of altered dark green amphibole and chlorite with a relict spotted texture like the unit above. Probably represents alteration of the "gabbro".
110.3 - 112.7	<u>Greywacke?</u>
EOH	More siliceous than layers above. Layers of light grey very fine grained possible greywacke form the original rock. Zones of dark grey to black chlorite-amphibole alteration from 1 to 5 cm thick form up to 50% of the rock. Garnets are restricted to the black alteration fractures within fine grained greywacke. NOTE: This entire segment from 109.3 m to the end of the hole may represent a variably altered greywacke metasediment.

Core hole M-3-97

- 95.9 3 m lost core at contact. Last section Paleozoic rock is a mature quartz sand with some zones of pyrite cement..
- 105.9 - 109.6 Serpentinized peridotite
Pseudomorphed 1 to 2 mm olivine (laminated serpentine) with rare 1 to 2 mm pyrite and disseminated 0.1 mm opaques - probably chromite - non magnetic.
- 109.6 - 109.8 Talc serpentine schist with minor phlogopite?
Very fine grained homogeneous schist lacks opaques. Is a pale green mix of very fine grained greenserpetine and white talc with scattered red brown phlogopite?
- 109.8 - 110.3 Serpentinized peridotite
Well developed joints with 1 to 5 cm layered joint parallel alteration - common feature to many dunites. Minor magnetite.
- 110.3 - 113.0 Serpentinized peridotite
As previous but with patchy purple red hematite alteration blotches from 0.5 cm to 2 cm. Lacks the distinct joint pattern.
- 113.0 - 115.1 Dominantly talc serpentine schist with serpentinite layers up to 15 cm thick. Looks like drilling down dip

(NOTE: Entire core is variations on serpentinite - Peridotite)

GS -20 GEOCHEMICAL CHARACTERIZATION OF BLACK SHALES IN MANITOBA'S PHANEROZOIC

by M.A.F. Fedikow, R.K. Bezys, and J.D. Bamburak and R.G. Garrett¹

Fedikow, M.A.F., Bezys, R.K., Bamburak, J.D. and Garrett, R.G. (1997): Geochemical characterization of black shales in Manitoba's Phanerozoic; in Manitoba Energy and Mines, Minerals Division, Report of Activities, 1997, p. 129-130.

SUMMARY AND CONCLUSIONS

Neutron activation and inductively coupled plasma - atomic emission spectrometry analytical approaches are being used to develop a multielement geochemical database for black shale samples collected from drill core, percussion well chips and outcrop chips. Initial data assessment for greater than 600 samples indicates characteristic chemical signatures are present for black shales throughout the stratigraphic record. The chemistry of these unique rocks will provide new metallogenetic concepts relevant to mineral exploration in Phanerozoic sequences.

INTRODUCTION

The development of a black shale geochemical database for metallogenetic studies throughout the province was initiated in 1995 (Fedikow *et al.*, 1995). Its usefulness demonstrated in 1996 (Schmidtke and Fedikow, 1996), when mineralogical studies, supplementing geochemical data, at Black Island in Lake Winnipeg indicated a probable link between metal-rich encrustations on black shales and a gold-enriched near solid pyrite stratum at Black Island.

In 1996, about 300 outcrop samples were collected along the Manitoba Escarpment and in the Precambrian River Valley in Southern Manitoba (Bamburak, 1996). Sampling sites for outcrop chips, drill core and archived percussion well chips is presented in Figure GS-20-1. All samples will be analysed for a wide range of trace and major elements with the aim of developing a chemical stratigraphy for black shales, initially in the Phanerozoic sequences in Manitoba, as well as screening the black shales for potential metal-source rocks.

Data will be released as open file reports with tabled analyses and geochemical maps. The database will also permit an evaluation of the relationship between black shales and Prairie-type microdisseminated mineralization (see GS-17, Bamburak *et al.*, this volume).

SAMPLE COLLECTION, PREPARATION AND ANALYSIS

Representative samples of drill core, outcrop chips and archived percussion well chips were submitted for multi-element analysis. Analytical

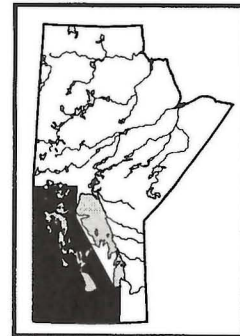
methods include neutron activation (NA) and atomic emission spectrometry (ICP-AES) undertaken by Activation Laboratories Ltd. (Ancaster, Ontario) and a second ICP-AES analysis based upon a hydrochloric acid-potassium chlorate digestion ("UT-10"; Chemex Laboratories Ltd., North Vancouver, British Columbia). The latter analytical approach is designed for samples that are not highly mineralized.

ACKNOWLEDGMENTS

Thanks are extend to staff at the Midland Core Storage facility and to the Petroleum Branch (Energy and Mines) for permission to sample the well cuttings.

REFERENCES

- Bamburak, J.D.
1996: Bentonite investigations and industrial mineral mapping of the Brandon map area (NTS 62G) in Manitoba Energy and Mines, Minerals Division, Report of Activities 1996, p. 127-133.
- Fedikow, M.A.F., Bamburak, J.D. and Weitzel, J.
1995: Geochemistry of Ordovician Winnipeg Formation black shale, sandstone and their metal-rich encrustations, Black Island, Lake Winnipeg (NTS 62P/1); in Manitoba Energy and Mines, Minerals Division, Report of Activities 1995, p. 128-135.
- Schmidtke, B.E. and Fedikow, M.A.F.
1996: Mineralogy of metal-rich encrustations on Ordovician Winnipeg Formation black shales and sandstones, Black Island, Lake Winnipeg (NTS 62 P/1); in Manitoba Energy and Mines, Minerals Division, Report of Activities 1996, p. 139-152.



¹ Geological Survey of Canada, Ottawa, Ontario

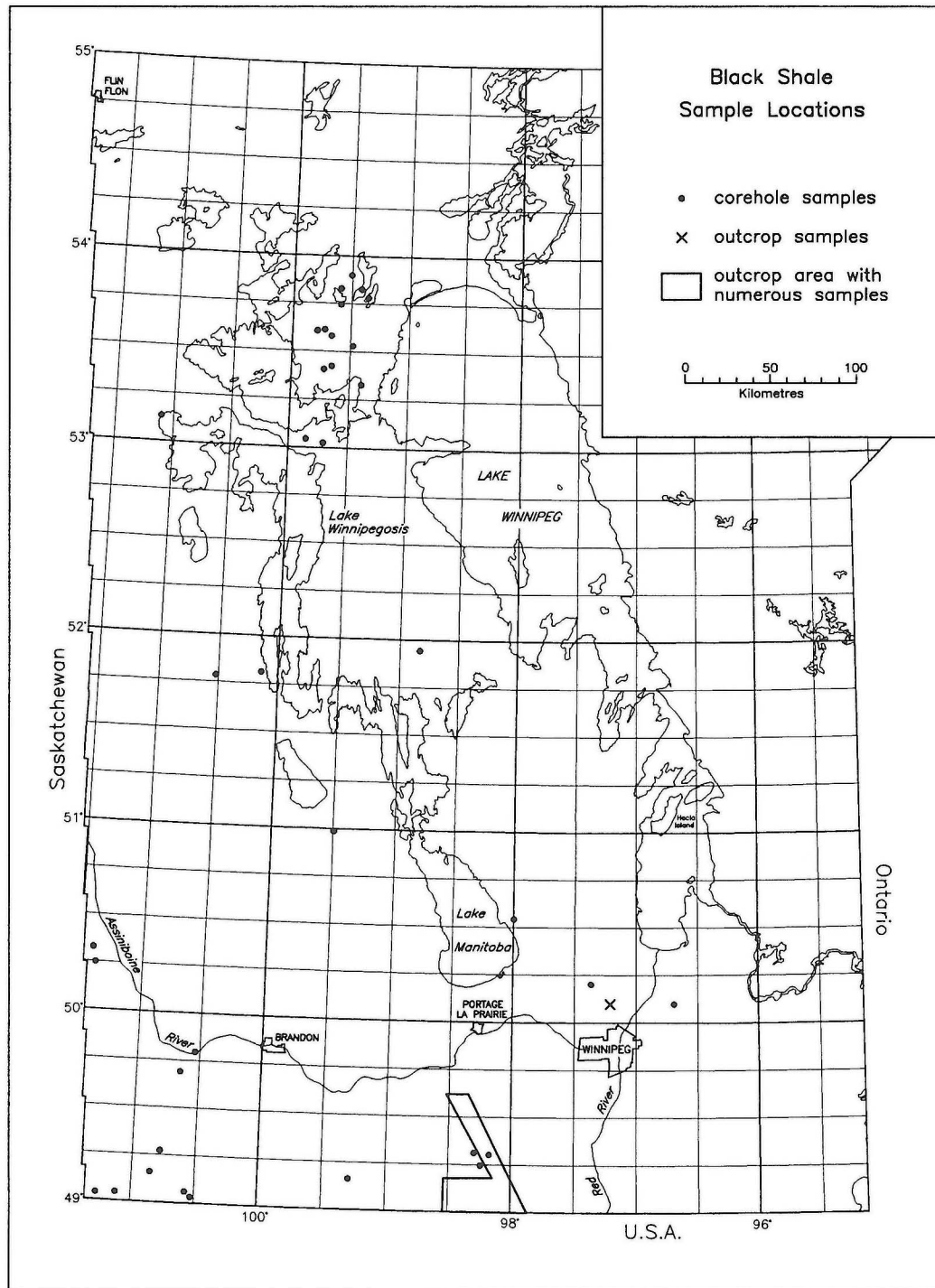
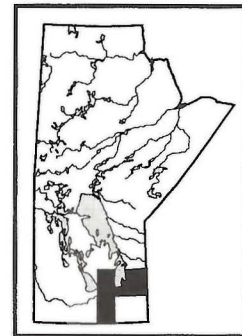


Figure GS-20-1: Sampling sites for outcrop, drill core and well chip samples in Manitoba. GS-20-1: Sampling sites for outcrop, drill core and well chip samples in Manitoba.

GS-21 QUATERNARY GEOLOGICAL, ENGINEERING GEOLOGICAL, AND HYDROGEOLOGICAL INITIATIVES IN THE RED RIVER VALLEY, INTERLAKE, AND SOUTHEASTERN MANITOBA

by G. L. D. Matile and L. H. Thorleifson

Matile, G.L.D. and Tholeifson, L.H. (1997): Quaternary geological, engineering geological, and hydrogeological initiatives in the Red River Valley, Interlake, and southern Manitoba; in Manitoba Energy and Mines, Minerals Division, Report of Activities, 1997, p. 131-132.



INTRODUCTION

Field activities conducted by the Manitoba Geological Services Branch (MGSB) in support of engineering and environmental geology in southern Manitoba intensified during 1997. New initiatives are being carried out in cooperation with the Geological Survey of Canada (GSC), the Manitoba Water Resources Branch (MWRB), and several other agencies.

New surficial geological mapping is underway in the Red River Valley, the southern Interlake, and southeastern Manitoba under the banner of the National Geoscience Mapping Program (NATMAP). This work is following standards established between 1991 and 1996 under the southeastern Manitoba component of Prairie NATMAP I, which included a Canada-Manitoba Partnership Agreement on Mineral Development (MDA) project.

Regional hydrogeological investigations of the intensively utilized bedrock aquifers in the Winnipeg region, and the Quaternary sediments that control their recharge, were initiated in 1997 as a contribution to a program being conducted with the GSC and MWRB. This work is addressing long-term and regional aspects of the saline waters discharging at the base of the Manitoba Escarpment, the freshwater system of the Interlake, and freshwater recharge in the Sandilands of southeastern Manitoba.

MGSB also is contributing to the Lake Winnipeg project, a comprehensive program of surveys and research stimulated by concerns regarding shoreline erosion and water quality. Furthermore, in response to the disastrous flooding of spring 1997, MGSB has initiated research into the fluvial geomorphology of the Red River.

MAPPING

The NATMAP program was established to promote multidisciplinary, cooperative, computer-based programs of new geological mapping, that include opportunities to address mineral resource development, environmental and societal concerns, as well as fundamental geological knowledge, along with ensuring the training of student geologists in mapping procedures.

Under Prairie NATMAP I, 1:100,000 surficial geology maps were completed for the Falcon Lake/Whitemouth Lake area (52E, west half; Matile and Thorleifson, 1995; 1996a) and the Steinbach/St. Malo area (62I, east half; Matile and Thorleifson, 1996b; 1996c). This work included synthesis of data previously collected by the former Aggregate Resources Section of the Mines Branch. Also included was a till geochemical and indicator mineral survey, based on surface till sampling and coring of the Quaternary sequence at 23 sites (Thorleifson and Matile, 1993).

Under Prairie NATMAP II, similar mapping and glacial sediment sampling will be completed, from 1997 to 2000, in the Winnipeg/Morris area (62H, west half), the Stonewall/Arborg area (62I, west half), the Selkirk/Pine Falls area (62I, east half), and the Pinawa/Nopiming area (52L, west half).

The objectives of the new NATMAP project are 1. To obtain an enhanced understanding of the environmental framework and geological history of the Winnipeg region through the collection of new field data, and to communicate this knowledge to users primarily in the form of new, computer-based geological maps, 2. To make major strides in understanding major geological features in the area such as the Belair/Sandilands glaciofluvial complex, 3. To further the establishment of a Winnipeg- and Ottawa-based infrastructure for the rapid production of high-quality, interactive digital cartographic products, 4. To support the training of field geologists in the production of new maps 5. To facilitate mineral exploration, particularly in the exposed shield east of the Winnipeg River, by producing new geological and geochemical maps of the area, 6. To provide an upgraded information base designed to support construction and other engineering activity, 7. To better define geological factors that control the quantity, quality, and long term sustainability of groundwater resources in the Winnipeg region, 8. To support efforts to manage the Lake

Winnipeg basin, by interpreting the evolution of the lake in recent geological time, and the role played by geology in controlling shoreline erosion, and 9. To support environmental and land use management, by mapping the composition and extent of lithological units that are relevant to issues such as waste disposal, soil geochemistry, and vulnerability of aquifers to contamination.

Fieldwork was initiated by a seven-person team during the summer of 1997. Data collection and sampling were carried out by G. Matile of MGSB in the Winnipeg area, by N. Grant of the University of Manitoba in the Stonewall area, and by A. Burt of the University of Waterloo in the Selkirk area. Plans call for systematic coverage to extend to the Morris, Arborg, Pine Falls, Pinawa, and Nopiming areas in 1998, with final follow-up investigations being completed in 1999.

Surficial mapping in the Winnipeg region is being coordinated with the MGSB Capital Region study, an effort to upgrade mapping of the Phanerozoic sequence in the Winnipeg area, and to inventory extractable industrial mineral resources. On the shield to the east, work will be coordinated with synthesis of available Precambrian geological data.

MGSB participants in NATMAP and Capital Region programming are cooperating with the GSC, the MWRB, and the City of Winnipeg to use existing drillhole databases in the mapping efforts. These databases include the Manitoba Stratigraphic Database (MSD) managed by MGSB, the water well database held by MWRB (GWDrill), and an engineering drillhole database originally compiled in the early 1970's by the City of Winnipeg and the GSC.

HYDROGEOLOGICAL INVESTIGATIONS

MGSB also is a participant, with GSC, MWRB, and the University of Manitoba, in a new program of hydrogeological investigations in the Red River Valley and Interlake. The objective of this work is to define geological factors that control groundwater in the Winnipeg region, thereby enhancing the knowledge base that will facilitate sustainable development of groundwater resources through better management and public education.

Communities and farms to the east and north of Winnipeg rely on groundwater from bedrock aquifers. To the west, saline groundwaters are a major constraint to groundwater usage (Betcher et al, 1995). A better knowledge of the factors that control discharge of these saline waters from the sedimentary basin to the west, and the replenishment of freshwater, largely from the Sandilands to the east, will facilitate management and protection of this resource.

Surveys and research under the program will include regional elements that encompass the area from the Escarpment to the Shield, as well as sub-regional and more focussed projects. Regional efforts have included transient electromagnetic soundings, coordinated by C. Hyde of GSC Ottawa, which have been successful in independently indicating the stratigraphic level, and approximate salinity, of saline groundwaters east of the Escarpment, as well as profiling the Precambrian surface below Phanerozoic cover. Also addressing groundwater composition and flow across the region are modeling initiatives coordinated by A. Woodbury of the University of Manitoba Faculty of Engineering, K. Osadetz of GSC Calgary, and A. Desbarats of GSC Ottawa.

In summer 1997, a helicopter survey designed to address the Interlake freshwater system was carried out by W. D. McRitchie and C. A. Kaszycki of MGSB, in cooperation with D. Boyle and A. Desbarats of GSC Ottawa. Research addressing saline waters west of Winnipeg is being initiated by S. Grasby of GSC Calgary, while work on recharge in southeastern Manitoba is being coordinated by M. Hinton of GSC Ottawa.

In all components of the hydrogeological program, major roles are being played by R. Betcher and F. Render of MWRB, along with a coordinating role contributed by H. Thorleifson of GSC Ottawa.

LAKE WINNIPEG PROJECT

The Lake Winnipeg Project was launched in 1994 with the support of Manitoba Hydro and several cooperating agencies, and under the coordination of E. Nielsen of MGSB and H. Thorleifson of GSC Ottawa. The primary objective of the work was to carry out the first comprehensive geological survey of the lake, in order to define the structure and history of the basin. A four-week cruise on board the Canadian Coast Guard Ship *Namoo* in 1994, led by B. Todd of GSC Ottawa and M. Lewis of GSC Atlantic, was followed by a similar, follow-up effort in 1996. Low frequency air gun seismic, high frequency seismic, side scan sonar and coring operations guided by real-time differential GPS navigation were supplemented by biological and limnological sampling carried out in cooperation with the Freshwater Institute of Fisheries and Oceans Canada. It was determined that all or most of the Phanerozoic sequence terminates at a buried escarpment extending from just offshore of Long Point to south of Hecla Island (Todd *et al.*, 1996). Furthermore, evidence was found that much of the lake was dry land until the late Holocene, and it was recognized that pressure ridges formed in ice play a major role in plowing the lake floor. Background knowledge such as this is now influencing topics such as shoreline erosion and groundwater studies.

The principal onshore effort has been research on shoreline processes led by D. Forbes of GSC Atlantic. Reconnaissance surveys in 1994, followed by targeted investigations in 1996, culminated in a month-long intensive effort of surveys and instrumental data collection in September 1997. Meanwhile, previously acquired wave data, supplemented by data from three waverider buoys deployed in 1996, are being analyzed under the direction of J. Doering of the University of Manitoba Faculty of Engineering. Coordinated with the Lake Winnipeg Project is a five-year program, led by A. Lambert of GSC Pacific, of absolute gravity measurements, and GPS measurement of uplift, along a transect from Iowa to Churchill.

FLOODING

Flooding along the Red River during the spring of 1997 was a major disaster that caused much damage and disruption. Attempts to better understand flood risk, and to better prepare the area for potential future

flooding, are now being carried out by many agencies. As a contribution to this effort, G. Brooks of GSC Ottawa and E. Nielsen of MGSB are coordinating research into the fluvial geomorphology and stratigraphy of the river. The work includes an attempt to locate stratigraphic records of past flooding, mapping and sampling of alluvial sediments, and quantification of evolutionary trends influencing the river, including the role of postglacial uplift, which has been causing the river to lose gradient throughout postglacial time.

REFERENCES

- Betcher, R. N., G. Grove, and C. Pupp, C.
1995: Groundwater in Manitoba: hydrogeology, quality concerns, management. National Hydrology Research Institute Contribution CS93017, 43 p.
- Matile, G. L. D. and Thorleifson L. H.
1995: Surficial geology, Whitemouth Lake area, Manitoba, Ontario, and Minnesota. Geological Survey of Canada Open File 2993, Manitoba Energy and Mines Open File 95-1, Scale 1: 100,000.
1996a: Surficial geology, Falcon Lake area, Manitoba and Ontario. Geological Survey of Canada Open File 3030, Manitoba Energy and Mines Open File 95-2, Scale 1: 100,000.
1996b: Surficial geology, Steinbach area, Manitoba. Geological Survey of Canada Open File 3270, Manitoba Energy and Mines Open File 96-6, Scale 1: 100,000.
1996c: Surficial geology, St. Malo area, Manitoba. Geological Survey of Canada Open File 3327, Manitoba Energy and Mines Open File 96-9, Scale 1: 100,000.
- Thorleifson, L. H. and Matile, G. L. D.
1993: Till geochemical and indicator mineral reconnaissance of southeastern Manitoba. Geological Survey of Canada Open File 2750.
- Todd, B. J., Lewis, C. F. M., Thorleifson L. H. and Nielsen, E.
1996: Lake Winnipeg Project: cruise report and scientific results. Geological Survey of Canada Open File 3113, 656 p.

GS-22 TUFA MOUNDS, UPWELLINGS AND GRAVITY SPRINGS IN THE CENTRAL AND NORTHERN INTERLAKE REGION, MANITOBA (PARTS OF NTS AREAS 62O, 62P, 63B AND 63G).

By W. D. McRitchie and C. A. Kaszycki.

McRitchie, W.D. and Kaszycki, C. (1997): Tufa mounds, upwellings and gravity springs in the central and northern Interlake region, Manitoba (parts of NTS areas 62O, 62P, 63B and 63G); in Manitoba Energy and Mines, Minerals Division, Report of Activities, 1997, p. 133-146.

SUMMARY

Groundwater geochemical surveys in Manitoba's Interlake region were expanded under a new joint federal/provincial program to encompass the terrain between Little Limestone Lake (north of Grand Rapids) and Riverton. A range of water, marl, iron oxide and tufa samples were collected from 116 sites (including 70 springs and 12 creeks and rivers) to determine if these media contain anomalous metal concentrations indicative of concealed mineralization in the Paleozoic bedrock.

INTRODUCTION

Manitoba's Paleozoic bedrock has drawn the attention of explorationists for several decades, looking for evidence of Mississippi-Valley-Type lead-zinc mineralization. More recently, groundwater and marls from the Grand Rapids region have been analyzed to search for evidence of anomalous metal concentrations that might point to concealed mineralization in the carbonate rocks of the hinterland (McRitchie, 1989, 1994, 1995, 1996).

Ongoing discussions between the federal and provincial survey organizations identified an opportunity to expand the groundwater geochemical investigations as part of a new NATMAP and Hydrogeological initiative, under the umbrella of Manitoba's new Bilateral Geoscience Accord. Accordingly, a nine day helicopter-supported project was initiated in the Interlake region during the latter part of August. This period of the year was selected to optimize the base flow component of the spring waters, thereby minimizing potential dilution by surface runoff or shallow meteoric systems.

The locations of marly fen pools were initially identified from aerial photos and photomosaics (Fig. GS-22-1a). In this survey, a total of 116 sites were visited. Marls were collected at 94 sites (Fig. GS-22-1b), as well as 22 iron oxide samples from tufa mounds and 6 tufa samples (Table GS-22-1). Water samples were collected at 94 sites, including 70 springs and 12 creeks and rivers (Fig. GS-22-2a, 2b). The survey included repeat analyses of some sites previously sampled in the Grand Rapids region in order to establish a standardized (time-specific) regional database. Additional bedrock fracture measurements were also collected from five sites to expand the bedrock fracture database covering the Interlake (Preliminary Geological Map 1997P-3).

METHODOLOGY

On-site measurements of pH, T°C and conductivity were taken using a Hach I pH meter and a Hach conductivity meter. GPS coordinates were determined using an Eagle Explorer GPS unit (version 1.8). Five aliquots of water were collected at each site. Two 60 ml samples, scheduled for ICP-MS analysis at the GSC, were field filtered and the cation sample acidified with 0.2% by volume Ultrex II nitric acid each evening. A 250 ml sample, scheduled for hydride (antimony, arsenic, selenium and mercury) analysis at the Manitoba Technology Center (MTC,) was filtered and acidified in the field, and a second 250 ml sample for anions and alkalinity determinations was filtered in the laboratory, prior to analysis. An unfiltered and unacidified 500 ml sample was also collected for isotope analysis (Tritium, Deuterium and O¹⁸) at the University of Waterloo.

Marl and iron oxide samples (500-1000 gm) were scooped from fen pools using a melamine ladle. Each sample was pressure filtered/dried in a perforated freezer bag and enclosed in a ziplock bag for transfer to the laboratory for air drying and analysis.

FIELD OBSERVATIONS

Very few westward flowing springs have been identified in the Grand Rapids region. Further south, thick Quaternary cover and a dominating ridge and swale topography west of Provincial Highway #6 (Manitoba Soil Surveys Report, Waterhen area) obscures all evidence of resurgences upwelling to the west of the height of land. Accordingly, this survey focused

entirely on those emergent points flowing generally eastwards into Lake Winnipeg.

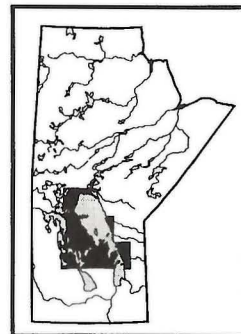
A distinct contrast in the nature of the springs north and south of Long Point was recognized, those to the north being dominantly gravity springs flowing out of the base of a well developed regional escarpment (Figs. GS-22-3m, 3n), those to the south being mainly artesian (Figs. GS-22-3a-3i), with upwellings and tufa mounds (Ford and Williams, 1989) heading up distinctive "Tadpole" shaped drainage elements (Fig. GS-22-4).

The emergent points north of Grand Rapids typically drain into a series or chain of ephemeral fen pools that display a well defined zone of marl precipitation ("paludal tufa", Ford and Pedley, 1996). Linear surge channels are overprinted on the entire system giving way to untreed spring fens in their lower reaches (McRitchie, 1994).

South of Long Point, surficial deposits are much more prevalent and the overall topographic relief is more muted, with extensive water-saturated treeless fens and ribbon bogs. Groundwater comes to surface in circular upwellings, many being the site of tufa mounds (19 in this survey) (Figs. GS-22-3i). The upwellings range in diameter from 3-200 m and in relief from 0-5 m above the surrounding fen pools. The surrounding fen pools are commonly arranged concentrically around the central upwelling, with several rings, separated by low relief peaty ridges, around the larger springs (Fig. GS-22-3d, 3e, 3f). Water flows radially out of the mounds and then down slope in narrow untreed sedge-lined surge channels with isolated islands of peat, covered with typical trees and shrubs (e.g. black spruce, tamarack, cedar and birch).

The central pools in the core of the mounds range up to 25 meters in diameter and 5 meters in depth (e.g. the "Bluehole" west of Sturgeon Bay) (Fig. GS-22-3a, 3c). East of Lake St. Martin, at station M1095 (UTM 558558E, 5726885N), nested craters caused by periodically emerging gases, were observed in sediments on the floor of a well developed spring pool. Elsewhere the emerging waters in the pools are a limpid, clear, green or blue colour with rust-brown iron oxide coatings and flocculents on the surrounding floating mosses and vegetation, and down the radially draining channels. On the upper reaches of the mounds, the iron oxide-rich zone forms a 2-4 cm thick layer encompassing the root zone of the surface mosses. Beneath it, a 1-5 cm thick, commonly friable tufa layer forms a blanket that embraces the entire elevated portion of the mound. Where buried, the tufa is cream coloured and intimately intergrown with the roots of the mosses, on which it appears to have been accreted. On the flanks of the mounds, highly skeletal and porous masses of white and buff tufa are commonly exposed on small ledges and in the walls of narrow, radial erosional channels. On the terraced slopes, small seepages and shallow pools are typical, many with "oily" films thought to reflect the presence of iron oxides. In the proximal fen pools flanking the mounds, carbonate-bearing algal mats and flocculants are typical, these giving way to thin white marly sediments, and thicker creamy marls in the more distal pools (50-100 m from the resurgence).

The area of each upwelling displays a regular zonation in both vegetation and physical characteristics (Fig. GS-22-5 and GS-22-6). Typically the emergent pool is surrounded by floating mats of bright, lime-green moss (*Scorpidium scorpioides* and *Dicranum undulatum*), and common butterwort (*Pinguicula vulgaris*), with sporadic sundew plants (*Drosera rotundifolia*). This zone gives way to one in which tufted grass mounds (*Carex aquatilis*) are dominant, these overgrow the entire resurgence where the vegetative mats are thicker. Outside of the tufted grass zone, dwarf birch (*Betula pumila*), dwarf and silverleaf willow (*Salix candida*), potentilla (*Potentilla fruticosa*), tamarack (*Larix laricina*), black spruce (*Picea mariana*), cedar (*Thuja occidentalis*), creeping juniper (*Juniperus horizontalis*), labrador tea (*Ledum groenlandica*) and bunchberry (*Cornus canadensis*) predominate. Down on the marly fen pools (with their interspersed peaty ridges), sedges predominate (*Carex prairea*), together



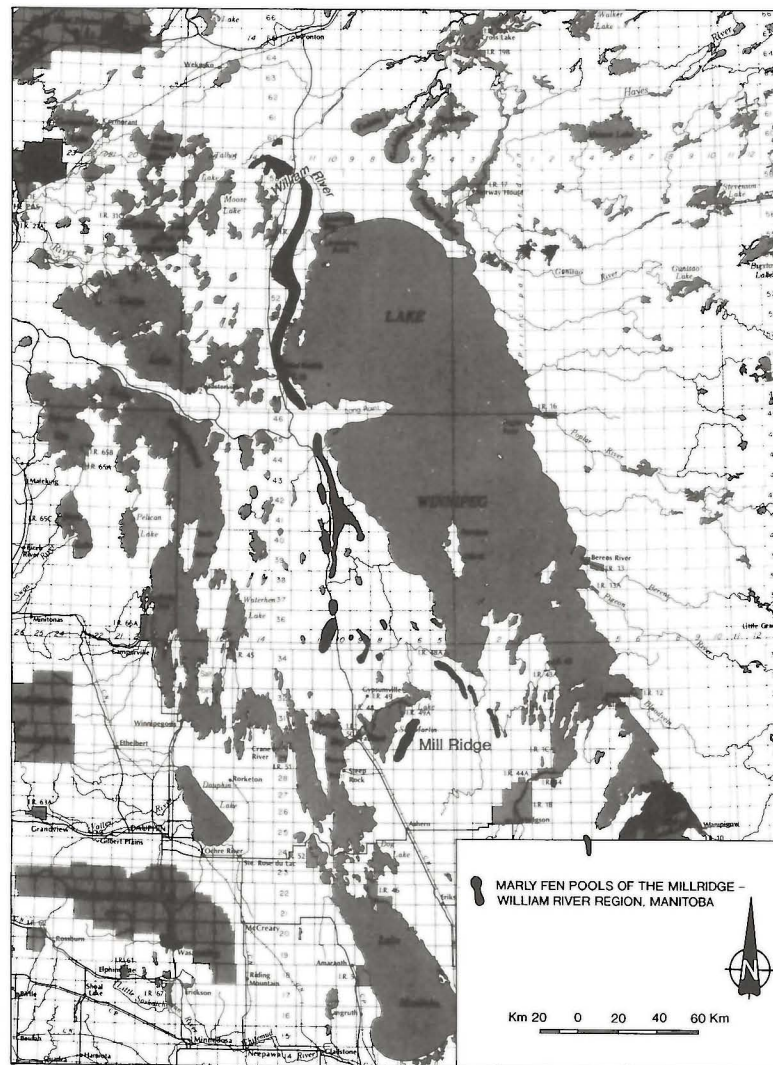


Figure GS-22-1a: Marly fen pools of the Mill Ridge-William River region, Manitoba. 1b: Location of marl sample sites.

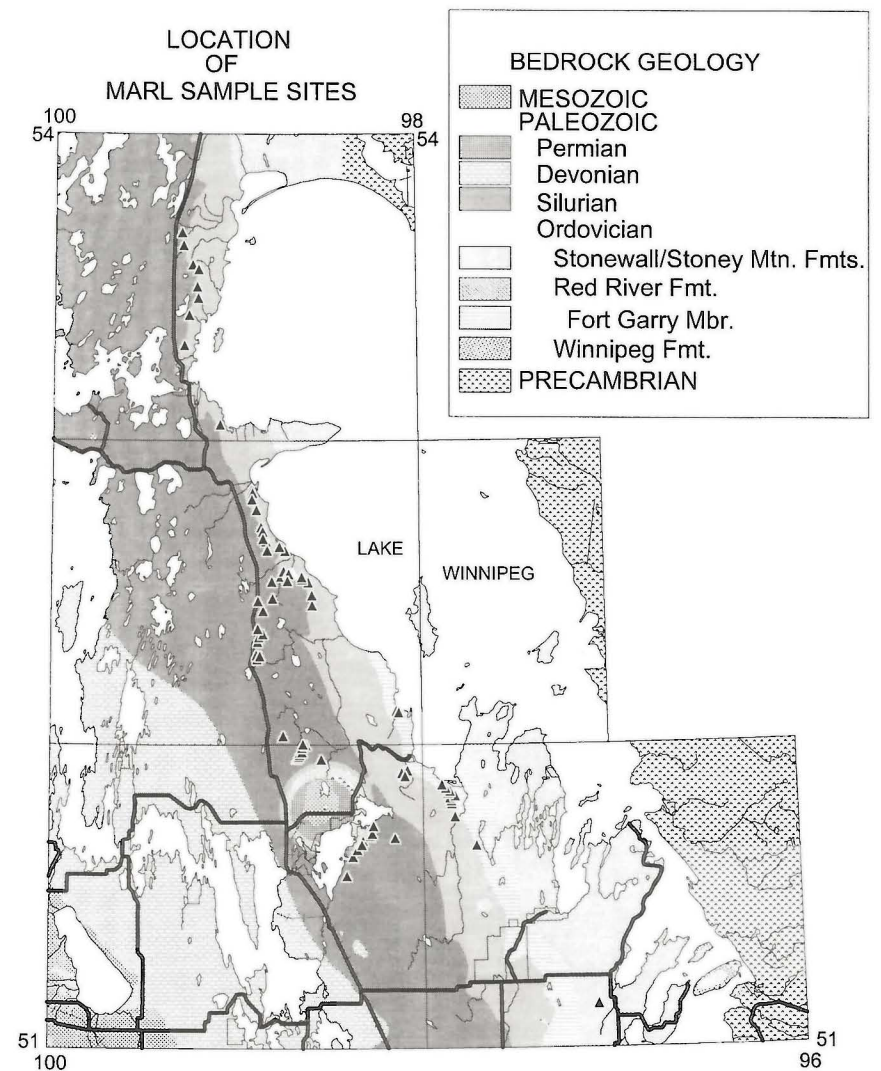


Figure GS-22-1b: Location of spring sample sites.

Table GS-22-1a

Station number, sample type, UTM coordinates, pH, ToC, conductivity and anion concentrations for spring and creek waters

Sample #	Easting	Northing	Sample Type	Class.	ToC	Cond.	pH	Tufa	pH (lab)	Bicarb.	Chloride	Nitrate/Nitrite	Sulphate	Fluoride
1001	507925	5852555	creek	C	14.7	486	7.29	no	7.83	332	1.2	0.01	11	0.1
1002	505611	5857048	creek	C	15	261	7.88	no	7.83	172	1.2	0.02	13	0.1
1003	505791	5857378	creek	C	16	280	7.7	no	7.69	178	2.5	0.04	14	0.1
1004	494156	5877925	upwelling	Sk	10.5	488	8.2	no	7.76	322	3.71	0.32	5	0.2
1005	507599	5847218	marly fen pool	P	17.3	430	8.71	no	8.45	265	0.9	0.01	5	0.1
1006	510004	5839311	upwelling	Sm	14.4	620	7.72	no	7.8	428	0.8	0.03	5	0.2
1008	512305	5840461	creek	C	16.5	422	8.21	no	8.12	289	1.2	0.01	13	0.1
1009	521626	5830483	creek	C	16.3	342	8.3	no	8.09	151	23	0.01	17	0.1
1010	521209	5828713	creek	C	16.1	294	7.93	no	7.9	196	1.81	0.01	14	0.3
1011	518117	5832142	marly fen pool	P	16.9	371	7.75	no	7.94	251	1.2	0.01	12	0.4
1012	518092	5832066	upwelling	Sm	12.6	573	7.8	no	7.97	390	1.3	0.03	5	0.6
1013	516665	5833568	marly fen pool	P	18.9	411	7.77	no	7.83	274	1	0.07	10	0.4
1014	511594	5832332	upwelling	Sm	5.8	660	7.97	yes	7.79	464	1.4	0.01	5	0.2
1015	511594	5832332	marly fen pool	P	20.7	425	8.15	yes	8.2	318	1.3	0.01	10	0.1
1016	516959	5822852	upwelling	Sm	5.4	614	7.82	no	7.9	425	1.5	0.05	5	0.7
1017	517662	5824688	upwelling	Sm	4.9	633	7.66	no	7.5	417	1.6	0.02	10	0.8
1018	588587	5724416	upwelling	Sm	4.4	730	7.31	yes	7.43	481	1.2	0.03	16	0.3
1019	588645	5724446	marly fen pool	P	15	679	8.18	no	8.27	457	1.2	0.06	13	0.2
1020	588587	5724416	outflow channel	Sm	9	705	7.78		7.97	484	1.1	0.01	14	0.2
1021	588587	5724416	outflow channel	Sm	6.3	718	7.5		7.49	485	1.3	0.02	14	0.2
1022	580719	5735164	marly fen pool	P	19.4	662	8.26	no	8.29	316	4.5	0.03	126	0.4
1023	580719	5735164	upwelling	Sm	5.7	944	7.43	yes	7.9	392	5	0.07	195	0.4
1024	579227	5740848	upwelling	Sm	4.3	760	7.22	no	7.5	431	2.2	0.03	73	0.3
1025	578828	5742060	upwelling	Sm	4.3	733	7.35	no	7.67	433	1.8	0.02	50	0.2
1026	578057	5743807	upwelling	Sm	6.3	670	7.39	yes	7.67	409	1.3	0.04	32	0.2
1027	578830	5744498	upwelling	Sm	6.3	684	7.54	yes	7.63	414	1.6	0.02	45	0.2
1028	577222	5745598	upwelling	Sm	5	666	7.4	yes	7.62	409	1.3	0.01	25	0.3
1029	575854	5746742	upwelling	Sm	15.4	610	7.64	yes	7.77	379	1.5	0.03	22	0.3
1030	480277	5947831	spring	Sk	7.3	532	7.44	no	7.81	352	0.8	0.09	5	0.1
1031	480872	5943177	spring	Sk	7.4	497	7.56	no	7.65	326	0.9	0.11	5	0.2
1033	484137	5935884	spring/brook	Sk	5.4	463	7.6	no	7.58	307	0.8	0.2	5	0.2
1034	484396	5936188	spring/creek	Sk	6	458	7.56	no	7.63	302	0.8	0.24	5	0.2
1035	486367	5934260	spring/brook	Sk	8.1	477	7.97	no	7.95	317	0.7	0.1	5	0.2
1036	485760	5927901	spring/brook	Sk	7.6	453	7.66	no	7.72	297	0.6	0.22	5	0.1
1037	486137	5923746	spring/brook	Sk	4.9	521	7.62	no	7.71	349	1	0.12	5	0.3
1038	482810	5917512	spring/brook	Sk	4.8	516	7.57	no	7.74	349	0.8	0.1	5	0.3
1039	477430	5918106	spring/brook	Sk	4.6	524	7.63	no	7.66	349	1	0.25	5	0.2
1040	482346	5906218	marly fen pool	P	14.4	535	7.4	no	7.99	351	2.7	0.02	5	0.2
1042	481006	5906452	upwelling	Sm	4.9	556	7.61	no	7.66	364	2.8	0.04	5	0.2
1043	528038	5812316	upwelling	Sm	3.4	645	7.53	no	7.5	426	0.7	0.02	5	0.4
1044	527642	5817601	spring/brook	Sk	7.3	474	7.6	no	7.77	296	0.7	0.19	5	0.2
1046	524309	5822671	upwelling	Sk	3.6	604	7.62	no	7.6	388	3.7	0.03	5	0.4
1047	521250	5823485	upwelling	Sm	5.4	639	7.61	no	7.49	433	10	0.05	5	1.3
1048	520579	5824117	upwelling	Sm	3.9	678	7.14	no	7.46	429	7.4	0.01	5	1
1049	519988	5823946	upwelling	Sm	5.2	679	7.35	no	7.45	432	5.5	0.16	5	0.9
1050	520028	5823790	upwelling	Sm	5.1	674	7.33	no	7.45	433	6	0.09	5	1

Table GS-22-1a

Station number, sample type, UTM coordinates, pH, ToC, conductivity and anion concentrations for spring and creek waters

1051	519511	5823721	upwelling	Sm	5.2	670	7.36	no	7.59	431	4.8	0.03	5	1
1053	519486	5821621	upwelling	Sm	3.5	682	7.3	no	7.44	428	7.2	0.03	5	1.1
1054	519092	5821181	upwelling	Sm	6.2	668	7.37	no	7.62	431	6.1	0.03	5	1.1
1055	518754	5818077	spring/brook	Sm	8	521	7.87	no	7.62	346	0.9	0.06	5	0.1
1056	513587	5814773	upwelling	Sm	2.5	673	7.45	no	7.52	423	2.7	0.05	5	0.6
1057	507709	5792554	upwelling	Sm	4.9	600	7.74	no	7.53	392	1.7	0.02	5	1.3
1058	507495	5793994	upwelling	Sm	5.7	571	7.7	no	7.68	374	1.1	0.02	5	0.9
1059	508823	5796578	upwelling	Sm	4.3	584	7.69	no	7.87	374	1.6	0.02	5	0.2
1060	508005	5798856	upwelling	Sm	4.5	552	7.74	yes	7.8	366	1.4	0.1	5	0.1
1061	508442	5800532	upwelling	Sm	4.4	578	7.44	yes	7.71	382	1.1	0.08	5	0.2
1062	509967	5801564	upwelling	Sm	4.8	577	7.3	yes	7.64	379	1.1	0.03	5	0.4
1063	539178	5800589	river	C	21.9	210	8	no	7.86	133	1.7	0.04	17	0.1
1064	508084	5803508	upwelling	Sm	4.8	600	7.52	no	7.77	397	0.9	0.18	5	0.2
1065	510073	5810146	upwelling	Sm	4.7	494	7.59	no	7.61	324	1.9	0.15	5	0.2
1066	509015	5810981	spring pool	Sm	4.8	524	7.56	no	7.63	338	1.1	0.09	5	0.2
1067	508168	5813722	upwelling	Sm	4.1	566	7.57	no	7.7	371	1.3	0.12	5	0.1
1068	539947	5799886	creek	C	18.6	128	7.48	no	7.48	94	1.7	0.005	22	0.1
1069	558521	5775016	river	C	22.2	562	8.06	no	7.91	161	80	0.01	11	0.1
1070	559092	5773780	upwelling	Sm	4.3	788	7.23	yes	7.31	530	3.3	0.04	5	0.7
1073	523405	5757341	seep	Ss	9.9	578	7.31	no	7.44	399	1.4	0.005	12	0.2
1074	524292	5758303	seep	Ss	16.7	544	7.51	no	7.52	444	1.7	0.08	12	0.2
1075	524608	5761247	upwelling	Sm	3.6	688	7.53	no	7.5	417	3.7	0.01	25	0.6
1076	531287	5755606	upwelling	Sm	4.9	672	7.56	yes	7.62	449	1.5	0.01	5	0.4
1077	545577	5760189	upwelling	Sm	5.1	613	7.64	no	7.69	420	0.9	0.13	5	0.2
1078	562283	5749677	upwelling	Sm	7.8	854	7.59	no	7.96	424	9.7	0.05	130	0.3
1079	562075	5749892	upwelling	Sm	4.5	880	7.38	no	7.46	442	9.8	0.02	124	0.4
1080	562096	5751269	upwelling	Sm	6.9	810	7.59	yes	7.66	379	17	0.13	136	0.4
1081	562819	5751364	upwelling	Sm	4.6	816	7.58	no	7.58	392	12	0.08	129	0.4
1082	563234	5751796	upwelling	Sm	4.6	806	7.51	no	7.68	393	8.4	0.02	110	0.4
1083	561060	5750902	upwelling	Sm	3.7	1086	7.49	no	7.6	396	43	0.01	215	0.4
1084	562194	5754142	creek	C	21.9	302	8.11	no	7.98	189	4.1	0.01	15	0.1
1085	563613	5769246	spring pool	Sm	16.3	705	7.53	no	7.56	463	4.6	0.04	5	0.7
1086	560819	5773082	upwelling	Sm	5.7	812	7.29	no	7.28	535	3.6	0.05	5	1
1087	559991	5773212	upwelling	Sm	4.7	795	7.4	yes	7.43	540	3.5	0.02	5	0.7
1088	541862	5714400	spring pool	Sm	7.7	571	7.56	no	7.67	387	1.2	0.13	5	0.3
1090	544545	5722383	spring pool	Sm	13.9	610	7.69	no	7.96	424	1.2	0.02	5	0.1
1091	546161	5724162	upwelling	Sm	5.4	590	7.65	yes	7.75	418	1.5	0.13	5	0.2
1092	549982	5728451	marly fen pool	P	20.4	598	7.8	no	7.95	434	15	0.04	5	0.1
1094	556971	5728423	upwelling	Sm	5.3	589	7.7	no	7.6	381	1.3	0.08	5	0.2
1095	558558	5726885	upwelling	Sm	6.5	627	7.44	no	7.59	399	1.9	0.05	13	0.3
1096	580633	5742825	upwelling	Sm	4.9	710	7.42	yes	7.49	424	2.4	0.04	51	0.3
1097	584017	5739875	river	C	21.4	363	8.05	no	8.02	238	1.8	0.13	14	0.1
1098	618081	5694022	spring pool	P	13.9	494	7.52	no	7.75	327	1	0.04	5	0.2

Table GS-22-1b

Station number, sample type and UTM coordinates for marl and iron oxide samples

Sample	Easting	Northing	Sample Type	Environment	Sample	Easting	Northing	Sample Type	Environment
04-97-1	505663	5854174	marl	marly fen pool	04-97-60	508823	5793578	marl	marly fen pool
04-97-2	505759	5854422	marl	marly fen pool	04-97-61	522382	5756103	marl	marly fen pool
04-97-3	506178	5853462	marl	marly fen pool	04-97-62	508005	5798856	marl	edge of mound
04-97-4	505966	5851091	marl	marly fen pool	04-97-63	508442	5800532	marl	marly fen pool
04-97-5	494157	5877907	marl	creek marl	04-97-64	509967	5801564	marl	marly fen pool
04-97-6	507599	5847218	marl	algal mat	04-97-65	508084	5803508	marl	marly fen pool
04-97-7	509321	5840951	marl	marly fen pool	04-97-66	510073	5810146	marl	marly fen pool
04-97-8	510004	5839311	marl	marly fen pool	04-97-67	508168	5813722	marl	marly fen pool
04-97-9	510026	5836659	marl	marly fen pool	04-97-68	559092	5773780	marl	marly fen pool
04-97-10	511109	5835777	marl	marly fen pool	04-97-69	559092	5773780	Fe Ox	side of mound
04-97-11	518117	5832142	marl	brook	04-97-70	523011	5756633	marl	marly fen pool
04-97-12	518117	5832142	marl	brook	04-97-71	523405	5757341	marl	marly fen pool
04-97-13	518175	5832290	marl	marly fen pool	04-97-72	523488	5758242	marl	marly fen pool
04-97-14	516083	5833675	marl	marly fen pool	04-97-73	523469	5758209	marl	marly fen pool
04-97-15	511594	5832332	marl	upwelling	04-97-74	523404	5758168	marl	marly fen pool
04-97-16	513277	5820905	marl	marly fen pool	04-97-75	524297	5758320	marl	rivulet
04-97-17	516595	5822852	marl	marly fen pool	04-97-76	524288	5759975	marl	marly fen pool
04-97-18	517662	5824688	marl		04-97-77	525609	5760912	marl	marly fen pool
04-97-19	519286	5823952	marl	marly fen pool	04-97-78	524608	5761247	marl	marly fen pool
04-97-20	588645	5724446	marl	marly fen pool	04-97-79	517319	5764239	marl	marly fen pool
04-97-21	588587	5724416	Fe Ox	outflow channel	04-97-80	535225	5758303		marly fen pool
04-97-22	588587	5724416	grey clastics	outflow channel	04-97-81	546614	5725680	marl	marly fen pool
04-97-23	580719	5735164	marl	marly fen pool	04-97-82	531287	5755606	marl	marly fen pool
04-97-24	579468	5739944	marl	marly fen pool	04-97-83	531287	5755606	tufa	mound
04-97-25	579301	5740950	marl	marly fen pool	04-97-84	562283	5749677	marl	marly fen pool
04-97-26	578828	5742060	marl	marly fen pool	04-97-85	562283	5749677	Fe Ox	side of mound
04-97-27	578057	5743807	marl	marly fen pool	04-97-86	562075	5749892	marl	marly fen pool
04-97-28	578830	5744498	marl	marly fen pool	04-97-87	562093	5750035	marl	marly fen pool
04-97-29	577222	5745598	marl	marly fen pool	04-97-88	562096	5751269	marl	marly fen pool
04-97-30	575854	5746742	marl	marly fen pool	04-97-89	562096	5751269	Fe Ox	side of mound
04-97-31	480277	5947831	marl	marly fen pool	04-97-90	562819	5751364	marl	flocculent
04-97-32	480872	5943177	marl	brook	04-97-91	562819	5751364	Fe Ox	30cm from vent
04-97-33	484132	5936012	marl	creek	04-97-92	562819	5751364	anoxic prec	at vent
04-97-34	486367	5934260	marl	marly fen pool	04-97-93	563234	5751796	marl	inner fen pool
04-97-35	485760	5927901	marl	marly fen pool	04-97-94	563234	5751796	marl	outer fen pool
04-97-36	486137	5923746	marl	marly fen pool	04-97-95	563234	5751796	Fe Ox	side of mound
04-97-37	482810	5917512	marl	marly fen pool	04-97-96	561060	5750902	marl	marly fen pool
04-97-38	481006	5906452	marl	marly fen pool	04-97-97	561060	5750902	Fe Ox	side of mound
04-97-39	528038	5812316	Fe Ox	rivulet	04-97-98	560819	5773082	marl	marly fen pool
04-97-40	528038	5812316	marl	marly fen pool	04-97-99	560819	5773082	Fe Ox	side of mound
04-97-41	527937	5816032	marl	marly fen pool	04-97-100	559991	5773212	marl	marly fen pool
04-97-42	526638	5820720	marl	marly fen pool	04-97-101	559991	5773212	Fe Ox	side of mound
04-97-43	524415	5821821	marl	marly fen pool	04-97-102	540622	5712610	marl	marly fen pool

Table GS-22-1b

Station number, sample type and UTM coordinates for marl and iron oxide samples

04-97-44	524309	5822671	marl	marly fen pool	04-97-103	542897	5719735	marl	marly fen pool
04-97-46	520579	5824117	marl	marly fen pool	04-97-104	544545	5722383	marl	marly fen pool
04-97-47	520579	5824117	Fe Ox	side of mound	04-97-105	546161	5724162	marl	marly fen pool
04-97-48	519995	5823845	marl	marly fen pool	04-97-106	546614	5725680	marl	marly fen pool
04-97-49	519995	5823845	Fe Ox	side of mound	04-97-107	546161	5724162	tufa	edge of mound
04-97-50	519511	5823721	marl	marly fen pool	04-97-108	549177	5727546	marl	marly fen pool
04-97-51	519511	5823721	Fe Ox	side of mound	04-97-109	549982	5728451		marly fen pool
04-97-52	519092	5821181	Fe Ox	side of mound	04-97-110	562283	5749677	Fe Ox	field dup 85
04-97-53	519092	5821181	marl	marly fen pool	04-97-111	550464	5731333	marl	marly fen pool
04-97-54	513587	5814773	marl	brook	04-97-112	550464	5731333	marl	marly fen pool
04-97-55	513587	5814773	Fe Ox	channel	04-97-113	558558	5726885	marl	marly fen pool
04-97-56	480277	5947831	marl	field dup (31)	04-97-114	580633	5742825	marl	marly fen pool
04-97-57	507709	5792554	marl	marly fen pool	04-97-115	580633	5742825	Fe Ox	side of mound
04-97-58	507495	5793994	marl	marly fen pool	04-97-116	580633	5742825	tufa	side of mound
04-97-59	507495	5793994	Fe Ox	side of mound	04-97-117	633652	5667216	marl	marly fen pool

with pitcher plants (*Sarracenia purpurea*), cattails (*Typha latifolia*), wet or aquatic mosses (*Drepanocladus spp.*), horsetails (*Equisetum fluviatile*), common reed grass (*Phragmites australis*) and rushes (*Scirpus spp.*).

White carbonate slimes and encrustations ("fringe cements", Ford and Pedley, 1996), readily apparent on the exposed roots of peaty and grassy tussocks in and surrounding most pools, indicate that water levels were approximately 20 cm below flood levels. Aggregates of circular, indurated "lozenges" locally litter the surface of the marly precipitates. They appear to be tufa-like residues that were originally formed on the underside of 1-4 cm black algal growths that form colonies in areas of continued surface run-off.

TOPOGRAPHIC/GEOLOGIC RELATIONSHIPS

Springs appear to be clustered in three distinct groupings. As mentioned previously, those north of Grand Rapids are gravity springs and their distribution closely follows the Silurian escarpment in this region (Figure GS-22-2a).

A second group of springs is clustered in the central part of the study area, just south of Long Point. These springs are all classified as artesian, forming tufa mounds and upwellings and some precipitating tufa and/or iron oxide. These springs also tend to follow the Silurian escarpment (Fig. GS 22-2a), but unlike the gravity springs to the north, they occur at a variety of elevations (Fig. GS-22-2b) and extend a significant distance westward across the Silurian upland. The digital elevation model for this area, reveals that the westernmost extent of springs sampled in this study is coincident with the edge of the Silurian upland plateau. The occurrence of marly fen pools has been mapped further west on the upland plateau, but these sites were not investigated in this survey.

The third cluster of springs is centred on Gypsumville in the west and extend eastward to the shore of Lake Winnipeg. Similar to group II, these springs are all artesian, forming tufa mounds and upwellings. Springs within this cluster occur at a variety of elevations, bounded by the Silurian upland plateau to the west (Fig. GS 22-2a,2b). A significant number of springs in this group occur within the Fort Garry Member of the Red River Formation, or adjacent to its contact with the Stonewall/Stony Mountain Formations to the east.

Although many of the upwellings in any one area appear to emerge at about the same elevation (slightly downslope from muted upland ridges), two distinct tiers of resurgences were observed west of Dancing Point (group I) and west of Sturgeon Bay (group II) (Fig. GS-22-4d).

SPRING WATER GEOCHEMISTRY

Although spring waters are being analyzed for a variety of trace and major elements, the only water quality data currently available are those parameters measured in the field, as well as anions and alkalinity. Preliminary observations and interpretations have been based on this limited data set.

Preliminary data analysis indicates that all waters collected in this study are consistent with parameters identified by Betcher *et al.* (1995) for the fresh water facies of the carbonate-evaporite unit within the Interlake area (Table GS-22-2). Samples were divided into three subpopulations based on the type of water sampled (gravity spring, artesian spring, standing pool). Subtle, but distinct, differences between sample subpopulations have been observed in the average values of several water quality parameters. In general water in artesian springs tends to be colder, has a higher conductivity and lower pH than gravity springs. These also tend to be elevated with respect to bicarbonate, chloride, fluoride and sulphate and depleted in nitrate/nitrite when compared with gravity springs. This may reflect a longer subsurface residence time for water emerging from mounds than water issuing from gravity flow systems.

Water collected from marly fen pools is significantly warmer, with elevated pH as compared to either type of spring water. These observations are consistent with those derived from serial sampling at Station M97-1018, where a gradual decrease in conductivity, and parallel increases in pH and T°C were observed from the emergent point downstream into the surrounding fen pools (Table GS-22-3). In general, in well developed upwellings, water temperatures at the point of emergence are typically 3.5-4.9°C, rising to >20°C in the outlying marly fen pools. The pH values, close to 7.4 in the springs, increase to over 8.0 in the marly fen pools, similar to trends observed at Grand Rapids (McRitchie, 1994).

Regional Trends

On a regional scale, distinct patterns in the distribution of several water quality parameters have been observed (Fig. GS-22-7a-7d). Although quantitatively the variability is very subtle, the strong regional trends observed in the data suggest differences may be related to variations in lithology along gradient.

Conductivity A pronounced southwardly increasing gradient in conductivity (Fig. GS-22-7a) is marked by: 1) low values for gravity springs north of Grand Rapids; 2) moderate to high values for the artesian springs south of Long Point and in the Gypsumville area, where artesian springs emerge at the Silurian escarpment or within the Silurian

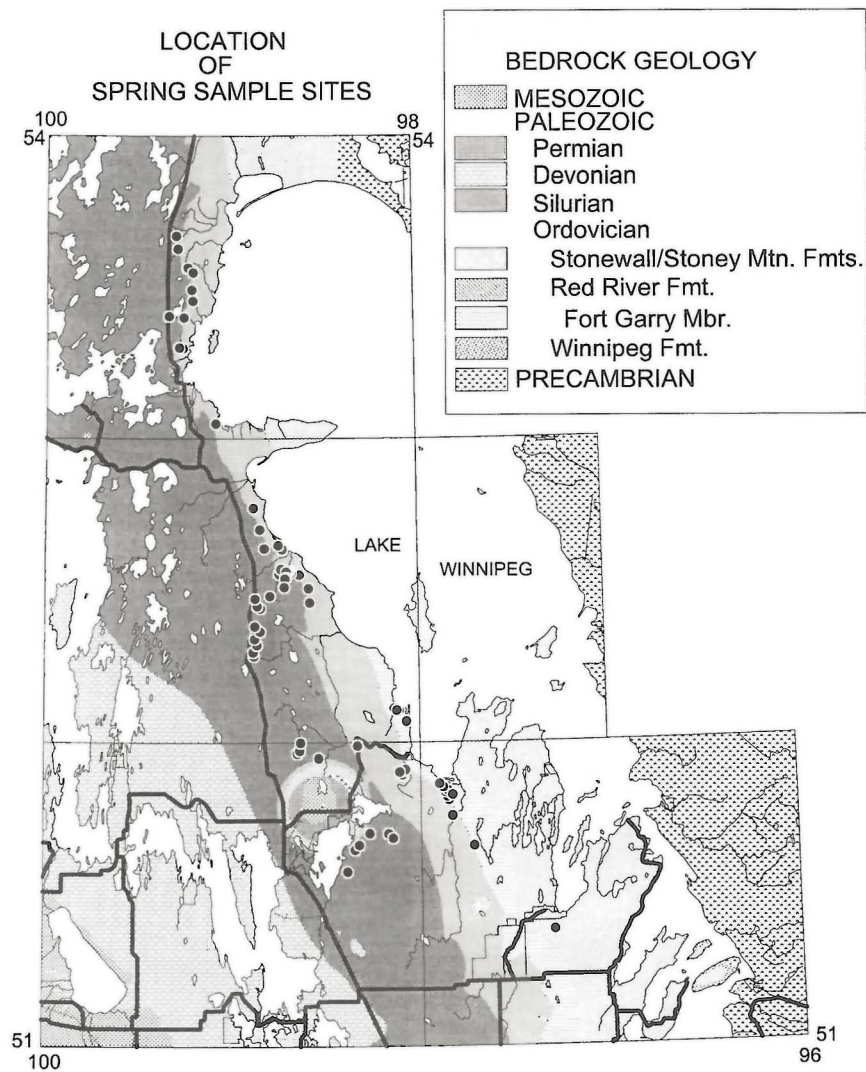


Figure GS-22-2a: Location of spring sample sites

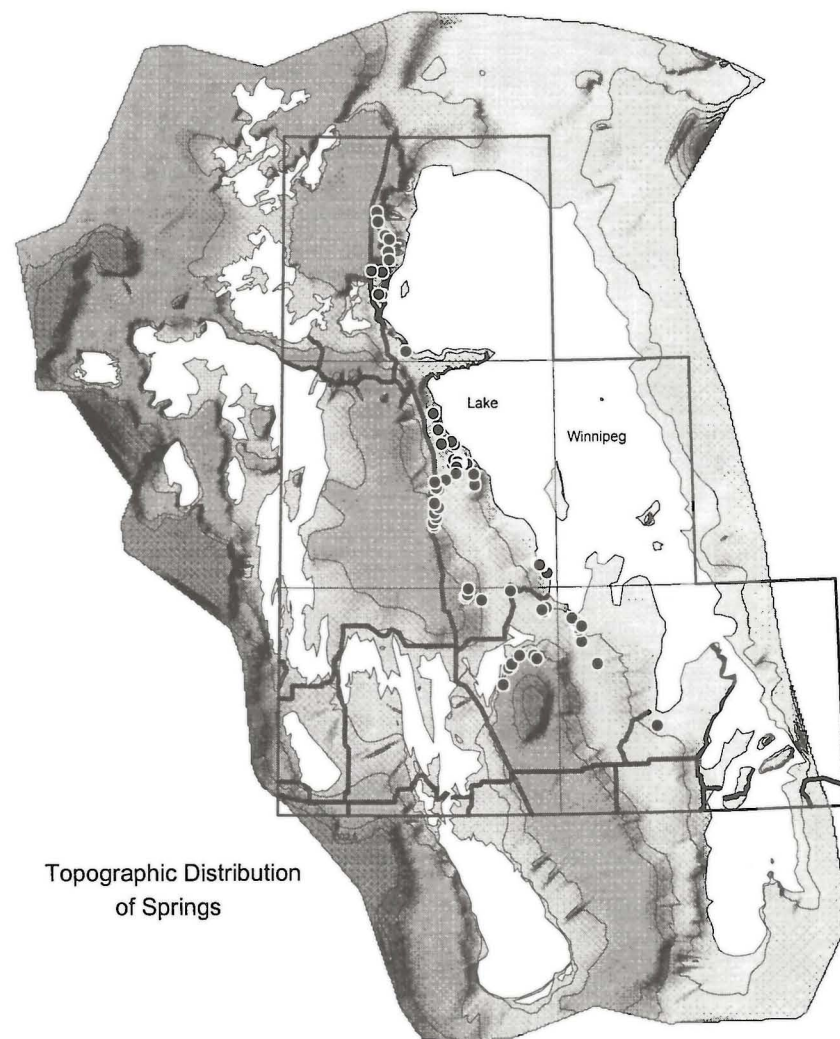


Figure GS 22-2b Topographic distribution of springs sampled in Manitoba's central and northern Interlake regions.



Figure GS-22-3a: "Bluehole # 1", a 5m deep, 7 X 12 m diameter spring pool perched in the core of a 2 m high tufa mound, west of Sturgeon Bay, Lake Winnipeg. (Site 1027. UTM 578830E 5744498N).



Figure GS-22-3b: "Bluehole #2", spring pool in core of tufa mound with vegetation mats around the periphery of the pool, and marly fen pools in surrounding flats. 275 m NNW of Bluehole #1.



Figure GS-22-3d: Upwelling with distinctive, concentric vegetation rings. Core of floating tufted grass and moss is 16 m diameter. Structure is elevated 2 m above surrounding marly fen pools. (Site 1050. UTM 520028E 5823970N).



Figure GS-22-3f: Upwelling with central elevated zone covered by labrador tea, dwarf birch and sporadic 3 m tamarack surrounded by intermediate zone with tufted grass and moss and outer zone of marly fen pools with pitcher plants, grasses, cattails. Structure 60 m diameter and 1.5 m elevation. (Site 1048. UTM 520579E 5824117N).

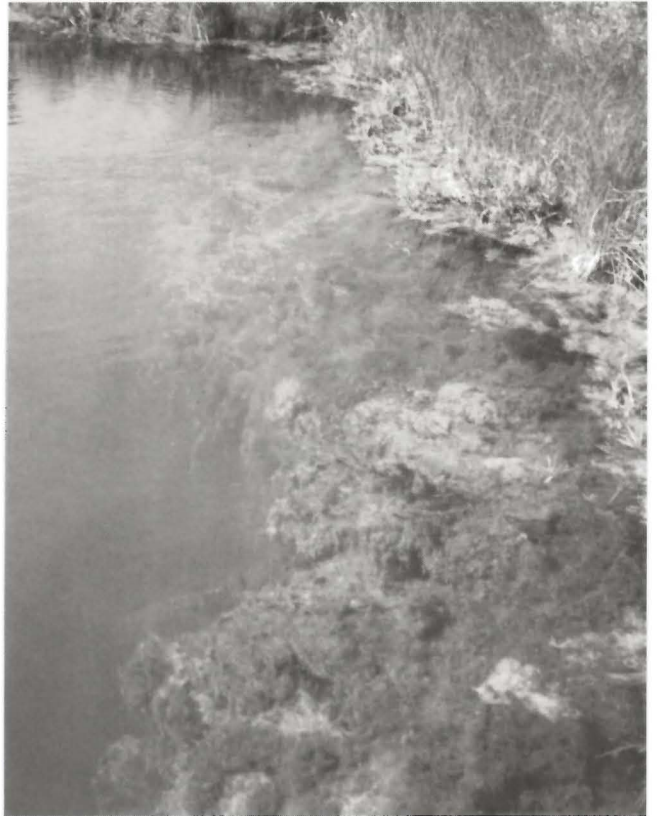


Figure GS-22-3c: Vertical to overhanging walls extending to depth of 5 m on east shore of "Bluehole #1", a 2 m high tufa mound associated with an artesian spring west of Sturgeon Bay, Lake Winnipeg. Note typical tufted grass build up on shoreline.



Figure GS-22-3e: Upwelling with concentric rings of fen pools and interspersed low peaty ridges. Overall diameter 200 m. (Site 1049. UTM 519988E 5823946N).



Figure GS-22-3g: Isolated upwelling, 1.5 m high and 20 m diameter. Central mossy caldera 6 m diameter. Well defined water-saturated surge channel draining eastwards (to left) through chain of ephemeral fen pools. (Site 1017. UTM 517662E 5824688N).



Figure GS-22-3h: "The Twins", paired upwellings (Sites 1049 and 1050) at the head of a typical "tadpole-shaped" drainage element feeding into the South Twin River. A cluster of at least twenty four springs feed into this system.



Figure GS-22-3k: Radial drainage channels on flanks of tufa mound. (Site 1018. UTM 588587E 5724416N).



Figure GS-22-3n: Typical, gravity spring-fed fen pools at base of bedrock escarpment and beach ridges, north of Menauhswun (Honeymoon) Lake, north of Grand Rapids. Ordovician in low ground to right of fen pools.



Figure GS-22-3i: Classic 10 m diameter tufa mound with 1.5 m relief, steep sides and 4 m diameter, mossy, actively upwelling vent pool. Flanks of mound and surrounding proximal fen pools are covered by gravelly tufa. (Site 1060. UTM 508005E 5798856N).



Figure GS-22-3j: Typical tufted grass on quaking ground covering artesian upwelling at Site 1053 (UTM 519486E 5821621N).



Figure GS-22-3l: Lozenge-shaped tufa pebbles forming thin lensoid aggregates on the surface of the marly precipitates. (Site 1014. UTM 511594E 5832332N).



Figure GS-22-3m: "Lothlorien" a pool fed by gravity springs flowing out from base of escarpment, north of Grand Rapids. Clogs in middle distance formed by Silurian, Moose Lake Formation capped by Atikameg Formation. Fisher Branch Formation is 20 m elevation above the pool. (Site 1034. UTM 484396E 5936188N).

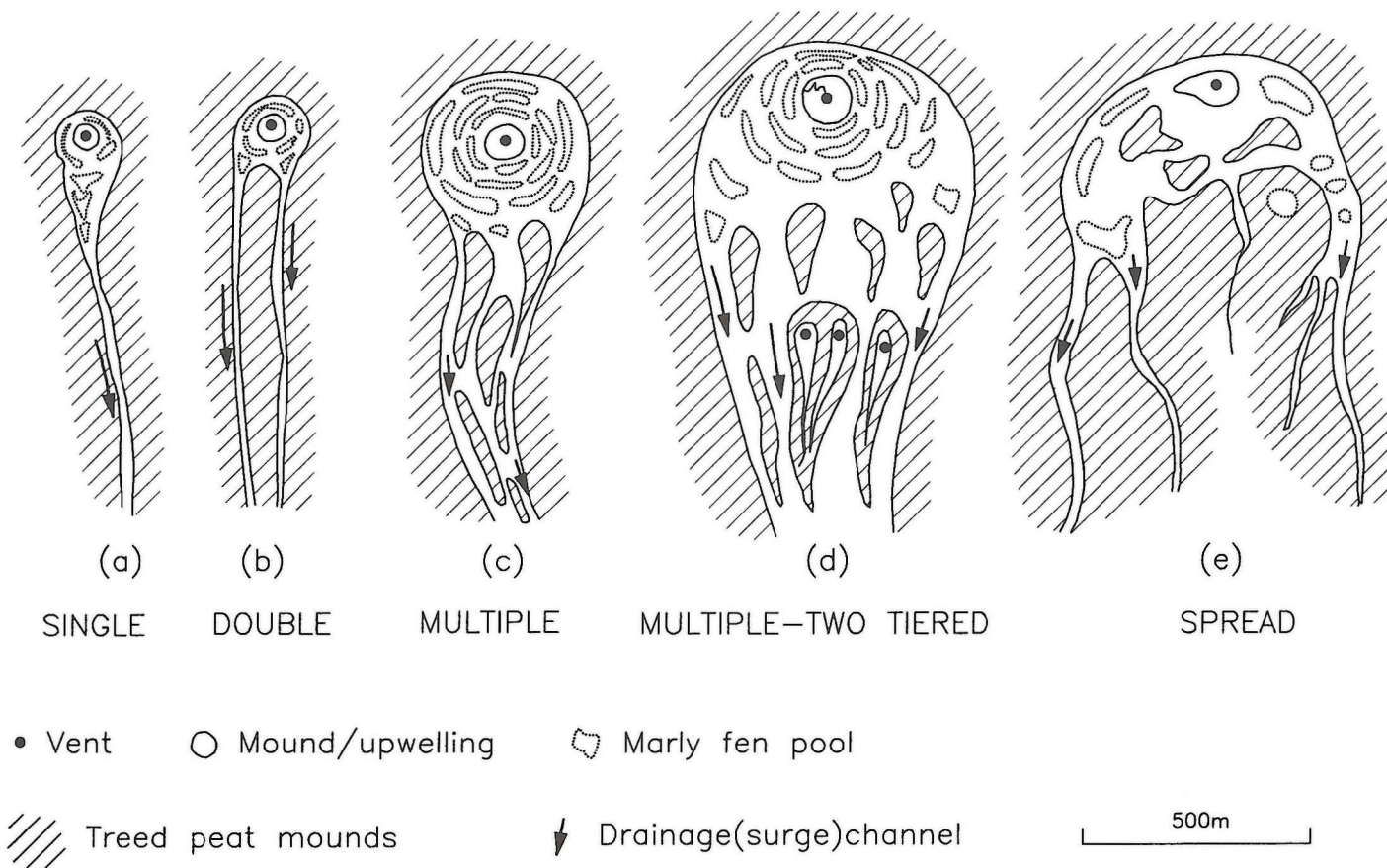


Figure GS-22-4: Generalized physical characteristics of drainage elements associated with upwellings and tufa mounds in the Central Interlake Region (plan views), a) single; b) double; c) multiple; d) multiple-two tiered; e) spread.

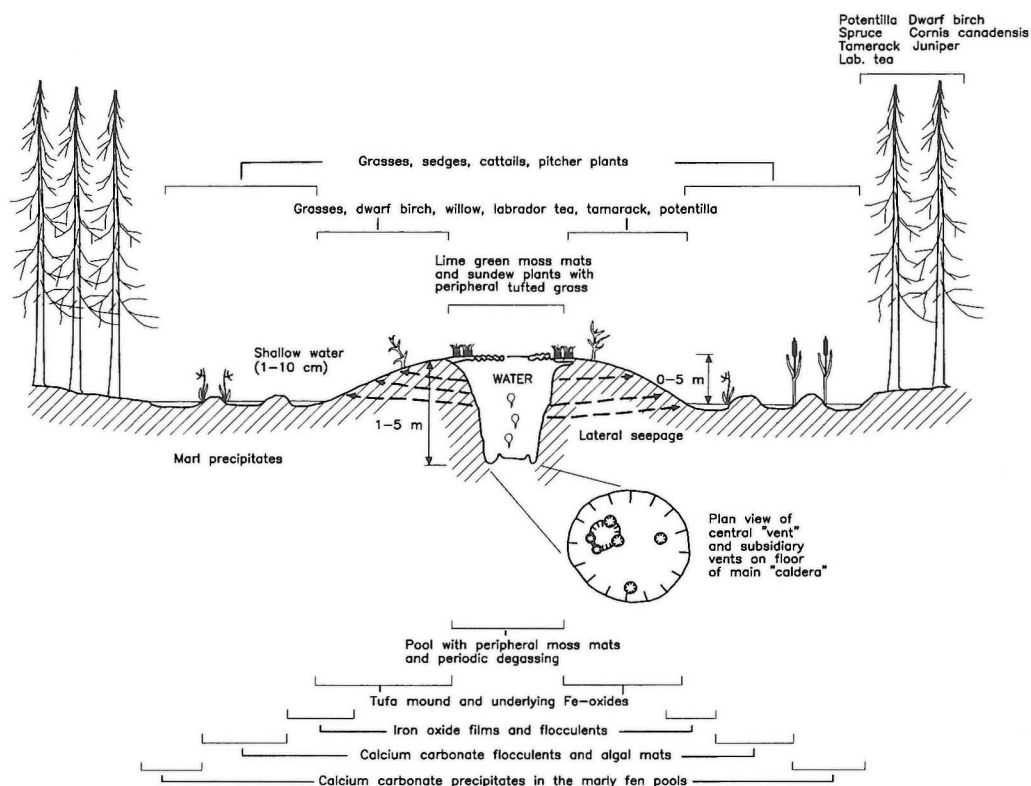


Figure GS-22-5: Zoned vegetation and physical characteristics associated with the upwellings and tufa mounds.

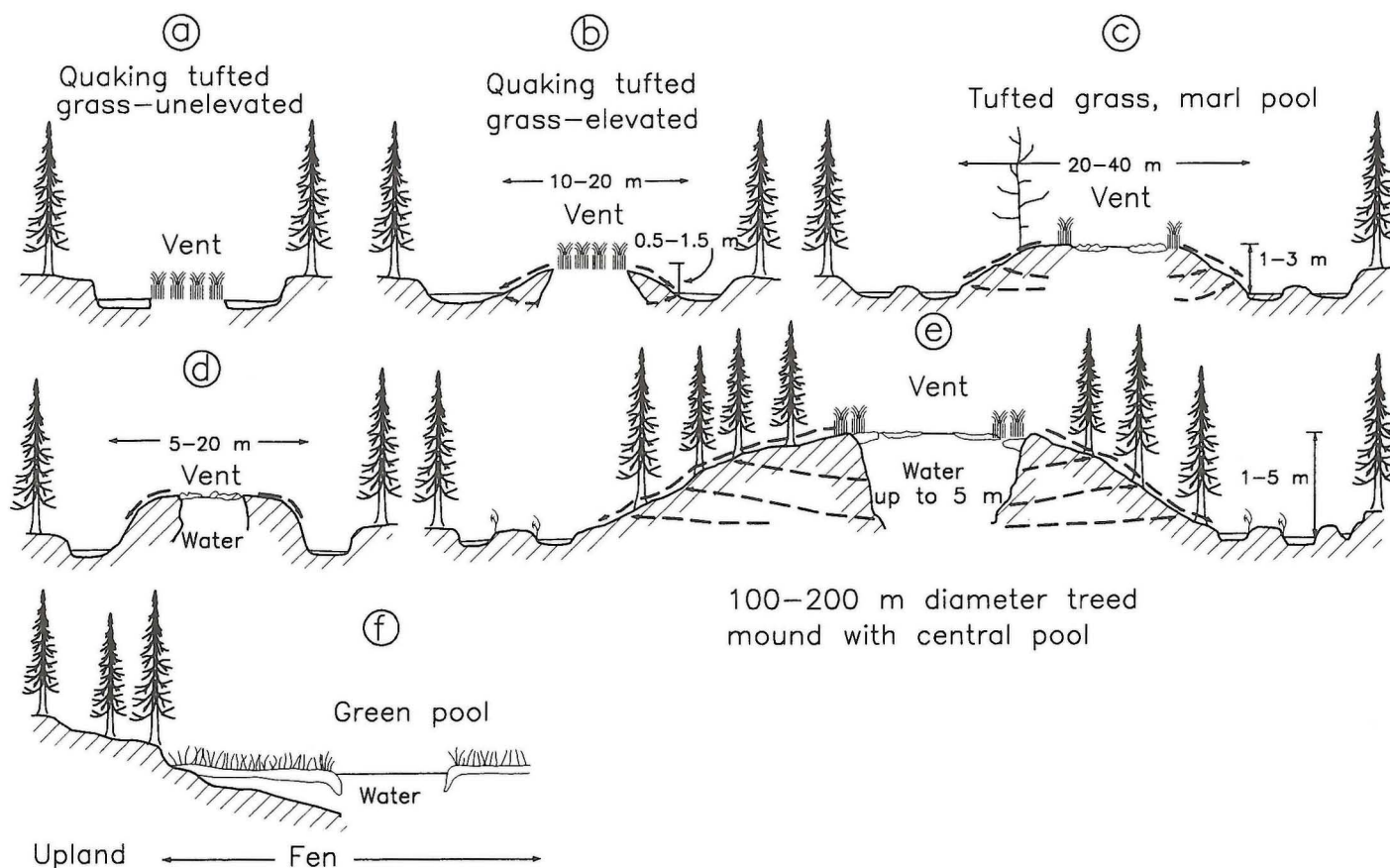


Figure GS-22-6: Generalized cross sections of upwellings and tufa mounds associated with resurgent zones in the Central Interlake.

Table GS-22-2
Average composition of spring waters, Interlake spring sampling survey

PARAMETER	Upwellings/ Mounds	Gravity Springs	Pools	Total	Carbonate* Aquifer
Field					
Temp (o C)	6.02	6.46	17.43	7.59	6.8
Cond (micro-siemens/sec)	674.06	500.58	511.67	625.73	N/A
pH	7.53	7.67	7.95	7.60	7.71
Lab					
pH (lab)	7.63	7.71	8.07	7.69	N/A
Bicarbonate (mg/L)	416.85	329.50	332.56	393.81	415.2
Chloride (mg/L)	4.05	1.29	3.20	3.46	46.4
Nitrate+ Nitrite (mg/L)	0.05	0.16	0.03	0.07	0.93
Sulphate (mg/L)	29.16	5.00	21.22	24.09	87.9
Fluoride (mg/L)	0.47	0.22	0.23	0.39	0.45
Observations (N)	55	12	10	79	500

* Data from Betcher et al., 1995; Table 2, pg. 18

Table GS-22-3 C

Changes in physical parameters away from the central vent of a tufa mound in the region south of Sturgeon Bay, Lake Winnipeg, Manitoba.

Sample #	Distance from vent/features	pH	T°C	Conductivity (mS/cm)
1018	0 m Vent pool (resurgence)	7.31	4.4	730
1021	5 m Outflow channel (cascading), abundant iron oxides	7.50	6.3	718
	10 m "Oily" films on flank and near base of tufa mound			
1020	20 m Outflow channel on marly fen pool flats	7.78	9.0	705
1019	70 m Marly fen pool	8.18	15.0	679

outcrop belt; and 3) high to very high values east of Gypsumville in the Sturgeon Bay area, where springs emerge within the Fort Garry and/or Stonewall/Stony Mountain formations.

Sulphate In general, anomalously high sulphate concentrations occur in those springs east of Gypsumville that emerge within the Fort Garry and/or Stonewall/Stony Mountain formations (Fig. GS-22-7b). Proximity to Gypsumville and location down flow gradient may indicate that this signature is related to the gypsum deposits in this area.

Chloride Like conductivity, chloride concentration appears to increase from north to south (Fig. GS-22-7c). Moderate concentrations occur within the artesian springs along the Silurian escarpments south of Long Point and in the Gypsumville area. The highest observed concentration (43 mg/L) was observed east of Gypsumville. These relationships, although subtle, may reflect eastward migration of the saline front within the carbonate-evaporite aquifer, or upward migration of saline fluids from the underlying Winnipeg Formation.

Fluoride Overall concentrations of fluoride are very low, however subtle variations in concentration suggest a regional trend slightly different to those observed for other parameters. Highest concentrations are observed in the central part of the region, where artesian springs emerge along the Silurian outcrop belt (Fig. GS-22-7d). Moderate concentrations are also observed in the same stratigraphic position north of Gypsumville and within springs emerging within the Fort Garry and Stonewall/Stony Mountain formations. The significance of this distribution is currently unknown, but could potentially be reflective of fluoride associated with Mississippi-Valley-Type mineralization.

CONCLUSIONS

The extension of the groundwater geochemical surveys into the central Interlake region has confirmed the existence of numerous resurgent points along the eastern flank of the drainage divide (Fig. GS-22-6), surfacing at elevations ranging from 218 m (715') to 266 m (873') (only a fraction of those observed were actually sampled during the current survey). Resurgences south of Long Point appear to be mainly artesian, in contrast to those in the Grand Rapids region, which are dominantly (though not exclusively) gravity springs. The apparently widespread occurrence of tufa mounds in the region south of Long Point, confirms and enlarges upon the only other known reference to these features in Manitoba made by Hutt in 1926.

At their point of emergence the artesian flows are driven by the potentiometric head of the groundwaters in the higher elevations nearby, or on a more regional basis, in the hinterland along the crest of the Interlake. All mounds were flowing at the time of the survey, but there was widespread evidence of more vigorous flow at other times in the year, presumably during

spring run-off and following summer storms. The mounds appear to be self-perpetuating structures resulting from the degassing of the cold subterranean waters when they reach the surface, and the associated precipitation of their carbonate-rich solutes. It seems probable that in the mounds themselves, this process is augmented by photosynthetic interaction with the associated mosses (and algae?) surrounding the vents, since the physico-chemical precipitation of the marls in the nearby fen pools is delayed until the waters have travelled some distance from the resurgent points, and warmed up significantly with an attendant increase in pH.

Conductivity measurements in the spring waters increase southwards from Grand Rapids to Anama Bay, the highest levels (>900 and >1000 mS/cm) being recorded west of Sturgeon Bay, together with elevated sulphate and chloride contents.

Geochemical data stemming from the survey of springwaters and associated marls will add substantially to the regional database on groundwater composition and distribution in this relatively remote area, as well as providing additional insights of potential interest to explorationists searching for evidence of buried mineralization in the Interlake.

ACKNOWLEDGMENTS:

Geological Survey of Canada personnel were particularly helpful in developing the initial framework for this project and arranging for sharing of operational costs. Harvey Thorleifson's organizational skills and enthusiasm were crucial to gaining acceptance for the broader hydrogeological initiative and the new federal/provincial NATMAP project in southern Manitoba. Dan Boyle (GSC), Bob Betcher (MWR), Alex Desbarats (GSC) and Gail Hill (MTC) provided technical guidance on methodologies for sample collection and analysis. Dan Boyle also provided all of the equipment for field filtering the water samples. Sample collection in the field was ably assisted by David Wright, Jeff Gutsall and Alex Desbarats. Natural Resources Officers at Gypsumville and Grand Rapids provided logistical support and bases for the operation. Finally thanks are extended to Darren O'Donnell of Provincial Helicopters whose piloting skills with the Bell 206B Jet Ranger helicopter enabled us to access the remote locations where most of the springs occur.

Thanks are also extended to Dr. John Stewart, Department of Botany, University of Manitoba, who assisted in the interpretation of some of the plant species collected during this survey.

REFERENCES:

- Betcher, R., Grove, G. and Pupp, C.
1995: Groundwater in Manitoba, Hydrogeology, Quality Concerns, Management. National Hydrology Research Institute Contribution No. CS-93017, p. 47.

REGIONAL VARIATION OF CONDUCTIVITY IN SPRING WATER

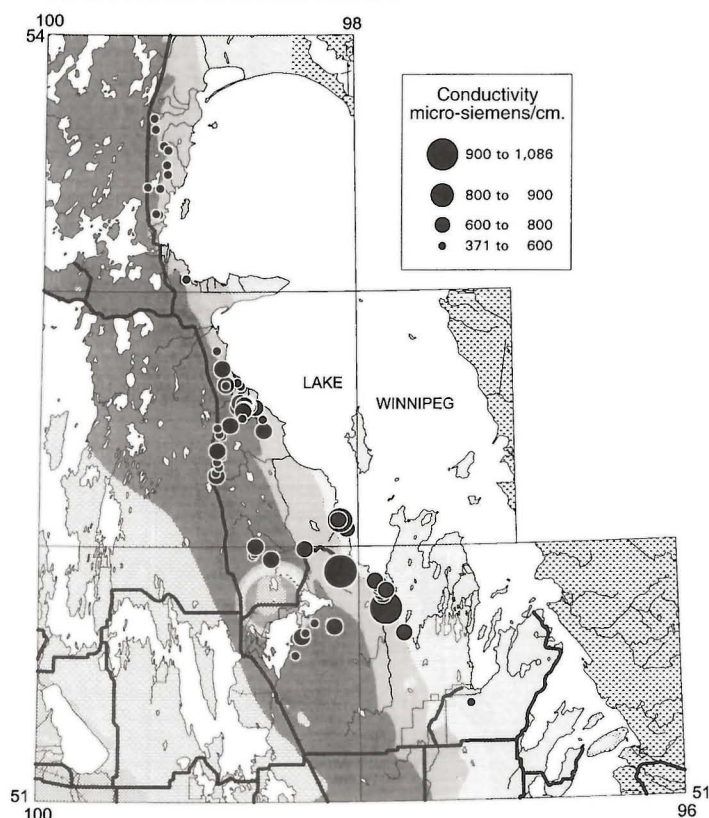
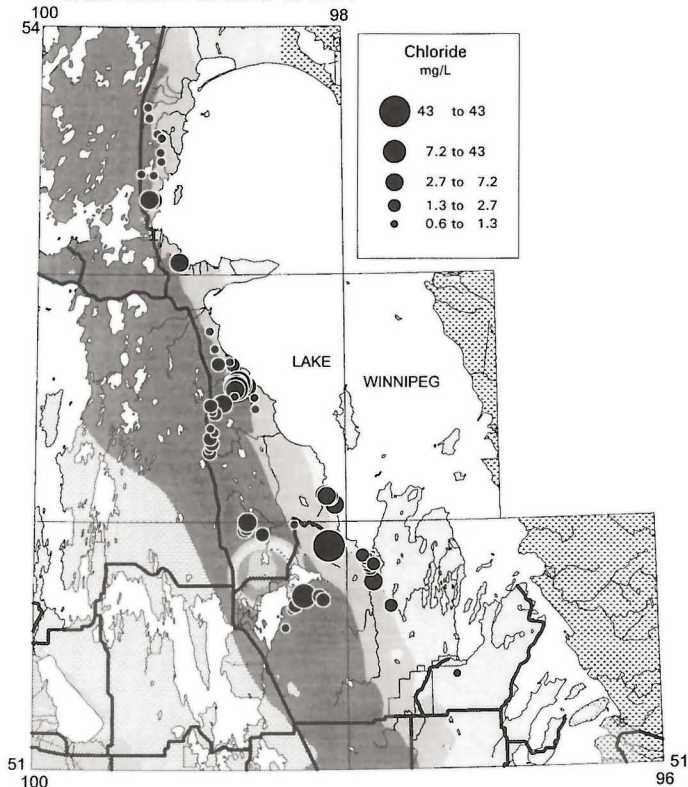


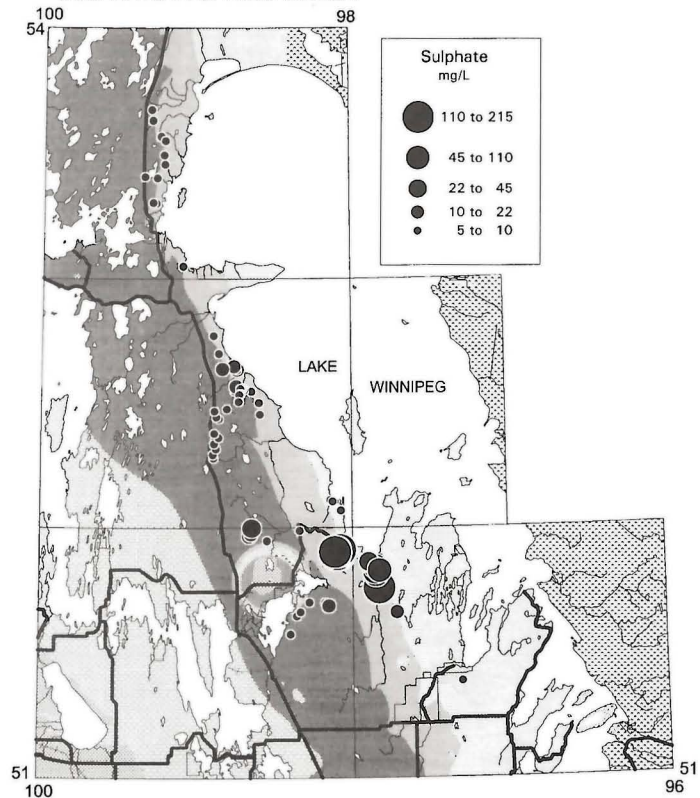
Figure GS-22-7a: Regional variation in conductivity of spring water.

REGIONAL VARIATION OF CHLORIDE IN SPRING WATER



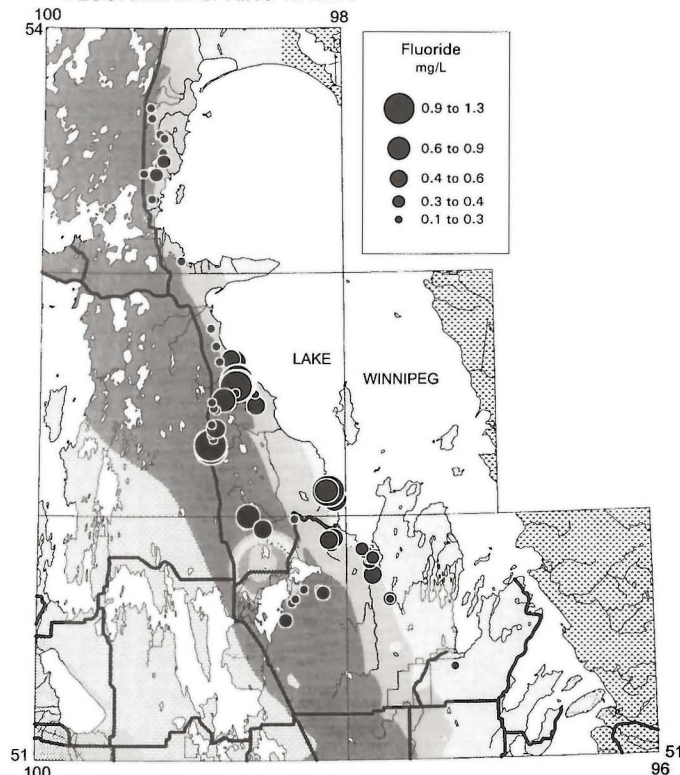
7c: Regional variation of chloride in spring water.

REGIONAL VARIATION OF SULPHATE IN SPRING WATER



7b: Regional variation of sulphate in spring water.

REGIONAL VARIATION OF FLUORIDE IN SPRING WATER



7d: Regional variation of fluoride in spring water.

- Ford, D. C. and Williams P. W.
1989: Karst Geomorphology and Hydrology, Unwin Hyman Ltd., London.
- Ford, T. D., and Pedley, H. M.
1996: A review of tufa and travertine deposits of the world. *Earth Science Reviews* 41, 1996, p. 117-175. Elsevier Science, B. V.
- Fraser, W. R., Hopkins, L. A., Smith, R. E., LeSann, A. and Mills, G. F.
1985: Soils of the Waterhen area, Canada-Manitoba Soil Survey, Agriculture Canada, Manitoba Department of Agriculture, Soils Report No. 23., p. 136.
- Hutt, G. M.
1926: Development Branch Survey - Fisher River - Grand Rapids; Manitoba Energy and Mines, Unpublished report.
- McRitchie, W. D.
1989: Lead-zinc potential in Paleozoic rocks; northern Interlake region, spring and creek waters and sediments; **in** Manitoba Energy and Mines, Minerals Division, Report of Activities, 1989, p. 95-102.

1994: Spring water and marl geochemical investigations, Grand Rapids Uplands (NTS 63G); **in** Manitoba Energy and Mines, Minerals Division, Report of Activities, 1994, p. 148-162.
- 1995: Spring water and marl geochemical investigations, Grand Rapids region, 1995 status report (NTS 63G); **in** Manitoba Energy and Mines, Minerals Division, Report of Activities, 1995, p. 109-119.
- 1996: Groundwater geochemistry and structural investigations of Paleozoic carbonates in Manitoba's Interlake Region; **in** Manitoba Energy and Mines, Report of Activities, 1996, p. 143-152.
- 1997: Bedrock Fracture Orientations, Manitoba Interlake Region. Manitoba Energy and Mines, Geological Services Branch, Preliminary Geological Map 1997P-3
- National Wetlands Working Group
1988: Wetlands of Canada. Ecological Land Classification Series, No. 24. Sustainable Development Branch, Environment Canada, Ottawa, Ontario and Polyscience Publications Inc. Montreal, Quebec.
- Rutulis, M.
1985: Springs in southern Manitoba. Unpublished Report, Manitoba Natural Resources, Water Resources Branch.

GS-23 THE USE OF RARE EARTH ELEMENT ANALYSES IN THE EXPLORATION FOR MASSIVE SULPHIDE TYPE DEPOSITS IN VOLCANIC ROCKS-PROGRESS REPORT.

by G. H. Gale, L.B. Dabek¹ and M.A.F. Fedikow

Gale, G.H., Dabek, L.B. and Fedikow, M.A.F. (1997): The use of rare earth element analyses in the exploration for massive sulphide type deposits in volcanic rocks - progress report; in Manitoba Energy and Mines, Minerals Division, Report of Activities, 1997, p. 147-155.

SUMMARY

Rare earth element data for rhyolites and sulphide-bearing rocks from massive sulphide deposits and occurrences in the Flin Flon - Snow Lake area indicates that the rare earth element contents are leached by the mineralizing fluids and redeposited together with the sulphides and silicates on the ocean floor and in the uppermost parts of the alteration zones. REE data may be useful in determining the presence of metal-bearing strata, distinguishing barren from 'economic' metal-poor sulphide layers, and as a means of correlating strata in some volcanic rocks.

INTRODUCTION

Several researchers have reported rare earth element (REE) data for mineralized rocks and host rocks around volcanogenic massive sulphide (VMS) deposits (e.g., Graf, 1977; Bence and Taylor, 1985; Adair, 1992; Campbell *et al.*, 1984). Graf (1977) not only reported positive Eu anomalies in samples of sulphides and chlorite-rich iron formation from the Brunswick Number 6 deposit, but also reasoned that the observed patterns were the result of hydrothermal fluids leaching Eu from the footwall rocks and depositing it together with other constituents in the chemical sediments and sulphides. Campbell *et al.* (1984) indicated that the hydrothermal solutions that formed VMS ore deposits selectively leached REE from the underlying volcanic rocks and that Eu was more mobile than other REE.

Michard and Albarede (1986) report measurements of hydrothermal fluids from submarine vents that revealed strong positive Eu anomalies and enriched light REE (LREE) relative to the heavy REE (HREE). Bence and Taylor (1985) reported the selective mobilization of Eu and LREE in the vicinity of feeder systems and deposition of Eu adjacent to the hydrothermal vents associated with the Middle Devonian metavolcanic rocks from the West Shasta district, California, but Whitford *et al.* (1988) found only a small positive Eu anomaly in sulphides and phengitic rocks from the Cambrian Que River deposit in the Mt. Read volcanic rocks of Tasmania.

We present here the results from samples of sulphide ores, alteration zones, exhalite-tuff and 'barren sulphides' from producing mines and prospects in the Proterozoic Flin Flon - Snow Lake district of Manitoba (Gale and Eccles, 1988; Fedikow *et al.*, 1989; 1991; Bailes and Galley, 1996). Our initial studies indicate that not only are positive Eu anomalies common in some VMS ores and associated exhalite-tuff, but the positive Eu signature extends well beyond the limits of the known mineralization. In addition, the REE profiles for rocks from stratigraphically underlying

alteration zones and barren sulphides are distinctively different from the exhalite-tuff.

ANALYTICAL METHODS

Samples were analyzed for REE by Activation Laboratories Ltd. (Ancaster) using neutron activation techniques and inductively coupled plasma-mass spectrometry (ICP/MS). Data obtained by neutron activation methods proved unsatisfactory for a number of the sulphide-rich samples because some of the elements were below the lower limits of determination. Although several samples with negligible amounts of silicates also have concentrations of HREE that are below the detection limits, in general the ICP/MS data provides complete profiles. Because our initial objective was to investigate the use of REE in exploration we have used Activation Laboratories 'standard grade' method of analyses instead of the more expensive and precise 'research grade'.

REE IN ALTERED RHYOLITES

Campbell *et al.* (1984) indicated that Eu and other REE were mobilized in the footwall alteration zone of the Kidd Creek deposit, but it is not certain that they were comparing the same rhyolite flows or magmatic events. Our studies (Gale and Dabek, 1996) have shown variations in REE contents not only within cogenetic rhyolites, but also within individual flows. For example, in the vicinity of the Don Jon, a small copper-rich VMS deposit (Gale and Eccles, 1988), the lobes, breccia and tuff of a subaqueous rhyolite flow are clearly cogenetic and both Ti and Zr are conserved elements (Stanley and Madeisky, 1994). All samples from this flow plot on a single line that passes through the origin (Fig. GS-23-1). On Figure GS-23-2 the individual samples exhibit variable degrees of alkali alteration because least altered samples plot on or near the feldspar model line (slope $m = 1$) whereas the strongly chloritized samples plot below the sericite line (slope $m = 1/3$) and towards the abscissa; rocks without sericite and only chlorite plot on the abscissa (Stanley and Madeisky, 1994). Consequently, the variations in REE, including Eu contents, observed in Figure GS-23-3 are the result of hydrothermal fluids differentially affecting the rhyolite flow.

This data supports the conclusions of Campbell *et al.* (1984) and Bence and Taylor (1985) that Eu is indeed depleted in zones of alteration by hydrothermal activity related to VMS activity. In addition, Adair (1992) and others have published rock/chondrite profiles that indicate the presence of negative Eu anomalies in rocks that stratigraphically underlie VMS deposits.

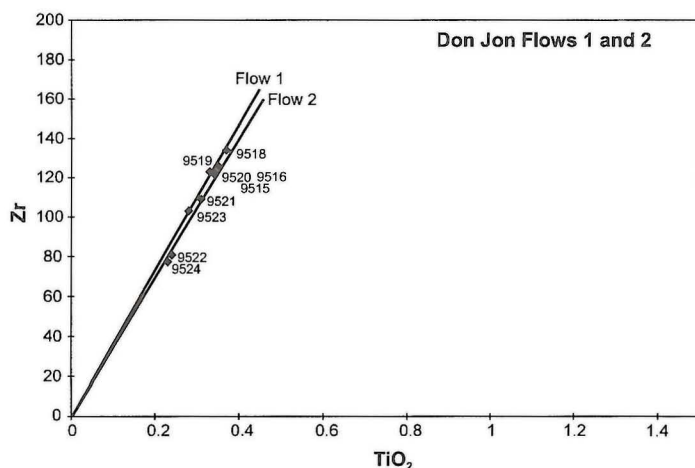


Figure GS-23-1: Zr-TiO₂ plot of samples from flows 1 (9518) and 2 (9522) to illustrate the comagmatic nature of the units sampled. Samples from the same rhyolite flow plot on a line that passes through the origin on this diagram (Gale *et al.*, 1996).

¹ Department of Geology, University of Regina, Regina, Saskatchewan

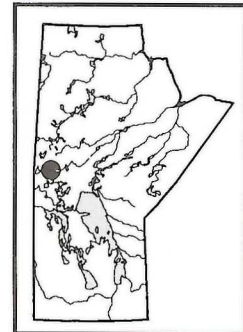


Figure GS-23-2: (Na+K)/Zr vs Al/Zr molar plots of samples of Don Jon flows 1 and 2 (after Stanley and Madeisky, 1994). Unaltered rhyolites plot along the feldspar model line ($m=1$), completely sericitized rhyolites plot along or near the sericite model line ($m=a$), whereas chloritized and sericitized rhyolites plot between $m=a$ and $m=0$. Note the difference in molar Al/Zr ratio of the two flows.

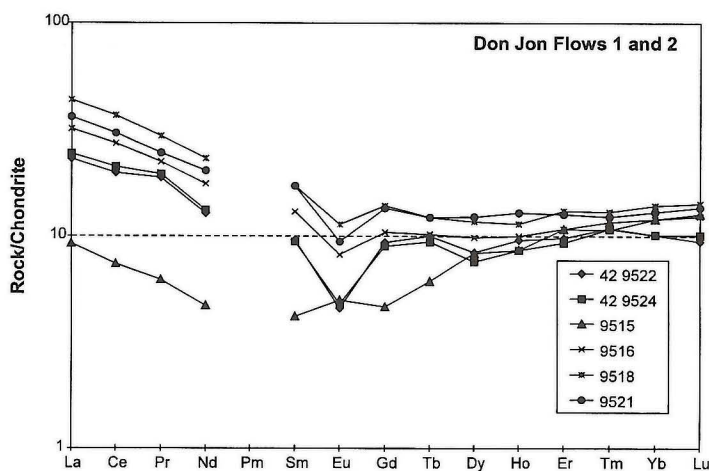
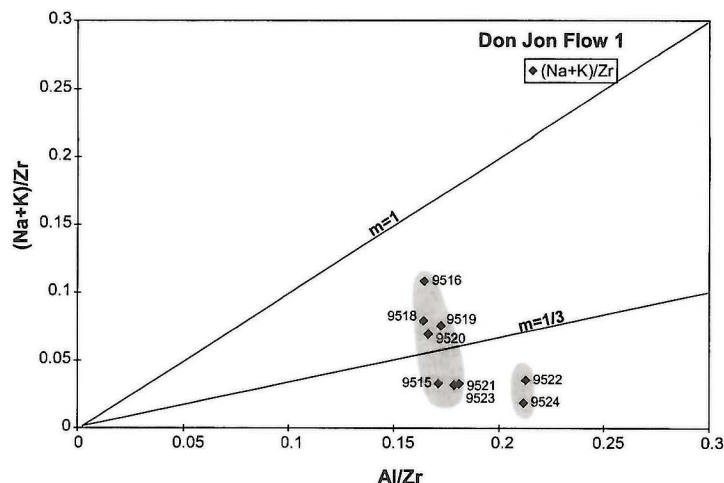


Figure GS-23-3: REE patterns for the variably altered Don Jon flows.

Experimental evidence presented by Haas *et al.* (1995) and measurements from geothermal fields (Michard, 1989) indicate that REE mobility and Eu enrichment in hydrothermal fluids increases with decreasing pH and increasing temperatures ($>230^{\circ}\text{C}$, Michard, 1989). These observations are the most probable explanation for the variability in Eu contents and light REE contents observed in alteration zones related to VMS deposits; namely, the cooler peripheral portions of the alteration zones should exhibit less REE mobility than the hotter and more acidic central portions of the same system.

REE PATTERNS IN ORES AND SULPHIDE-BEARING ROCKS.

If REE, including Eu, are being leached from the volcanic rocks by hydrothermal fluids responsible for the alteration zones that stratigraphically underlie a massive sulphide deposit, then it follows that these elements should be concentrated in the hydrothermal fluids and deposited together with other elements transported by the fluids at or close to the fluid discharge sites, *i.e.*, together with the exhalite products and ores. Michard (1989) has shown that fluids from submarine hydrothermal vents on the East Pacific Rise are indeed enriched in Eu relative to Sm and Gd and are also enriched in LREE relative to the HREE. Barrett *et al.* (1990) present data for massive sulphide-sulphate samples and gossan samples from the Southern Explorer Ridge that have Eu enriched patterns and are enriched in LREE. In addition, they also suggest that positive Eu anomalies in gossanous sediments would indicate the presence of nearby hydrothermal sites and that this could be used as an exploration guide in ancient volcano-sedimentary sequences (Barrett *et al.*, 1990).

The presence of positive Eu anomalies in sulphides and associated sedimentary rocks was recorded by Graf (1977) for samples from the Brunswick VMS deposit, by Lottermoser (1989) for exhalites and ores from the Broken Hill sedimentary rock-hosted deposit, by Adair (1992) for the Halfmile Lake VMS deposit, and by Liaghat and MacLean (1992) for the Matagami Key Tuffite.

RESULTS

Layered solid sulphide and near solid sulphide ores

In general, samples of sulphide ores with more than 90% sulphide minerals have enriched LREE and a positive Eu anomaly relative to Sm, but commonly have HREE concentrations that are below detection limits (Figs. GS-23-4, -5, -6). There does not appear to be any correlation between sulfide mineral species and Eu contents. However, sulphide-rich ore samples with a significant ($>25\%$) silicate component commonly contain elevated HREE contents, have LREE that are the same or higher than the HREE Yb and Lu and higher Eu contents than near solid sulphide samples.

Positive, negative and flat Eu patterns occur in the sulphide ores from massive sulphide deposits (Figs. GS-23-5, -6). The patterns observed in these figures represent grab samples collected from various parts of the deposits. The ores in these deposits have been metamorphosed and deformed (Fedikow *et al.*, 1989, 1991) and, in addition to layered sulphides, commonly include abundant mobilized sulphides and chalcopyrite-pyrrhotite-chlorite ores in proximity to the 'feeder zones'. The variation in REE patterns from these deposits is considered to reflect not only the original

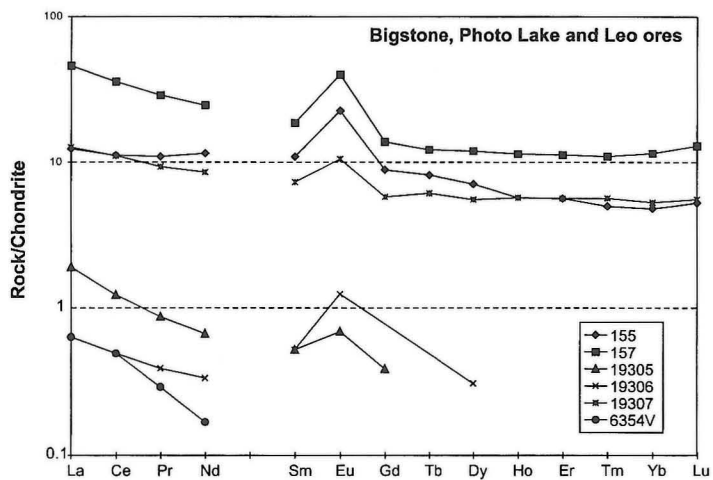


Figure GS-23-4: REE patterns for sulphide-rich ores from the Bigstone, Photo Lake and Leo deposits.

Figure GS-23-5: REE patterns for sulphide-rich samples from the Stall Lake and Rod deposits. Note these deposits contain abundant mobilized ores.

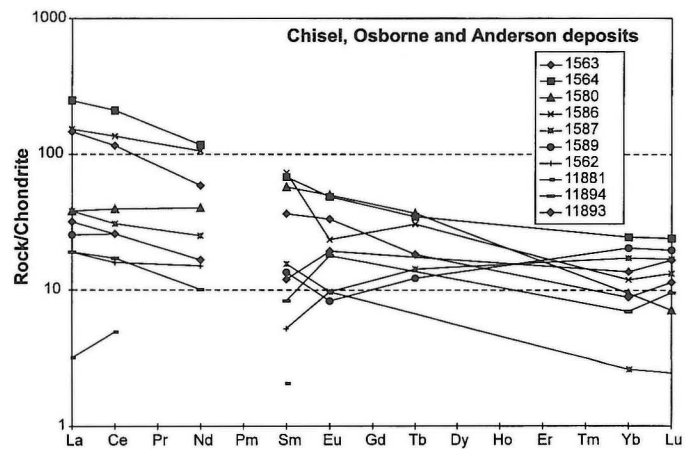
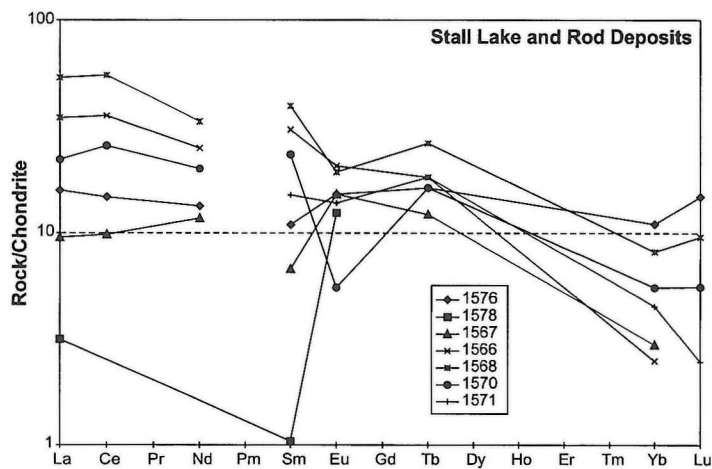


Figure GS-23-6: REE patterns for sulphide-rich ores from the Chisel, Osborne and Anderson deposits.

REE contents, but also changes in the contents of silicates and REE during mobilization and recrystallization of sulphides within different types of ores.

Footwall alteration zones

Sulphide-bearing samples collected from known footwall alteration zones exhibit patterns that are characterized by a negative Eu anomaly and LREE enrichment, e.g., the Leo and Bigstone deposits (Fig. GS-23-7). The HREE patterns can be distinctive in that the HREE portions of the profiles can be lower than either Eu or Gd. These samples are from the sulphide-rich uppermost portions of the alteration zones.

The observed patterns are similar to those from other footwall alteration zones (Adair, 1992; Whitford *et al.*, 1988) and suggest that this type of REE profile may be diagnostic in distinguishing different portions of alteration zones. Samples from the Chartier Lake and Dowling Lake mineral occurrences classified as 'VMS type alteration' (Fedikow *et al.*, 1991) also have negative Eu profiles (Fig. GS-23-7).

Exhalite-tuff ore equivalent zones

Material locally known as 'exhalite' that consists of a mixture of chemical sedimentary rocks, tuff and tuffaceous rocks and often containing sulphides is referred to here as 'exhalite-tuff'. This material has been sampled along strike from several deposits and prospects. The profiles (Fig. GS-23-8) in general have flat HREE profiles, are enriched in LREE and have a distinctive Eu anomaly similar to the VMS 'exhalative' ores. Material from base metal prospects that have been classified as exhalite-

tuff, with and without low base metal contents have similar patterns, e.g. Puella Bay (Fig. GS-23-8). The unusual profile for sample 19310 represents strong fractionation of the LREE and middle REE relative to the HREE. This sample, collected 400 m from known mineralization, is not unique because it resembles the profiles of the Puella Bay occurrence and samples 6355V and 6367V-A that are both base metal-rich. Of particular interest, even though firm conclusions cannot be drawn at this time, is sample 19302 that was collected 1800 m along strike from known mineralization at the Photo Lake mine. The implication from this sample is that there is a definite decrease in Eu contents and minimal enrichment in LREE laterally away from known sulphide deposits as found by Lottermoser (1989, 1991) for sediment hosted deposits and as predicted by Barrett *et al.* (1991).

Barren sulphide zones

A graphitic tuff (Fig. GS-23-9), sampled along strike from the Bigstone deposit does not exhibit a Eu anomaly although there is an increase in LREE relative to HREE. The Sneath Lake 'barren' sulphide zone has a relatively flat REE pattern in both the HREE and LREE; the Tb spike on the profile is probably analytical error. The data for a number of other samples of 'barren' sulphides is incomplete in that most of the values were below the lower limits of detection of the INAA method used. Consequently the data for this sulphide sample type is not conclusive. Further studies are required to determine if 'barren' sulphides have consistently flat profiles.

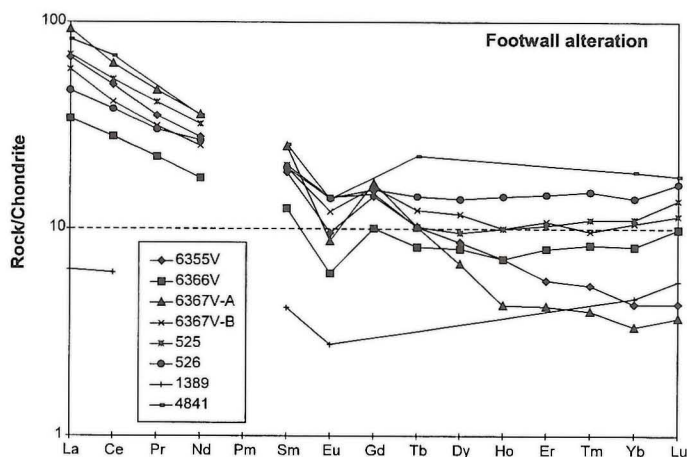
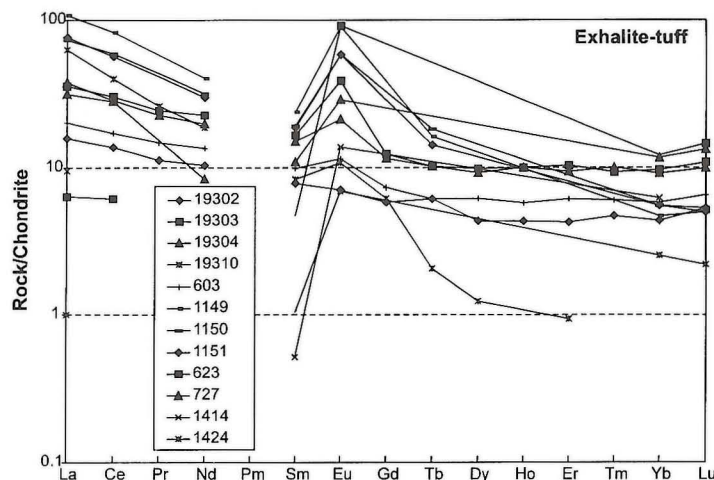


Figure GS-23-7: REE patterns for samples from the footwall alteration zones of the Leo and Bigstone deposits and the Chartier and Dowling occurrences.

Figure GS-23-8: REE patterns for exhalite-tuff from various deposits and occurrences.



DISCUSSION:

Sulphide-bearing rocks from different parts of VMS deposits show different REE profiles. In general, altered rocks stratigraphically underlying a deposit exhibit variable and negative Eu profiles, whereas exhalative ores and related exhalite-tuff material have positive Eu anomalies. However, interpretation of the data is not straightforward, because some 'stringer' ores adjacent to the solid sulphide lense and mobilized sulphides exhibit Eu negative, Eu positive and flat profiles. Sulphide ores with low silicate contents have correspondingly low HREE contents.

The REE variability is substantiated and typified by the results for the Spruce Point deposit. We have examined two sections across the strata hosting the Spruce Point copper-zinc deposit. The 274 m drift was cut adjacent to an ore lense and the 574 m drift was cut 140 m from the nearest known ore lense. Figures GS-23-10 and -11 show that both the footwall and hanging wall felsic rocks exhibit Eu negative anomalies whereas the rocks immediately above the ore (Figure GS-23-10) and along strike from the ore exhibit positive Eu anomalies. In addition, not only does the zone identified as the 'ore equivalent' have a positive Eu anomaly, but Eu enriched exhalite-tuff occur for an additional 20 m into the hanging wall. A REE geochemical profile from a drillhole that missed the ore lenses would have alerted the explorationist to the proximity of the nearby VMS deposit.

Both measurements of hydrothermal fluids and experimental data indicate that Eu anomalies should be common around VMS deposits. Positive Eu anomalies and enriched LREE contents occur in low pH and hot vent fluids, but in general low temperature geothermal solutions do not contain positive Eu anomalies (Michard, 1989). These measurements of vent fluids at active hydrothermal sites suggest that it may be possible to distinguish base and precious metal-bearing sulphide systems from barren systems. In addition, experimental evidence suggests that Eu in East Pacific Rise hydrothermal vent fluids with a positive Eu anomaly exists mainly as EuCl_4^{-2} and EuCl_3^{-3} complexes at 300°C whereas in low temperature geothermal solutions, dissolved Eu occurs as Eu^{+3} (Haas *et al.*, 1995).

Consequently, it should be feasible to use REE data to identify laterally distal exhalite-tuff units that are associated with base metal deposits during exploration that is focused on drilling geophysical anomalies. Strata that contain hydrothermal exhalative products related to hot acidic and presumably metal-bearing fluids should have distinctive Eu positive anomalies whereas those related to colder non acidic and presumably metal-poor fluids should have flat or negative Eu anomalies. The presence of Eu positive anomalies in sulphidic exhalite-tuff several hundred metres from known deposits and in the low sulphide-bearing portions of the 'ore-equivalent' rocks at the Spruce Point Mine, versus the flat Eu profile for barren sulphide, suggests that REE data can be useful in determining whether sulphide-bearing tuff/sedimentary rocks are related to 'economic' or barren hydrothermal systems.

It may be possible to detect the proximity of base metal mineralization from the REE data. Positive Eu anomalies in layered sulphides should decrease away from a vent site and Eu contents of footwall rocks should

decrease in altered rocks towards a vent site. Although our present data is too limited in scope to validate this contention, the findings of Lottermoser (1989, 1991) suggest that the use of Eu as a vector in the location of VMS deposits has considerable potential.

The identification and tracing of 'ore equivalent' strata within faulted and folded rocks in the vicinity of some known deposits is often a major problem in mine scale exploration for additional ore. The recognition of a hydrothermal signature from REE data could provide an additional tool that will increase the confidence level of mine property exploration.

It appears from these preliminary data that further studies of REE data from VMS deposits is warranted. Further data will be reported as acquired.

REFERENCES

- Barrett, T.J., Jarvis, I., and Jarvis, K.E.
1990: Rare earth element geochemistry of massive sulfides-sulfates and gossans on the Southern Explorer Ridge; *Geology*, v. 18, p.583-586.
- Bailes, A.H., and Galley, A.G.
1996: Setting of Paleoproterozoic volcanic-hosted massive base metal sulphide deposits, Snow Lake; in *EXTech I: A Multidisciplinary Approach to Massive Sulphide Research in the Rusty Lake-Snow Lake Greenstone Belts, Manitoba*, (ed.) G.F. Bonham-Carter, A.G. Galley, and G.E.M. Hall, Geological Survey of Canada, Bulletin 426, p. 105-138.
- Bence, A.E., and Taylor, B.E.
1985: Rare element systematics of West Shasta metavolcanic rocks: Petrogenesis and hydrothermal alteration; *Economic Geology*, v. 80, p. 2164-2176.
- Campbell, I.H., Leshner, C.M., Coad, P., Franklin, J.M., Gorton, M.P., and Thurston, P.C.
1984: Rare-earth element mobility in alteration pipes below massive Cu-Zn-sulfide deposits; *Chemical Geology*, v. 45, p. 181-202.
- Fedikow, M.A.F., Ostry, G., Ferreira, K.J. and Galley, A.G.
1989: Mineral deposits and occurrences in the File Lake area, NTS 63K/16; Manitoba Energy and Mines, Geological Services, Mineral Deposit Series, Report No.5, 277 p.
- Fedikow, M.A.F., Athayde, P. and Galley, A.G.
1993: Mineral deposits and occurrences in the Wekusko Lake area, NTS 63J/13; Manitoba Energy and Mines, Geological Services, Mineral Deposit Series, Report No.14, 460 p.

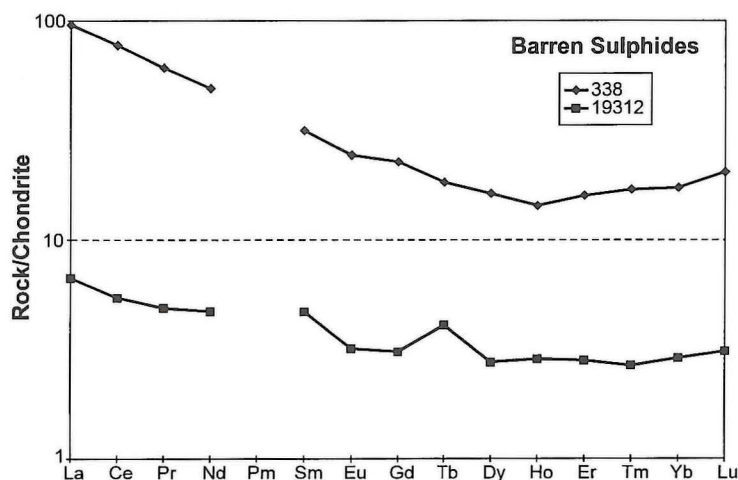


Figure GS-23-9: REE patterns for two barren sulphide occurrences in proximity to known ore deposits.

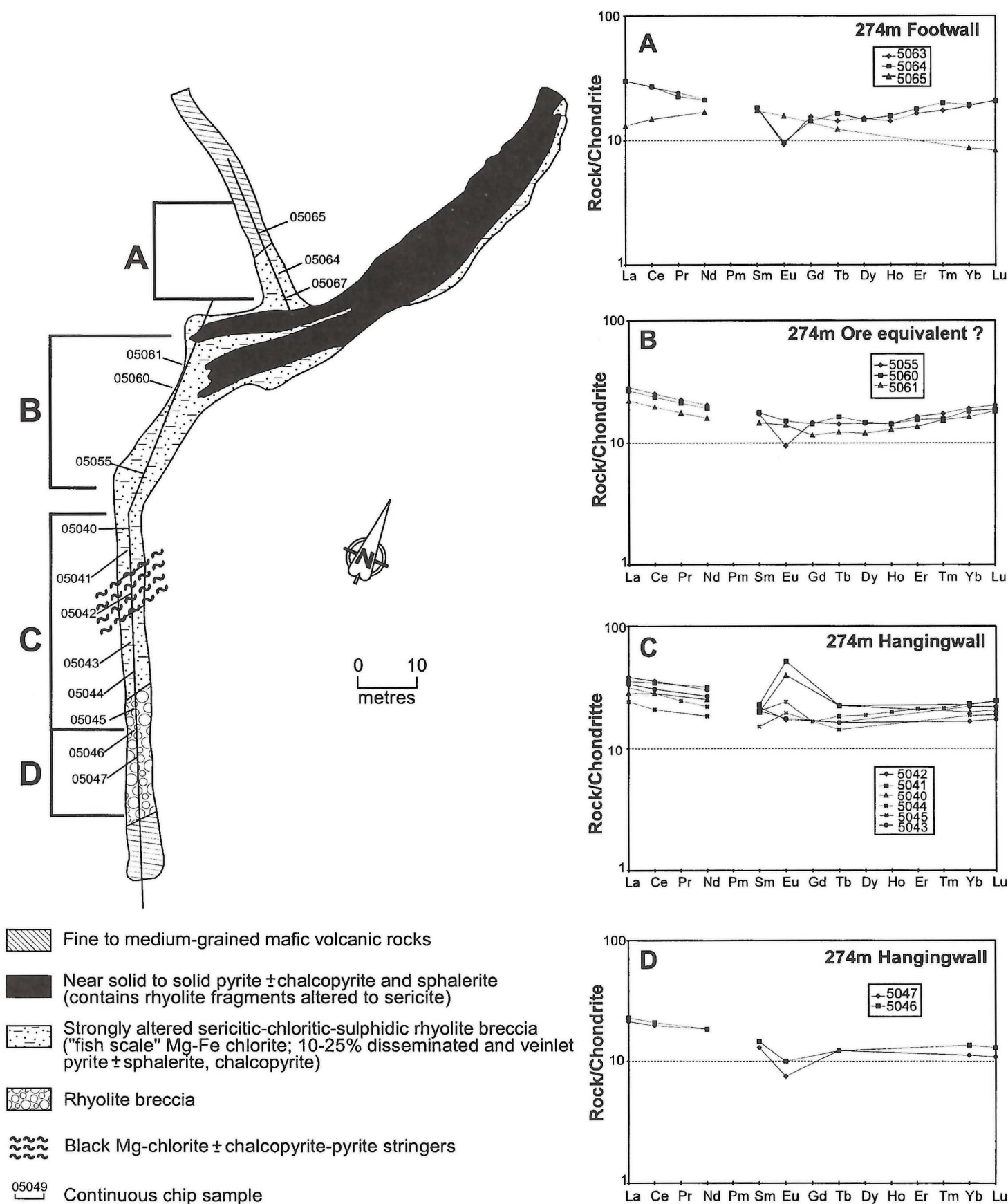


Figure GS-23-10: Geology, sample locations and REE profiles from the 274 m level of the Spruce Point deposit.

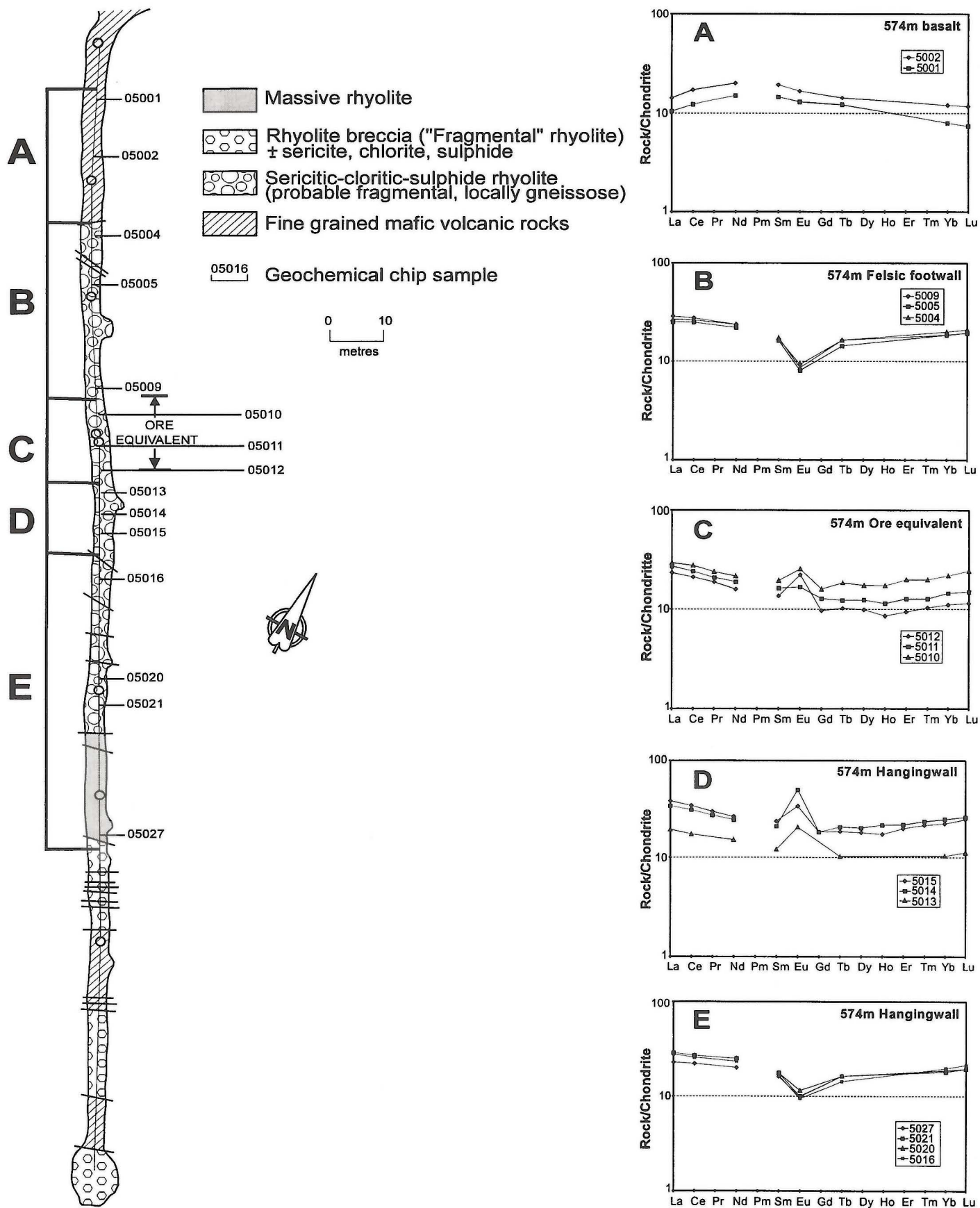


Figure GS-23-11: Geology, sample locations and REE profiles from the 574 m level of the Spruce Point deposit.

- Gale, G.H., and Dabek, L.B.
1996: The Baker Patton Complex (parts of 63K/12 and 63K/13) - rhyolites, dacites and rare earth element chemistry; in Manitoba Energy and Mines, Minerals Division, Report of Activities 1996, p. 47-51.
- Gale, G.H., and Eccles, D.R.
1988: Mineral Deposits and Occurrences in the Flin Flon Area NTS 63K/13: Part 1, Mikanagan Lake Area (63K/13SE); Manitoba Energy and Mines, Geological Services, Mineral Deposit Series Report No.1, 133 p.
- German, C.R., Higgs, N.C., Thomson, J., Mills, R., Elderfield, H., Blusztajn, J., Fleer, A.P., and Bacon, M.P.
1993: A geochemical Study of Metalliferous Sediment From the TAG Hydrothermal Mound, 26° 08'N, Mid-Atlantic Ridge; Journal of Geophysical Research, v. 98, No. B6, p. 9683-92.
- Graf, J.L.,
1977: Rare earth elements as hydrothermal tracers during the formation of massive sulfide deposits in volcanic rocks; Economic Geology, v. 72, p. 527-548.
- Haas, J.R., Shock, E.L., and Sassani, D.C.
1995: Rare earth elements in hydrothermal systems: Estimates of standard partial molal thermodynamic properties of aqueous complexes of the rare earth elements at high pressures and temperatures; Geochimica et Cosmochimica Acta, v. 59, p. 4329-4350.
- Lottermoser, B.G.
1989: Rare earth element study of exhalites within the Willyama Supergroup, Broken Hill block, Australia; Mineralium Deposita, v. 24, p. 92-99.
- Lottermoser, B.G.
1991: Trace element composition of exhalites associated with the Broken Hill sulfide deposit, Australia; Economic Geology, v. 86, p. 870-877.
- Michard, A.
1989: Rare earth element systematics in hydrothermal fluids; Geochimica et Cosmochimica Acta, v. 53, p. 745-50.
- Michard, A., and Albarede, F.
1986: The REE content of some hydrothermal fluids; Chemical Geology, v. 55, p.51-60.
- Stanley, C.R., and Madeisky, H.E.
1994: Lithogeochemical exploration for hydrothermal ore deposits using Pearce element ratio analysis; Geological Association of Canada Short Course Notes, v. 11, p. 193-211.
- Whitford, D.J., Korsch, M.J., Porritt, P.M., and Craven, S.J.
1988: Rare-earth element mobility around the volcanogenic polymetallic massive sulfide deposit at Que River, Tasmania, Australia; Chemical Geology, v. 68, p. 105-119.

Table GS-23-1

Location and description of sulphide samples. NSS - near solid sulfide, SS - solid sulphide.

(Fig. GS-23-4, etc) indicates where the REE profile is plotted.

Sample Deposit	Description
(Fig. GS-23-4)	
525 Bigstone	Main Zone sulphides and altered andesite
526 Bigstone	Main Zone sulphides and altered andesite
19305 Photo Lake	Cu-rich ore, NSS
19306 Photo Lake	Zn-rich ore, NSS
19307 Photo Lake	Silica-rich ore, 50% py, cp, sp
6354V Leo Lake	NSS in siliceous matrix, 30% sp, 30% py, 1% cp
(Fig. GS-23-5)	
1576 Stall	Silica-rich disseminated and stringer ore, 15%cp, 5%py
1578 Stall	SS, cu-rich ore
1567 Rod	SS, cu-rich ore
1566 Rod	NSS, cu-rich ore, fine grained
1568 Rod	SS, cu-rich ore, medium grained
1570 Rod	SS, cu-rich ore, medium grained
1571 Rod	NSS, cu-rich ore, fine- to medium- grained
(Fig. GS-23-6)	
1563 Chisel	Dissem. and veinlet py-cp (25%) in chlorite schist
1564 Chisel	Quartz -chlorite schist, <1% dissem. pyrite
1580	Anderson Dissem., fine grained sp and cp (15%) in fine grained siliceous matrix
1586 Osborne	Dissem. py and po (10%) in biotite-anthophyllite rock
1587 Osborne	Disseminated po (10%) in matrix of anthophyllite, biotite, quartz, staurolite and cordierite
1589 Osborne	Dissem. po (5%) in matrix of anthophyllite, cordierite and staurolite
1562 Chisel	Dissem. and veinlets of sp-py-cp (25%) in sugary textured siliceous matrix
11881 Anderson	NSS ore, 1775 west stope
11894 Prospect 1	NSS
11893 Prospect 1	NSS
(Fig. GS-23-7)	
6355V Leo Lake	Aphyric rhyolite, banded and brecciated, 3-5%sp, 3-5% py in a chloritic matrix
6366V Leo Lake	Aphyric rhyolite, chloritic, trace sulphides
6367V-A Leo Lake	NSS, cp, py with 1-2 cm dark green to black chlorite fragments

Table GS-23-1

Location and description of sulphide samples. NSS - near solid sulfide, SS - solid sulphide.

(Fig. GS-23-4, etc) indicates where the REE profile is plotted.

Sample Deposit	Description
6367V-B Leo Lake	Veins of cp and py in dark green chloritic rhyolite
525 Bigstone	Altered andesite and sulphides
526 Bigstone	Altered andesite and sulphides
1389 Chartier Lake	Dissem. py, po and asp
4841 Dowling Lake	Dissem. cp, py and mt in garnet-anthophyllite rich matrix
(Fig. GS-23-8)	
19302 Photo Lake	Felsic tuff (quartz-chlorite-sericite schist) with trace py; 1800 m north of mine
19303 Photo Lake	Felsic tuff with 15-20% py; chlorite and biotite-rich layers; 250 m into HW from mine
19304 Photo Lake	Felsic tuff with 10% py; trace cp and sp as mobilizate veinlets; 120 m north from mine
19310 Prospect 2	Fine grained silicic rock with 10% biotite and trace py; 400 m south from orebody
603 Bigstone sample 525	Felsic and intermediate tuff; 17 m into HW from
1149 Puella Bay	Quartz vein with 5% dissem. cp, py and sp mobilizate
1150 Puella Bay	Quartz vein with 10 % dissem. py, cp and sp mobilizate
1151 Puella Bay	Quartz vein with 10% dissem. py, cp and sp mobilizate
623 Ruby Zone	Dissem. py and ga (5%) in siliceous quartz-carbonate altered rhyolite
727 Ruby Zone	Dissem. sp, ga and py (15%)
1414 Ruby Zone	SS py, ga, sp, and cp
1424 Ruby Zone	Quartz vein with 5% ga and py mobilizate
(Fig. GS-23-9)	
338 Bigstone	Graphitic and pyrrhotitic sedimentary rocks
19312 Sneath Lake	Po with trace cp and sp, <5% silicates

N.B.

1. Prospect 1 and Prospect 2 are 'economic' massive sulphide type deposits (J. Kitzler, HBMS, pers. comm.)
2. Chartier Lake, Dowling Lake, Puella Bay, Ruby Zone are mineral occurrences.
3. Sneath Lake is a zone of 'barren' NSS mobilizate(?).

Table GS-23-2

**Grades and tonnages of massive sulphide deposits
sampled for the rare earth element study (From Bailes and
Galley, 1996).**

Deposit	Cu %	Zn %	Au g/t	Ag g/t	Production and Reserves (tonnes)
Chisel Lake	0.6	10.94			7299816
Stall Lake	4.39	0.5			7 000 000
Osborne Lake	3.14	1.52			3 380 061
Anderson Lake	3.41	0.1			3 189 601
Spruce Point	2.36	2.8	2	25	1 931 000
Photo Lake	5.6	6.2	5.1	20	660 000
Rod No. 2	6.63	2.9			810 440
Don Jon	3.07		96	15.2	79 313
Bigstone	2.57	0.21	12.18		1 462 400
Bigstone	0.23	6.08	12.58		627 000
Leo Lake	3.65	1.94			80 000

GS-24 GEOSCIENCE INFORMATION SERVICES PROJECTS

by P. G. Lenton

Lenton, P.G. (1997): Geoscience Information Services Projects; in Manitoba Energy and Mines, Minerals Division, Report of Activities, 1997, p. 156.

SUMMARY

Manitoba Energy and Mines has expanded GIS technology into all areas of land-related information management. Production of all maps and land-based databases is now handled digitally. This technology allows rapid production of many new products, such as the NATMAP geological compilation maps, wetlands database, and new or updated geological compilations at various scales.

GIS SYSTEMS

Geological Services Branch continues to expand GIS capabilities. The principal GIS platform is still ArcInfo version 7.1.1 running on a SPARC work station with PC ArcInfo/ArcView stations as secondary systems. To supplement the main systems in the Winnipeg office, an additional PC ArcInfo workstation has been added to support operation in the Thompson office.

In addition to the dedicated GIS workstations, extensive use is made of desktop GIS software. The software chosen for this task includes MapInfo and ArcView, which are used directly by geologists for data management and analysis. The report on the multimedia geochemistry survey released at the end of May (Fedikow *et al.*, 1997) was produced almost entirely using MapInfo software.

ArcInfo software is also the standard GIS platform for other branches of Energy and Mines including Petroleum Branch (oil well information system) and Mines Branch (claims administration function and land management).

NATMAP SHIELD MARGIN PROJECT

The 1:100 000 compilation of the Fin Flon-Snow Lake belt in Manitoba and Saskatchewan has been completed. The geology maps were displayed as a poster at the Ottawa '97 GAC/MAC meeting and have subsequently undergone final editing. This concludes the map production phase of the project that started in 1991.

The 1:100 000 map package comprises 3 maps of exposed Precambrian geology and interpreted sub-Phanerozoic Precambrian geology, 3 maps of exposed Precambrian and Phanerozoic geology, one legend sheet and a sheet of marginal notes, figures and references. The package is complemented with complete coverage of surficial geology at 1:100 000.

The final product resulting from this project will be a release of bulk data and digital versions of the maps on CD-ROM to follow late in 1998. Development of this package of digital information will proceed through the remainder of the year.

WETLANDS PROJECT

The previously reported Wetlands Map of Manitoba (1:1 000 000) project is now complete. This joint project with the University of Alberta comprises a compilation map portraying wetland classifications for Manitoba based on 15 units ranging from dry ground and outcrop through various content of fen, bog and open water to peat complexes. The map includes marginal notes and a figure demonstrating the classification scheme used for the project. The map was compiled by Energy and Mines using ArcInfo GIS and printed by Linnet Geomatics Ltd.

BEDROCK GEOLOGY COMPILATION MAP SERIES

The 1:250 000 Bedrock Geology Compilation program continues with NTS 62I (Selkirk) now available for purchase. Norway House (NTS 63H) is available for viewing in preliminary form with final release to follow in 1998. These two maps represent the last to be produced by conventional drafting methods; all subsequent products of Manitoba Energy and Mines will be produced using GIS and full digital techniques. Compilation work, using GIS, has begun for Island Lake (NTS 53E) and Opasquia Lake (NTS 53F).

Digital compilation of the geology of the northern Superior in support of Superior Province programming continued with addition of 54D (Kettle Rapids), re-interpretation of the contacts of existing maps 63P (Sipiwek Lake) and 53M (Knee Lake) and inclusion of parts of 53E and 53F.

Digital conversion of all existing 1:250 000 maps of the Bedrock Geology Compilation Map Series will continue both to facilitate update and reprinting of maps and to provide a base for planned revisions to the 1:1 000 000 Geology of Manitoba map, which has not been revised since its release in 1979.

Concomitant with revision to Geology of Manitoba is a complete update of the Surficial Geology of Manitoba map at 1:1 000 000, currently underway under direction of geologists in the Stratigraphic and Industrial Minerals Section.

INTERNET PROJECTS

Energy and Mines is committed to maintaining a web site that is useful to all clients. To this end the department site is currently undergoing a complete redesign and expansion. Over the next few months the department will add both map data in GIS and image format for such features as claim information, some geological projects, as well as integrating searchable databases of geoscience data.

REFERENCE

- Fedikow, M.A.F., E. Nielsen, G.G. Conley and G.L.D. Matile
1997: Operation Superior: Multimedia Geochemistry Survey Results from the Echimamish River, Carrot River and Munro Lake Greenstone Belts, Northern Superior Province, Manitoba (NTS 53L and 63I), Manitoba Energy and Mines, Open File Report 97-2, parts 1 to 6.

**PUBLICATIONS
AND
GEOLOGICAL STAFF**

Publications Released
November 1996 - November 1997
Manitoba Energy and Mines
Geological Services Branch

- Abercrombie, H.J., 1996:
Low temperature Prairie-type gold and PGM mineralization, western Canada sedimentary basin; Manitoba Mining and Minerals Convention 1996, Program and Abstracts.
- Aelick, R., 1996:
A time of growth and change for Inco and the nickel industry; Manitoba Energy and Mines, Manitoba Mining and Minerals Convention 1996, Program and Abstracts.
- Ansdell, K.M., 1996:
Isotopes as guides to alteration and stratigraphy in volcanogenic massive sulphide camps; Manitoba Energy and Mines, Manitoba Mining and Minerals Convention 1996, Program and Abstracts.
- Ash and Associates, 1996:
Sodium silicate study; bench scale tests with silica sands of Manitoba; Manitoba Energy and Mines, Open File OF96-4, 46p.
- Bailes, A.H., 1996:
Setting of Cu-Zn-Au mineralization at Photo Lake; in Manitoba Energy and Mines, Minerals Division, Report of Activities 1996, p. 66-74.
- Bailes, A.H., Simms, D., Galley, A.G. and Young, J., 1996:
Photo Lake (NTS 63K16); Manitoba Energy and Mines, Preliminary Geological Map 1996F-1, 1:10 000
- Bamburak, J.D., 1996:
Bentonite investigations and industrial mineral mapping of the Brandon map area (NTS 62G); in Manitoba Energy and Mines, Minerals Division, Report of Activities 1996, p. 127-133.
- Bamburak, J.D. and Bezys, R.K., 1996:
Manitoba's capital region mineral assessment: 1996 update; Manitoba Energy and Mines, Manitoba Mining and Minerals Convention 1996, Program and Abstracts.
- Bamburak, J.D. and Bezys, R.K., 1996:
Capital region study: update 1996 (NTS 62H and 62I); in Manitoba Energy and Mines, Minerals Division, Report of Activities 1996, p. 103 107.
- Bamburak, J.D. and Nielsen, E., 1996:
Scoriaceous clinker in Swan River Valley gravel pits (NTS 63C/2 and C/3); in Manitoba Energy and Mines, Minerals Division, Report of Activities 1996, p. 134-138.
- Bezys, R.K., 1996:
Stratigraphic mapping (NTS 63G) and core hole drilling program 1996; in Manitoba Energy and Mines, Minerals Division, Report of Activities 1996, p. 96-102.
- Bezys, R.K., 1996:
Sub-Paleozoic structure in Manitoba's northern Interlake along the Churchill-Superior boundary zone: a detailed investigation of the Falconbridge William Lake study area; Manitoba Energy and Mines, Open File OF94-3, 32p.
- Bezys, R.K., Fedikow, M.A.F. and Kjarsgaard, B.A., 1996:
Evidence of Cretaceous(?) volcanism along the Churchill Superior boundary zone, Manitoba (NTS 63G/4); in Manitoba Energy and Mines, Minerals Division, Report of Activities 1996, p. 122-126.
- Bianchini, E., 1996:
Globalization of the gold mining industry; Manitoba Energy and Mines, Manitoba Mining and Minerals Convention 1996, Program and Abstracts.
- Bleeker, W. and Ansdell, K., 1996:
Geology of the Thompson nickel belt: a progress report; Manitoba Energy and Mines, Manitoba Mining and Minerals Convention 1996, Program and Abstracts.
- Breukelman, M., 1996:
Raising capital and valuation of mining companies; Manitoba Energy and Mines, Manitoba Mining and Minerals Convention 1996, Program and Abstracts.
- Brown, T., 1996:
The future for commercial peat moss development in the interlake region of Manitoba; Manitoba Energy and Mines, Manitoba Mining and Minerals Convention 1996, Program and Abstracts.

- Campbell, R.C., 1996:
Manitoba aboriginal issues - aboriginal and corporate relations; Manitoba Energy and Mines, Manitoba Mining and Minerals Convention 1996, Program and Abstracts.
- Clemmer, S. and Tirschmann, P., 1996:
An overview of Falconbridge Limited exploration activities in the Thompson nickel belt; Manitoba Energy and Mines, Manitoba Mining and Minerals Convention 1996, Program and Abstracts.
- Canadian Ceramic Consultant Inc., 1996:
Manitoba whiteware market study; Manitoba Energy and Mines, Open File OF96-5, 161p.
- Conley, G.G., 1996:
Status of the Manitoba Stratigraphic Database; in Manitoba Energy and Mines, Minerals Division, Report of Activities 1996, p. 153.
- Corkery, M.T., 1996:
North East Edmond Lake (NTS 53K/11 NE); Manitoba Energy and Mines, Preliminary Geological Map 1996S-1, 1:20 000
- Corkery, M.T., 1996:
Geology of the Edmund Lake area (53K/11NE); in Manitoba Energy and Mines, Minerals Division, Report of Activities 1996, p. 11-13.
- Chackowsky, L. and Lenton, P.G., 1996:
Geoscience information services projects; in Manitoba Energy and Mines, Minerals Division, Report of Activities 1996, p. 154.
- Cummings, G., 1996:
Overview of the white paper on sustainable development act and the impact on Manitoba's mining industry; Manitoba Energy and Mines, Manitoba Mining and Minerals Convention 1996, Program and Abstracts.
- Darbyshire, P., 1996:
Lime production and its use; Manitoba Energy and Mines, Manitoba Mining and Minerals Convention 1996, Program and Abstracts.
- Dorish, A., 1996:
Market segments, dollar size, traditional uses of peat and peat based mixes; Manitoba Energy and Mines, Manitoba Mining and Minerals Convention 1996, Program and Abstracts.
- Fedikow, M.A.F., Bezys, R.K., Bamburak, J.D. and Abercrombie, H.J., 1996:
Prairie-type microdisseminated Au mineralization - a new deposit type in Manitoba's Phanerozoic rocks (NTS 63C/14); in Manitoba Energy and Mines, Minerals Division, Report of Activities 1996, p. 108-121.
- Fedikow, M.A.F., Bezys, R.K., Bamburak, J.D. and Abercrombie, H.J., 1996:
Prairie-type microdisseminated Au mineralization - a new deposit type in Manitoba's Phanerozoic rocks; Manitoba Energy and Mines, Manitoba Mining and Minerals Convention 1996, Program and Abstracts.
- Fedikow, M.A.F., Ferreira, K.J. and Chackowsky, L., 1996:
Geochemistry of Black Spruce (Picea Mariana) needles and twigs growing over zones of gold mineralization and associated induced polarization responses, Dot Lake area, Agassiz Metaltect; Manitoba Energy and Mines, Economic Geology Report ER96-1, 207p.
- Fedikow, M.A.F., Nielsen, E. and Conley, G.G. 1996:
Operation Superior: 1996 Multimedia Geochemical Data from the Max Lake Area, NTS 63I/8,9 and 53L/5,12; Manitoba Energy and Mines, Open File OF97-1, 37p.
- Fedikow, M.A.F., Nielsen, E. and Sailerova, E., 1996:
Operation Superior: multimedia geochemical surveys in the Echimamish River, Carrot River and Munro Lake greenstone belts, northern Superior Province, Manitoba (NTS 53L and 63I); in Manitoba Energy and Mines, Minerals Division, Report of Activities 1996, p. 5-8.
- Fedikow, M.A.F., Nielsen, E., Conley, G.G. and Matile, G.L.D. 1997:
Operation Superior: Multimedia Geochemical Survey Results From The Echimamish River, Carrot River and Munro Lake Greenstone Belts, Northern Superior Province, Manitoba (NTS 53L and 63I): Manitoba Energy and Mines, Open File OF97-2, 1500p.
- Ferreira, K.J., 1996:
Mineral deposits and occurrences in the Uhlman Lake (northwest) area, NTS 64B/11 to 14.; Manitoba Energy and Mines, Mineral Deposit Series Report No. 29, 104p.
- Ferreira, K.J., Mitchell, J. and Gula, D., 1996
Mineral deposits and occurrences in the south half of the Cormorant Lake area, NTS 63K/1 to 63K/8; Manitoba Energy and Mines, Mineral Deposit Series Report No. 33, 150p.
- Fraser, W., 1996:
ISO 14000: environment management system; Manitoba Energy and Mines, Manitoba Mining and Minerals Convention 1996, Program and Abstracts.

- Frazer, G.R., 1996:
Experience with spectrem - an advanced airborne geophysical unit in northern Manitoba; Manitoba Energy and Mines, Manitoba Mining and Minerals Convention 1996, Program and Abstracts.
- Gale, G.E. and Dabek, L.B., 1996:
The Baker Patton Complex (parts of 63K/12 and 63K/13) - rhyolites, dacites and rare earth element chemistry; in Manitoba Energy and Mines, Minerals Division, Report of Activities 1996, p. 47-51.
- Gale, G.H. and Norquay, L.I., 1996:
Mineral deposits and occurrences in the Cranberry Portage area, NTS 63K/11; Manitoba Energy and Mines, Mineral Deposit Series Report No. 16, 163p.
- Gale, G.H. and Norquay, L.I., 1996:
Mineral Deposits and Occurrences in the Naosap lake area, NTS 64K/14; Manitoba Energy and Mines, Mineral Deposit Series Report No. 20, 91p.
- Gale, G.H., 1996:
Gold in the Churchill Province; Manitoba Energy and Mines, Manitoba Mining and Minerals Convention 1996, Program and Abstracts.
- Gibb, A., 1996:
Progress report on Tanco's efforts to exploit their cesium reserves; Manitoba Energy and Mines, Manitoba Mining and Minerals Convention 1996, Program and Abstracts.
- Gilbert, H.P., 1996:
Geology of the Lac Aimée-Naosap Lake area (63K/13SE and 63K/14SW); in Manitoba Energy and Mines, Minerals Division, Report of Activities 1996, p. 32-39.
- Gilbert, H.P., 1996:
Lac Aimée-Naosap Lake (parts of NTS 63K/13SW, 14SW); Manitoba Energy and Mines, Preliminary Geological Map 1996F-2, 1:20 000.
Golightly, P., Hannila, J., Larson, L., Lyons, R., Stewart, R., Somerville, R. and Toderian, M., 1996:
New developments in the Pipe-Thompson-Moak zone of the Thompson nickel belt; Manitoba Energy and Mines, Manitoba Mining and Minerals Convention 1996, Program and Abstracts.
- Halverson, G., 1996:
TVX Gold Inc: a global operations review; Manitoba Energy and Mines, Manitoba Mining and Minerals Convention 1996, Program and Abstracts.
- Heine, T.H., 1996:
Geology of the Alberts Lake Area, Flin Flon (NTS 63K/13); in Manitoba Energy and Mines, Minerals Division, Report of Activities, 1996, p. 40-42.
- Heslop, J.B., 1996:
Canada's current mining environment; Manitoba Energy and Mines, Manitoba Mining and Minerals Convention 1996, Program and Abstracts.
- Hogan, J., 1996:
R.O.I. on incentives is A-O.K.; Manitoba Energy and Mines, Manitoba Mining and Minerals Convention 1996, Program and Abstracts.
International Technologies Consultants, Inc., 1996
Manitoba float glass project feasibility study; Manitoba Energy and Mines, Open File OF96-7, 77p.
- James, D.R., 1996:
Gold supply and demand, and prices: separate issues?; Manitoba Energy and Mines, Manitoba Mining and Minerals Convention 1996, Program and Abstracts.
- Jobin-Bevans, L.S., Peck, D.C. and Halden, N.M., 1996:
Detailed geological mapping in the central portion of the Pipestone Lake Anorthosite Complex: in Manitoba Energy and Mines, Mineral Resources Division, Report of Activities, 1996, p. 75-84.
- Kuzyk, G.W., 1996:
Geotechnologies at the underground research laboratory; Manitoba Energy and Mines, Manitoba Mining and Minerals Convention 1996, Program and Abstracts.
- Lin, S., 1996:
Gold deposit potential in the western Superior Province: lessons from Ontario and Quebec; Manitoba Energy and Mines, Manitoba Mining and Minerals Convention 1996, Program and Abstracts.
- Lucas, S.B., White D. J., Bleeker, W., Hajnal, Z., Weber, W. and Lewry, J., 1996:
Contrasts in crustal structure and tectonic history along the strike of the Thompson nickel belt: new insights from lithoprobe seismic reflection data; Manitoba Energy and Mines, Manitoba Mining and Minerals Convention 1996, Program and Abstracts.
- Macek, J.J., 1996:
Thompson Nickel Belt Project: A new compilation map; in Manitoba Energy and Mines, Minerals Division, Report of Activities, 1996, p. 93.

- Macek, J., 1996:
Geological Services Branch objectives in the Thompson nickel belt; Manitoba Energy and Mines, Manitoba Mining and Minerals Convention 1996, Program and Abstracts.
- Mani, H., Xu, M., Stratton-Crawley, R. and MacDonald, R., 1996:
Determination of characteristics of troublesome ultramafic ores; Manitoba Energy and Mines, Manitoba Mining and Minerals Convention 1996, Program and Abstracts.
- Manitoba Energy and Mines, 1996:
Cross Lake NTS 63I; Manitoba Energy and Mines, Bedrock Geology Compilation Map Series, 1:250 000 with marginal notes.
- Manitoba Energy and Mines, 1996:
Georeference information package for the Northern Superior Geologic Province (Second Edition); Manitoba Energy and Mines, Open File OF95-8.
- Matile, G.L.D. and Thorleifson, L.H., 1996:
Regional till compositional trends, northeastern Manitoba; in Manitoba Energy and Mines, Minerals Division, Report of Activities 1996, p. 9-10.
- Matile, G.L.D. and Thorleifson, L.H. 1997:
Till Geochemical and Indicator Mineral Reconnaissance of Northeastern Manitoba; Manitoba Energy and Mines, Open File OF97-3, 120p.
- Matile, G.L.D., Nielsen, E., Lewis, C.F.M., Thorleifson, L.H. and Todd, B.J., 1997:
Holocene Evolution of the Manitoba Great Lakes Region; Manitoba Energy and Mines, Open File OF96-8.
- McGregor, C.R. 1996:
Documentation of Sub-Phanerozoic Precambrian exploration drill core in NTS 63J/SW and parts of NTS 63K/SE; Manitoba Energy and Mines, Preliminary Geological Report PR96-1.
- McGregor, C.R., 1996:
Relogged drill core from sub-Phanerozoic Precambrian basement in NTS 63J/SW and parts of NTS 63K/SE; in Manitoba Energy and Mines, Minerals Division, Report of Activities 1996, p. 94-95.
- McRitchie, W.D., 1996:
Introductory summary; in Manitoba Energy and Mines, Minerals Division, Report of Activities 1996, p. 1-4.
- McRitchie, W.D., 1996:
Groundwater geochemistry and structural investigations of Paleozoic carbonates in Manitoba's Interlake Region; in Manitoba Energy and Mines, Minerals Division, Report of Activities, 1996, p. 143-152.
- Morris, D. and Lesguillier, J.C., 1996:
Technological analyses of industrial processes for the production of magnesium metal; Manitoba Energy and Mines, Manitoba Mining and Minerals Convention 1996, Program and Abstracts.
- Oswald, R., 1996:
Mining Recording's information system: a new approach; Manitoba Energy and Mines, Manitoba Mining and Minerals Convention 1996, Program and Abstracts.
- Parres, J.R.B., 1996:
The Baker Patton felsic complex....exploration potential; Manitoba Energy and Mines, Manitoba Mining and Minerals Convention 1996, Program and Abstracts.
- Pearson, J., 1996:
Exploration, geophysics and geology of the Winnipegosis basin, Thompson nickel belt; Manitoba Energy and Mines, Manitoba Mining and Minerals Convention 1996, Program and Abstracts.
- Peck, D.C., Cameron, H.D.M., Layton-Matthews, D. and Bishop, A., 1996:
Geological investigations of anorthosite, gabbro and pyroxenite occurrences in the Pikwitonei granulite domain and the Cross Lake region; in Manitoba Energy and Mines, Minerals Division, Report of Field Activities, 1996, p. 85-90.
- Poulsen, K.H., 1996:
Future gold exploration targets in southwestern Superior Province in Manitoba; Manitoba Energy and Mines, Manitoba Mining and Minerals Convention 1996, Program and Abstracts.
- Prouse, D.E., 1996:
The Hotstone - Persian Lake project, North Arm, Lake Athapapuskow, (NTS 63K/12); in Manitoba Energy and Mines, Minerals Division, Report of Activities 1996, p. 43-46.
- Schledewitz, D.C.P., 1996:
Perspectives on the structural geology along the north margin of the Flin Flon volcanic belt; in Manitoba Energy and Mines, Minerals Division, Report of Activities, 1996, p. 29-31.

- Schmidtke, B.E. and Fedikow, M.A.F., 1996:
Mineralogy of metal-rich encrustations on Ordovician Winnipeg Formation black shales and sandstones, Black Island, Lake Winnipeg (NTS 62P/1); in Manitoba Energy and Mines, Minerals Division, Report of Activities 1996, p. 139-142.
- Stephens, R.A., 1996:
Environmental management harmonization: an update; Manitoba Energy and Mines, Manitoba Mining and Minerals Convention 1996, Program and Abstracts.
- Sutherland, B., 1996:
The changing dynamics of the nickel industry; Manitoba Energy and Mines, Manitoba Mining and Minerals Convention 1996, Program and Abstracts.
- Syme, E.C. and Bailes, A.H., 1996:
Geochemistry of arc and ocean-floor metavolcanic rocks in the Reed Lake area, Flin Flon belt; in Manitoba Energy and Mines, Minerals Division, Report of Activities 1996. p. 52-65.
- Syme, E.C., Bailes, A.H., Lucas, S.B. and Stern, R.A., 1996:
Significance of tectonostratigraphic setting and intra-arc extension in localizing volcanogenic massive sulphide deposits in the Paleoproterozoic Flin Flon belt, Manitoba; Manitoba Energy and Mines, Manitoba Mining and Minerals Convention 1996, Program and Abstracts.
- Symons, D.T.A., Lewchuk, M.T., and Harris, M.J., 1996:
Paleomagnetism of the Paleoproterozoic Baldock Batholith (NTS 64B/14); in Manitoba Energy and Mines, Minerals Division, Report of Activities, 1996, p. 14-20.
- Theyer, P., 1996:
Stratigraphy and lithologies of selected drill core from the sub-Paleozoic portion of the Thompson Nickel belt (parts of 63B, 63C and 63G); in Manitoba Energy and Mines, Minerals Division, Report of Activities, 1996, p. 91-92.
- Theyer, P., 1996:
Komatiite hosted nickel copper deposits; Manitoba Energy and Mines, Manitoba Mining and Minerals Convention 1996, Program and Abstracts.
- Turner, A., 1996:
Establishing a ferrous alloy and stainless steel industry in Manitoba, Canada; Manitoba Energy and Mines, Manitoba Mining and Minerals Convention 1996, Program and Abstracts.
- Prouse, D.E., 1996:
North Arm-Athapapuskow Lake and Persian Lake (NTS 63K/12); Manitoba Energy and Mines, Preliminary Geological Map 1996F-3, 1:10000
- Zwanzig, H.V., 1996:
Geology of the Dow Lake - Martell Lake area (parts of NTS 63K/15 and 63N/2); in Manitoba Energy and Mines, Minerals Division, Report of Activities 1996, p. 21-28.
- Zwanzig, H.V., 1996:
Dow Lake-Martell Lake (parts of 63K/15, 63N/2); Manitoba Energy and Mines, Preliminary Geological Map 1996K-1, 1:20 000
- Zwanzig, H., 1996:
Applying the lessons learned in the Flin Flon-Snow Lake Belt to the Kisseynew gneisses; Manitoba Energy and Mines, Manitoba Mining and Minerals Convention 1996, Program and Abstracts.

EXTERNAL PUBLICATIONS

- Corkery, M.T., 1996:
Exploration and a Proposal for a NATMAP Mapping Project in the NW Superior Province; in GAC/MAC Winnipeg 96 Program with Abstracts p. A-19.
- Corkery, M.T., 1996:
Manitoba; in The Geography of Manitoba (J. Welsted, J. Everitt and C. Stadel ed.), University of Manitoba press 1996, p 11-30.
- David, J., Bailes, A.H. and Machado, N., 1996:
Evolution of the Snow Lake portion of the Paleoproterozoic Flin Flon and Kisseynew Belts, Trans Hudson Orogen, Manitoba, Canada; Precambrian Research, V. 80 (1/2), p. 10 7-124.
- Heaman, L.M. and Corkery, M.T., 1996:
Evolution of the Eastern Trans Hudson Margin: Preliminary Results from the Split Lake Block, in GAC/MAC Winnipeg 96 Program with Abstracts p A-42.
- Heaman, L.M. and Corkery, M.T., 1996:
Split Lake Block, Manitoba: Preliminary Results; in Lithoprobe Trans-Hudson Orogen transect report of sixth annual meeting (Z. Hajnal and J. Lewry ed.) Report #55, p 60-687.
- White D.J., Lucas, S.B., Hajnal, Z., Weber, W., Corkery M.T. and Lewry, J.F., 1996:
Images Across the Superior Boundary Zone, Trans-Hudson Orogen, in GAC/MAC Winnipeg 96 Program with Abstracts p A-102.

PRELIMINARY MAPS

GEOLOGICAL SERVICES BRANCH

SCALE

1997F-1	Geology of the Lac Aimée-Naosap Lake area (NTS 63K/14SW) by H.P. Gilbert	1:20 000
1997F-2	Compilation of the geology of the Squall Lake area (NTS 63K/16NE) by D.C.P. Schledewitz	1:20 000
1997P-1	Geological setting of Prairie-type Au mineralization, Mafeking Quarry, west central Manitoba, 1996 work (NTS 63C) by R.K. Bezys, M.A.F. Fedikow, J.D. Bamburak and H.J. Abercrombie	1:5 000
1997P-2	Geological setting of Prairie-type Au mineralization, Mafeking Quarry, west central Manitoba, 1997 work (NTS 63C) by R.K. Bezys, J.D. Bamburak and M.A.F. Fedikow	1:5 000
1997P-3	Bedrock fracture orientations, Manitoba Interlake Region (parts of NTS 62O, 62P, 63B and 63G) by W.D. McRitchie	1:750 000
1997S-1	Geology of the Little Stull Lake area (NTS 53K/10) by M.T. Corkery, T. Skulski and J.B. Whalen	1:20 000
1997S-2	Preliminary geological map of the High Rock Island gold deposit, Island Lake, Manitoba (NTS 53E/15) by S. Lin and H.D.M. Cameron	1:75
1997S-3	Geology of the Assean Lake area (parts of NTS 64A/1,2,7,8) by Ch. Böhm	1:50 000

GEOLOGICAL STAFF, GEOLOGICAL SERVICES BRANCH

POSITION	PERSONNEL	PHONE / E-MAIL	AREAS OF INTEREST
A/Director	Dr. Christine Kaszycki	(204) 945-6549 ckaszycki@em.gov.mb.ca	Manitoba
Precambrian Section			
Chief Geologist	Ric Syme	(204) 945-6556 esyme@em.gov.mb.ca	Manitoba, Flin Flon Belt
Geologist	Dr. Alan Bailes	(204) 945-6555 abailes@em.gov.mb.ca	Flin Flon Belt
Geologist	Tim Corkery	(204) 945-6554 tcorkery@em.gov.mb.ca	Superior Province
Geochemist/mineral deposit geologist	Dr. Mark Fedikow	(204) 945-6562 mfedikow@em.gov.mb.ca	Multimedia geochemical survey, Superior Province
Mineral deposit geologist	Dr. George Gale	(204) 945-6561 ggale@em.gov.mb.ca	Flin Flon Belt, Superior Province
Geologist	Paul Gilbert	(204) 945-6547 pgilbert@em.gov.mb.ca	Flin Flon Belt
Geophysicist	Ifiti Hosain	(204) 945-6540 ihosain@em.gov.mb.ca	Manitoba
Geologist	Cathy McGregor	(204) 945-6543 cmcgregor@em.gov.mb.ca	Thompson Belt compilation
Geologist	Dr. Josef Macek	(204) 945-6548 jmacek@em.gov.mb.ca	Thompson Belt compilation
Geologist	Dave Schledewitz	(204) 945-6566 dschledewitz@em.gov.mb.ca	Kisseynew Belt/Flin Flon Belt
Geologist	Dr. Herman Zwanzig	(204) 945-6552 hzwanzig@em.gov.mb.ca	KisseynewBelt/Churchill Superior Boundary Zone
Thompson office:			
Regional geologist	Dr. Peter Theyer	(204) 677-6886 ptheyer@norcom.mb.ca	Thompson Belt, Superior Province
Regional geologist	Dr. Shoufa Lin	(204) 677-6880 slin@norcom.mb.ca	Superior Province
Regional geologist	Dr. Dave Peck	(204) 677-6885 dpeck@norcom.mb.ca	Thompson Belt, Superior Province
Geologist	Malcolm Cameron	(204) 677-6884 hdmcameron@norcom.mb.ca	Superior Province
Flin Flon office:			
Regional geologist	Tom Heine	(204) 687-4222 theine@gov.mb.ca	Flin Flon Belt
Resident geologist	Dave Prouse	(204) 687-4221 theine@gov.mb.ca	Flin Flon Belt
Sedimentary and Industrial Minerals Section			
Chief Geologist	Dr. Christine Kaszycki	(204) 945-6549 ckaszycki@em.gov.mb.ca	Manitoba
Industrial minerals geologist	Jim Bamburak	(204) 945-6534 jbamburak@em.gov.mb.ca	Capital region, Cretaceous
Phanerozoic stratigrapher	Ruth Bezys	(204) 945-6563 rbezys@em.gov.mb.ca	Southern Manitoba, Interlake
Quaternary geologist	Gaywood Matile	(204) 945-6530 gmatile@em.gov.mb.ca	Manitoba
Quaternary geologist	Dr. Erik Nielsen	(204) 945-6506 enielsen@em.gov.mb.ca	Manitoba;multimedia geochemical survey
Geoscience Information Section			
Section Head	Paul Lenton	(204) 945-6553 plenton@em.gov.mb.ca	Geological data management and analysis
Database geologist	Glen Conley	(204) 945-7255 gconley@em.gov.mb.ca	Stratigraphic data files
GIS specialist	Len Chackowsky	(204) 945-8204 lchackowsky@em.gov.mb.ca	Geographic Information Systems
Geological compiler	Dorne Lindal	(204) 945-0661 dlindal@em.gov.mb.ca	1:250 000 bedrock compilation map series



Printed in Canada



XIII Pan Am Games
Winnipeg '99